

Optimal Placement and Effect of a Wind Farm on Load Flow and Protection Systems in a Municipal Distribution Network



Dissertation by:

Mogamat Noer Martin

MRTMOG009

Department of Electrical Engineering
University of Cape Town

Supervised by:

Mrs K. O. Awodele

Department of Electrical Engineering
University of Cape Town

February 2019

Submitted to the Department of Electrical Engineering at the University of Cape Town in fulfilment of the academic requirements for a Master of Science degree in Electrical Engineering.

Key Words: Wind farm, economic analysis, evolutionary algorithm, optimisation, municipal network, distribution system.

The copyright of this thesis vests in the author. No quotation from it or information derived from it is to be published without full acknowledgement of the source. The thesis is to be used for private study or non-commercial research purposes only.

Published by the University of Cape Town (UCT) in terms of the non-exclusive license granted to UCT by the author.

Declaration

I know the meaning of plagiarism and declare that all the work in the document, save for that which is properly acknowledged, is my own. This dissertation has been submitted to the Turnitin module (or equivalent similarity and originality checking software) and I confirm that my supervisor has seen my report and any concerns revealed by such have been resolved with my supervisor.

Name: Mogamat Noer Martin

Signature: Signed by candidate

Date: 14 October 2019

Acknowledgements

I would like to thank my entire family, my father and mother, Mogamat Yusuf and Zulaiga, as well as my brothers, Mogamat Junaid, Mogamat Yaaseen, and Mughammad. You have all done so much for me that words cannot do justice. I will never be able to thank you all for all the encouragement, support, making sure I got to school every day, helping me with whatever I needed, and everything else in between. I love you all. May Allah grant you all Jannah for all of your efforts, Ameen.

I'd like to thank all my teachers, from pre-school to university. I would not be the person I am today were it not for the knowledge you imparted to me. I also thank my supervisor, Mrs. Awodele, for her assistance during the course of this research.

I'd also like to thank Tyrone for supporting me through life and always raising the bar for me to aim towards, academically.

Finally, I'd like to thank my wife, Nausheena. You have been a rock, my strength throughout the course of this dissertation. You've kept me going when I felt overwhelmed and comforted me whenever I needed it. I fall in love with you more and more each day that we spend together. Marrying you was the best thing I've ever done and I can't wait to see what our future together holds. Shukran for being you.

List of abbreviations

A	Amps
AC	Alternating Current
CFL	Compact Fluorescent Lamp
CSIR	Council for Scientific and Industrial Research
DC	Direct Current
DE	Differential Evolution
DFIG	Doubly-Fed Induction Generator
DG	Distributed Generator
EF	Earth-fault
GA	Genetic Algorithm
GHG	Greenhouse Gas
HV	High Voltage
Hz	Hertz
IEEE	Institute of Electrical and Electronics Engineers
IPP	Independent Power Producer
kA	Kilo-Amps
kV	Kilo-Volts
MPPT	Maximum Power Point Tracking
MS	Main Substation
MV	Medium Voltage
MVA	Mega-Volt-Ampere
MVA _r	Mega-Volt-Ampere Reactive
MW	Mega-Watt
NER	Neutral-Earthing Resistor
NERSA	National Energy Regulator of South Africa
NRS	National Regulatory Standard
OC	Overcurrent
PBIL	Probability-based Incremental Learning
PILC	Paper Insulated Lead Sheath Cable
PMSG	Permanent-Magnet Synchronous Generator
PSO	Particle-Swarm Optimisation
pu	per-unit
PU	Pick Up
PV	Photovoltaic
R-APF	Resistive-Active Power Filter
REFIT	Renewable Energy Feed-In Tariff
RMS	Root Mean Square
SANEDI	South African National Energy Development Institute
SCADA	Supervisory Control and Data Acquisition
SCIM	Squirrel-Cage Induction Machine
SMES	Super-Conducting Magnetic Energy Storage
SS	Substation
THD	Total Harmonic Distortion
TSR	Tip-Speed Ratio
V	Volts
WECS	Wind Energy Conversion System
XLPE	Cross-Linked Polyethylene

Abstract

Much research has been done on the effects of distributed generation on network characteristics. However, little research has been done on the effects of this distributed generation on current network protection schemes.

An IPP has approached a South African municipality regarding the connection of a wind farm that would be connected to the municipality's existing grid. This presented a unique opportunity to simulate and study the impact and effect that this wind farm would have on a real-life network in terms of network operation and protection schemes. This also presents the possibility of connecting the wind farm in a different configuration, possibly resulting in better network operation at a lower cost.

The network optimisation in this research was done using the probability-based incremental learning (PBIL) and differential evolution (DE) optimisation techniques. These algorithms were programmed and modelled according to the desired IPP wind farm requirements using the MATLAB and MATPOWER simulation packages. The networks used in these algorithms were modelled in the text-based MATPOWER format.

This research goes on to study a modified 14-bus IEEE test network in terms of network characteristics and protection performance so that an idea of the performance of the optimisation algorithms can be obtained. Protection data for the IEEE network was not available. The network was thus graded for use in this study.

The research then continues to model the existing and proposed network configuration, and proposes various other points of connection to the municipal network using the PBIL and DE algorithms. These studies were conducted using the DIgSILENT PowerFactory simulation package, with the networks and protection data being modelled in this package. Network and protection performance results were recorded for each case in both networks under study.

The results show that in the case of the modified IEEE network, the DE algorithm provides a better solution in terms of improving power losses while the PBIL algorithm provides a better solution in terms of improving the voltage profile. In the case of the municipality network, the DE algorithm provides the best performance, with the DE result managing to reduce power losses by 83.89% compared to the current and proposed network configurations. The overall voltage profile was also seen to improve by over 23%.

The research also found that the change in fault level for the various cases are minimal. This is due to the limitation in fault current contribution imposed by the use of an inverter system connecting the wind farm to the grid. This means that, as the results shows, network grading is not very much affected by the addition of the wind farm connections. However, it is seen that the municipal network is not optimally graded in the base case. Finally, it is also seen that, though not often used in research, the MATPOWER package works well as a network simulation tool.

A costing analysis was also conducted and shows that the DE solution is the most cost-effective solution, in addition to being the best-performing solution. The study recommends that the results produced by the DE algorithm be implemented instead of the proposed implementation. The municipal network should also be regraded and new protection settings should be implemented.

Table of Contents

Declaration	i
Acknowledgements	ii
List of abbreviations	iii
Abstract	iv
Table of Contents	v
List of Figures and Tables	vii
1. Introduction	1
1.1 Background to the study.....	1
1.2 Objectives of the study.....	1
1.2.1 Problems to be investigated.....	1
1.2.2 Purpose of the study.....	1
1.3 Scope and limitations.....	2
1.4 Plan of development.....	2
2. Literature Review	3
2.1 Distributed generation.....	3
2.1.1 Impacts of renewable energy in South Africa.....	3
2.1.2 Components in a distributed generation system.....	4
2.2 Distributed Generators in South Africa.....	5
2.2.1 Distributed generation uptake in South Africa.....	5
2.2.2 Connecting DGs to the utility grid.....	5
2.2.3 Connection Standards.....	6
2.3 Wind generation systems.....	8
2.3.1 Wind turbine theory.....	8
2.3.2 Types of wind turbines.....	9
2.3.3 Generators.....	12
2.3.4 Wind resources in South Africa.....	15
2.4 Impacts of adding distributed generators to an existing grid.....	15
2.4.1 Factors influencing the impact of distributed generation on a power network.....	15
2.4.2 Advantages of implementing distributed generation with an existing grid.....	16
2.4.3 Impacts and disadvantages of integrating distributed resources into the network.....	16
2.4.4 Review of other research involving the impact of DGs on the network.....	20
2.5 Energy storage technologies.....	21
2.5.1 Storage techniques.....	21
2.5.2 Common terms and battery specifications.....	21
2.5.3 Comparison of battery technologies.....	22
2.5.4 Advantages and disadvantages of using battery storage.....	23
2.5.5 Other energy storage developments.....	23
2.6 Renewable system electronics.....	24
2.6.1 Conversion technologies.....	24
2.6.2 System controllers.....	25
2.7 Wind turbine system control.....	26
2.7.1 Aerodynamic torque control.....	26
2.7.2 Electrical torque control.....	27
2.7.3 Inverter technology.....	27
2.8 Common DG placement techniques.....	27

2.8.1	Analytical methods.....	27
2.8.2	Evolutionary algorithms.....	28
2.9	Types of evolutionary algorithms.....	29
2.9.1	Genetic algorithms.....	29
2.9.2	Advantages and disadvantages of genetic algorithms.....	30
2.9.3	Population-based Incremental Learning (PBIL).....	30
2.9.4	Advantages and disadvantages of PBIL.....	31
2.9.5	Differential evolution.....	31
2.9.6	Advantages and disadvantages of DE.....	34
2.9.7	Review of research done using optimisation techniques for DG placement.....	34
3.	Case study system design and methodology.....	37
3.1	IEEE test case methodology.....	37
3.1.1	Test case network modelling.....	37
3.1.2	Protection system modelling for the test case.....	38
3.1.1	Test case methodology breakdown.....	39
3.2	Municipal case study methodology.....	40
3.2.1	Case study background.....	40
3.2.2	Case study methodology breakdown.....	41
3.2.3	The current network topology.....	41
3.2.4	Cable modelling for the case study.....	42
3.2.5	Transformer modelling for the case study.....	44
3.2.6	Load modelling for the case study.....	45
3.2.7	Protection system modelling for the case study.....	46
3.3	Generation farm specifications.....	46
3.3.1	Wind generator specifications.....	46
3.3.2	Wind farm modelling.....	47
3.4	Optimisation modelling.....	47
3.4.1	Optimisation criteria.....	47
3.4.2	Algorithm modelling.....	48
3.5	Selecting the fault positions for the study.....	50
3.6	Detailed case studies.....	51
4.	Test System Results and Discussion.....	53
4.1	Network simulator verification.....	53
4.2	Modified IEEE 14-bus system: Case 1 – Base case.....	54
4.2.1	Load flow results.....	54
4.2.2	Protection grading results.....	54
4.3	Modified IEEE 14-bus system: Case 2 – PBIL optimisation.....	56
4.3.1	Optimisation results.....	56
4.3.2	Load flow results.....	57
4.3.3	Protection grading results.....	57
4.4	Modified IEEE 14-bus system: Case 3 – DE optimisation.....	60
4.4.1	Optimisation results.....	60
4.4.2	Load flow results.....	60
4.4.3	Protection grading results.....	61
4.5	Discussion of load flow results.....	64
4.6	Discussion of protection grading results.....	65
4.6.1	Fault at Bus 4.....	65
4.6.2	Fault at Bus 10.....	66
4.6.1	Fault at Bus 11.....	66

4.6.2	Fault at Bus 13.....	67
4.6.3	Summary of IEEE network protection.....	68
4.7	Discussion of the performance of the optimisation algorithms	68
5.	Municipal Case Study Results and Discussion	69
5.1	Case 1: Pre-DG installation network state	69
5.1.1	Load flow results	69
5.1.2	Protection grading results.....	72
5.2	Case 2: DG installed at Utility substation.....	75
5.2.1	Load flow results	75
5.2.2	Protection grading results.....	79
5.3	Case 3: PBIL optimal DGs installed at the busbars.....	81
5.3.1	Optimal DG placement results.....	81
5.3.2	Load flow results	82
5.3.3	Protection grading results.....	86
5.4	Case 4: Differential evolution optimal DGs installed at the busbars.....	89
5.4.1	Optimal DG placement results.....	89
5.4.2	Load flow results	90
5.4.3	Protection grading results.....	93
5.5	Discussion of load flow results	95
5.6	Discussion of case study protection grading results.....	98
5.6.1	Fault at the 33 kV Utility substation rear busbar.....	98
5.6.2	Fault at the Bushes substation	99
5.6.3	Fault at the Addition substation	100
5.6.4	Fault at the Tortoise substation.....	102
5.6.5	Fault at the Winelands RMU 1 substation.....	104
5.6.6	Fault at the Steve LHS substation	105
5.6.7	Fault at the Mine substation.....	107
5.6.8	Fault at the Short substation.....	108
5.6.9	Fault at the Paste RMU 1 substation.....	110
5.6.10	Summary of Case Study protection	111
5.7	Discussion of the performance of the optimisation algorithms	112
5.8	Costing analysis	113
5.9	Chapter summary	115
6.	Conclusions.....	116
7.	Recommendations.....	119
	References	120
	Appendix A: IEEE 14-bus network data	125
	Appendix B: Review of protection systems	127
	Appendix C: Single-line diagrams and busbar loads for the municipal network.....	137
	Appendix D: Network cable datasheets	144
	Appendix E: Municipal network protection settings	149
	Appendix F: Optimisation algorithm MATLAB code	157
	Appendix G: Additional results for the network simulations.....	187
	Appendix H: IDMT curve results.....	221

List of Figures and Tables

List of Figures

Figure 2.1: Solar resource availability in South Africa [4]	4
Figure 2.2: 2010 energy generation mix in South Africa [3].	5
Figure 2.3: The connection of a DG system to the utility grid [9].....	6
Figure 2.4: The cross-section of a wind energy conversion system [12].....	8
Figure 2.5: Block diagram of a fixed-speed wind turbine system [14]	9
Figure 2.6: Block diagram of a narrow-speed wind turbine system [14].....	10
Figure 2.7: Block diagram of a broad-speed wind turbine system [14]	11
Figure 2.8: A HAWT system [16].....	11
Figure 2.9: A VAWT system [16].....	12
Figure 2.10: The DC wind turbine generator system setup [17].....	13
Figure 2.11: The cross-section of a PMSG [17].....	13
Figure 2.12: A block diagram of the implementation of a DFIG [17].....	14
Figure 2.13: Typical interconnecting transformer connections [2].....	17
Figure 2.14: Typical voltage profile along a feeder with and without a DG [2].....	19
Figure 2.15: Undistorted and distorted sine waves [2].....	20
Figure 2.16: Buck-boost converter and inverter circuits [41].....	25
Figure 2.17: Typical graphical relationship between TSR, Pitch, and Cp for a 600kW, dual blade, HAWT [45].	26
Figure 2.18: General analytical method algorithm for optimal DG placement [47].....	28
Figure 2.19: Flowchart showing the general DE algorithm [51].....	32
Figure 3.1: The standard IEEE 14-bus test system [63].....	37
Figure 3.2: The modified IEEE 14-bus test system	39
Figure 3.3: The main substation layout of the municipal network	42
Figure 3.4: Flow chart of the PBIL optimisation algorithm used for the study	49
Figure 3.5: Flow chart of the DE optimisation algorithm used for the study	50
Figure 4.1: The voltage profile for the modified IEEE 14-bus system for Case 1	54
Figure 4.2: The voltage profile for the modified IEEE 14-bus system for Case 2	57
Figure 4.3: The voltage profile for the modified 14-bus IEEE system for Case 3	61
Figure 4.4: Imported power from the grid across the three cases for the modified IEEE 14-bus network.....	64
Figure 4.5: The percentage power loss reduction across the three cases for the modified IEEE 14-bus network.....	65
Figure 4.6: Total trip times for a three-phase fault at Bus 4 for the three cases for the modified IEEE 14-bus network.....	66
Figure 4.7: Total trip times for a three-phase fault at Bus 10 for the three cases for the modified IEEE 14-bus network.....	67
Figure 4.8: Total trip times for a three-phase fault at Bus 11 for the three cases for the modified IEEE 14-bus network.....	67
Figure 4.9: Total trip times for a three-phase fault at Bus 13 for the three cases for the modified IEEE 14-bus network.....	68
Figure 5.1: Graph showing the voltage profile for the main substations in the municipal network for Case 1.....	69
Figure 5.2: The voltage profile for the Utility substation group of busbars in the municipal network for Case 1	70
Figure 5.3: The voltage profile for the Atlantic MS group of busbars in the municipal network for Case 1.....	70
Figure 5.4: The voltage profile for the Delilah MS group of busbars in the municipal network for Case 1	70
Figure 5.5: The voltage profile for the Gardens MS group of busbars in the municipal network for Case 1.....	71
Figure 5.6: The voltage profile for the Wozniak group of busbars in the municipal network for Case 1	71
Figure 5.7: The voltage profile for the Sunset Vista MS group of busbars in the municipal network for Case 1	71
Figure 5.8: The voltage profile for the Workplace MS group of busbars in the municipal network for Case 1	72
Figure 5.9: The voltage profile for the Winery MS group of busbars in the municipal network for Case 1.....	72
Figure 5.10: Graph showing the voltage profile for the main substations in the municipal network for Case 2.....	75
Figure 5.11: The voltage profile for the Utility substation group of busbars in the municipal network for Case 2	76
Figure 5.12: The voltage profile for the Atlantic MS group of busbars in the municipal network for Case 2	76
Figure 5.13: The voltage profile for the Delilah MS group of busbars in the municipal network for Case 2.....	76
Figure 5.14: The voltage profile for the Gardens MS group of busbars in the municipal network for Case 2.....	77
Figure 5.15: The voltage profile for the Wozniak group of busbars in the municipal network for Case 2.....	77
Figure 5.16: The voltage profile for the Sunset Vista MS group of busbars in the municipal network for Case 2	77
Figure 5.17: The voltage profile for the Workplace MS group of busbars in the municipal network for Case 2	78
Figure 5.18: The voltage profile for the Winery MS group of busbars in the municipal network for Case 2.....	78
Figure 5.19: Graph showing the voltage profile for the main substations in the municipal network for Case 3	83
Figure 5.20: The voltage profile for the Utility substation group of busbars in the municipal network for Case 3	83

Figure 5.21: The voltage profile for the Atlantic MS group of busbars in the municipal network for Case 3.....	84
Figure 5.22: The voltage profile for the Delilah MS group of busbars in the municipal network for Case 3.....	84
Figure 5.23: The voltage profile for the Gardens MS group of busbars in the municipal network for Case 3.....	84
Figure 5.24: The voltage profile for the Wozniak group of busbars in the municipal network for Case 3.....	85
Figure 5.25: The voltage profile for the Sunset Vista MS group of busbars in the municipal network for Case 3.....	85
Figure 5.26: The voltage profile for the Workplace MS group of busbars in the municipal network for Case 3.....	85
Figure 5.27: The voltage profile for the Winery MS group of busbars in the municipal network for Case 3.....	86
Figure 5.28: Graph showing the voltage profile for the main substations in the municipal network for Case 4.....	90
Figure 5.29: The voltage profile for the Utility substation group of busbars in the municipal network for Case 4.....	90
Figure 5.30: The voltage profile for the Atlantic MS group of busbars in the municipal network for Case 4.....	91
Figure 5.31: The voltage profile for the Delilah MS group of busbars in the municipal network for Case 4.....	91
Figure 5.32: The voltage profile for the Gardens MS group of busbars in the municipal network for Case 4.....	91
Figure 5.33: The voltage profile for the Wozniak group of busbars in the municipal network for Case 4.....	92
Figure 5.34: The voltage profile for the Sunset Vista MS group of busbars in the municipal network for Case 4.....	92
Figure 5.35: The voltage profile for the Workplace MS group of busbars in the municipal network for Case 4.....	92
Figure 5.36: The voltage profile for the Winery MS group of busbars in the municipal network for Case 4.....	93
Figure 5.37: Total MW and MVAR imported and exported to the grid across the various cases for the municipal network.....	96
Figure 5.38: Total power loss reduction across the cases under study for the municipal network.....	96
Figure 5.39: Overall network voltage profile improvement across the four cases for the municipal network.....	98
Figure 5.40: Total trip times for a three-phase fault at the Utility substation for the four cases for the municipal network.....	99
Figure 5.41: Total trip times for a three-phase fault at the Bushes SS for the four cases for the municipal network.....	100
Figure 5.42: Total trip times for a single-phase fault at the Bushes SS for the four cases for the municipal network.....	101
Figure 5.43: Total trip times for a three-phase fault at the Addition SS for the four cases for the municipal network.....	101
Figure 5.44: Total trip times for a single-phase fault at the Addition SS for the four cases for the municipal network.....	102
Figure 5.45: Total trip times for a three-phase fault at the Tortoise SS for the four cases for the municipal network.....	103
Figure 5.46: Total trip times for a single-phase fault at the Tortoise SS for the four cases for the municipal network.....	103
Figure 5.47: Trip times for a three-phase fault at the Winelands RMU 1 SS for the four cases for the municipal network.....	105
Figure 5.48: Trip times for a single-phase fault at the Winelands RMU 1 SS for the four cases for the municipal network.....	105
Figure 5.49: Trip times for a three-phase fault at the Steve LHS SS for the four cases for the municipal network.....	106
Figure 5.50: Total trip times for a single-phase fault at the Steve LHS SS for the four cases for the municipal network.....	107
Figure 5.51: Total trip times for a three-phase fault at the Mine SS for the four cases for the municipal network.....	108
Figure 5.52: Total trip times for a single-phase fault at the Mine SS for the four cases for the municipal network.....	108
Figure 5.53: Total trip times for a three-phase fault at the Short SS for the four cases for the municipal network.....	109
Figure 5.54: Total trip times for a single-phase fault at the Short SS for the four cases for the municipal network.....	110
Figure 5.55: Total trip times for a three-phase fault at the Paste RMU 1 SS for the four cases for the municipal network.....	111
Figure 5.56: Total trip times for a single-phase fault at the Paste RMU 1 SS for the four cases for the municipal network.....	111
Figure 5.57: Total cost of implementation for each case for the municipal network.....	115

List of Tables

Table 2-1: Frequency deviations allowed for network compatibility [10]	7
Table 3-1: The IEEE 14-bus system protection setting data.....	40
Table 3-2: The 11 kV cables used through the network [65] [66] [67] [68].....	43
Table 3-3: Transformer specifications for main substations in the network.....	44
Table 3-4: Transformer tap changer settings for all transformers in the network.....	45
Table 3-5: NER specifications at each of the main substations in the network.....	45
Table 3-6: Feeder load specifications at the Atlantic main substation	46
Table 3-7: The wind generator specifications given by the IPP.....	47
Table 4-1: The network overview results for the network simulator verification case.....	53
Table 4-2: The bus results for the 33 kV network for the network simulator verification case	53
Table 4-3: The network overview results for the modified IEEE 14-bus system for Case 1.....	54
Table 4-4: The branch currents and trip times for a three-phase fault at Bus 4 in the modified IEEE network for Case 1.....	55
Table 4-5: The branch currents and trip times for a three-phase fault at Bus 10 in the modified IEEE network for Case 1.....	55
Table 4-6: The branch currents and trip times for a three-phase fault at Bus 11 in the modified IEEE network for Case 1.....	56
Table 4-7: The branch currents and trip times for a three-phase fault at Bus 13 in the modified IEEE network for Case 1.....	56
Table 4-8: The optimal DG placement results and protection settings for the modified 14-bus IEEE system for Case 2	56
Table 4-9: The MATPOWER network overview results for the modified IEEE 14-bus system for Case 2	57
Table 4-10: The DigSILENT PowerFactory network overview results for the modified IEEE 14-bus system for Case 2.....	57
Table 4-11: The branch currents and trip times for a three-phase fault at Bus 4 in the modified IEEE network for Case 2.....	58
Table 4-12: The branch currents and trip times for a three-phase fault at Bus 10 in the modified IEEE network for Case 2.....	59
Table 4-13: The branch currents and trip times for a three-phase fault at Bus 11 in the modified IEEE network for Case 2.....	59
Table 4-14: The branch currents and trip times for a three-phase fault at Bus 13 in the modified IEEE network for Case 2.....	60
Table 4-15: The optimal DG placement results settings for the modified 14-bus IEEE system for Case 3	60
Table 4-16: The MATPOWER network overview results for the modified 14-bus IEEE system for Case 3	61
Table 4-17: The DigSILENT PowerFactory network overview results for the modified 14-bus IEEE system for Case 3.....	61
Table 4-18: The branch currents and trip times for a three-phase fault at Bus 4 in the modified IEEE network for Case 3.....	62
Table 4-19: The branch currents and trip times for a three-phase fault at Bus 10 in the modified IEEE network for Case 3.....	63
Table 4-20: The branch currents and trip times for a three-phase fault at Bus 11 in the modified IEEE network for Case 3.....	63
Table 4-21: The branch currents and trip times for a three-phase fault at Bus 13 in the modified IEEE network for Case 3.....	64
Table 5-1: The network overview results for the municipal network for Case 1.....	69
Table 5-2: Branch currents and trip times for a three-phase fault at Bushes SS for the municipal network for Case 1.....	73
Table 5-3: Branch currents and trip times for a single-phase fault at Bushes SS for the municipal network for Case 1	73
Table 5-4: Currents and trip times for a three-phase fault at Winelands RMU 1 SS for the municipal network for Case 1	73
Table 5-5: Currents and trip times for a single-phase fault at Winelands RMU 1 SS for the municipal network for Case 1	74
Table 5-6: Branch currents and trip times for a three-phase fault at Short SS for the municipal network for Case 1	74
Table 5-7: Branch currents and trip times for a single-phase fault at Short SS for the municipal network for Case 1	75
Table 5-8: The network overview results for the municipal network for Case 2.....	75
Table 5-9: Branch currents and trip times for a three-phase fault at Bushes SS for the municipal network for Case 2.....	79
Table 5-10: Branch currents and trip times for a single-phase fault at Bushes SS for the municipal network for Case 2	79
Table 5-11: Currents and trip times for a three-phase fault at Winelands RMU 1 SS for the municipal network for Case 2.....	80
Table 5-12: Currents and trip times for a single-phase fault at Winelands RMU 1 SS for the municipal network for Case 2.....	80
Table 5-13: Branch currents and trip times for a three-phase fault at Short SS for the municipal network for Case 2	81
Table 5-14: Branch currents and trip times for a single-phase fault at Short SS for the municipal network for Case 2	81
Table 5-15: PBIL placement results and definite-time protection settings for the municipal network for Case 3	82
Table 5-16: The MATPOWER network overview results for the municipal network for Case 3	82
Table 5-17: The DigSILENT PowerFactory network overview results for the municipal network for Case 3	83
Table 5-18: Branch currents and trip times for a three-phase fault at Bushes SS for the municipal network for Case 3.....	86
Table 5-19: Branch currents and trip times for a single-phase fault at Bushes SS for the municipal network for Case 3	87
Table 5-20: Currents and trip times for a three-phase fault at Winelands RMU 1 SS for the municipal network for Case 3.....	87
Table 5-21: Currents and trip times for a single-phase fault at Winelands RMU 1 SS for the municipal network for Case 3.....	88
Table 5-22: Branch currents and trip times for a three-phase fault at Short SS for the municipal network for Case 3	88
Table 5-23: Branch currents and trip times for a single-phase fault at Short SS for the municipal network for Case 3	89
Table 5-24: DE DG placement results and definite-time protection settings for the municipal network for Case 4.....	89
Table 5-25: The MATPOWER network overview results for the municipal network for Case 4.....	90
Table 5-26: The DigSILENT PowerFactory network overview results for the municipal network for Case 4	90
Table 5-27: Branch currents and trip times for a three-phase fault at Bushes SS for the municipal network for Case 4.....	93
Table 5-28: Branch currents and trip times for a single-phase fault at Bushes SS for the municipal network for Case 4	93
Table 5-29: Currents and trip times for a three-phase fault at Winelands RMU 1 SS for the municipal network for Case 4.....	94

Table 5-30: Currents and trip times for a single-phase fault at Winelands RMU 1 SS for the municipal network for Case 4	94
Table 5-31: Branch currents and trip times for a three-phase fault at Short SS for the municipal network for Case 4	95
Table 5-32: Branch currents and trip times for a single-phase fault at Short SS for the municipal network for Case 4	95
Table 5-33: Cable types and associated costs	113
Table 5-34: Cables and inverters required for implementing Case 3 in the municipal network.....	114
Table 5-35: Cables and inverters required for implementing Case 4 in the municipal network.....	114
Table 5-36: Total costs for implementing the three possible cases for the municipal network.....	114

1. Introduction

1.1 Background to the study

Since the advent of renewable energy generation technologies, the world has begun shifting towards abandoning the use of fossil fuels in favour of renewable energy generation technologies. These technologies have improved in terms of cost and efficiency, resulting in increased uptake. This has also resulted in the use of microgrids and independent power producers (IPP) becoming more widespread, changing the way traditional power grids work.

Recently, an IPP approached a South African municipality to connect up to 72 MW of wind farm generation to the existing municipal grid. This triggered an investigation to determine the impact that the proposed wind farm would have on the municipal network in terms of load flows, fault levels, and protection grading. This also prompted further research into the optimal sizing and placement of generation from the IPP to best suit the municipality in terms of power loss reduction and voltage profile improvement. This aims to allow the municipality in question to be able to make an informed decision regarding the IPP application.

1.2 Objectives of the study

1.2.1 *Problems to be investigated*

The study aims to investigate the electrical feasibility and effect of the proposed IPP generation on the power flows, voltage profiles, and protection grading in the existing grid. The study also intends to extend further into finding the optimal size and placement of the wind farm connection. This results in the following research questions being posed.

- What is the effect of the proposed wind farm installation on the current network voltage profile, power loss performance, fault levels, and protection grading?
- What other optimisation placement options exist for this network and how do they compare to the proposed installation in terms of overall network improvement?
- What other installations could be proposed instead, in order to result in better network and protection performance, and how can these solutions be generated?
- What is the effect of the different solutions on the network fault levels?
- Does any of the various solutions result in incorrect protection grading?
- Is the proposed solution more cost-effective than other possible solutions?

1.2.2 *Purpose of the study*

This study aims to fulfil the following objectives.

- Successfully model the IEEE 14-bus network as well as the existing municipal network in the MATPOWER and DigSILENT PowerFactory software packages. This will be done to compare the simulation packages. Additionally, the MATPOWER models will be used to interface with optimisation algorithms in MATLAB, and the DigSILENT PowerFactory models will be used to test the protection performance of the networks.
- Run power flows on the IEEE 14-bus network and modify the network accordingly such that protection settings can be designed for the network. This constitutes the first case for the IEEE network.

- Run power flows and establish the correctness of the current protection grading for the case study network before distributed generators are added, constituting the first case for the case study. Add the proposed wind farm generation into the existing grid and run power flows and check protection grading, constituting the second case for the case study.
- Create both a Probability-Based Incremental Learning (PBIL) and Differential Evolution (DE) algorithm in order to optimise the placement of distributed generators throughout the IEEE 14-bus network and the case study network. The PBIL algorithm results constitute the second case for the IEEE network and the third case for the case study network, while the DE algorithm results constitute the third case for the IEEE network and the fourth case for the case study network.
- Validate the protection settings for both networks.
- Validate the use of the MATPOWER library and method of optimisation for the applicable cases by comparing the results to those produced by DlgSILENT PowerFactory.
- Assess and critically compare the load flow and protection grading results across the cases in each network.
- Conclude the research so that the research questions are answered, based on the analysis across the networks and cases.
- Make recommendations on the research, based on the conclusions drawn, and comment on the solution that should be implemented for the case study network.

1.3 Scope and limitations

This research deals with the IPP wind farm connection only, and does not consider renewable generation technologies that may be used by consumers and installed on their property. The loads modelled in the case study are average loads taken over a month during the peak usage season. The research also only considers wind turbine technology fed through an inverter system, as was specified by the IPP. The case study is conducted on an existing municipal network, thus the results obtained are specific to this grid and may not be applicable to other municipal grids.

1.4 Plan of development

This dissertation consists of seven chapters, each of which is explained below.

Chapter 1 provides an introduction to the dissertation, detailing the background, objectives, and scope of the study. Chapter 2 then goes on to review relevant literature on the topic. It goes on to review the current energy status and potential of South Africa and future plans. Distributed generation, wind turbine technologies, controllers, inverters, the impact of these technologies, optimisation techniques, and research done in these areas are reviewed. Chapter 3 then provides detailed insight into the methodology followed in this research. This includes the inputs required by DlgSILENT PowerFactory, MATPOWER, and the optimisation techniques. Chapters 4 and 5 provide a record of the results obtained for each of the cases of each of the networks under study, and provides a discussion of the results recorded. Chapter 6 provides conclusions on the objectives of the research based on the discussions in Chapters 4 and 5. Finally, Chapter 7 makes recommendations, based on the conclusions drawn from the research.

2. Literature Review

2.1 Distributed generation

Distributed generation refers to the interconnection of on-site, small-scale energy resources with the utility power grid. These small-scale generators are usually connected at distribution voltage levels, which decreases transmission and distribution losses, and the costs involved.

Due to the global increase in power demand, increased awareness of carbon emissions and global warming, and the efforts to decrease environmental pollution, renewable distributed generation (DG) is seeing an increased uptake across the globe and is becoming increasingly mainstream. According to [1], South Africa has the potential to become the global renewable energy leader should the right political decisions be made.

Even though most types of distributed generators are environmentally friendly, they are also unreliable due to the way in which they generate power. They are dependent on environmental and weather conditions, such as the solar or wind availability on a particular day. However, when added to a larger network incorporating multiple generation technologies, they become more reliable, as they act as a support to the larger network.

Distributed generators can run in tandem with one another separated from the grid, in order to provide power to a small cluster of consumers. This is known as a microgrid. Microgrids are usually able to be connected to the larger utility grid, such that it may support the utility grid during peak times, with the utility grid acting to stabilise the microgrid when the DGs are providing less power than expected due to environmental conditions. However, the connection of DGs into an existing distribution network influences the load flow and voltage profile in the existing network, which could have adverse effects on the protection and voltage regulation systems in the network [2].

2.1.1 Impacts of renewable energy in South Africa

As has been the case globally, the average electricity usage of a single household in South Africa has increased in line with providing a better quality of life to the citizens of the country [3]. Following urbanisation, electricity usage in South Africa has previously reached a point where demand outstrips supply, leading to the implementation of load shedding [3]. This fact, coupled with the fact that most of the generation in the country comes from burning fossil fuels, the shift towards cleaner, renewable energy is incumbent to ensure a sustainable future for generations to come [3].

Solar resources, as well as wind resources, are widely available to South Africans due to the geographical position of the country, and the country is said to have the most promising solar resources in Africa [1]. A measurement of the country's solar resources can be seen in Figure 2.1.

A study done by Dekker *et al.* [5] into the economic feasibility of implementing PV schemes in South Africa also found that incorporating solar PV generation into the South African grid would be ideal in terms of irradiation and technology, but points out that the initial cost of implementing

these generation schemes would need to be subsidized by the government to encourage its implementation.

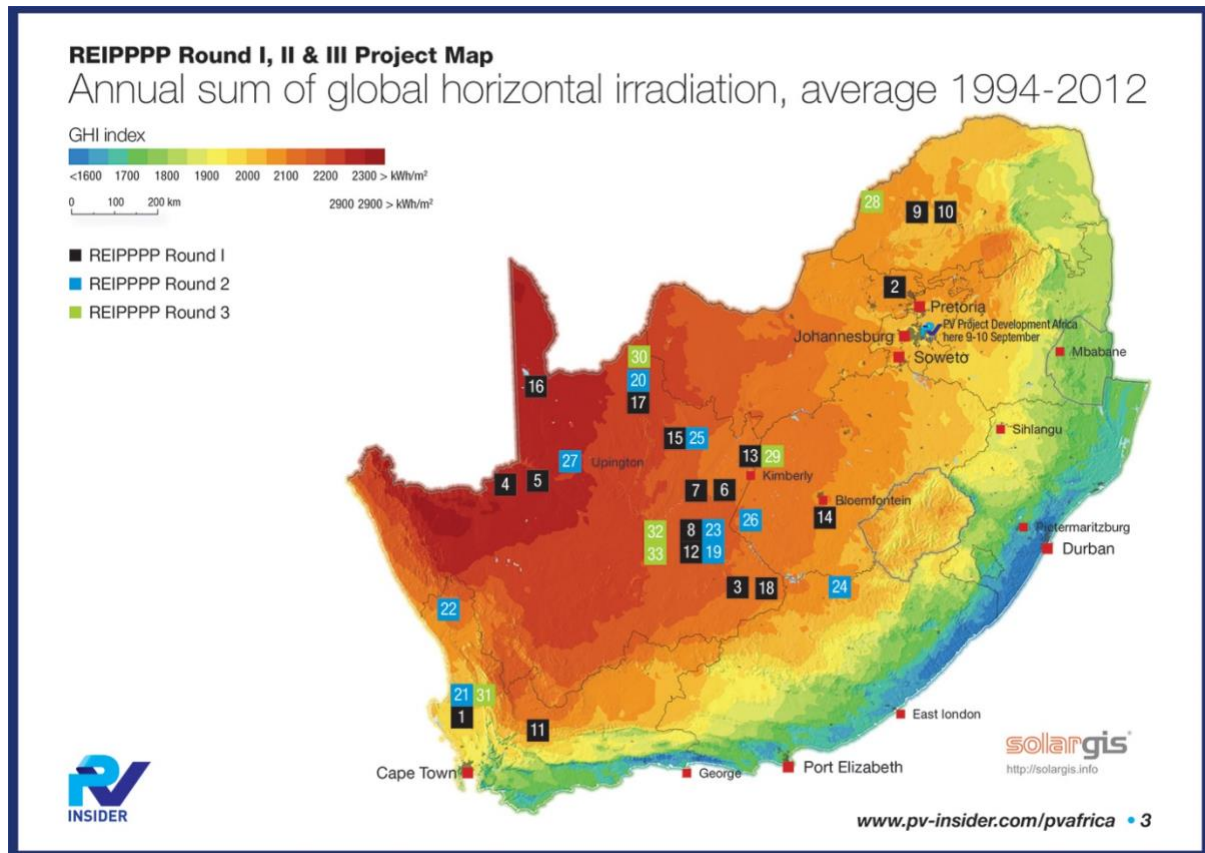


Figure 2.1: Solar resource availability in South Africa [4]

However, a study done by Mulaudzi *et al.* [6] in 2016 suggests that even though South Africa has an abundance of solar irradiation, the solar panel conditions, such as efficiency and degradation could make these panels unsuitable for a large-scale rollout in South Africa. This is found to be mainly due to the fact that dust and soiling would likely cover these panels during the seasons where solar irradiation is most available in the inland provinces, which has an extremely negative impact on the efficiency of the panels.

The study also found that the scheme would be most suitable for implementation in the Eastern and Northern Cape provinces due to the large amount of land available. However, these provinces were found to consume less than 5% of the total energy usage in South Africa. Thus, if PV generation farms were constructed in these provinces, most of the energy generated would need to be exported to the other provinces over long transmission lines.

2.1.2 Components in a distributed generation system

A distributed generation system consists of multiple components which make it able to supply electricity to a single user, a microgrid, or the power system as a whole. These general components are as follows, but actual implementation depends on the type of generation unit.

- **PV Solar Panels:** Photovoltaic arrays are used to generate an electric voltage using solar energy.

- **Wind Turbines:** Wind turbines are designed to cause a generator to generate electrical energy by converting the kinetic energy carried by wind into mechanical energy to turn a generator shaft.
- **Battery Packs:** Arrays of batteries are used to store the DC power generated from the solar panels.
- **Charge Controller:** The charge controller is used to control charge rates.
- **DC-AC Inverter:** The inverter converts the DC power generated by the rest of the system to an AC voltage.

2.2 Distributed Generators in South Africa

2.2.1 Distributed generation uptake in South Africa

In South Africa, electricity is generated primarily by the national electricity utility Eskom. Eskom generates electricity and either distributes it to different government municipalities who resell the power to the consumers, or sell to consumers directly. The energy generation mix as of 2010 is shown in Figure 2.2.

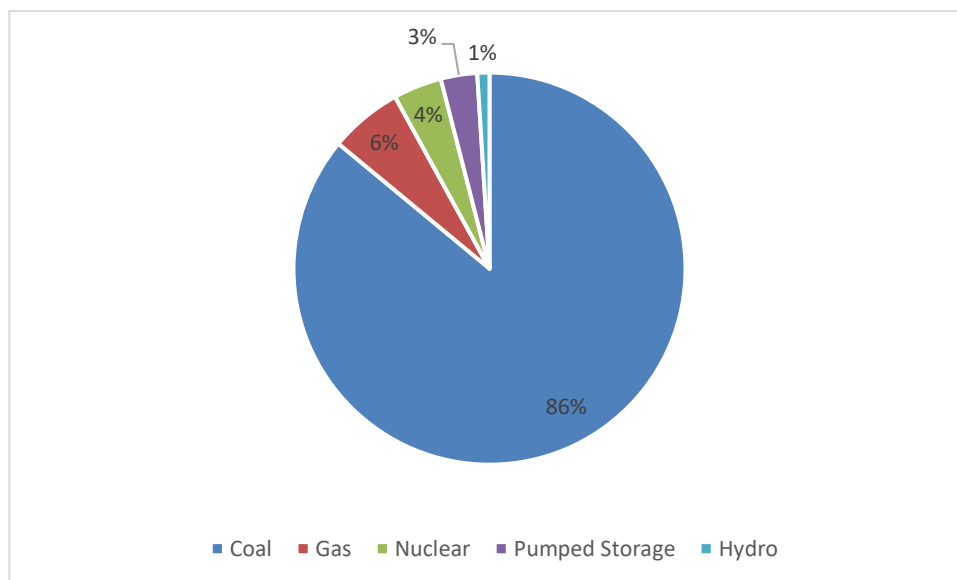


Figure 2.2: 2010 energy generation mix in South Africa [3].

As can be seen in Figure 2.2, the vast majority of generated energy comes through coal-fired power stations. Eskom is looking to decrease the energy contribution from coal-fired power stations by increasing energy production from other energy sources.

However, Eskom is currently the only major power producer in the country [3]. This is partly due to the abundance of cheap coal in the country, for its coal-fired power stations. This results in a completely deregulated market due to the much higher cost of producing energy using renewable resources. However, NERSA has recognised this fact and has since urged IPPs to come forward by introducing the Renewable Energy Feed-In Tariff (REFIT), which aims to ensure that renewable energy investments are financially viable for IPPs. This aims to create a regulated energy market over time as more IPPs come forward [7].

2.2.2 Connecting DGs to the utility grid

In many cases, distributed generation owned by entities other than the utility may be used in their personal capacity by using multiple distributed generators to feed a complex of flats, houses,

or other buildings. This microgrid may possibly operate in two modes, namely grid-connected mode or isolated mode. As the name suggests, grid-connected mode means that the microgrid and the utility grid are connected and support each other. When operating in isolated mode, the microgrid and the utility grid operate independently of each other.

In order for the distributed generator or microgrid to be able to connect to the utility grid, they need to abide by the standards and specifications of the utility grid, such as the DG output being set at the correct voltage level and frequency [8]. This is important as an incorrect voltage level or frequency output of the DG could compromise the quality of supply of the utility grid. In South Africa, 50 Hz is used throughout the country, and distributed generators are normally connected to the medium voltage network. A typical DG connection is shown in Figure 2.3.

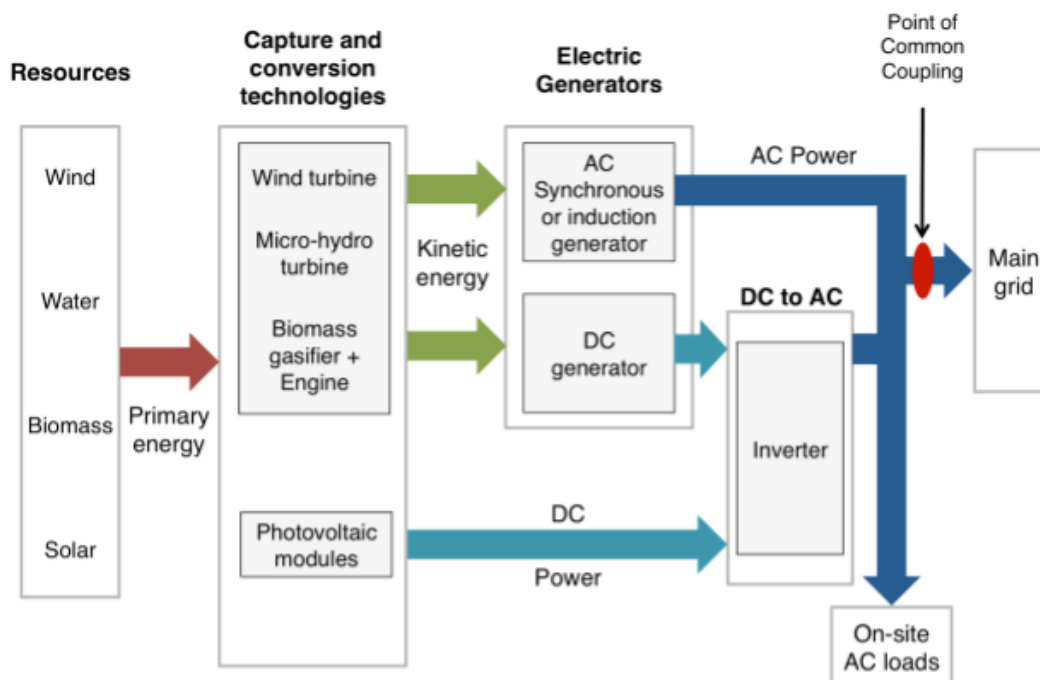


Figure 2.3: The connection of a DG system to the utility grid [9]

2.2.3 Connection Standards

Distributed generators and microgrids need to abide by a set standard used by the utility grid in order to be connected to the grid without causing instability. Grid interconnection standards are laid out in the IEEE1547 standard. The standard lays out the technical specifications for interconnection as well as the commissioning and testing procedures to be followed.

However, in South Africa, the NRS 048-2 standard dictates the voltage standards, allowed voltage dip, harmonics, and more. These are explored in further detail below [10].

i. Voltage Levels

The nominal voltage levels of the power system is generally determined by Eskom. However, the NRS 048-2 standard was set so that electricity providers maintain the voltage at an expected level, so that customers are not negatively affected and network equipment is not damaged.

The standard states that this nominal voltage level may not exceed a band of +/-5% for a system in which the nominal voltage is over 500 V, for more than 10 minutes. This can be equated to a voltage band of 1.05-0.95 pu on the per-unit scale and extends to all phases in a power system [10].

The standard also states that an event of the voltage falling below 0.85 pu for more than 3 seconds is considered an under-voltage event [10].

ii. Frequency Conditions

The NRS 084-2 standard states that the agreed-upon power network frequency for South Africa is 50 Hz. However, it allows for some deviation from this value, which is shown in Table 2-1 [10].

Table 2-1: Frequency deviations allowed for network compatibility [10]

Network Type	Compatibility Level
Grid	± 2 % (± 1 Hz)
Island	± 2.5 % (± 1.25 Hz)

iii. Voltage Unbalance Conditions

Voltage unbalance is a network condition that occurs when the voltages or phase angles between phases in a multi-phase power system are not equal, causing a zero-sequence and negative sequence voltage component to be present in the system [10].

Voltage unbalance in a three-phase system can be calculated as per Equations 2-1 to 2-3 below [11].

$$V_{ave} = \frac{V_{A-B} + V_{B-C} + V_{C-A}}{3} \quad (2-1)$$

$$V_{maxdev.} = V_{ave} - \text{max voltage diff. from } V_{ave} \quad (2-2)$$

$$\%V_{unbalance} = \frac{V_{maxdev.}}{V_{ave}} \quad (2-3)$$

The NRS 084-2 standard defines a voltage unbalance condition when the result of the voltage unbalance calculation is greater than or equal to 2% [10].

iv. Voltage harmonics

Voltage harmonics in an electrical power system is defined as sinusoidal components of the primary 50 Hz voltage waveform. Harmonics in a specified voltage waveform occur in integer multiples of the primary waveform.

Voltage harmonics normally occur due to current harmonics which are caused by non-linear loads, such as switched-mode power supplies and CFLs [2].

The main effect of unfiltered harmonics in a power system is the thermal effect, which can cause heating of transformers and cables, lowering current-carrying capacities and delivery of real power [11].

The total harmonic distortion (THD) in a waveform can be calculated using Equation 2-4, where V_n is the total harmonic component of the voltage in harmonic n .

$$\% \text{ Total Harmonic Distortion (THD)} = \frac{\sqrt{\sum_{n=2}^N V_n^2}}{V_1} \times 100\% \quad (2-4)$$

The NRS 084-2 standard dictates that the THD of the supply voltage, up to the 40th harmonic, must not be greater than 8% [10].

v. ***Voltage swells***

A voltage swell is defined as an overvoltage condition, where, according to the NRS 084-2 standard, the voltage is greater than or equal to 15% above the nominal voltage, or 1.15 pu [10].

Voltage swells can occur when large loads are lost due to protection relay tripping or switching out loads for maintenance. However, voltages can also increase when distributed generation is added to a network, due to the bidirectional currents that are introduced.

2.3 Wind generation systems

Wind resources in an area can be used to generate electrical energy by erecting a wind turbine, which spins when subjected to wind, converting this kinetic energy into electrical energy. This section explores wind turbines and wind technologies in further detail.

2.3.1 Wind turbine theory

Wind turbines are capable of generating large amounts of energy and are thus used for both low and high energy requirements.

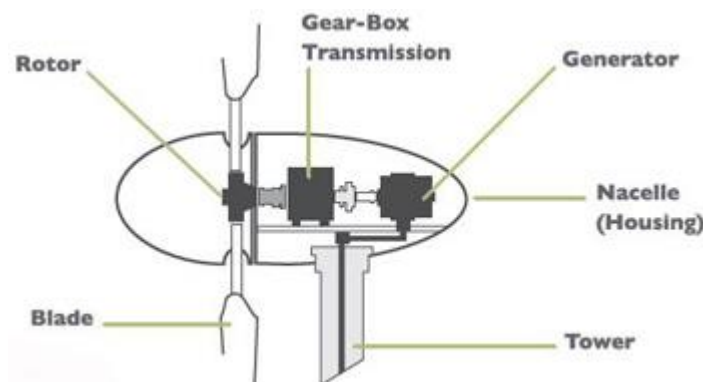


Figure 2.4: The cross-section of a wind energy conversion system [12]

Once the blades, shown in Figure 2.4, are subjected to streams of wind, they rotate, causing the rotor to rotate. This rotational energy is then passed through the transmission gearbox to the generator, which rotates and produces electrical energy. This is usually transmitted through a copper cable down the turbine's tower, which can be of varying height. The gearbox converts the slower rotational speed of the rotor to a higher speed that is used by the generator. This entire system is known as a wind energy conversion system (WECS) [13].

The wind power, P , of the wind blowing through the sweep area of the rotor blades, A , is given by Equation 2-5 [14].

$$P = \frac{1}{2} \rho A v^3 \quad (2-5)$$

In Equation 2-5, P is the power, A is the sweep area of the rotor blades, ρ is the air density, and v is the speed of the wind. The actual power captured by the wind turbine is obtained by multiplying the wind power, given by Equation 2-5, by the power coefficient, C_p . This coefficient has a maximum theoretical Betz limit of 59.3%, as proposed by Albert Betz [14].

Losses incurred by the wind turbine are attributed to the aerodynamic losses experienced through the transfer of energy from the wind to the blades and rotor mechanism, frictional losses along the transmission shaft, losses incurred by the generator itself, as well as electrical transmission losses in the conducting copper wires connecting the generator to the grid or load.

2.3.2 Types of wind turbines

The term 'wind turbine' refers to the entirety of the WECS system enclosed in the nacelle as well as the tower on which it stands. Two different types of wind turbines exist. These are explored in further detail below.

i. Fixed-Speed Wind Turbine (FSWT)

Fixed-speed wind turbines (FSWTs) were the first type of wind turbines made commercially available to the market. These types of turbines operate on the fundamental of keeping the rotor speed constant, so that electricity generated by the turbine is generated at the grid frequency, while the fixed speed for which they are designed is in order to keep the tip speed to wind speed ratio at an optimum [14]. These types of wind turbines usually use an induction machine to act as the system generator, as shown in Figure 2.5.

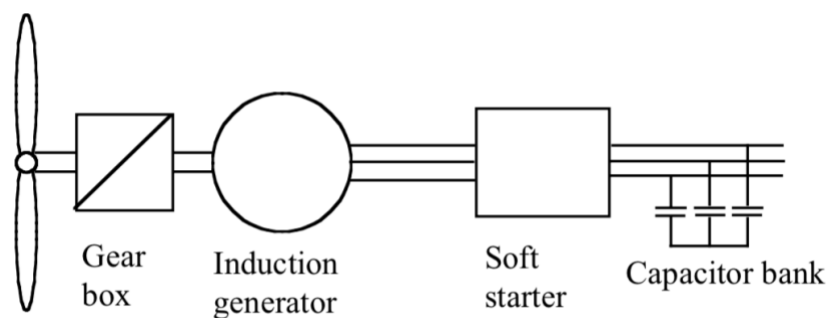


Figure 2.5: Block diagram of a fixed-speed wind turbine system [14]

A device known as a soft-starter is connected on the grid side of the turbine, which limits the inrush current from the grid upon start-up connection to the grid. FSWTs also usually have capacitor banks connected on the generating side. This is done to compensate for the high reactive power consumption to generate the rotating magnetic field required to generate active power from the induction generator [15].

FSWTs are used quite commonly due to their simplicity in design, reliability, and low cost of manufacture and maintenance. They also have high efficiency at the constant speed for which they are designed to operate [15].

However, they do not operate optimally for a range of wind speeds causing their efficiencies to drop when the wind speed changes from the nominal design speed [14]. They also cause voltage fluctuations from the nominal voltage due to the fluctuations in wind speed, which causes mechanical stress and torque on the generator. This can cause voltage fluctuations outside the allowable legal limits, and will affect the quality of power being generated. This has prompted the development of the Variable-Speed Wind Turbine (VSWT).

ii. **Variable-Speed Wind Turbine (VSWT)**

Variable-Speed Wind Turbines (VSWTs) allows the wind turbine to operate efficiently at a wide range of wind and rotor speeds, unlike FSWTs. These wind turbines use either synchronous or induction machines to act as the system generator, and come in the form of both narrow and broad-speed variations, the latter of which is designed for greater variation in wind speeds than the former. The generator's speed, as well as the rotor speed can be controlled in this case using power electronics to keep the generator torque constant while varying the rotor speed when the wind speed changes [15].

For narrow speed variations, doubly-fed induction generators are normally used [14]. A typical block diagram of a narrow-speed wind turbine is shown in Figure 2.6.

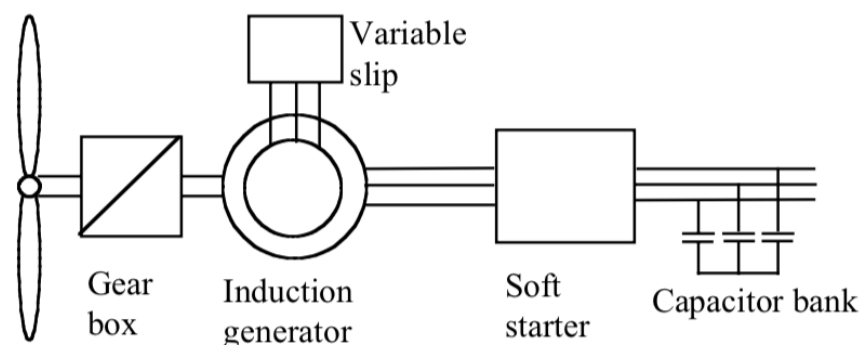


Figure 2.6: Block diagram of a narrow-speed wind turbine system [14]

The system depicted in Figure 2.6 uses variable rotor resistances, which are able to be externally controlled depending on the current wind speed [14].

Broad-speed wind turbines allow the turbine to operate efficiently at a broader range of wind speeds than narrow-speed variations. These systems use frequency converters. The AC current generated from the turbine is converted to DC using a rectifier, and then converted again to AC using an inverter, set at the correct grid frequency [14]. The inverter introduces harmonics into the AC signal due to the high switching rates of the power electronics used in the device. These harmonics must be filtered out before being introduced to the grid.

Broad-speed wind turbines sometimes do not have gearbox systems, and instead use multipole direct-driven generators [15]. A block diagram of a typical broad-speed wind turbine system is shown in Figure 2.7.

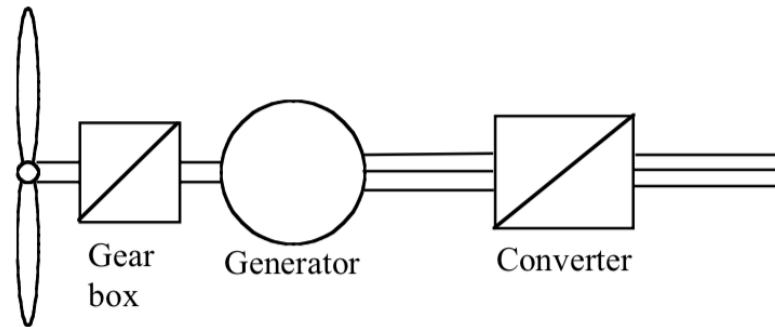


Figure 2.7: Block diagram of a broad-speed wind turbine system [14]

Variable-speed wind turbines, due to their controllable and variable nature, provide better efficiencies at differing ranges of wind speeds. They also result in much lower mechanical stress and fewer and lower voltage fluctuations are experienced at the point of grid connection. However, these turbines are costlier than their fixed-speed counterparts [14].

iii. **Horizontal-axis wind turbine**

Wind turbines are also available in configurations where the rotor is designed to rotate on either the horizontal axis, or the vertical axis, each with their own advantages and disadvantages.

Horizontal-axis wind turbines are wind turbines which rotate on the horizontal axis, parallel to the ground, as shown in Figure 2.8.



Figure 2.8: A HAWT system [16]

Horizontal-axis wind turbines (HAWT) are currently the most commonly-used type of wind turbine [16]. They have the advantage of having a variable blade pitch, which allows the turbine to adjust the blades in a manner in which they are able to operate efficiently for different wind directions [16]. HAWTs also have higher efficiencies than vertical-axis wind turbines (VAWTs) due to the power received from the rotation of the entire blade [16]. The tall tower on which the turbines are mounted also allow them to capture more wind, as wind speed increases with distance from the ground [15].

However, HAWTs require a higher initial wind speed to start rotating than VAWTs, which are normally found at higher altitudes. This results in the turbine being required to be mounted on a long tower [15]. HAWTs are also very dependent on wind direction and operates less efficiently at non-optimal wind directions.

iv. Vertical-axis wind turbine

Vertical-axis wind turbines (VAWTs) rotate on the vertical axis, relative to the ground, as shown in Figure 2.9.



Figure 2.9: A VAWT system [16]

Vertical-axis wind turbines do not need to be mounted on long towers, as they require lower wind speeds to begin rotating and generating electrical energy [16]. A VAWT is also independent of wind direction [15].

However, the VAWT generally provides a lower power output and lower efficiencies at the same wind speeds when compared to HAWTs [15]. VAWTs may require input energy to start turning [15]. VAWTs also require frequent maintenance due to the wires holding the structure up, which causes thrust on the blades as they spin, causing wear and tear [16].

2.3.3 Generators

The generator in the WECS is responsible for the conversion of kinetic mechanical energy to electrical energy. The generator is driven by the secondary, faster shaft of the gearbox. There are different types of generators used in WECS systems in both fixed-speed and variable-speed variations. These are detailed below.

i. DC machines

DC machines can be used as DC generators in wind turbines, so that the output of the turbine will be a DC current, which is fed to an inverter before being connected to the grid, as shown in Figure 2.10.

DC machines are only used as wind turbine generators in cases where a low power output is required and the load is close to the generator [17].

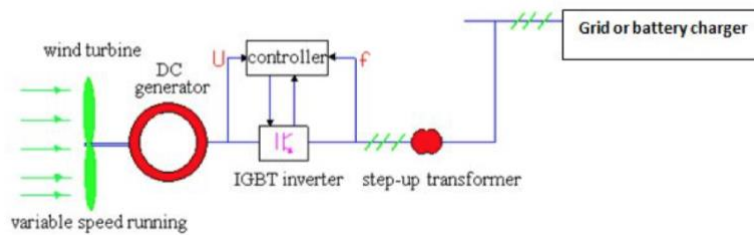


Figure 2.10: The DC wind turbine generator system setup [17]

ii. ***The permanent-magnet synchronous generator***

Synchronous machines are AC machines where the magnetic field generated and the rotor move at a synchronised speed. The magnetic field is normally generated by a separate winding known as a “field winding”, which is subjected to an AC current. Permanent-magnet synchronous generators (PMSGs) are a type of synchronous machine that uses permanent magnets mounted on the surface or inside the rotor in order to create the rotating magnetic field instead of using a field winding [17]. A cross-section of a PMSG is shown in Figure 2.11.

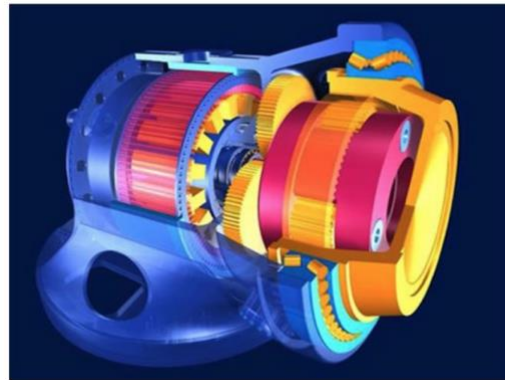


Figure 2.11: The cross-section of a PMSG [17]

The removal of the field winding in PMSGs, which is present in regular synchronous machines, improves efficiency [18]. This also results in the machine being cheaper to produce [18].

However, the removal of the field winding and addition of permanent magnets also causes a loss of controllability of the speed of the magnetic field. The cost of the permanent magnets can also become considerably high when implemented in large machines [17]. Additionally, the output of the generator cannot be kept stable for varying wind speeds. The output of the PMSG thus needs to be rectified and inverted at the correct grid frequency in order to be connected to the grid [18]. Demagnetisation of the permanent magnets can also occur at high temperatures [15].

PMSGs are a commonly used type of generator used in smaller, low-power wind turbines [17].

iii. ***The squirrel-cage induction generator***

Induction machines are a type of AC machine which, when used as a generator, produces power when the rotating magnetic field of the stator and the rotor are operating at different speeds. Induction machines are a proven technology which has been thoroughly researched and well-designed. They are thus very reliable, simple, and cheap to manufacture [17]. However, induction machines need reactive power in order to establish the rotating magnetic field that is required

for it to generate power. This means that it generally requires reactive power compensation while also drawing some reactive power from the grid [17].

Until 1998, induction generators that were used were of the fixed-speed variety in that they operated at fixed rotational speeds only [17]. However, these machines were limited to operate within a very narrow band of speeds and were large, noisy, and unreliable. This led to the development of the Squirrel-cage Induction Machine (SCIM).

The lower maintenance cost and variable speed ability allowed the SCIM to dominate the market for a time, being widely used in wind turbines as well as other applications [17]. However, the development of the Doubly-fed Induction Machine (DFIM) saw the adoption of the SCIM being lowered, so much so that the DFIM is currently used in 85% of wind turbines worldwide to date [17].

iv. The doubly-fed induction generator

The doubly-fed induction generator (DFIG) was developed following the SCIG and improves on it in many ways.

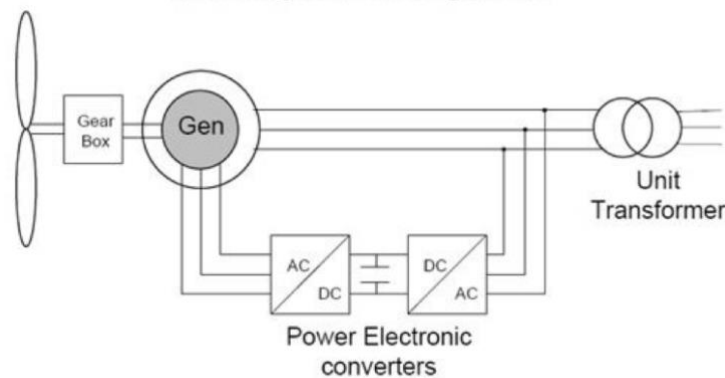


Figure 2.12: A block diagram of the implementation of a DFIG [17]

The DFIG topology consists of the stator being connected to the grid through step-up transformers and controllers, while the rotor is connected to the grid through a series of power electronic converters and controllers as shown in Figure 2.12 [17]. The term “doubly-fed” originates from this dual connection to the grid on both the stator and the rotor.

The rotor electronic controllers control the current, phase angle, and frequency of the rotor circuit [17]. This allows the machine to operate within a wide slip range of the machine’s synchronous speed, resulting in a high efficiency [19] [20]. This also allows DFIGs to offer good controllability [20].

The DFIG however, requires large amounts of reactive power to maintain its rotating magnetic field. This can be obtained directly from the grid or from reactive power compensation devices [17].

The DFIG topology’s reliance on power electronics causes it to be vulnerable to voltage fluctuations [20] which can cause instability on the network it is connected to. A study done by Barendse *et al.* [20] finds that the time taken to detect a voltage sag is the defining factor that separates inconvenience from catastrophic failure. The study identifies that current voltage sag

detection techniques, such as the root mean square (RMS) method, are too slow to quickly detect a fault condition. The proposed method of using a non-linear adaptive filter to detect voltage sags in real-time shows much improved results over traditional methods.

2.3.4 *Wind resources in South Africa*

A study done by the CSIR in 2016 found that over 80% of the land in South Africa has adequate wind resources to support low-cost wind energy [21]. The study also found that, in South Africa, wind resource potential is on par with that of solar resources. The short-term generation fluctuations were also found to be easily solved by distributing the generation over a large spatial area.

However, a study done by SANEDI in 2017 [22] on the hybridisation of fossil fuel generation technologies with renewable technologies found that solar PV generation was the most suitable candidate for hybridisation with the current grid configuration. This was due to the country's vast amount of solar resources, and the fact that the study had found that the generation cost of a solar PV system was equivalent to buying electricity from a municipality. However, the study noted that this was based on consumers having both a solar PV system and a grid connection, as energy storage was not considered as part of the system.

The study also found that the installation of wind generation should be done in locations where no grid connection currently exists and where the cost of a grid connection being installed is high. This recommendation was made due to the high cost of maintenance.

2.4 Impacts of adding distributed generators to an existing grid

Adding distributed generation to an already established distribution network has multiple impacts which affect the grid and distributed generator in multiple ways.

2.4.1 *Factors influencing the impact of distributed generation on a power network*

In order to be able to evaluate the impact of distributed generation on the distribution network, data that properly describes the distributed resources as well as the distribution network needs to be collected and analysed [2]. The data that is required is stated below [2].

- Rated size of the distributed resource.
- The type of the energy source that is used.
- The type of converter that is used.
- The contribution of the distributed resource to the fault current.
- The contribution of system harmonics from the distributed resource.
- Operating cycles.
- The power factor of the distributed resource.
- Location of the distributed resource on the established power network.
- Location and settings of the protection systems on the power network.
- Location of the voltage regulators on the power network.
- Network parameters such as cable types and ratings.

2.4.2 Advantages of implementing distributed generation with an existing grid

Implementing distributed generation, especially in grid-connected mode, has the following advantages [23].

- Renewable technologies are often employed, making distributed generation environmentally friendly and thus receives a good political response to its implementation.
- The country's dependency on fossil fuels can be reduced.
- Distributed generation helps the country to reach its GHG target and helps to combat climate change.
- Distributed generation generally has lower investments than building traditional power plants and transmission lines.
- Distributed generators are normally connected near load centres, reducing transmission cost and losses.
- Distributed generation helps IPPs to be able to erect distributed resources and step forward to sell electricity to the system controller.

2.4.3 Impacts and disadvantages of integrating distributed resources into the network

This section deals with some issues in integrating distributed resources into the power network, and presents some solutions to these issues.

i. Interconnecting transformer connections

A DG is normally connected to the network through a transformer, as the network voltage is much higher than the voltage provided by the DG. However, the transformer chosen for this purpose has a large impact on the distribution system to which it is connected, as the DG has to appear as a grounded source to the rest of the network [2]. Each type of connection, shown in Figure 2.13, affects the protection coordination differently.

The delta winding on a delta-wye transformer ensures that no zero-sequence currents are transferred from the primary to the secondary side of the transformer in the case of a single-phase fault. Because the delta winding is normally used on the utility side, the single-phase fault levels will remain the same on the utility network side, as the DG will not contribute any fault current in this case [24]. Also, it is seen in [24] that the absence of a ground connection on the delta winding means that the ground faults on the primary and secondary windings are completely isolated and protection settings for single-phase faults can remain the same. For these reasons, the delta-wye connection transformer type is often used for connecting generators to transmission and distribution networks. However, an ungrounded primary winding results in a risk of overvoltage [24].

Neither of the connections are said to be the “best” connection as they each affect the system in different ways [2].

i. Generation with ungrounded transformer primary windings

If a DG is connected to the network through a transformer without a grounded primary winding, the utility transformer would be the only ground connection available to the system and thus it would be the only ground current source for the DG. Thus, if a line-to-ground fault were to occur

on a utility feeder connected to the utility substation, this breaker would trip with the generator still connected to the utility bus, resulting in incorrect grounding [2]. This would cause the line-to-neutral voltages on the un-faulted lines to approach the normal line-to-line system voltage, causing a large overvoltage on these lines and equipment connected between these lines and neutral [24]. This could result in astronomical damage to the system [24].

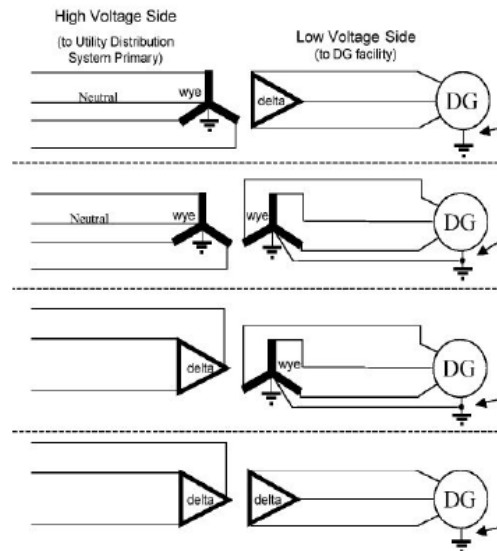


Figure 2.13: Typical interconnecting transformer connections [2]

However, it is generally known that a generator rated at half of the minimum load on the system would not suffer from this overvoltage condition, and thus, ungrounded primary winding transformers should only be used in this circumstance [2].

ii. **Fault current contribution from distributed generation**

With distributed generation connected to the power system, its contribution to the possible fault currents must be analysed. Thus, the utility system and DG system must be analysed together. Relays need to be properly co-ordinated whether the distributed generators are connected to the system or not.

The following facts must be noted when investigating the effects of DGs on the fault current level in an established power system.

- The fault current levels must not exceed the short-time ratings of the equipment in the system.
- Overcurrent relays need to be properly sized to include the presence of DGs.
- Co-ordination of protection devices needs to be set correctly.
- The direction of power flow would change when DGs are added to the system and needs to be accounted for in the protection scheme [24].

If the DG added to the system is small compared to the main system source, the contribution of fault current from the DG would be small. However, the contribution from the DG could decrease the fault current that would normally be fed from the substation source, due to the opposing direction of power flow, hence making the fault more difficult to detect.

PV panels are connected to the utility grid through inverters which feeds a step-up transformer. The inverter specification thus plays a large part in determining the magnitude of the fault

current contribution of this type of DG system. However, it is seen in [25] that the fault current contribution of these inverters lies between the rated current as a minimum contribution, and 120% of the rated current, as the maximum contribution until the fault is isolated. Janssen *et al.* [26] also state that the limitation for fault current from a DG connected to the grid through a converter unit is limited by the design specification of the converter unit and not by the generator. In this case, the study set the converter fault contribution to 150% of the rated converter capacity.

Wind generators, as previously discussed in this dissertation, are usually connected to the grid through inverters and power electronic controllers as well [18] [19]. This means that large wind turbines would contribute to fault current levels in a similar manner as PV panels, and would thus be dependent on inverter specification.

iii. Protection co-ordination and sensitivity issues

Classical existing power systems have not been designed with distributed generation in mind, and thus protection systems generally do not make provision for it. The existing co-ordination between protection relays in the network can cause issues in the network when DGs are added, thus the co-ordination might have to be changed, likely on the protection devices downstream of the DGs [2].

This would be the case where the interconnection transformer's primary winding is grounded. Grounding the transformer primary winding would link the DG circuit to the rest of the grid during earth-fault conditions, causing the earth-fault current on the utility side to change, possibly resulting in incorrect grading [24].

The effects of DGs on the protection co-ordination is not limited to the circuit to which the DG is connected. Rather, any faults that occur on the adjacent circuit may trigger a trip on the DG circuit due to the presence of the DG [24]. Thus, time co-ordination must be maintained on the adjacent circuits as well.

Sensitivity issues can also arise when DGs are added, as the protection settings might not pick up a fault in the network due to reverse power flow.

iv. System voltage and frequency

The addition of distributed generation in a power system affects both the voltage and frequency, though the impact of the DGs on the voltage is much greater than the effect on the frequency [2]. This is due to the fact that the addition of a DG at a certain point in the network would change the voltage at that local point in the network, whereas a change in frequency would require a network-wide change, requiring the DG to make up a large part of the total network capacity [2].

Because DGs can have a large impact on the voltage at different points in the network, due to the changing power flows, it becomes necessary to maintain the voltage at +/- 5% of the nominal voltage level, as per the NRS 048. Voltage regulation is used to achieve this. Figure 2.14 shows a general voltage profile along a feeder, with and without DGs connected to the feeder.

As can be seen in Figure 2.14, the voltage does fall below the required +/- 5% band after a DG is added. This issue needs to be checked and fixed to ensure an adequate quality of supply. It is

proposed in [24] to employ a rate-of-change of frequency protection in order to act as a type of frequency protection instead of traditional over-frequency and under-frequency methods. This allows for fast tripping for extreme overloads when the rate-of-change of frequency is high, while maintaining the DG connection to the grid for low rates-of-change of frequency for less severe conditions [24].

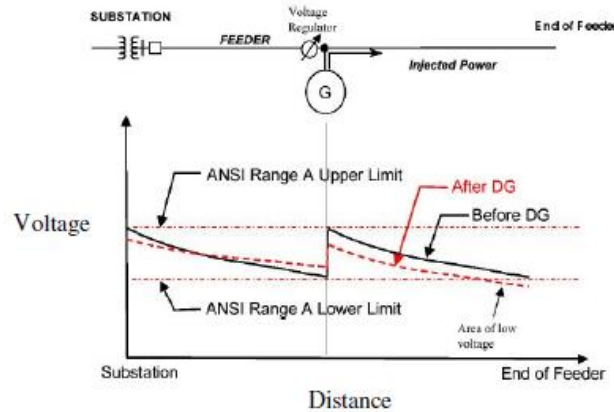


Figure 2.14: Typical voltage profile along a feeder with and without a DG [2]

v. Harmonics

Harmonics are contained in an AC wave that is not perfectly sinusoidal and causes distortion in the network. Harmonics are always present in any power system but are maintained at acceptable levels [2]. Harmonics are introduced into a system where non-linear loads are present, such as CFLs and switched-mode circuits [27]. Figure 2.15 shows the difference between a distorted and undistorted sine wave.

The fast-switching nature of modern DC to AC converters means that harmonics will be introduced into the system, which is undesirable due to the negative effects harmonics has on power systems. Harmonics can cause an increase in current flow via an increase in the zero sequence current in the network. Harmonics can also cause the heating of transformers and other network elements which can cause them to deteriorate in performance, malfunction, or break down in extreme circumstances.

Harmonics are unavoidable in a large power system due to the types of modern devices used by consumers [27]. Harmonics therefore need to be mitigated as much as possible. This is normally done using filtering techniques.

Filters are devices consisting of reactive and capacitive components which are designed to only allow signals of a certain range of frequencies through it.

Filters are generally tuned to the frequencies for which it needs to operate but can be generally grouped into the following filter types [28].

- **Low-pass filter:** A low-pass filter is a type of filter which allows signals of a low frequency through them while filtering out signals of a higher than specified frequency.
- **High-pass filter:** A high-pass filter acts in the same way as a low-pass filter, but filters out lower than specified frequency signals while allowing high frequency signals to pass through.

- **Band-pass filter:** As the name suggests, this type of filter allows a band of frequencies through while filtering out any frequency signal outside this band. Two threshold frequencies are specified for this type of filter.

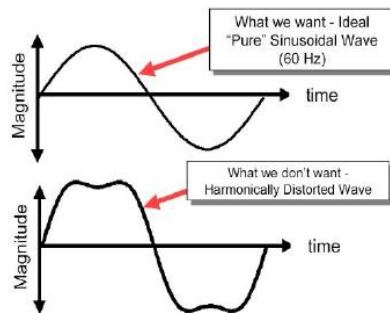


Figure 2.15: Undistorted and distorted sine waves [2]

In power system applications, utilities generally want to filter out any high frequency signal while allowing low frequency signals through. Thus, low pass filters are normally used.

In [27], Lu *et al.* discuss the resistive-active power filter (R-APF) and describes it as a promising method to filter harmonics in a DG configuration. However, the authors note that it has been reported that installing these filters at one node could amplify the filtered harmonic at network nodes where the filter is not installed. Wada *et al.* [29] states that using an active filter on a feeder exceeding $0.25\gamma_h$ in length for the h^{th} harmonic would result in inadequate filtering of the harmonic and can result in the given harmonic being amplified on other network nodes.

2.4.4 Review of other research involving the impact of DGs on the network

In [30], Newman *et al.* propose the use of a dynamic power transmission model to investigate the impact of connecting additional distributed generation to the grid on the overall grid robustness. The research finds that as the reliability of the distributed generation increases, the power grid characteristics improve. The study also found that in the case of the distributed generation being more variable in its reliability and availability, the overall network is seen to become much less robust and more prone to blackouts. The study concludes that the addition of distributed generation into the network has both positive and negative impacts. It is also noted that impacts of variable distributed generation on an existing grid should be investigated for any specific grid to which the generation is planned on being connected.

In [31], Momoh *et al.* discusses the feasibility of centralised and distributed generation and compares them from an economic impact point of view. The study also compares the advantages of co-optimising these generation technologies and identifies the extent to which the technologies should be used in a future network. The study concludes that a combination network consisting of both centralised, traditional generation, and distributed generation is desirable and should be promoted, and that network studies in terms of reliability, sustainability, and economics should be done for any given network.

In [32], Sheikhi *et al.* conduct a study on the impact of distributed generation penetration on overall network power losses in a distribution network. The study was conducted using the IEEE 30-bus test network and the IEEE 34-node test feeder. The study found that the increase in the

distributed generation penetration level resulted in an increase in distributed generation production cost but decreased centralised generation costs and network transmission costs. The overall network power losses were found to occur when the distributed generation penetration level is 6.8% of the total network electricity production.

In [33], Pourarab *et al.* present a case study analysing the harmonics involved in the connection of a distributed generator to an existing, real MV distribution network. The study concludes that the integration of the given distributed generator would be permitted and would not negatively affect the overall total harmonic distortion in the network significantly. The total harmonic distortion is calculated as 2.81% with the distributed generator installed. This is below the desired 5% that the study aims to achieve. However, the study also recommends that further research be done.

In [34], Caramia *et al.* studies the impact of distributed generation on the voltage sag in a transmission network. The study proposes a systematic method to study the voltage sag for a transmission network to which large distributed generators are connected. The study found that the addition of distributed generator units in a transmission network does not always improve the voltage sag performance of that network.

2.5 Energy storage technologies

Electrical energy generated using renewable technologies are usually designed to output a DC voltage of varying magnitudes. Also, due to the unpredictable nature of the natural sources driving these technologies, they are not always available. Thus, the generated DC power should be stored to account for the instances where the driving source is not available.

2.5.1 Storage techniques

The storage of electrical energy is a major focus of recent research. Various new technologies are being researched and proposed, including super-capacitors, compressed air energy storage, flywheels, pumped-hydro storage, superconducting magnetic energy storage, and hydrogen fuel cells [35].

However, distributed generation systems usually employ battery technology due to its cost and variety of technologies.

2.5.2 Common terms and battery specifications

Some of the terms used to describe batteries and their specifications are stated below [36].

- **Capacity:** The capacity of a battery is the maximum amount of energy that can be stored in the battery at any instance in time. Battery capacities are usually measured in Amp-hours.
- **Cells, modules, and packs:** A cell is the smallest form of a battery, and usually has a terminal voltage ranging from one to six volts. Multiple cells are usually connected in series or parallel to create a battery module. Battery modules are then connected in series or parallel to form a battery pack. Battery packs and modules are connected in series or parallel depending on the voltage and current requirements for which the packs or modules will be used.

- **Internal Resistance:** Internal resistance is a resistance found within the battery that is introduced to the circuit when the battery is connected. The internal resistance is dependent on the battery's state of charge, and changes depending on whether the battery is discharging or charging.
- **Secondary and Primary cells:** Primary cells are cells which cannot be recharged. Secondary cells are cells which can be recharged.
- **State of Charge (SOC %):** The state of charge is a measurement used to indicate the current capacity of a battery, as a percentage of the maximum capacity of the battery.
- **Depth of Discharge (DOD %):** The depth of discharge is a measurement used to indicate the total discharged capacity of a battery as a percentage of the maximum capacity of the battery.
- **Cycle life:** The cycle life of a battery refers to the amount of charge-discharge cycles the battery can endure before its performance fails to meet specific performance criteria. The cycle life is estimated for specific charge and discharge conditions.
- **Power density:** The power density of a battery refers to the nominal power held by the battery, per unit volume.
- **Energy density:** The energy density of a battery refers to the nominal energy held by the battery, per unit volume.
- **Self-discharge:** Self-discharge occurs when a battery is not connected to any loads, while being in a charged state. The battery would then lose charge over time.

2.5.3 Comparison of battery technologies

There are a wide variety of battery technologies available, each with their own advantages and disadvantages for different ranges of applications.

The lead-acid battery technology possesses an average efficiency while possessing a relatively low cycle life [37]. However, the relatively low cost of this technology makes it desirable.

The lithium-ion battery technology provides very high cycle life, high efficiency, and a relatively high depth of discharge [35]. This battery technology thus possesses highly desirable qualities for the battery bank for a distributed generation system. However, the high cost and the required advanced monitoring and control methods associated with the technology [37] makes it highly uneconomical for use in large capacities.

The sodium-sulphur battery technology provides high efficiencies, high cycle life, high depth of discharge, and negligible self-discharge. The costs associated with this technology are high, however, due to the initial cost of the cells being high, as well as the fact that these types of batteries require auxiliary heating systems to function properly [35].

The nickel-cadmium battery technology has a high depth of discharge and cycle life, but couples high cost, relatively lower efficiencies, and high self-discharge rates [35].

The zinc-bromine battery technology possesses high depth of discharge, relatively high cycle life, average efficiencies, and negligible self-discharge rates. The cost associated with these types of cells are high [35].

2.5.4 Advantages and disadvantages of using battery storage

The following advantages come with using battery storage in distributed generation scheme [37].

- Response times are in the millisecond range.
- Batteries can be sited near residential areas due to low environmental footprints.
- Batteries can be installed anywhere and are not restricted in their use by geographical location, such as hydro systems.
- They are modular in design, and can be interconnected for additional capacity.

The following disadvantages come with using battery storage in distributed generation.

- The batteries will need to be replaced as the batteries reach the end of their designed cycle life [35].
- Some battery technologies employ dangerous substances, which can result in fires or explosions if subjected to negative conditions [37].

2.5.5 Other energy storage developments

Developments have been made in the area of energy storage technologies. Some of these are explored below.

i. Flywheels

A flywheel is a mechanical form of energy storage. A flywheel consists of a rotating cylinder, bearings, and an energy transmission device. The energy in a flywheel is stored in the rotational energy of the rotating cylinder, by keeping the rotational speed constant. The transmission device either provides electrical energy to the wheel, thereby accelerating it, or extracts the energy from the wheel, thereby decelerating it [38].

Flywheels are designed to possess a fast response time. However, flywheels present relatively low cycle life, and average efficiency [37].

ii. Double-layer Capacitors

Double-layer capacitors (DLCs) are forms of electrical energy storage. They work similarly as traditional capacitors but offer extremely high power density, very large capacitance, and low internal resistance [39]. However, they are better suited and more likely to be used in instances where very fast charge and discharge cycles are required [38].

iii. Super-conducting Magnetic Energy Storage (SMES)

Super-conducting Magnetic Energy Storage (SMES) is another type of electrical storage technology. The energy is stored in a magnetic field which is created by running a DC current through a superconducting material kept below its superconducting critical temperature [38].

SMES possesses a very short response time, allowing the energy to be available very quickly [40]. However, storing the energy for long periods of time is made difficult by the fact that refrigeration systems are required to meet the low temperature requirements that the system requires [38] [40].

SMES systems offer very high efficiencies, power densities, and cycle life. It possesses zero resistance, adding to its excellent efficiency. It also involves no moving parts, chemical reactions, and produces no toxic substances in its operation [40].

2.6 Renewable system electronics

In order for a solar PV system to connect to the grid, its DC output voltage needs to be converted to an AC voltage of the appropriate voltage level. For a wind turbine system, the low voltage AC output needs to be stepped up.

In addition to this, controllers are also required to control both the charge and discharge of the battery system, as well as the wind turbines themselves.

2.6.1 Conversion technologies

The DC voltage produced by the distributed generator needs to be converted to an AC voltage to be able to connect to the grid. This AC voltage can then be stepped up or down as required, using a transformer. The conversion process for converting a DC voltage to an AC voltage is done by an electronic circuit known as an inverter.

Distributed generators generally provide a very small output voltage compared to the RMS voltage on a low-voltage AC circuit. For this reason, it is preferable that the DC input to the inverter be increased before it is rectified. This is done using a DC-to-DC converter. There are many types of DC converters available, such as the buck, boost, and buck-boost types, all of which have different characteristics which are discussed below [41].

- **Buck converters:** Buck converters are converters which output a voltage lower than the input voltage.
- **Boost converters:** Boost converters are converters which output a voltage higher than the input voltage.
- **Buck-boost converters:** Buck-boost converters are converters which are flexible enough to be able to output a voltage lower or higher than a given input voltage.

In [41], the buck-boost DC-DC converter is proposed due to the flexibility it provides. This converter can then be coupled to a full-bridge inverter circuit to obtain the desired AC voltage. The complete circuit diagram for this implementation is shown in Figure 2.16.

Q_A is a MOSFET designed to withstand high power levels. This MOSFET is switched at high frequencies to properly shape the sinusoidal output voltage. The inductor (L) and capacitor (C) are used to construct a low-pass filter that extracts the 50Hz sinusoidal waveform while leaving high frequency components behind.

Distributed generators are connected to the grid through a switch. Grid-tie inverters can be used to connect the DG to the grid, and also feature multiple protection functions which would normally be performed by protection relays [9]. However, most of these inverters do not allow off-grid inversion, and most off-grid inverters do not allow grid-tie inversion [9]. Inverters which perform both functions are available [9].

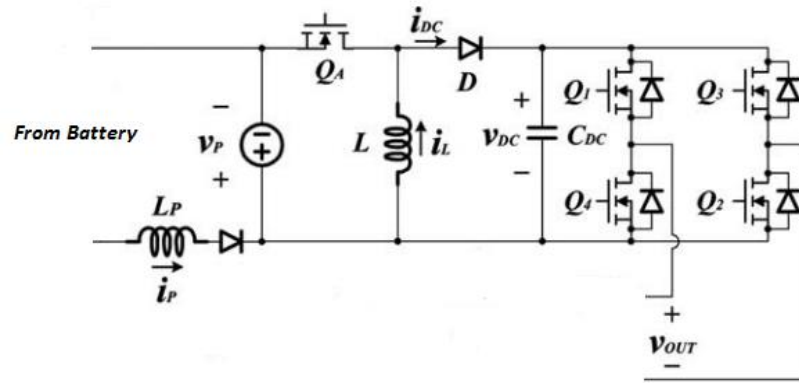


Figure 2.16: Buck-boost converter and inverter circuits [41].

2.6.2 System controllers

In a system as complex with multiple components, such as solar PV systems, controllers are required to regulate and control processes within the system, so that the individual components, and thus the system as a whole, perform optimally.

i. MPPT controllers

The solar PV array and wind turbines are seen to perform best when operating at the maximum power point (MPP). Thus, maximum power point tracking (MPPT) techniques need to be incorporated into the controller to ensure that the MPP is tracked consistently and accurately. The algorithms need to be implemented in physical hardware to enact them.

ii. Battery charge controllers

The state of charge of the battery needs to be monitored and controlled according to the current status of the battery at a moment in time, such as preventing the battery from charging when it is fully charged or preventing the battery from reaching a state of severe undercharge in order to avoid damaging the battery [42]. This is done by the battery charge controller.

In wind turbine applications, once the battery has reached its full capacity, the controller is generally diverted to another useful load so that the batteries are not damaged. In PV applications, the controller shorts the PV array terminals once the batteries are charged. However, this approach would cause damage to the wind turbine if implemented in this way [43].

iii. Complete system controllers

Modern PV system controllers provide both battery charge controller as well as MPPT functionality. These system controllers generally include over-voltage as well, to protect the system from voltage surges due to lightning strikes. In [42], Tesfahunegn *et al.* propose a complete system controller to perform the MPPT function while ensuring voltage stability.

The proposed controller model works by calculating an error value continuously, which is calculated as the difference between the setpoint value and the actual value at that point in time. Once the error value is found, adjustments are made so that the system approaches the setpoint value. These changes are made based on the P and I elements – Proportional and Integrator elements, which give the controller its name. Derivative (D) elements are also sometimes added to these types of controllers when required.

The study concludes to find that the proposed controller possesses a very fast transient response with minimal voltage overshoot [42].

In [44], Hsieh *et al.* expand on this idea by employing a fuzzy logic controlled algorithm to improve a state-of-charge controller for a lithium-ion battery. This incorporation is found to improve the charging speed by 23%.

2.7 Wind turbine system control

A wind turbine farm consists of multiple wind turbines working in conjunction to support a cluster of loads or export power to the grid. These farms, as well as the individual turbines, use controllers to ensure that the farm operates optimally.

The wind farm controller's main function is to control the farm dispatch based on current requirements or other network changes, or changes in wind speed, direction, and other natural conditions.

The wind turbine supervisory controller is a separate controller that controls each individual turbine. It manages power production and operation of each individual turbine, manages start-up and shut-down conditions, and provides control input to any sub-system controller that the turbine may have [45].

2.7.1 Aerodynamic torque control

For any given wind turbine, there exists an optimal tip-speed-ratio, γ , that maximises the power coefficient [45]. The power coefficient is defined as the ratio of the electrical power produced by the wind turbine to the wind power used as an input to the wind turbine. The typical relationship between the power coefficient, tip-speed-ratio (TSR), and rotor pitch angle is shown in Figure 2.17.

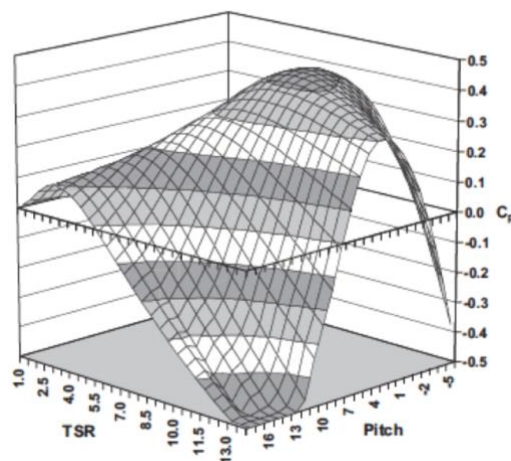


Figure 2.17: Typical graphical relationship between TSR, Pitch, and C_p for a 600kW, dual blade, HAWT [45].

The relationship between γ and the power coefficient motivates a closed-loop control system to focus on the rotational frequency [45]. Aerodynamic control is thus achieved by controlling γ , which can be achieved by controlling the rotor's lift and drag. This can be achieved in the following two ways.

i. Stall-regulated rotor designs

Stall-regulated rotors are designed in a manner that results in the rotor being able to stall at wind speeds higher than the rated wind speed of the wind turbine [45]. This is achieved by adjusting the pitch angle at higher wind speeds [43].

ii. Pitch-regulated rotor designs

Pitch-regulated rotors are designed in order to reduce the torque experienced by reducing the pitch, which in turn, reduces the lift experienced by the rotor blades [45]. This control only initiates once the wind speed is at an acceptable level so that the turbine is able to produce rated power [45].

2.7.2 Electrical torque control

The TSR can also be controlled electrically. The fundamental of this type of control comes from controlling the magnetic field of the generator by controlling the current that creates this field.

2.7.3 Inverter technology

Ozdemir *et al.* [19] discusses the effect of using back-to-back power electronic inverters in wind turbine systems. This allows the output to be controlled when fed to the grid, and is found to improve the overall turbine system efficiency.

2.8 Common DG placement techniques

The placement of the DGs at different points in the network affects the network in different ways, depending on the point of connection. The connection of DGs at a point can affect the power system voltage profile and can either increase or decrease the network losses depending on the direction of power flow [46]. The placement of a DG in the network may also require reconfiguration of protection systems and settings due to the design of the protection system being specific to the network configuration at the time of setting implementation. The placement of DGs thus plays a vital role in ensuring an adequate level of performance from the entire network.

2.8.1 Analytical methods

Many analytical methods have been proposed for finding the optimal placement and sizing of DGs with respect to optimising the power flow, minimising losses, and improving the voltage profile [47]. These methods are based on theory, mathematical analysis, and calculations. A general algorithm for these methods are shown in Figure 2.18.

The objective functions shown in Equations 2-6 and 2-7 has been proposed for bus 'j' [47].

$$f_j = \sum_{i=1}^{j-1} (R_{1i}(j) |S_{Li}|^2) + \sum_{i=1}^N R_{1i}(j) |S_{Li}|^2, j = 2, 3, 4, 5 \dots, N \quad (2-6)$$

$$\text{Where } R_{1i}(j) = \begin{cases} \text{Real}(Z_{11} + Z_{ii} - 2Z_{1i}), & i < j \\ \text{Real}(Z_{11} + Z_{(i-1)(i-1)} - 2Z_{1(i-1)}), & i > j \end{cases} \quad (2-7)$$

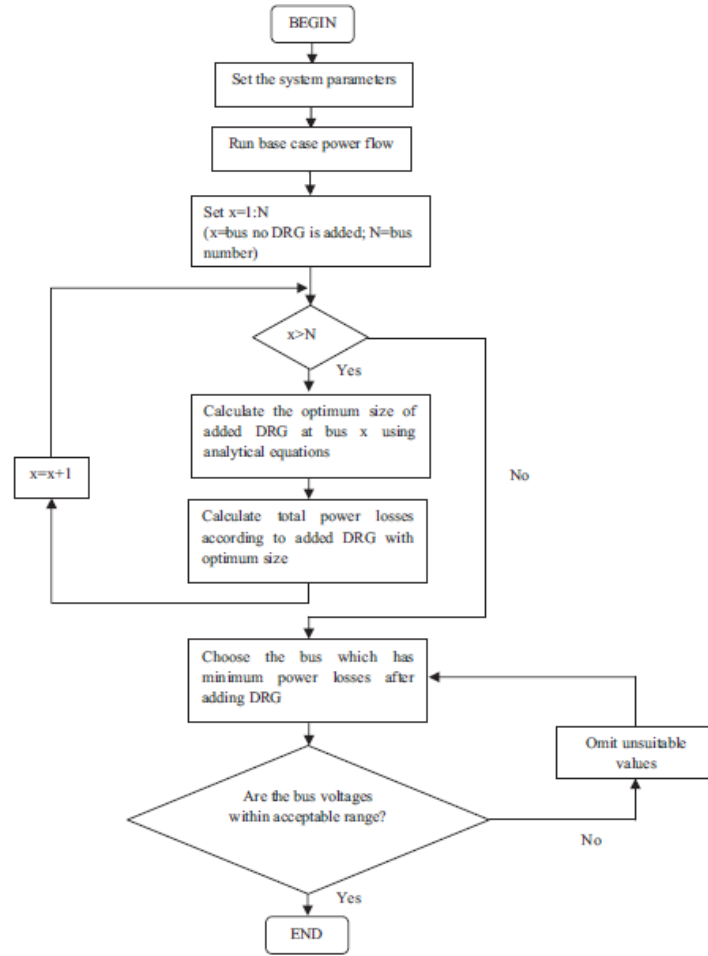


Figure 2.18: General analytical method algorithm for optimal DG placement [47]

In the above formulae, Z_{xy} are the elements of the bus impedance matrix. The goal of the above formulae is to find the optimal bus, Bus M, on which to install the required DG by finding the minimum value of f_j for all values of j , as shown in Equation 2-8 [47].

$$f_M = \min(f_j), j = 1, 2, 3, \dots, N \quad (2-8)$$

2.8.2 Evolutionary algorithms

Evolutionary algorithms have become very popular and are often used for optimisation problems. The algorithm creates trial solutions that aim to satisfy a given fitness function defined by the specifics of the problem. The fitness function combines the objective function along with any system constraints that the solution needs to abide by. These trial solutions are evaluated and evolved with each generation until a satisfying solution is found and the termination conditions are met [48].

With regards to DG sizing and placement, the evolutionary algorithm will propose different DG sizes and placement as possible solutions. A power flow analysis will then be carried out and evaluated for each solution and the best solutions will undergo evolution to find even better solutions to the problem. System constraints would include the allowable power losses in the system, DG size constraints, as well as the maximum and minimum bus voltages in the system.

2.9 Types of evolutionary algorithms

This section focusses on the different types of evolutionary algorithms that are used, as well as their advantages and disadvantages.

2.9.1 Genetic algorithms

One of the most popular evolutionary algorithms is known as the genetic algorithm. Genetic algorithms work by randomly creating multiple solution vectors, in the form of bit-strings, to a particular problem. This is called the solution population. Each of these solution vectors are substituted into the objective function and its performance is evaluated [48]. Once the best solutions are found, they are mutated in some form and used to create the next generation of solutions, while the rest of the solutions are discarded. This concludes what is known as one generation. Multiple generations are run until the solution vectors converge and the best solution is found.

The key component of evolutionary algorithms is the ability of the solution vectors to mutate, evolve, and become more suitable to solve the problem. These mutations occur in an organised way via different methods. The steps followed in the genetic algorithm as well as the methods of mutation are discussed in detail below.

i. Creation

The population is initialised as a list of vectors consisting of binary numbers if there are no existing populations. The population is made up of vectors of binary numbers which are possible solutions of the defined objective function [46].

ii. Selection

The selection operator is used to determine which individuals from a current generation will survive and reproduce to create the next generation. The individuals are selected based on their performance in satisfying the objective function [48]. There are multiple ways this operator is used, the most common of which are deterministic selection, stochastic selection, and roulette-wheel selection [48].

iii. Crossover

The crossover operation takes two 'parent' solution vectors and produces an 'offspring' solution vector which forms part of the next generation [46]. The parents are taken from the breeding pool of the fittest solutions of the previous generation in order to create offspring which would result in good solution vectors. These can be done in multiple ways called "crossover operators" [48]. Euclidean distance is sometimes used.

Crossover is the most common method used to introduce change into the population. The nature of crossover introduces convergence of the solutions to a common point [48].

iv. Mutation

The mutation operation introduces random changes to the previous generation of solution vectors in order to create the new generation. The random changes are kept small in each generation, usually below 10% [48].

The nature of mutation introduces genetic variety into the population to counter the convergence of solutions created by the crossover operation [48]. This ensures that the optimal point that is found is the global optimum, not the local optimum. The mutation and crossover operators are normally used in conjunction.

2.9.2 Advantages and disadvantages of genetic algorithms

Some of the advantages of genetic algorithms are listed below [46] [49].

- Genetic algorithms are able to search multiple points in the vector space in parallel.
- Genetic algorithms are more likely to find the global optimum and less likely to get stuck at a local optimum.
- Genetic algorithms require no explicit knowledge of the problem, only the fitness function and the required performance information.

Some of the disadvantages of genetic algorithms are listed below [49].

- The convergence of the genetic algorithm is generally slower than other evolutionary algorithms.
- Genetic drift may cause the population to lose diversity. This is combatted by using mutation, but not to the extent that the genetic drift has no effect.

2.9.3 Population-based Incremental Learning (PBIL)

Population-based incremental learning (PBIL) is an evolutionary algorithm based on genetic algorithms, which combines genetic algorithms with the concept of competitive learning [49]. In PBIL, the method of crossover and the role of the population is redefined. PBIL has been shown to be extremely useful for solving many difficult optimisation problems [50].

i. Implementing PBIL

PBIL works by implementing a real-valued vector known as the 'probability vector' which is initialised as a vector with M elements as is required in the solution vector, where each element is set to 0.5 [50]. The probability vector defines the probability of selecting a '1' for each bit in the bit-string of the solution vectors [49].

A population of N random solutions are created, each containing M elements of real numbers. Each individual in the population is compared with the probability vector, element-by-element [49]. Each element where the corresponding element in the probability vector is greater than that of the solution vector, a '1' is generated, while each element where the corresponding element in the probability vector is smaller than that of the solution vector, a '0' is generated. Each bit-string generated in this way is treated as a solution to the problem and evaluated.

Once the best solution vector is found, the probability vector is updated by comparing the best solution with the probability vector, element-by-element, increasing the probability vector element where a '1' occurs in the corresponding element in the solution vector, and decreasing it wherever a '0' occurs. The amount by which the probability vector is increased or decreased is known as the learning rate [49]. A new population is then created using the updated probability vector and the process is repeated.

ii. **The learning rate**

The updated probability vector can be given by Equation 2-9 [49].

$$PV(i)_{n+1} = (PV(i)_n \times (1 - LR)) + (LR \times V(i)) \quad (2-9)$$

In the equation above, $PV(i)$ is the probability of generating a '1' bit in bit position i , LR is the learning rate, and $V(i)$ is the i -th position in the solution vector towards which the probability vector is moved.

The numerical value of the learning rate has a greater effect than the learning rate used in standard competitive learning, due to the fact that the probability vector is used to generate sample solutions in the future generation [49]. However, a higher learning rate would increase the speed at which convergence occurs but decreases the search space in which solutions are explored [50].

iii. **Maintaining diversity in PBIL**

Because the probability vector is continuously moving towards the vector which performs the best in each generation, it is likely to lose diversity using this method alone. For this reason, a 'mutation' operator is employed in PBIL in order to maintain diversity while searching for the best solution vector [49].

Mutation in PBIL works using a 'forgetting factor' which relaxes the probability vector back to the neutral values of 0.5 by applying a mutation. This mutation can be given by Equation 2-10, where FF is the forgetting factor [49].

$$PV(i) = PV(i) - FF \times (PV(i) - 0.5) \quad (2-10)$$

This ensures that the search space remains diverse throughout the search and helps to find the global optimum instead of a local optimum.

2.9.4 Advantages and disadvantages of PBIL

Some of the advantages of PBIL are listed below [49] [50].

- Operations are done on the probability vector itself, not on the overall population.
- PBIL is easier to implement than traditional genetic algorithms.
- PBIL outperforms genetic algorithms on a variety of benchmark tests.
- The processing overhead for PBIL operations are significantly lower than that of genetic algorithms.

Some of the disadvantages of PBIL are listed below [49].

- Because the algorithm uses a single probability vector for a given variable, a large number of points can be argued to cause deteriorating performance.

2.9.5 Differential evolution

Differential evolution (DE) is an evolutionary algorithm that closely represents genetic algorithms, but does not introduce random change to the population. Instead, it introduces arithmetic changes with each generation. DE has very few tuneable parameters compared to other evolutionary algorithms, namely the mutation co-efficient (F), crossover co-efficient (CR),

and the population size (NP) [51]. The solutions generated by this algorithm are real-valued solutions instead of binary-based. Figure 2.19 shows the general algorithm followed by DE.

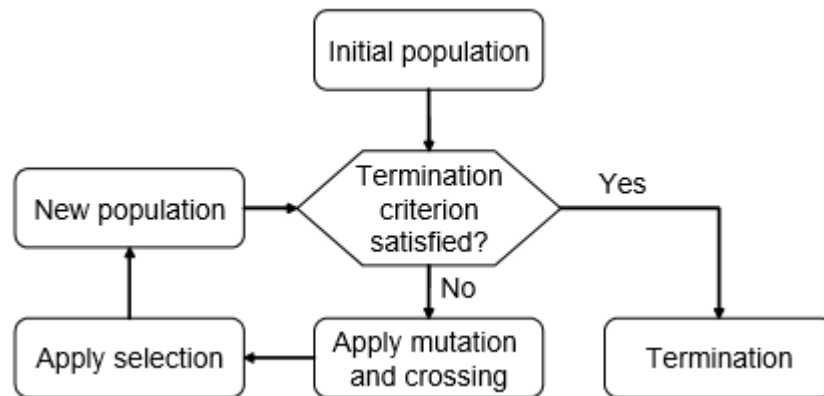


Figure 2.19: Flowchart showing the general DE algorithm [51]

As seen in Figure 2.19, DE follows a similar algorithm to other evolutionary algorithms. The stages in DE are discussed below.

i. Initialisation

The initial population is created and their fitness is tested against the defined fitness function. The population is carefully initialised between the lower and upper bounds defined for each of the parameters [52].

ii. Mutation

Mutation in DE makes use of a difference vector, which is a vector whose elements are determined by the differences between two randomly selected vectors in the population. This difference vector is then scaled and added to the base vector to create the mutant vector [51]. The mutant vector can be mathematically expressed by Equation 2-11, employing the ‘current’ operator [51].

$$V_{i,G} = X_{r1,G} + F(X_{r2,G} - X_{r3,G}) \quad (2-11)$$

In the above equation, $V_{i,G}$ is the mutant vector, F is the mutation co-efficient between 0 and 1, $X_{r1,G}$ is the base vector, and $X_{r2,G}$ and $X_{r3,G}$ are two random vectors in the population which are used to create the difference vector [51].

The first step in mutating a vector is to select the base vector. There are multiple ways of selecting it from within the entire population. Some of these methods are discussed below.

The ‘rand’ operator

The ‘rand’ operator selects a base vector from the established population at random. A problem with this method of selection is that a single vector in the population can be selected multiple times to act as a base vector, which is undesirable. To overcome this problem, it is suggested that a random starting point is selected instead of selecting vectors completely at random [51].

The 'best' operator

The 'best' operator selects the best-performing vector as the base vector for mutation. This, however, may lead to premature convergence and thus should be used when the global optimum is easy to find [51].

The 'rand-to-best' operator

The 'rand-to-best' operator is a combination of the 'rand' and 'best' operators. This method illustrates the mutant vector as in Equation 2-12 [51].

$$V_{i,G} = X_{r1,G} + F(X_{r2,G} - X_{r3,G}) + \gamma_W(X_{best,G} - X_{r1,G}) \quad (2-12)$$

In the mathematical equation above, $X_{r1,G}$ is a randomly selected vector within the population and $X_{best,G}$ is the best performing vector from the population. γ_W is a scaling factor ranging between 0 and 1. A high value of γ_W results in a mutant vector which is closer to the best vector, compared to the random vector, while low values of γ_W results in a mutant vector which is closer to the random vector, compared to the best vector. For simplicity, it is suggested that γ_W takes on the same value as F [51].

The 'current' operator

The 'current' operator uses the target vector as the base vector, which allows the search to become isolated. This is desirable when multiple global optima exist in the search space [51].

The 'current-to-best' and 'current-to-rand' operators

The 'current-to-best' and 'current-to-rand' operators use a base vector which lies between two chromosomes. The 'current-to-best' method uses a base vector which lies between the target vector and the best vector [51]. The mutant vector is expressed as in Equation 2-13 [51].

$$V_{i,G} = X_{i,G} + F(X_{r2,G} - X_{r3,G}) + \gamma_W(X_{best,G} - X_{i,G}) \quad (2-13)$$

The 'current-to-rand' method uses a base vector which lies between a randomly selected vector and the target vector. The mutant vector can be expressed as in Equation 2-14 [51].

$$V_{i,G} = X_{i,G} + F(X_{r2,G} - X_{r3,G}) + \gamma_W(X_{r1,G} - X_{i,G}) \quad (2-14)$$

iii. Crossover

In differential evolution, crossover is applied after mutation. A trial vector is obtained by combining the mutant and target vectors using a specific crossover method. Thus, results would vary depending on the value of the crossover co-efficient (CR) and which crossover method is used. Some of the common crossover methods are discussed below.

Binomial crossover

Binomial crossover employs probabilistic methods. An element in the mutant vector is taken to the corresponding element in the trial vector with the probability given by the crossover co-efficient (CR). If the mutant element is not carried over to the trial vector, the corresponding element from the target vector is carried over to the trial vector instead. In order to ensure the

target vector is not completely duplicated in the trial vector, at least one element from the mutant vector is forced to be carried over to the trial vector [53].

Exponential crossover

Exponential crossover in differential evolution is similar to crossover in genetic algorithms. Exponential crossover takes random elements from the mutant vector, starting from a random point, and places them in the trial vector [53]. The rest of the elements in the trial vector are taken from the target vector.

iv. Selection

Selection in DE is applied to select which chromosomes are placed into the next generation and which are discarded. The target vector is usually either selected randomly or the best performing vector is used [53].

2.9.6 Advantages and disadvantages of DE

DE presents the following advantages [51].

- DE is said to be simple and can thus be easily applied due to a minimal amount of tuning.
- DE is seen to perform well in large, complex problems.
- The algorithm uses real values.
- DE provides a much faster convergence in fewer generations.

DE presents the following disadvantages [51].

- The tuning parameters used are seen to vary widely in other research depending on requirements, and can thus be difficult to select.

2.9.7 Review of research done using optimisation techniques for DG placement

In [54], Ayodele *et al.* describes different approaches taken by different researchers regarding the optimal placement problem of DGs in an electrical network. This study goes on to propose the use of the genetic algorithm. The study found that the GA technique was successful in meeting its optimisation criteria to reduce power losses in the IEEE 14-bus network.

In [46], Kotb *et al.* also proposes the use of genetic algorithms for use in the optimisation of DG placement in order to find the optimal placement and sizing of network DGs to reduce power losses and improve the cumulative voltage profile. Kotb *et al.* however, identifies 8 nodes at which the voltage is relatively low, and limits the amount of DG installations to three, so that the GA would need to find the optimal placement between the 8 identified busses instead of the 69-bus system as a whole. This study finds that using GA for optimal DG sizing and placement produces good results, reducing active power losses by 56.6% and reducing reactive power losses by 48.3%. This is better than the results obtained by the same authors from using analytical methods on the same network.

Zhan *et al.* propose including protection grading considerations into the genetic algorithm itself in [55]. This proposal identifies that little research has been done into the protection aspects of optimal DG placement using heuristic techniques, and investigates using the fault levels at the busses as constraints in both a 14-node and 33-node radial network. The study concludes that the proposed method has worked and provided optimal DG placement and sizing with the

additional constraints. However, the study does not mention relay trip times for faults throughout the network before and after the proposed DGs have been added.

Kotb *et al.* [46], Ayodele *et al.* [54], and Zhan *et al.* [55] have explored the use of genetic algorithms to optimise DG sizing and placement in different networks. However, none have ventured into using PBIL.

In [56], Montoya *et al.* have proposed a 'master-slave' combination of parallel PBIL (PPBIL) with Particle Swarm Optimisation (PSO) in order to solve the DG placement and sizing problem. The PBIL-PSO algorithm was tested on a radial 69-bus network, with three case studies varying by the number of DGs added. The study found that the PPBIL-PSO algorithm provided the best balance between power loss reduction, voltage profile improvement, and processing time compared to the genetic algorithm.

Tusar *et al.* [57] directly compares the DE and GA algorithms on multiple different problems and finds that DE significantly outperforms GA on 20% of the problems it was given. GA performed better on only 3% of the problems it was given, while the solutions were comparable for the rest of the problems.

Manafi *et al.* [52] and Ravi *et al.* [58] have ventured into using DE algorithms in order to optimise DG sizing and placement, using load flows on specific networks. Ravi *et al.* uses the algorithm to optimise sizing and placement while taking operating costs into account as well. Manafi *et al.* on the other hand, uses DE to only optimise power losses, but compares it to the performance of the more complicated PSO algorithm. Manafi *et al.* finds that the DE and PSO algorithms perform excellently for finding the global optima, however, the complex PSO algorithm does it slightly faster than the DE algorithm. Manafi *et al.* and Ravi *et al.* have implemented DE simply to find the optimal placement and sizing of the DGs with between two to three objectives. However, Tusar *et al.* [57] states that the DE algorithm performs well optimising four objectives as well. DE is also seen to be easily scalable for multi-objective problems. Ravi *et al.* also proposes the idea of parallel computation, taking advantage of multiple processing cores.

Lui *et al.* [59] have implemented DE with the objective of optimising the costs and effects of implementing voltage control systems into the network under study, completely steering away from other researchers' focus on minimising power losses itself, but rather minimising the cost impact of power losses. The research concludes the effectiveness of the proposed approach, and goes on to state that their implementation has more potential than traditional voltage improvement techniques, such as reactive compensation.

Yang *et al.* [60] investigates using the DE algorithm to place DGs optimally according to their concern which lies mainly in the effect that distributed generation has on the protection system. However, their focus is strictly on the directional overcurrent protection scheme, and optimising the settings of these relays, as replacement of these schemes may not be cost effective. The problem is formulated by focussing on each relay being co-ordinated only with their neighbour. The proposed method is tested on a five-bus system and successfully grades the relays in the network to perform their function when exposed to network faults.

It is noted in this study that previous studies observed in [46] and [56] have predominantly dealt with mostly radial feeder networks with few single interconnections between a vast minority of busses. The network topologies used generally consist of a main bus feeding three radial circuits with busses located between the lines on these circuits.

To this researcher's knowledge, three-feeder groups, however, are not seen to be implemented in these algorithms. It is also noted that most studies surrounding the DG placement problem have opted to use the GA algorithm and not much research has been done in terms of implementing PBIL and DE to solve this problem. Research has also not been done on the direct effect of heuristic algorithm-based DG sizing and placement techniques on current network protection schemes, without directly taking the protection scheme into the algorithm itself, as is evident by the reviews of work done by Alarcon-Rodriguez *et al.* [61] and Georgilakis *et al.* [62]. Finally, the MATPOWER power system simulation package is not seen to be used in conjunction with heuristic DG placement techniques in any published work.

Of these algorithms, it is seen that DE and PSO are generally the better performing algorithms for a multitude of problems. However, due to the complexity of the PSO algorithm and the fact that the performance difference between it and the DE algorithm comes down to a slightly faster convergence using PSO as per Manafi *et al.*, this study will opt to use the PBIL and DE algorithms in further investigations.

3. Case study system design and methodology

This section details the design of the networks and systems that will be investigated in the remainder of this dissertation.

3.1 IEEE test case methodology

This section explores the methodology used to model the IEEE 14-bus test system, which was used to test the optimisation algorithms to be used on the case study, as well as to provide some insight into results that can be expected from the case study.

3.1.1 Test case network modelling

The network was modelled according to the topology and component characteristics provided by the IEEE for the 14-bus test system. A system diagram of this network is shown in Figure 3.1.

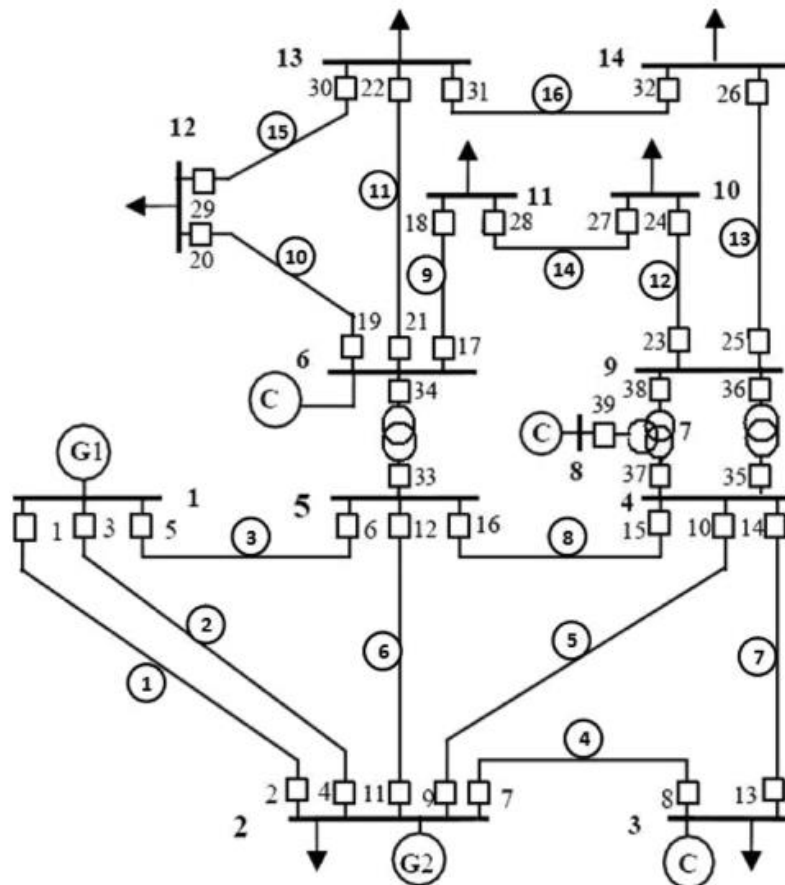


Figure 3.1: The standard IEEE 14-bus test system [63]

The generator, load, bus, transformer, and line data were modelled as given in [64]. These details are shown in the tables in Appendix A.

The network was modelled in both DlgSILENT PowerFactory and as a MATPOWER input script for simulation. The results were compared against the standard results obtained for this network in order to ensure correct modelling methodologies are used for this case and the case study used further in this dissertation.

3.1.2 Protection system modelling for the test case

Because the protection settings for the IEEE 14-bus system are not provided as part of the standard, it was decided to grade the network for the purposes of this study. The PBIL and DE algorithms were then used to optimally place distributed generators in this network. The effect of these additional distributed generators was then observed and compared to the base case, where no additional generation is placed in the network.

The protection settings were designed based on the furthest downstream feeders tripping in 0.4 seconds. Current pickup was set based on the nominal current flow through a given feeder under normal load flow conditions, and was rounded to the next highest amps. The time multipliers were set so that relays were given grading margins of between 300 ms and 400 ms.

Relay settings were tested in the network and it was found that the network could not be properly graded for a fault at any given bus in the network due to discrimination issues associated with the network running in a closed ring topology in both the MV and HV parts of the network without directional relay elements. Non-directional relays were used in the grading of this network so as to match the types of relays used in the municipal network. Thus, it was decided to modify the given network and run normally open points in the network so that proper non-directional overcurrent grading could be possible. The modified network and the normally open points are shown in Figure 3.2.

Faults were placed at Bus 10 and Bus 13 so that the network downstream of the transformers could be graded. These busses were chosen as their fault levels were the largest in their respective groups. Choosing a bus with a lower fault level for grading purposes could result relays tripping too quickly for a fault at a bus with a higher fault level.

Another municipal standard that was used was to trip opposite ends of a given line at the same time for a given fault. The designed protection settings are shown in Table 3-1. Relay numbering refers back to Figure 3.1.

The time multipliers above assume modern relays are installed in the network, capable of accepting time multipliers between 0.05 and 1, rounded to two decimal places. All settings are based on the use of the IEC Standard Inverse curve as is standard practice within the municipality to which the case study network belongs, as discussed in section 3.2.

An overview of protection systems and faults is given in Appendix B.

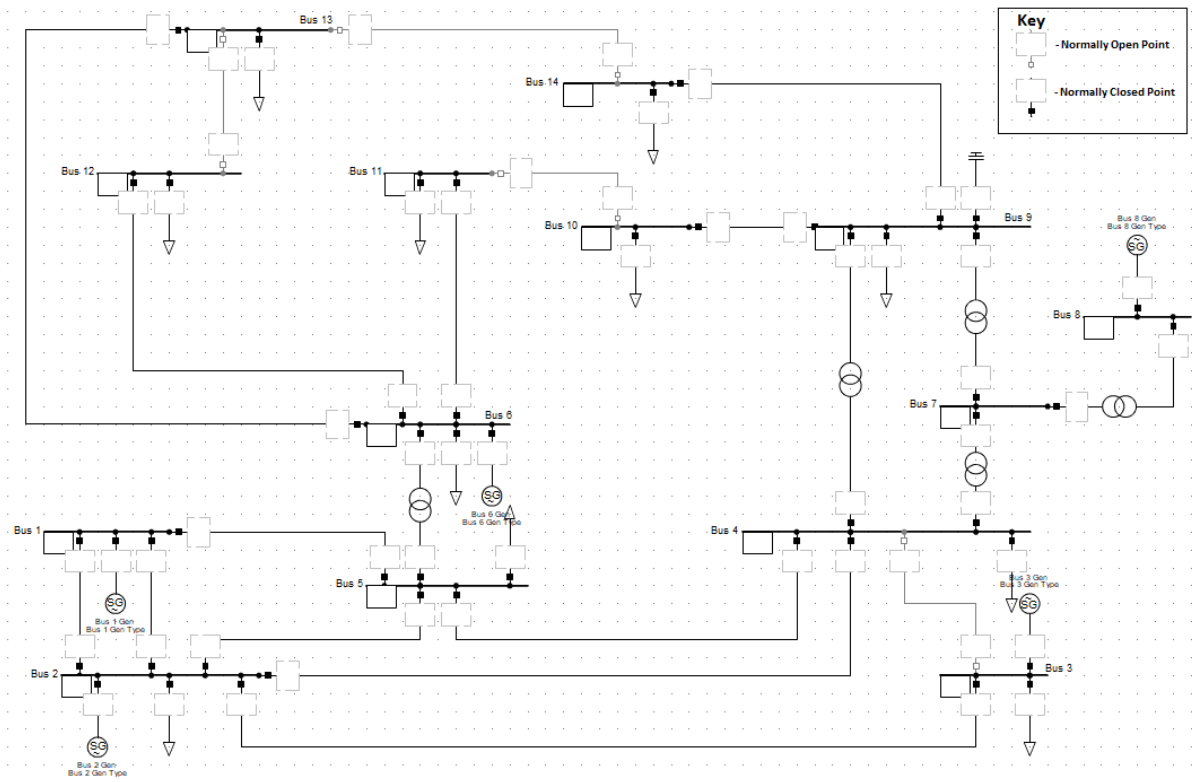


Figure 3.2: The modified IEEE 14-bus test system

3.1.1 Test case methodology breakdown

The network was modelled in both Digsilent PowerFactory and MATPOWER as described by the parameters in Appendix A. Based on the test case presented, the wind turbines which will be added to the modified IEEE 14-bus system were modelled, allowing them to be switched in and out at will. This allows the network to be simulated with the wind turbines being considered when switched in, and without the wind turbines being considered when switched out. Wind turbine positions and sizing were determined by means of optimisation algorithms in terms of optimising the voltage profile and power losses in the network. These are discussed later in this Chapter.

A load flow study was run for each of the case studies for this network, as discussed further in this Chapter. Results in terms of bus voltages, power flows, and power line losses were recorded to compare them at a later stage. Faults were also simulated at the busbars close to the source, slightly further from the source, and even further from the source, as discussed further in section 3.5, for each of the case studies. Relay grading results were recorded. These simulations were done for each of the optimisation algorithms that were used.

The Digsilent PowerFactory 15 software package was used for the simulation of the network and wind turbine system, as well as the protection grading. The MATLAB 2016b software package in conjunction with the MATPOWER 6.0 library was used in the optimisation. These simulation packages were chosen due to their availability for the duration of the study.

Table 3-1: The IEEE 14-bus system protection setting data

Relay No.	Pickup Current (A)	Time Setting	Multiplier
1	350	0.07	
2	350	0.07	
3	350	0.07	
4	350	0.07	
5	400	0.11	
6	400	0.11	
7	420	0.05	
8	420	0.05	
9	300	0.19	
10	300	0.19	
11	300	0.15	
12	300	0.15	
15	400	0.11	
16	400	0.11	
17	300	0.17	
18	300	0.17	
19	200	0.19	
20	200	0.19	
21	400	0.17	
22	400	0.17	
23	300	0.15	
24	300	0.15	
25	300	0.13	
26	300	0.13	
33	200	0.20	
34	800	0.14	
35	100	0.18	
36	300	0.20	
37	200	0.21	
38	1000	0.15	
39	6000	0.14	
G1	600	0.21	
G2	200	0.44	
G3	200	0.44	
G6	100	0.71	
G8	6000	0.18	

3.2 Municipal case study methodology

3.2.1 Case study background

A single IPP has submitted a proposal to build and connect a wind farm to a utility network, which feeds an area that is starting to grow in its energy usage.

The proposed project will provide an additional generation capacity up to 72 MW. This capacity was decided by the IPP based on the amount of land available and the generation capacity and

physical size of the most cost-effective wind turbines that could be installed. The type of wind turbine that will be used is not yet known, though the company intends on utilising inverters and battery storage in the configuration. This means that it must be of the asynchronous type fed through a converter system. As found in [25] and [26], the fault contribution of these converter systems are limited by a built-in current limiter. This contribution is set to 120% of the full inverter rating as shown in [25].

The capacity will be generated using wind turbines only. The specifications of the wind turbines have been decided upon by the IPP based on the historical wind patterns in the area, and have been provided by the IPP as part of the environmental impact assessment.

The project has been approved in terms of the environmental impact assessment, and no objections have been raised by citizens of the area or by the utility in question. The project is thus likely to be implemented in the coming years.

3.2.2 Case study methodology breakdown

Based on the case study presented, the dissertation will go on to detail the utility network as currently in operation and model it in both DiGSILENT PowerFactory and MATPOWER. The wind turbines were modelled according to the proposed implementation and the results obtained from the optimisation algorithms, and added to the models, allowing them to be switched in and out at will.

A load flow study and network faults were simulated and results were recorded for each of the case studies for this network as done for the IEEE 14-bus system case.

The same software packages were used as in the IEEE 14-bus system case.

3.2.3 The current network topology

The network was modelled according to the single-line diagram provided by the municipality under study. Due to the need for anonymity in this study, the actual single-line diagrams are not given and substation names were changed. However, the network topology and elements remain exactly the same as the actual network being studied. A single line diagram of the main network is shown in Figure 3.3.

As shown in Figure 3.3, the Utility substation is the only main substation (MS) in the area being fed from the major utility from which the municipality buys electricity. Thus, for the purposes of this study, the fault level at this station is of utmost importance. The current three-phase fault level is 13.001 kA at an angle of -49.8° , while the current single-phase-to-ground fault level is 4.849 kA at an angle of -52.2° at the 33 kV side of the Utility substation. The low earth-fault current is due to the Utility substation 33 kV side being fed through a wye-delta transformer.

The utility's network will be modelled as a positive-sequence and negative-sequence impedance. In order to obtain the given three-phase fault magnitude and angle, the positive-sequence and negative-sequence impedance were adjusted through the trial-and-error approach. The zero-sequence impedances were then adjusted in the same manner to obtain the required earth-fault current. The equivalent impedance was found to be a positive-sequence and negative-sequence

impedance of $1.875 + j2.176 \Omega$, while the zero-sequence impedance was found to be $10.65 + j13.905 \Omega$. These impedances were connected between the 33 kV side of the Utility substation and the external grid as source impedances.

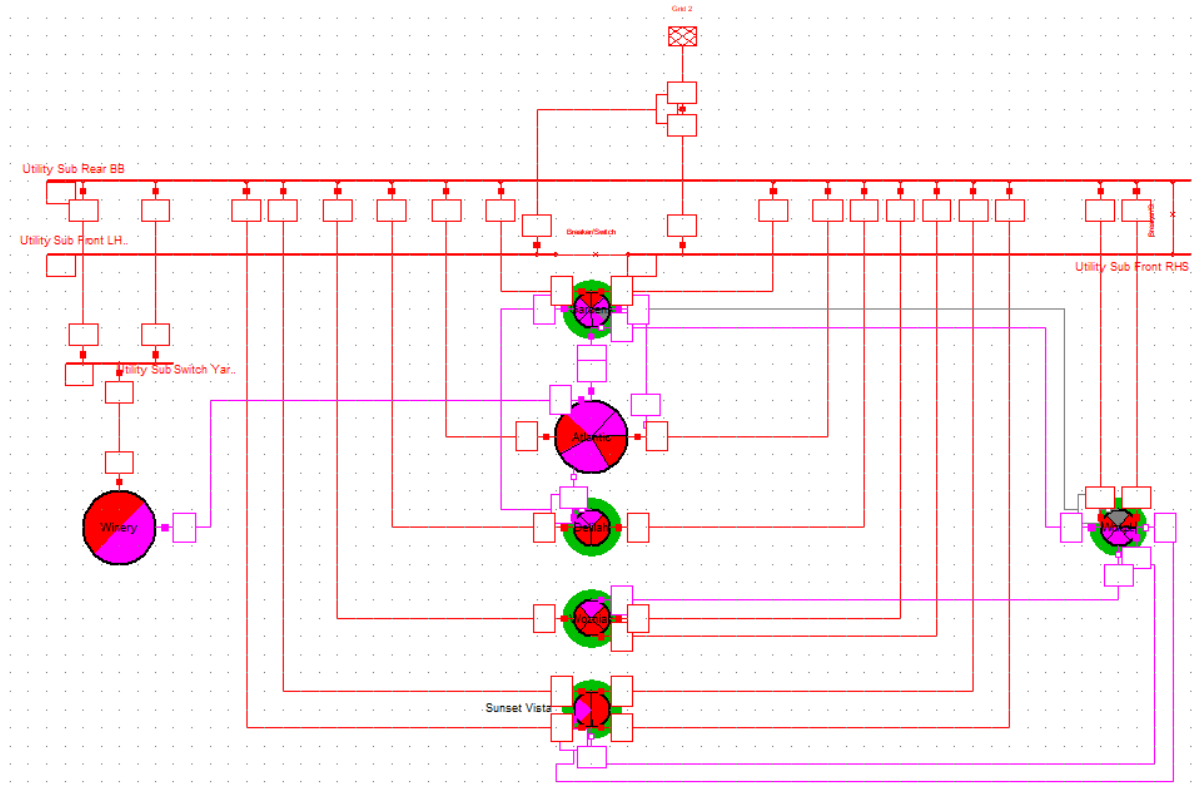


Figure 3.3: The main substation layout of the municipal network

Single line diagrams of each main substation's MV network are shown in Appendix C.

Unprotected mini-substations fed from the main substations mostly occurred in the ring topology throughout this network. This was changed in the model to only include the two mini-substations on the two ends of the ring for simplicity and to reduce clutter. The lines connecting the mini-substations were then modelled as they occurred in the actual network, while ensuring that the different types and lengths of lines were individually modelled by connecting them to nodes in place of mini-substations, as DigSILENT PowerFactory distinguishes between substations and nodes. Nodes are seen as being a single point in the network while substations are modelled as buses. This group of nodes and lines would then be carefully combined by grouping them as a new, single line in the software. This freed up clutter and got rid of substations which would not affect the results, while still being able to place faults at these mini-substations by placing them along the amalgamated line, if desired.

Radial unprotected mini-substations were modelled similarly, by modelling the first and last substations along the radial feeder, with the lines between these stations modelled individually and grouped to create a single line between the substations.

3.2.4 Cable modelling for the case study

Multiple types of cables are used in the network being studied. Overhead lines in the area were replaced as the area grew in size and scope.

Different cable manufacturers provide slightly different cable specifications for the same types of cables, whether copper, aluminium, or grouped by core diameter. Thus, due to record not being kept of the manufacturers of each cable in the network, but rather the cable type, the study will assume that the specifications provided by the African Cables datasheets correspond to the real-world cable specifications.

The cable insulation type is also not kept in records within the municipality. However, it is known that most of the 11 kV cables in the area are of the 3-core PILC type. Thus, these insulation types were assumed for the corresponding voltage levels in this study.

The types of underground cable used through the 11 kV network is as shown in Table 3-2.

Table 3-2: The 11 kV cables used through the network [65] [66] [67] [68]

Cable Conductor Type	Cable Area (mm²)	Resistance (Ohms/km)	Reactance (Ohms/km)
Aluminium	50	0.641	0.115
Aluminium	95	0.32	0.102
Aluminium	120	0.253	0.098
Aluminium	150	0.206	0.095
Aluminium	185	0.164	0.092
Aluminium	300	0.1	0.86
Copper	16	1.15	0.105
Copper	25	0.727	0.11
Copper	35	0.524	0.105
Copper	50	0.387	0.101
Copper	70	0.268	0.082
Copper	95	0.193	0.077
Copper	185	0.0991	0.07
Copper	240	0.0754	0.068
Copper	300	0.0601	0.066
Copper	400 (single-core)	0.047	0.103

The data sheets for these cables can be found in Appendix D. All of the cable types tabulated above were modelled in DigSILENT PowerFactory as cable types, with specifications as found in Appendix D. Cables were modelled in the MATPOWER model as complete impedances by multiplying the cable specifications with the line length.

The only type of 33 kV cable used in the network is of the 300 mm² Aluminium, PILC, single-core type. These cables have a resistance of 0.1 Ω/km and a reactance of 0.095 Ω/km, respectively, and were modelled as such.

Specifications that were used as input in each cable type include the rated voltage, rated current in the ground and in the air, positive, negative, and zero sequence resistance, reactance, and capacitance. The maximum operational temperature for each cable was left at its default of 80°C, as this was deemed within specification by the manufacturer for these cables.

3.2.5 Transformer modelling for the case study

Transformers were modelled according to their manufacturer specifications. Transformer specifications were obtained through data capturing from transformer nameplates. These parameters were then used in the DIGSILENT PowerFactory transformer models for the transformers at each MS and as reactances in the MATPOWER model.

The transformer specifications for the network are as shown in Table 3-3.

Table 3-3: Transformer specifications for main substations in the network

Main Substation Transformer	Voltage Rating (primary/secondary)	Power Rating (MVA)	Vector Group	Percent Impedance (Neutral Tap)
Gardens 1	33 kV/11.66 kV	10	Dyn1	10.5%
Gardens 2	33 kV/11.66 kV	10	Dyn1	10.6%
Atlantic 1 & 2	33 kV/11.66 kV	20	Dyn11	22.4%
Wozniak 1	33 kV/11.66 kV	10	Dyn1	9.63%
Wozniak 2	33 kV/11.66 kV	10	Dyn1	10.05%
Wozniak 3	33 kV/11.66 kV	10	Dyn1	10.6%
Sunset Vista 1 & 2	33 kV/11.66 kV	20	Dyn11	11.2%
Sunset Vista 3	33 kV/11.66 kV	20	Dyn11	11.9%
Sunset Vista 4	33 kV/11.66 kV	20	Dyn11	11.1%
Workplace 1	33 kV/11.66 kV	20	Dyn1	12.32%
Workplace 2	33 kV/11.66 kV	20	Dyn1	12.75%
Delilah 1	33 kV/11.66 kV	10	Dyn1	10.2%
Delilah 2	33 kV/11.66 kV	10	Dyn1	10.04%
Winery 1	33 kV/11.66 kV	10.2	Dyn1	10.4%

The zero sequence impedances of these transformers are not specified and were thus left at zero in the model. This is justified by the delta primary windings found in these transformers, which prevents zero-sequence current passing through the transformer during an earth fault, eliminating the zero-sequence contribution from the primary winding. This is shown in [69].

i. Tap Changer Modelling

Due to the fact that this research focusses mainly on the 11 kV side of the network and the grading therein, it was decided to model the tap changer, as voltage drops on the 33 kV network would affect the fault levels and overcurrent and earth fault grading on the 11 kV network. DIGSILENT PowerFactory, however, does not use a specific model for tap changers, and instead builds them in as part of the transformer element. Thus, all tap changers were set up as automatic tap changers controlling the HV transformer voltage with an operating band of 1.3% and a controller time constant of 0.5 seconds, as the tap changers are set up through the network. The network tap changer settings are shown in Table 3-4.

These settings were chosen to ensure that the tap changer models operate as they do on-site.

Table 3-4: Transformer tap changer settings for all transformers in the network

Tap Changer Setting Description	Setting
Controlled Node (voltage tracking)	HV Side
Control Mode	Voltage
Setpoint	Local
Voltage Setpoint	1 p.u.
Lower Bound	0.987 p.u.
Upper Bound	1.013 p.u.
Controller Time Constant	0.5 seconds

ii. NER Modelling

Each MS in this network also has separate neutral earthing resistors (NERs) installed for each of the transformers in order to mitigate and limit high levels of earth fault current. The NER data for each station is as shown in Table 3-5.

Table 3-5: NER specifications at each of the main substations in the network

MS and Transformer	Voltage Rating (kV)	Current Rating (A)	Resistance (Ohms)
Gardens MS Transformer 1	6.358	800	6.1
Gardens MS Transformer 2	6.358	800	6.2
Atlantic MS Transformer 1 and 2	6.358	800	6.2
Delilah MS Transformer 1	6.358	800	6.2
Delilah MS Transformer 2	6.358	800	6.1
Wozniak MS Transformer 1 and 2	6.358	800	6.2
Wozniak MS Transformer 3	6.358	800	6.1
Sunset Vista MS Transformer 1, 2, and 3	6.650	800	6.31
Sunset Vista MS Transformer 4	6.650	500	13.3
Workplace MS Transformer 1 and 2	6.650	1.000	6.65
Winery MS Transformer 1	6.358	800	6.1

NERs were modelled according to their specifications as shown in Table 3-5, and connected to the disconnected transformer neutrals on the 11 kV sides at each MS. The NER was added to the model by adding the NER resistance value to the transformer model as a zero-sequence resistance.

3.2.6 Load modelling for the case study

Loads were modelled as general load types in the network. However, it is not possible to model each individual load in the network for the purposes of this study due to SCADA data only being recorded at the main substations in the area, and not being recorded with corresponding phasor angles. For this reason, it was decided to reduce the network as lumped loads, as seen in [70]. Thus, for system and fault level accuracy, loads were modelled as general loads out of the main substations from which they are fed, at the furthest point in a feeder ring or group. The power factor of the loads were modelled according to the type of area which a given station feeds. Unity power factor was used for residential loads, while an inductive power factor of 0.9 was used for industrial loads, as these values are seen to be the average power factor for the different types of

loads throughout the rest of the municipal network. The load for the Atlantic main substation and feeders are shown in Table 3-6. Other main substation loads are shown in Appendix C. Zero-valued loads are a result of normally-open points.

Table 3-6: Feeder load specifications at the Atlantic main substation

Feeder	Voltage Rating (kV)	Load (A)	Power Factor
Parcel	11.66	16.9414	1
Queen	11.66	5.8152	1
Forest	11.66	14.0293	1
Squad	11.66	16.8951	1
Ares	11.66	13.2642	1
Hula	11.66	11.2161	1
Youth	11.66	4.4725	1
Poles	11.66	14.9145	1
Yellow	11.66	65.1219	1
Spring	11.66	8.1068	1
Royalty	11.66	0	1
Bushes	11.66	6.0989	1
Delilah	11.66	0	1
Gym	11.66	48.3987	1
Twenty	11.66	11.2725	1

3.2.7 Protection system modelling for the case study

The effect of the wind farm on the network protection grading was also studied in this research. As such, the overcurrent and earth-fault protection relay settings were added to the model. These protection settings and current transformer information are detailed in Appendix E.

In the DiGSILENT PowerFactory model, the current transformers were modelled as current transformer types, of different ratios, classes, and burdens as specified in Appendix E. The relays were modelled as generic IDMT relay types, which allowed a selection of the standard IEC IDMT curves, pickup current, and time multiplier to be set as inputs. Separate relays were modelled for overcurrent and earth-fault functionality.

3.3 Generation farm specifications

The proposed generation farm will consist of multiple components to allow it to generate and link onto the existing municipal grid. These components and their specifications, as given by the IPP, are described below.

3.3.1 Wind generator specifications

The wind generators to be used in the proposed project have not been specifically identified as yet, as the exact turbines have not been installed or ordered. However, the IPP has provided the design specifications that the turbines will have to meet, and the fact that they will be fed to the grid through an inverter conversion system. The turbine specifications are shown in Table 3-7 below.

Table 3-7: The wind generator specifications given by the IPP

Turbine Height:	120m
Blade Length:	60m per blade
Shaft Dimensions:	Tapering tubular steel towers being 6m at the base
Turbine Foundation Dimensions:	An octagonal foundation shall be used. The diameter shall be 20m. The height shall be 1.2m at the edge and 3m at the centre.
Generation Capacity:	2 MW – 4 MW per unit

Because the specifications given are not exact, for the purposes of protection studies, the worst possible case has to be assumed. Since the farm will consist of 18 generation units, the worst case scenario would occur when all 18 units are 4 MW in capacity, resulting in a maximum total generation capacity of 72 MW for the farm.

3.3.2 Wind farm modelling

The wind turbines will form the generation basis of the farm, generating a peak of 72 MW of power. This will be fed through an inverter system when implemented. Since the DigSILENT PowerFactory package was used for network modelling, the generic static wind turbine object included in the PowerFactory library was used for the study, changing parameters as they need to be changed, while leaving the rest at their default settings. This was chosen due to the object including the inverter system in its parameters. The object was connected directly to the network so that a worst-case fault contribution can be seen for the protection analysis. The wind turbines were modelled as generators in the MATPOWER model during the execution of the optimisation algorithms. The following settings and assumptions were changed in the models for both the IEEE 14-bus network and the case study.

- The generic static generator was set to the “Wind Generator” category.
- The wind turbines were modelled collectively as a single 72 MW wind turbine fed through an inverter system set to operate at 0.8 power factor lagging. This was done only for the proposed IPP implementation for the case study network, and not for the optimisation cases. The power factor was selected on the basis of the inverter system absorbing VArS from the network in the evening when the network is lightly loaded. This has been apparent in predominantly cable networks where overvoltage problems may exist during minimum load conditions. A setting of 0.85 was also seen to produce excellent results for large networks, as seen in [52].
- Wind turbine specifications for the optimisation cases were modelled depending on the sizing and power factor results obtained from the respective optimisation algorithms.
- The inverters that will be used in the project were also not yet specified. Thus, for the purposes of this research, the fault contribution for these wind turbines were set to a maximum of 120% of the generation capacity of the turbine, as found in [25].
- The R/X ratio of the wind turbine determines the ratio of real and reactive fault current components under a fault condition. This value was set to 1.614, so that the fault components from the wind turbine would be at a 0.8 lagging power factor.

3.4 Optimisation modelling

3.4.1 Optimisation criteria

In order to determine whether the wind turbine system is placed in the optimal position from an electrical standpoint, the optimal place needs to be defined by a set of criteria.

The optimal placement of the turbines was defined as the point at which power losses are reduced to its lowest value possible, while simultaneously improving the voltage profile towards the nominal voltage for the purposes of this research.

3.4.2 Algorithm modelling

The MATLAB software package and MATPOWER extension library were used for optimisation.

It was decided to perform the optimisation using two algorithms, namely the Probability-Based Incremental Learning (PBIL) and Differential Evolution (DE) algorithms. These algorithms were chosen due to their superior performance in terms of fast convergence and robust solutions over genetic algorithms, their ease of implementation, and their lack of comparison in other works, regarding the optimisation of placement and sizing of distributed generators.

i. Probability-Based Incremental Learning (PBIL) algorithm modelling

First, optimisation was done using the PBIL algorithm.

The traditional PBIL algorithm was used for this study and no modifications were made to the algorithm. Probability vectors were created for each individual generator that would be added to a given network for both the IEEE 14-bus system and the case study network. Seven bits were used to represent a given generator at a given bus, so that the limitation of a total of 72 MW of additional generation is observed. Thus, the probability vectors were set to contain seven elements, each starting at a probability value of 0.5 to give the creation of either a 1 or a 0 an equal likelihood. The same was done for probability vectors for the optimisation of the power factor. Probability vectors were programmed to be modified independently.

The learning factor was set to 0.1 and the forgetting factor was set to 0.05. This was done in order to allow the algorithm to deviate from the first generation solutions while also ensuring that the algorithm does not get stuck at any local maxima.

The algorithm was programmed as shown in Figure 3.4. The MATLAB code implementing the PBIL algorithm is shown in Appendix F. The algorithm was programmed and run 10 times, using a population of 50 solutions in each of the 100 generations over which the algorithm was run. These 10 results were compared.

The best result was then placed in the DlgSILENT PowerFactory simulation, and power flows and fault studies were conducted. The results in terms of bus voltages, power flows, and power line losses were recorded to compare them at a later stage. Faults were then simulated at the points discussed in section 3.5 and recorded to compare at a later stage.

i. Differential Evolution (DE) algorithm modelling

Optimisation was also done by means of the DE algorithm.

The rand-to-best operator was used in order to ensure that the best trial solutions are used as the generations progress, while also ensuring an element of randomness is kept in the solutions. This operator in the DE algorithm uses three user-defined variables to determine its performance.

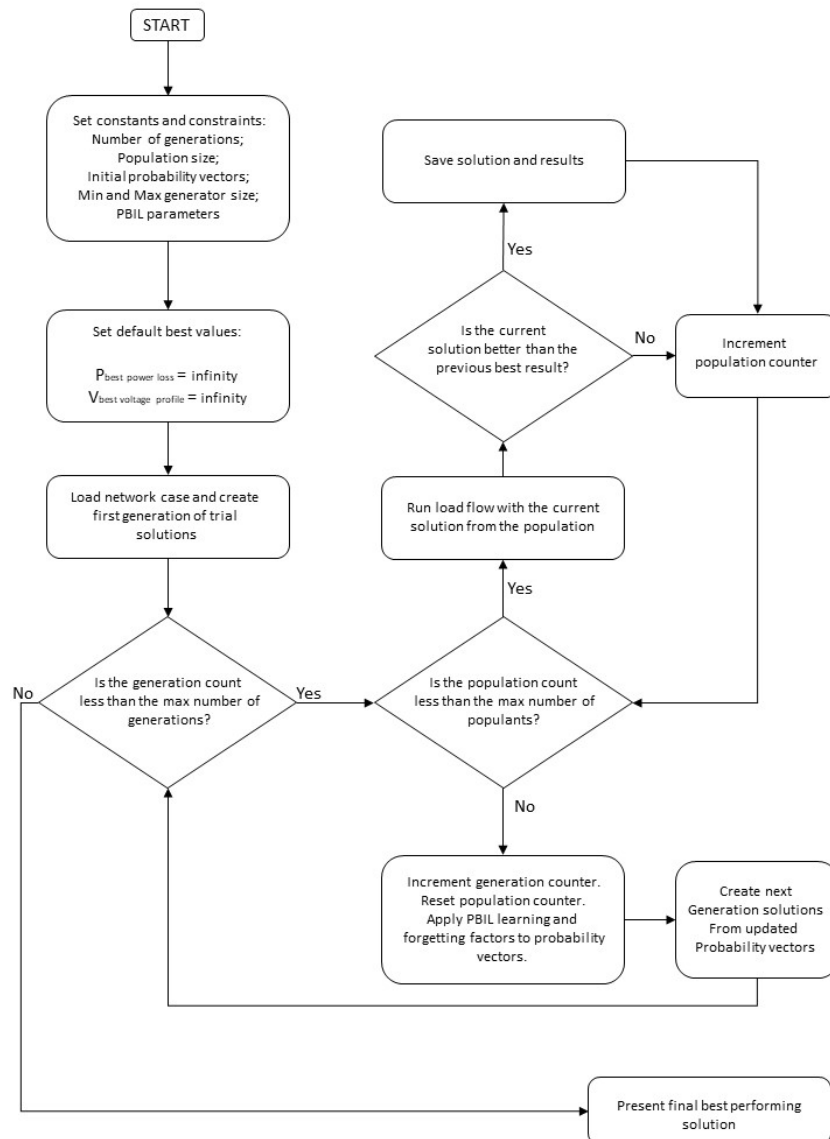


Figure 3.4: Flow chart of the PBIL optimisation algorithm used for the study

The mutation co-efficient, F , was set to 0.5 for this study, allowing the mutation process to have an impact on the population without the impact being too minute or large. The scaling factor, γ_W , was also set to 0.5 for this same reason. The crossover co-efficient was set to 0.5 to allow an equal probability for the creation of a 1 or 0 in the probability matrix.

The algorithm was programmed as shown in Figure 3.5.

The MATLAB code implementing the DE algorithm shown in Figure 3.5 is shown in Appendix F. The algorithm was also run 10 times, using the same population and generation sizes as in the PBIL algorithm. The results were then compared.

The best result was then placed in the DiGSILENT PowerFactory simulation, and power flows and fault studies were conducted. Network power flow and protection grading results were recorded as done for the PBIL algorithm results.

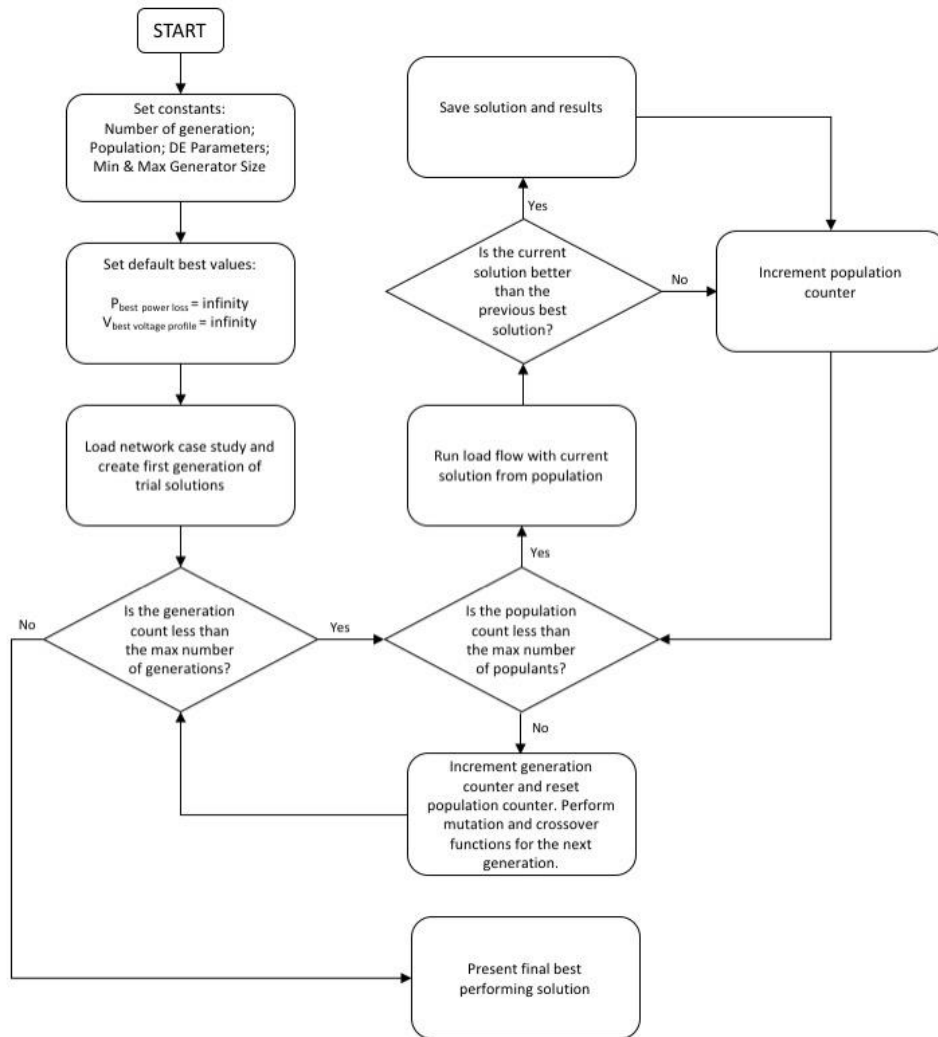


Figure 3.5: Flow chart of the DE optimisation algorithm used for the study

3.5 Selecting the fault positions for the study

In order for a thorough study to be done in terms of the protection grading in the network, the positions of the faults to be simulated in the network were chosen to include different voltage levels, different network topologies, and different line distances from the source.

For the modified IEEE 14-bus network, it was decided to simulate at least one fault in each feeder group. The faults were thus simulated at the following busbars in the modified IEEE 14-bus network.

- Bus 4
- Bus 10
- Bus 11
- Bus 13

For the case study, in addition to the above criteria, it was also decided to simulate at least one fault within the feeder groups of each MS in the study. The faults were thus simulated at the following busbars in the case study network.

- The 33 kV Utility substation rear busbar
- The Bushes substation fed from the Atlantic MS

- The Addition substation fed from the Gardens MS
- The Tortoise substation fed from the Delilah MS
- The Winelands RMU 1 substation fed from the Wozniak MS
- The Steve substation fed from the Sunset Vista MS
- The Mine substation fed from the Sunset Vista MS
- The Short substation fed from the Workplace MS
- The Paste RMU1 substation fed from the Winery MS

3.6 Detailed case studies

The cases that were considered in this research are detailed below. Optimisation algorithms were programmed so that the voltage constraints detailed in the grid code and the NRS 048 standard, as discussed in Chapter 2 of this dissertation, were adhered to at all times.

For the IEEE 14-bus test network, three cases were defined as detailed below.

- **Network simulator verification:** This case is used for verifying the correctness of the modelling methodology in both DIgSILENT PowerFactory and MATPOWER. The standard IEEE 14-bus test network was modelled in DIgSILENT PowerFactory and MATPOWER. Load flows were run using both of these simulation tools and the results were recorded for comparison to the results obtained from the standard, built-in IEEE 14-bus example system model found in the DIgSILENT PowerFactory simulation package. The network was then modified as specified in the preceding sections for the case studies detailed below.
- **Case 1:** This is the base case for the IEEE 14-bus test network, without any distributed generation added to the network. Load flows and three-phase faults were run and load flow and protection results were recorded.
- **Case 2:** This case investigates the use of the PBIL algorithm to find the optimal sizing for placing distributed generation sources at each of the busbars in the network, as placement at multiple points in the network is seen to improve power losses rather than placement at a single point in [56]. The results from the algorithm were recorded and added to the model, where load flow and protection grading results were recorded for comparison to Case 1. The wind turbines were set to trip in 400 ms on definite-time protection for 110% of their nominal generation rating. This was done so that the turbines would not trip for voltage dips at 300 ms, as described in the NRS 048, while also allowing secondary circuit relays to be able to trip first for faults on these feeders. The 110% pickup level was decided due to the turbines generally operating at 100% of their capacity when simulated in the previous cases, and due to their maximum fault contribution being set to 120% of their nominal capacity. The PBIL algorithm was allowed to optimise the power factor of the individual distributed generators. They were allowed to range between 0.8 and 1 so that the power losses and voltage profile of the network is optimised. The power factor was always set to lag if not set to unity, so that VARs may be absorbed during lightly-loaded conditions.
- **Case 3:** This case investigates the use of the DE algorithm to find the optimal sizing for placing distributed generation sources at each of the busbars in the network, as in Case 2. Settings and constraints used for protection relays and wind turbines were done as in Case 2, with the sizing of the distributed generation and their power factors changing to be in line with the results produced by the DE algorithm.

For the case study, it was necessary to research the IPP proposed implementation in addition to the optimal placement and sizing results produced by the probability-based incremental learning and differential evolution algorithms. Thus, the following cases were researched for the case study network.

- **Case 1:** This is the base case for the network. This case details the network conditions without any distributed generation added in terms of load flow results and protection grading.
- **Case 2:** This is the case where the wind farm is added to the network at the Utility substation, as the IPP has proposed. The power factor for the turbine in this case was set to 0.8 lagging, so that the inverter and turbine system is capable of absorbing network VArS during lightly-loaded conditions. The load flow results and protection grading results for this case were also recorded for comparison to Case 1 above. The protection settings for the Wind Turbine were set to pick up at 110% of its capacity as the inverter would operate under normal conditions at 100%, while allowing for discrimination, and set to trip as fast as possible. These settings are detailed in Appendix E.
- **Case 3:** This case investigates the use of the PBIL algorithm to find the optimal sizing for placing distributed generation sources at each of the switching stations and main substation busbars in the network. The results from the algorithm were recorded and added to the model, where load flow and protection grading results were recorded. The protection settings were done as outlined in the IEEE 14-bus system case above, based on the NRS 048 voltage restriction. The power factor of the individual distributed generators were also set to be optimised by the algorithm, set to range between 0.8 and 1 so that the power losses and voltage profile of the network are optimised.
- **Case 4:** This case investigates the use of the DE algorithm to find the optimal sizing for placing distributed generation sources at each of the switching stations and main substation busbars in the network. Settings used for protection relays and wind turbines were done as in Case 3, with the sizing of the distributed generators and their power factors changing to be in line with the results produced by the differential evolution algorithm.

4. Test System Results and Discussion

This section details the results obtained from the methodology of the test system network study outlined in Chapter 3.

4.1 Network simulator verification

The IEEE 14-bus network with network data as given in Chapter 3 was modelled in order to verify the method of modelling and validity of the simulation tools used in the study. The results for the load flow done for the DigSILENT PowerFactory example system (Case A), DigSILENT PowerFactory modelled system (Case B), and the MATPOWER system (Case C) are shown in Tables 4-1 and 4-2.

Table 4-1: The network overview results for the network simulator verification case

<i>Case</i>	<i>Active Power Generation (MW)</i>	<i>Reactive Power Generation (MVar)</i>	<i>Active Load (MW)</i>	<i>Reactive Load (MVar)</i>	<i>Active Power Losses (MW)</i>	<i>Reactive Power Losses (MVar)</i>
Case A	272.386	78.497	258.999	73.499	13.386	54.498
Case B	272.386	78.497	258.999	73.499	13.386	54.498
Case C	272.390	79.570	259.000	73.500	13.385	54.480

Table 4-2: The bus results for the 33 kV network for the network simulator verification case

<i>Busbar</i>	<i>3-phase Voltage Magnitude (pu) – Case A</i>	<i>3-phase Voltage Angle (°) – Case A</i>	<i>3-phase Voltage Magnitude (pu) – Case B</i>	<i>3-phase Voltage Angle (°) – Case B</i>	<i>3-phase Voltage Magnitude (pu) – Case C</i>	<i>3-phase Voltage Angle (°) – Case C</i>
Bus 1	1.060	0.000	1.060	0.000	1.060	0.000
Bus 2	1.045	-4.981	1.045	-4.981	1.045	-4.982
Bus 3	1.010	-12.718	1.010	-12.718	1.010	-12.723
Bus 4	1.019	-10.324	1.019	-10.324	1.018	-10.321
Bus 5	1.020	-8.783	1.020	-8.783	1.020	-8.776
Bus 6	1.070	-14.223	1.070	-14.222	1.070	-14.197
Bus 7	1.062	-13.368	1.062	-13.368	1.063	-13.374
Bus 8	1.090	-13.368	1.090	-13.368	1.090	-13.374
Bus 9	1.056	-14.947	1.056	-14.947	1.059	-14.953
Bus 10	1.051	-15.104	1.051	-15.104	1.053	-15.106
Bus 11	1.057	-14.795	1.057	-14.795	1.058	-14.785
Bus 12	1.055	-15.077	1.055	-15.077	1.055	-15.052
Bus 13	1.050	-15.159	1.050	-15.159	1.051	-15.138
Bus 14	1.036	-16.039	1.036	-16.039	1.037	-16.031

The simulators and network construction methodology can thus be verified as being correct.

4.2 Modified IEEE 14-bus system: Case 1 – Base case

4.2.1 Load flow results

Upon running the load flow for the modified IEEE 14-bus system for Case 1, the overview results shown in Table 4-3 and Figure 4.1 were obtained. Detailed voltage profile tables for the three modified IEEE network cases are shown in Appendix G.

Table 4-3: The network overview results for the modified IEEE 14-bus system for Case 1

<i>Active Power Generation (MW)</i>	<i>Reactive Power Generation (MVar)</i>	<i>Active Load (MW)</i>	<i>Reactive Load (MVar)</i>	<i>Active Power Losses (MW)</i>	<i>Reactive Power Losses (MVar)</i>
272.814	85.802	259.000	73.500	13.813	57.989

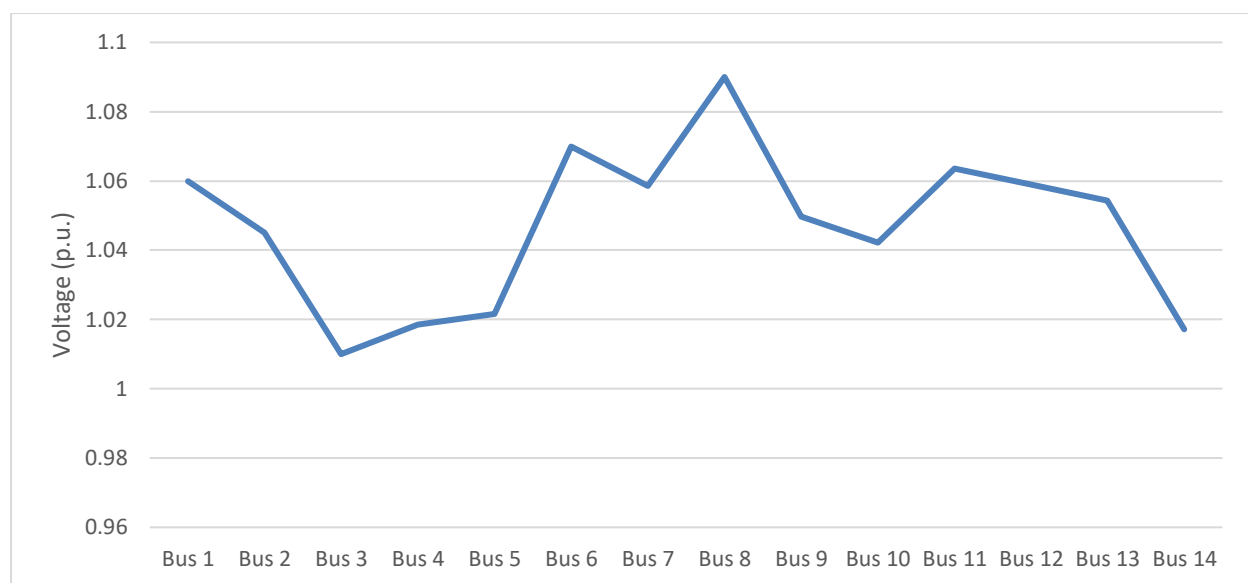


Figure 4.1: The voltage profile for the modified IEEE 14-bus system for Case 1

4.2.2 Protection grading results

Four faults were placed throughout the modified network for the purposes of studying the protection grading. The results for each of these faults are detailed below. IDMT curves for the modified IEEE network grading across the three cases is shown in Appendix H.

a) Protection grading results for Bus 4

For a fault at Bus 4, the fault consists of multiple stages. This is due to a change in the network configuration as different circuit breakers trip without the fault being isolated. This phenomena is seen in both the modified IEEE 14-bus network and in the municipal network cases. IDMT curves for the modified IEEE network grading across the three cases is shown in Appendix H.

The grading for a three-phase fault of 5.197 kA at Bus 4 is shown in Table 4-4.

Table 4-4: The branch currents and trip times for a three-phase fault at Bus 4 in the modified IEEE network for Case 1

<i>Subst.</i>	<i>Feeder</i>	<i>Voltage Level (kV)</i>	<i>Stage 1 Fault Level Mag. Contribution (kA)</i>	<i>Stage 1 OCEF relay calc. trip time (s)</i>	<i>Stage 2 Fault Level Mag. Contribution (kA)</i>	<i>Stage 2 OCEF relay calc. trip time (s)</i>	<i>Stage 3 Fault Level Mag. Contribution (kA)</i>	<i>Stage 3 OCEF relay calc. trip time (s)</i>	<i>Stage 4 Fault Level Mag. Contribution (kA)</i>	<i>Stage 4 OCEF relay calc. trip time (s)</i>	<i>Overall Trip Time (s)</i>
Bus 4	Bus 2	132	1.595	0.783	1.958	0.696	0	N/A	0	N/A	0.740
Bus 5	Bus 4	132	2.723	0.394	0	N/A	0	N/A	0	N/A	0.394
Bus 5	Bus 1	132	1.037	0.801	0.208	N/A	0.140	N/A	0.140	N/A	N/A
Bus 5	Bus 2	132	0.963	0.890	0.158	N/A	0.047	N/A	0.047	N/A	N/A
Bus 4	Transf. 4 – 9 HV	132	0.226	1.535	0.228	1.518	0.231	1.491	0.502	0.768	1.323
Bus 9	Transf. 4 – 9 MV	33	0.875	1.294	0.883	1.283	0.896	1.266	1.946	0.735	1.215
Bus 4	Transf. 4 – 7 HV	132	0.717	1.136	0.725	1.127	0.735	1.115	0	N/A	1.126
Bus 6	Transf. 5 – 6 MV	33	3.006	0.730	0.579	N/A	0.603	N/A	0.603	N/A	N/A
Bus 5	Transf. 5 – 6 HV	132	0.806	0.990	0.155	N/A	0.162	N/A	0.162	N/A	N/A
Bus 1	Bus 2-1	132	0.542	1.116	0.511	1.289	0.190	N/A	0.190	N/A	N/A
Bus 1	Bus 2-2	132	0.542	1.116	0.511	1.289	0.190	N/A	0.190	N/A	N/A
Bus 2	Bus 3	132	0.494	2.142	0.434	10.671	0.412	N/A	0.412	N/A	N/A
Bus 1	G1	132	2.046	1.184	1.214	2.071	0.513	N/A	0.513	N/A	N/A
Bus 2	G2	132	1.412	1.545	0.969	1.921	0.183	N/A	0.183	N/A	N/A
Bus 3	G3	132	0.530	3.127	0.362	5.170	0.131	N/A	0.131	N/A	N/A
Bus 6	G6	33	3.207	1.610	0.610	2.700	0.065	N/A	0.065	N/A	N/A
Bus 8	G8	1	11.182	2.011	11.305	1.976	11.448	1.938	6.391	19.946	9.699

b) Protection grading results for Bus 10

The grading for a three-phase fault of 6.083 kA at Bus 10 is shown in Table 4-5.

Table 4-5: The branch currents and trip times for a three-phase fault at Bus 10 in the modified IEEE network for Case 1

<i>Substation</i>	<i>Feeder</i>	<i>Voltage Level (kV)</i>	<i>Fault Level Magnitude Contribution (kA)</i>	<i>OCEF relay calculated trip time (s)</i>
Bus 9	Bus 10	33	6.083	0.340
Bus 9	Transformer 9 – 7 MV	33	4.500	0.688
Bus 9	Transformer 9 – 4 MV	33	1.677	0.800
Bus 4	Transformer 9 – 4 HV	132	0.433	0.848
Bus 4	Transformer 7 – 4 HV	132	0.526	1.504
Bus 7	Transformer 7 – 8 LV	11	7.615	4.102
Bus 6	Transformer 5 – 6 MV	33	0.821	N/A
Bus 6	Transformer 5 – 6 HV	132	0.220	14.459
Bus 4	Bus 5	132	0.595	1.934
Bus 4	Bus 2	132	0.386	5.247
Bus 1	G1	132	0.964	3.085
Bus 2	G2	132	0.478	3.504
Bus 3	G3	132	0.220	32.285
Bus 6	G6	33	0.798	2.343
Bus 8	G8	11	7.615	5.274

c) Protection grading results for Bus 11

The grading for a three-phase fault of 5.542 kA at Bus 11 is shown in Table 4-6.

Table 4-6: The branch currents and trip times for a three-phase fault at Bus 11 in the modified IEEE network for Case 1

Substation	Feeder	Voltage Level (kV)	Fault Level Contribution (kA)	Magnitude	OCEF relay calculated trip time (s)
Bus 6	Bus 11	33	5.542		0.396
Bus 6	Transformer 5 – 6 MV	33	2.275		0.928
Bus 6	Transformer 5 – 6 HV	132	0.610		1.241
Bus 1	G1	132	0.988		2.933
Bus 2	G2	132	0.384		4.693
Bus 6	G6	33	3.621		1.610

d) Protection grading results for Bus 13

The grading for a three-phase fault of 7.122 kA at Bus 13 is shown in Table 4-7.

Table 4-7: The branch currents and trip times for a three-phase fault at Bus 13 in the modified IEEE network for Case 1

Substation	Feeder	Voltage Level (kV)	Fault Level Contribution (kA)	Magnitude	OCEF relay calculated trip time (s)
Bus 6	Bus 11	33	7.122		0.401
Bus 6	Transformer 5 – 6 MV	33	2.772		0.779
Bus 6	Transformer 5 – 6 HV	132	0.744		1.052
Bus 1	G1	132	0.996		2.886
Bus 2	G2	132	0.418		4.145
Bus 6	G6	33	4.582		1.610

4.3 Modified IEEE 14-bus system: Case 2 – PBIL optimisation

4.3.1 Optimisation results

The optimisation results obtained from running the PBIL algorithm on the modified IEEE 14-bus system is shown in Table 4-8. The solution converged in the 100th generation.

Table 4-8: The optimal DG placement results and protection settings for the modified 14-bus IEEE system for Case 2

Turbine Location	Turbine Apparent Power Generation (MVA)	Turbine Real Generation (MW)	Turbine Reactive Generation (MVar)	Power Factor	Definite Time Current Pickup (A)	Definite Trip Time (s)
Bus 1	1.654	1.654	0	1.00	7.968	0.400
Bus 2	2.960	2.368	1.776	0.80	14.259	0.400
Bus 3	11.057	11.057	0	1.00	53.260	0.400
Bus 4	7.574	6.060	4.545	0.80	36.485	0.400
Bus 5	2.612	2.090	1.567	0.80	12.581	0.400
Bus 6	10.186	10.186	0	1.00	196.266	0.400
Bus 7	0.697	0.557	0.418	0.80	442.861	0.400
Bus 8	7.400	7.400	0	1.00	427.757	0.400
Bus 9	5.050	4.444	2.398	0.88	97.294	0.400
Bus 10	5.398	4.318	3.239	0.80	104.005	0.400
Bus 11	8.271	7.609	3.242	0.92	159.362	0.400
Bus 12	2.177	1.741	1.306	0.80	41.936	0.400
Bus 13	4.266	3.925	1.672	0.92	82.196	0.400
Bus 14	2.698	2.159	1.619	0.80	52.001	0.400

4.3.2 Load flow results

Upon running the load flow using MATPOWER for the modified IEEE 14-bus system for Case 2, the network overview results shown in Tables 4-9, 4-10, and Figure 4.2 were obtained.

Table 4-9: The MATPOWER network overview results for the modified IEEE 14-bus system for Case 2

<i>Grid Active Power Generation (MW)</i>	<i>Grid Reactive Power Generation (MVar)</i>	<i>Turbine Active Power Generation (MW)</i>	<i>Turbine Reactive Power Generation (MVar)</i>	<i>Active Load (MW)</i>	<i>Reactive Load (MVar)</i>	<i>Active Power Losses (MW)</i>	<i>Reactive Power Losses (MVar)</i>
202.159	47.115	65.568	21.781	259.000	73.500	8.727	35.704

Table 4-10: The DigSILENT PowerFactory network overview results for the modified IEEE 14-bus system for Case 2

<i>Grid Active Power Generation (MW)</i>	<i>Grid Reactive Power Generation (MVar)</i>	<i>Turbine Active Power Generation (MW)</i>	<i>Turbine Reactive Power Generation (MVar)</i>	<i>Active Load (MW)</i>	<i>Reactive Load (MVar)</i>	<i>Active Power Losses (MW)</i>	<i>Reactive Power Losses (MVar)</i>
202.328	47.115	65.569	21.781	259.000	73.500	8.896	36.406

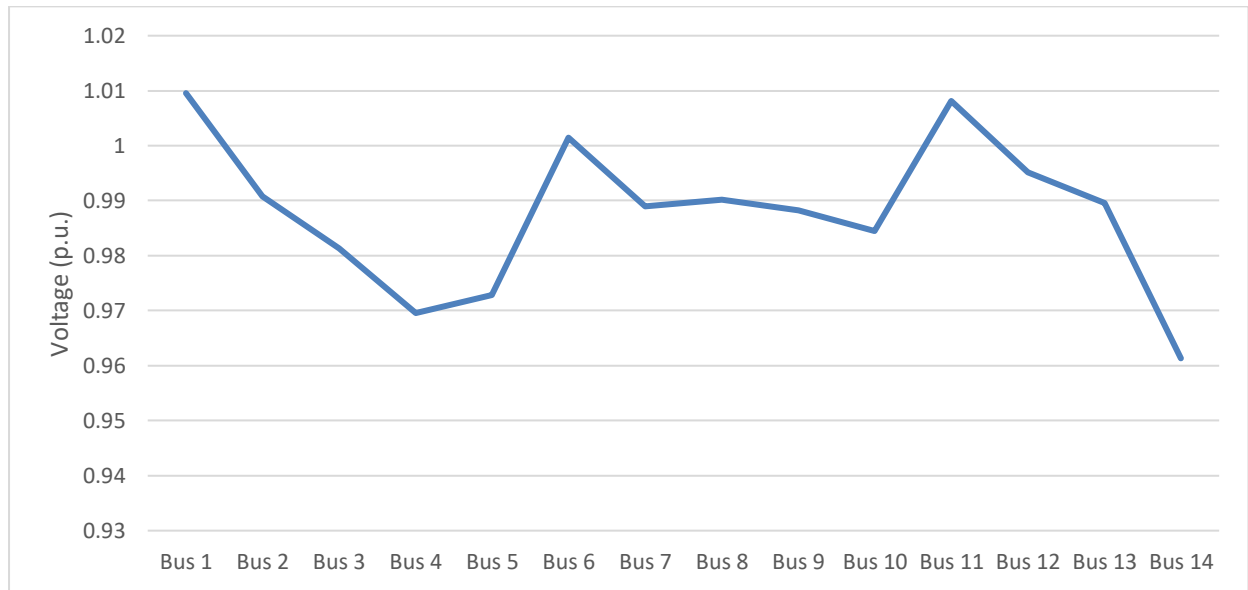


Figure 4.2: The voltage profile for the modified IEEE 14-bus system for Case 2

4.3.3 Protection grading results

As detailed in Chapter 3 of this dissertation, four faults were placed throughout the network for the purposes of studying the protection grading. The results for each of these four fault positions are detailed below.

a) Protection grading results for Bus 4

The grading for a three-phase fault of 4.980 kA at Bus 4 is shown in Table 4-11.

Table 4-11: The branch currents and trip times for a three-phase fault at Bus 4 in the modified IEEE network for Case 2

Subst.	Feeder	Volt. Level (kV)	Stage 1 Fault Level Mag. Contr (kA)	Stage 1 OCEF relay calc. trip time (s)	Stage 2 Fault Level Mag. Contr (kA)	Stage 2 OCEF relay calc. trip time (s)	Stage 3 Fault Level Mag. Contr (kA)	Stage 3 OCEF relay calc. trip time (s)	Stage 4 Fault Level Mag. Contr (kA)	Stage 4 OCEF relay calc. trip time (s)	Stage 5 Fault Level Mag. Contr (kA)	Stage 5 OCEF relay calc. trip time (s)	Overall Trip Time (s)
Bus 4	Bus 2	132	1.512	0.809	1.952	0.697	2.211	0.653	0	N/A	0	N/A	0.732
Bus 5	Bus 4	132	2.606	0.403	0	N/A	0	N/A	0	N/A	0	N/A	0.403
Bus 5	Bus 1	132	0.983	0.849	0.143	N/A	0.143	N/A	0.093	N/A	0.093	N/A	N/A
Bus 5	Bus 2	132	0.907	0.939	0.188	N/A	0.222	N/A	0.032	N/A	0.032	N/A	N/A
Bus 4	Transf. 4 - 9 HV	132	0.211	1.670	0.219	1.591	0.232	1.486	0.235	1.464	0.563	0.717	1.331
Bus 9	Transf. 4 - 9 MV	33	0.819	1.379	0.851	1.330	0.899	1.262	0.910	1.248	2.183	0.692	1.228
Bus 4	Transf. 4 - 7 HV	132	0.653	1.228	0.677	1.191	0.734	1.116	0.745	1.103	0	N/A	1.149
Bus 6	Transf. 5 - 6 MV	33	2.755	0.783	0.301	N/A	0.391	N/A	0.388	N/A	0.388	N/A	N/A
Bus 5	Transf. 5 - 6 HV	132	0.739	1.057	0.081	N/A	0.105	N/A	0.104	N/A	0.104	N/A	N/A
Bus 1	Bus 2-1	132	0.504	1.339	0.487	1.479	0.527	N/A	0.164	N/A	0.163	N/A	N/A
Bus 1	Bus 2-2	132	0.504	1.339	0.487	1.479	0.527	N/A	0.164	N/A	0.163	N/A	N/A
Bus 2	Bus 3	132	0.502	1.968	0.420	N/A	0.414	N/A	0.426	24.671	0.408	N/A	N/A
Bus 1	G1	132	1.933	1.242	1.095	2.428	1.173	2.179	0.401	N/A	0.401	N/A	N/A
Bus 2	G2	132	1.218	1.674	0.764	2.267	0.836	2.123	0.201	617.508	0.201	N/A	N/A
Bus 3	G3	132	0.553	2.999	0.398	4.443	0.408	4.294	0.198	N/A	0.188	N/A	N/A
Bus 6	G6	132	2.795	1.610	0.443	3.288	0.523	2.953	0.116	32.912	0.116	32.912	21.758
Bus 8	G8	132	9.677	2.623	10.036	2.437	11.288	1.981	11.461	1.934	6.570	13.871	7.617
Bus 4	Wind G4	132	0.040	0.420	0.040	0.420	0	N/A	0	N/A	0	N/A	0.420
Bus 5	Wind G5	132	0.013	0.420	0.011	N/A	0.010	N/A	0.013	0.420	0	N/A	1.569
Bus 7	Wind G7	1	0.459	0.420	0.455	0.420	0	N/A	0	N/A	0	N/A	0.420
Bus 9	Wind G9	33	0.102	0.420	0.101	0.420	0	N/A	0	N/A	0	N/A	0.420
Bus 10	Wind G10	33	0.109	0.420	0.108	0.420	0	N/A	0	N/A	0	N/A	0.420
Bus 14	Wind G14	33	0.055	0.420	0.054	0.420	0	N/A	0	N/A	0	N/A	0.420

b) Protection grading results for Bus 10

The grading for a three-phase fault of 5.810 kA at Bus 10 is shown in Table 4-12.

Table 4-12: The branch currents and trip times for a three-phase fault at Bus 10 in the modified IEEE network for Case 2

<i>Substation</i>	<i>Feeder</i>	<i>Voltage Level (kV)</i>	<i>Stage 1 Fault Level Magnitude Contribution (kA)</i>	<i>Stage 1 OCEF relay calculated trip time (s)</i>	<i>Stage 2 Fault Level Magnitude Contribution (kA)</i>	<i>Stage 2 OCEF relay calculated trip time (s)</i>	<i>Overall Trip Time (s)</i>
Bus 9	Bus 10	33	5.730	0.346	0	N/A	0.340
Bus 9	Transformer 9 – 7 MV	33	4.125	0.730	0	N/A	0.730
Bus 9	Transformer 9 – 4 MV	33	1.600	0.822	0	N/A	0.822
Bus 4	Transformer 9 – 4 HV	132	0.413	0.876	0	N/A	0.876
Bus 4	Transformer 7 – 4 HV	132	0.520	1.524	0	N/A	1.524
Bus 7	Transformer 7 – 8 LV	1	6.344	17.569	0	N/A	17.569
Bus 4	Bus 5	132	0.567	2.195	0	N/A	2.195
Bus 4	Bus 2	132	0.351	8.429	0	N/A	8.429
Bus 1	G1	132	0.774	5.764	0	N/A	5.764
Bus 2	G2	132	0.337	5.862	0	N/A	5.862
Bus 3	G3	132	0.260	11.632	0	N/A	11.632
Bus 6	G6	33	0.527	2.941	0	N/A	2.941
Bus 8	G8	1	6.278	27.807	0	N/A	27.807
Bus 9	Wind G9	33	0.101	0.420	0	N/A	N/A
Bus 10	Wind G10	33	0.113	0.420	0.171	0.420	0.420
Bus 14	Wind G14	33	0.054	0.420	0	N/A	N/A

c) Protection grading results for Bus 11

The grading for a three-phase fault of 5.317 kA at Bus 11 is shown in Table 4-13.

Table 4-13: The branch currents and trip times for a three-phase fault at Bus 11 in the modified IEEE network for Case 2

<i>Substation</i>	<i>Feeder</i>	<i>Voltage Level (kV)</i>	<i>Stage 1 Fault Level Magnitude Contribution (kA)</i>	<i>Stage 1 OCEF relay calculated trip time (s)</i>	<i>Stage 2 Fault Level Magnitude Contribution (kA)</i>	<i>Stage 2 OCEF relay calculated trip time (s)</i>	<i>Overall Trip Time (s)</i>
Bus 6	Bus 11	33	5.185	0.406	0	N/A	0.406
Bus 6	Transformer 5 – 6 MV	33	2.124	0.994	0	N/A	0.994
Bus 6	Transformer 5 – 6 HV	132	0.570	1.323	0	N/A	1.323
Bus 1	G1	132	0.769	5.892	0	N/A	5.892
Bus 2	G2	132	0.270	10.245	0	N/A	10.245
Bus 3	G3	132	0.220	31.695	0	N/A	31.695
Bus 6	G6	33	3.193	1.610	0	N/A	1.610
Bus 11	Wind G11	33	0.173	0.420	0.174	0.420	0.420

d) Protection grading results for Bus 13

The grading for a three-phase fault of 6.759 kA at Bus 13 is shown in Table 4-14.

Table 4-14: The branch currents and trip times for a three-phase fault at Bus 13 in the modified IEEE network for Case 2

<i>Substation</i>	<i>Feeder</i>	<i>Voltage Level (kV)</i>	<i>Stage 1 Fault Level Magnitude Contribution (kA)</i>	<i>Stage 1 OCEF relay calculated trip time (s)</i>	<i>Stage 2 Fault Level Magnitude Contribution (kA)</i>	<i>Stage 2 OCEF relay calculated trip time (s)</i>	<i>Overall Trip Time (s)</i>
Bus 6	Bus 13	33	6.692	0.411	0	N/A	0.411
Bus 6	Transformer 5 – 6 MV	33	2.590	0.824	0	N/A	0.824
Bus 6	Transformer 5 – 6 HV	132	0.695	1.110	0	N/A	1.110
Bus 1	G1	132	0.787	5.407	0	N/A	5.407
Bus 2	G2	132	0.295	7.890	0	N/A	7.890
Bus 3	G3	132	0.232	20.645	0	N/A	20.645
Bus 6	G6	33	5.058	1.610	0	N/A	1.610
Bus 6	Wind G6	33	0.197	0.420	0	N/A	N/A
Bus 13	Wind G13	33	0.090	0.420	0.090	0.420	0.420

4.4 Modified IEEE 14-bus system: Case 3 – DE optimisation

4.4.1 Optimisation results

The optimisation results obtained from running the DE algorithm on the modified network is shown in Table 4-15. The solution converged in the 2nd generation.

Table 4-15: The optimal DG placement results settings for the modified 14-bus IEEE system for Case 3

<i>Turbine Location</i>	<i>Turbine Apparent Power Generation (MVA)</i>	<i>Turbine Real Generation (MW)</i>	<i>Turbine Reactive Generation (MVA_r)</i>	<i>Power Factor</i>	<i>Definite Time Current Pickup (A)</i>	<i>Definite Trip Time (s)</i>
Bus 1	1.875	1.605	0.970	0.856	9.033	0.400
Bus 2	8.286	8.174	1.358	0.986	39.913	0.400
Bus 3	13.205	12.527	4.178	0.949	63.610	0.400
Bus 4	0.916	0.872	0.281	0.952	4.413	0.400
Bus 5	3.337	3.302	0.480	0.990	16.073	0.400
Bus 6	1.736	1.604	0.665	0.924	33.456	0.400
Bus 7	8.592	7.573	4.059	0.881	5463.245	0.400
Bus 8	4.677	3.918	2.555	0.838	270.374	0.400
Bus 9	2.629	2.572	0.546	0.978	50.661	0.400
Bus 10	11.861	9.991	6.393	0.842	228.542	0.400
Bus 11	1.220	1.082	0.564	0.887	23.510	0.400
Bus 12	2.163	1.824	1.162	0.843	41.670	0.400
Bus 13	6.879	6.004	3.358	0.873	132.548	0.400
Bus 14	4.622	4.584	0.592	0.992	89.057	0.400

4.4.2 Load flow results

Upon running the load flow using MATPOWER and DigSILENT PowerFactory for the network for Case 3, the results shown in Tables 4-16, 4-17, and Figure 4.3 were obtained.

Table 4-16: The MATPOWER network overview results for the modified 14-bus IEEE system for Case 3

<i>Grid Active Power Generation (MW)</i>	<i>Grid Reactive Power Generation (MVar)</i>	<i>Turbine Active Power Generation (MW)</i>	<i>Turbine Reactive Power Generation (MVar)</i>	<i>Active Load (MW)</i>	<i>Reactive Load (MVar)</i>	<i>Active Power Losses (MW)</i>	<i>Reactive Power Losses (MVar)</i>
201.992	41.438	67.632	27.161	259.000	73.500	8.623	35.485

Table 4-17: The DigSILENT PowerFactory network overview results for the modified 14-bus IEEE system for Case 3

<i>Grid Active Power Generation (MW)</i>	<i>Grid Reactive Power Generation (MVar)</i>	<i>Turbine Active Power Generation (MW)</i>	<i>Turbine Reactive Power Generation (MVar)</i>	<i>Active Load (MW)</i>	<i>Reactive Load (MVar)</i>	<i>Active Power Losses (MW)</i>	<i>Reactive Power Losses (MVar)</i>
201.470	41.683	66.302	27.161	259.000	73.500	8.772	36.121

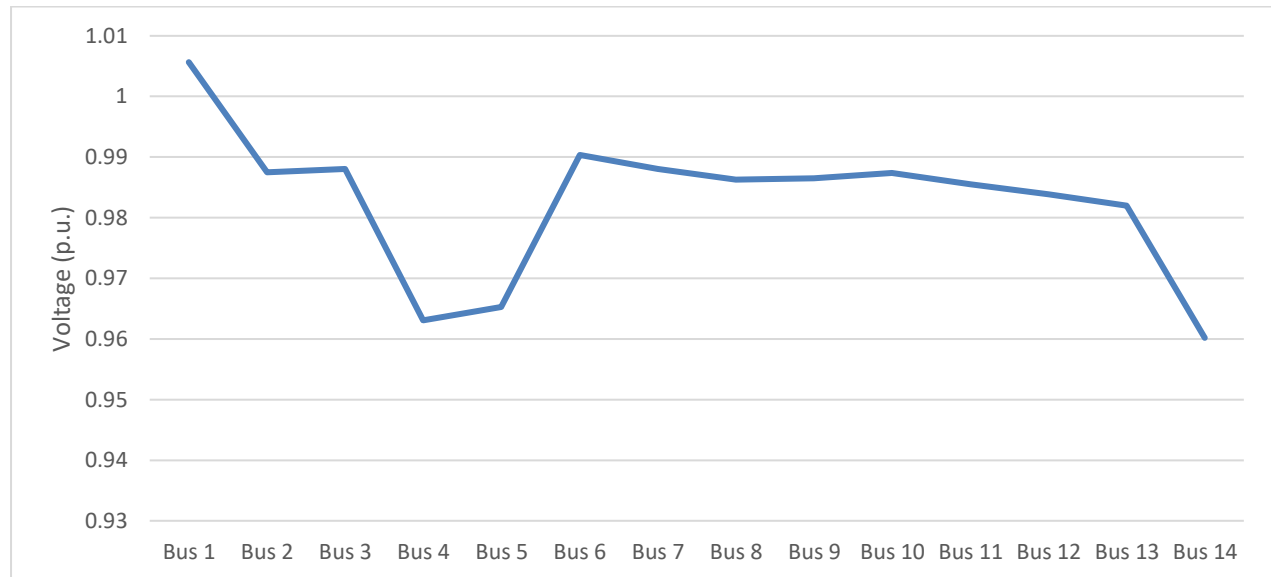


Figure 4.3: The voltage profile for the modified 14-bus IEEE system for Case 3

4.4.3 Protection grading results

Faults were simulated at the same positions as in previous cases. The protection grading results are detailed below.

a) Protection grading results for Bus 4

The grading for a three-phase fault of 4.957 kA at Bus 4 is shown in Table 4-18.

Table 4-18: The branch currents and trip times for a three-phase fault at Bus 4 in the modified IEEE network for Case 3

Substation	Feeder	Voltage Level (kV)	Stage 1 Fault Level Magnitude Contribution (kA)	Stage 1 OCEF relay calculated trip time (s)	Stage 2 Fault Level Magnitude Contribution (kA)	Stage 2 OCEF relay calculated trip time (s)	Stage 3 Fault Level Magnitude Contribution (kA)	Stage 3 OCEF relay calculated trip time (s)	Stage 4 Fault Level Magnitude Contribution (kA)	Stage 4 OCEF relay calculated trip time (s)	Stage 5 Fault Level Magnitude Contribution (kA)	Stage 5 OCEF relay calculated trip time (s)	Stage 6 Fault Level Magnitude Contribution (kA)	Stage 6 OCEF relay calculated trip time (s)	Overall Trip Time (s)
Bus 4	Bus 2	132	1.511	0.810	1.923	0.703	2.239	0.648	0	N/A	0	N/A	0	N/A	0.730
Bus 5	Bus 4	132	2.580	0.405	0	N/A	0	N/A	0	N/A	0	N/A	0	N/A	0.405
Bus 5	Bus 1	132	0.985	0.847	0.164	N/A	0.161	N/A	0.119	N/A	0.119	N/A	0.126	N/A	N/A
Bus 5	Bus 2	132	0.912	0.934	0.168	N/A	0.211	N/A	0.052	N/A	0.052	N/A	0.057	N/A	N/A
Bus 4	Transformer 4 – 9 HV	132	0.218	1.601	0.224	1.546	0.232	1.482	0.288	1.178	0.664	0.653	0.664	0.653	1.298
Bus 9	Transformer 4 – 9 MV	33	0.846	1.336	0.870	1.301	0.901	1.259	1.117	1.051	2.575	0.637	2.575	0.637	1.151
Bus 4	Transformer 4 – 7 HV	132	0.665	1.208	0.684	1.181	0.735	1.114	0.907	0.959	0	N/A	0	N/A	1.088
Bus 6	Transformer 5 – 6 MV	33	2.698	0.796	0.385	N/A	0.439	N/A	0.580	N/A	0.580	N/A	0.574	N/A	N/A
Bus 5	Transformer 5 – 6 HV	132	0.724	1.075	0.103	N/A	0.118	N/A	0.156	N/A	0.156	N/A	0.154	N/A	N/A
Bus 1	Bus 2-1	132	0.497	1.396	0.477	1.577	0.530	1.177	0.162	N/A	0.162	N/A	0.164	N/A	N/A
Bus 1	Bus 2-2	132	0.497	1.396	0.477	1.577	0.530	1.177	0.162	N/A	0.162	N/A	0.164	N/A	N/A
Bus 2	Bus 3	132	0.513	1.742	0.427		0.422	N/A	0.419	N/A	0.419	N/A	0.415	N/A	N/A
Bus 1	G1	132	1.919	1.249	1.092	2.439	1.192	2.128	0.421	N/A	0.052	N/A	0.432	N/A	N/A
Bus 2	G2	132	1.203	1.686	0.750	2.300	0.836	2.123	0.200	N/A	0.200	N/A	0.198	N/A	N/A
Bus 3	G3	132	0.550	3.013	0.396	4.479	0.408	4.290	0.196	N/A	0.196	N/A	0.194	N/A	N/A
Bus 6	G6	33	2.797	1.610	0.437	3.321	0.534	2.917	0.119	29.230	0.119	29.230	0.117	31.112	32.196
Bus 8	G8	1	9.409	1.788	9.690	2.616	11.265	1.988	13.763	1.505	7.370	6.114	7.370	6.114	3.374
Bus 4	Wind G4	132	0.005	0.420	0.005	0.420	0	N/A	0	N/A	0	N/A	0	N/A	0.420
Bus 5	Wind G5	132	0.017	0.420	0.015	N/A	0.013	N/A	0.017	0.420	0.017	0.420	0	N/A	1.150
Bus 7	Wind G7	1	5.652	0.420	5.608	0.420	0	N/A	0	N/A	0	N/A	0	N/A	0.420
Bus 9	Wind G9	33	0.052	0.420	0.052	0.420	0	N/A	0	N/A	0	N/A	0	N/A	0.420
Bus 10	Wind G10	33	0.239	0.420	0.237	0.420	0	N/A	0	N/A	0	N/A	0	N/A	0.420
Bus 14	Wind G14	33	0.091	0.420	0.090	0.420	0	N/A	0	N/A	0	N/A	0	N/A	0.420

b) Protection grading results for Bus 10

The grading for a three-phase fault of 5.868 kA at Bus 10 is shown in Table 4-19.

Table 4-19: The branch currents and trip times for a three-phase fault at Bus 10 in the modified IEEE network for Case 3

<i>Substation</i>	<i>Feeder</i>	<i>Voltage Level (kV)</i>	<i>Stage 1 Fault Level Magnitude Contribution (kA)</i>	<i>Stage 1 OCEF relay calculated trip time (s)</i>	<i>Stage 2 Fault Level Magnitude Contribution (kA)</i>	<i>Stage 2 OCEF relay calculated trip time (s)</i>	<i>Overall Trip Time (s)</i>
Bus 9	Bus 10	33	5.693	0.346	0	N/A	0.346
Bus 9	Transformer 9 - 7 MV	33	4.128	0.730	0	N/A	0.730
Bus 9	Transformer 9 - 4 MV	33	1.577	0.830	0	N/A	0.830
Bus 4	Transformer 9 - 4 HV	132	0.407	0.885	0	N/A	0.885
Bus 4	Transformer 7 - 4 HV	132	0.503	1.580	0	N/A	1.580
Bus 7	Transformer 7 - 8 MV	1	6.247	24.283	0	N/A	24.283
Bus 4	Bus 5	132	0.560	2.281	0	N/A	2.281
Bus 4	Bus 2	132	0.363	7.013	0	N/A	7.013
Bus 1	G1	132	0.780	5.591	0	N/A	5.591
Bus 2	G2	132	0.334	5.959	0	N/A	5.959
Bus 3	G3	132	0.259	11.816	0	N/A	11.816
Bus 6	G6	33	0.530	2.930	0	N/A	2.930
Bus 8	G8	1	6.102	74.733	0	N/A	74.733
Bus 9	Wind G9	33	0.053	0.420	0	N/A	N/A
Bus 10	Wind G10	33	0.249	0.420	0.249	0.420	0.420
Bus 14	Wind G14	33	0.093	0.420	0	N/A	N/A

c) Protection grading results for Bus 11

The grading for a three-phase fault of 5.155 kA at Bus 11 is shown in Table 4-20.

Table 4-20: The branch currents and trip times for a three-phase fault at Bus 11 in the modified IEEE network for Case 3

<i>Substation</i>	<i>Feeder</i>	<i>Voltage Level (kV)</i>	<i>Stage 1 Fault Level Magnitude Contribution (kA)</i>	<i>Stage 1 OCEF relay calculated trip time (s)</i>	<i>Stage 2 Fault Level Magnitude Contribution (kA)</i>	<i>Stage 2 OCEF relay calculated trip time (s)</i>	<i>Overall Trip Time (s)</i>
Bus 6	Bus 11	33	5.135	0.407	0	N/A	0.407
Bus 6	Transformer 5 - 6 MV	33	2.192	0.962	0	N/A	0.962
Bus 6	Transformer 5 - 6 HV	132	0.588	1.284	0	N/A	1.284
Bus 1	G1	132	0.757	6.301	0	N/A	6.301
Bus 2	G2	132	0.260	11.768	0	N/A	11.768
Bus 3	G3	132	0.219	33.907	0	N/A	33.907
Bus 6	G6	33	3.131	1.610	0	N/A	1.610
Bus 11	Wind G11	33	0.026	0.420	0.026	0.420	0.420

d) Protection grading results for Bus 13

The grading for a three-phase fault of 6.686 kA at Bus 13 is shown in Table 4-21.

Table 4-21: The branch currents and trip times for a three-phase fault at Bus 13 in the modified IEEE network for Case 3

Substation	Feeder	Voltage Level (kV)	Stage 1 Fault Level Magnitude Contribution (kA)	Stage 1 OCEF relay calculated trip time (s)	Stage 2 Fault Level Magnitude Contribution (kA)	Stage 2 OCEF relay calculated trip time (s)	Overall Trip Time (s)
Bus 6	Bus 13	33	6.577	0.413	0	N/A	0.413
Bus 6	Transformer 5 – 6 MV	33	2.678	0.801	0	N/A	0.801
Bus 6	Transformer 5 – 6 HV	132	0.718	1.081	0	N/A	1.081
Bus 1	G1	132	0.777	5.685	0	N/A	5.685
Bus 2	G2	132	0.286	8.556	0	N/A	8.556
Bus 3	G3	132	0.231	21.174	0	N/A	21.174
Bus 6	G6	33	4.045	1.610	0	N/A	1.610
Bus 6	Wind G6	33	0.034	0.420	0	N/A	N/A
Bus 11	Wind G11	33	0.024	0.420	0	N/A	N/A
Bus 13	Wind G13	33	0.144	0.420	0.144	0.420	0.420

4.5 Discussion of load flow results

Due to the addition of the distributed generation in Cases 2 and 3, all three cases present different load flow results. Slight differences in load flow results are noted in both networks between the MATPOWER and DIgSILENT PowerFactory simulation results. This is likely due to MATPOWER rounding values in its output but not internally.

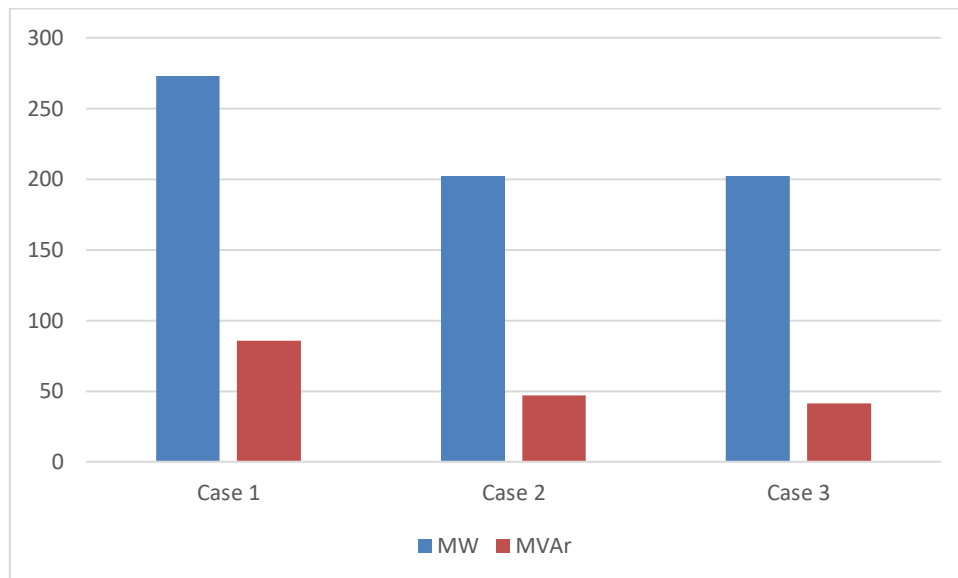


Figure 4.4: Imported power from the grid across the three cases for the modified IEEE 14-bus network

As seen graphically in Figure 4.4, Case 1 presents a total generated power of 272.814 MW and 85.802 MVar. The additional generation added using the PBIL algorithm in Case 2 reduces the required power generated by the generators to 202.159 MW and 47.115 MVar, adding a total wind turbine generation of 65.568 MW and 21.781 MVar to the grid. This equates to a 27.42% reduction in MVA being provided by the system generators. Case 3 further reduces the power generated by the system generators using the DE algorithm to 201.992 MW and 41.438 MVar by adding wind turbines to the system totalling 67.632 MW and 27.161 MVar. This results in a 27.90% reduction in power being provided by the system generators.

The load remains constant through the three cases at 259 MW and 73.5 MVar.

The total power losses in Case 1 is calculated as 13.813 MW and 57.989 MVar. This is reduced in Case 2 to 8.727 MW and 35.704 MVar using the PBIL algorithm, resulting in a 38.34% reduction in MVA losses. This is further reduced in Case 3 to 8.623 MW and 35.485 MVar, resulting in a 38.74% reduction in MVA losses from Case 1. This reduction in power losses can be seen graphically in Figure 4.5.

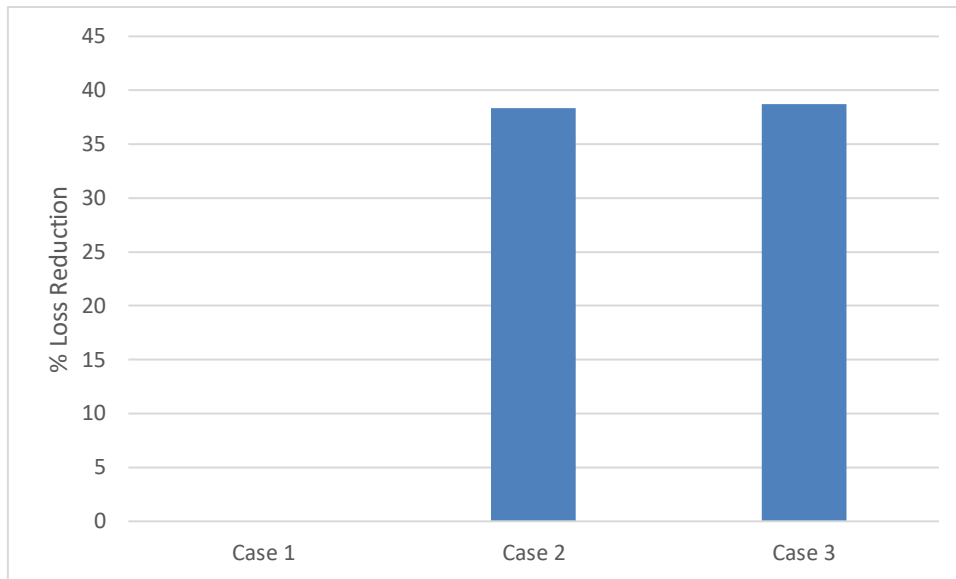


Figure 4.5: The percentage power loss reduction across the three cases for the modified IEEE 14-bus network

Both algorithms are thus seen to significantly reduce network power losses while providing a maximum total generation of 72 MVA. The solution obtained from the DE algorithm is seen to produce slightly better results in this case in terms of power loss reduction, but both algorithms perform similarly.

Voltage profile improvements were tracked using the RMS of the difference of the voltages at the busses between Case 1, 2 and 3. The busbar voltage levels in Case 1 are seen to vary more than those seen in Cases 2 and 3. The total RMS error from the nominal voltages is calculated as 3.12% in Case 1. The results produced by the PBIL algorithm in Case 2 results in this error being reduced to 1.70%, a 45.51% reduction in RMS error between these two cases. Case 3 results in a slightly higher 1.96% total RMS error, a 37.18% reduction in error over Case 1.

The results produced by the PBIL algorithm are seen to result in voltages closer to nominal, and is thus seen to produce the better result in terms of overall voltage profile improvement in the case of the modified IEEE 14-bus network.

4.6 Discussion of protection grading results

This section outlines the protection grading results for the different cases in the modified IEEE 14-bus network.

4.6.1 Fault at Bus 4

In Case 1, the three-phase fault level is calculated as 5.197 kA. The fault is isolated in 1.215 seconds when the Transformer 4-9 MV relay trips. The grading margin with the HV relay on the same transformer is calculated as 108 ms. Other relays are not seen to trip due to insufficient pickup current as the fault stages progress.

In Case 2, the three-phase fault level is seen to decrease to 4.980 kA and is isolated in 1.228 seconds, when the Transformer 4-9 MV relay trips. The grading margin with the HV relay on the same transformer remains similar to that seen in Case 1.

In Case 3, the three-phase fault level is seen to decrease to 4.957 kA and is isolated in 1.150 seconds. This case is seen to trip sooner than the other cases despite a decrease in total fault level due to the cables experiencing higher current levels case due to sizing of the Wind Turbines.

The trip times are graphically shown in Figure 4.6.

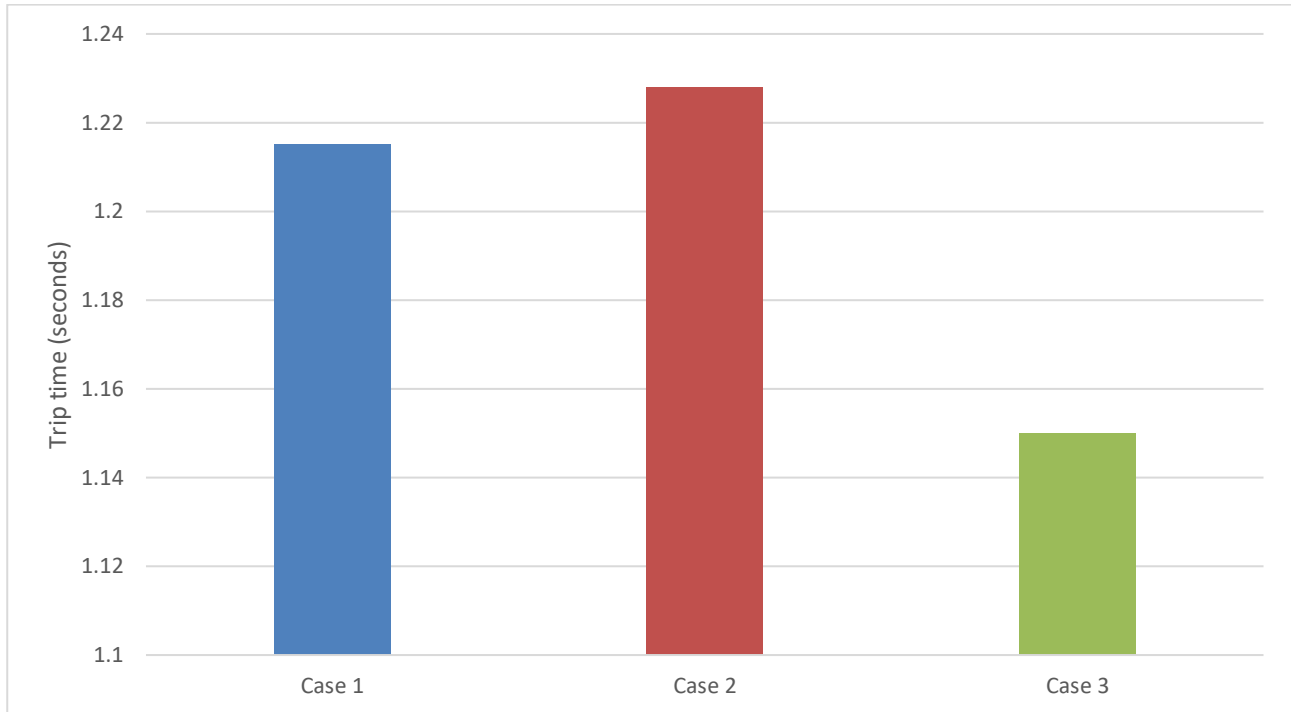


Figure 4.6: Total trip times for a three-phase fault at Bus 4 for the three cases for the modified IEEE 14-bus network

4.6.2 Fault at Bus 10

In Case 1, the three-phase fault level for a fault at Bus 10 is calculated as 6.083 kA and is isolated in 0.340 seconds. Bus 10 is fed directly from Bus 9 and therefore, grading is done with the Transformer 9-4 MV relay which trips in 0.800 seconds, and with the Transformer 9-7 MV relay which trips in 0.688 seconds. The grading margin is sufficient in this case.

The three-phase fault level for a fault at Bus 10 is calculated as 5.810 kA in Case 2 and 5.868 kA in Case 3, both of which are isolated in 0.420 seconds. The grading margins are similar to those in Case 1. The trip times are graphically shown in Figure 4.7.

4.6.1 Fault at Bus 11

In Case 1, the three-phase fault level for a fault at Bus 11 is calculated as 5.452 kA and is isolated in 0.396 seconds. Bus 11 is fed directly from Bus 6 and therefore, grading is done with the Transformer 5-6 MV relay, which trips in 0.928 seconds, and with the Transformer 5-6 HV relay, which trips in 1.241 seconds. The grading margin is sufficient in this case.

In Case 2, the three-phase fault level for a fault at Bus 11 is calculated as 5.317 kA and is isolated in 0.420 seconds due to the Wind G11 relay tripping in 0.420 seconds. Bus 11 is fed directly from Bus 6, and therefore, grading is done with the Transformer 5-6 MV relay, which trips in 0.994 seconds, and with the Transformer 5-6 HV relay, which trips in 1.323 seconds. In Case 3, the fault level is calculated as 5.155 kA and is also isolated in 0.420 seconds, with similar grading margins as seen in Case 2. The grading margin is thus sufficient in these cases. The trip times are graphically shown in Figure 4.8.

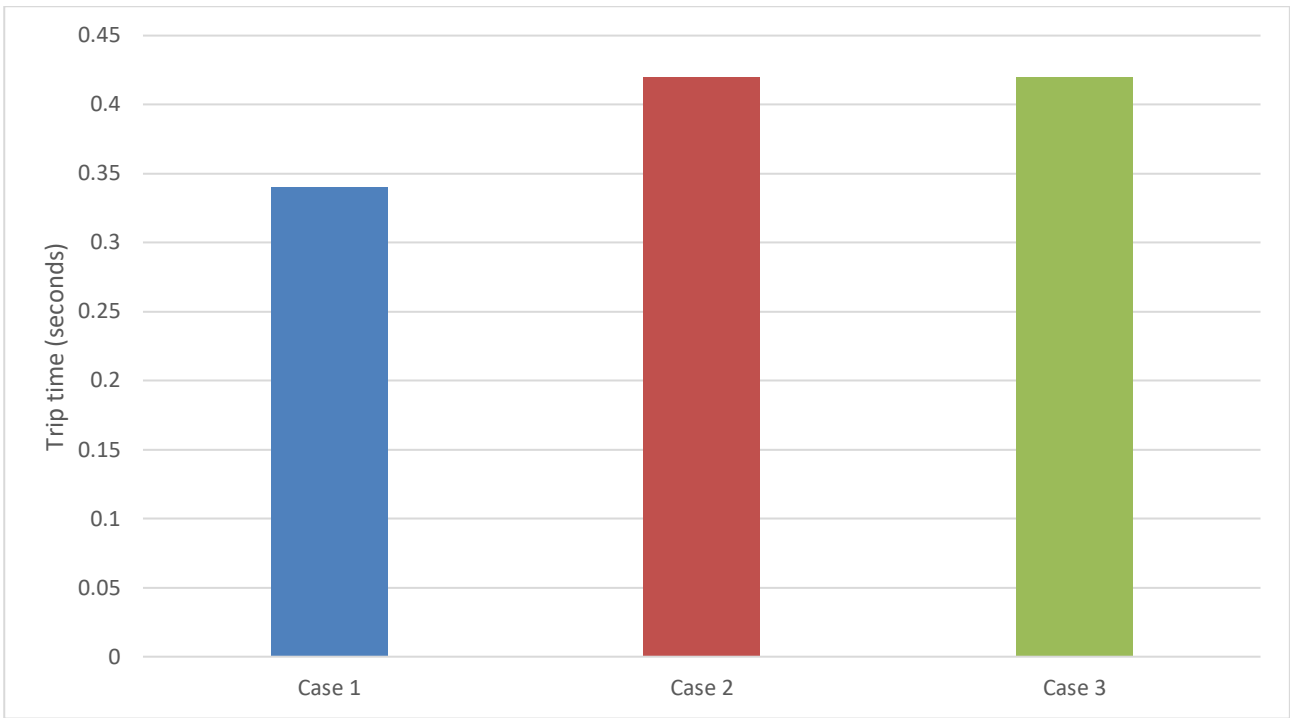


Figure 4.7: Total trip times for a three-phase fault at Bus 10 for the three cases for the modified IEEE 14-bus network

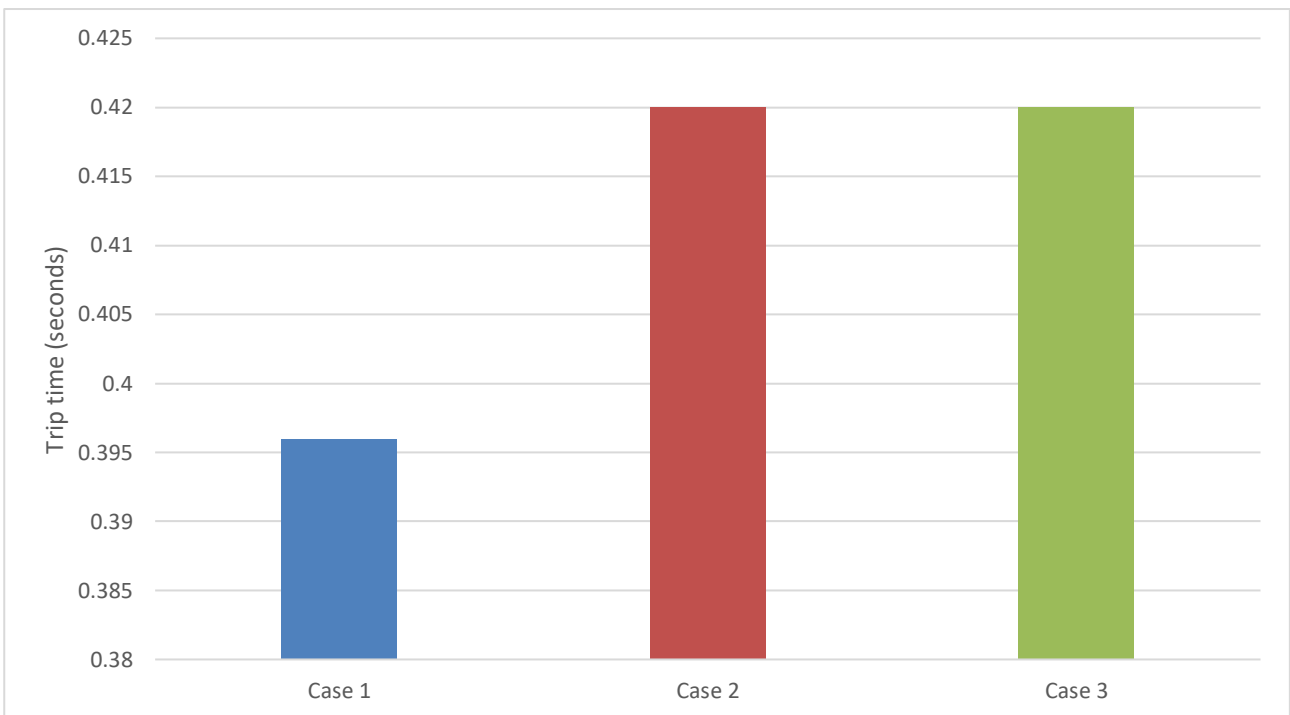


Figure 4.8: Total trip times for a three-phase fault at Bus 11 for the three cases for the modified IEEE 14-bus network

4.6.2 Fault at Bus 13

In Case 1, the three-phase fault level for a fault at Bus 13 is calculated as 7.122 kA and is isolated in 0.401 seconds. Bus 13 is fed directly from Bus 6 and therefore, grading is done with the Transformer 5-6 MV relay which trips in 0.779 seconds, and with the Transformer 5-6 HV relay which trips in 1.052 seconds. The grading margin is sufficient in this case.

In Case 2, the three-phase fault level for a fault at Bus 13 is calculated as 6.759 kA and is isolated in 0.420 seconds, due to the Wind G13 relay tripping in 0.420 seconds. In Case 3, the fault level is calculated as

6.686 kA and is also isolated in 0.420 seconds. Grading margins are similar to Case 1 for both of these cases, though trip times are slightly longer. The trip times are graphically shown in Figure 4.9.

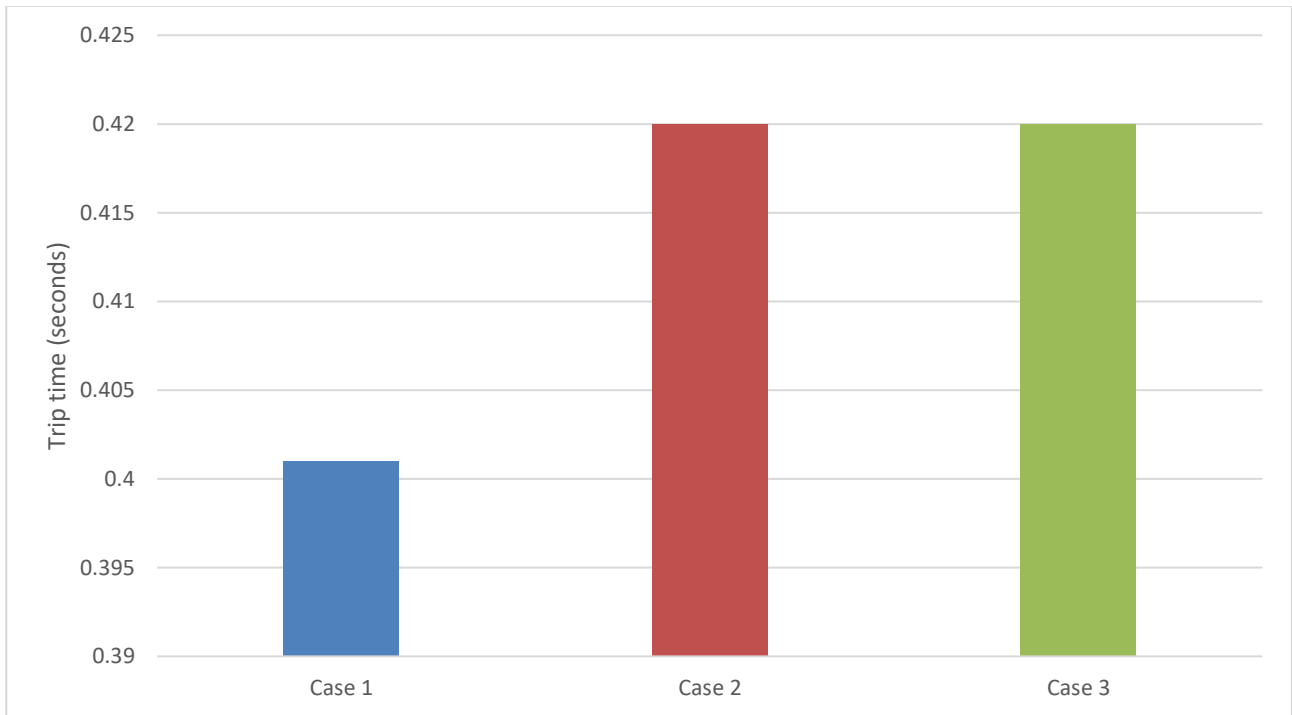


Figure 4.9: Total trip times for a three-phase fault at Bus 13 for the three cases for the modified IEEE 14-bus network

4.6.3 Summary of IEEE network protection

Throughout all three cases in all of the faults studied, it is found that the fault levels in Cases 2 and 3 are lower than those in Case 1. This is likely due to the method by which PowerFactory calculates the fault levels, by first running a load flow. Thus the current network generators would contribute less to the fault when the DGs are installed. The standard network generators provide less power in load flows for Cases 2 and 3. This different, lower initial power output is then taken into account when calculating the fault level.

Grading is essentially unaffected between the three Cases for the faults under study.

4.7 Discussion of the performance of the optimisation algorithms

As per the discussion in section 4.5, the combination of each optimisation algorithm with the MATPOWER simulation package is seen to produce impressive optimisation gains over Case 1.

The PBIL algorithm is seen to produce better results in terms of improving the voltage profile, while the DE algorithm produces better results in terms of power loss improvement. The two algorithms were seen to place very different sizes of distributed generation at the nodes throughout the network.

5. Municipal Case Study Results and Discussion

This section details the results obtained from the methodology of the municipal network study outlined in Chapter 3. The results from each of the four cases are then discussed and compared in terms of improvement in voltage profile, reduction in power losses, and the effect on the protection schemes.

5.1 Case 1: Pre-DG installation network state

5.1.1 Load flow results

Upon running the load flow for Case 1, the network overview results shown in Table 5-1 and Figures 5.1 through 5.9 were obtained.

Table 5-1: The network overview results for the municipal network for Case 1

<i>Active Power Generation (MW)</i>	<i>Reactive Power Generation (MVar)</i>	<i>Active Load (MW)</i>	<i>Reactive Load (MVar)</i>	<i>Active Power Losses (MW)</i>	<i>Reactive Power Losses (MVar)</i>
43.208	11.774	41.551	8.684	1.656	3.323

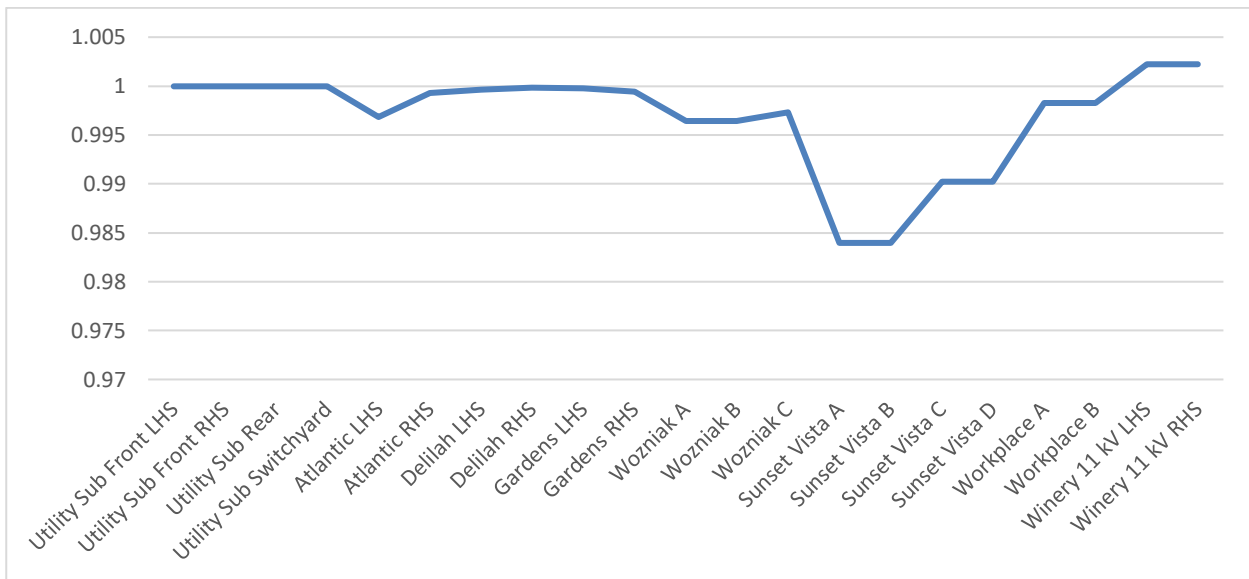


Figure 5.1: Graph showing the voltage profile for the main substations in the municipal network for Case 1

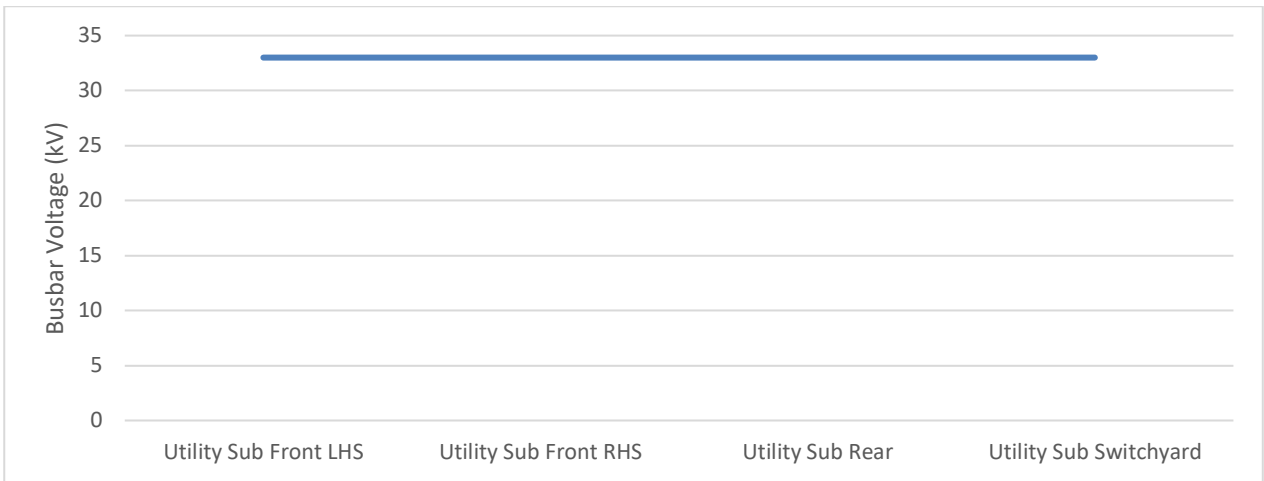


Figure 5.2: The voltage profile for the Utility substation group of busbars in the municipal network for Case 1

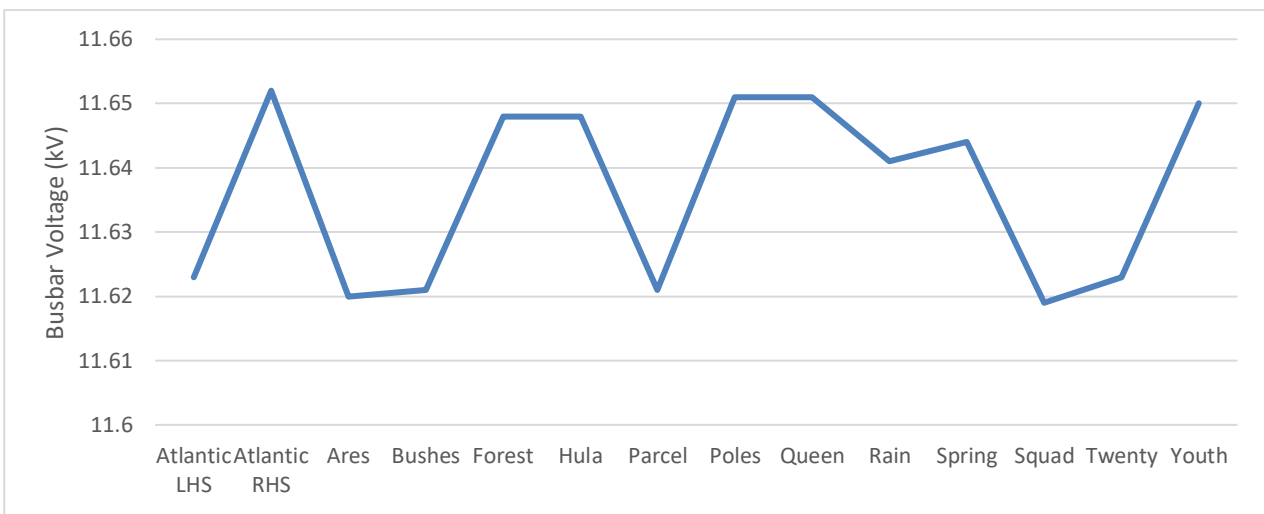


Figure 5.3: The voltage profile for the Atlantic MS group of busbars in the municipal network for Case 1

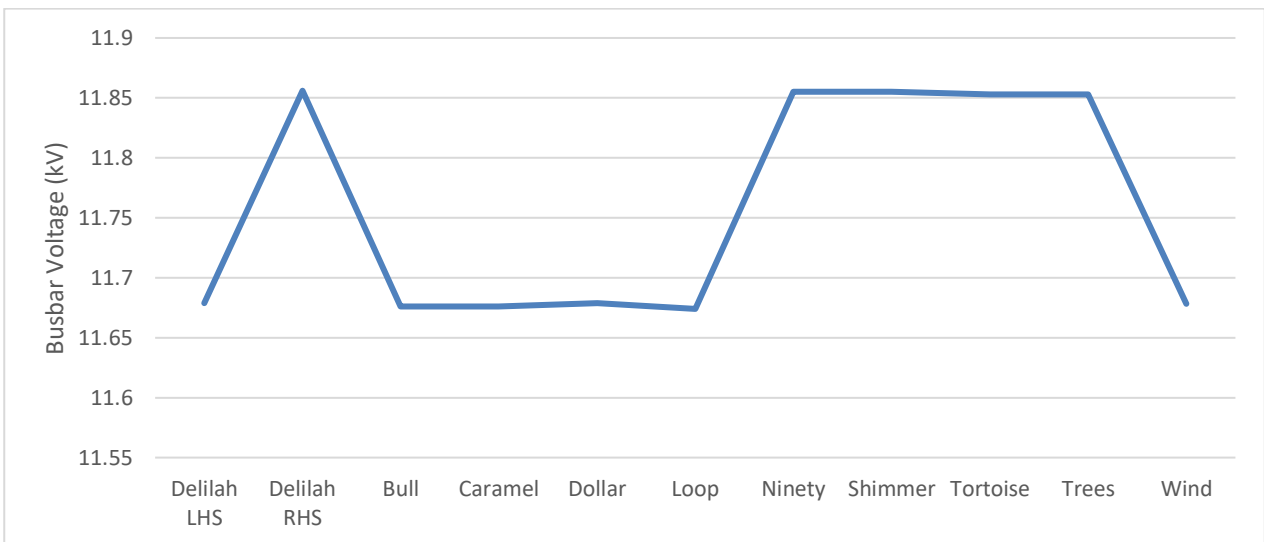


Figure 5.4: The voltage profile for the Delilah MS group of busbars in the municipal network for Case 1

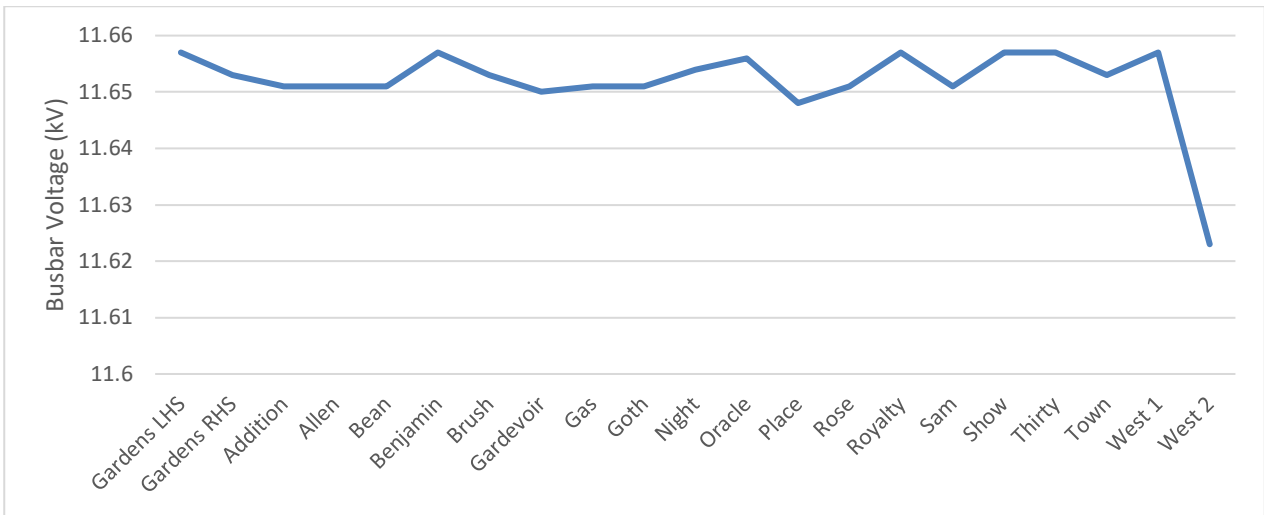


Figure 5.5: The voltage profile for the Gardens MS group of busbars in the municipal network for Case 1

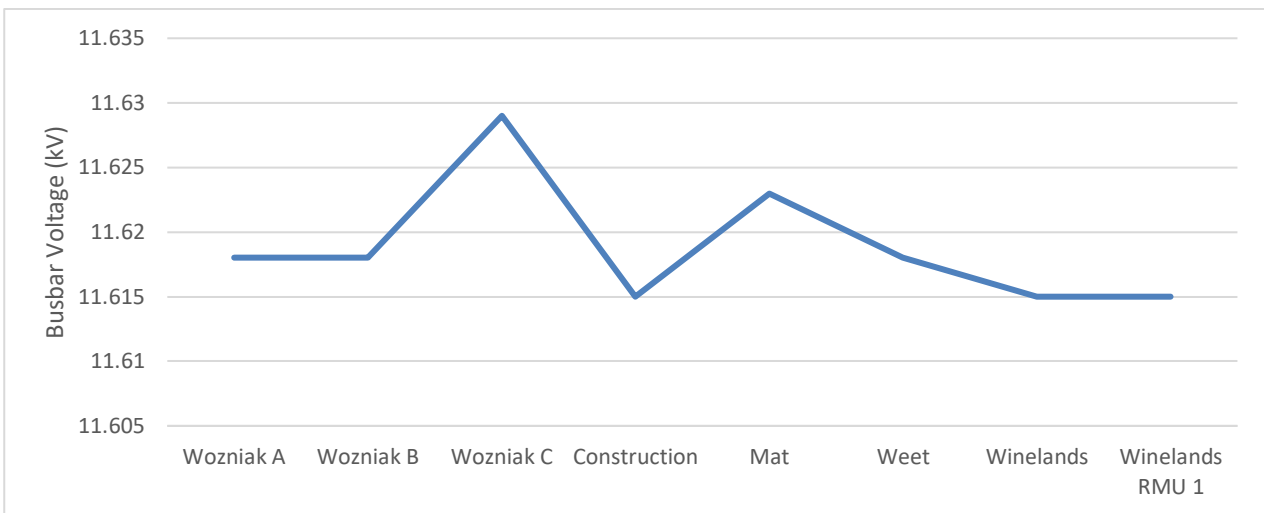


Figure 5.6: The voltage profile for the Wozniak group of busbars in the municipal network for Case 1

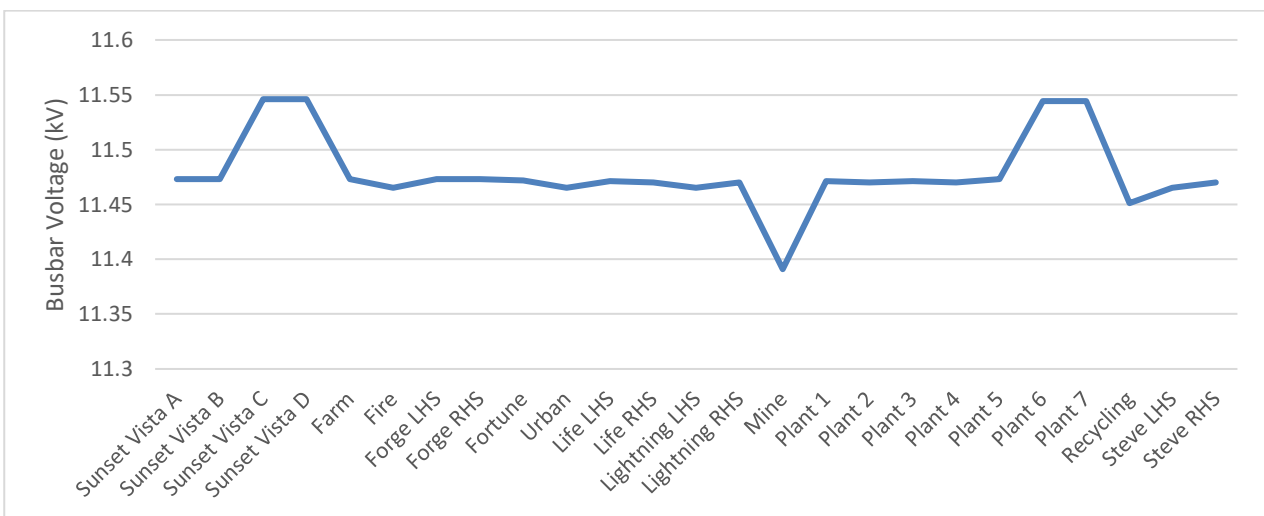


Figure 5.7: The voltage profile for the Sunset Vista MS group of busbars in the municipal network for Case 1

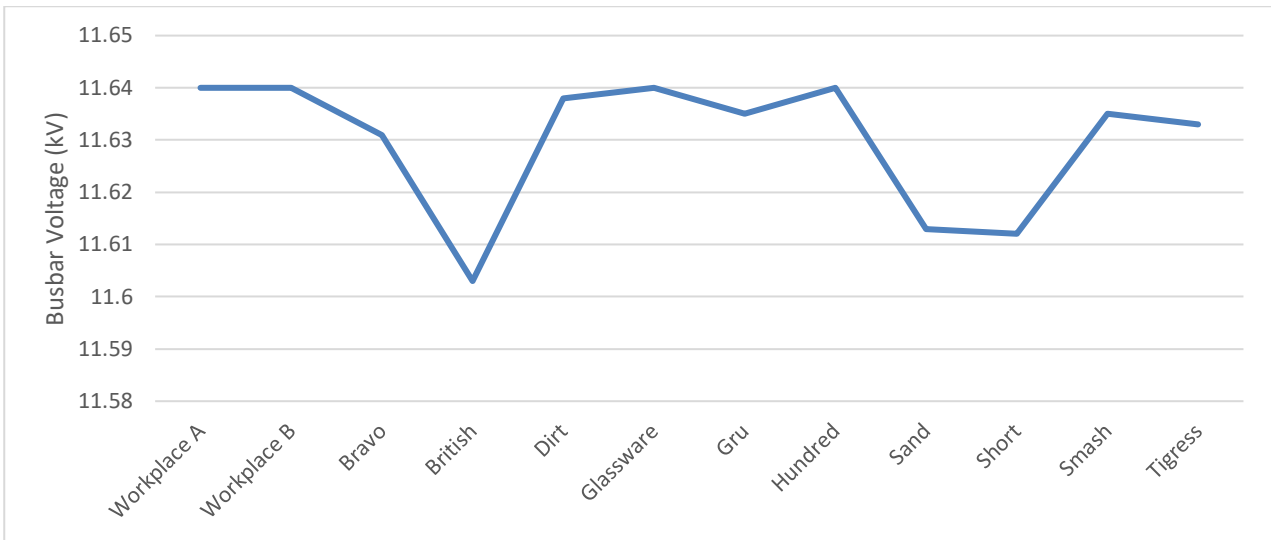


Figure 5.8: The voltage profile for the Workplace MS group of busbars in the municipal network for Case 1

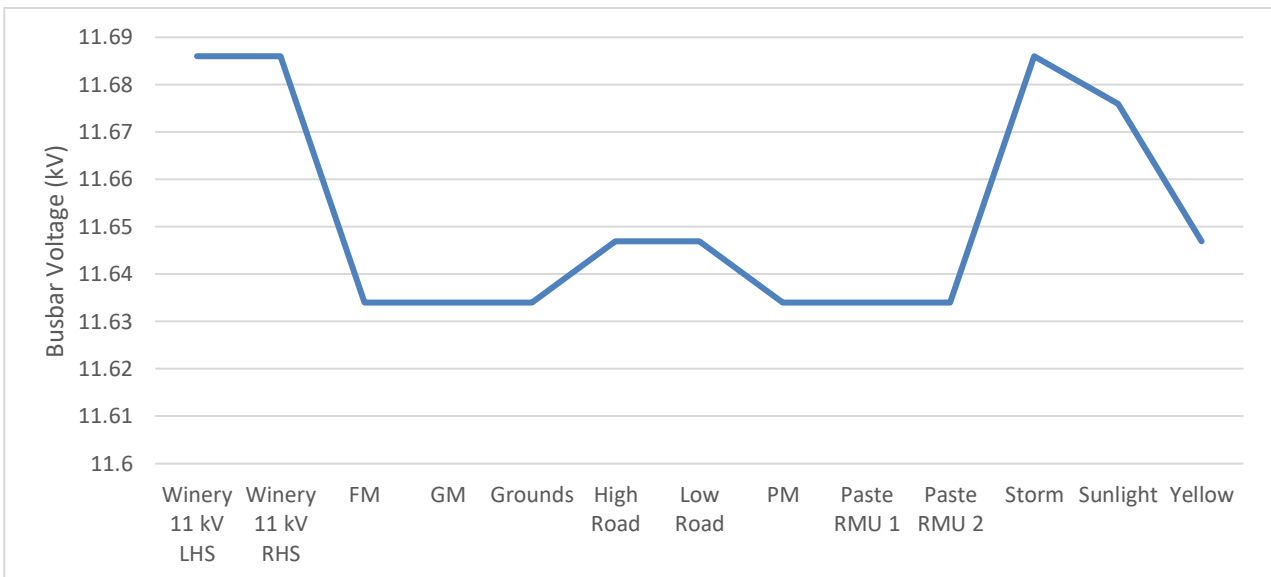


Figure 5.9: The voltage profile for the Winery MS group of busbars in the municipal network for Case 1

5.1.2 Protection grading results

As detailed in Chapter 3, nine faults were placed throughout the network for the purposes of studying the protection grading for this case study. The results for three of the nine selected faults are detailed below. The grading results for the remaining fault locations are shown in Appendix G. Results are organised in this manner in the remaining cases for the municipal network as well. IDMT curves for the municipal network grading across the four cases is shown in Appendix H.

It should also be noted that, in this research, the term ‘single-phase fault’ and ‘earth-fault’ are interchangeable.

a) Protection grading results for the Bushes substation

The grading for a three-phase fault of 4.182 kA and a single-phase-to-ground fault of 1.169 kA at the Bushes substation is shown in Tables 5-2 and 5-3.

Table 5-2: Branch currents and trip times for a three-phase fault at Bushes SS for the municipal network for Case 1

Substation	Feeder	Voltage Level (kV)	Fault Level Magnitude Contribution (kA)	OCEF relay calculated trip time (s)
Atlantic	Bushes	11.66	4.182	0.120
Atlantic	Transformer 1 MV	11.66	3.337	1.239
Atlantic	Grounds	11.66	1.198	0.316
Winery	Yellow	11.66	1.198	0.221
Winery	Transformer 1 MV	11.66	1.199	3.241
Atlantic	Transformer 1 HV	33	1.179	1.595
Winery	Transformer 1 HV	33	0.424	3.961
Utility Sub	Utility Sub Switch Yard 1	33	0.211	N/A
Utility Sub	Utility Sub Switch Yard 2	33	0.213	N/A
Utility Sub	Atlantic 1	33	1.179	2.206
Utility Sub	Incomer 1	33	0.969	N/A
Utility Sub	Incomer 2	33	0.969	N/A

Table 5-3: Branch currents and trip times for a single-phase fault at Bushes SS for the municipal network for Case 1

Substation	Feeder	Voltage Level (kV)	Fault Level Magnitude Contribution (kA)	OCEF relay calculated trip time (s)
Atlantic	Bushes	11.66	1.169	0.150
Atlantic	Transformer 1 MV	11.66	0.914	1.907
Atlantic	Grounds	11.66	0.255	0.460
Winery	Yellow	11.66	0.255	0.238
Winery	Transformer 1 MV	11.66	0.255	5.020
Atlantic	Transformer 1 HV	33	0.207	N/A
Winery	Transformer 1 HV	33	0.074	N/A
Utility Sub	Utility Sub Switch Yard 1	33	0.037	N/A
Utility Sub	Utility Sub Switch Yard 2	33	0.038	N/A
Utility Sub	Atlantic 1	33	0.207	N/A
Utility Sub	Incomer 1	33	0.476	N/A
Utility Sub	Incomer 2	33	0.476	N/A

b) Protection grading results for the Winelands RMU 1 substation

The grading for a three-phase fault of 7.668 kA and a single-phase-to-ground fault of 1.977 kA at the Winelands RMU 1 substation is shown in Tables 5-4 and 5-5.

Table 5-4: Currents and trip times for a three-phase fault at Winelands RMU 1 SS for the municipal network for Case 1

Substation	Feeder	Voltage Level (kV)	Fault Level Magnitude Contribution (kA)	OCEF relay stage 1 calculated trip time (s)	Fault Level Magnitude Contribution (kA)	OCEF relay stage 2 calculated trip time (s)	Fault Level Magnitude Contribution (kA)	OCEF relay stage 3 calculated trip time (s)	Overall Trip Time (s)
Winelands	Winelands RMU 1	11.66	7.597	0.120	0	N/A	0	N/A	0.120
Winelands	Weet	11.66	1.116	1.688	0.876	2.214	4.357	0.715	1.147
Wozniak	Winelands	11.66	6.552	0.609	5.142	0.668	0	N/A	0.656
Wozniak	Weet	11.66	1.116	1.688	0.876	2.214	4.357	0.715	1.147
Wozniak	Transformer A MV	11.66	3.918	1.692	3.083	1.952	2.240	2.452	2.261
Wozniak	Transformer B MV	11.66	3.755	1.733	2.955	2.007	2.146	2.538	2.340
Wozniak	Transformer A HV	33	1.384	0.947	1.089	1.108	0.791	1.430	1.213
Wozniak	Transformer B HV	33	1.327	0.972	1.044	1.142	0.758	1.488	1.262
Utility Sub	Wozniak A	33	1.384	1.852	1.089	2.167	0.791	2.799	2.581
Utility Sub	Wozniak B	33	1.327	1.902	1.044	2.235	0.758	2.911	2.685
Utility Sub	Incomer 1	33	1.474	N/A	1.272	N/A	1.025	N/A	N/A
Utility Sub	Incomer 2	33	1.474	N/A	1.272	N/A	1.025	N/A	N/A

Table 5-5: Currents and trip times for a single-phase fault at Winelands RMU 1 SS for the municipal network for Case 1

Substation	Feeder	Voltage Level (kV)	Fault Level Stage 1 Magnitude Contribution (kA)	OCEF relay stage 1 calculated trip time (s)	Fault Level Stage 2 Magnitude Contribution (kA)	OCEF relay stage 2 calculated trip time (s)	Fault Level Stage 3 Magnitude Contribution (kA)	OCEF relay stage 3 calculated trip time (s)	Overall Trip Time (s)
Winelands	Winelands RMU 1	11.66	1.966	0.120	0	N/A	0	N/A	0.120
Winelands	Weet	11.66	0.249	1.221	0.189	1.614	1.178	0.507	0.822
Wozniak	Winelands	11.66	1.728	0.453	1.314	0.486	0	N/A	0.477
Wozniak	Weet	11.66	0.249	1.221	0.189	1.614	1.178	0.507	0.822
Wozniak	Transformer A MV	11.66	0.996	1.407	0.758	1.680	0.594	2.029	1.902
Wozniak	Transformer B MV	11.66	0.980	1.421	0.746	1.699	0.584	2.057	1.928
Wozniak	Transformer A HV	33	0.219	N/A	0.170	N/A	0.136	N/A	N/A
Wozniak	Transformer B HV	33	0.210	N/A	0.163	N/A	0.130	N/A	N/A
Utility Sub	Wozniak A	33	0.219	N/A	0.170	N/A	0.136	N/A	N/A
Utility Sub	Wozniak B	33	0.210	N/A	0.163	N/A	0.130	N/A	N/A
Utility Sub	Incomer 1	33	0.549	N/A	0.507	N/A	0.477	N/A	N/A
Utility Sub	Incomer 2	33	0.549	N/A	0.507	N/A	0.477	N/A	N/A

c) Protection grading results for the Short substation

The grading for a three-phase fault of 10.444 kA and a single-phase-to-ground fault of 1.718 kA at the Short substation is shown in Tables 5-6 and 5-7.

Table 5-6: Branch currents and trip times for a three-phase fault at Short SS for the municipal network for Case 1

Substation	Feeder	Voltage Level (kV)	Stage 1 Fault Level Magnitude Contribution (kA)	Stage 1 OCEF relay calculated trip time (s)	Stage 2 Fault Level Magnitude Contribution (kA)	Stage 2 OCEF relay calculated trip time (s)	Stage 3 Fault Level Magnitude Contribution (kA)	Stage 3 OCEF relay calculated trip time (s)	Overall Trip Time (s)
Short	Workplace	11.66	5.162	0.694	7.505	0.603	9.504	0.590	0.640
Short	Glassware	11.66	1.677	0.481	2.439	0.380	0	N/A	0.445
Short	British	11.66	3.619	0.311	0	N/A	0	N/A	0.311
Workplace	Glassware	11.66	1.677	1.252	2.439	0.989	0	N/A	N/A
Workplace	British 1	11.66	1.263	1.505	0	N/A	0	N/A	N/A
Workplace	British 2	11.66	2.382	0.963	0	N/A	0	N/A	N/A
Workplace	Transformer 1 MV	11.66	5.220	1.275	4.984	1.325	4.776	1.374	1.345
Workplace	Transformer 2 MV	11.66	5.263	1.267	5.025	1.316	4.816	1.364	1.335
Workplace	Transformer 1 HV	33	1.844	1.270	1.761	1.318	1.688	1.364	1.336
Workplace	Transformer 2 HV	33	1.860	1.262	1.776	1.309	1.702	1.355	1.327
Utility Sub	Workplace 1	33	1.844	2.184	1.761	2.268	1.688	2.351	2.322
Utility Sub	Workplace 2	33	1.860	2.169	1.776	2.252	1.702	2.334	2.305
Utility Sub	Incomer 1	33	1.942	199.842	1.868	N/A	1.801	N/A	N/A
Utility Sub	Incomer 2	33	1.942	199.842	1.868	N/A	1.801	N/A	N/A

Table 5-7: Branch currents and trip times for a single-phase fault at Short SS for the municipal network for Case 1

Substation	Feeder	Voltage Level (kV)	Stage 1 Fault Level Magnitude Contribution (kA)	Stage 1 OCEF relay calculated trip time (s)	Stage 2 Fault Level Magnitude Contribution (kA)	Stage 2 OCEF relay calculated trip time (s)	Stage 3 Fault Level Magnitude Contribution (kA)	Stage 3 OCEF relay calculated trip time (s)	Overall Trip Time (s)
Short	Workplace	11.66	0.707	1.047	1.158	0.815	1.480	0.734	0.878
Short	Glassware	11.66	0.258	0.909	0.422	0.549	0	N/A	0.697
Short	British	11.66	0.754	0.374	0	N/A	0	N/A	0.374
Workplace	Glassware	11.66	0.258	2.455	0.422	1.483	0	N/A	N/A
Workplace	British 1	11.66	0.533	0.869	0	N/A	0	N/A	N/A
Workplace	British 2	11.66	0.221	1.636	0	N/A	0	N/A	N/A
Workplace	Transformer 1 MV	11.66	0.859	3.590	0.790	3.974	0.740	4.340	4.232
Workplace	Transformer 2 MV	11.66	0.859	3.590	0.790	3.974	0.740	4.340	4.232
Workplace	Transformer 1 HV	33	0.295	N/A	0.281	N/A	0.271	N/A	N/A
Workplace	Transformer 2 HV	33	0.297	N/A	0.284	N/A	0.274	N/A	N/A
Utility Sub	Workplace 1	33	0.295	N/A	0.281	N/A	0.271	N/A	N/A
Utility Sub	Workplace 2	33	0.297	N/A	0.284	N/A	0.274	N/A	N/A
Utility Sub	Incomer 1	33	0.526	N/A	0.513	N/A	0.504	N/A	N/A
Utility Sub	Incomer 2	33	0.526	N/A	0.513	N/A	0.504	N/A	N/A

5.2 Case 2: DG installed at Utility substation

5.2.1 Load flow results

Upon running the load flow for Case 2, the network overview results shown in Table 5-8 and Figures 5.10 through 5.18 were obtained.

Table 5-8: The network overview results for the municipal network for Case 2

Grid Active Power Generation (MW)	Grid Reactive Power Generation (MVar)	Turbine Active Power Generation (MW)	Turbine Reactive Power Generation (MVar)	Active Load (MW)	Reactive Load (MVar)	Active Power Losses (MW)	Reactive Power Losses (MVar)
-14.798	-31.897	57.600	43.200	41.551	8.684	1.251	2.852

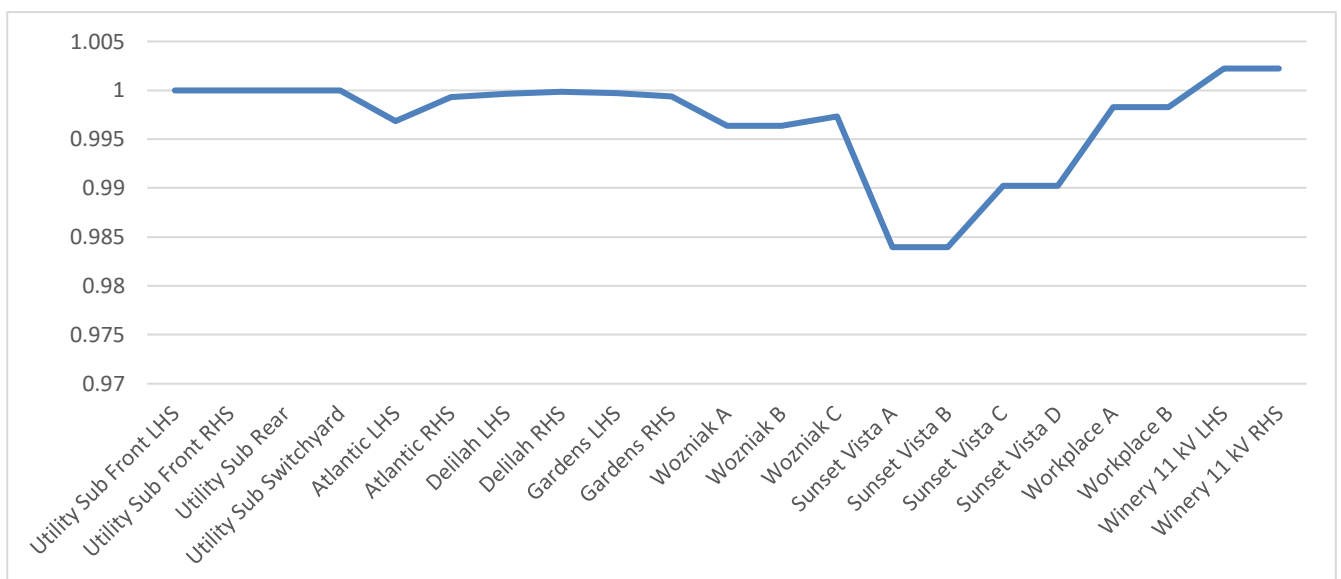


Figure 5.10: Graph showing the voltage profile for the main substations in the municipal network for Case 2

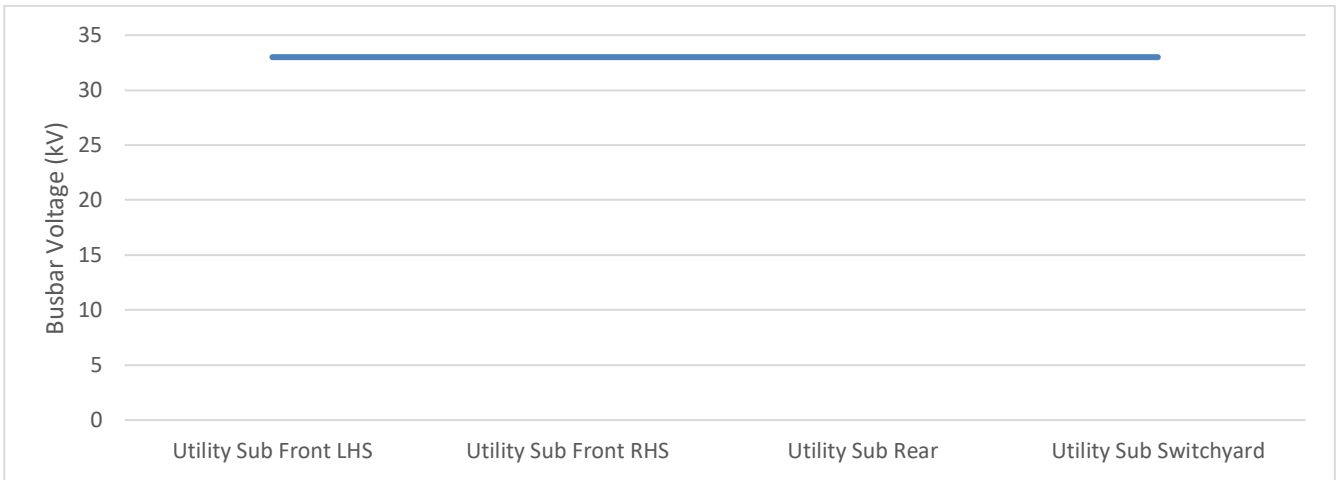


Figure 5.11: The voltage profile for the Utility substation group of busbars in the municipal network for Case 2

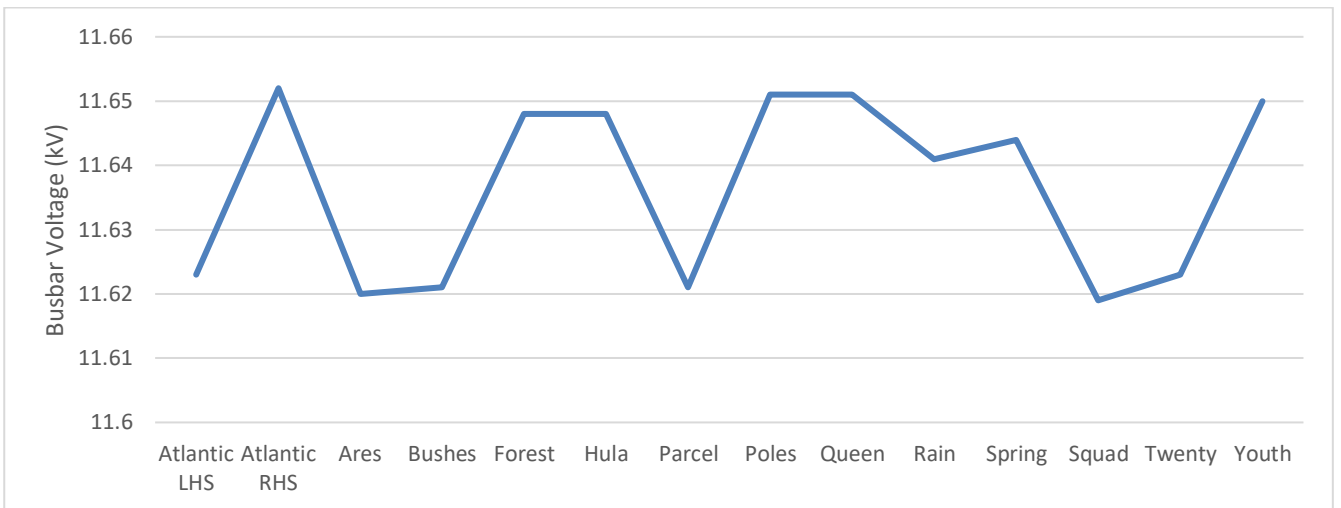


Figure 5.12: The voltage profile for the Atlantic MS group of busbars in the municipal network for Case 2

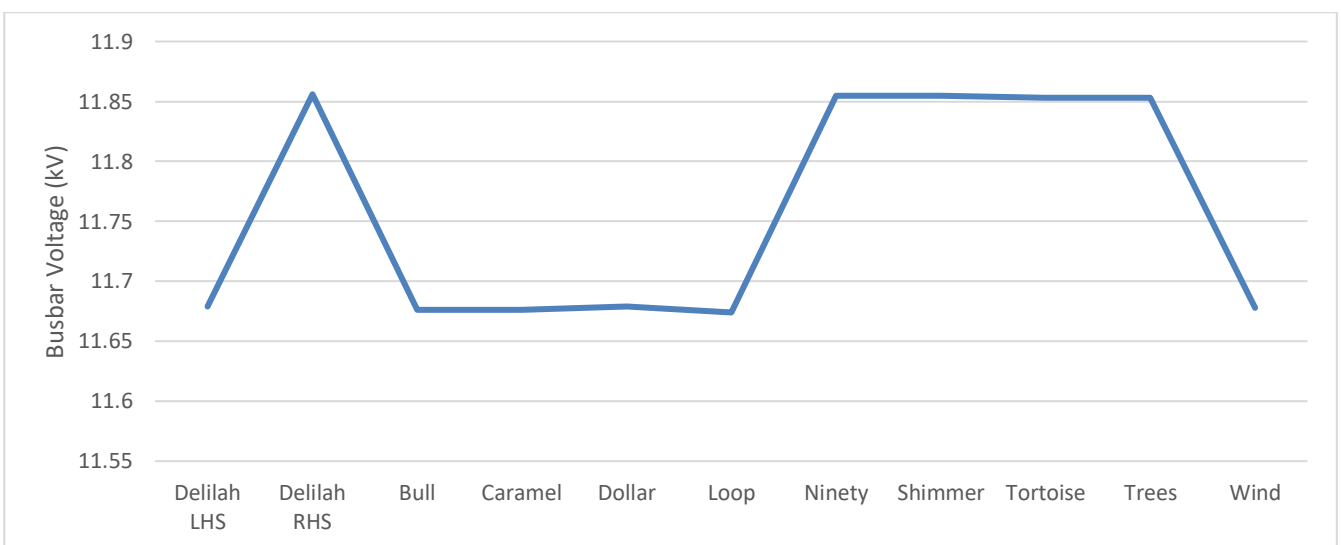


Figure 5.13: The voltage profile for the Delilah MS group of busbars in the municipal network for Case 2

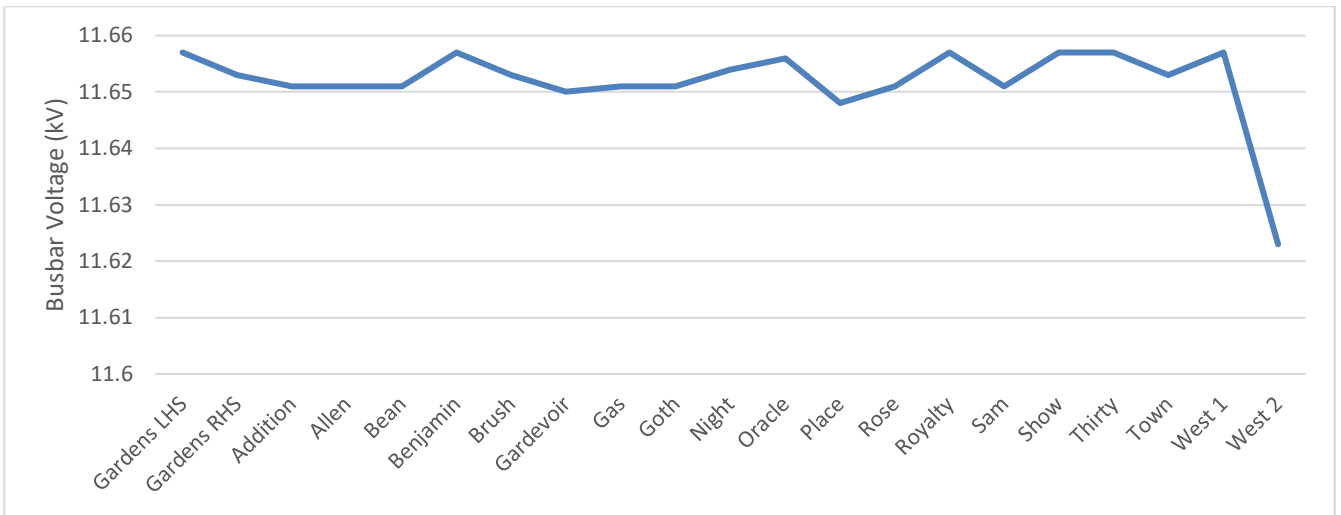


Figure 5.14: The voltage profile for the Gardens MS group of busbars in the municipal network for Case 2

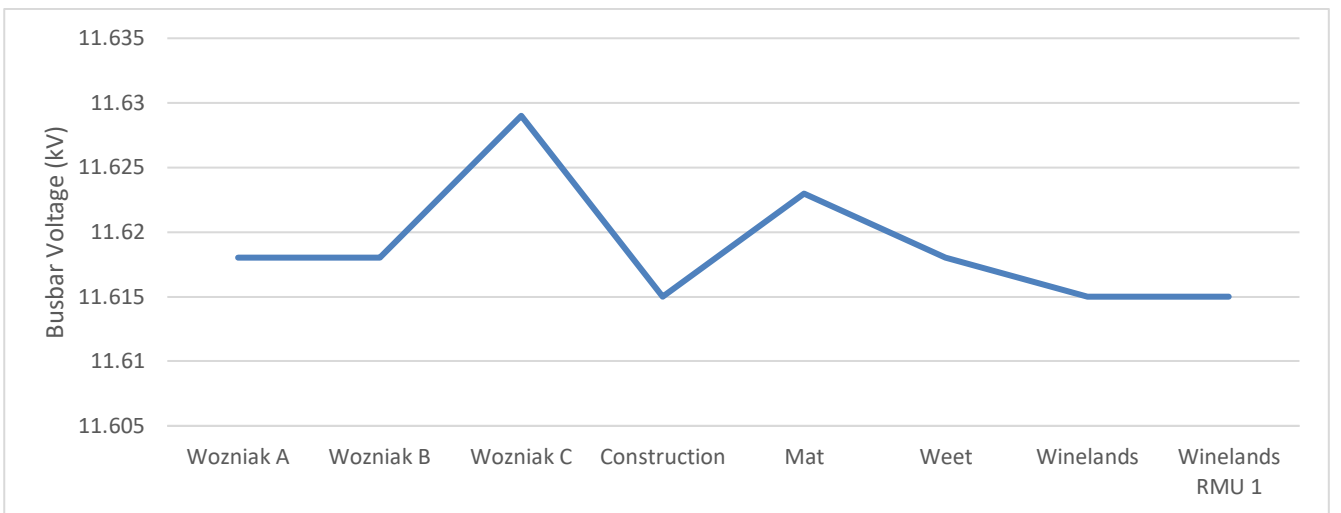


Figure 5.15: The voltage profile for the Wozniak group of busbars in the municipal network for Case 2

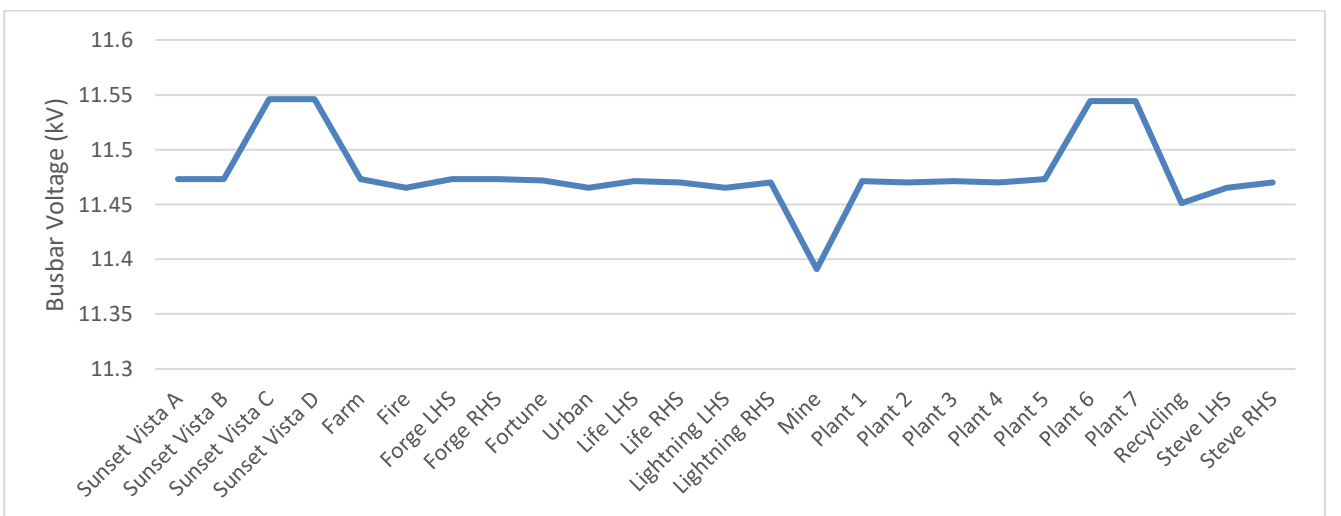


Figure 5.16: The voltage profile for the Sunset Vista MS group of busbars in the municipal network for Case 2

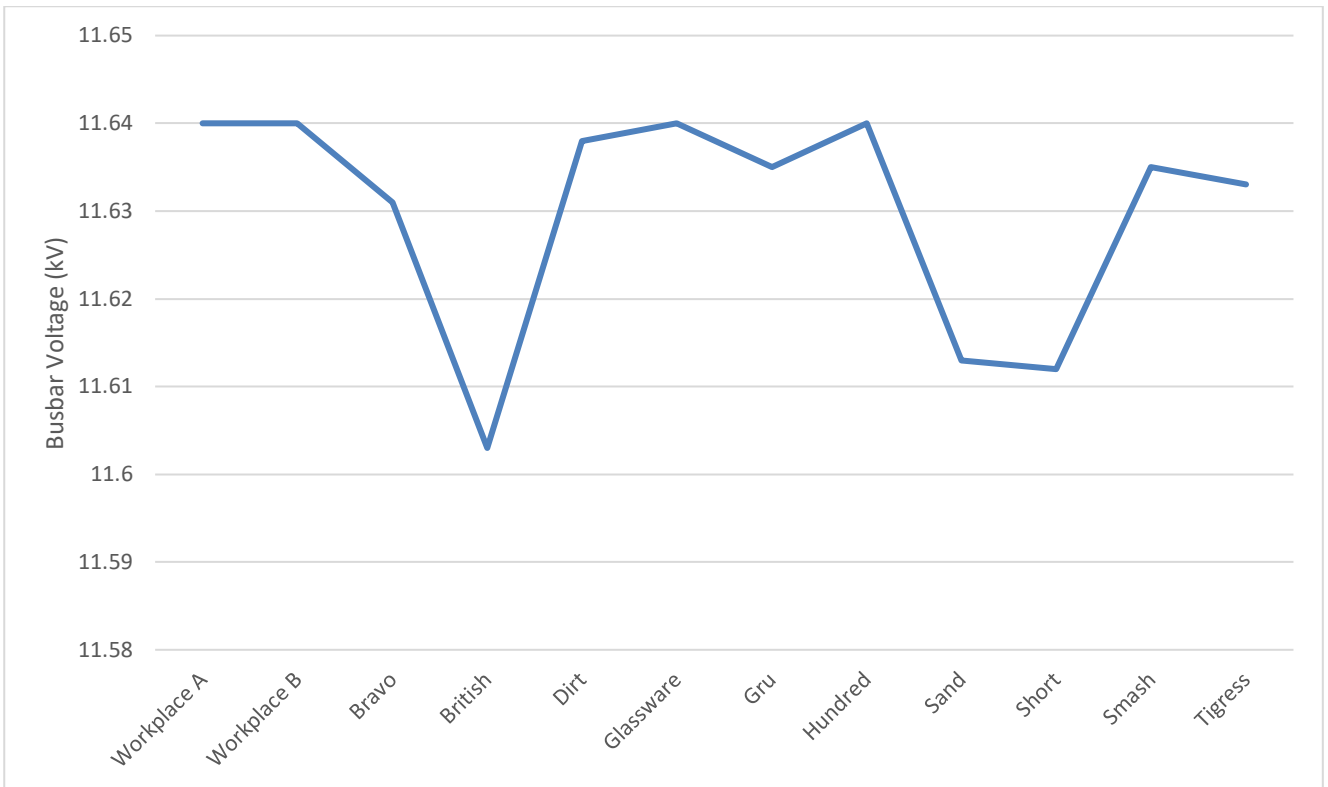


Figure 5.17: The voltage profile for the Workplace MS group of busbars in the municipal network for Case 2

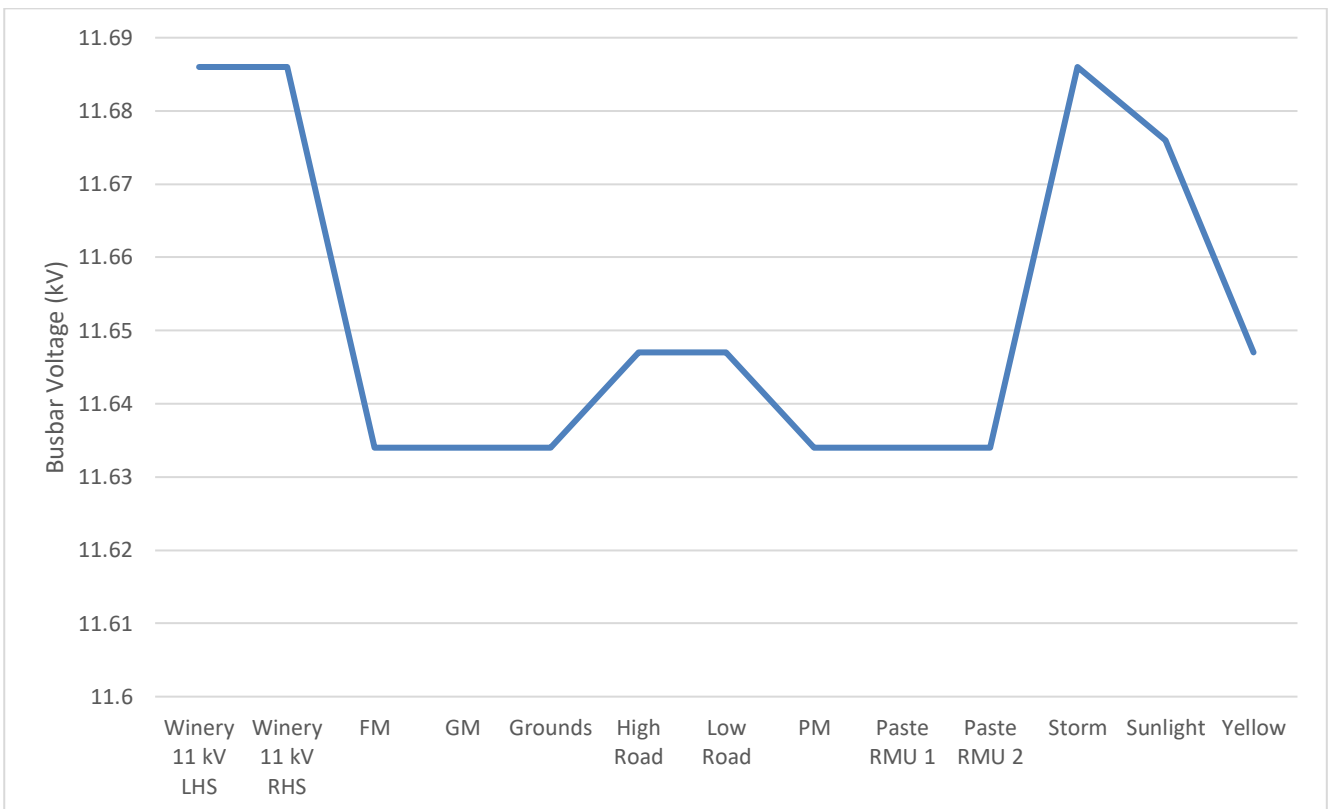


Figure 5.18: The voltage profile for the Winery MS group of busbars in the municipal network for Case 2

5.2.2 Protection grading results

The results for three of the nine selected faults are detailed below. The grading results for the remaining fault locations are shown in Appendix G.

a) Protection grading results for the Bushes substation

The grading for a three-phase fault of 4.191 kA and a single-phase-to-ground fault of 1.169 kA at the Bushes substation is shown in Tables 5-9 and 5-10.

Table 5-9: Branch currents and trip times for a three-phase fault at Bushes SS for the municipal network for Case 2

Substation	Feeder	Voltage Level (kV)	Fault Level Magnitude (kA)	Contribution	OCEF relay calculated trip time (s)
Atlantic	Bushes	11.66	4.191		0.120
Atlantic	Transformer 1 MV	11.66	3.344		1.237
Atlantic	Grounds	11.66	1.200		0.315
Winery	Yellow	11.66	1.200		0.221
Winery	Transformer 1 MV	11.66	1.202		3.230
Atlantic	Transformer 1 HV	33	1.182		1.593
Winery	Transformer 1 HV	33	0.425		3.948
Utility Sub	Utility Sub Switch Yard 1	33	0.211		N/A
Utility Sub	Utility Sub Switch Yard 2	33	0.213		N/A
Utility Sub	Atlantic 1	33	1.181		2.200
Utility Sub	Wind Turbine	33	1.290		N/A
Utility Sub	Incomer 1	33	0.372		N/A
Utility Sub	Incomer 2	33	0.372		N/A

Table 5-10: Branch currents and trip times for a single-phase fault at Bushes SS for the municipal network for Case 2

Substation	Feeder	Voltage Level (kV)	Fault Level Magnitude (kA)	Contribution	OCEF relay calculated trip time (s)
Atlantic	Bushes	11.66	1.169		0.150
Atlantic	Transformer 1 MV	11.66	0.914		1.907
Atlantic	Grounds	11.66	0.255		0.460
Winery	Yellow	11.66	0.255		0.238
Winery	Transformer 1 MV	11.66	0.255		5.020
Atlantic	Transformer 1 HV	33	0.207		N/A
Winery	Transformer 1 HV	33	0.074		N/A
Utility Sub	Utility Sub Switch Yard 1	33	0.037		N/A
Utility Sub	Utility Sub Switch Yard 2	33	0.038		N/A
Utility Sub	Atlantic 1	33	0.207		N/A
Utility Sub	Wind Turbine	33	1.261		N/A
Utility Sub	Incomer 1	33	0.324		N/A
Utility Sub	Incomer 2	33	0.324		N/A

b) Protection grading results for the Winelands RMU 1 substation

The grading for a three-phase fault of 7.701 kA and a single-phase-to-ground fault of 1.977 kA at the Winelands RMU 1 substation is shown in Tables 5-11 and 5-12.

Table 5-11: Currents and trip times for a three-phase fault at Winelands RMU 1 SS for the municipal network for Case 2

Substation	Feeder	Voltage Level (kV)	Fault Level Stage 1 Magnitude Contribution (kA)	OCEF relay stage 1 calculated trip time (s)	Fault Level Stage 2 Magnitude Contribution (kA)	OCEF relay stage 2 calculated trip time (s)	Fault Level Stage 3 Magnitude Contribution (kA)	OCEF relay stage 3 calculated trip time (s)	Overall Trip Time (s)
Winelands	Winelands RMU 1	11.66	7.630	0.120	0	N/A	0	N/A	0.120
Winelands	Weet	11.66	1.121	1.680	0.879	2.205	4.367	0.715	1.145
Wozniak	Winelands	11.66	6.580	0.608	5.158	0.667	0	N/A	0.655
Wozniak	Weet	11.66	1.121	1.680	0.879	2.205	4.367	0.715	1.145
Wozniak	Transformer A MV	11.66	3.935	1.688	3.093	1.948	2.244	2.448	2.257
Wozniak	Transformer B MV	11.66	3.771	1.729	2.964	2.003	2.151	2.534	2.336
Wozniak	Transformer A HV	33	1.390	0.944	1.093	1.105	0.793	1.428	1.210
Wozniak	Transformer B HV	33	1.332	0.969	1.047	1.140	0.760	1.485	1.259
Utility Sub	Wozniak A	33	1.390	1.847	1.093	2.163	0.793	2.793	2.576
Utility Sub	Wozniak B	33	1.332	1.896	1.047	2.230	0.760	2.905	2.679
Utility Sub	Wind Turbine	33	1.317	N/A	1.303	N/A	1.290	N/A	N/A
Utility Sub	Incomer 1	33	0.968	N/A	0.674	N/A	0.398	N/A	N/A
Utility Sub	Incomer 2	33	0.968	N/A	0.674	N/A	0.398	N/A	N/A

Table 5-12: Currents and trip times for a single-phase fault at Winelands RMU 1 SS for the municipal network for Case 2

Substation	Feeder	Voltage Level (kV)	Fault Level Stage 1 Magnitude Contribution (kA)	OCEF relay stage 1 calculated trip time (s)	Fault Level Stage 2 Magnitude Contribution (kA)	OCEF relay stage 2 calculated trip time (s)	Fault Level Stage 3 Magnitude Contribution (kA)	OCEF relay stage 3 calculated trip time (s)	Overall Trip Time (s)
Winelands	Winelands RMU 1	11.66	1.966	0.120	0	N/A	0	N/A	0.120
Winelands	Weet	11.66	0.249	1.221	0.189	1.614	1.178	0.507	0.740
Wozniak	Winelands	11.66	1.728	0.453	1.315	0.486	0	N/A	0.357
Wozniak	Weet	11.66	0.249	1.221	0.189	1.614	1.178	0.507	0.740
Wozniak	Transformer A MV	11.66	0.996	1.407	0.758	1.680	0.594	2.029	1.927
Wozniak	Transformer B MV	11.66	0.980	1.421	0.746	1.699	0.584	2.057	1.953
Wozniak	Transformer A HV	33	0.219	N/A	0.170	N/A	0.136	N/A	N/A
Wozniak	Transformer B HV	33	0.210	N/A	0.163	N/A	0.130	N/A	N/A
Utility Sub	Wozniak A	33	0.219	N/A	0.170	N/A	0.136	N/A	N/A
Utility Sub	Wozniak B	33	0.210	N/A	0.163	N/A	0.130	N/A	N/A
Utility Sub	Wind Turbine	33	1.262	N/A	1.261	N/A	1.261	N/A	N/A
Utility Sub	Incomer 1	33	0.349	N/A	0.334	N/A	0.324	N/A	N/A
Utility Sub	Incomer 2	33	0.349	N/A	0.334	N/A	0.324	N/A	N/A

c) Protection grading results for the Short substation

The grading for a three-phase fault of 10.505 kA and a single-phase-to-ground fault of 1.718 kA at the Short substation is shown in Tables 5-13 and 5-14.

Table 5-13: Branch currents and trip times for a three-phase fault at Short SS for the municipal network for Case 2

Substation	Feeder	Voltage Level (kV)	Stage 1 Fault Level Magnitude Contribution (kA)	Stage 1 OCEF relay calculated trip time (s)	Stage 2 Fault Level Magnitude Contribution (kA)	Stage 2 OCEF relay calculated trip time (s)	Stage 3 Fault Level Magnitude Contribution (kA)	Stage 3 OCEF relay calculated trip time (s)	Overall Trip Time (s)
Short	Workplace	11.66	5.192	0.692	7.547	0.602	9.554	0.590	0.640
Short	Glassware	11.66	1.687	0.479	2.542	0.379	0	N/A	0.444
Short	British	11.66	3.640	0.310	0	N/A	0	N/A	0.310
Workplace	Glassware	11.66	1.687	1.246	2.542	0.986	0	N/A	N/A
Workplace	British 1	11.66	1.270	1.497	0	N/A	0	N/A	N/A
Workplace	British 2	11.66	2.396	0.960	0	N/A	0	N/A	N/A
Workplace	Transformer 1 MV	11.66	5.250	1.269	5.011	1.319	4.802	1.368	1.339
Workplace	Transformer 2 MV	11.66	5.294	1.261	5.053	1.310	4.842	1.358	1.329
Workplace	Transformer 1 HV	33	1.855	1.265	1.771	1.312	1.697	1.358	1.331
Workplace	Transformer 2 HV	33	1.871	1.257	1.785	1.303	1.711	1.349	1.322
Utility Sub	Workplace 1	33	1.855	2.174	1.771	2.257	1.696	2.340	2.311
Utility Sub	Workplace 2	33	1.871	2.159	1.785	2.242	1.711	2.323	2.295
Utility Sub	Wind Turbine	33	1.338	N/A	1.334	N/A	1.331	N/A	N/A
Utility Sub	Incomer 1	33	1.426	N/A	1.340	N/A	1.264	N/A	N/A
Utility Sub	Incomer 2	33	1.426	N/A	1.340	N/A	1.264	N/A	N/A

Table 5-14: Branch currents and trip times for a single-phase fault at Short SS for the municipal network for Case 2

Substation	Feeder	Voltage Level (kV)	Stage 1 Fault Level Magnitude Contribution (kA)	Stage 1 OCEF relay calculated trip time (s)	Stage 2 Fault Level Magnitude Contribution (kA)	Stage 2 OCEF relay calculated trip time (s)	Stage 3 Fault Level Magnitude Contribution (kA)	Stage 3 OCEF relay calculated trip time (s)	Overall Trip Time (s)
Short	Workplace	11.66	0.707	1.047	1.158	0.815	1.480	0.734	0.878
Short	Glassware	11.66	0.258	0.909	0.422	0.549	0	N/A	0.697
Short	British	11.66	0.754	0.374	0	N/A	0	N/A	0.374
Workplace	Glassware	11.66	0.258	2.455	0.422	1.483	0	N/A	N/A
Workplace	British 1	11.66	0.533	0.869	0	N/A	0	N/A	N/A
Workplace	British 2	11.66	0.221	1.635	0	N/A	0	N/A	N/A
Workplace	Transformer 1 MV	11.66	0.859	3.590	0.790	3.974	0.740	4.340	4.232
Workplace	Transformer 2 MV	11.66	0.859	3.590	0.790	3.974	0.740	4.340	4.232
Workplace	Transformer 1 HV	33	0.295	N/A	0.281	N/A	0.271	N/A	N/A
Workplace	Transformer 2 HV	33	0.297	N/A	0.284	N/A	0.274	N/A	N/A
Utility Sub	Workplace 1	33	0.295	N/A	0.281	N/A	0.271	N/A	N/A
Utility Sub	Workplace 2	33	0.297	N/A	0.284	N/A	0.274	N/A	N/A
Utility Sub	Wind Turbine	33	1.261	N/A	1.261	N/A	1.261	N/A	N/A
Utility Sub	Incomer 1	33	0.337	N/A	0.333	N/A	0.330	N/A	N/A
Utility Sub	Incomer 2	33	0.337	N/A	0.333	N/A	0.330	N/A	N/A

5.3 Case 3: PBIL optimal DGs installed at the busbars

5.3.1 Optimal DG placement results

Upon running the PBIL algorithm, the results shown in Table 5-15 were obtained.

Table 5-15: PBIL placement results and definite-time protection settings for the municipal network for Case 3

<i>Turbine Location</i>	<i>Turbine Apparent Power Generation (MVA)</i>	<i>Turbine Real Generation (MW)</i>	<i>Turbine Reactive Generation (MVar)</i>	<i>Power Factor</i>	<i>Maximum fault contribution (MVA)</i>	<i>Definite-time protection pickup (A)</i>	<i>Definite trip time (s)</i>
Bus 1 – Utility Sub Source	0	0	0	N/A	0	0	0.400
Bus 2 – Utility Sub	0.591	0.473	0.355	0.800	0.710	11.381	0.400
Bus 3 – LHS Gardens HV	3.098	3.098	0	1.000	3.718	59.621	0.400
Bus 4 – RHS Gardens HV	3.061	2.449	1.837	0.800	3.674	58.917	0.400
Bus 5 – LHS Atlantic HV	2.330	2.330	0	1.000	2.796	44.841	0.400
Bus 6 – RHS Atlantic HV	3.896	3.896	0	1.000	4.675	74.979	0.400
Bus 7 – LHS Delilah HV	2.121	1.697	1.273	0.800	2.546	40.826	0.400
Bus 8 – RHS Delilah HV	3.479	2.783	2.087	0.800	4.174	66.946	0.400
Bus 9 – LHS Wozniak B HV	2.713	2.170	1.628	0.800	3.255	52.208	0.400
Bus 10 – LHS Wozniak A HV	3.339	2.705	1.958	0.810	4.007	64.264	0.400
Bus 11 – RHS Wozniak C HV	4.070	3.256	2.442	0.800	4.884	78.327	0.400
Bus 12 – LHS Sunset Vista B HV	3.548	3.548	0	1.000	4.258	68.281	0.400
Bus 13 – LHS Sunset Vista A HV	1.252	1.252	0	1.000	1.502	24.095	0.400
Bus 14 – RHS Sunset Vista C HV	1.183	1.029	0.583	0.870	1.419	22.761	0.400
Bus 15 – RHS Sunset Vista D HV	0.591	0.473	0.355	0.800	0.710	11.381	0.400
Bus 16 – LHS Workplace HV	2.365	1.892	1.419	0.800	2.838	45.514	0.400
Bus 17 – RHS Workplace HV	2.087	1.670	1.252	0.800	2.505	40.168	0.400
Bus 18 – Utility Sub Switch Yard	2.991	2.692	1.304	0.900	3.589	57.566	0.400
Bus 19 – Winery HV	1.670	1.336	1.002	0.800	2.004	32.139	0.400
Bus 20 – LHS Gardens LV	0.348	0.278	0.209	0.800	0.417	18.944	0.400
Bus 21 – RHS Gardens LV	0.556	0.445	0.334	0.800	0.668	30.305	0.400
Bus 22 – LHS Atlantic LV	3.026	3.026	0	1.000	3.631	164.817	0.400
Bus 23 – RHS Atlantic LV	2.017	2.017	0	1.000	2.420	109.860	0.400
Bus 24 – LHS Delilah LV	3.757	3.757	0	1.000	4.508	204.633	0.400
Bus 25 – RHS Delilah LV	2.470	2.025	1.414	0.820	2.964	134.524	0.400
Bus 26 – LHS Wozniak LV	0.383	0.306	0.230	0.800	0.459	20.850	0.400
Bus 27 – RHS Wozniak LV	3.409	3.409	0	1.000	4.091	185.678	0.400
Bus 28 – LHS Sunset Vista LV	3.930	3.144	2.358	0.800	4.716	214.055	0.400
Bus 29 – RHS Sunset Vista LV	2.783	2.226	1.670	0.800	3.339	151.571	0.400
Bus 30 – Workplace LV	3.687	3.687	0	1.000	4.424	200.820	0.400
Bus 31 – Winery LV	1.252	1.002	0.751	0.800	1.503	68.204	0.400

This configuration was installed in the DigSILENT PowerFactory case file and results were recorded in the following sections.

5.3.2 Load flow results

The load flow results obtained from the MATPOWER and DigSILENT PowerFactory load flow are shown in Tables 5-16 and 5-17. Network voltage profiles are shown in Figures 5.19 through 5.27.

Table 5-16: The MATPOWER network overview results for the municipal network for Case 3

<i>Grid Active Power Generation (MW)</i>	<i>Grid Reactive Power Generation (MVar)</i>	<i>Turbine Active Power Generation (MW)</i>	<i>Turbine Reactive Power Generation (MVar)</i>	<i>Active Load (MW)</i>	<i>Reactive Load (MVar)</i>	<i>Active Power Losses (MW)</i>	<i>Reactive Power Losses (MVar)</i>
-21.879	-14.371	64.071	24.461	41.552	8.864	0.639	1.665

Table 5-17: The DigSILENT PowerFactory network overview results for the municipal network for Case 3

<i>Grid Active Power Generation (MW)</i>	<i>Grid Reactive Power Generation (MVar)</i>	<i>Turbine Active Power Generation (MW)</i>	<i>Turbine Reactive Power Generation (MVar)</i>	<i>Active Load (MW)</i>	<i>Reactive Load (MVar)</i>	<i>Active Power Losses (MW)</i>	<i>Reactive Power Losses (MVar)</i>
-21.800	-14.204	64.071	24.459	41.552	8.864	0.719	1.803

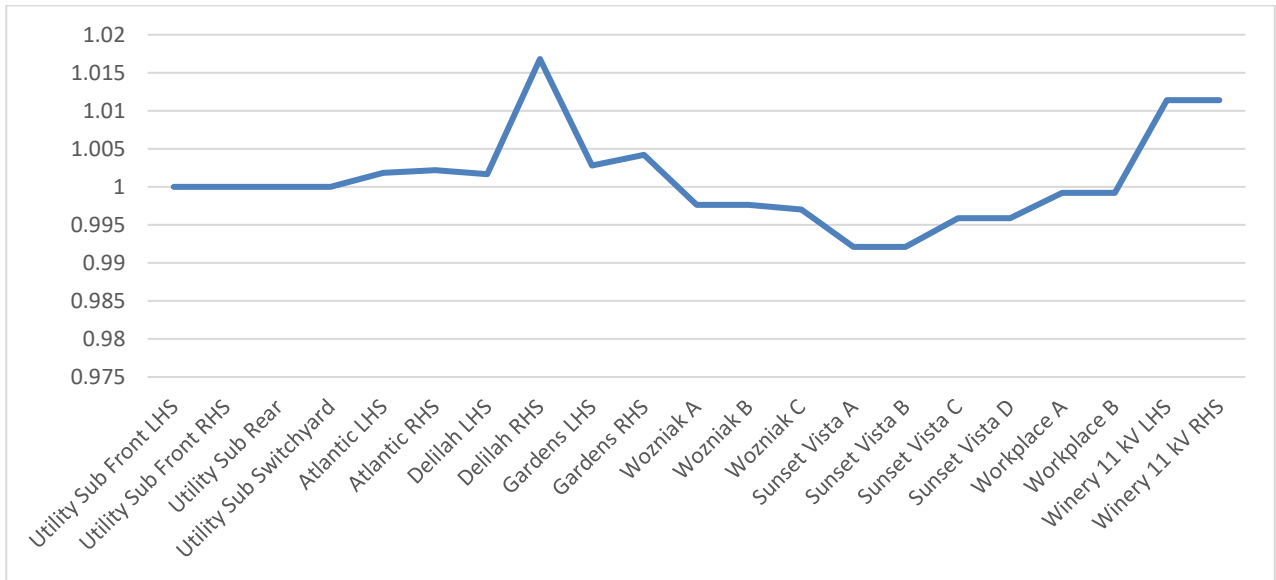


Figure 5.19: Graph showing the voltage profile for the main substations in the municipal network for Case 3

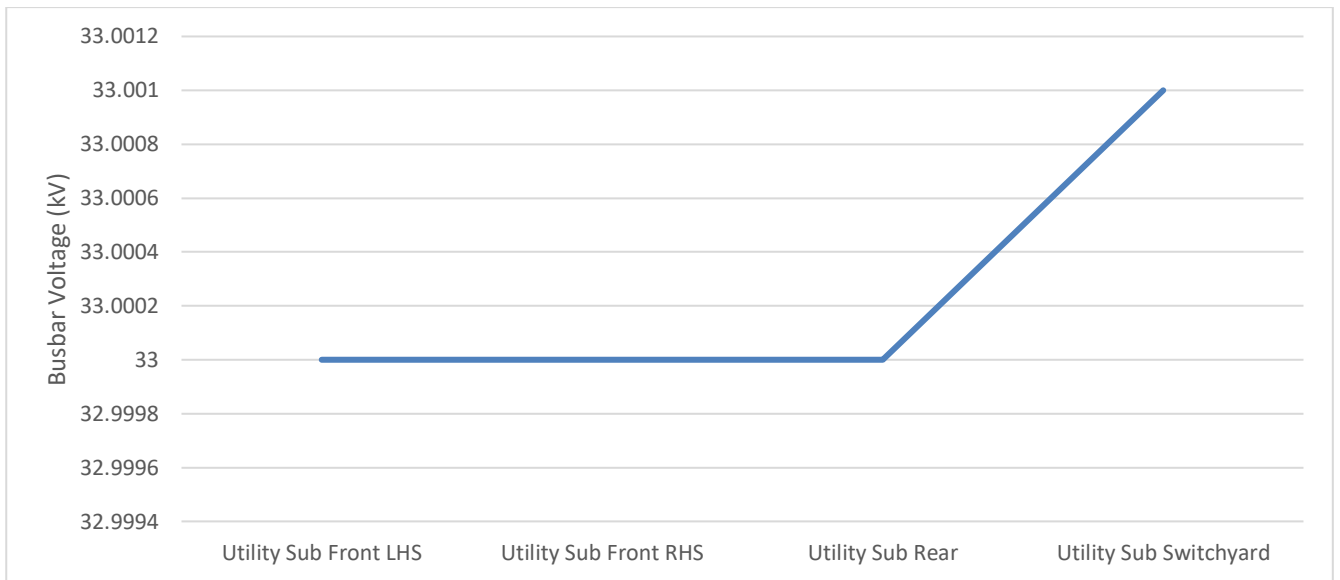


Figure 5.20: The voltage profile for the Utility substation group of busbars in the municipal network for Case 3

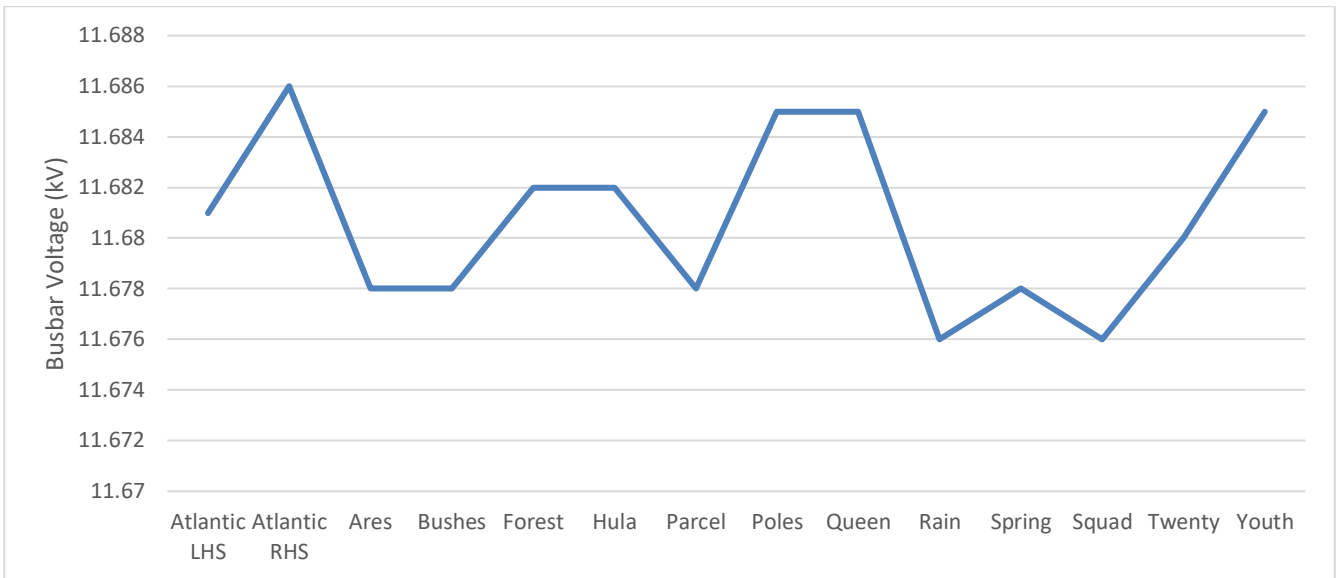


Figure 5.21: The voltage profile for the Atlantic MS group of busbars in the municipal network for Case 3

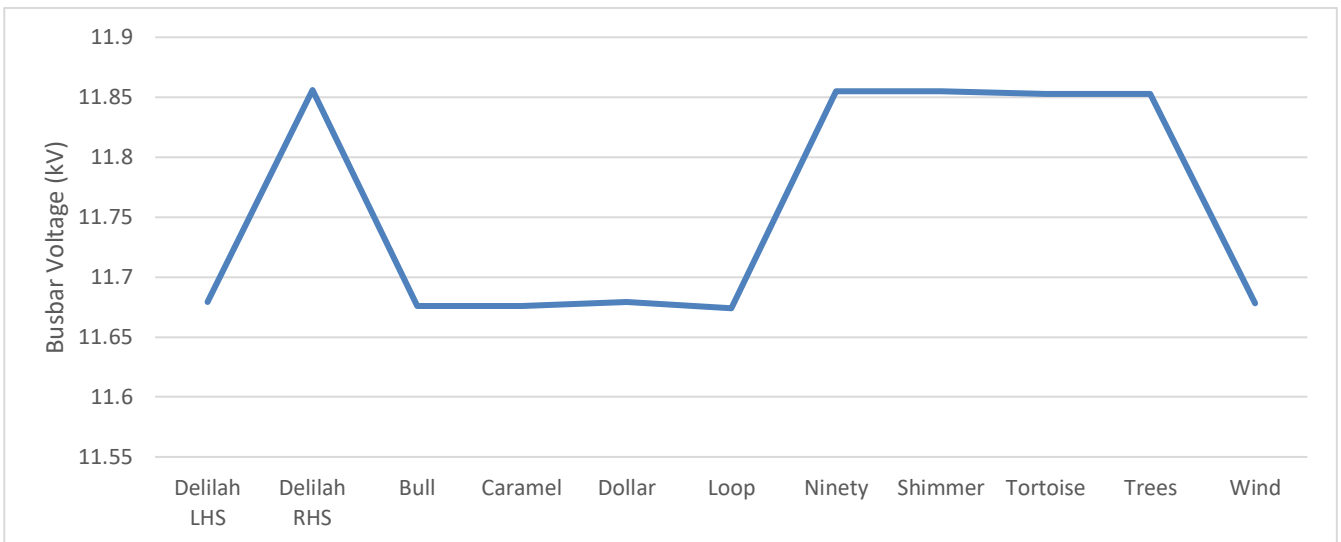


Figure 5.22: The voltage profile for the Delilah MS group of busbars in the municipal network for Case 3

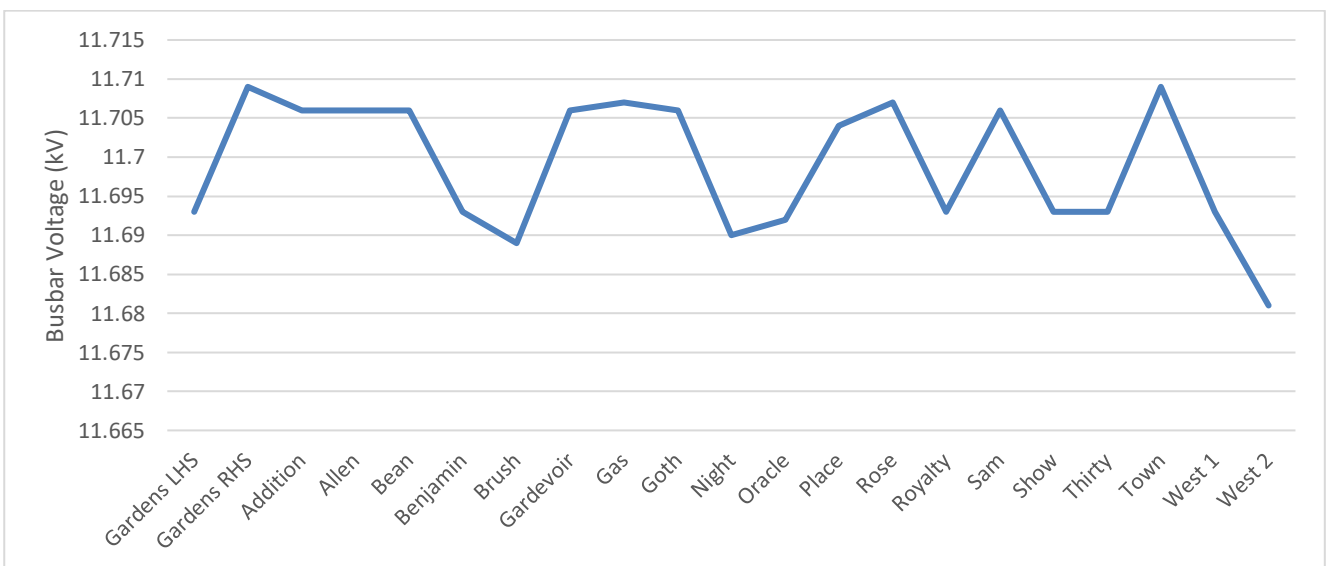


Figure 5.23: The voltage profile for the Gardens MS group of busbars in the municipal network for Case 3

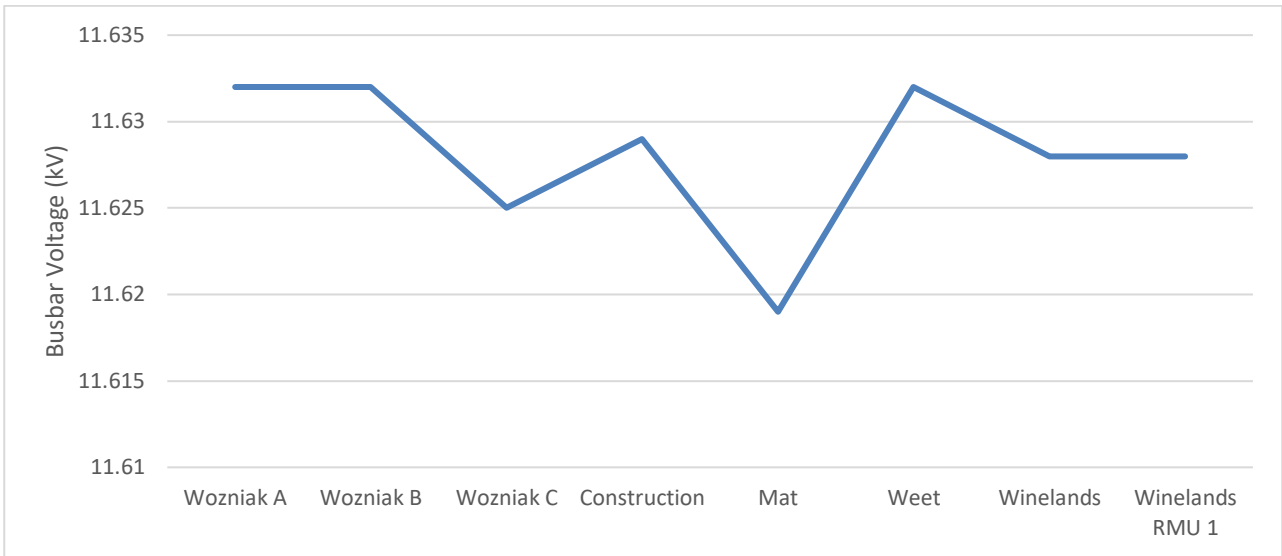


Figure 5.24: The voltage profile for the Wozniak group of busbars in the municipal network for Case 3

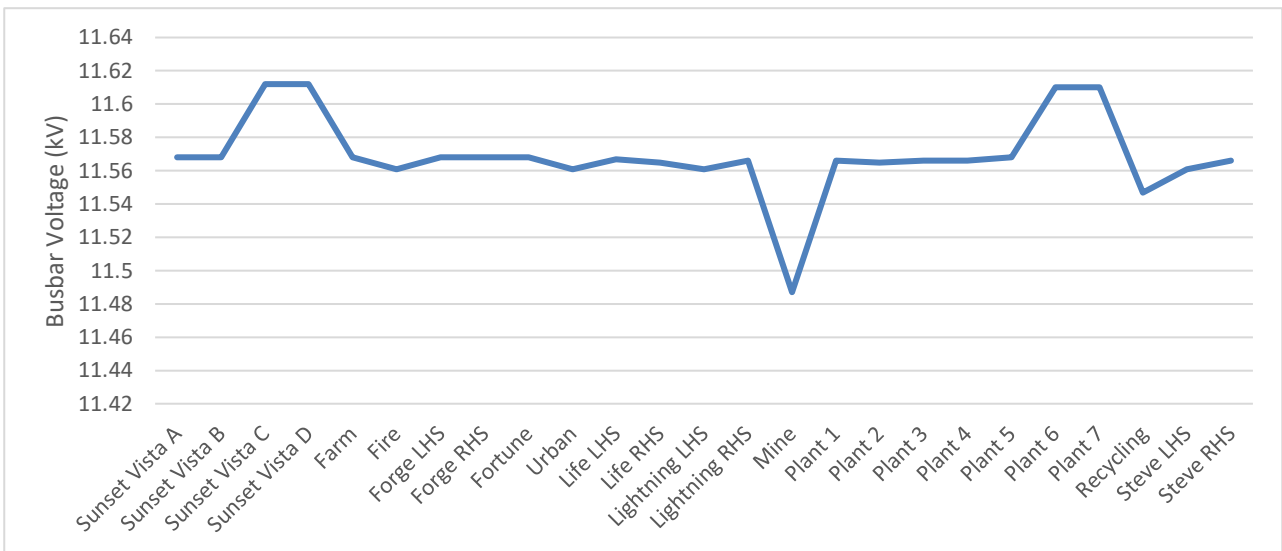


Figure 5.25: The voltage profile for the Sunset Vista MS group of busbars in the municipal network for Case 3

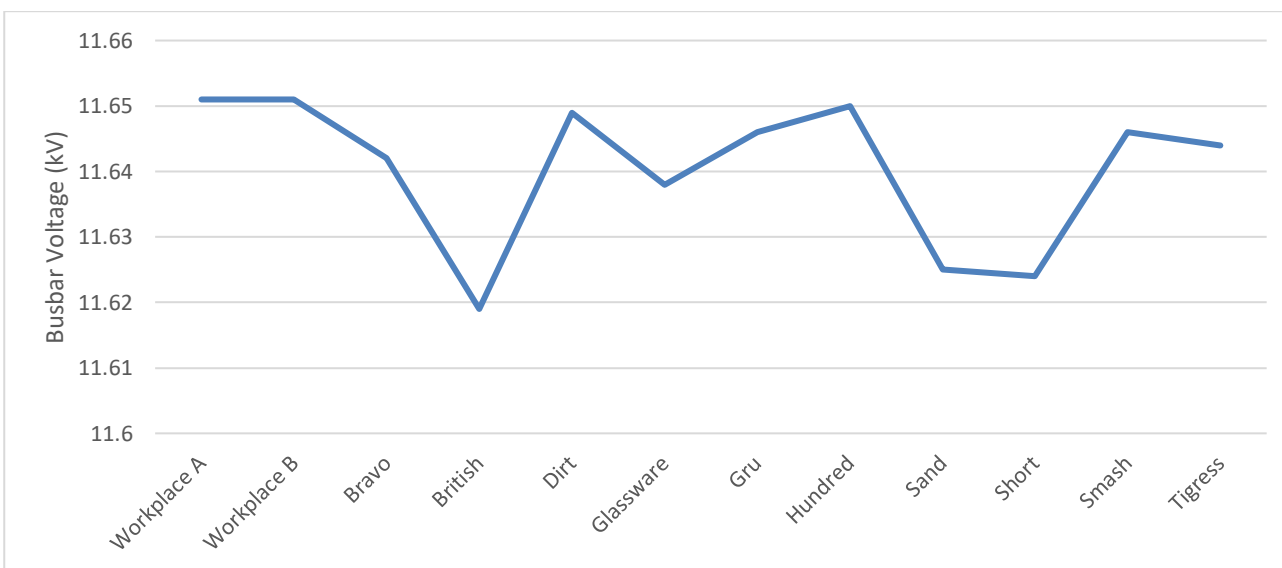


Figure 5.26: The voltage profile for the Workplace MS group of busbars in the municipal network for Case 3

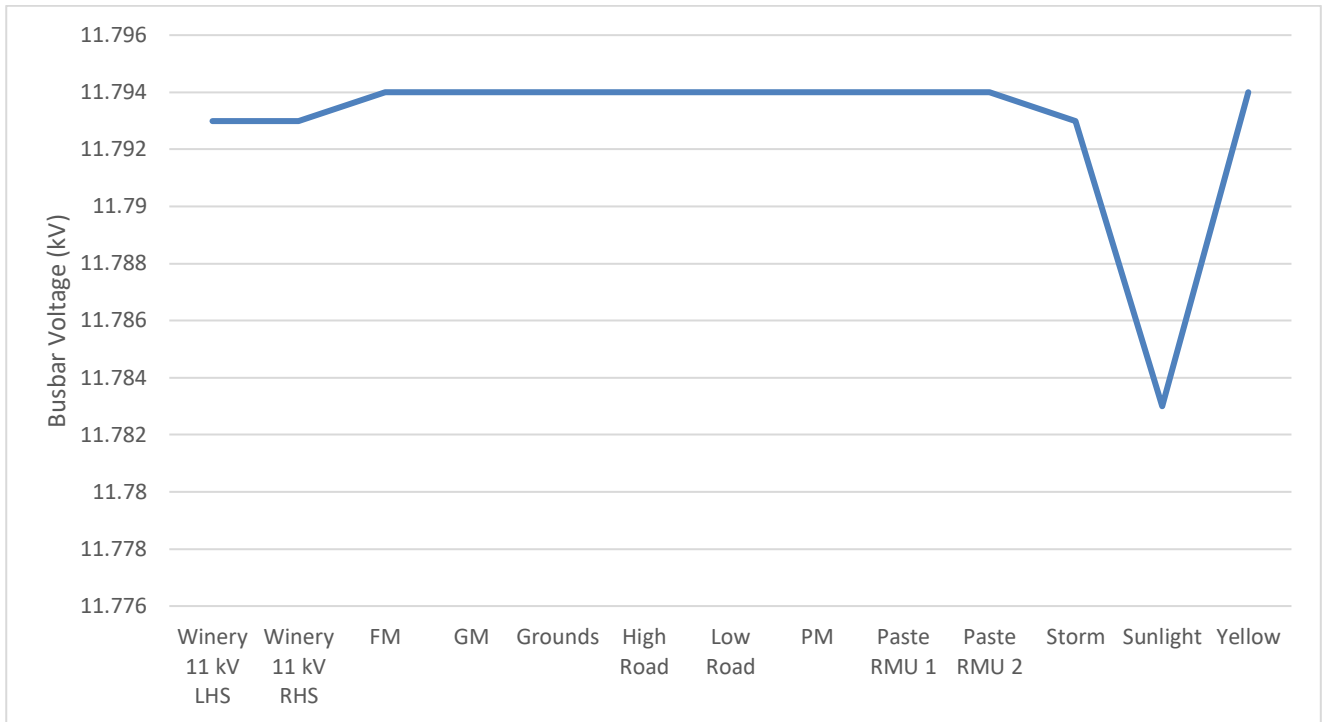


Figure 5.27: The voltage profile for the Winery MS group of busbars in the municipal network for Case 3

5.3.3 Protection grading results

The results for three of the nine selected faults are detailed below, as previously discussed. The grading results for the remaining fault locations are shown in Appendix G.

a) Protection grading results for the Bushes substation

The grading for a three-phase fault of 4.304 kA and a single-phase-to-ground fault of 1.182 kA at the Bushes substation is shown in Tables 5-18 and 5-19.

Table 5-18: Branch currents and trip times for a three-phase fault at Bushes SS for the municipal network for Case 3

Substation	Feeder	Voltage Level (kV)	Fault Level Magnitude Contribution (kA)	OCEF relay calculated trip time (s)
Atlantic	Bushes	11.66	4.304	0.120
Atlantic	Transformer 1 MV	11.66	3.316	1.243
Atlantic	Grounds	11.66	1.208	0.313
Winery	Yellow	11.66	1.208	0.220
Winery	Transformer 1 MV	11.66	1.146	3.488
Atlantic	Wind Turbine - LHS LV	11.66	0.182	0.420
Atlantic	Transformer 1 HV	33	1.172	1.601
Winery	Transformer 1 HV	33	0.405	4.236
Utility Sub	Utility Sub Switch Yard 1	33	0.160	N/A
Utility Sub	Utility Sub Switch Yard 2	33	0.162	N/A
Utility Sub	Atlantic 1	33	1.160	2.249
Utility Sub	Incomer 1	33	0.507	N/A
Utility Sub	Incomer 2	33	0.507	N/A

Table 5-19: Branch currents and trip times for a single-phase fault at Bushes SS for the municipal network for Case 3

<i>Substation</i>	<i>Feeder</i>	<i>Voltage Level (kV)</i>	<i>Fault Level Contribution (kA)</i>	<i>Magnitude</i>	<i>OCEF relay calculated trip time (s)</i>
Atlantic	Bushes	11.66	1.182		0.150
Atlantic	Transformer 1 MV	11.66	0.924		1.895
Atlantic	Grounds	11.66	0.258		0.454
Winery	Yellow	11.66	0.258		0.236
Winery	Transformer 1 MV	11.66	0.258		5.020
Atlantic	Wind Turbine - LHS LV	11.66	0.156		N/A
Atlantic	Transformer 1 HV	33	0.168		N/A
Winery	Transformer 1 HV	33	0.067		N/A
Utility Sub	Utility Sub Switch Yard 1	33	0.059		N/A
Utility Sub	Utility Sub Switch Yard 2	33	0.060		N/A
Utility Sub	Atlantic 1	33	0.151		N/A
Utility Sub	Incomer 1	33	0.239		N/A
Utility Sub	Incomer 2	33	0.239		N/A

b) Protection grading results for the Winelands RMU 1 substation

The grading for a three-phase fault of 7.710 kA and a single-phase-to-ground fault of 1.980 kA at the Winelands RMU 1 substation is shown in Tables 5-20 and 5-21.

Table 5-20: Currents and trip times for a three-phase fault at Winelands RMU 1 SS for the municipal network for Case 3

<i>Subst.</i>	<i>Feeder</i>	<i>Volt. Level (kV)</i>	<i>Stage 1 Fault Level Mag. Contr (kA)</i>	<i>Stage 1 OCEF relay calc. trip time (s)</i>	<i>Stage 2 Fault Level Mag. Contr (kA)</i>	<i>Stage 2 OCEF relay calc. trip time (s)</i>	<i>Stage 3 Fault Level Mag. Contr (kA)</i>	<i>Stage 3 OCEF relay calc. trip time (s)</i>	<i>Stage 4 Fault Level Mag. Contr (kA)</i>	<i>Stage 4 OCEF relay calc. trip time (s)</i>	<i>Overall Trip Time (s)</i>
Winelands	Winelands RMU 1	11.66	7.639	0.120	0	N/A	0	N/A	0	N/A	0.120
Winelands	Weet	11.66	1.123	1.678	0.881	2.199	0.880	2.203	4.371	0.714	1.144
Wozniak	Winelands	11.66	6.588	0.607	5.169	0.667	5.163	0.667	0	N/A	0.655
Wozniak	Weet	11.66	1.123	1.678	0.881	2.199	0.880	2.203	4.371	0.714	1.144
Wozniak	Transformer A MV	11.66	3.932	1.689	3.090	1.949	3.096	1.947	2.247	2.446	2.255
Wozniak	Transformer B MV	11.66	3.768	1.730	2.961	2.004	2.967	2.002	2.153	2.532	2.335
Wozniak	Wind Turbine - LHS LV	11.66	0.022	0.420	0.021	0.420	0	N/A	0	N/A	0.420
Wozniak	Transformer A HV	33	1.389	0.945	1.092	1.106	1.094	1.105	0.794	1.426	1.210
Wozniak	Transformer B HV	33	1.331	0.970	1.046	1.140	1.048	1.139	0.761	1.483	1.258
Utility Sub	Wozniak A	33	1.345	1.886	1.039	2.242	1.041	2.239	0.739	2.986	2.738
Utility Sub	Wozniak B	33	1.295	1.931	1.003	2.302	1.005	2.299	0.716	3.080	2.827
Utility Sub	Incomer 1	33	1.110	N/A	0.796	N/A	0.798	N/A	0.511	N/A	N/A
Utility Sub	Incomer 2	33	1.110	N/A	0.796	N/A	0.798	N/A	0.511	N/A	N/A

Table 5-21: Currents and trip times for a single-phase fault at Winelands RMU 1 SS for the municipal network for Case 3

<i>Subst.</i>	<i>Feeder</i>	<i>Volt. Level (kV)</i>	<i>Stage 1 Fault Level Mag. Contr (kA)</i>	<i>Stage 1 OCEF relay calc. trip time (s)</i>	<i>Stage 2 Fault Level Mag. Contr (kA)</i>	<i>Stage 2 OCEF relay calc. trip time (s)</i>	<i>Stage 3 Fault Level Mag. Contr (kA)</i>	<i>Stage 3 OCEF relay calc. trip time (s)</i>	<i>Overall Trip Time (s)</i>
Winelands	Winelands RMU 1	11.66	1.969	0.120	0	N/A	0	N/A	0.120
Winelands	Weet	11.66	0.249	1.219	0.189	1.612	1.180	0.506	0.821
Wozniak	Winelands	11.66	1.731	0.453	1.316	0.486	0	N/A	0.477
Wozniak	Weet	11.66	0.249	1.219	0.189	1.612	1.180	0.506	0.821
Wozniak	Transformer A MV	11.66	0.998	1.406	0.759	1.678	0.595	2.026	1.899
Wozniak	Transformer B MV	11.66	0.982	1.420	0.747	1.698	0.585	2.054	1.926
Wozniak	Wind Turbine - LHS LV	11.66	0.019	N/A	0.019	N/A	0.019	N/A	N/A
Wozniak	Transformer A HV	33	0.216	N/A	0.167	N/A	0.133	N/A	N/A
Wozniak	Transformer B HV	33	0.207	N/A	0.160	N/A	0.127	N/A	N/A
Utility Sub	Wozniak A	33	0.184	N/A	0.137	N/A	0.104	N/A	N/A
Utility Sub	Wozniak B	33	0.181	N/A	0.135	N/A	0.103	N/A	N/A
Utility Sub	Incomer 1	33	0.239	N/A	0.238	N/A	0.238	N/A	N/A
Utility Sub	Incomer 2	33	0.239	N/A	0.238	N/A	0.238	N/A	N/A

c) Protection grading results for the Short substation

The grading for a three-phase fault of 10.609 kA and a single-phase-to-ground fault of 1.721 kA at the Short substation is shown in Tables 5-22 and 5-23.

Table 5-22: Branch currents and trip times for a three-phase fault at Short SS for the municipal network for Case 3

<i>Subst.</i>	<i>Feeder</i>	<i>Volt. Level (kV)</i>	<i>Stage 1 Fault Level Mag. Contr (kA)</i>	<i>Stage 1 OCEF relay calc. trip time (s)</i>	<i>Stage 2 Fault Level Mag. Contr (kA)</i>	<i>Stage 2 OCEF relay calc. trip time (s)</i>	<i>Stage 3 Fault Level Mag. Contr (kA)</i>	<i>Stage 3 OCEF relay calc. trip time (s)</i>	<i>Stage 4 Fault Level Mag. Contr (kA)</i>	<i>Stage 4 OCEF relay calc. trip time (s)</i>	<i>Overall Trip Time (s)</i>
Short	Workplace	11.66	5.243	0.689	7.620	0.600	7.550	0.601	9.559	0.590	0.637
Short	Glassware	11.66	1.704	0.476	2.476	0.377	2.453	0.379	0	N/A	0.441
Short	British	11.66	3.676	0.309	0	N/A	0	N/A	0	N/A	0.309
Workplace	Glassware	11.66	1.704	1.238	2.476	0.980	2.453	0.985	0	N/A	N/A
Workplace	British 1	11.66	1.282	1.485	0	N/A	0	N/A	0	N/A	N/A
Workplace	British 2	11.66	2.420	0.955	0	N/A	0	N/A	0	N/A	N/A
Workplace	Transformer 1 MV	11.66	5.223	1.275	4.980	1.326	5.014	1.316	4.805	1.367	1.340
Workplace	Transformer 2 MV	11.66	5.265	1.266	5.020	1.317	5.054	1.309	4.843	1.358	1.331
Workplace	Wind Turbine - LV	11.66	0.220	0.420	0.219	0.420	0	N/A	0	N/A	0.420
Workplace	Transformer 1 HV	33	1.845	1.270	1.760	1.318	1.772	1.311	1.698	1.358	1.332
Workplace	Transformer 2 HV	33	1.860	1.262	1.774	1.310	1.786	1.303	1.711	1.349	1.324
Utility Sub	Workplace 1	33	1.810	2.217	1.724	2.308	1.736	2.295	1.661	2.383	2.355
Utility Sub	Workplace 2	33	1.829	2.198	1.742	2.288	1.754	2.275	1.679	2.360	2.333
Utility Sub	Incomer 1	33	1.557	N/A	1.469	N/A	1.479	N/A	1.404	N/A	N/A
Utility Sub	Incomer 2	33	1.557	N/A	1.469	N/A	1.479	N/A	1.404	N/A	N/A

Table 5-23: Branch currents and trip times for a single-phase fault at Short SS for the municipal network for Case 3

Subst.	Feeder	Volt. Level (kV)	Stage 1 Fault Level Mag. Contr (kA)	Stage 1 OCEF relay calc. trip time (s)	Stage 2 Fault Level Mag. Contr (kA)	Stage 2 OCEF relay calc. trip time (s)	Stage 3 Fault Level Mag. Contr (kA)	Stage 3 OCEF relay calc. trip time (s)	Overall Trip Time (s)
Short	Workplace	11.66	0.708	1.046	1.160	0.814	1.482	0.733	0.877
Short	Glassware	11.66	0.258	0.907	0.423	0.549	0	N/A	0.697
Short	British	11.66	0.755	0.374	0	N/A	0	N/A	0.374
Workplace	Glassware	11.66	0.258	2.450	0.423	1.482	0	N/A	N/A
Workplace	British 1	11.66	0.534	0.868	0	N/A	0	N/A	N/A
Workplace	British 2	11.66	0.221	1.633	0	N/A	0	N/A	N/A
Workplace	Transformer 1 MV	11.66	0.860	3.584	0.792	3.967	0.741	4.331	4.223
Workplace	Transformer 2 MV	11.66	0.860	3.584	0.792	3.967	0.741	4.331	4.223
Workplace	Wind Turbine - LV	11.66	0.188	N/A	0.188	N/A	0.187	N/A	N/A
Workplace	Transformer 1 HV	33	0.263	N/A	0.249	N/A	0.239	N/A	N/A
Workplace	Transformer 2 HV	33	0.265	N/A	0.251	N/A	0.241	N/A	N/A
Utility Sub	Workplace 1	33	0.237	N/A	0.223	N/A	0.213	N/A	N/A
Utility Sub	Workplace 2	33	0.242	N/A	0.228	N/A	0.218	N/A	N/A
Utility Sub	Incomer 1	33	0.239	N/A	0.239	N/A	0.239	N/A	N/A
Utility Sub	Incomer 2	33	0.239	N/A	0.239	N/A	0.239	N/A	N/A

5.4 Case 4: Differential evolution optimal DGs installed at the busbars

5.4.1 Optimal DG placement results

Upon running the DE algorithm, the results shown in Table 5-24 were obtained.

Table 5-24: DE DG placement results and definite-time protection settings for the municipal network for Case 4

Turbine Location	Turbine Apparent Power Generation (MVA)	Turbine Real Generation (MW)	Turbine Reactive Generation (MVar)	Power Factor	Maximum fault contribution (MVA)	Definite-time protection pickup (A)	Definite trip time (s)
Bus 1 – Utility Sub Source	0	0	0	N/A	N/A	N/A	N/A
Bus 2 – Utility Sub	0.117	0.097	0.066	0.829	0.141	2.261	0.400
Bus 3 – LHS Gardens HV	1.450	1.450	0	1	1.740	27.903	0.400
Bus 4 – RHS Gardens HV	0.559	0.559	0	1	0.671	10.764	0.400
Bus 5 – LHS Atlantic HV	0.541	0.541	0	1	0.649	10.408	0.400
Bus 6 – RHS Atlantic HV	1.799	1.799	0	1	2.159	34.626	0.400
Bus 7 – LHS Delilah HV	2.686	2.149	1.612	0.8	3.223	51.692	0.400
Bus 8 – RHS Delilah HV	0	0	0	N/A	N/A	N/A	N/A
Bus 9 – LHS Wozniak B HV	0.665	0.665	0	1	0.798	12.806	0.400
Bus 10 – LHS Wozniak A HV	0.858	0.801	0.307	0.934	1.029	16.508	0.400
Bus 11 – RHS Wozniak C HV	3.028	3.028	0	1	3.63	58.276	0.400
Bus 12 – LHS Sunset Vista B HV	1.095	0.876	0.657	0.800	1.314	21.076	0.400
Bus 13 – LHS Sunset Vista A HV	1.015	1.015	0	1	1.218	19.541	0.400
Bus 14 – RHS Sunset Vista C HV	1.624	1.624	0	1	1.948	31.244	0.400
Bus 15 – RHS Sunset Vista D HV	3.302	3.302	0	1	3.961	63.539	0.400
Bus 16 – LHS Workplace HV	1.611	1.611	0	1	1.933	31.008	0.400
Bus 17 – RHS Workplace HV	0.407	0.325	0.244	0.800	0.488	7.825	0.400
Bus 18 – Utility Sub Switch Yard	2.944	2.902	0.495	0.986	3.533	56.660	0.400
Bus 19 – Winery HV	0.524	0.419	0.315	0.800	0.629	10.091	0.400
Bus 20 – LHS Gardens LV	0.860	0.770	0.383	0.895	1.031	46.824	0.400
Bus 21 – RHS Gardens LV	0.628	0.541	0.3194	0.861	0.754	34.214	0.400
Bus 22 – LHS Atlantic LV	0.545	0.545	0	1	0.654	29.663	0.400
Bus 23 – RHS Atlantic LV	1.712	1.712	0	1	2.054	93.220	0.400
Bus 24 – LHS Delilah LV	0.036	0.029	0.0218	0.800	0.044	1.980	0.400
Bus 25 – RHS Delilah LV	0	0	0	N/A	N/A	N/A	N/A
Bus 26 – LHS Wozniak LV	1.698	1.501	0.795	0.884	2.038	92.487	0.400
Bus 27 – RHS Wozniak LV	2.441	2.441	0	1	2.929	132.949	0.400
Bus 28 – LHS Sunset Vista LV	3.842	3.707	1.009	0.965	4.610	209.237	0.400
Bus 29 – RHS Sunset Vista LV	2.137	2.137	0	1	2.565	116.418	0.400
Bus 30 – Workplace LV	8.138	8.138	0	1	9.766	443.252	0.400
Bus 31 – Winery LV	0	0	0	N/A	N/A	N/A	N/A

5.4.2 Load flow results

The load flow results obtained from the MATPOWER and DigSILENT PowerFactory load flow are shown in Tables 5-25 and 5-26. Network voltage profiles are shown in Figures 5.28 through 5.36.

Table 5-25: The MATPOWER network overview results for the municipal network for Case 4

Grid Active Power Generation (MW)	Grid Reactive Power Generation (MVar)	Turbine Active Power Generation (MW)	Turbine Reactive Power Generation (MVar)	Active Load (MW)	Reactive Load (MVar)	Active Power Losses (MW)	Reactive Power Losses (MVar)
-3.104	2.786	44.684	6.222	41.552	8.684	0.029	0.569

Table 5-26: The DigSILENT PowerFactory network overview results for the municipal network for Case 4

Grid Active Power Generation (MW)	Grid Reactive Power Generation (MVar)	Turbine Active Power Generation (MW)	Turbine Reactive Power Generation (MVar)	Active Load (MW)	Reactive Load (MVar)	Active Power Losses (MW)	Reactive Power Losses (MVar)
-3.065	2.831	44.685	6.216	41.552	8.684	0.069	0.594

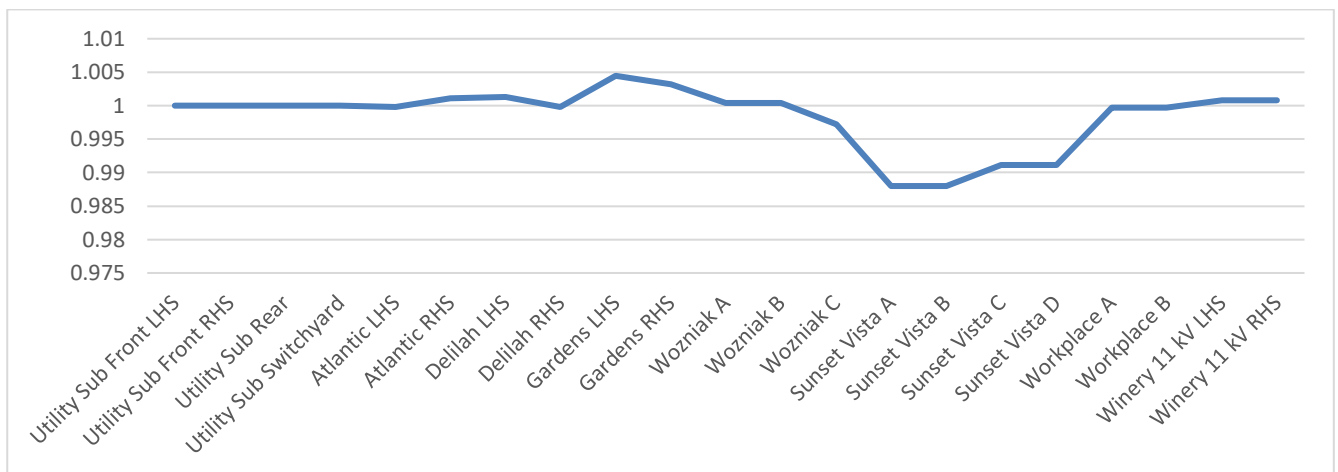


Figure 5.28: Graph showing the voltage profile for the main substations in the municipal network for Case 4

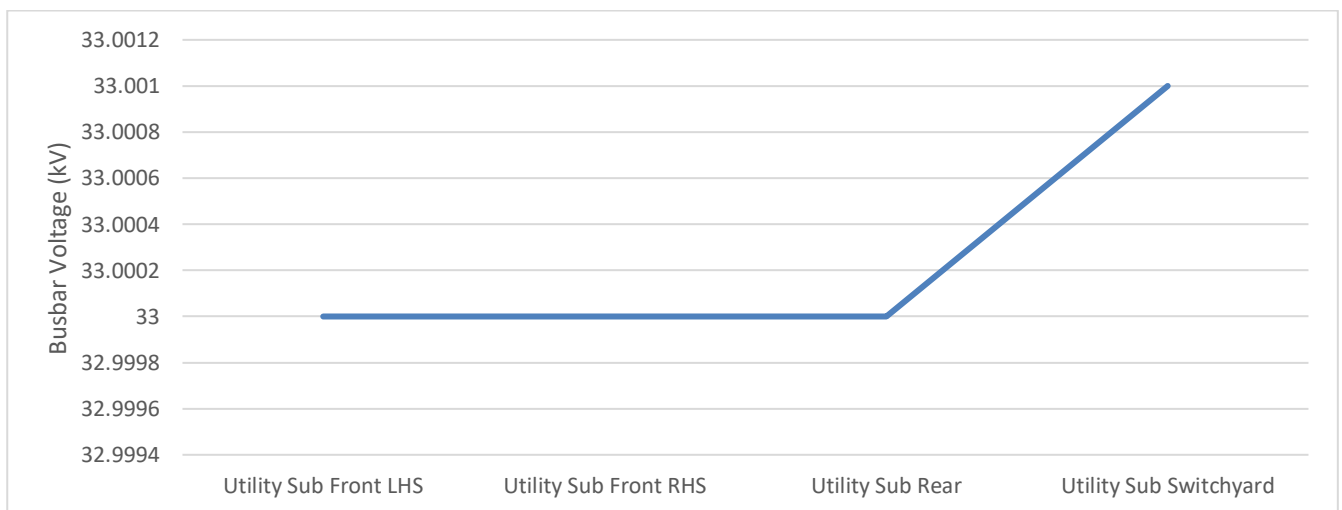


Figure 5.29: The voltage profile for the Utility substation group of busbars in the municipal network for Case 4

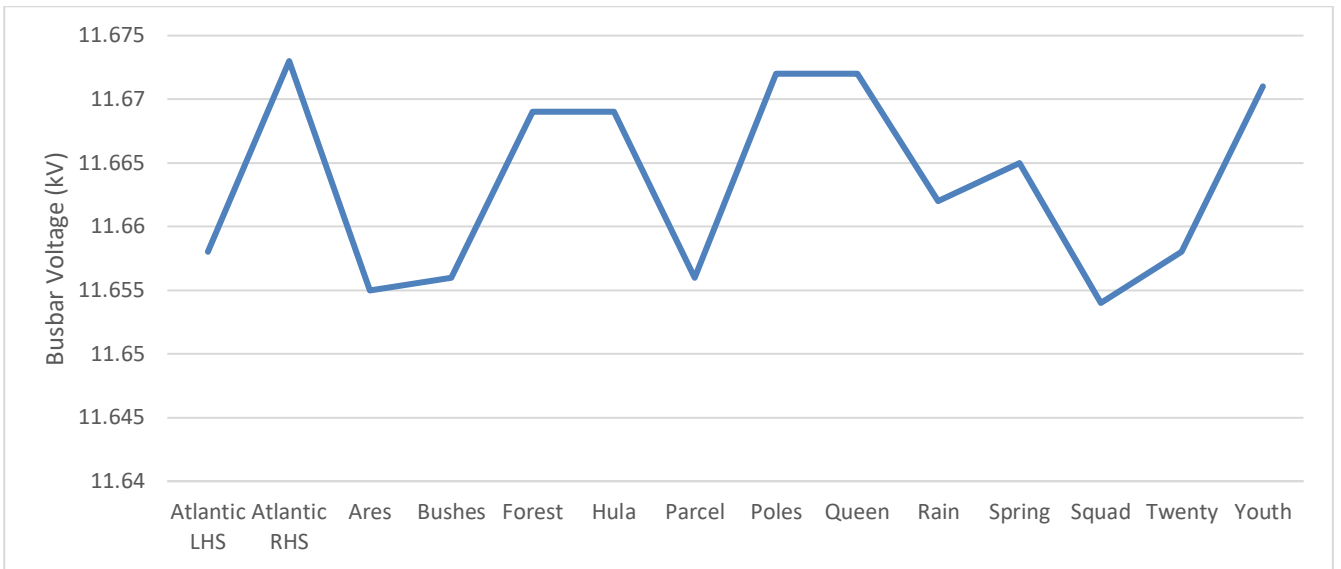


Figure 5.30: The voltage profile for the Atlantic MS group of busbars in the municipal network for Case 4

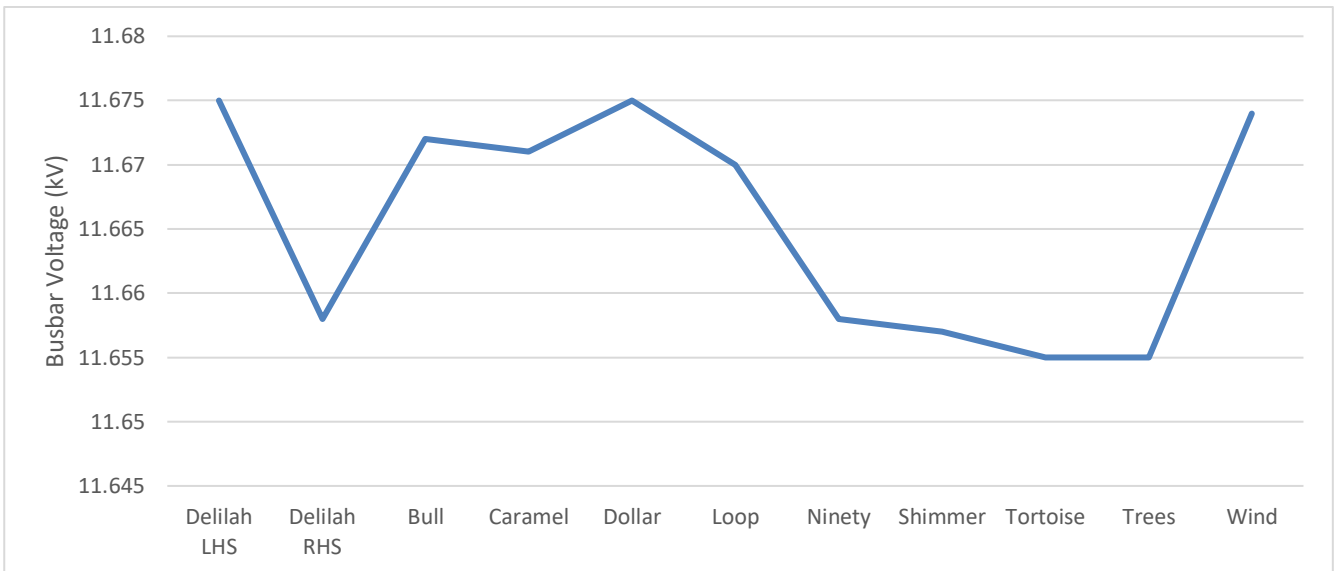


Figure 5.31: The voltage profile for the Delilah MS group of busbars in the municipal network for Case 4

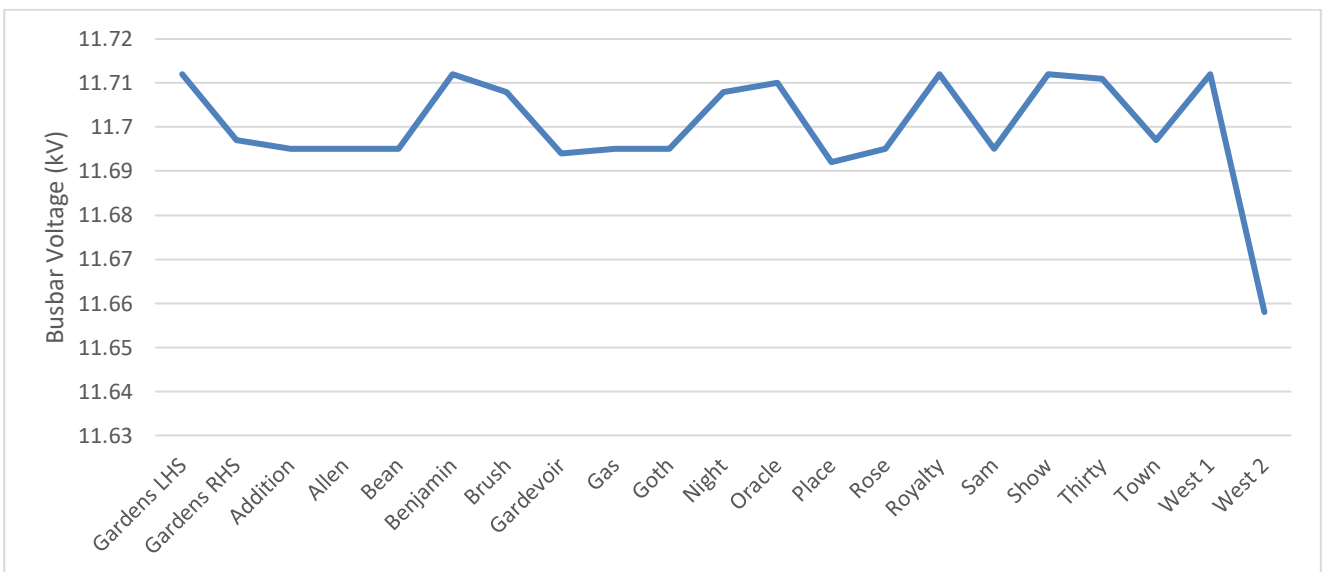


Figure 5.32: The voltage profile for the Gardens MS group of busbars in the municipal network for Case 4

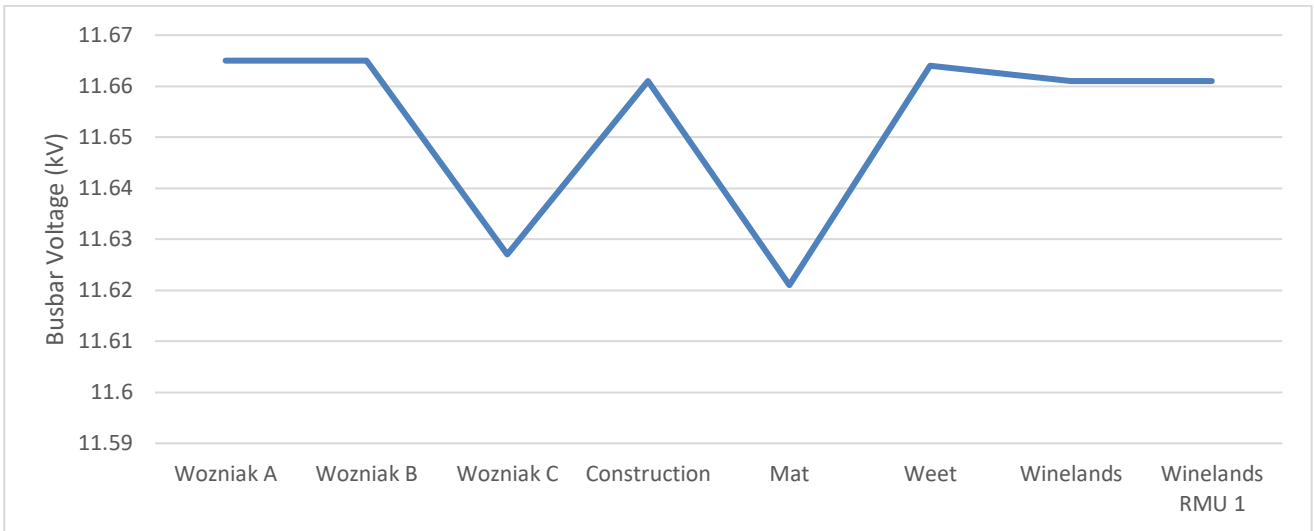


Figure 5.33: The voltage profile for the Wozniak group of busbars in the municipal network for Case 4

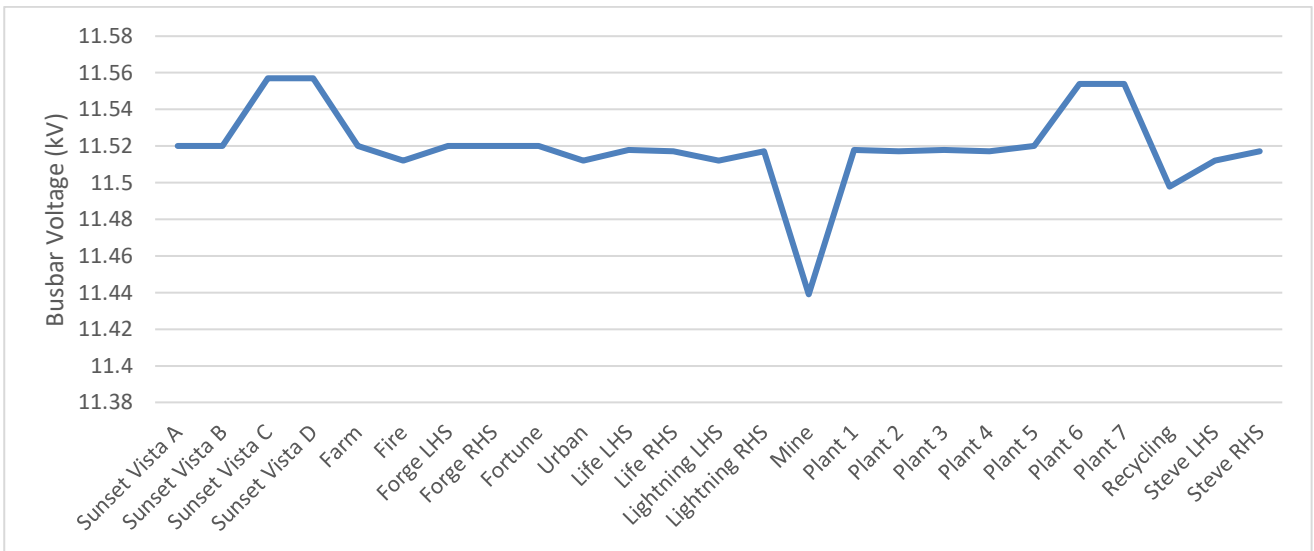


Figure 5.34: The voltage profile for the Sunset Vista MS group of busbars in the municipal network for Case 4

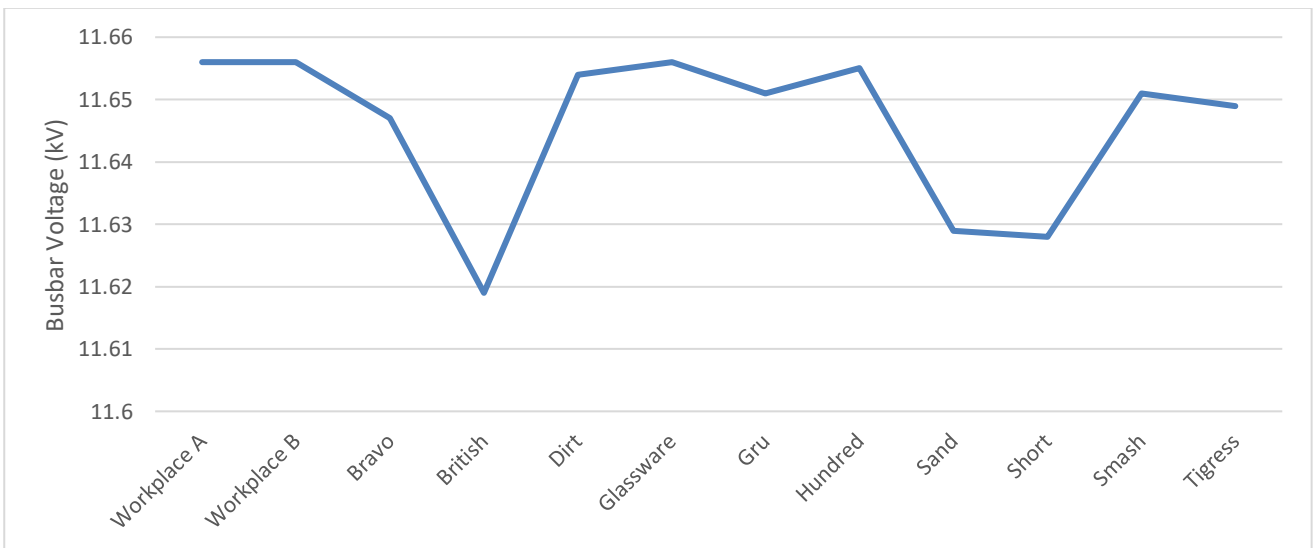


Figure 5.35: The voltage profile for the Workplace MS group of busbars in the municipal network for Case 4

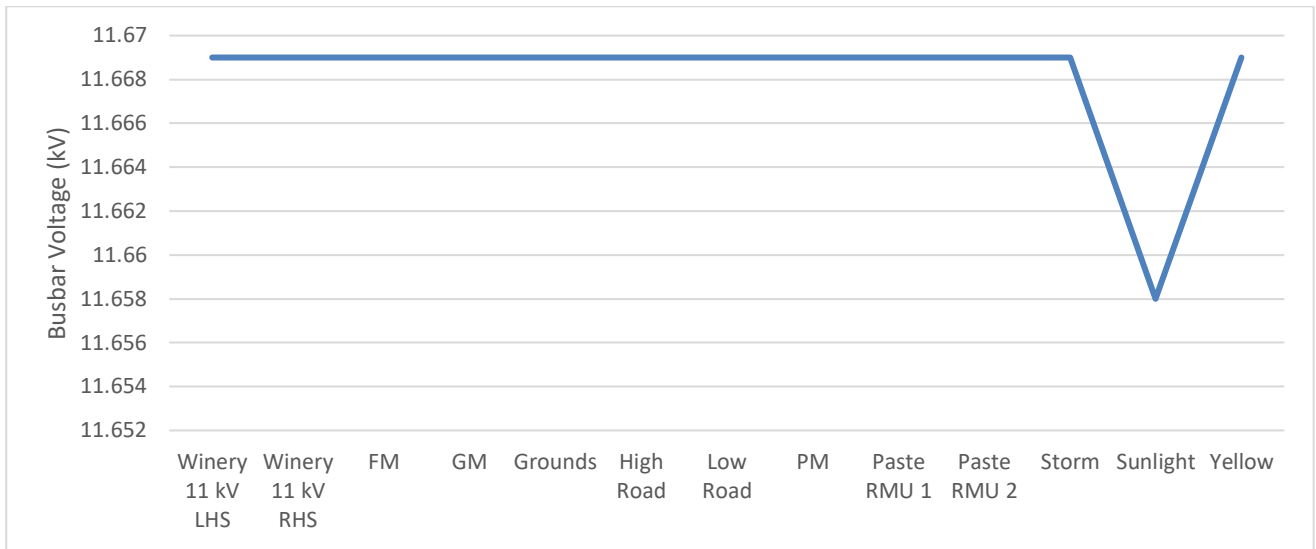


Figure 5.36: The voltage profile for the Winery MS group of busbars in the municipal network for Case 4

5.4.3 Protection grading results

The results for three of the nine selected faults are detailed below, as previously discussed. The grading results for the remaining fault locations are shown in Appendix G.

a) Protection grading results for the Bushes substation

The grading for a three-phase fault of 4.212 kA and a single-phase-to-ground fault of 1.172 kA at the Bushes substation is shown in Tables 5-27 and 5-28.

Table 5-27: Branch currents and trip times for a three-phase fault at Bushes SS for the municipal network for Case 4

Substation	Feeder	Voltage Level (kV)	Fault Level Magnitude Contribution (kA)	OCEF relay calculated trip time (s)
Atlantic	Bushes	11.66	4.212	0.120
Atlantic	Transformer 1 MV	11.66	3.339	1.238
Atlantic	Grounds	11.66	1.199	0.315
Winery	Yellow	11.66	1.199	0.221
Winery	Transformer 1 MV	11.66	1.201	3.235
Atlantic	Wind Turbine – LHS LV	11.66	0.033	0.420
Atlantic	Transformer 1 HV	33	1.180	1.594
Winery	Transformer 1 HV	33	0.424	3.954
Utility Sub	Utility Sub Switch Yard 1	33	0.181	N/A
Utility Sub	Utility Sub Switch Yard 2	33	0.183	N/A
Utility Sub	Atlantic 1	33	1.177	2.210
Utility Sub	Incomer 1	33	0.701	N/A
Utility Sub	Incomer 2	33	0.701	N/A

Table 5-28: Branch currents and trip times for a single-phase fault at Bushes SS for the municipal network for Case 4

Substation	Feeder	Voltage Level (kV)	Fault Level Magnitude Contribution (kA)	OCEF relay calculated trip time (s)
Atlantic	Bushes	11.66	1.172	0.150
Atlantic	Transformer 1 MV	11.66	0.916	1.905
Atlantic	Grounds	11.66	0.256	0.459
Winery	Yellow	11.66	0.256	0.238
Winery	Transformer 1 MV	11.66	0.256	5.020
Atlantic	Wind Turbine – LHS LV	11.66	0.028	N/A
Atlantic	Transformer 1 HV	33	0.199	N/A
Winery	Transformer 1 HV	33	0.072	N/A
Utility Sub	Utility Sub Switch Yard 1	33	0.038	N/A
Utility Sub	Utility Sub Switch Yard 2	33	0.038	N/A
Utility Sub	Atlantic 1	33	0.191	N/A
Utility Sub	Incomer 1	33	0.115	N/A
Utility Sub	Incomer 2	33	0.115	N/A

b) Protection grading results for the Winelands RMU 1 substation

The grading for a three-phase fault of 7.731 kA and a single-phase-to-ground fault of 1.986 kA at the Winelands RMU 1 substation is shown in Tables 5-29 and 5-30.

Table 5-29: Currents and trip times for a three-phase fault at Winelands RMU 1 SS for the municipal network for Case 4

Subst.	Feeder	Volt. Level (kV)	Stage 1 Fault Level Mag. Contr (kA)	Stage 1 OCEF relay calc. trip time (s)	Stage 2 Fault Level Mag. Contr (kA)	Stage 2 OCEF relay calc. trip time (s)	Stage 3 Fault Level Mag. Contr (kA)	Stage 3 OCEF relay calc. trip time (s)	Stage 4 Fault Level Mag. Contr (kA)	Stage 4 OCEF relay calc. trip time (s)	Overall Trip Time (s)
Winelands	Winelands RMU 1	11.66	7.660	0.120	0	N/A	0	N/A	0	N/A	0.120
Winelands	Weet	11.66	1.126	1.674	0.883	2.191	0.879	2.205	4.369	0.715	1.145
Wozniak	Winelands	11.66	6.606	0.607	5.184	0.666	5.158	0.667	0	N/A	0.655
Wozniak	Weet	11.66	1.126	1.674	0.883	2.191	0.879	2.205	4.369	0.715	1.145
Wozniak	Transformer A MV	11.66	3.915	1.693	3.067	1.959	3.093	1.948	2.245	2.447	2.259
Wozniak	Transformer B MV	11.66	3.752	1.734	2.940	2.014	2.964	2.003	2.152	2.533	2.338
Wozniak	Wind Turbine - LHS LV	11.66	0.100	0.420	0.097	0.420	0	N/A	0	N/A	0.420
Wozniak	Transformer A HV	33	1.383	0.947	1.084	1.112	1.093	1.105	0.793	1.427	1.213
Wozniak	Transformer B HV	33	1.326	0.972	1.039	1.146	1.047	1.140	0.760	1.484	1.261
Utility Sub	Wozniak A	33	1.275	1.860	1.072	2.192	1.081	2.179	0.781	2.833	2.612
Utility Sub	Wozniak B	33	1.322	1.905	1.033	2.253	1.041	2.239	0.753	2.929	2.702
Utility Sub	Incomer 1	33	1.285	N/A	1.003	N/A	1.011	N/A	0.734	N/A	N/A
Utility Sub	Incomer 2	33	1.285	N/A	1.003	N/A	1.011	N/A	0.734	N/A	N/A

Table 5-30: Currents and trip times for a single-phase fault at Winelands RMU 1 SS for the municipal network for Case 4

Subst.	Feeder	Volt. Level (kV)	Stage 1 Fault Level Mag. Contr (kA)	Stage 1 OCEF relay calc. trip time (s)	Stage 2 Fault Level Mag. Contr (kA)	Stage 2 OCEF relay calc. trip time (s)	Stage 3 Fault Level Mag. Contr (kA)	Stage 3 OCEF relay calc. trip time (s)	Overall Trip Time (s)
Winelands	Winelands RMU 1	11.66	1.975	0.120	0	N/A	0	N/A	0.120
Winelands	Weet	11.66	0.250	1.216	0.190	1.606	1.183	0.506	0.821
Wozniak	Winelands	11.66	1.736	0.453	1.320	0.486	0	N/A	0.477
Wozniak	Weet	11.66	0.250	1.216	0.190	1.606	1.183	0.506	0.821
Wozniak	Transformer A MV	11.66	1.001	1.404	0.761	1.675	0.596	2.021	1.895
Wozniak	Transformer B MV	11.66	0.985	1.417	0.749	1.694	0.587	2.049	1.921
Wozniak	Wind Turbine - LHS LV	11.66	0.085	N/A	0.085	N/A	0.085	N/A	N/A
Wozniak	Transformer A HV	33	0.205	N/A	0.156	N/A	0.122	N/A	N/A
Wozniak	Transformer B HV	33	0.197	N/A	0.150	N/A	0.117	N/A	N/A
Utility Sub	Wozniak A	33	0.194	N/A	0.145	N/A	0.111	N/A	N/A
Utility Sub	Wozniak B	33	0.187	N/A	0.140	N/A	0.108	N/A	N/A
Utility Sub	Incomer 1	33	0.189	N/A	0.145	N/A	0.116	N/A	N/A
Utility Sub	Incomer 2	33	0.189	N/A	0.145	N/A	0.116	N/A	N/A

c) Protection grading results for the Short substation

The grading for a three-phase fault of 10.702 kA and a single-phase-to-ground fault of 1.722 kA at the Short substation is shown in Tables 5-31 and 5-32.

Table 5-31: Branch currents and trip times for a three-phase fault at Short SS for the municipal network for Case 4

Subst.	Feeder	Volt. Level (kV)	Stage 1 Fault Level Mag. Contr (kA)	Stage 1 OCEF relay calc. trip time (s)	Stage 2 Fault Level Mag. Contr (kA)	Stage 2 OCEF relay calc. trip time (s)	Stage 3 Fault Level Mag. Contr (kA)	Stage 3 OCEF relay calc. trip time (s)	Stage 4 Fault Level Mag. Contr (kA)	Stage 4 OCEF relay calc. trip time (s)	Overall Trip Time (s)
Short	Workplace	11.66	5.289	0.687	7.684	0.598	7.531	0.602	9.537	0.590	0.635
Short	Glassware	11.66	1.719	0.473	2.497	0.375	2.447	0.380	0	N/A	0.439
Short	British	11.66	3.709	0.307	0	N/A	0	N/A	0	N/A	0.307
Workplace	Glassware	11.66	1.719	1.230	2.497	0.976	2.447	0.987	0	N/A	N/A
Workplace	British 1	11.66	1.294	1.473	0	N/A	0	N/A	0	N/A	N/A
Workplace	British 2	11.66	2.441	0.950	0	N/A	0	N/A	0	N/A	N/A
Workplace	Transformer 1 MV	11.66	5.174	1.284	4.928	1.337	5.002	1.321	4.793	1.370	1.346
Workplace	Transformer 2 MV	11.66	5.216	1.276	4.968	1.328	5.042	1.312	4.832	1.360	1.336
Workplace	Wind Turbine - LV	11.66	0.485	0.420	0.483	0.420	0	N/A	0	N/A	0.420
Workplace	Transformer 1 HV	33	1.828	1.279	1.741	1.330	1.767	1.314	1.694	1.360	1.337
Workplace	Transformer 2 HV	33	1.843	1.271	1.755	1.321	1.781	1.305	1.707	1.351	1.328
Utility Sub	Workplace 1	33	1.816	2.211	1.729	2.303	1.755	2.274	1.681	2.359	2.335
Utility Sub	Workplace 2	33	1.837	2.191	1.749	2.280	1.775	2.252	1.701	2.335	2.311
Utility Sub	Incomer 1	33	1.742	N/A	1.657	N/A	1.682	N/A	1.610	N/A	N/A
Utility Sub	Incomer 2	33	1.742	N/A	1.657	N/A	1.682	N/A	1.610	N/A	N/A

Table 5-32: Branch currents and trip times for a single-phase fault at Short SS for the municipal network for Case 4

Subst.	Feeder	Volt. Level (kV)	Stage 1 Fault Level Mag. Contr (kA)	Stage 1 OCEF relay calc. trip time (s)	Stage 2 Fault Level Mag. Contr (kA)	Stage 2 OCEF relay calc. trip time (s)	Stage 3 Fault Level Mag. Contr (kA)	Stage 3 OCEF relay calc. trip time (s)	Overall Trip Time (s)
Short	Workplace	11.66	0.708	1.046	1.161	0.814	1.483	0.733	0.877
Short	Glassware	11.66	0.258	0.906	0.423	0.548	0	N/A	0.695
Short	British	11.66	0.756	0.373	0	N/A	0	N/A	0.373
Workplace	Glassware	11.66	0.258	2.447	0.423	1.481	0	N/A	N/A
Workplace	British 1	11.66	0.535	0.868	0	N/A	0	N/A	N/A
Workplace	British 2	11.66	0.222	1.632	0	N/A	0	N/A	N/A
Workplace	Transformer 1 MV	11.66	0.861	3.580	0.792	3.963	0.742	4.326	4.219
Workplace	Transformer 2 MV	11.66	0.861	3.580	0.792	3.963	0.742	4.326	4.219
Workplace	Wind Turbine - LV	11.66	0.415	N/A	0.414	N/A	0.413	N/A	N/A
Workplace	Transformer 1 HV	33	0.225	N/A	0.211	N/A	0.201	N/A	N/A
Workplace	Transformer 2 HV	33	0.226	N/A	0.212	N/A	0.202	N/A	N/A
Utility Sub	Workplace 1	33	0.197	N/A	0.184	N/A	0.174	N/A	N/A
Utility Sub	Workplace 2	33	0.222	N/A	0.208	N/A	0.198	N/A	N/A
Utility Sub	Incomer 1	33	0.164	N/A	0.151	N/A	0.142	N/A	N/A
Utility Sub	Incomer 2	33	0.164	N/A	0.151	N/A	0.142	N/A	N/A

5.5 Discussion of load flow results

Case 1 presents a grid import of 43.208 MW and 11.774 MVar. Case 2 presents a grid export of 14.798 MW and 31.897 MVar. Case 3 presents a grid export of 21.800 MW and 14.204 MVar, a 26.00% reduction in exported MVA compared to Case 2. Finally, Case 4 shows a grid export of 3.065 MW and a grid import of 2.831 MVar. The power imported or exported to the grid across the four cases is shown graphically in Figure 5.37.



Figure 5.37: Total MW and MVAr imported and exported to the grid across the various cases for the municipal network

Case 2 shows a 3.114 MVA total power loss. This results in a 16.13% power loss reduction over the 3.713 MVA total seen in Case 1. Case 3 results in a total power loss of 1.941 MVA, resulting in a reduction of 47.72% over Case 1. However, Case 4 results in a total power loss of only 0.598 MVA, resulting in a total reduction of 83.89% over Case 1. The total power loss reduction across the four cases can be seen graphically in Figure 5.38.

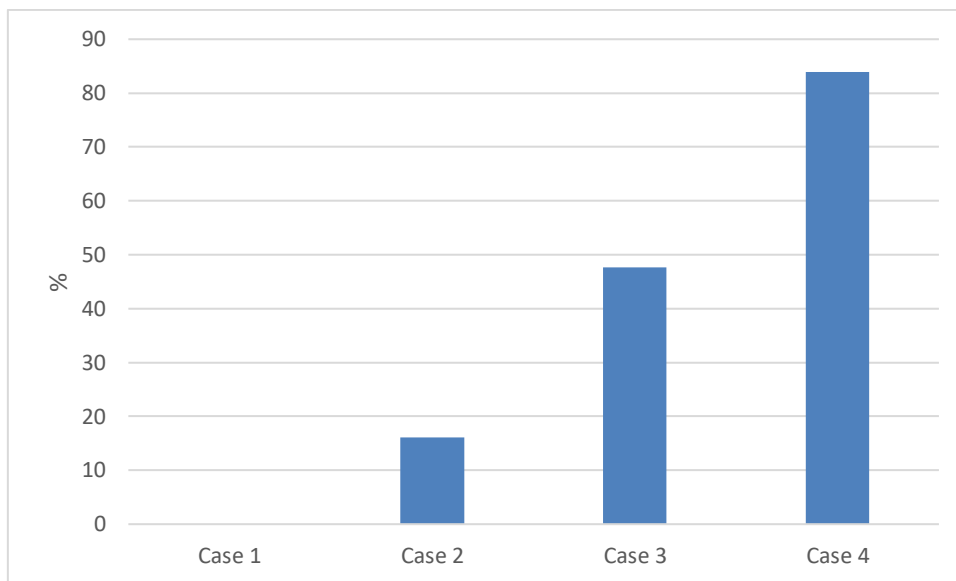


Figure 5.38: Total power loss reduction across the cases under study for the municipal network

The wind turbine generation obtained from Case 2 totals 72 MVA, the full capacity that the wind farm could provide. Case 3 results in 68.58 MVA being produced by the wind farm, while Case 4 results in only 45.12 MVA being generated by the wind farm. However, the large influx of generation in Case 2 at the Utility substation results in less power being imported from the major utility, resulting in lower line losses on the Utility substation incomers without impacting other network feeders. However, distributing the generators throughout the network shows a larger reduction in total network power losses in both Cases 3 and 4.

Both algorithms are seen to significantly reduce overall power losses. The solution obtained from the DE algorithm is seen to perform much better than the solution obtained from the PBIL algorithm in

terms of overall network power losses. Based on the results seen in the IEEE cases, this significant performance difference between the two algorithms is likely due to the reduced performance experienced by the PBIL algorithm due to its weakness in multi-objective and multi-variable optimisation.

At the 33 kV Utility substation, the voltage magnitudes and angles are seen to stay consistent at 33 kV and at an angle of zero degrees throughout Cases 1, 2, 3, and 4, as it is the network slack bus. The Utility Switch Yard is seen to rise in voltage in Cases 3 and 4 by 1V.

The voltage levels between Case 1 and Case 2 are seen to be identical in magnitude and phase. This is due to the wind farm incomer in Case 2 being connected directly to the slack bus.

The voltage of many busses in the Atlantic MS network are seen to hover around the 11.62 kV and 11.64 kV marks in Cases 1 and 2, resulting in an overall RMS error of 2.71% from the nominal voltage. In Case 3, this error is slightly reduced to 2.10%, marking a 22.51% improvement over Cases 1 and 2. However, in Case 4, this improves to an overall RMS error of 0.79%, a 70.85% improvement over Cases 1 and 2.

In the Gardens MS feeder group, the total RMS error is seen to increase from 1.08% in Cases 1 and 2, to 4% in Case 3 and 4.18% in Case 4. Even though this is within the tolerable range according to the NRS 048 requirements, the group does see a substantial change in voltage. This is mainly explained by the closeness of the voltage to the nominal value in Cases 1 and 2. This means that any additional generation at the bus will result in a voltage increase away from the nominal value.

In the Delilah MS feeder group, the voltage is seen to deviate further from the nominal value in Case 3, when compared to Cases 1 and 2. In Cases 1 and 2, the total RMS error is calculated as 0.51%, while this is seen to increase to 1.317% in Case 3 and 0.99% in Case 4. This can be explained in the same way as the deviation in the Gardens MS feeder group. It is noted in this case that the voltage of the only bus not within the 11.65-11.66 kV range in Cases 1 and 2, the West 2 substation, is seen to improve.

The Wozniak MS feeder group sees an overall RMS error improvement of over two times, with a total RMS error of 4.14% in Cases 1 and 2 to 1.83% in Case 4. Case 3 also sees an improvement with a total RMS error of 3.21%. The busses in this feeder group all see a large improvement, with voltages very close to the nominal 11.66 kV in Case 4, with the exception of the Mat substation, whose voltage is seen to decrease slightly from 11.623 kV in Cases 1 and 2 to 11.621 kV in Case 4.

The total RMS error in the Sunset Vista MS feeder group is seen to decrease from 18.48% in Cases 1 and 2 to 9.42% in Case 3, a 49.03% improvement over Cases 1 and 2, and to 14.23% in Case 4, a 23% improvement over Cases 1 and 2. The voltage level at all busses in this network is seen to increase. This is due to the radial nature of this network.

The Workplace MS feeder group sees an overall RMS error improvement, from 3.24% in Cases 1 and 2 to 2.24% in Case 3 and 1.88% in Case 4, a 41.98% improvement over Cases 1 and 2. The voltages in all three cases are very close to the nominal voltage. The voltage level improved at all substations in Cases 3 and 4, though the voltages presented in Case 4 is closer to the nominal voltage.

Finally, the Winery MS feeder group shows an overall improvement as well, with a total RMS error of 2.29% in Cases 1 and 2 to an error of 1.33% in Case 3 and 0.87% in Case 4, marking a 62.01% improvement over Cases 1 and 2. Voltages are seen to be closer to the nominal voltage. This is most

notable on the Winery 11 kV LHS and RHS busbars, dropping from 11.686 kV in Cases 1 and 2 to 11.669 kV in Case 4.

Overall, the network as a whole is seen to improve its voltage profile in both Cases 3 and 4, compared to Cases 1 and 2. Only the Atlantic and Gardens MS feeder groups are seen to deviate slightly further from the nominal voltage in Case 3. However, the average total network RMS error is seen to decrease from 4.64% in Cases 1 and 2 to 3.54% in Case 4, showing a 23.71% voltage profile improvement. In Case 3, however, due to the large deviations experienced at the Gardens and Delilah MS feeder groups, the average total RMS error is seen to increase to 6.77% from Cases 1 and 2. This results in a 45.91% voltage profile deterioration in Case 3. The overall voltage profile improvement seen across the four cases are shown in Figure 5.39.

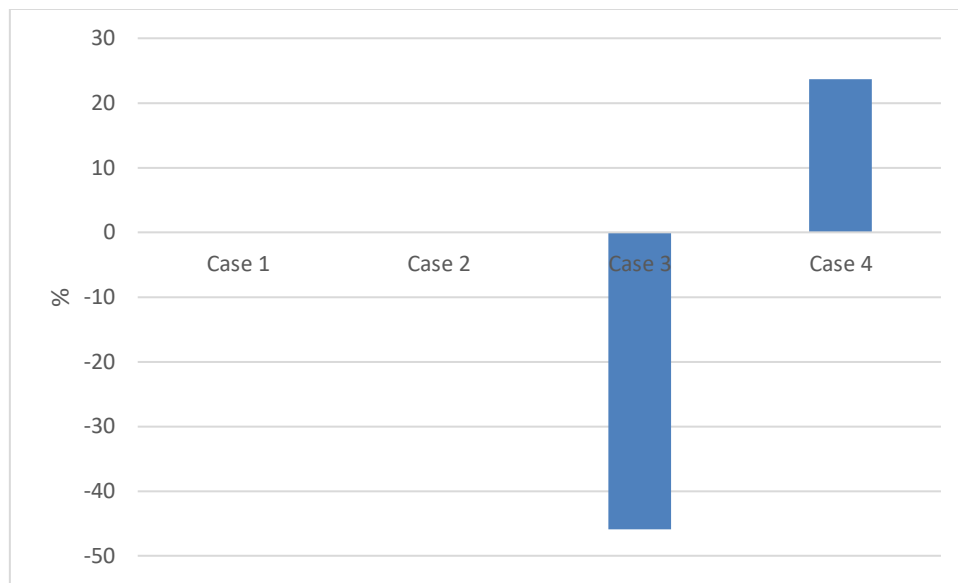


Figure 5.39: Overall network voltage profile improvement across the four cases for the municipal network

Thus, the DE algorithm is seen to produce results which perform better overall in terms of voltage profile improvement than the PBIL algorithm.

5.6 Discussion of case study protection grading results

5.6.1 Fault at the 33 kV Utility substation rear busbar

In Case 1, the three-phase fault level is calculated as 13.001 kA, splitting equally between the two Utility substation incomers. This results in a trip time of 1.928 seconds to isolate the fault.

Case 2 sees the three-phase fault level rise to 13.212 kA, but with the Utility substation incomers providing only 5.888 kA to the fault, resulting in the incomers tripping in 2.100 seconds. The wind turbine provides 1.512 kA towards the fault level both before and after the Utility substation incomers have tripped. This results in the turbine tripping in 4.019 seconds from fault inception. The wind turbine is seen to only pick up for this fault in Case 2 and none of the other faults observed result in this relay picking up a fault condition downstream.

In Case 3, the three-phase fault level is calculated as 13.376 kA. All of the wind turbines contribute their maximum 120% of their rating towards the fault while the Utility substation incomers each contribute 5.979 kA. Each turbine trips after 0.42 seconds. The Utility substation incomers then trip 1.537 seconds later.

Case 4 sees a similar response as in Case 3, with the total fault level seen to decrease to 13.324 kA. The Utility substation incomer contributions are seen to increase in this case to 6.206 kA. The fault is isolated in a similar time as in Case 3.

The total trip times are graphically shown in Figure 5.40.

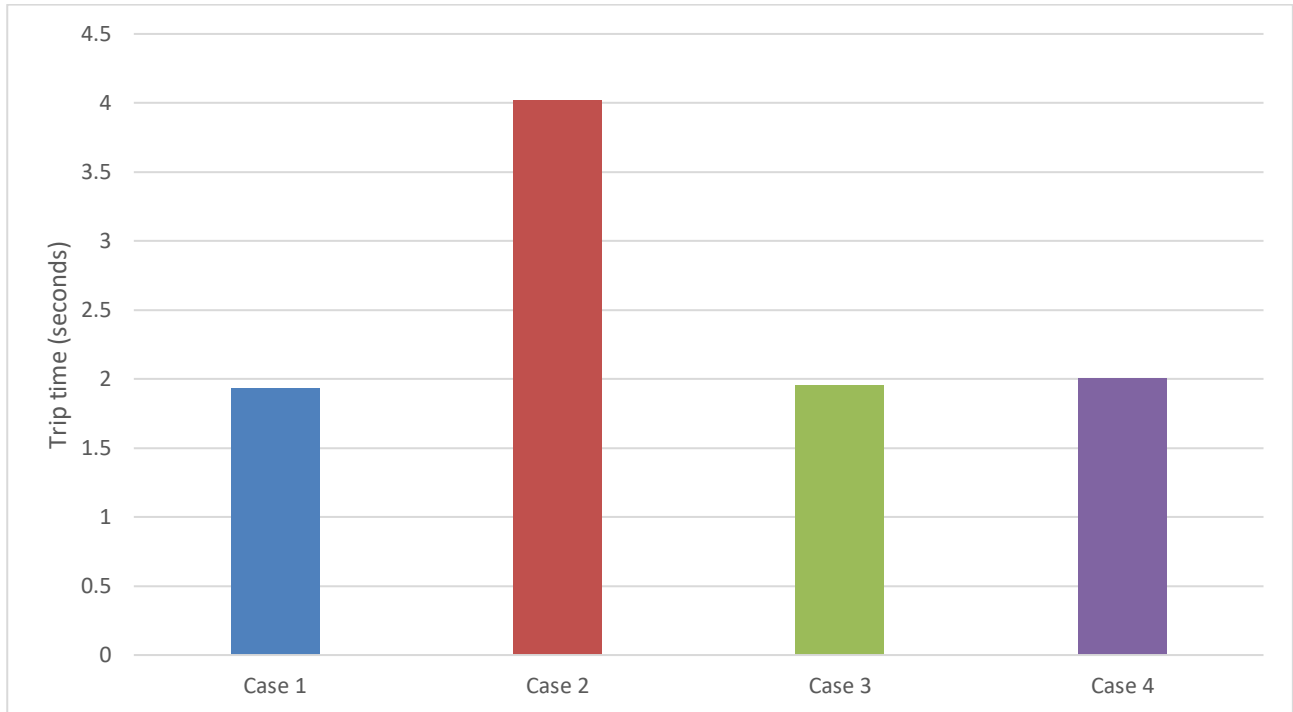


Figure 5.40: Total trip times for a three-phase fault at the Utility substation for the four cases for the municipal network

The earth fault levels through the four cases are not affected as much as the three-phase fault levels. In Case 1, the Utility substation incomers split the fault level of 4.849 kA equally into 2.425 kA each, and trip in 0.907 seconds. In Case 2, the fault level rises to 4.859 kA, with each incomer contributing 2.430 kA and tripping in 0.907 seconds. In Case 3, the earth-fault level is calculated as 4.866 kA, with the fault being isolated in 0.907 seconds. Finally, in Case 4, the fault level is increased slightly to 4.863 kA, split by the Utility substation incomers, also tripping in 0.907 seconds. The wind turbines do not affect the earth fault level and do not contribute to the earth fault condition in Cases 2, 3, and 4.

The relay grading for the earth fault condition is thus unaffected.

5.6.2 Fault at the Bushes substation

In Case 1, the three-phase fault level is calculated as 4.182 kA. The Bushes feeder at the Atlantic substation is the only feeder that directly feeds the fault. This feeder trips in 0.120 seconds, isolating the fault. However, the grading margin for a fault at this location is not acceptable due to grading margins of 0.101 and 0.196 seconds with the Yellow feeder at the Winery substation and the Grounds feeder at the Atlantic substation, respectively.

Transformer trip times show that there is ample margin available to be able to increase these grading margins.

In Case 2, the three-phase fault level is calculated as 4.191 kA, slightly increasing from Case 1. In Case 3, the fault level is observed to increase to 4.304 kA. Finally, the fault level is seen to decrease to 4.212 kA

in Case 4. The fault is isolated in 0.120 seconds in each of these cases. The same issue from Case 1 is seen to present itself in this case. The fault level and grading margin remain similar. The total trip times are graphically shown in Figure 5.41.

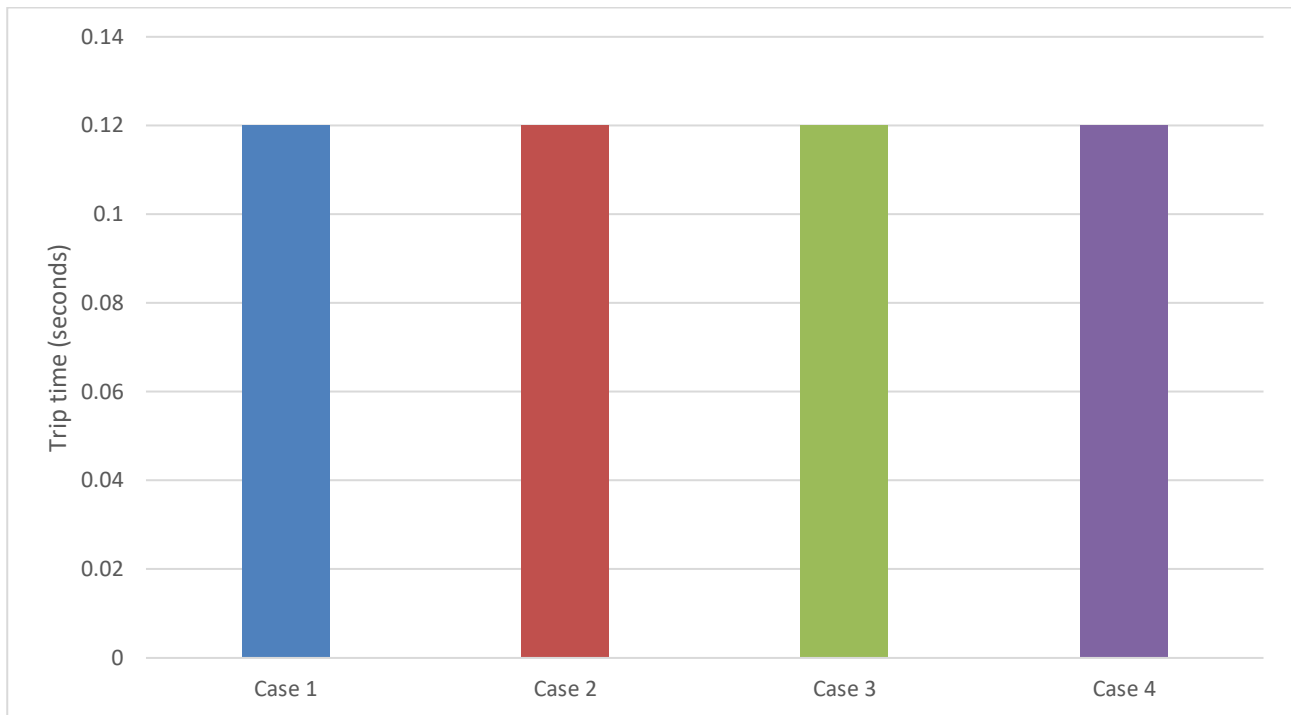


Figure 5.41: Total trip times for a three-phase fault at the Buses SS for the four cases for the municipal network

The earth-fault level in Case 1 is calculated as 1.169 kA. This results in the Buses feeder at the Atlantic substation tripping in 0.150 seconds, isolating the fault. However, a similar grading issue is observed in this case, where the Yellow feeder at the Winery substation would trip after 0.238 seconds, resulting in a grading margin of just 0.088 seconds. This should be increased to match the Grounds feeder at the Atlantic substation, as the trip time of the MV-side of the Winery transformer relay would allow for the implementation of a better grading margin as it is seen to trip in 5.020 seconds.

The earth-fault level in Case 2 is calculated to be the same as in Case 1. This is due to the turbine not directly contributing to a network earth-fault condition, but does result in the Utility substation incomer fault contribution decreasing from 0.476 kA to 0.324 kA per incomer.

The earth-fault level in Case 3 is seen to increase to 1.182 kA, due to the addition of a direct DG incomer at the Atlantic MV substation. The trip times and grading margins remain extremely similar to Cases 1 and 2 due to the very slight increase in fault level and the contribution from the Atlantic LHS MV DG incomer.

The earth-fault level in Case 4 is calculated as 1.172 kA. The same observations are made for Case 4 as in Case 3. The total trip times are graphically shown in Figure 5.42.

5.6.3 Fault at the Addition substation

In Case 1, the three-phase fault level is calculated as 4.112 kA. This fault is fed from the Addition feeder at the Allen substation which trips in 0.120 seconds, isolating the fault. The Gardens feeder at the Allen substation trips in 0.528 seconds, resulting in an adequate grading margin with the Addition feeder at the same station. However, the Allen feeder at the Gardens substation trips in 0.734 seconds. This means

that there are conflicting protection settings on the two ends of the same cable. Should the Allen feeder at the Gardens substation be changed to match the trip time of 0.528 seconds, the rest of the relays involved in the fault would be well-graded.

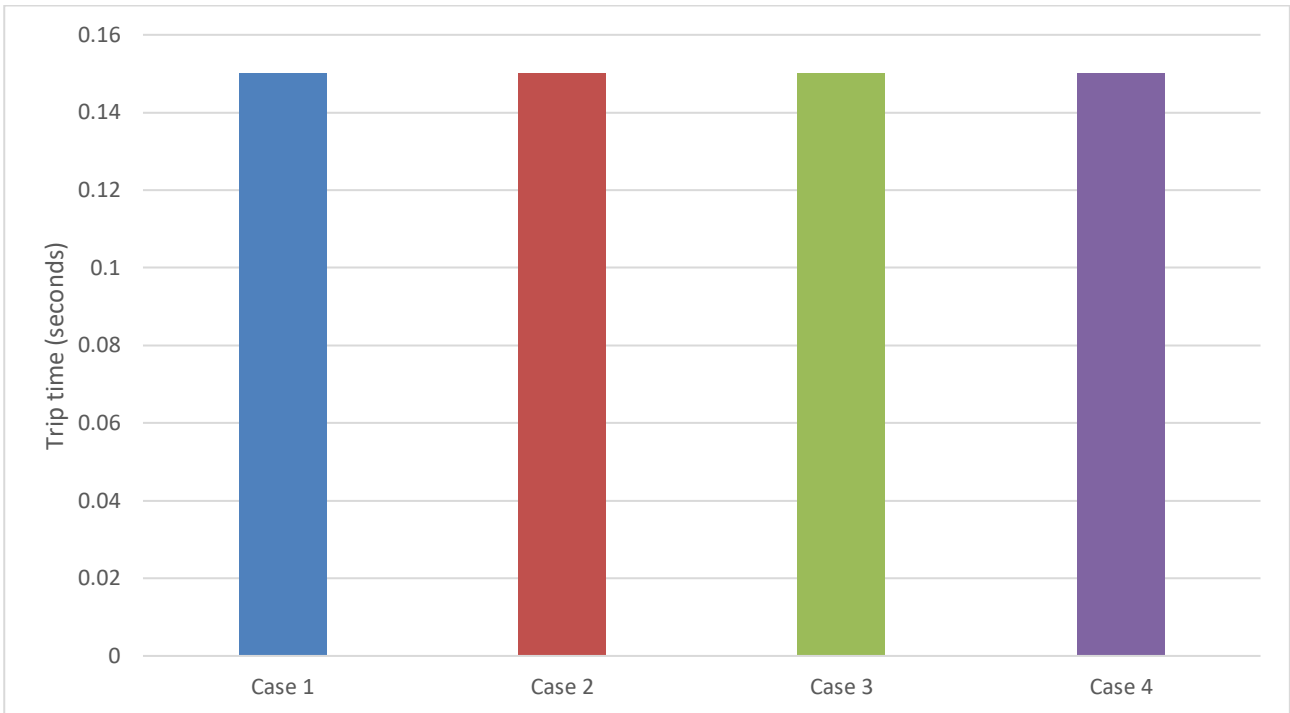


Figure 5.42: Total trip times for a single-phase fault at the Buses SS for the four cases for the municipal network

The three-phase fault level in Case 2 is observed to increase slightly to 4.121 kA, 4.141 kA in Case 3, and 4.136 kA in Case 4. These fault levels result in a trip time of 0.120 seconds for the Addition feeder at the Allen substation and is subject to the same grading margins and issues as in Case 1. The total trip times are graphically shown in Figure 5.43.

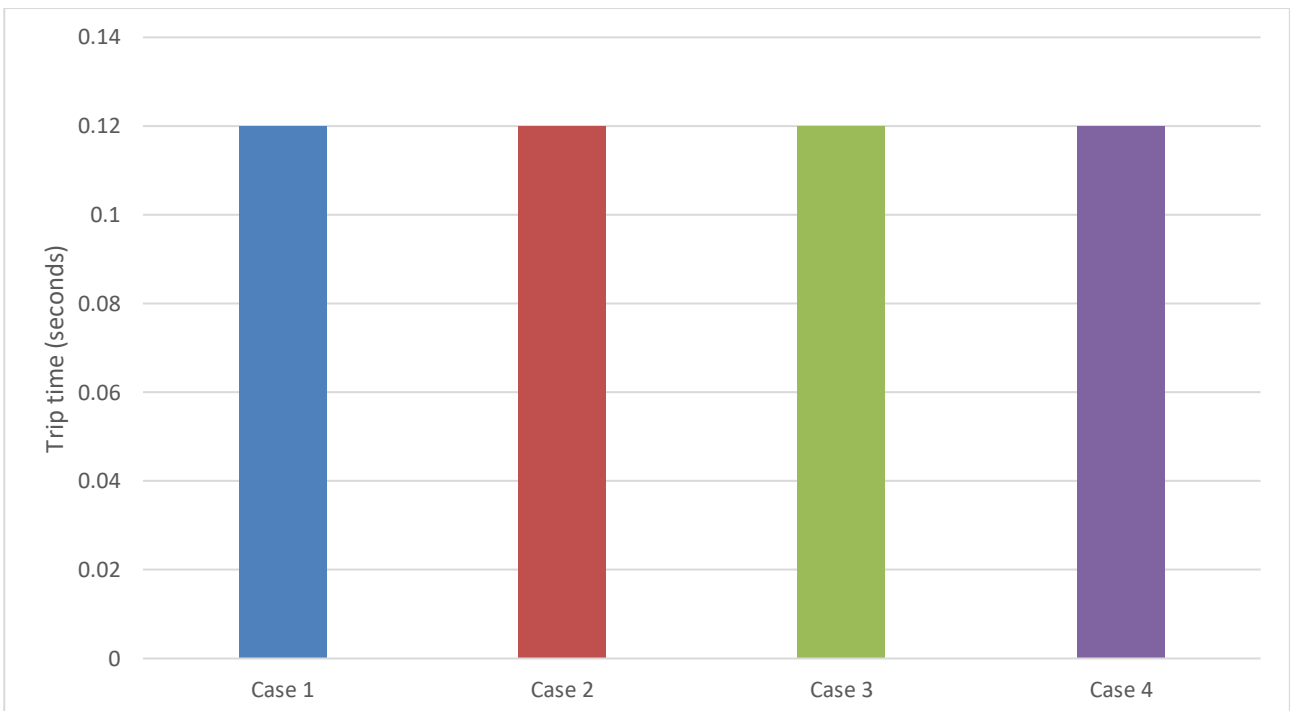


Figure 5.43: Total trip times for a three-phase fault at the Addition SS for the four cases for the municipal network

The earth-fault level for Cases 1 and 2 is calculated as 1.000 kA. The Addition feeder at the Allen substation trips in 0.120 seconds. The same grading issue on the two ends of the Gardens – Allen line persists in terms of earth-fault settings. The trip time on the Gardens Transformer 2 MV relay is slightly too long, depending on the grading with the other feeders in the group, and could be changed to accommodate a better grading margin with the Gardens – Allen line relays.

The earth-fault level is calculated as 1.005 kA in Case 3 due to the direct connection of a DG incomer at the Gardens RHS MV busbar. This results in a slightly decreased grading margin between the Allen – Addition feeder relay, which trips in 0.120 seconds, and the upstream relays. The same issue on the Gardens – Allen feeder relays is observed.

The earth-fault level is calculated as 1.004 kA in Case 4 and is isolated in 0.120 seconds. The same observations are made for Case 4 as in Case 3. The total trip times are graphically shown in Figure 5.44.

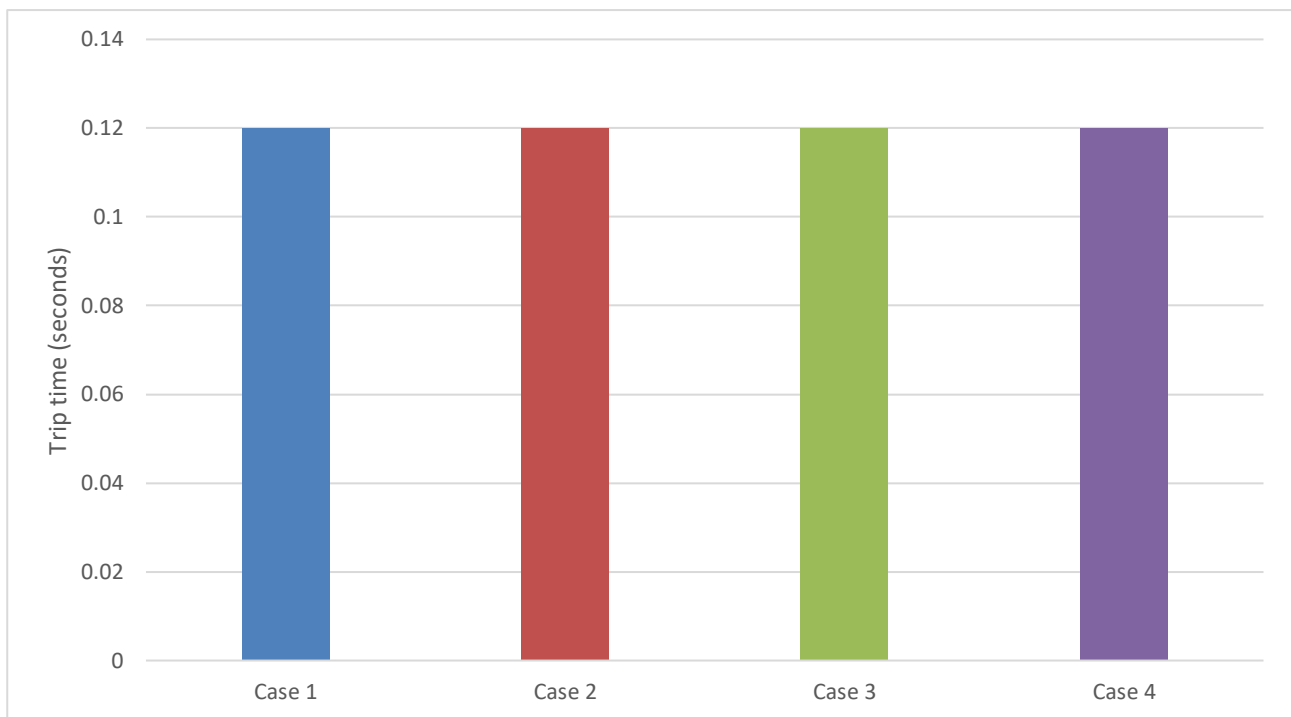


Figure 5.44: Total trip times for a single-phase fault at the Addition SS for the four cases for the municipal network

5.6.4 Fault at the Tortoise substation

For Case 1, the three-phase fault level is calculated as 3.981 kA at the Tortoise substation. The Tortoise substation is fed directly out of the Delilah substation. This feeder relay is seen to trip in 0.120 seconds. The Delilah Transformer 2 MV relay is seen to trip in 0.857 seconds, should the Tortoise feeder relay fail to trip. Thus, this grading margin is slightly too large but adequate to avoid spurious tripping.

The three-phase fault level for Case 2 is increased slightly to 3.989 kA at the Tortoise substation. However, the grading margin is seen to remain essentially constant compared to Case 1.

The three-phase fault level in Case 3 increases to 4.064 kA due to the relatively large DG connection made at the Delilah RHS MV MS. The Tortoise relay at the Delilah MS is seen to trip in 0.120 seconds, allowing for an adequate grading margin between it and the Transformer 2 MV relays, tripping in 0.859 seconds.

The three-phase fault level for Case 4 is calculated as 3.986 kA. Thus, the grading margins are observed to remain the same as in Case 2. The total trip times are graphically shown in Figure 5.45.

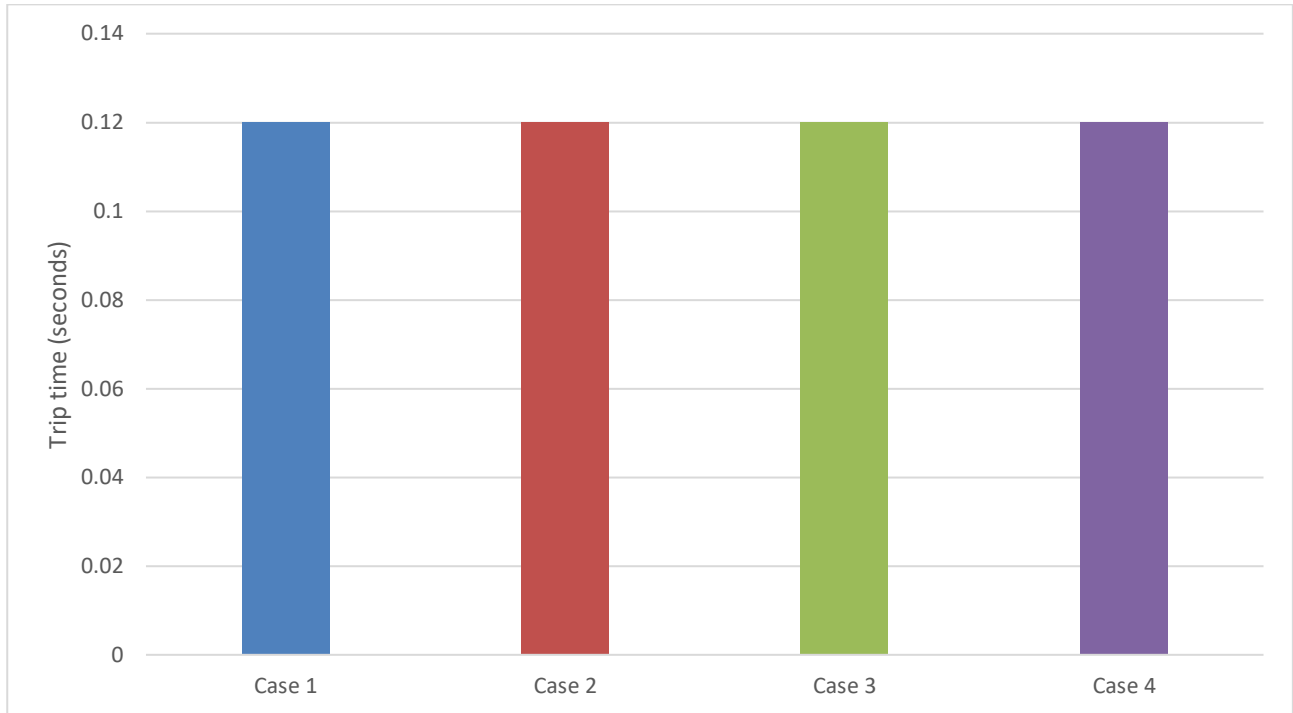


Figure 5.45: Total trip times for a three-phase fault at the Tortoise SS for the four cases for the municipal network

The earth-fault level for Cases 1, 2 and 4 is calculated as 1.163 kA at the Tortoise substation. This results in the Tortoise feeder relay tripping in 0.120 seconds, while the Delilah Transformer 2 MV relay would trip in 1.289 seconds should the Tortoise relay fail to trip. This results in a large grading margin.

The earth-fault level for Case 3 is calculated as 1.183 kA. The fault remains to be isolated in 0.120 seconds, and the same observations are made as in the other cases. The total trip times are graphically shown in Figure 5.46.

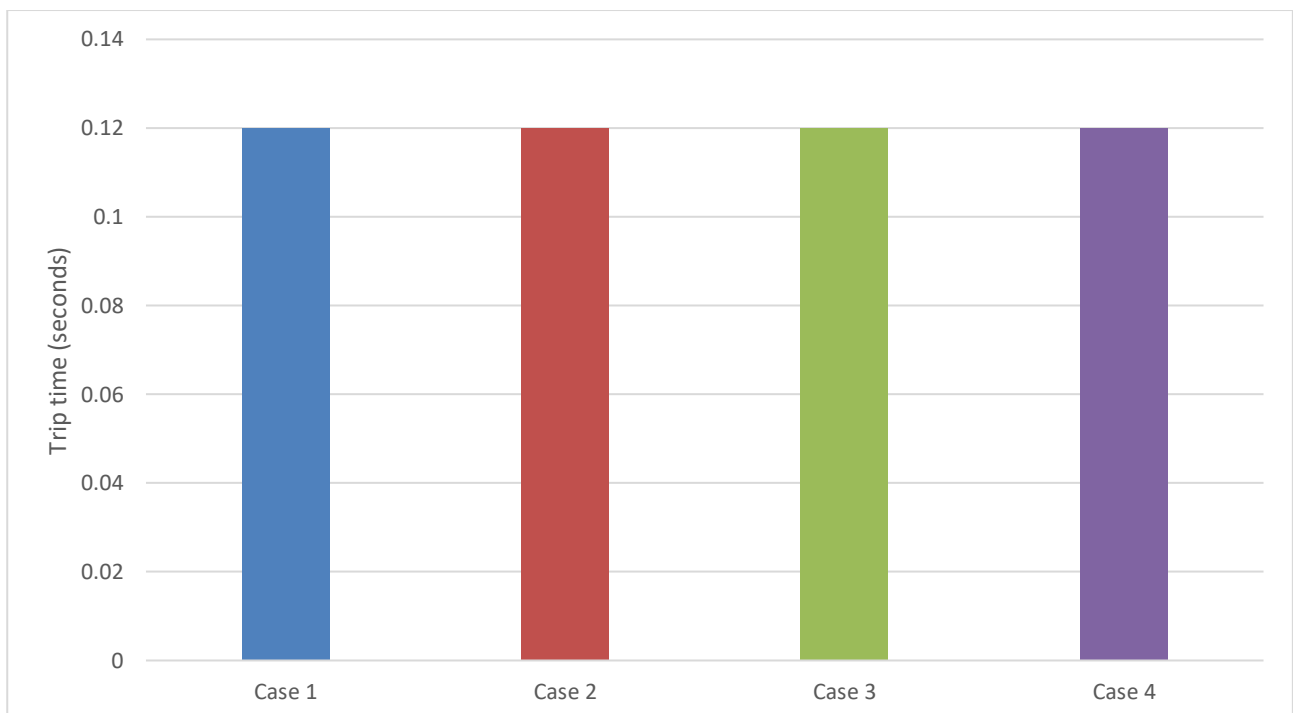


Figure 5.46: Total trip times for a single-phase fault at the Tortoise SS for the four cases for the municipal network

5.6.5 Fault at the Winelands RMU 1 substation

The fault at the Winelands RMU 1 substation consists of different fault stages due to the network configuration and fault level changing after a given breaker has tripped without isolating the fault. This is due to a lack of protection relays installed on certain feeders in the network.

In Case 1, the three-phase fault level is calculated as 7.668 kA, being fed from two sides to the busbar. The Winelands RMU 1 feeder at the Winelands substation has a protection relay installed, which is seen to trip first in 0.120 seconds, concluding the first fault stage. The fault is then fed through the T-off connection on the Weet – Winelands line, which does not have a protection relay installed at the Winelands substation. This means that the fault will only be isolated after the Winelands substation is completely disconnected from the grid. This occurs through the tripping of the Wozniak – Winelands feeder in 0.656 seconds from fault inception, followed by the tripping of the Weet – Winelands and Wozniak - Weet feeders in 1.147 seconds from fault inception. This means that any load fed from the Weet substation will be shed should a fault occur at the Winelands RMU 1 substation.

The Wozniak Transformer A and B MV relays trip in 2.261 and 2.340 seconds, respectively, allowing for a large grading margin. However, it is noted that the Wozniak Transformer A and B HV relays trip in 1.213 and 1.262 seconds, respectively, before the MV side relays while also allowing for an extremely narrow grading margin with the Weet – Winelands feeder relays that isolate the fault after 1.147 seconds. This will likely lead to tripping the HV transformer relays should a fault occur at this substation.

In Case 2, the three-phase fault level slightly increases to 7.701 kA. Due to this increase, the time to isolate the fault is calculated as 1.145 seconds. The Wozniak Transformer A and B HV relays trip in 1.210 and 1.259 seconds, remaining instrumental in a small grading margin between the MV network and the transformers tripping times.

In Case 3, the three-phase fault level is calculated as 7.710 kA while it increases to 7.731 kA in Case 4. The overall trip time to isolate the fault in the MV network is thus calculated as 1.144 seconds in Case 3 and 1.145 seconds in Case 4. The same grading issue is observed as in previous cases. Thus, the wind turbine placed at the LHS Wozniak MV busbar is noted to have little effect on the overall trip time. The total trip times are graphically shown in Figure 5.47.

In Cases 1 and 2, the earth-fault level is calculated as 1.977 kA at this substation. A similar issue is encountered as in the three-phase fault case regarding the unnecessary tripping of the Weet substation for a fault at the Winelands RMU 1 substation. The fault is seen to follow the same three stages as in the case of a three-phase fault in Cases 1 and 2, where the third breaker trips and isolates the fault in 0.822 seconds. However, the Wozniak Transformers A and B MV relays trip in 1.902 and 1.928 seconds, respectively. This allows a large grading margin which could be shortened if other relays in the network are graded accordingly.

The earth-fault level in Case 3 and 4 is seen to vary slightly to 1.980 kA and 1.968 kA, respectively. The fault is isolated in 0.821 seconds in both cases. The Wozniak Transformers A and B MV relays still allow for a large grading margin as seen in Cases 1 and 2. The wind turbine at this bus is seen to not contribute to the earth-fault level, as seen in other fault locations. The total trip times are graphically shown in Figure 5.48.

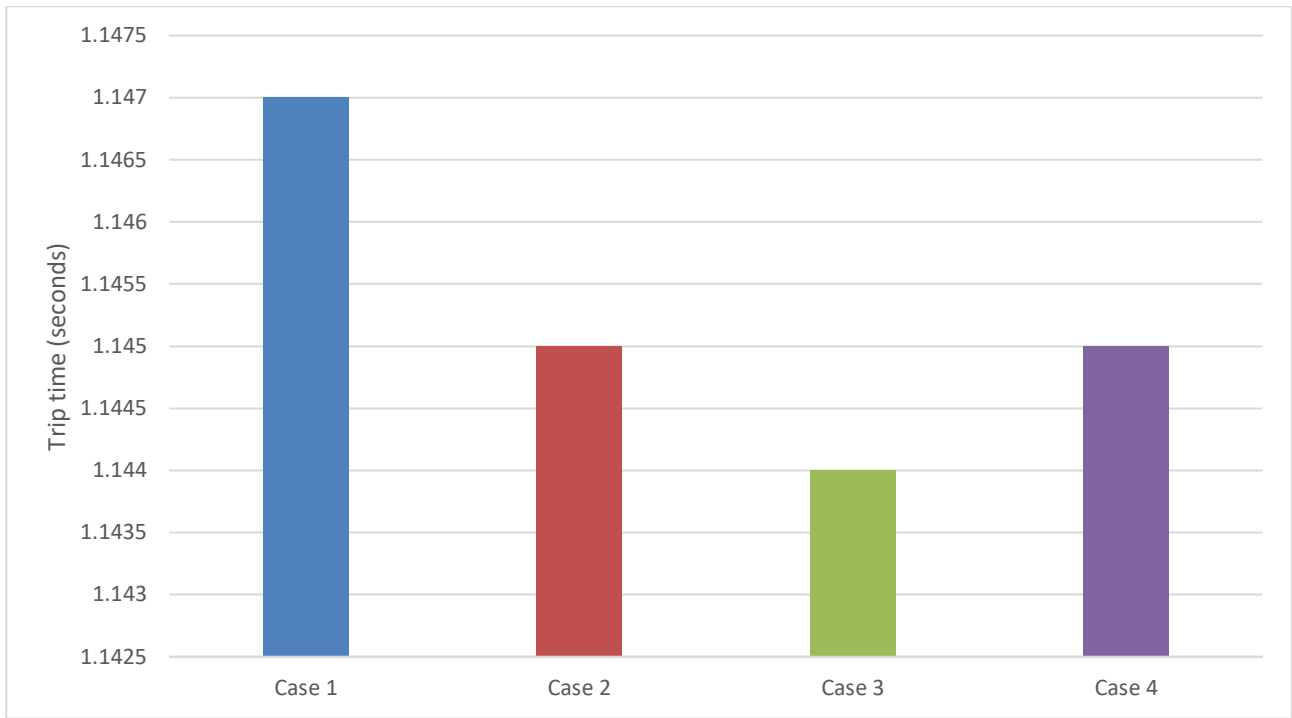


Figure 5.47: Trip times for a three-phase fault at the Winelands RMU 1 SS for the four cases for the municipal network

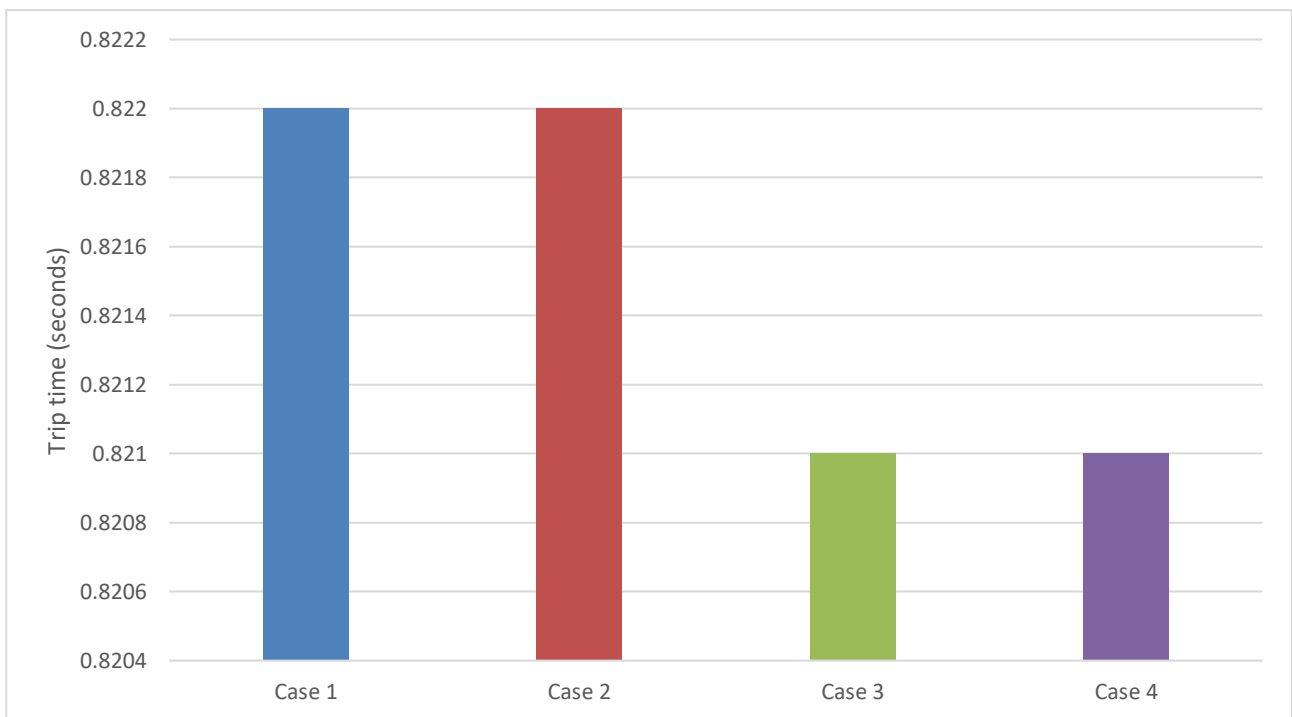


Figure 5.48: Trip times for a single-phase fault at the Winelands RMU 1 SS for the four cases for the municipal network

5.6.6 Fault at the Steve LHS substation

In Case 1, the three-phase fault level is calculated as 9.387 kA at the Steve LHS substation, fed directly from the Steve LHS feeder at the Lightning substation. This feeder is seen to trip in 0.340 seconds, isolating the fault from the network. The relay pair on the Sunset Vista – Lightning LHS feeder is seen to trip in 0.635 seconds, allowing for a barely adequate grading margin of 295 ms should the first relay fail to trip. The Sunset Vista Transformer A and B MV relays are seen to trip in 1.346 seconds, with the HV side relays and Utility substation relays tripping in 1.761 seconds. This allows for an adequate grading

margin in this group, though the Sunset Vista – Lightning LHS feeder relay pair should be made to allow for a slightly longer grading margin.

The three-phase fault level in Case 2 is calculated as 9.433 kA. The trip times and grading margins are similar to Case 1.

The three-phase fault level in Case 3 is calculated as 9.524 kA, with the same trip times as in Cases 1 and 2 on the Lightning and Steve LHS feeders, isolating the fault in 0.340 seconds and allowing for a 295 ms grading margin. This is due to CT saturation.

The three-phase fault level in Case 4 is calculated as 9.505 kA from Cases 1 and 2, with the same trip times and observations as in Case 3. The transformer MV relays trip slightly later, in 1.353 seconds, due to these transformers contributing slightly less current to the fault. The total trip times are graphically shown in Figure 5.49.

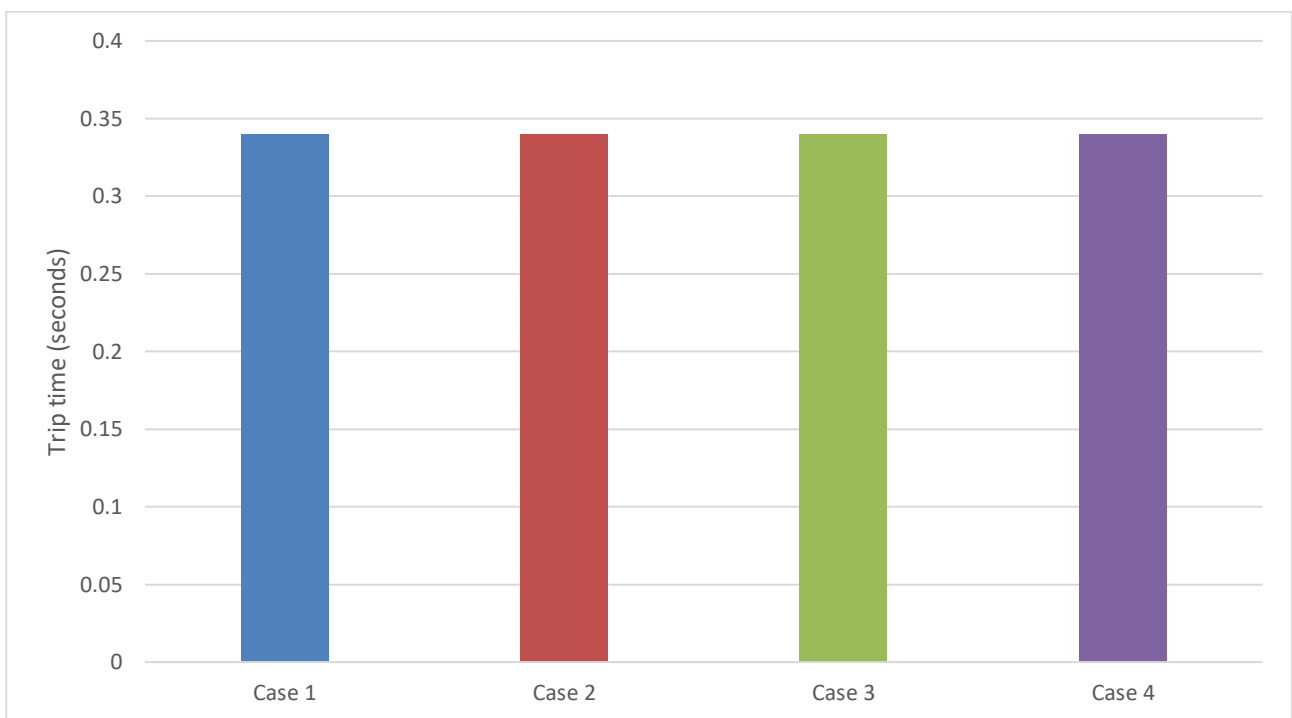


Figure 5.49: Trip times for a three-phase fault at the Steve LHS SS for the four cases for the municipal network

The earth-fault level in Cases 1 and 2 is calculated as 1.167 kA at the Steve LHS substation. This is fed directly through the Steve LHS feeder at the Lightning substation, which is seen to trip in 0.812 seconds. Should this relay fail to operate, the relay pair on the Sunset Vista – Lightning LHS feeder will trip in 1.203 seconds, allowing for a perfectly adequate grading margin between these relays. However, the Sunset Vista Transformers A and B MV relays are seen to trip in 3.460 seconds, resulting in a large grading margin between it and the Sunset Vista – Lightning LHS feeder relay pair. This should be shortened, if possible.

The earth-fault level in Case 3 is calculated as 1.177 kA and 1.173 kA in Case 4. The Steve LHS feeder relay pair is seen to trip in 0.809 seconds and 0.810 seconds in Cases 3 and 4, respectively, isolating the fault. Grading margins and trip times remain similar to previous cases. The total trip times are graphically shown in Figure 5.50.

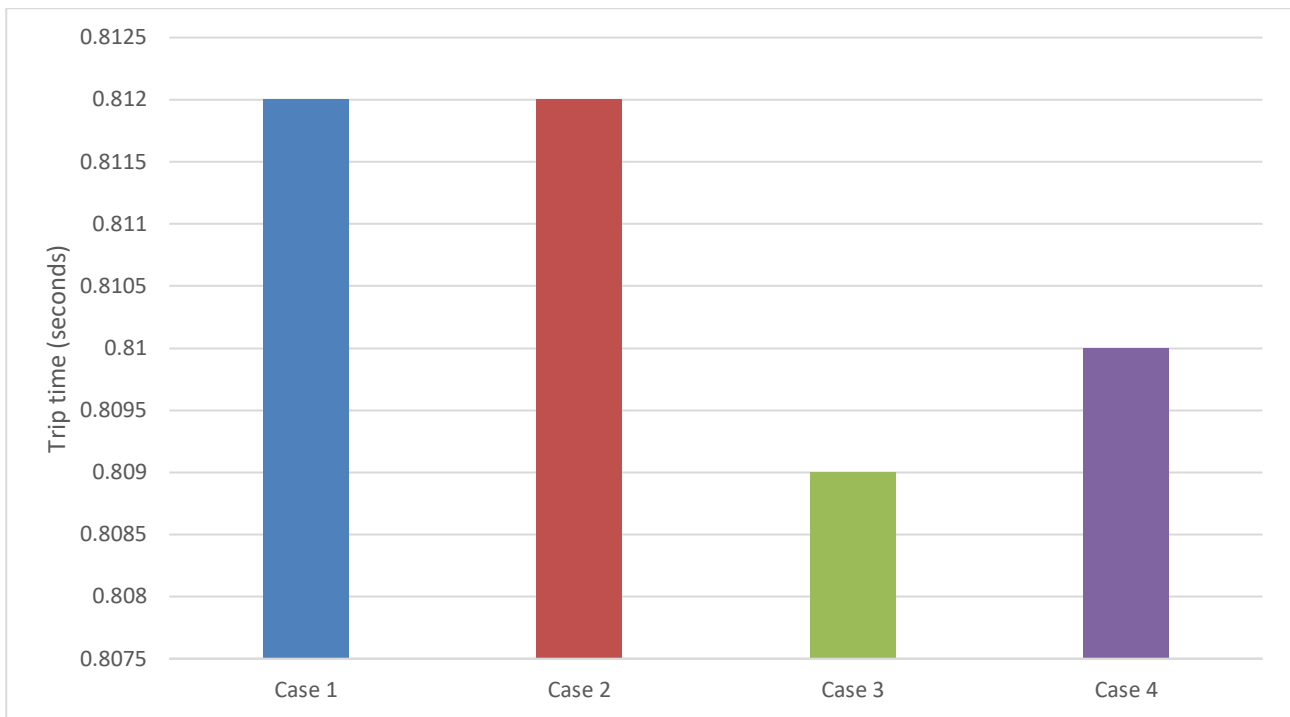


Figure 5.50: Total trip times for a single-phase fault at the Steve LHS SS for the four cases for the municipal network

5.6.7 Fault at the Mine substation

In Case 1, the three-phase fault level is calculated as 3.576 kA at the Mine substation. This fault consists of only one stage, only being directly fed from the Mine feeder at the Recycling substation. This feeder trips in 0.112 seconds, isolating the fault. The relay pair on the Recycling – Sunset Vista feeder trips in 0.566 seconds, allowing for a good grading margin between these two relays. However, the Sunset Vista Transformer A and B MV relays are seen to trip in 3.717 and 3.718 seconds, respectively. This results in over a 3 second grading margin between these incomers and the Recycling feeder relay at the same substation. The Transformer A and B HV relays also time for almost double the period of the MV side relays before tripping, which could cause the fault to be sustained for longer than necessary and possibly result in equipment damage.

The three-phase fault level in Case 2 shows a slight increase at 3.580 kA. The Mine feeder at the Recycling substation trips in 0.113 seconds for this fault, while the Transformer A and B incomers are seen to trip in 3.710 and 3.711 seconds. The grading issues thus persist in Case 2, as in Case 1.

The three-phase fault level in Case 3 increases slightly to 3.615 kA, resulting in the fault being isolated in 0.113 seconds. This results in the relay pair on the Recycling – Sunset Vista feeder to trip slightly faster at 0.564 seconds. However, the Transformer A and B MV relays are seen to trip over a longer period of sustaining the fault, tripping in 4.069 and 4.044 seconds, respectively. This is due to the addition of the wind turbine at the Sunset Vista LHS busbar contributing towards the fault.

The three-phase fault level in Case 4 is calculated as 3.605 kA, resulting in the fault being isolated in 0.113 seconds. The same observation is made in this case as in Case 3. The total trip times are graphically shown in Figure 5.51.

The earth-fault level in Case 1 is calculated as 0.761 kA for a fault at the Mine substation. This causes the Mine feeder at the Recycling substation to trip in 0.120 seconds while causing the relay pair on the Sunset Vista – Recycling feeder to trip in 0.433 seconds, resulting in an adequate grading margin. The Sunset Vista Transformer A and B both trip in 29.962 seconds for this fault, resulting in an enormous

grading margin with the rest of the network that these incomers feed. The earth-fault level in Case 2 increases slightly to 0.762 kA, resulting in similar trip times and the same grading issues as in Case 1.

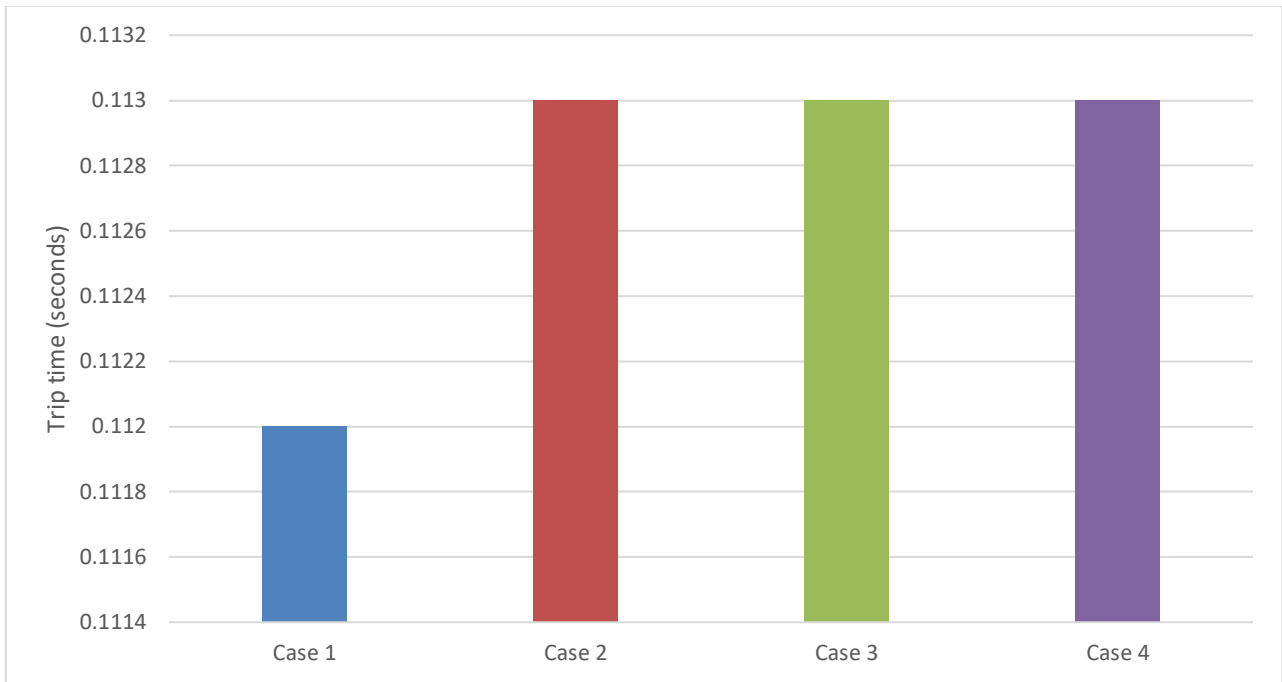


Figure 5.51: Total trip times for a three-phase fault at the Mine SS for the four cases for the municipal network

The earth-fault level in Case 3 is calculated as 0.768 kA and as 0.765 kA in Case 4. This results in similar network trip times and grading. The total trip times are graphically shown in Figure 5.52.

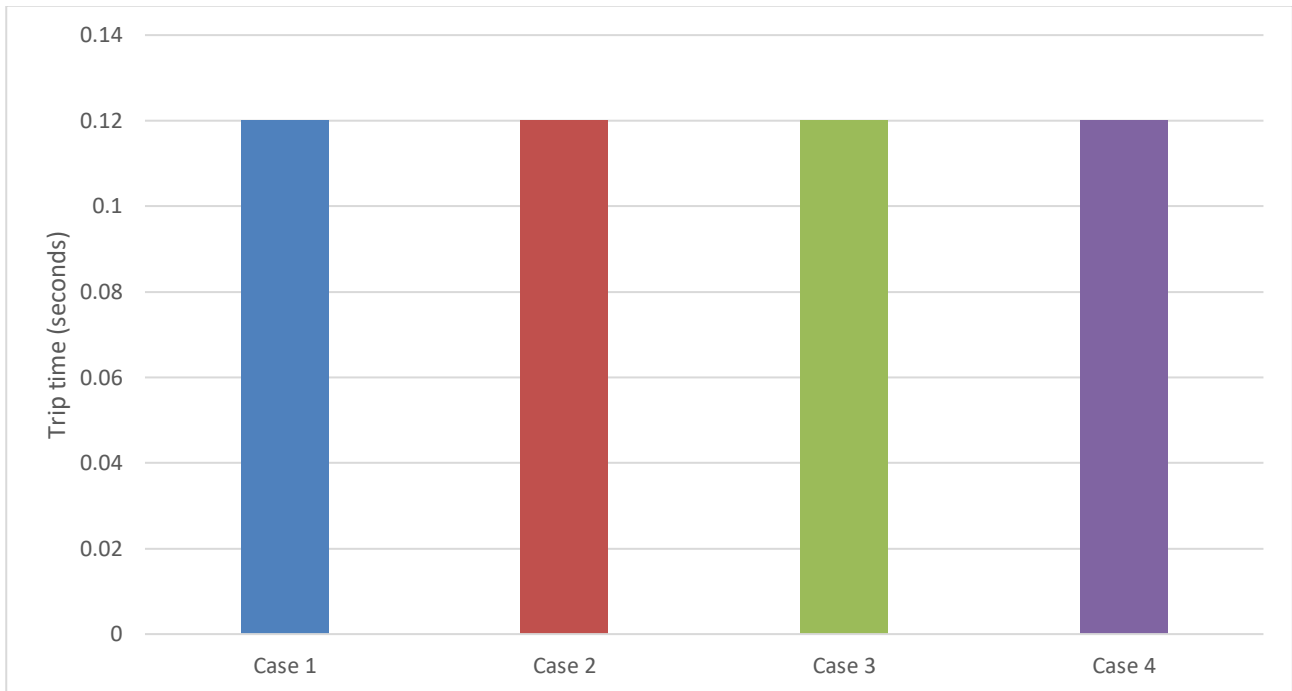


Figure 5.52: Total trip times for a single-phase fault at the Mine SS for the four cases for the municipal network

5.6.8 Fault at the Short substation

In Case 1, the stage 1 three-phase fault level is calculated as 10.444 kA, with the fault level reducing as breakers trip in order to isolate the fault. The three-phase fault consists of three stages with the first

breaker tripping in 0.311 seconds, followed by the second breaker tripping in 0.445 seconds and finally, the third breaker tripping in 0.613 seconds. Thus, the time to isolation of the fault from inception is 0.640 seconds. The Workplace MV Transformer 1 and 2 relays are seen to trip in 1.345 and 1.335 seconds, respectively, with the HV relays tripping in a similar time. This allows for a grading margin of 714 ms. This could be shortened depending on the trip times for other faults in the feeder group.

The stage 1 three-phase fault level in Case 2 is calculated as 10.505 kA, a slight increase from Case 1, also consisting of three fault stages. Similar trip times and grading margins are observed as in Case 1.

The stage 1 three-phase fault level in Case 3 is calculated as 10.609 kA. The fault persists for four stages, due to the additional tripping of the wind turbine in 0.420 seconds. The overall trip time to isolate the fault was calculated as 0.637 seconds. This includes the isolation of the wind turbine incomer at the MV main substation. The Transformer incomer 1 and 2 MV relays are calculated to trip in 1.340 and 1.331 seconds due to the wind turbine feeding the fault for 0.42 seconds of its duration.

The stage 1 three-phase fault level in Case 4 is calculated as 10.702 kA. Similar trip times and grading margins are experienced as in Case 3. The total trip times are graphically shown in Figure 5.53.

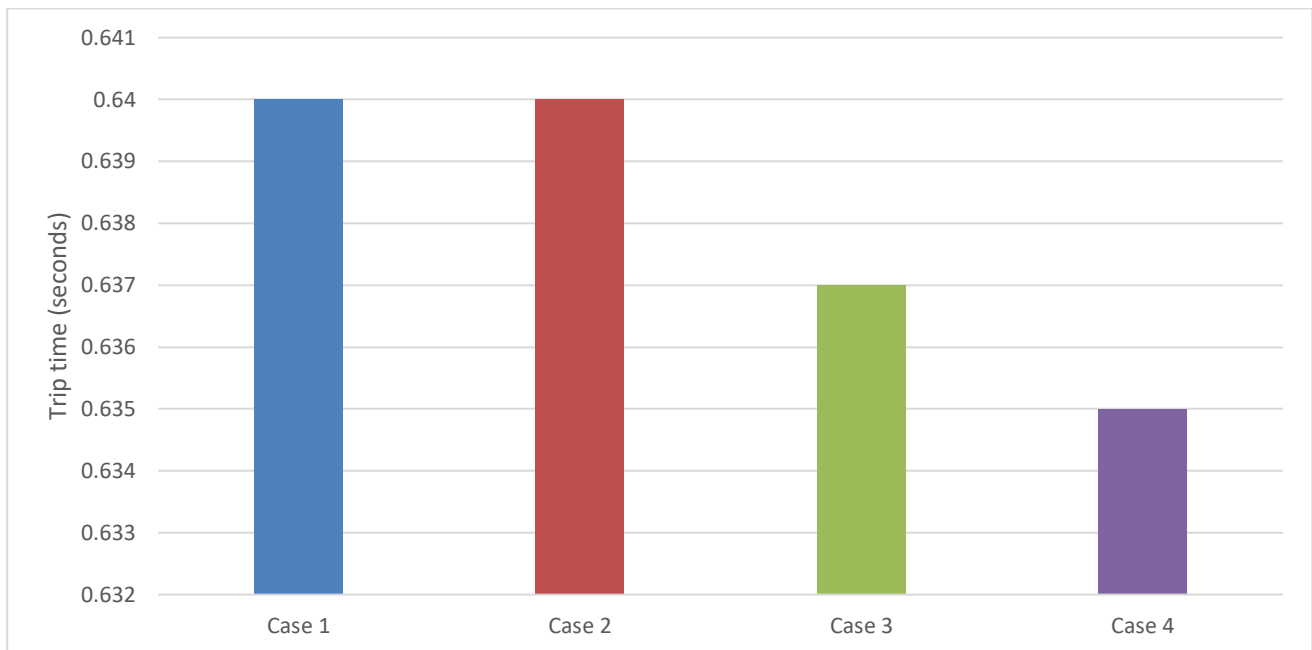


Figure 5.53: Total trip times for a three-phase fault at the Short SS for the four cases for the municipal network

The stage 1 earth-fault level in Cases 1 and 2 are calculated as 1.718 kA, with the fault level reducing as breakers trip in order to isolate the fault. The earth-fault also consists of three stages, with the overall trip time calculated as 0.878 seconds from fault inception. The Transformer 1 and 2 relays both trip in 4.232 seconds, allowing for a large grading margin. This margin could be shortened depending on the trip times for the other feeders in this feeder group.

The stage 1 earth-fault level in Case 3 is calculated as 1.721 kA and 1.722 kA in Case 4. The fault persists for three stages. The overall trip time is calculated as 0.877 seconds. Similar trip times and grading margins are experienced as in previous cases. The total trip times are graphically shown in Figure 5.54.

5.6.9 Fault at the Paste RMU 1 substation

In Case 1, the stage 1 three-phase fault level is calculated as 2.848 kA with the fault persisting over two stages. The Grounds feeder relay at the Atlantic MS is seen to trip first in 0.216 seconds. The Yellow feeder relay at the Winery MS is then seen to trip 32 ms later, isolating the fault. The grading margin with the MV Transformer relays at the Atlantic and Winery main substations are seen to be quite large, with the Winery Transformer MV relay tripping in 2.835 seconds, should the Yellow relay not operate. Should the Grounds relay not operate, the Atlantic Transformer MV relay is seen to trip in 1.788 seconds. These margins should be shortened if possible.

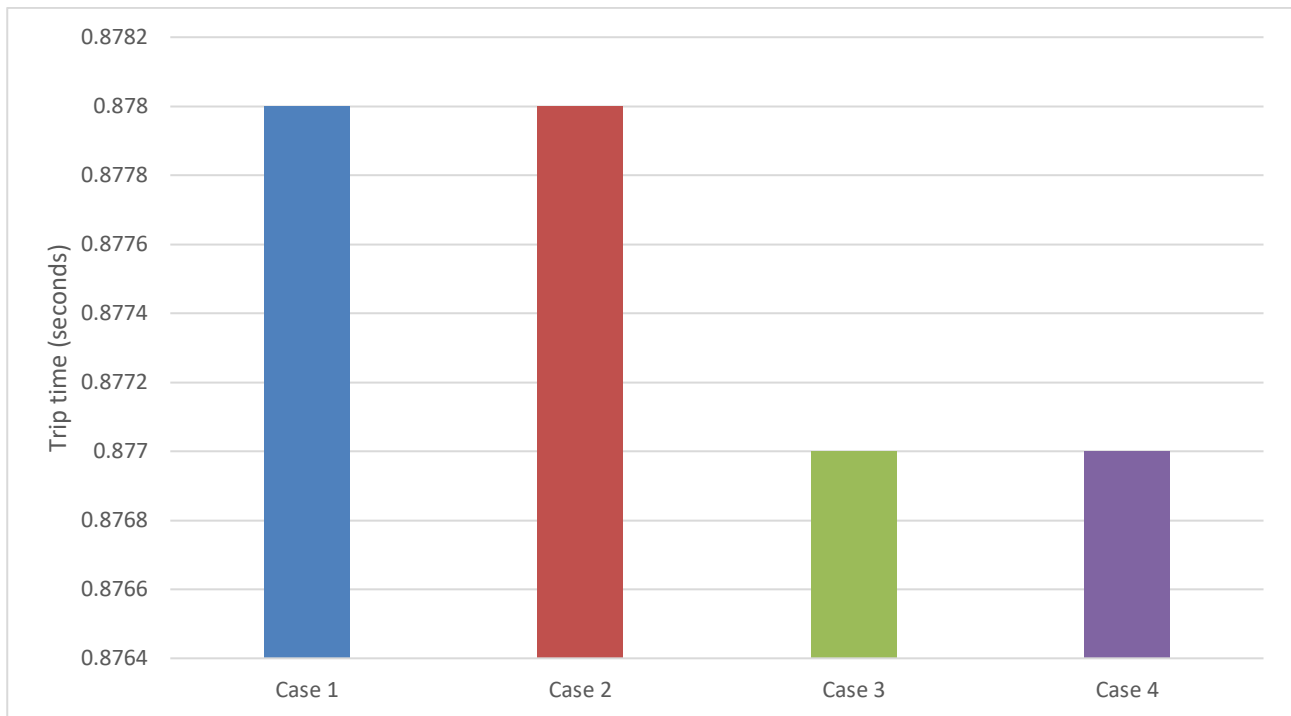


Figure 5.54: Total trip times for a single-phase fault at the Short SS for the four cases for the municipal network

The three-phase fault level in Case 2 is calculated as 2.851 kA. The fault is isolated in 0.248 seconds. However, the same grading issue with the transformer MV relays at the Atlantic and Winery main substations is observed as in Case 1.

The three-phase fault level in Case 3 is calculated as 2.904 kA. The trip time is thus similar to previous cases, with the fault being isolated in 0.247 seconds. The Atlantic Transformer MV relay is seen to trip slightly later than in previous cases, due to the addition of the direct wind turbine connection at the Atlantic LHS MV busbar. The fault level in Case 4 decreases to 2.863 kA. The trip times, grading margins, and observations are similar to Case 3 with the fault being isolated in 0.249 seconds. The total trip times are graphically shown in Figure 5.55.

The earth-fault level in Cases 1 and 2 is calculated as 0.754 kA, with the fault being isolated by the two relays as explained above. The Grounds relay at the Atlantic main substation is seen to trip first in 0.237 seconds, while the Yellow relay at the Winery main substation is seen to trip 11 ms later. Should one of these relays fail to trip, the transformer MV relay at the corresponding main substation would then trip. The trip time for the Atlantic Transformer MV relay is calculated as 2.971 seconds, while the Winery Transformer MV relay trip time is calculated as 4.599 seconds. Both of these scenarios result in extremely large grading margins that should be shortened if possible.

The earth-fault level in Cases 3 and 4 is calculated as 0.761 kA and 0.755 kA, respectively. This results in similar trip times and grading margins as in Cases 1 and 2. The fault is isolated in 0.246 and 0.248 seconds, respectively. The total trip times are graphically shown in Figure 5.56.

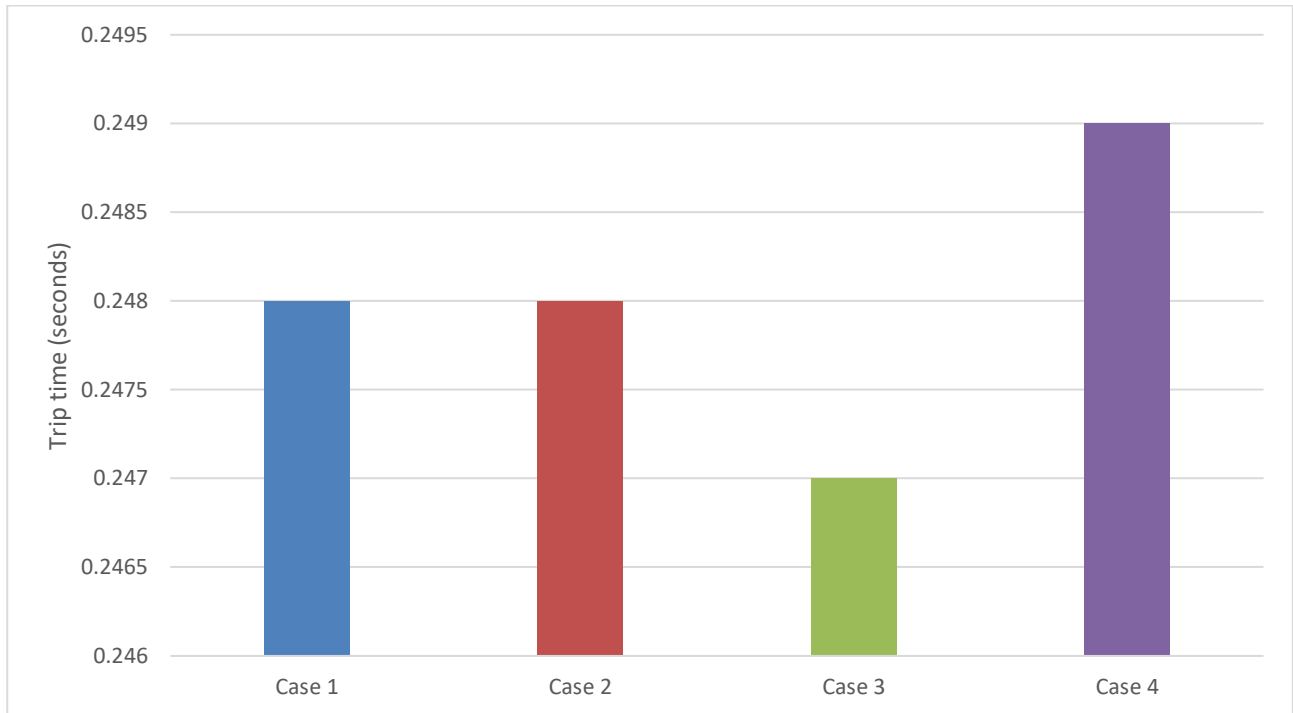


Figure 5.55: Total trip times for a three-phase fault at the Paste RMU 1 SS for the four cases for the municipal network

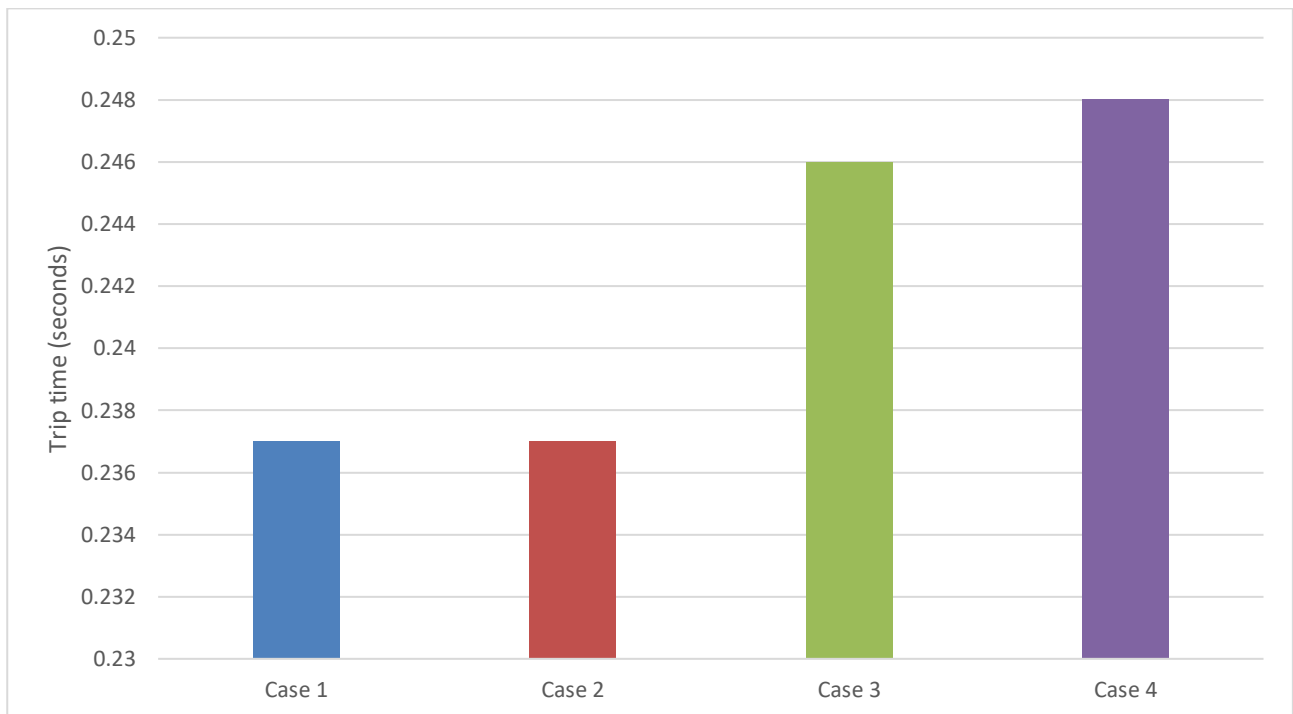


Figure 5.56: Total trip times for a single-phase fault at the Paste RMU 1 SS for the four cases for the municipal network

5.6.10 Summary of Case Study protection

In general, it is seen that the three-phase fault levels in Cases 1 and 2 remain very similar throughout the faults under study. This is expected due to the Utility substation incomers and the wind turbine

source essentially feeding the network from the same point. Thus, the MV network experiences similar fault levels due to little change in the HV source.

The three-phase fault levels shown in Cases 3 and 4, however, are generally seen to be slightly larger than the fault levels shown in Cases 1 and 2. This is also expected, due to the direct connection of a wind turbine incomer at the MV level main substation out of which the rest of the MV network is fed. However, as seen with the fault at the Tortoise substation in Case 4, this is not always the case, as the fault level at this substation remains relatively constant.

The limiting factor is seen to be the inverter units through which the wind farm is connected to the grid. Should the 120% inverter capacity be removed and the wind turbines connected directly to the busbar through a transformer, the fault levels are likely to increase. Also, due to the large amounts of power flowing in the network, the small wind turbine connections in Cases 3 and 4 have very little impact due to the inverter capacity constraint.

Transformer MV relays are generally seen to not grade well with faults further down in the networks which these transformers feed. This is seen in the case of three-phase and single-phase network faults. The transformer HV and MV relays are also generally seen to not be graded correctly, where a grading margin of around 300 ms is usually allowed, in the majority of the cases observed the margin is generally much larger than this, such as in the case for the faults at the Mine and Paste RMU 1 substations. In the case of the fault at the Winelands RMU 1 substation, the HV and MV transformer relays are completely ungraded, with the MV relays set to trip over a second later than the HV relays.

It is also seen that the Utility substation feeder trip times and the main substation HV transformer relays do not coincide in many cases, such as in the case of faults at the Winelands RMU 1, Mine, and Bushes substations. In these cases, the Utility substation feeders are seen to trip over a second later than the HV transformer relays.

The earth-fault levels for Cases 1 and 2 are also seen to be essentially the same in most of the faults studied. This is expected due to the lack of the inverter-fed wind turbine incomers contributing directly to network single-phase faults.

Fault trip times are generally seen to remain constant, even with slight increases in fault current throughout the cases under study. This is due to CT saturation, resulting in the relay thinking that the same fault current is flowing through it, even though the fault level has increased.

5.7 Discussion of the performance of the optimisation algorithms

As per the discussion above, the combination of each optimisation algorithm with the MATPOWER simulation package is seen to produce impressive optimisation gains over the both Cases 1 and 2.

The DE algorithm is seen to produce better results than the PBIL algorithm in terms of reducing network power losses and in terms of voltage profile improvement. This result differs from the results obtained from the modified IEEE 14-bus test network, in that the PBIL algorithm was seen to perform better in terms of voltage profile improvement in this case. This is likely due to the weakness of PBIL in multi-objective optimisation, as the municipal network is much larger than the modified IEEE 14-bus test network. The generator sizing results between the algorithms were mostly different, as seen in the modified IEEE network.

5.8 Costing analysis

In order to find the most suitable solution for the municipal network in terms of real-world implementation, the costs involved in each proposed solution should be analyzed.

Due to the lack of actual pricing information being available from the IPP, estimated costs were used. As seen in [71], the costs associated with commercial wind turbines can be estimated at \$2.2 million per installed MW of capacity in the worst case, including installation.

In [72], it is seen that the cost of an inverter unit capable of converting 11 kW at the desired voltage level could cost \$100 000 per set. Cables were chosen for these implementations from Appendix D based on the current-carrying requirements at full load from the municipal network Cases 2, 3 and 4. Aluminium cables were chosen based on their lower cost and contract availability. Costs for cables, obtained from the municipality, and their current-carrying capacity per km, including installation, are shown in Table 5-33. Costs for laying cables were added to the actual cable cost per km instead of the installation cost for simplicity.

Table 5-33: Cable types and associated costs

<i>Cable Type Number</i>	<i>Cable Type</i>	<i>Current-carrying Capacity (A) (in ground)</i>	<i>Cost per m (ZAR)</i>	<i>Installation Cost (ZAR)</i>
1	33 kV PILC 95 mm ² Al	180	1 172	6 584
2	11 kV XLPE 400 mm ² Al	444	701	6 741
3	11 kV XLPE 95 mm ² Al	214	289	6 584
4	11 kV XLPE 50 mm ² Al	147	126	6 517
5	11 kV XLPE 25 mm ² Al	105	73	6 517
6	11 kV XLPE 16 mm ² Al	82	51	6 517

For Case 2, only a single cable is required from the source to the Utility substation. This cable must be able to carry 1260 A based on the DG capacity. For this reason, four pairs of Type 1 cable should be used to support this. The distance from the source to the Utility substation is 15.724 km on their preferred cable route, resulting in a total cost of R18 435 112 for cabling and installation for this case.

The types of cable required for each wind turbine connection in Cases 3 and 4 are shown in Tables 5-34 and 5-35. These tables also show the total length of cable required from the source to the point of connection and the total cost associated with the physical connection. Costs for inverter units were based on a forward rate of R16.00/USD as was reasonable at the time of writing.

From Tables 5-34 and 5-35, it is seen that the total cost of cabling and cable installation is R18 435 112 for Case 2, R434 004 957 for Case 3, and R403 733 444 for Case 4. For the inverter units required, the total cost for Case 2 is R10 473 600 000, R10 480 000 000 for Case 3, and R6 729 600 000 for Case 4.

The wind turbine cost remains constant at \$2.2 million per MW of generation. Cases 2 and 3 require totals of 72 MW of generation capacity. At a forward rate of R16.00/USD, this results in a total wind turbine cost for these cases of R2 534 400 000. For Case 4, the total generation capacity required is considerably less at 46.262 MW of generation capacity. This results in a lower cost of R1 628 422 400.

Thus, the total costs for each case is shown in Table 5-36 and Figure 5.57.

Table 5-34: Cables and inverters required for implementing Case 3 in the municipal network

<i>Turbine Location</i>	<i>Turbine full load current (A)</i>	<i>Cable type number</i>	<i>Length of cable required (km)</i>	<i>Cable Cost (ZAR)</i>	<i>Number of inverter units required</i>	<i>Cost of inverter units</i>
Bus 2 – Utility Sub	10.346	1	15.724	18 435 112	54	86 400 000
Bus 3 – LHS Gardens HV	54.201	1	18.373	21 539 740	282	451 200 000
Bus 4 – RHS Gardens HV	53.561	1	18.363	21 528 020	278	444 800 000
Bus 5 – LHS Atlantic HV	40.765	1	21.032	24 656 088	212	339 200 000
Bus 6 – RHS Atlantic HV	68.163	1	21.039	24 664 292	354	566 400 000
Bus 7 – LHS Delilah HV	37.115	1	19.634	23 017 632	193	308 800 000
Bus 8 – RHS Delilah HV	60.860	1	19.916	23 348 136	316	505 600 000
Bus 9 – LHS Wozniak B HV	47.462	1	15.817	18 544 108	247	395 200 000
Bus 10 – LHS Wozniak A HV	58.422	1	15.829	18 558 172	304	486 400 000
Bus 11 – RHS Wozniak C HV	71.206	1	15.833	18 562 860	370	592 000 000
Bus 12 – LHS Sunset Vista B HV	62.074	1	18.098	21 217 440	323	516 800 000
Bus 13 – LHS Sunset Vista A HV	21.905	1	18.090	21 208 064	114	182 400 000
Bus 14 – RHS Sunset Vista C HV	20.692	1	18.146	21 273 696	108	172 800 000
Bus 15 – RHS Sunset Vista D HV	10.346	1	18.111	21 232 676	54	86 400 000
Bus 16 – LHS Workplace HV	41.376	1	16.946	19 867 296	215	344 000 000
Bus 17 – RHS Workplace HV	36.516	1	16.336	19 152 376	190	304 000 000
Bus 18 – Utility Sub Switch Yard	52.333	1	15.821	18 548 796	272	435 200 000
Bus 19 – Winery HV	29.217	1	25.812	30 258 248	152	243 200 000
Bus 20 – LHS Gardens LV	17.222	6	18.373	943 540	32	51 200 000
Bus 21 – RHS Gardens LV	27.550	6	18.363	943 030	51	81 600 000
Bus 22 – LHS Atlantic LV	149.834	3	21.032	6 084 832	275	440 000 000
Bus 23 – RHS Atlantic LV	99.873	4	21.039	2 657 431	183	292 800 000
Bus 24 – LHS Delilah LV	186.030	3	19.634	5 680 810	342	547 200 000
Bus 25 – RHS Delilah LV	122.295	4	19.916	2 515 933	225	360 000 000
Bus 26 – LHS Wozniak LV	18.955	6	15.817	813 184	35	56 000 000
Bus 27 – RHS Wozniak LV	168.798	3	15.833	4 582 321	310	496 000 000
Bus 28 – LHS Sunset Vista LV	194.595	2	18.098	12 693 439	357	571 200 000
Bus 29 – RHS Sunset Vista LV	137.792	3	18.146	5 250 778	253	404 800 000
Bus 30 – Workplace LV	182.564	3	16.946	4 903 978	335	536 000 000
Bus 31 – Winery LV	62.004	6	25.812	1 322 929	114	182 400 000

Table 5-35: Cables and inverters required for implementing Case 4 in the municipal network

<i>Turbine Location</i>	<i>Turbine full load current (A)</i>	<i>Cable type number</i>	<i>Length of cable required (km)</i>	<i>Cable Cost (ZAR)</i>	<i>Number of inverter units required</i>	<i>Cost of inverter units</i>
Bus 2 – Utility Sub	2.055	1	15.724	18 435 112	11	17 600 000
Bus 3 – LHS Gardens HV	25.366	1	18.373	21 539 740	132	211 200 000
Bus 4 – RHS Gardens HV	9.785	1	18.363	21 528 020	51	81 600 000
Bus 5 – LHS Atlantic HV	9.462	1	21.032	24 656 088	49	78 400 000
Bus 6 – RHS Atlantic HV	31.478	1	21.039	24 664 292	164	262 400 000
Bus 7 – LHS Delilah HV	46.993	1	19.634	23 017 632	244	390 400 000
Bus 9 – LHS Wozniak B HV	11.642	1	15.817	18 544 108	60	96 000 000
Bus 10 – LHS Wozniak A HV	15.007	1	15.829	18 558 172	78	124 800 000
Bus 11 – RHS Wozniak C HV	52.978	1	15.833	18 562 860	275	440 000 000
Bus 12 – LHS Sunset Vista B HV	19.160	1	18.098	21 217 440	100	160 000 000
Bus 13 – LHS Sunset Vista A HV	17.765	1	18.090	21 208 064	92	147 200 000
Bus 14 – RHS Sunset Vista C HV	28.404	1	18.146	21 273 696	148	236 800 000
Bus 15 – RHS Sunset Vista D HV	57.763	1	18.111	21 232 676	300	480 000 000
Bus 16 – LHS Workplace HV	28.189	1	16.946	19 867 296	146	233 600 000
Bus 17 – RHS Workplace HV	7.114	1	16.336	19 152 376	37	59 200 000
Bus 18 – Utility Sub Switch Yard	51.509	1	15.821	18 548 796	268	428 800 000
Bus 19 – Winery HV	9.174	1	25.812	30 258 248	48	76 800 000
Bus 20 – LHS Gardens LV	42.567	6	18.373	943 540	78	124 800 000
Bus 21 – RHS Gardens LV	31.104	6	18.363	943 030	57	91 200 000
Bus 22 – LHS Atlantic LV	26.966	3	21.032	6 084 832	50	80 000 000
Bus 23 – RHS Atlantic LV	84.745	4	21.039	2 657 431	156	249 600 000
Bus 24 – LHS Delilah LV	1.800	3	19.634	5 680 810	3	4 800 000
Bus 26 – LHS Wozniak LV	84.079	5	15.817	1 161 158	154	246 400 000
Bus 27 – RHS Wozniak LV	120.863	3	15.833	4 582 321	222	355 200 000
Bus 28 – LHS Sunset Vista LV	190.215	3	18.098	5 236 906	349	558 400 000
Bus 29 – RHS Sunset Vista LV	105.835	4	18.146	2 292 913	194	310 400 000
Bus 30 – Workplace LV	402.956	2	16.946	11 885 887	740	1 184 000 000

From Table 5-36 and Figure 5.57, it is seen that Case 4 is the most cost-efficient overall case for implementation. This is mainly due to the reduction in generation capacity, and thus inverter capacity required for this case. This excludes the fact that Case 4 will result in additional savings over the other two cases due to the reduction in power losses associated with the case.

Table 5-36: Total costs for implementing the three possible cases for the municipal network

<i>Case</i>	<i>Total Cabling Cost (ZAR)</i>	<i>Total Inverter Cost (ZAR)</i>	<i>Total Turbine Cost (ZAR)</i>	<i>Total Project Cost (ZAR)</i>
Case 2	18 435 112	10 473 600 000	2 534 400 000	13 026 435 112
Case 3	434 004 957	10 480 000 000	2 534 400 000	13 448 404 957
Case 4	403 733 444	6 729 600 000	1 628 422 400	8 761 755 844

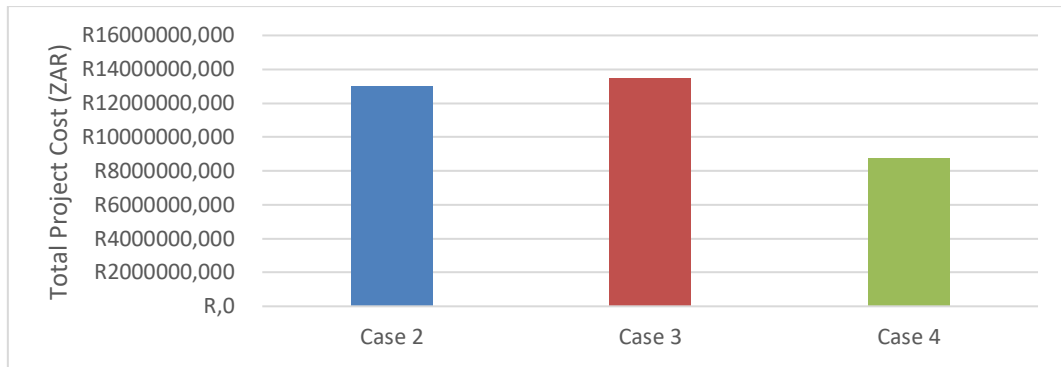


Figure 5.57: Total cost of implementation for each case for the municipal network

5.9 Chapter summary

In summary, the results shown in the municipal network show that the use of either of the two optimisation algorithms produce excellent results. Both algorithms result in less power being required from the grid. The DE algorithm result is seen to outperform the PBIL algorithm result in terms of voltage profile improvement and reduction in network power losses. In terms of protection, the four cases all result in similar fault levels. Thus, the network grading remains essentially unaffected.

The DE algorithm result is also seen to be the most economical result in terms of cost of implementation.

6. Conclusions

This section concludes the study based on the discussion in the preceding sections. The main conclusions drawn from the case studies are summarised below.

6.1 The MATPOWER library works well as a network simulation tool

The MATPOWER network simulation library works well and produces very similar results to a DlgSILENT PowerFactory simulation, though the text-based modelling makes network modelling more complex. This tool does work well, however, and could be used in future research.

6.2 In the modified IEEE network, the DE algorithm presents the best power loss reduction

The power flow results for the DE algorithm in the modified IEEE network show that the solution presented by the algorithm produces the best results, reducing power losses by 38.74% compared to the base modified IEEE network, though the solution produced by the PBIL algorithm also performs similarly well.

6.3 In the modified IEEE network, the PBIL algorithm presents the best overall voltage profile

The power flow results for the modified IEEE network shows that the solution presented by the PBIL algorithm produces the best overall voltage profile improvement.

6.4 In the municipal network, the DE algorithm presents the best power loss reduction

The power flow results for the proposed implementation, the PBIL algorithm, and the DE algorithm show that the overall network power loss is reduced in all three cases from the base case. However, the solution presented by the DE algorithm results in the power losses being reduced by 83.89% compared to both the base case and the proposed implementation, and 69.19% compared to the PBIL solution.

6.5 In the municipal network, the DE algorithm presents the best overall voltage profile

The power flow results for the cases show that the voltage profiles in base case and the proposed implementation are the same due to the wind turbine in the latter case being connected to the network slack bus. The PBIL solution is shown to introduce voltage profile deterioration from the first two cases. However, in the solution presented by the DE algorithm, the connections of the wind turbines throughout the network results in a definite voltage profile improvement, with the total RMS error improving by 23.71%.

6.6 The Differential Evolution minimisation algorithm produces excellent results

The DE algorithm used in conjunction with the MATPOWER library produces excellent results and improvements as detailed in preceding sections. The performance of this algorithm is seen to supersede the performance demonstrated by the PBIL algorithm in both objectives in the municipal network, likely due to the algorithm's inherent difficulty in dealing with many variables in multi-objective problems.

The PBIL algorithm is observed to result in better voltage profile improvement in the modified IEEE 14-bus test system, though the improvement over the DE algorithm is slight.

6.7 Fault levels are extremely similar between the cases

The three-phase and single-phase to ground fault levels at the various substations in the network are not seen to vary much throughout the two networks and across the respective cases, though the fault levels in the cases involving the algorithms are generally slightly higher or slightly lower than in the cases without them due to the direct turbine incomer connections on the 11 kV network. This is due to the fault contribution limit created by the inverters through which the wind turbines are connected to the network. This limit is good in terms of limiting change in fault levels with inverter installations, so that sensitivity issues could be minimised if these inverters are used on a larger scale.

6.8 The case study network is not optimally graded

It is observed in most of the simulated fault locations that the case study network is not optimally graded. Many of the observed faults show that grading margins are either too large or too small between network relays or are incorrectly graded.

6.9 Relay grading remains unaffected by the addition of the wind farm incomers

The slight differences in fault current observed in both networks through the multiple cases leads to the grading between the cases remaining extremely similar in each respective network, without any need to completely change any protection settings should any of the cases be implemented.

6.10 The most cost-effective solution for the Case Study network is produced by the Differential Evolution algorithm

The total project costs for the solution produced by the DE algorithm is observed to be the lowest of all the cases studied. This, coupled with the improved performance of the solution over the proposed implementation and the solution produced by the PBIL algorithm make it the best choice for implementation.

6.11 Chapter summary

This research has investigated the proposed connection of a wind farm to an existing municipal grid, and has compared it to the current configuration. The PBIL and DE optimisation algorithms were then used to find the optimal placement of the wind farm connections in terms of voltage profile improvement and power loss reduction. The results presented by these algorithms were then compared to the proposed and current configurations.

As seen in this chapter, the PBIL algorithm solution produces the best voltage profile in the case of the IEEE network, but is observed to be dramatically outperformed by the DE algorithm in the Case Study network in terms of both voltage profile improvement and network power loss reduction. The DE algorithm also presents the most cost-effective solution in the Case Study network due to the lower total generation required.

The Case Study network is observed to not be optimally graded, as grading margins at some of the fault locations are either too large or too small. However, the proposed solution and the solutions produced by the PBIL and DE algorithms are observed to minimally impact the protection grading performance compared to the protection performance in the base case. This is due to very similar fault levels

experienced between the different proposed solutions because of the limited fault contribution from the wind farm inverter units.

Both algorithms are observed to perform well and provide good solutions in terms network improvement and cost-effectiveness for the Case Study network. Fault levels and protection grading are observed to be minimally impacted by the addition of the DGs in these networks.

7. Recommendations

This section details recommendations based on the conclusions made in the previous chapter.

7.1 Regrade the case study network

Grading studies need to be done to grade the entire municipal network. This will ensure proper grading margins are allowed for, so that the network protection scheme would be ready for a connection to the proposed wind farm.

7.2 Implement the Differential Evolution solution for the wind farm connection

The configuration obtained by the DE algorithm for the municipal network is seen to provide the best electrical results. The costs for this case are also observed to be substantially lower than the other cases under study. It is thus recommended that this configuration be implemented.

7.3 Investigate the effect of the wind farm connection with higher fault contributions

To further the work done in this research, an investigation can be done in order to observe the differences in the implementation of the wind farm with higher fault contributions from the wind turbines, either with the turbines being directly connected to the grid through step-up transformers, or by increasing the allowable fault contribution from the inverters.

7.4 Conduct further research

It is recommended that further research be done to investigate the possibility of connecting the proposed wind farm to the major utility network instead of the municipal network. Further research can also be done to investigate the effect of distributed generators on different networks. Finally, an investigation can be done to the effect of non-inverter connected wind turbines on the municipal network.

References

- [1] J. Krupa and S. Burch, "A New Energy Future for South Africa: The Political Ecology of South African Renewable Energy," *Elsevier Energy Policy*, vol. 39, no. 10, pp. 6254-6261, 2011.
- [2] U. Khan, "Impact of Distributed Generation on Electrical Power Network," 15 December 2015. [Online]. Available: <https://pdfs.semanticscholar.org/4724/7d27fc19df1755274c65ce8581b807e6c9c9.pdf>. [Accessed 29 September 2018].
- [3] M. Martin, "Economic Analysis of a Stand-Alone Solar PV System for Different Sizes of Middle Income Residential Load Clusters In South Africa," B. Sc. (Eng.) Thesis, University of Cape Town, Cape Town, 2014.
- [4] PV Insider, "Annual Sum of Global Horizontal Irradiation," 20 June 2014. [Online]. Available: <http://www.ee.co.za/wp-content/uploads/2014/06/PV-insider-191-07-2014.jpg>. [Accessed 29 September 2018].
- [5] J. Dekker, S. Chowdhury and S. P. Chowdhury, "Economic Viability of PV/Diesel Hybrid Power Systems in Different Climatic Zones in South Africa," in *IEEE PES General Meeting*, Providence, USA, 2010.
- [6] S. K. Mulaudzi and S. Bull, "An Assessment of the Potential of Solar Photovoltaic (PV) Application in South Africa," in *International Renewable Energy Conference*, Hammamet, 2016.
- [7] SANews, "Energy to Launch IPP Bid Window," 1 June 2018. [Online]. Available: <https://www.sanews.gov.za/south-africa/energy-launch-new-ipp-bid-window>. [Accessed 29 September 2018].
- [8] NERSA, "Grid Connection Code for Renewable Power Plants (RPPs) Connected to the Electricity Transmission System (TS) or the Distribution System (DS) in South Africa," NERSA, Pretoria, 2010.
- [9] C. Greacen, R. Engel and T. Quetchenbach, "A Guidebook on Grid Interconnection and Islanded Operation of Mini-Grid Power Systems up to 200kW," April 2013. [Online]. Available: https://ies.lbl.gov/sites/default/files/a_guidebook_for_minigrids-serc_lbnl_march_2013.pdf. [Accessed 29 September 2018].
- [10] NERSA, "Electricity Supply — Quality of Supply Part 2: Voltage Characteristics, Compatibility Levels, Limits and Assessment Methods," NERSA, Pretoria, 2010.
- [11] Pacific Gas and Electric Company, "Voltage Unbalance and Motors," 24 March 2017. [Online]. Available: https://www.pge.com/includes/docs/pdfs/mybusiness/customerservice/energystatus/powerquality/voltage_unbalance_rev2.pdf. [Accessed 29 September 2018].
- [12] Yukon Government, "Turbine Parts," [Online]. Available: http://www.energy.gov.yk.ca/images/turbine_parts.JPG. [Accessed 19 February 2018].
- [13] S. Chowdhury and S. Chowdhury, *Microgrids and Active Distribution Networks*, India: Macmillan Publishing Solutions, 2009.
- [14] A. Larsson, "The Power Quality of Wind Turbines," PhD Thesis, Chalmers University of Technology, Gothenburg, 2000.
- [15] R. Mittal, K. S. Sandhu and D. K. Jain, "An Overview of Some Important Issues Related to Wind Energy Conversion System (WECS)," *International Journal of Environmental Science and Development*, vol. 1, no. 4, pp. 352-363, 2010.
- [16] T. Dang, "Introduction, History, and Theory of Wind Power," in *North American Power Symposium*, Starkville, 2009.

- [17] W. Cao, Y. Xie and Z. Tan, "Wind Turbine Generator Technologies," IntechOpen, London, 2012.
- [18] R. Bharanikumar, R. Senthilkumar and A. N. Kumar, "Impedance Source Inverter for Wind Turbine Driven Permanent Magnet Generator," in *Joint International Conference on Power System Technology and IEEE Power India Conference*, New Delhi, 2008.
- [19] S. Ozdemir, U. S. Selamogullari and O. Elma, "Analyzing the Effect of Inverter Efficiency Improvement in Wind Turbine Systems," in *International Conference on Renewable Energy Research and Application (ICRERA)*, Milwaukee, 2014.
- [20] P. Barendse, R. Naidoo, H. Douglas and P. Pillay, "A New Algorithm for Improved Dip/Sag Detection with Application to Improved Performance of Wind Turbine Generators," in *Conference Record of the 2006 IEEE Industry Applications Conference*, Tampa, 2006.
- [21] K. Knorr, B. Zimmerman, S. Bofinger, A. Gerlach, T. Bischof-Niemz and C. Mushwana, "Wind and Solar PV Resource Aggregation Study for South Africa," Fraunhofer IWES and CSIR, Pretoria, 2016.
- [22] SANEDI, "Appraisal of Implementation of Fossil Fuel and Renewable Energy Hybrid Technologies in South Africa," SANEDI, Sandton, 2017.
- [23] M. Esmaili, E. C. Firozjaee and H. A. Shayanfar, "Optimal Placement of Distributed Generations Considering Voltage Stability and Power Losses with Observing Voltage-Related Constraints," *Elsevier Applied Energy*, vol. 113, no. C, pp. 1252-1260, 2014.
- [24] C. J. Mozina, "Update on the Current Status of DG Interconnection Protection—What IEEE P-1547 Doesn't Tell You About DG Interconnection Protection," in *WSU Conference*, Washington, 2014.
- [25] F. Katiraei, J. Holbach, T. Chang, W. Johnson, D. Wills, B. Young, L. Marti, A. Yan, P. Baroutis, G. Thompson and J. Rajda, "Investigation of Solar PV Inverters Current Contributions During Faults on Distribution and Transmission Systems Interruption Capacity," in *Western Protective Relay Conference*, Washington, 2012.
- [26] A. Janssen, M. van Riet, J. Bozelie and J. Au-yeung, "Fault Current Contribution from State of the Art DG's and its Limitation," in *International Conference on Power System Transients*, Delft, 2011.
- [27] J. Lu, M. Savaghebi and J. M. Guerrero, "and Damping of Harmonic Propagation in DG-Penetrated Distribution Networks," in *IEEE Energy Conversion Congress and Exposition (ECCE)*, Milwaukee, 2016.
- [28] A. N. Z. Rashed, "Band Pass Filters with Low Pass and High Pass Filters Integrated With Operational Amplifiers in Advanced Integrated Communication Circuits," *International Journal of Advanced Research in Computer Engineering & Technology*, vol. 2, no. 3, pp. 861-866, 2013.
- [29] K. Wada, H. Fujita and H. Akagi, "Considerations of a Shunt Active Filter Based on Voltage Detection for Installation on a Long Distribution Feeder," *IEEE Transactions on Industry Applications*, vol. 38, no. 4, pp. 1123-1130, 2002.
- [30] D. E. Newman, B. A. Carreras, M. Kirchner and I. Dobson, "The Impact of Distributed Generation on Power Transmission Grid Dynamics," in *Hawaii International Conference on System Science*, Kauai, 2011.
- [31] J. A. Momoh, S. Meliopoulos and R. Saint, "Centralized and Distributed Generated Power Systems – A Comparison Approach," Future Grid Initiative, Washington, 2012.
- [32] A. Sheikhi, A. Maani, F. Safe and A. M. Ranjbar, "Distributed Generation Penetration Impact on Distribution Networks Loss," in *International Conference on Renewable Energies and Power Quality*, Bilbao, 2013.
- [33] M. H. Pourarab, M. H. Meshkini and A. Yektay, "Harmonic Analysis of Integrating a DG Unit to the Distribution Network – Case Study," in *International Conference on Electricity Distribution*, Stockholm, 2013.

- [34] P. Caramia, E. D. Mambro, P. Varilone and P. Verde, "Impact of Distributed Generation on the Voltage Sag Performance of Transmission Systems," *Energies*, vol. 10, pp. 1-19, 2017.
- [35] G. Coppez, S. Chowdhury and S. P. Chowdhury, "Battery Storage and Testing Protocols for CHP Systems," in *IEEE Power and Energy Society General Meeting*, San Diego, 2011.
- [36] MIT Electric Vehicle Team, "A Guide to Understanding Battery Specifications," December 2008. [Online]. Available: http://web.mit.edu/evt/summary_battery_specifications.pdf. [Accessed 29 September 2018].
- [37] M. Skyllas-Kazacos, M. H. Chakrabarti, S. A. Hajimolana, F. S. Mjalli and M. Saleem, "Progress in Flow Battery Research and Development," *Journal of the Electrochemical Society*, vol. 158, no. 8, pp. 55-79, 2011.
- [38] IEC, "Electrical Energy Storage," 2017. [Online]. Available: <https://www.iec.ch/whitepaper/pdf/iecWP-energystorage-LR-en.pdf>. [Accessed 29 September 2018].
- [39] Z. Stevic, M. Rajcic-Vujasinovic, S. Bugarinovic and A. Dekanski, "Construction and Characterisation of Double Layer Capacitors," in *Oxide Materials for Electronic Engineering*, Lviv, 2009.
- [40] R. V. Holla, "Energy Storage Methods - Superconducting Magnetic Energy Storage - A Review," *University of Illinois Journal of Undergraduate Research*, vol. 5, no. 1, pp. 49-54, 2015.
- [41] F. Kang, S. Park, S. E. Cho and J. Kim, "Photovoltaic Power Interface Circuit Incorporated with a Buck-Boost Converter and a Full-Bridge Inverter," *Elsevier Applied Energy*, vol. 82, no. 3, pp. 266-283, 2005.
- [42] S. G. Tesfahunegn, O. Ulleberg, T. M. Undeland and P. J. S. Vie, "A Simplified Battery Charge Controller for Safety and Increased Utilization in Standalone PV Applications," in *International Conference on Clean Electrical Power*, Ischia, 2011.
- [43] M. Ragheb, "Control of Wind Turbines," 2016. [Online]. Available: <https://www.mragheb.com/NPRE%20475%20Wind%20Power%20Systems/Control%20of%20Wind%20Turbines.pdf>. [Accessed 29 September 2018].
- [44] Hsieh, L. Chen and K. Huang, "Fuzzy-Controlled Li-ion Battery Charge System with Active State-of-Charge Controller," *IEEE Transactions on Industrial Electronics*, vol. 48, no. 3, pp. 585-593, 2011.
- [45] University of Notre Dame, "Wind Turbine Control," 2016. [Online]. Available: https://www3.nd.edu/~tcorke/w.WindTurbineCourse/WindTurbineControl_Presentation.pdf. [Accessed 29 September 2018].
- [46] M. F. Kotb, K. M. Shebl, M. El Khazendar and A. El Hussein, "Genetic Algorithm for Optimum Siting and Sizing of Distributed Generation," in *International Middle East Power Systems Conference*, Cairo, 2010.
- [47] W. Tan, M. Y. Hassan, M. S. Majid and H. Abdul Rahman, "Optimal Distributed Renewable Generation Planning: A Review of Different Approaches," *Elsevier Renewable and Sustainable Energy Reviews*, vol. 18, no. C, pp. 626-645, 2013.
- [48] N. Vijaysimha, C. Chengaiah and M. Venugopal, "Optimal Siting and Sizing of Distributed Generation for Radial Distribution System using Genetic Algorithm," *International Journal of Engineering and Science*, vol. 5, no. 4, pp. 39-46, 2015.
- [49] K. A. Folly and G. K. Venayagamoorthy, "Effects of Learning Rate on the Performance of the Population Based Incremental Learning Algorithm," in *International Joint Conference on Neural Networks*, Atlanta, 2009.
- [50] E. J. Hughes, "Optimisation Using Population Based Incremental Learning (PBIL)," in *IEE Colloquium on Optimisation in Control: Methods and Applications*, London, 1998.

- [51] A. Sorsa, A. Koskenniemi and K. Leiviska, "Evolutionary Algorithms in Nonlinear Model Identification," 2010. [Online]. Available: <http://jultika.oulu.fi/files/isbn9789514263323.pdf>. [Accessed 29 September 2018].
- [52] H. Manafi, N. Ghadimi, M. Ojaroudi and P. Farhadi, "Optimal Placement of Distributed Generations in Radial Distribution Systems Using Various PSO and DE Algorithms," *Elektronika IR Elektrotehnika*, vol. 19, no. 10, pp. 53-57, 2013.
- [53] A. P. Engelbrecht, *Computational Intelligence: An Introduction*, Second Edition, West Sussex: John Wiley & Sons, Ltd, 2007.
- [54] T. R. Ayodele, A. S. O. Ogunjuyigbe and O. O. Akinola, "Optimal Location, Sizing, and Appropriate Technology Selection of Distributed Generators for Minimizing Power Loss Using Genetic Algorithm," *Journal of Renewable Energy*, vol. 2015, pp. 1-9, 2015.
- [55] H. Zhan, C. Wang, Y. Wang, X. Yang, X. Zhang, C. Wu and Y. Chen, "Relay Protection Coordination Integrated Optimal Placement and Sizing of Distributed Generation Sources in Distribution Networks," *IEEE Transactions on Smart Grid*, vol. 7, no. 1, pp. 55-65, 2016.
- [56] L. F. Grisales-Norena, D. G. Montoya and C. A. Ramos-Paja, "Optimal Sizing and Location of Distributed Generators Based on PBIL and PSO Techniques," *Energies*, vol. 11, no. 4, pp. 1-27, 2018.
- [57] T. Tusar and B. Filipic, "Differential Evolution Versus Genetic Algorithms in Multiobjective Optimization," in *International Conference on Evolutionary Multi-Criterion Optimization*, Sendai, 2007.
- [58] Ravi and H. Sangwan, "Optimal Positioning and Sizing of DG Units Using Differential Evolution Algorithm," *International Journal of Innovative Research in Science, Engineering and Technology*, vol. 5, no. 9, pp. 17178-17185, 2016.
- [59] W. Lui, H. Xu, S. Niu and J. Xie, "Optimal Distributed Generator Allocation Method Considering Voltage Control Cost," *Sustainability*, vol. 8, no. 2, pp. 1-20, 2016.
- [60] H. Yang, F. Wen and G. Ledwich, "Optimal Coordination of Overcurrent Relays in Distribution Systems with Distributed Generators Based on Differential Evolution Algorithm," *European Transactions on Electrical Power*, vol. 23, pp. 1-12, 2011.
- [61] A. Alarcon-Rodriguez, G. Ault and S. Galloway, "Multi-Objective Planning of Distributed Energy Resources: A Review of the State-of-the-Art," *Elsevier Renewable and Sustainable Energy Reviews*, vol. 14, no. 5, pp. 1353-1366, 2010.
- [62] P. S. Georgilakis and N. D. Hatziargyriou, "Optimal Distributed Generation Placement in Power Distribution Networks: Models, Methods, and Future Research," *IEEE Transactions on Power Systems*, vol. 28, no. 3, pp. 3420-3428, 2013.
- [63] A. S. Noghabi, H. R. Mashhadi and J. Sadeh, "Optimal Coordination of Directional Overcurrent Relays Considering Different Network Topologies Using Interval Linear Programming," *IEEE Transactions on Power Delivery*, vol. 25, no. 3, pp. 1348-1354, 2010.
- [64] DlgSILENT PowerFactory, "14-Bus System Datasheet," DlgSILENT PowerFactory, Gomaringen, 2015.
- [65] CBI Electric, "MV XLPE Cable Data Sheet, 6350/11000V, Aluminium, 3 core, Type A," October 2016. [Online]. Available: <http://www.africancables.com/sites/default/files/11kV%20MV%20XLPE%20Aluminium%203%20Core%20Type%20A%20%28Armoured%29%20PVC.pdf>. [Accessed 5 October 2018].
- [66] CBI Electric, "Medium Voltage PILC Cables, 6350/11000V, Copper 3 core," May 2006. [Online]. Available: <http://www.africancables.com/sites/default/files/11kV%20MV%20PILC%20Copper%203%20Core%20DSTA%20Table%202017.pdf>. [Accessed 5 October 2018].

- [67] CBI Electric, "Medium Voltage PILC Cables, 6350/11000V, Copper 1 core," May 2006. [Online]. Available: <http://www.africancables.com/sites/default/files/11kV%20MV%20PILC%20Copper%201%20Core%20AWA%20Table%2010.pdf>. [Accessed 5 October 2018].
- [68] CBI Electric, "MV XLPE Cable Data Sheet, 6350/11000V, Copper 3 core, Type A," October 2016. [Online]. Available: <http://www.africancables.com/sites/default/files/11kV%20MV%20XLPE%20Copper%203%20core%20Type%20A%20PVC..pdf>. [Accessed 5 October 2018].
- [69] B. A. Mustaqim, E. A. Ambarani, A. K. Srivastava and Suwarno, "Influence of Zero-Sequence Removal on Transformer Fundamental Quantity Monitoring," in *Proceedings of the World Congress on Engineering*, London, 2016.
- [70] Univeristy of California, "Circuit Reduction Techniques," 2001. [Online]. Available: <http://aries.ucsd.edu/najmabadi/CLASS/MAE140/NOTES/reduce.pdf>. [Accessed 29 September 2018].
- [71] Windustry, "How Much Do Wind Turbines Cost?," 2017. [Online]. Available: http://www.windustry.org/how_much_do_wind_turbines_cost. [Accessed 24 December 2018].
- [72] Made-in-China.com, "11-35kV Frequency Inverter VFD," [Online]. Available: <https://simoncnc.en.made-in-china.com/product/pKYnESBxqicr/China-11kv-35kv-Frwquency-Inverter-VFD.html>. [Accessed 24 December 2018].
- [73] M. Sarma and J. Glover, *Power System Analysis and Design*, 5th ed., Stamford: Cengage Learning, 2011.
- [74] Circuit Globe, "Symmetrical and Unsymmetrical Faults," 20 May 2016. [Online]. Available: <https://circuitglobe.com/symmetrical-and-unsymmetrical-faults.html>. [Accessed 29 September 2018].
- [75] T. Agarwal, "Types of Faults and Effects in Electric Power Systems," February 2014. [Online]. Available: <https://www.elprocus.com/what-are-the-different-types-of-faults-in-electrical-power-systems/>. [Accessed 29 September 2018].
- [76] M. Eissa, "New Protection Philosophy for Protecting Complex Smart Grid with Renewable Resources Penetration," in *IEEE 2012 International Conference on Smart Grid*, Oshawa, 2012.
- [77] M. Rycroft, "Advantages of Optical Current and Voltage Sensors and Transformers," 13 March 2017. [Online]. Available: <http://www.ee.co.za/article/advantages-optical-current-voltage-sensors-transformers.html>. [Accessed 29 September 2018].
- [78] S. McFadyen, "Electromechanical Relays," 2 April 2012. [Online]. Available: <https://myelectrical.com/notes/entryid/159/electromechanical-relays>. [Accessed 29 September 2018].
- [79] Fecime.org, "Overcurrent Protection for Phase and Earth Faults," 4 May 2008. [Online]. Available: <https://www.fecime.org/referencias/npag/chap9-122-151.pdf>. [Accessed 29 September 2018].

Appendix A: IEEE 14-bus network data

Table A-1: The IEEE 14-bus system generator dispatch data [64]

Generator	Bus	P in MW	Q in MVAr
Gen_0001	Bus_0001	N/A	N/A
Gen_0002	Bus_0002	40.0	N/A
Gen_0003	Bus_0003	0.0	N/A
Gen_0006	Bus_0006	0.0	N/A
Gen_0008	Bus_0008	0.0	N/A

Table A-2: The IEEE 14-bus system generator controller data [64]

Generator	Bus Type	Voltage in p.u.	Minimum capability (MVA)	Maximum capability (MVA)
Gen_0001	Slack	1.060	N/A	N/A
Gen_0002	PV	1.045	-40.0	50.0
Gen_0003	PV	1.010	0.0	40.0
Gen_0006	PV	1.070	-6.0	24.0
Gen_0008	PV	1.090	-6.0	24.0

Table A-3: The IEEE 14-bus system load data [64]

Generator	Bus	P in MW	Q in MVAr
Load_0002	Bus_0002	21.7	12.7
Load_0003	Bus_0003	94.2	19.0
Load_0004	Bus_0004	47.8	-3.9
Load_0005	Bus_0005	7.6	1.6
Load_0006	Bus_0006	11.2	7.5
Load_0009	Bus_0009	29.5	16.6
Load_0010	Bus_0010	9.0	5.8
Load_0011	Bus_0011	3.5	1.8
Load_0012	Bus_0012	6.1	1.6
Load_0013	Bus_0013	13.5	5.8
Load_0014	Bus_0014	14.9	5.0

Table A-4: The IEEE 14-bus system line data [64]

From Bus	To Bus	r in p.u.	x in p.u.	q _c /2 in p.u.	b in p.u.
1	2	0.01938	0.05917	0.0264	0.0528
1	5	0.05403	0.22304	0.0246	0.0492
2	3	0.04699	0.19797	0.0219	0.0438
2	4	0.05811	0.17632	0.0187	0.0374
2	5	0.05695	0.17388	0.0170	0.0340
3	4	0.06701	0.17103	0.0173	0.0346
4	5	0.01335	0.04211	0.0064	0.0128
6	11	0.09498	0.19890	0.0000	0.0000
6	12	0.12291	0.25581	0.0000	0.0000
6	12	0.06615	0.13027	0.0000	0.0000
9	10	0.03181	0.08450	0.0000	0.0000
9	14	0.12711	0.27038	0.0000	0.0000
10	11	0.08205	0.19207	0.0000	0.0000
12	13	0.22092	0.19988	0.0000	0.0000
13	14	0.17093	0.34802	0.0000	0.0000

Table A-5: The IEEE 14-bus system transformer data [64]

Transformer	From Bus	To Bus	Ur HV in kV	Ur LV in kV	x in p.u.	Transformer Final Turns Ratio
Trf_0004_0007	4	7	132	1	0.20912	0.978
Trf_0004_0009	4	9	132	33	0.55618	0.969
Trf_0005_0006	5	6	132	33	0.25202	0.932
Trf_0007_0008	7	8	11	1	0.17615	0.000
Trf_0007_0009	7	9	33	1	0.11001	0.000

**The system is set on a 100 MVA base.

Appendix B: Review of protection systems

B.1 Faults in a power network

Power networks are made up of multiple components which work together to deliver electrical power from generation sources to multiple loads. These components include generators, power lines, underground cables, transformers, and more. Each of these components are subject to the possibility of a failure or external interference which could cause them to malfunction in some way.

A fault in a power network is defined as a short circuit from a specified point in the network to ground, or a short circuit between different phases. When a fault occurs, the fault current is usually several times greater than the normal operating current [73], which could cause damage to the equipment in the network if the fault is allowed to persist for long periods of time. This is due to stress, heat, and other magnetic forces introduced by excessively high currents. There are different types of faults that could occur in a power network. Some of these faults are explored below.

B.1.1 Symmetrical faults

Symmetrical faults, also known as three-phase faults, are characterised by a connection of each of the three phases to earth under balanced conditions. In practice, however, the connection between the three phases and earth is usually connected through a single, common impedance. This type of fault usually produces the largest fault currents compared to any other type of fault.

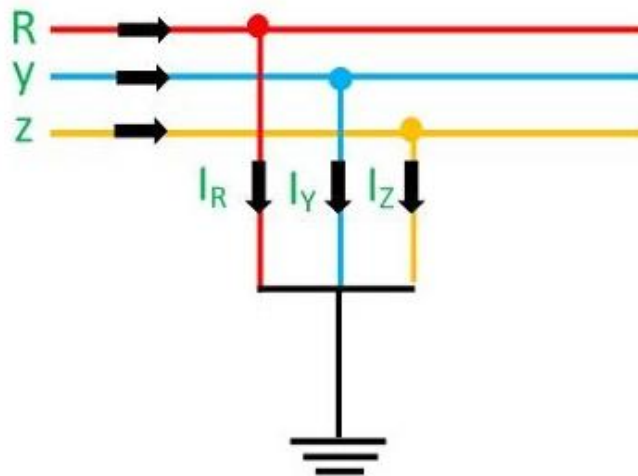


Figure B-1: Typical CT and VT connection on the power grid [74]

B.1.2 Unsymmetrical faults

Unsymmetrical faults are faults in which different combinations of the three system phases are shorted to earth [73]. This includes single-phase-to-ground (also known as a 'single-phase' or 'earth'), double-line-to-ground, and line-to-line faults. Unsymmetrical faults are not balanced on the three phases and hence comprise of positive, negative, and zero-sequence components [73]. The network connection of each type of unsymmetrical fault is shown below.

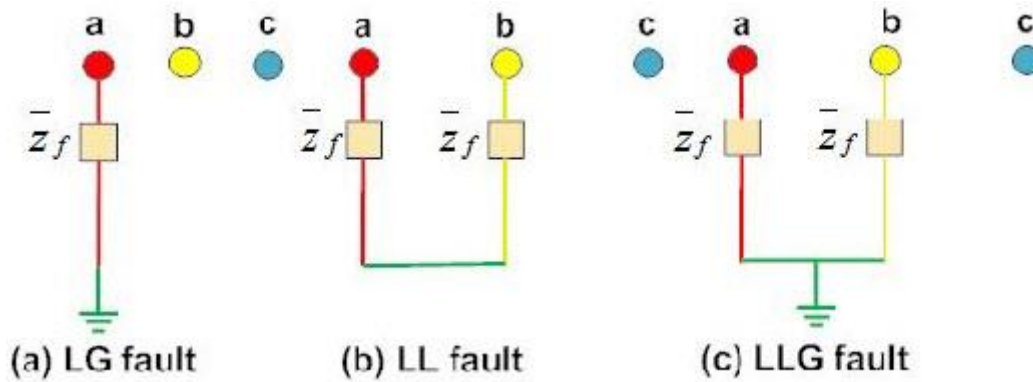


Figure B-2: Typical CT and VT connection on the power grid [75]

In practice, neutral-earthing resistors (NERs) are sometimes used at medium voltages to reduce the fault current levels flowing through the neutral connection of a generator or transformer under earth-fault conditions to a pre-set value determined by the design of the NER. This results in minimized equipment damage and generated heat under earth-fault conditions.

B.2 Protection systems

Protection systems are used to protect the power network from any possible component failures and faults on the network. The protection system cannot prevent faults from occurring, but can minimize and control them. Other characteristics of protection systems are stated below [76].

- **Speed:** The protection system must operate quickly in order to minimize damage to the remaining parts of the network.
- **Selectivity:** The protection system must keep the healthy part of the network alive, and not trip unnecessarily [73].
- **Sensitivity:** The protection system must be sensitive to fault conditions, and not operate under normal power system conditions.
- **Reliability:** The protection system must be known to work under fault conditions.

Protection systems can fall into one of two categories, namely Unit and Non-Unit protection.

- **Unit protection:** Unit protection, also known as primary protection, is the protection of a specific component or piece of equipment in the power system. It does not concern itself with the conditions outside the protected zone. Common unit protection used in the network include line differential protection and different types of transformer unit protection.
- **Non-unit protection:** Non-unit protection, also known as secondary protection, does not protect a specific part of the network, but rather provides a general protection for the entire system. For this reason, it is mainly used as backup protection in the case of a failure of the unit protection. Common types of non-unit protection used in the network include overcurrent and earth-fault relays.

B.2.1 Equipment used in protection systems

Protection systems are made up of multiple components. These components are explored below.

Fuses

Fuses are the simplest overcurrent devices; they consist of a metallic fusible link encapsulated in a glass tube with metallic sides, and filled with material to control arcing [73]. Once the current reaches a certain value, the metallic link begins to melt until it is completely disintegrated, disconnecting the circuit.

Measuring Equipment

Instrument transformers are used to scale high voltages and currents down to readable levels so that they can be measured using standard electronic equipment. Current transformers (CTs) are used to step high currents down to lower levels, and voltage transformers (VTs) are used to step high voltages down to lower levels [73]. The CT and VT ratios are generally standardised, usually with a secondary rating of either 5A or 1A. CTs are connected in series with the primary conductor while VTs are connected parallel to the conductor. This is shown in Figure B-3 below.

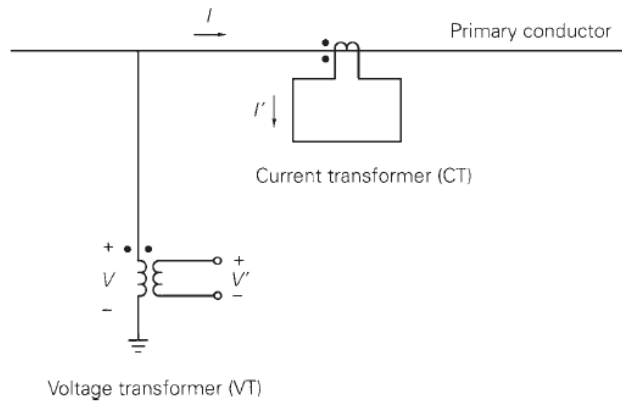


Figure B-3: Typical CT and VT connection on the power grid [73]

New types of CTs and VTs have recently made great strides based on the Faraday Effect. These are known as optical CTs and optical VTs, which uses fibre-optic technology coupled with the Faraday Effect instead of traditional transformer technology [77]. The Faraday Effect is detailed in the equation below and is only valid for materials which exhibit this effect [77].

$$\theta = \int_0^L V\beta \, dl \quad (\text{B-1})$$

In the equation above, θ is the angle of rotation of the polarized light, which is determined by the magnetic field strength. V is the Verdet constant which is dependant on the type of material used and β is the magnetic field strength. L is the distance over which the light and magnetic field interact with each other [77]. In a uniform, constant magnetic field, the equation above can be reduced to the following equation.

$$\theta = V\beta L \quad (\text{B-2})$$

Using CTs and VTs of an optical nature thus allows multiple advantages over traditional CTs and VTs. These include freedom from magnetic saturation, lower wiring cost, light-weight and small in size, interaction with modern relays and protection schemes where fibre connections are becoming more commonly used, and safety of field staff from dangers associated with purely electrical connections, among others [77].

Power supplies

A substation is usually fitted with a DC and AC power supply. The DC supply consists of a string of series-connected batteries and a battery charger which is also connected to the AC supply for charging purposes.

In terms of power supply usage, the DC supply is used to power the relays, contacts, and other related DC-powered components in the substation. DC power is usually set to 30 V for an 11 kV substation or 110V for a higher voltage main or switching substation in the municipality under study.

The AC power is used for charging the DC battery charger, as well as powering the circuit breaker spring recharging and panel heaters.

Circuit breakers

Circuit breakers are mechanically operated switches in the power system which are used to interrupt currents. They differ in comparison to fuses due to the fact that they are able to be reclosed and used again. When the circuit breaker's contacts open due to a fault current, an arc develops between the contacts which keeps the current flowing. This arc needs to be safely extinguished so that the fault can be cleared from the network. There are multiple ways in which this can be done, most of which employ a neutralising agent to quench the arc.

Relays

Relays are devices, either electronic or electromechanical, which issue a trip signal to a circuit breaker to open its contacts when the device detects abnormal system conditions. Relays generally sense abnormal system conditions by reading the outputs of CTs and VTs.

Relays were initially electromechanical devices, using the laws of electromagnetism to pick up an abnormal system condition, issue a trip signal through a mechanical contact. However, as technology has developed, and the need for more sophisticated protection systems grew, digital and numerical relays were developed, which provided better accuracy and allowed a wider range of possible settings. These sophisticated relays can also communicate with each other through either hard-wiring or fibre optic methods which allows larger protection schemes to be developed, such as reverse-busbar blocking.

There are different types of relays for different types of abnormal system conditions, though more modern relays incorporate multiple functions in a single device. The different types of relays and their functions are explored below.

Overcurrent relays

Overcurrent relays are relays designed specifically to detect a situation when the current flowing in a line on the power system becomes too high, in which case the relay issues a trip signal to the circuit breaker for that specific line. Overcurrent relays are a form of non-unit protection.

The value that determines an overcurrent condition is called the "pickup current" and varies based on system and network design and the normal operating current for that feeder. The currents are monitored on all three phases as well as the earth connection if one exists. Relays which monitor the current flowing to earth are known as earth-fault relays, which usually have different settings compared to the overcurrent settings for the same feeder.

Because the overcurrent condition may last for a very short amount of time when the current is slightly above the pickup current but is operating normally, it is undesirable for the circuit breaker to trip for any overcurrent condition. Therefore, there are different timing methods used to determine how long the overcurrent condition should last before the relay issues a trip signal. These are discussed in more detail below.

Instantaneous overcurrent relays

Instantaneous overcurrent relays issue the trip signal to the circuit breaker immediately when the overcurrent condition is reached. No timing mechanism is implemented in this case. However, because the laws of causality prevent anything from happening instantaneously, there is a very short delay before the trip signal is sent [73]. The characteristic of this type of relay is shown in Figure B-4 below.

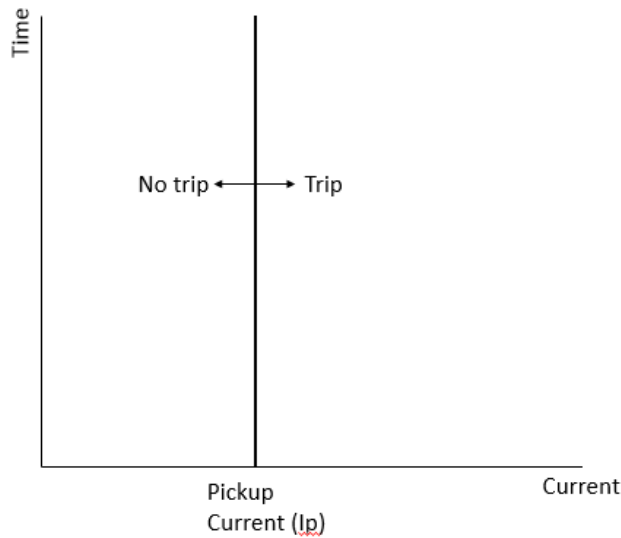


Figure B-4: Characteristic of the instantaneous overcurrent relay

Definite-time overcurrent relays

Definite-time overcurrent relays monitor the current for the overcurrent condition. Once this condition is reached, the relay starts timing as long as the current stays above the threshold. Once the timer has reached a pre-specified limit, the relay sends the trip signal to the circuit breaker.

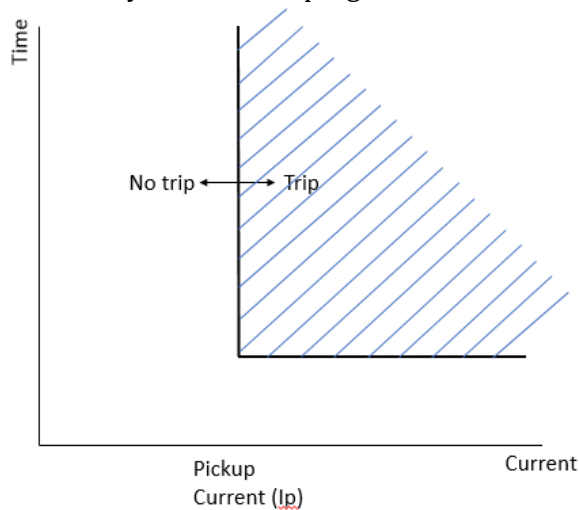


Figure B-5: Characteristic of the definite-time overcurrent relay

Indefinite-minimum-time (IDMT) overcurrent relays

IDMT overcurrent relays work similarly to definite-time overcurrent relays but use inverse curves to determine the tripping time for different levels of fault current. There are three standard IEC inverse curves which are used in South Africa, namely the Normal Inverse, Very Inverse, Extremely Inverse, and Long-time Inverse curves. The trip time is determined by an equation depending on which of the three curves are chosen to be used. Some of these curves are shown in Figure B-6 below.

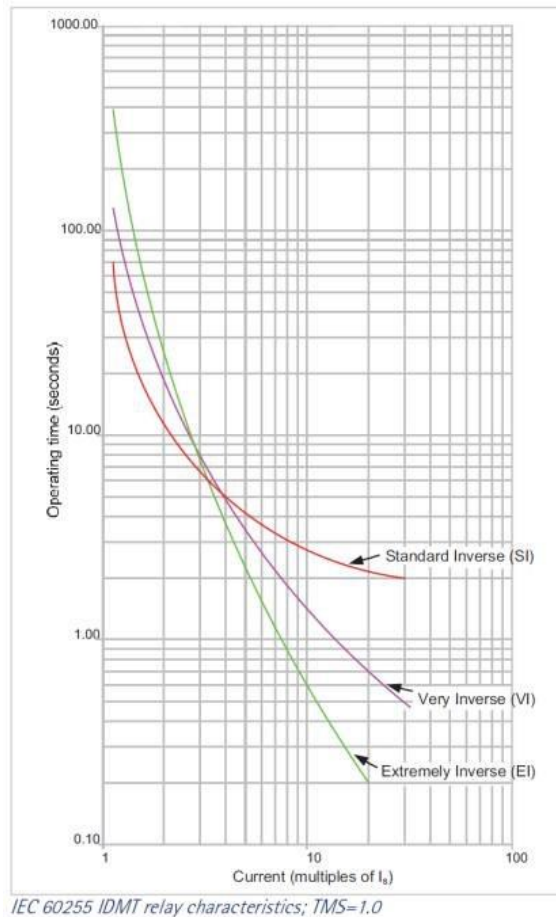


Figure B-6: Graph showing three IEC IDMT inverse curves [78]

The equation which determines the tripping time is given below [78].

$$t_{trip} = \frac{K}{\left(\frac{I}{I_s}\right)^{\alpha} - 1} \times TMS \quad (B-3)$$

In the above equation, t_{trip} is the trip time in seconds, K and α are constants which change depending on the type of curve that is being used, TMS is the time multiplier setting on the relay, I is the actual secondary current, and I_s is the relay setting for the secondary current [78]. Table B-1 gives the K and α values for the different types of IEC IDMT curves.

Table B-1: K and α values for the different IEC IDMT curves [78]

Type of IEC IDMT curve	α	K
Normal/Standard Inverse	0.02	0.14
Very Inverse	1.0	13.5
Extremely Inverse	2.0	80
Long-time Inverse	1.0	120

Combinations

In practice, a combination of the above curves are used. This occurs mainly in newer digital relays, as the curve and its chosen settings are highly programmable. IDMT curves are usually used for overcurrent protection up to a certain multiple of the normal load current. Instantaneous overcurrent settings usually take over from the IDMT curves after a certain multiple of the load current has been reached, which is normally 10 times the pickup current in the municipal network under study.

Overcurrent relay grading

Overcurrent relays need to be discriminated from each other in a network. This means that, in the case when multiple overcurrent relays see an overcurrent condition, they should time differently such that the overcurrent relays closer to the electricity source do not trip for a fault lower downstream, to preserve the power delivered to the healthy part of the network while disconnecting the faulty part. This is done by grading overcurrent relays. The time difference for a trip between two consecutive overcurrent relays is known as the ‘grading margin’ and must be set to adequately be able to discriminate a downstream fault from an upstream fault condition. An example of a simple relay grading between two relays is shown in Figure B-7 below.

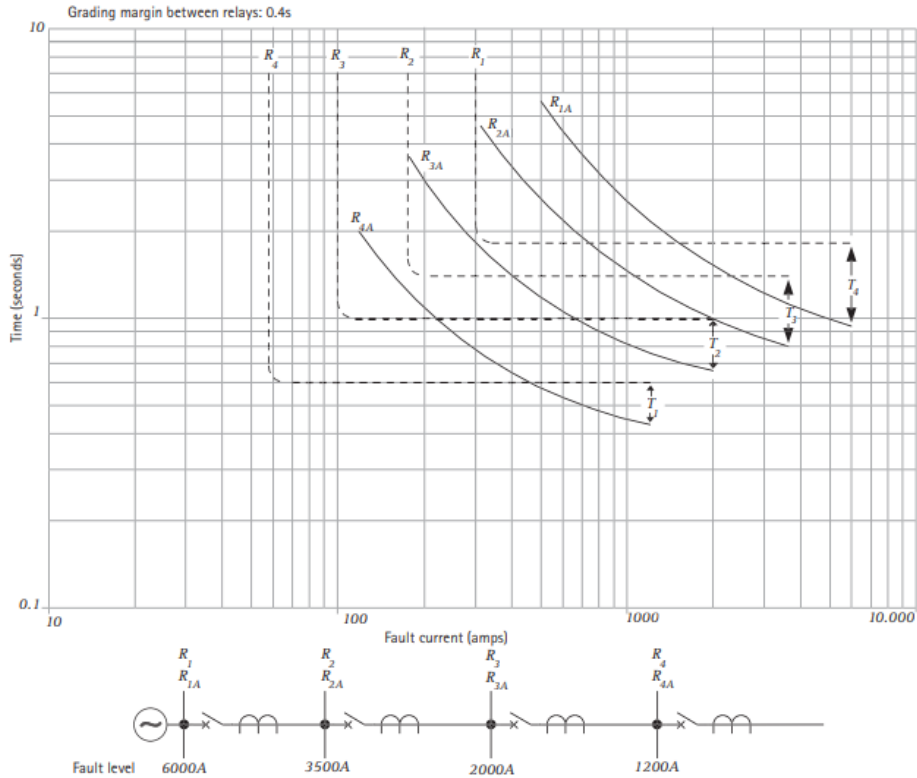


Figure B-7: The grading between two overcurrent relays [79]

Graded relays usually use the same IEC curve in the municipal network to make discrimination easier, while maintaining simplicity.

Grading mainly involves setting the time multiplier setting on overcurrent and earth-fault relays, as the pickup current is generally set based on the types of cable being used or the transformer rating. The IEC Normal Inverse curve is used throughout the municipality’s network.

Due to the complexity and scale of a functioning network, the overcurrent settings applied in the network are usually difficult to change, especially for a consumer like the municipality under study, where the utility’s protection settings determine how much leeway is available to grade with the upstream and downstream parts of the network. Thus, when adding additional components to the network, it would be desirable to leave the currently applied settings while only adding settings for the component or substation being added to the network.

Differential relays

Differential relays are pairs of relays which are used for the unit protection of generators, transformers, lines, and busses. They measure the current in and out of the protected zone and compare them. If there are any differences in current, the relays issue a trip on both sides of the protected zone. Figure B-8 below illustrates a practical implementation of differential relays for a single phase of a generator.

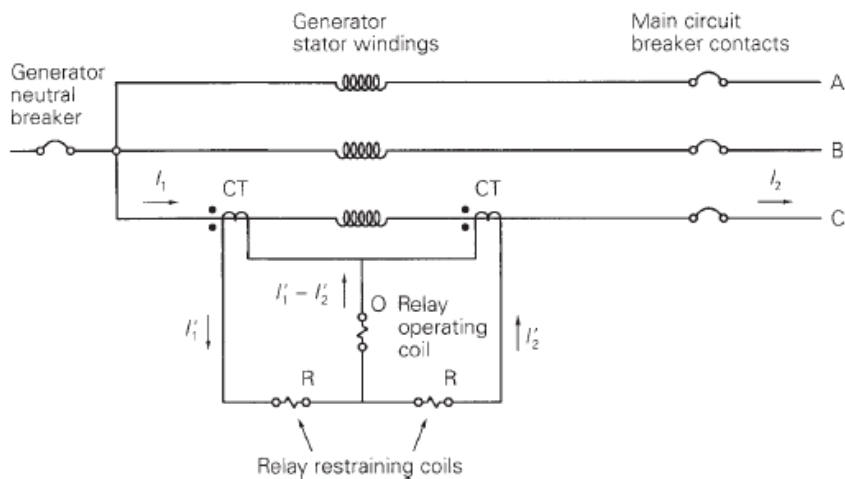


Figure B-8: Typical differential relay connection for a single phase of a generator [73]

Differential relays normally come in two main variants, namely “R” and “Rf” differential relays. The main difference between these two relays are the fact that R relays use half-wave rectification for measuring the current input from the CT, while Rf relays use full-wave rectification for this function. The types of differential relays on both ends of a protected zone must be the same so that the measured currents are equally measured on both ends of the protected zone and can be fairly compared.

Pairs of newer differential relays normally communicate with each other using fibre optics, but older relays use hardwired, physical connections between relays known as “pilot wires”.

Directional relays

Directional relays are used to detect a fault in only one “direction” in the power system, usually either on the left or right-hand side of the CT being used for measurement at a specific point in the network. A typical connection of a directional relay is shown in Figure B-9.

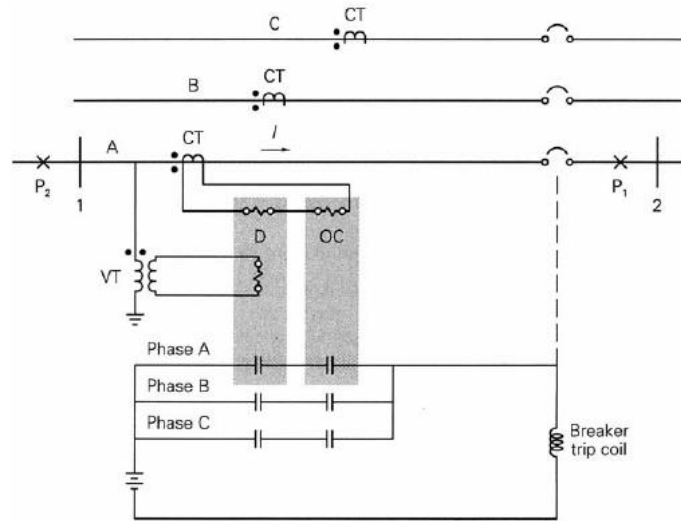


Figure B-9: Typical directional relay connection for a single phase [73]

Directional relays have two inputs, namely the reference voltage $V = |V| < 0^\circ$ and the reference current $I = |I| < \phi$ [73]. The line impedance is mostly reactive, and thus, if a fault were to occur at P1, the current would lag the bus voltage by almost 90° [73]. This defines the forward direction of the relay. If a fault were to occur at P2 however, the current would lead the bus voltage by almost 90° , defining the reverse direction of the relay [73]. The trip and block regions can thus be defined by the following set of equations [73].

$$\begin{aligned} -180^\circ < \phi - \phi_1 < 0^\circ & \quad (\text{Trip}) \\ \text{Otherwise} & \quad (\text{Block}) \end{aligned} \quad (\text{B-4})$$

Where ϕ_1 is the boundary between the boundary between the trip and block regions. This results in the following trip and block regions in the complex plane.

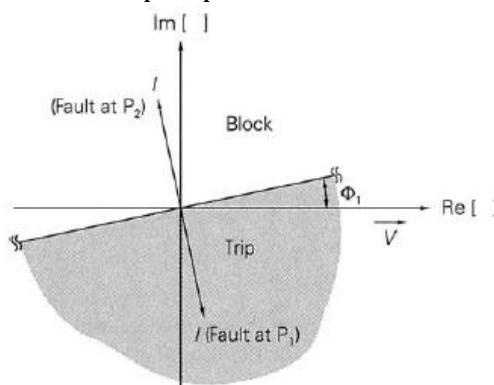


Figure B-10: Typical directional relay trip and block regions in the complex plane [73]

Directional relays are difficult to use when there are multiple sources in the network [73].

Distance relays

Distance relays, also known as impedance relays, are relays which use the voltage-to-current ratio to determine when an abnormal condition is present in the system. By Ohm's Law, the ratio of voltage to current is known as impedance, which consists of a resistive and reactive component. Thus, the trip and block regions for a distance relay can be seen as a circle in the impedance plane where the radius of the circle is the acceptable ratio of voltage to current set by the engineer. Thus, a point inside the circle

would issue a trip signal and a point outside the circle would not [73]. A The trip and block regions for distance relays are shown in Figure B-11 below.

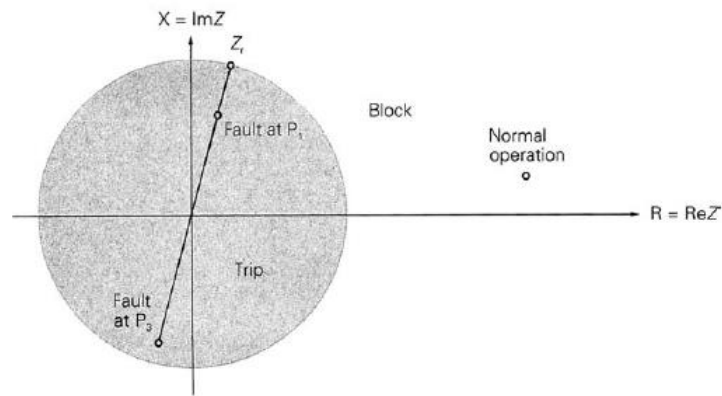


Figure B-11: Typical distance relay trip and block regions in the complex plane [73]

Distance relays are used to protect different “zones”. A zone of protection is defined in the complex plane as a circle with a certain radius. Multiple circles can be incorporated into a single distance relay, which allows for more discrimination. Circles with larger radii are usually set to have longer trip times.

Distance relays can also be made to incorporate directional discrimination, which would offset the centre of the circle and thus incorporate directional and distance protection.

Appendix C: Single-line diagrams and busbar loads for the municipal network

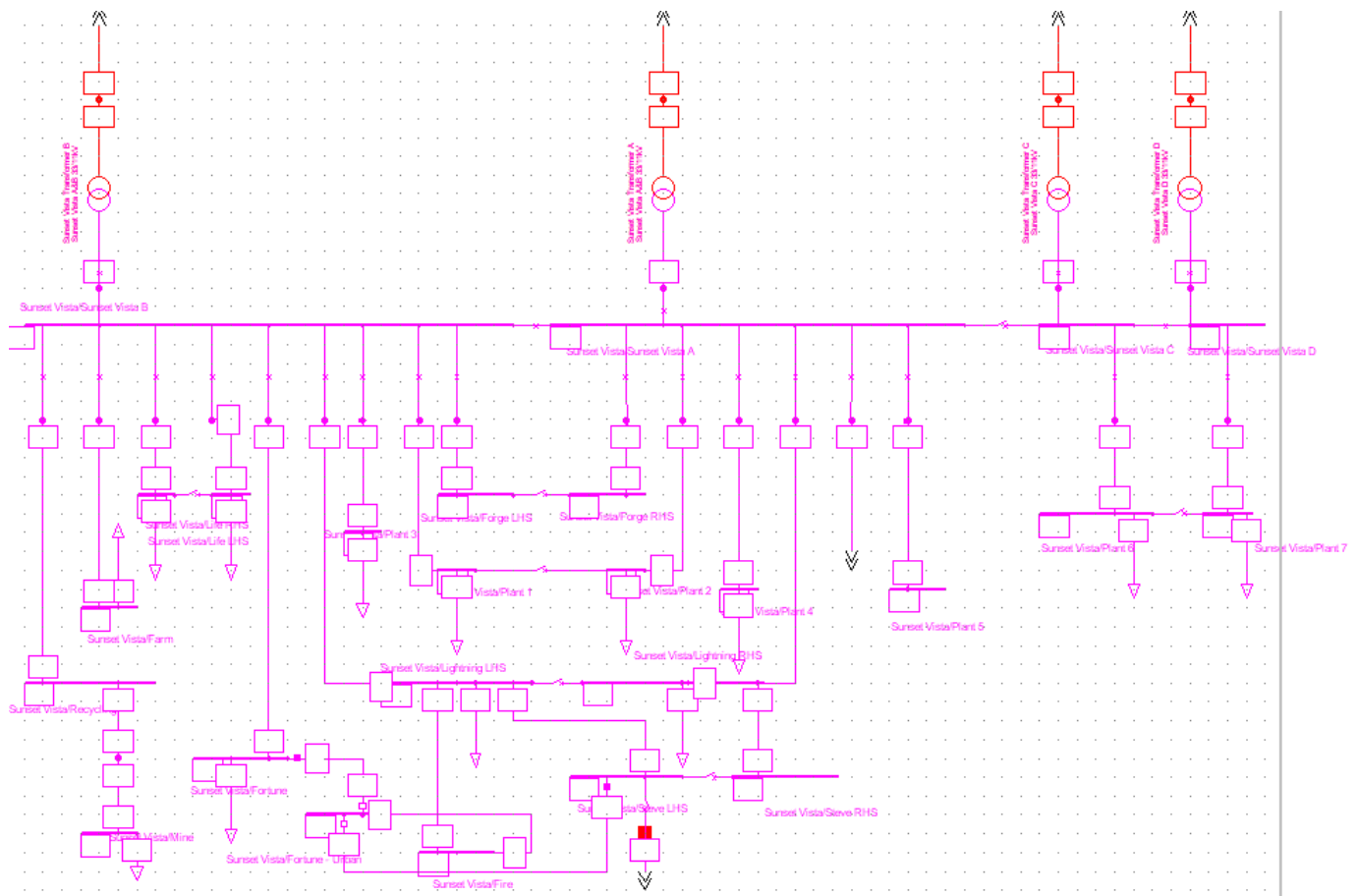


Figure C.1: Single-line diagram of the Sunset Vista MS feeder group

Table C-1: Feeder load specifications at the Sunset Vista MS

Feeder	Voltage Rating (kV)	Load (A)	Power Factor
Life LHS	11.66	31.9349	0.9
Life RHS	11.66	78.6283	0.9
Short	11.66	4.5457	0.9
Fortune	11.66	25.6497	0.9
Forge 1	11.66	0	0.9
Forge 2	11.66	0	0.9
Plant 1	11.66	86.8589	0.9
Plant 2	11.66	140.6093	0.9
Plant 3	11.66	79.5621	0.9
Plant 4	11.66	154.6042	0.9
Plant 5	11.66	0	0.9
Plant 6	11.66	160.1695	0.9
Plant 7	11.66	175.9824	0.9
Lightning 1	11.66	39.6835	0.9
Lightning 2	11.66	13.2884	0.9
Farm	11.66	0.1198	0.9
Recycling	11.66	33.9312	0.9

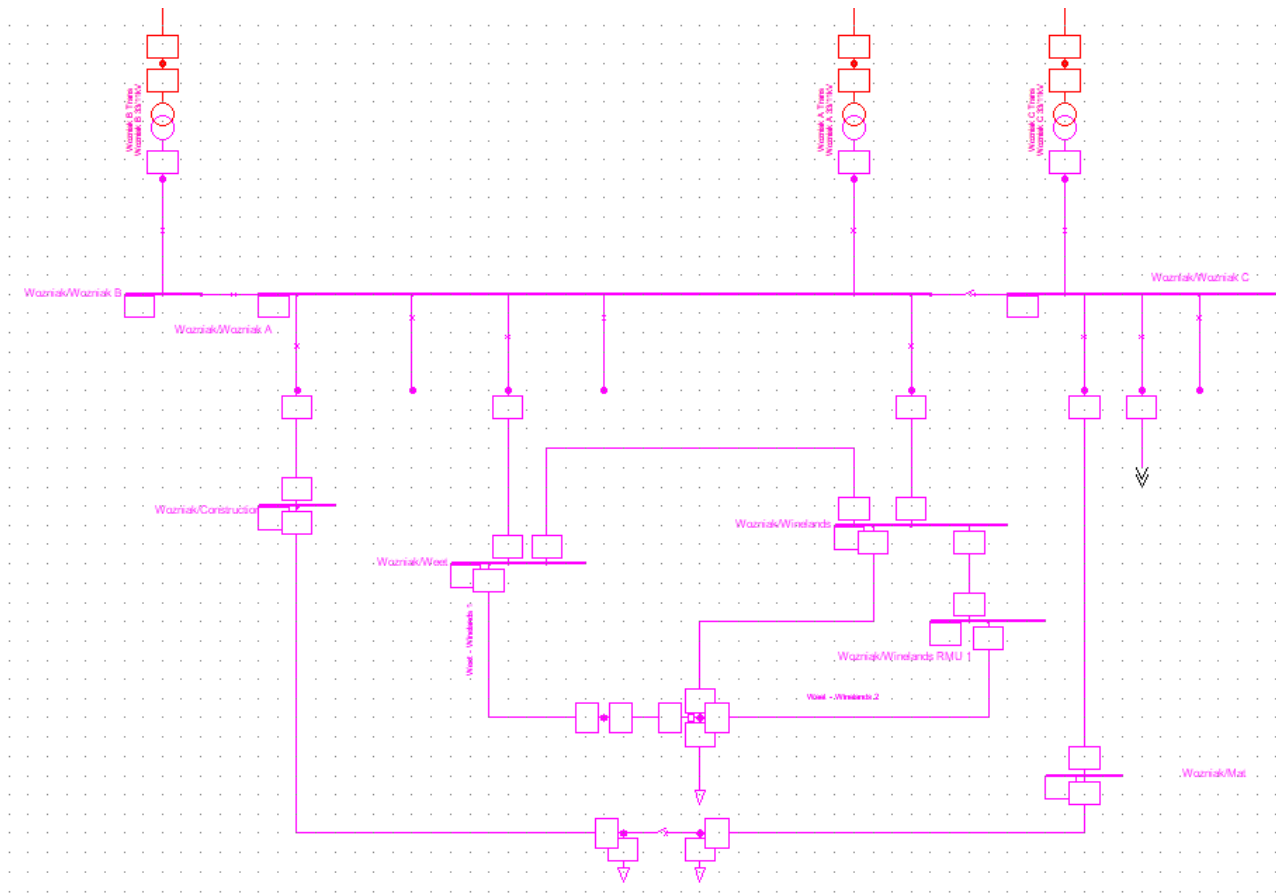


Figure C.2: Single-line diagram of the Wozniak MS feeder group

Table C-2: Table showing feeder load specifications at the Wozniak MS

Feeder	Voltage Rating (kV)	Load (A)	Power Factor
Construction	11.66	51.0026	0.9
Winlands	11.66	29.9663	0.9
Workplace	11.66	0	0.9
Mat	11.66	29.0924	0.9

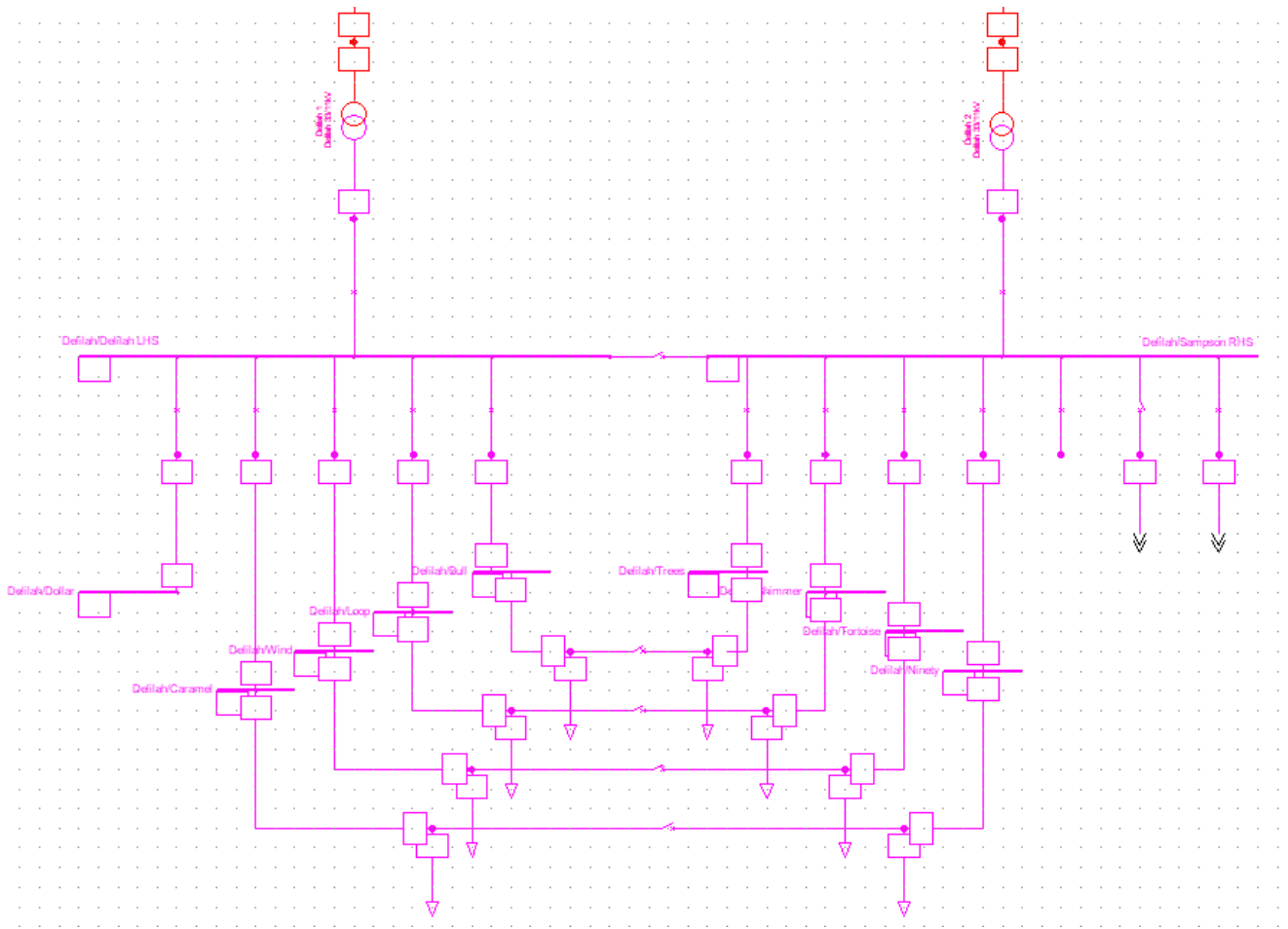


Figure C.3: Single-line diagram of the Delilah MS feeder group

Table C-3: Table showing feeder load specifications at the Delilah MS

Feeder	Voltage Rating (kV)	Load (A)	Power Factor
Caramel	11.66	10.6610	1
Atlantic	11.66	0	1
Loop	11.66	11.4834	1
Bull	11.66	11.5293	1
Medical	11.66	0	1
Dollar	11.66	0	1
Shimmer	11.66	5.2416	1
Wind	11.66	4.9741	1
Ninety	11.66	7.8421	1
Tortoise	11.66	6.8143	1
Trees	11.66	7.055	1

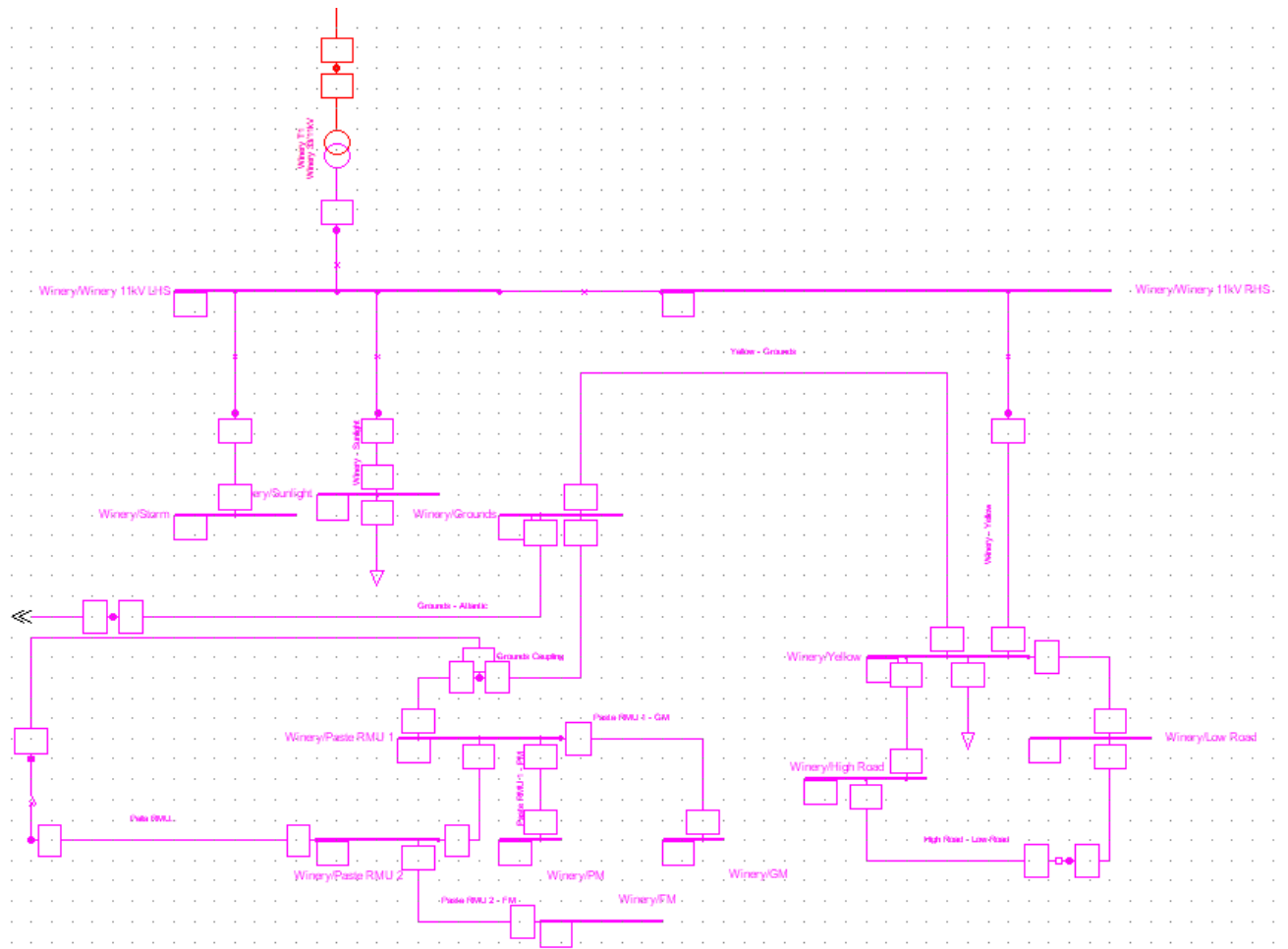


Figure C.4: Single-line diagram of the Winery MS feeder group

Table C-4: Table showing feeder load specifications at the Winery MS

Feeder	Voltage Rating (kV)	Load (A)	Power Factor
Yellow	11.66	0.03972	1
Storm	11.66	0	1
Sunlight	11.66	2.1657	1

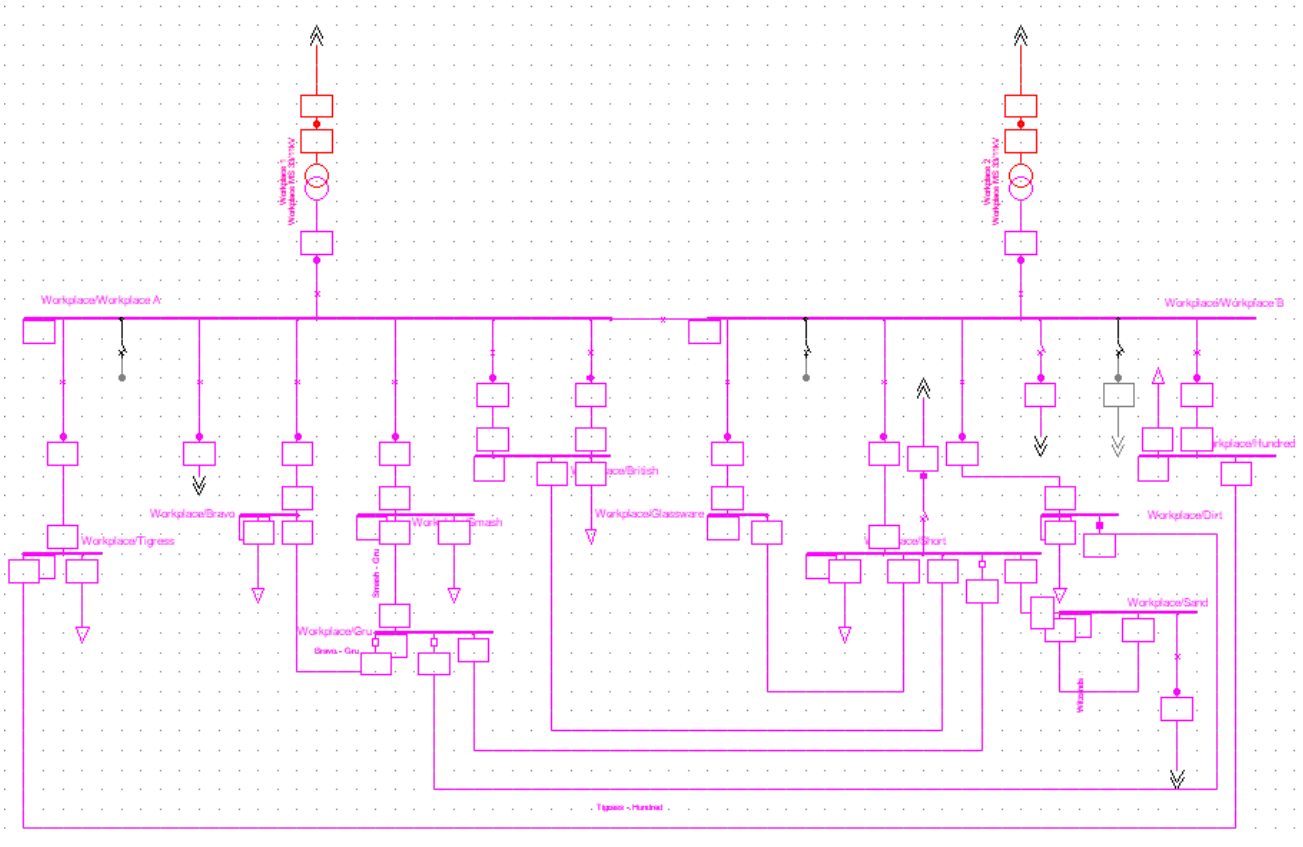


Figure C.5: Single-line diagram of the Workplace MS feeder group

Table C-5: Table showing feeder load specifications at the Workplace MS

Feeder	Voltage Rating (kV)	Load (A)	Power Factor
Allen	11.66	0	1
Short	11.66	146.9188	1
Hundred	11.66	116.1282	1
Gardens	11.66	0	1
Glassware	11.66	18.2423	1
British 1	11.66	131.6342	1
British 2	11.66	130.9322	1
Wozniak	11.66	0	1
Tigress	11.66	44.5260	1
Bravo	11.66	63.4869	1
Smash	11.66	71.8868	1
Dirt	11.66	18.4669	1

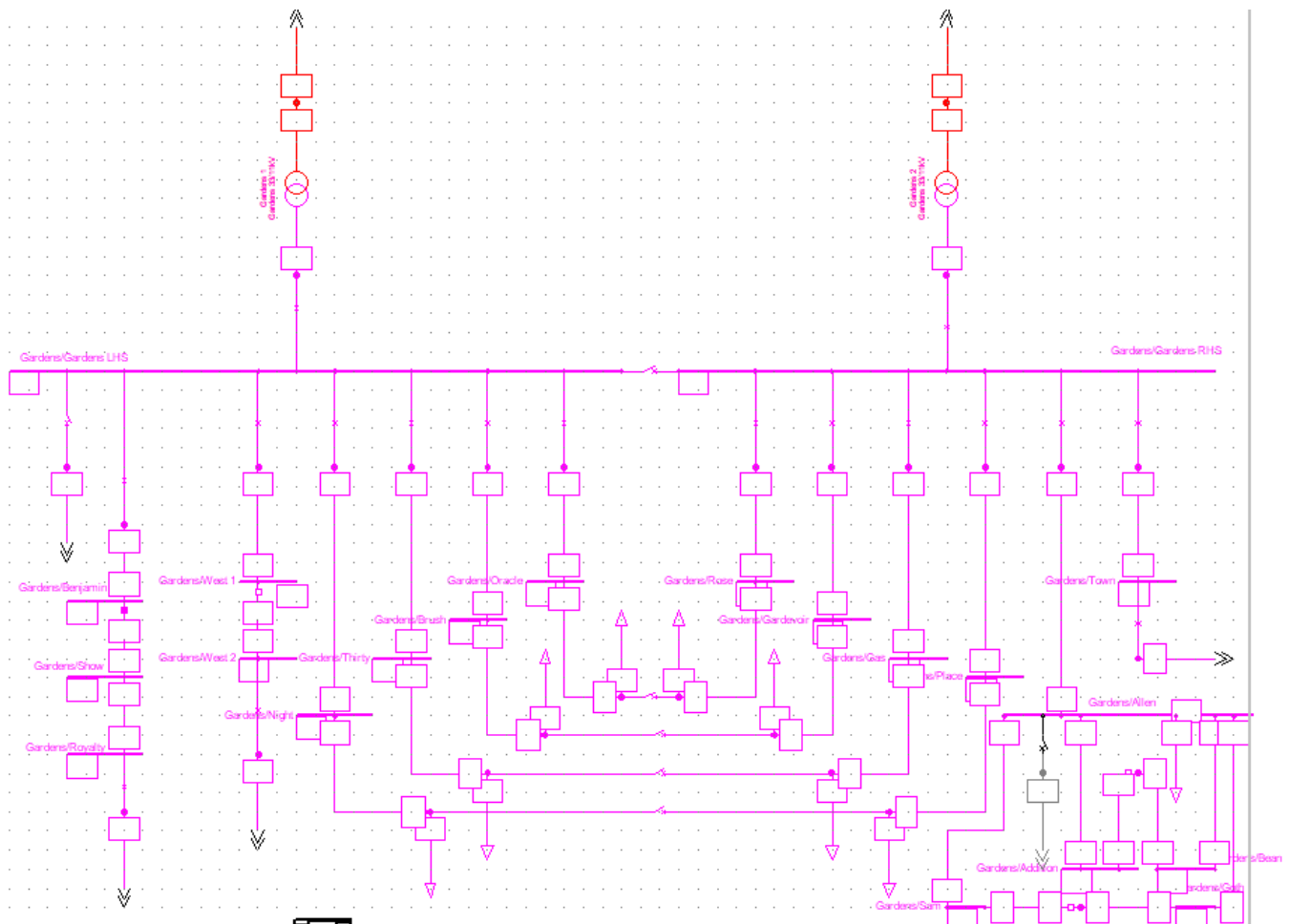


Figure C.6: Single-line diagram of the Gardens MS feeder group

Table C-6: Table showing feeder load specifications at the Gardens MS

Feeder	Voltage Rating (kV)	Load (A)	Power Factor
Allen	11.66	44.3581	1
Benjamin	11.66	6.3222	1
Brush	11.66	9.7210	1
Place	11.66	11.9240	1
Workplace	11.66	0	1
Oracle	11.66	9.8637	1
Gas	11.66	13.9091	1
Gardevoir	11.66	7.3639	1
Night	11.66	10.9924	1
Thirty	11.66	11.3032	1
Rose	11.66	5.8850	1
Town	11.66	6.1403	1
West	11.66	22.9860	1

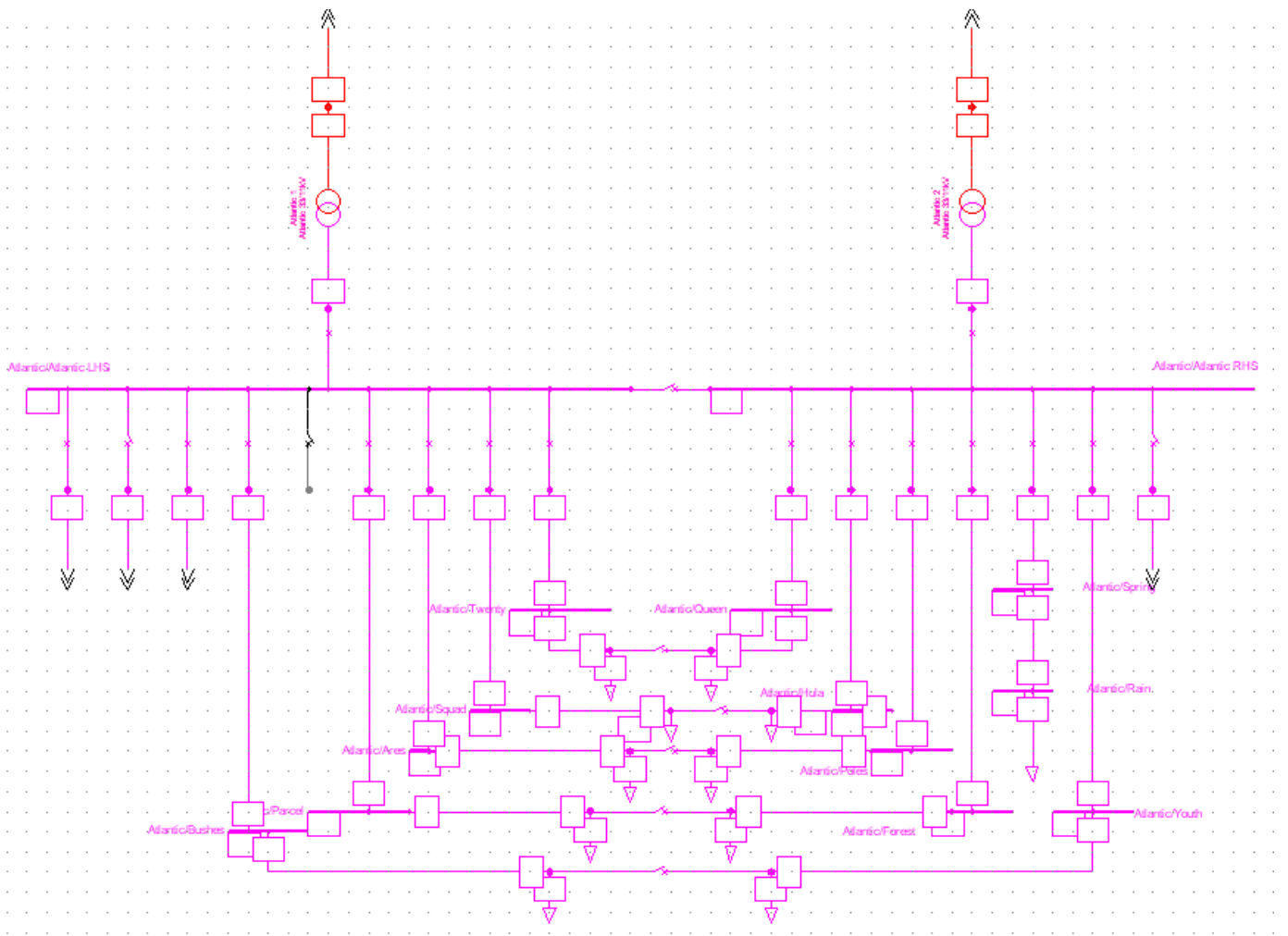


Figure C.7: Single-line diagram of the Atlantic MS feeder group

Table C-7: Table showing feeder load specifications at the Atlantic MS

Feeder	Voltage Rating (kV)	Load (A)	Power Factor
Parcel	11.66	16.9414	1
Queen	11.66	5.8152	1
Forest	11.66	14.0293	1
Squad	11.66	16.8951	1
Ares	11.66	13.2642	1
Hula	11.66	11.2161	1
Youth	11.66	4.4725	1
Poles	11.66	14.9145	1
Yellow	11.66	65.1219	1
Spring	11.66	8.1068	1
Royalty	11.66	0	1
Buses	11.66	6.0989	1
Delilah	11.66	0	1
Gym	11.66	48.3987	1
Twenty	11.66	11.2725	1

Appendix D: Network cable datasheets

Medium Voltage PILC Cables CBI electric african cables

PILC Aluminium 3 Core
 FRPVC DTA FRPVC (red stripe) ...21191 Table + Finish code 19000/33000V
 LHPVC DTA LHPVC (blue stripe) ...21292 Table 21
 SANS 97

Size code	...naaa...	3095	3120	3150	3185	3240	3300
Conductor size	mm ² nom	95	120	150	185	240	300
Conductor diameter	mm app.	11.6	13.6	14.4	15.9	18.4	20.5
Insulated diameter	mm app.	26.6	28.6	29.4	30.9	33.4	35.5
Diameter over lead sheath	mm app.	65.0	69.0	71.5	74.5	80.5	85.5
Bedding diameter	mm app.	68.5	73.0	75.5	78.5	84.5	90.0
Size of armour wires	mm	0.8	0.8	0.8	0.8	0.8	0.8
Overall diameter	mm app.	78.5	83.5	86.0	90.0	95.5	101.5
Normal drum length	m	300	300	300	300	300	300
Cable mass	kg/m app.	11.9	13.2	14.2	15.6	17.6	19.9
Gross mass (drum length)	kg app.	4070	4460	4760	5180	5780	6470
Bending radius	mm min.	1178	1253	1290	1350	1433	1523
Current rating							
In ground	Amps	180	205	230	260	300	335
In ducts	Amps	155	175	195	220	255	285
In air	Amps	200	230	255	290	340	390
Positive sequence							
Resistance dc @ 20°C	Ω/km max	0.320	0.253	0.206	0.164	0.125	0.100
ac @ 70°C	Ω/km max	0.385	0.304	0.248	0.198	0.151	0.121
Reactance	Ω/km	0.115	0.112	0.107	0.103	0.099	0.095
Impedance at	Ω/km	0.401	0.324	0.270	0.223	0.181	0.154
Zero sequence							
Resistance	Ω/km	1.812	1.583	1.440	1.292	1.129	0.978
Reactance	Ω/km	0.118	0.114	0.112	0.109	0.105	0.102
Impedance	Ω/km	1.816	1.588	1.445	1.296	1.134	0.983
Short circuit ratings							
Symmetrical	kA (1sec)	8.8	11.1	13.7	17.2	22.5	28.2
Earth fault(Symmetrical limit)	kA (1sec)	12.1(8.8)	13.5(11.1)	14.5(13.7)	15.9	17.8	20.3

Last updated May 2006

When ordering please quote: primary + size + table + finish code
 e.g. FIJA 3120 21 191



POWER BY INNOVATION... INNOVATION THROUGH PARTNERSHIPS

CBI Electric African Cables
 PO Box 172, Vereeniging 1930 • Tel: +27 16 430 6000 • Fax: +27 16 423 6103
 www.cbi-electric.com • afcab@cbi-electric.com

A member of the REUNERT Group



MV XLPE Cable Data Sheet



Description: 6350/11000V, Copper, 1 Core, Type A F2FC...
Bedding/Armouring/Sheathing: FRPVC/AWA/ FRPVC (red stripe) ...141
 LHPVC/AWA/ LHPVC (blue stripe) ...242
Specification: SANS 1339

Last updated: October 2016

Size code	...n/a...	1050	1070	1095	1120	1150	1185	1240	1300	1400	1500	1630	1800	1999
PHYSICAL DIMENSIONS														
Conductor size	mm ² nom	50	70	95	120	150	185	240	300	400	500	630	800	1000
Conductor diameter	mm app.	8.35	10.05	11.90	13.25	14.70	16.23	18.46	20.75	24.05	27.42	30.45	34.25	38.81
Scale document down	mm app.	17.02	18.72	20.57	21.92	23.37	24.90	27.13	29.42	33.52	37.67	40.70	44.50	49.06
Bedding diameter	mm app.	21.87	23.57	25.42	26.77	28.22	29.75	31.98	34.27	38.37	42.73	45.96	49.76	54.53
Armour diameter	mm app.	25.07	26.77	28.62	29.97	32.22	33.75	35.98	38.27	42.37	47.73	50.96	54.76	59.53
Cable diameter	mm app.	29.54	31.45	33.30	34.85	37.31	38.84	41.27	43.56	48.07	53.63	57.07	61.08	66.25
TECHNICAL DATA														
Normal drum length	m	500	500	500	500	500	500	500	500	500	500	500	500	500
Cable mass (approximate)	kg/m	1.353	1.634	1.955	2.258	2.692	3.096	3.743	4.417	5.527	6.936	8.481	10.35	12.61
Gross mass (500 m)	kg app.	780.5	921	1160	1311	1552	1742	2208	2466	3096	3868	4869	5645	6886
Bending radius	mm min.	591	629	666	697	746	777	825	871	961	1073	1141	1222	1325
DC Resistance @ 20°C	Ω/km	0.387	0.268	0.193	0.153	0.124	0.099	0.075	0.060	0.047	0.037	0.028	0.022	0.018
AC Resistance @ 90°C	Ω/km	0.494	0.342	0.247	0.196	0.159	0.128	0.098	0.080	0.064	0.052	0.042	0.036	0.031
Reactance	Ω/km	0.143	0.135	0.128	0.122	0.119	0.115	0.111	0.107	0.103	0.102	0.099	0.096	0.093
Impedance	Ω/km	0.514	0.368	0.278	0.231	0.199	0.172	0.148	0.133	0.121	0.114	0.108	0.103	0.098
Capacitance	µF/km	0.264	0.298	0.336	0.363	0.392	0.423	0.468	0.514	0.596	0.679	0.739	0.815	0.906
Zero Sequence Resistance	Ω/km	0.793	0.621	0.506	0.442	0.349	0.308	0.266	0.236	0.203	0.152	0.135	0.120	0.108
Zero Sequence Reactance	Ω/km	0.085	0.078	0.072	0.065	0.062	0.059	0.055	0.052	0.049	0.048	0.045	0.043	0.040
Current rating:														
In ground	Amps	206	251	298	336	371	414	470	519	574	617	665	707	742
In air in shade	Amps	241	298	361	412	465	526	608	684	775	857	941	1023	1095
In air in direct sunlight	Amps	192	237	287	327	368	416	480	539	609	670	734	796	850
Short circuit ratings:														
Symmetrical (250°C)	kA (1sec)	6.4	9.2	12.8	16.2	20.0	25.0	32.8	41.2	52.7	67.6	87.5	112.0	140.6
Earth fault (200°C)	kA (1sec)	9.7	10.4	11.1	11.7	15.3	16.0	17.2	18.4	20.5	28.1	30.2	32.5	35.5

Ratings above are based on standard laying conditions for a single circuit in isolation as follows:

Soil thermal resistance = 1.2Km/W

Soil temperature = 25°C

Depth of burial = 800mm

Air temperature = 30°C

5% tolerance on dimensions

Ratings for solid bonded, Trefoil formation

POWER BY INNOVATION... INNOVATION THROUGH PARTNERSHIPS

PO Box 172, Vereeniging 1930 | Steel Road, Peacehaven, Vereeniging 1939 | South Africa
 Tel: +27 16 430 6000 | Fax: +27 16 423 6103 | www.cbi-electric.com

Directors: AE Dickson, GW Eddey, TA Pooe, PJ Banda, Z Mjalli
 Alternate Director: PW de Villiers

B-BBEE Level 1

A member of the **REUNERT** Group
 A division of ATC (Pty) Ltd
 Registration No. 1955/003773/07



PILC/PILAC
 FRPVC DTA FRPVC(red stripe)
 LHPVC DTA LHPVC(blue stripe)

 FIEC...
 ...15191
 ...15292

 Primary group code
 Table + Finish code

 Copper 3 Core
 3800/6600V
 Table 15
 SANS 97

Size code	...naaa...	3016	3025	3035	3050	3070	3095	3120	3150	3185	3240	3300
Conductor size	mm ² nom	16*	25*	35*	50*	70	95	120	150	185	240	300
Conductor depth	mm nom	5.2	6.1	7.2	8.3	8.3	9.8	11.0	12.2	13.7	15.7	17.6
Insulated depth	mm nom	9.7	10.6	11.7	12.8	12.8	14.3	15.5	16.7	18.2	20.2	22.1
Diameter over lead sheath	mm nom	26.0	28.0	30.5	33.0	32.5	36.0	38.5	41.5	45.0	49.5	54.0
Bedding diameter	mm nom	28.0	31.0	33.5	36.0	35.5	39.0	42.0	44.5	48.5	53.0	57.5
Thickness of DSTA	mm	0.80	0.80	0.80	0.80	0.80	0.80	0.80	0.80	0.80	0.80	0.80
Overall diameter	mm nom	35.5	38.0	41.0	44.0	43.5	47.5	50.5	53.5	57.5	63.0	67.5
Normal drum length	m	500	500	500	300	300	300	300	300	300	300	300
Cable mass	kg/m app.	3.4	3.9	4.6	5.3	5.9	7.2	8.4	9.7	11.4	14.1	16.7
Gross mass (drum length)	kg app.	2080	2330	2680	1970	2150	2540	2900	3290	3800	4610	5390
Bending radius	mm min.	426	456	492	528	522	570	606	642	690	756	810
Current rating												
In ground	Amps	92	115	140	170	210	250	285	320	360	420	470
In ducts	Amps	76	98	115	140	170	210	240	265	300	350	395
In air	Amps	91	115	145	170	215	265	305	350	400	470	539
Positive sequence												
Resistance dc @ 20°C	Ω/km max	1.150	0.727	0.524	0.387	0.268	0.193	0.153	0.124	0.0991	0.0754	0.0601
ac @ 80°C	Ω/km max	1.421	0.899	0.648	0.479	0.332	0.239	0.190	0.155	0.124	0.0955	0.0773
Reactance	Ω/km	0.105	0.101	0.096	0.093	0.075	0.071	0.069	0.067	0.065	0.063	0.061
Impedance at 80°C	Ω/km	1.425	0.904	0.655	0.487	0.340	0.249	0.202	0.168	0.140	0.114	0.098
Zero sequence												
Resistance	Ω/km	7.851	6.821	5.687	5.120	4.747	3.993	3.466	3.037	2.643	2.159	1.882
Reactance	Ω/km	0.127	0.120	0.115	0.110	0.112	0.106	0.103	0.100	0.097	0.094	0.091
Impedance	Ω/km	7.852	6.822	5.689	5.121	4.749	3.995	3.468	3.039	2.645	2.161	1.884
Short circuit ratings												
Symmetrical	kA (1sec)	2.2	3.5	4.9	6.6	9.5	13.3	16.7	20.7	25.9	34.0	42.7
Earth fault(Symmetrical limit)	kA (1sec)	2.7	2.9	3.4	3.7	3.9	4.6	5.3	6.0	6.8	8.4	9.6

Last updated May 2006

* Circular Conductor

 When ordering please quote: primary + size + table + finish code
 e.g. FIEC 3120 15 191


POWER BY INNOVATION... INNOVATION THROUGH PARTNERSHIPS

 CBI Electric African Cables
 PO Box 172, Vereeniging 1930 • Tel: +27 16 430 6000 • Fax: +27 16 423 6103
 www.cbi-electric.com • afcab@cbi-electric.com

A member of the REUNERT Group



Copper 3 Core
6350/11000 V
Table 17
SANS 97

PILC FIFC... Primary group code
FRPVC DTA FRPVC (red stripe) ...17191 Table + Finish code
LHPVC DTA LHPVC (blue stripe) ...17292

Size code	...naaa...	3025	3035	3050	3070	3095	3120	3150	3185	3240	3300
Conductor size	mm ² nom	25*	35*	50*	70	95	120	150	185	240	300
Conductor depth	mm app.	6.1	7.2	8.3	8.3	9.8	11.0	12.2	13.7	15.7	17.6
Insulated depth	mm app.	12.4	13.5	14.6	14.6	16.0	17.2	18.4	19.9	21.9	23.9
Diameter over lead sheath	mm app.	32.5	34.5	37.0	36.5	40.0	42.5	45.5	49.0	53.0	57.5
Bedding diameter	mm app.	35.0	37.5	40.0	39.5	43.0	46.0	49.0	52.5	56.5	61.5
Thickness of DSTA	mm	0.80	0.80	0.80	0.80	0.80	0.80	0.80	0.80	0.80	0.80
Overall diameter	mm nom	43.0	45.5	48.5	48.5	52.0	55.0	58.5	62.0	66.5	72.0
Normal drum length	m	500	500	300	300	300	300	300	300	300	300
Cable mass	kg/m app.	4.7	5.2	6.0	6.7	8.0	9.3	10.7	12.4	14.7	17.4
Gross mass (drum length)	kg app.	2570	2840	1960	2170	2585	3190	3610	4290	4755	5650
Bending radius	mm min.	516	546	582	582	624	660	702	744	798	864
Current rating											
In ground	Amps	110	130	155	190	230	260	290	330	380	430
In ducts	Amps	91	110	130	160	190	220	245	280	320	360
In air	Amps	110	130	155	200	240	275	315	360	425	485
Positive sequence											
Resistance dc @ 20°C	Ω/km max	0.727	0.524	0.387	0.268	0.193	0.153	0.124	0.0991	0.0754	0.0601
ac @ 70°C	Ω/km max	0.870	0.627	0.463	0.321	0.232	0.184	0.149	0.1201	0.0924	0.0747
Reactance	Ω/km	0.110	0.105	0.101	0.082	0.077	0.075	0.073	0.070	0.068	0.066
Impedance	Ω/km	0.877	0.636	0.474	0.332	0.244	0.199	0.166	0.139	0.115	0.099
Zero sequence											
Resistance	Ω/km	5.325	4.769	4.314	4.004	3.406	2.985	2.638	2.316	2.104	1.841
Reactance	Ω/km	0.126	0.120	0.115	0.117	0.112	0.108	0.105	0.102	0.098	0.094
Impedance	Ω/km	5.326	4.771	4.316	4.006	3.408	2.987	2.640	2.318	2.106	1.843
Short circuit ratings											
Symmetrical	kA (1sec)	3.7	5.1	6.9	9.9	13.8	17.4	21.5	26.9	35.3	44.3
Earth fault(Symmetrical limit)	kA (1sec)	3.97)	4.2	4.5	4.7	5.5	6.2	7.0	7.9	8.6	9.8

Last updated May 2006

* Circular Conductor
When ordering please quote: primary + size + table + finish code
e.g. FIFC 3120 17 191



POWER BY INNOVATION... INNOVATION THROUGH PARTNERSHIPS

CBI Electric African Cables
PO Box 172, Vereeniging 1930 • Tel: +27 16 430 6000 • Fax: +27 16 423 6103
www.cbi-electric.com • afcab@cbi-electric.com

A member of the REUNERT Group



Description: 6350/11000V, Aluminium, 3 Core, Type A
Bedding/Sheathing: FRPVC/ SWA/ FRPVC (red stripe)
 LHPVC/ SWA/ FRPVC(blue stripe)
Specification: SANS 1339

F2FA...
 ...111
 ...212

Last updated: October 2016

Size code	...n/a...	3016	3025	3035	3050	3070	3095	3120	3150	3185	3240	3300	3400
PHYSICAL DIMENSIONS													
Conductor size	mm ² nom	16	25	35	50	70	95	120	150	185	240	300	400
Conductor diameter	mm app.	4.8	6.0	7.2	8.4	9.9	11.7	13.4	14.6	16.4	18.8	20.4	24.3
Insulation diameter	mm app.	13.5	14.7	15.9	17.1	18.6	20.4	22.1	23.3	25.1	27.5	29.1	33.8
Bedding diameter	mm app.	36.6	39.4	42.0	44.8	48.0	52.1	56.0	58.6	62.6	68.0	71.7	82.1
Armour diameter	mm app.	40.6	44.4	47.0	49.8	53.0	57.1	61.0	64.9	68.9	74.3	78.0	88.4
Cable diameter	mm app.	45.3	49.3	52.1	55.1	58.5	62.8	67.1	71.2	75.5	81.3	85.4	96.1
TECHNICAL DATA													
Normal drum length	m	300	300	300	300	300	300	300	300	300	300	300	300
Cable mass (approximate)	kg/m	3.3	4.2	4.5	4.9	5.4	6.1	6.8	8.1	8.8	9.9	11.2	13.1
Gross mass (300 m)	kg app.	1225	1620	1695	1820	2095	2320	2555	2940	3440	3820	4190	4675
Bending radius	mm min.	543	591	625	661	702	754	805	855	906	976	1025	1154
DC Resistance @ 20°C	Ω/km	1.910	1.200	0.868	0.641	0.443	0.320	0.253	0.206	0.164	0.125	0.100	0.078
AC Resistance @ 90°C	Ω/km	2.449	1.539	1.113	0.822	0.568	0.411	0.325	0.265	0.211	0.162	0.130	0.102
Reactance	Ω/km	0.137	0.128	0.121	0.115	0.107	0.102	0.098	0.095	0.092	0.088	0.086	0.084
Impedance	Ω/km	2.453	1.544	1.120	0.830	0.578	0.423	0.339	0.282	0.230	0.184	0.156	0.132
Capacitance	µF/km	0.191	0.215	0.240	0.265	0.295	0.332	0.366	0.390	0.426	0.475	0.507	0.601
Zero Sequence Resistance	Ω/km	3.917	2.721	2.222	1.864	1.540	1.307	1.160	0.945	0.848	0.748	0.687	0.589
Zero Sequence Reactance	Ω/km	0.154	0.149	0.142	0.137	0.130	0.124	0.120	0.119	0.115	0.110	0.108	0.103
Current rating:													
In ground	Amps	82	105	125	147	179	214	242	270	304	350	391	444
In air in shade	Amps	88	114	137	163	202	243	279	314	358	417	469	545
In air in direct sunlight	Amps	77	100	121	143	177	213	244	274	312	363	408	472
Short circuit ratings:													
Symmetrical (250°C)	kA (1sec)	1.4	2.2	3.0	4.0	5.8	8.1	10.2	12.6	15.8	20.7	25.9	33.3
Earth fault (200°C)	kA (1sec)	11.9	15.6	16.6	17.6	18.9	20.4	21.9	28.3	30.2	32.6	34.3	39.1

Ratings above are based on standard laying conditions for a single circuit in isolation as follows:

- Soil thermal resistance = 1.2 Km/W
- Soil temperature = 25 °C
- Depth of burial = 800 mm
- Air temperature = 30 °C
- Single circuit in isolation
- 5% tolerance on dimensions

POWER BY INNOVATION... INNOVATION THROUGH PARTNERSHIPS

PO Box 172, Vereeniging 1930 | Steel Road, Peacehaven, Vereeniging 1939 | South Africa
 Tel: +27 16 430 6000 | Fax: +27 16 423 6103 | www.cbi-electric.com

Directors: AE Dickson, GW Eddey, TA Pooe, PJ Banda, Z Mjali
 Alternate Director: PW de Villiers

B-BBEE Level 1

A member of the REUNERT Group
 A division of ATC (Pty) Ltd
 Registration No. 1955/003773/07



Appendix E: Municipal network protection settings

Table E-1: Protection settings for the Atlantic MS feeder group

<i>Substation</i>	<i>Feeder</i>	<i>CT Ratio</i>	<i>CT Class/ Burden</i>	<i>OC PU (A)</i>	<i>OC TM</i>	<i>EF PU (A)</i>	<i>EF TM</i>	<i>OC Inst.</i>	<i>EF Inst.</i>
Atlantic	Transf. 1 HV	200/5	10P10/15VA	210	0.4	-	-	2100A/ 20ms	-
Atlantic	Transf. 2 HV	200/5	10P10/15VA	210	0.4	-	-	2100A/ 20ms	-
Atlantic	Transf. 1 MV	600/1	10P15/15VA	630	0.3	180	0.45	-	-
Atlantic	Transf. 2 MV	600/1	10P15/15VA	630	0.3	180	0.45	-	-
Atlantic	West 2	300/5	10P10/15VA	300	0.15	120	0.18	3000A/ 100ms	1200A/ 100ms
Atlantic	Royalty	300/5	10P10/15VA	300	0.15	120	0.18	3000A/ 100ms	1200A/ 100ms
Atlantic	Grounds	400/5	10P10/15VA	400	0.05	120	0.05	-	-
Atlantic	Bushes	300/5	10P10/15VA	300	0.05	120	0.05	3000A/ 100ms	1200A/ 100ms
Atlantic	Parcel	300/5	10P10/15VA	225	0.05	90	0.05	2250A/ 100ms	900A/ 100ms
Atlantic	Ares	300/5	10P10/15VA	300	0.05	90	0.05	3000A/ 100ms	900A/ 100ms
Atlantic	Squad	300/5	10P10/15VA	225	0.05	90	0.05	2250A/ 100ms	900A/ 100ms
Atlantic	Twenty	300/5	10P10/15VA	225	0.05	90	0.05	2250A/ 100ms	900A/ 100ms
Atlantic	Queen	300/5	10P10/15VA	225	0.05	90	0.05	2250A/ 100ms	900A/ 100ms
Atlantic	Hula	300/5	10P10/15VA	225	0.05	90	0.05	2250A/ 100ms	900A/ 100ms
Atlantic	Poles	300/5	10P10/15VA	300	0.05	90	0.05	3000A/ 100ms	900A/ 100ms
Atlantic	Forest	300/5	10P10/15VA	225	0.05	90	0.05	2250A/ 100ms	900A/ 100ms
Atlantic	Spring	300/5	10P10/15VA	225	0.05	90	0.05	2250A/ 100ms	900A/ 100ms
Atlantic	Youth	300/5	10P10/15VA	225	0.05	90	0.05	2250A/ 100ms	900A/ 100ms
Atlantic	Delilah	300/5	10P10/15VA	300	0.05	120	0.05	3000A/ 100ms	1200A/ 100ms

Table E-2: Protection settings for the Gardens MS feeder group

<i>Substation</i>	<i>Feeder</i>	<i>CT Ratio</i>	<i>CT Class/ Burden</i>	<i>OC PU (A)</i>	<i>OC TM</i>	<i>EF PU (A)</i>	<i>EF TM</i>	<i>OC Inst.</i>	<i>EF Inst.</i>
Gardens	Transf. 1 HV	200/5	10P10/15VA	210	0.4	-	-	3000A/ 20ms	-
Gardens	Transf. 2 HV	200/5	10P10/15VA	210	0.4	-	-	3000A/ 20ms	-
Gardens	Transf. 1 MV	600/1	10P15/15VA	630	0.3	180	0.45	-	-
Gardens	Transf. 2 MV	600/1	10P15/15VA	630	0.3	180	0.45	-	-
Gardens	Workplace	400/5	10P10/15VA	400	0.25	120	0.35	-	-
Gardens	Benjamin	400/5	10P10/15VA	300	0.15	120	0.18	-	-
Gardens	West 1	400/5	10P10/15VA	300	0.15	120	0.2	-	-
Gardens	Night	200/5	10P10/15VA	200	0.1	60	0.1	2000A/ 100ms	600A/ 100ms
Gardens	Thirty	300/5	10P10/15VA	300	0.1	90	0.1	3000A/ 100ms	900A/ 100ms
Gardens	Brush	300/5	10P10/15VA	300	0.1	90	0.1	3000A/ 100ms	900A/ 100ms
Gardens	Oracle	300/5	10P10/15VA	225	0.1	66	0.1	2250A/ 100ms	660A/ 100ms
Gardens	Rose	300/5	10P10/15VA	225	0.1	75	0.1	2250A/ 100ms	750A/ 100ms
Gardens	Gardevoir	300/5	10P10/15VA	225	0.1	75	0.1	2250A/ 100ms	750A/ 100ms
Gardens	Gas	400/5	10P10/15VA	200	0.1	120	0.1	2000A/ 100ms	1200A/ 100ms
Gardens	Place	200/5	10P10/15VA	200	0.1	60	0.1	2000A/ 100ms	600A/ 100ms
Gardens	Allen	400/5	10P10/15VA	400	0.25	120	0.35	-	-
Gardens	Town	400/5	10P10/15VA	400	0.05	120	0.05	-	-
Allen	Sam	400/5	10P10/15VA	224.8	0.1	60	0.1	2249.6A/ 100ms	600A/ 100ms
Allen	Workplace	400/5	10P10/15VA	320	0.25	100	0.3	-	-
Allen	Addition	400/5	10P10/15VA	224.8	0.1	60	0.1	2249.6A/ 100ms	600A/ 100ms
Allen	Bean	400/5	10P10/15VA	224.8	0.1	60	0.1	2249.6A/ 100ms	600A/ 100ms
Allen	Goth	400/5	10P10/15VA	224.8	0.1	60	0.1	2249.6A/ 100ms	600A/ 100ms

Table E-3: Protection settings for the Delilah MS feeder group

<i>Substation</i>	<i>Feeder</i>	<i>CT Ratio</i>	<i>CT Class/ Burden</i>	<i>OC PU (A)</i>	<i>OC TM</i>	<i>EF PU (A)</i>	<i>EF TM</i>	<i>OC Inst.</i>	<i>EF Inst.</i>
Delilah	Transf. 1 HV	200/1	10P15/15VA	260	0.23	-	-	3000A/ 20ms	-
Delilah	Transf. 2 HV	200/1	10P15/15VA	260	0.23	-	-	3000A/ 20ms	-
Delilah	Transf. 1 MV	600/1	10P15/15VA	630	0.23	180	0.35	-	-
Delilah	Transf. 2 MV	600/1	10P15/15VA	630	0.23	180	0.35	-	-
Delilah	Dollar	300/5	10P10/15VA	30	0.1	30	0.1	240A/ 100ms	240A/ 100ms
Delilah	Caramel	300/5	10P10/15VA	225	0.1	60	0.1	2250A/ 100ms	600A/ 100ms
Delilah	Wind	300/5	10P10/15VA	225	0.1	60	0.1	2250A/ 100ms	600A/ 100ms
Delilah	Loop	300/5	10P10/15VA	285	0.1	84	0.1	2850A/ 100ms	840A/ 100ms
Delilah	Bull	300/5	10P10/15VA	225	0.1	60	0.1	2250A/ 100ms	600A/ 100ms
Delilah	Trees	300/5	10P10/15VA	225	0.1	60	0.1	2250A/ 100ms	600A/ 100ms
Delilah	Shimmer	300/5	10P10/15VA	285	0.1	84	0.1	2850A/ 100ms	840A/ 100ms
Delilah	Tortoise	300/5	10P10/15VA	225	0.1	60	0.1	2250A/ 100ms	600A/ 100ms
Delilah	Ninety	300/5	10P10/15VA	225	0.1	60	0.1	2250A/ 100ms	600A/ 100ms
Delilah	Town	400/5	10P10/15VA	320	0.2	100	0.4	-	-
Delilah	Youth	400/5	10P10/15VA	320	0.2	100	0.4	-	-

Table E-4: Protection settings for the Wozniak MS feeder group

<i>Substation</i>	<i>Feeder</i>	<i>CT Ratio</i>	<i>CT Class/ Burden</i>	<i>OC PU (A)</i>	<i>OC TM</i>	<i>EF PU (A)</i>	<i>EF TM</i>	<i>OC Inst.</i>	<i>EF Inst.</i>
Wozniak	Transf. 1 HV	200/1	10P15/15VA	260	0.23	-	-	3000A/ 20ms	-
Wozniak	Transf. 2 HV	200/1	10P15/15VA	260	0.23	-	-	3000A/ 20ms	-
Wozniak	Transf. 3 HV	200/1	10P15/15VA	260	0.23	-	-	3000A/ 20ms	-
Wozniak	Transf. 1 MV	600/1	10P15/15VA	630	0.45	180	0.35	-	120A/ 5000ms
Wozniak	Transf. 2 MV	600/1	10P15/15VA	630	0.45	180	0.35	-	120A/ 5000ms
Wozniak	Transf. 3 MV	600/1	10P15/15VA	630	0.45	180	0.35	-	120A/ 5000ms
Wozniak	Construction	400/5	10P10/15VA	400	0.1	120	0.1	4000A/ 100ms	1200A/ 100ms
Wozniak	Weet	400/5	10P10/15VA	400	0.25	80	0.2	-	-
Wozniak	Winelands	400/5	10P10/15VA	400	0.25	80	0.2	-	-
Wozniak	Mat	400/5	10P10/15VA	400	0.1	120	0.1	4000A/ 100ms	1200A/ 100ms
Wozniak	Workplace	400/5	10P10/15VA	400	0.2	120	0.35	-	-
Weet	Wozniak	400/5	10P10/15VA	400	0.25	80	0.2	-	-
Weet	Winelands	400/5	10P10/15VA	400	0.25	80	0.2	-	-
Weet	Winelands RMU	400/5	10P10/15VA	240	0.18	60	0.12	-	-
Winelands	Wozniak	400/5	10P10/15VA	400	0.25	80	0.2	-	-
Winelands	Weet	400/5	10P10/15VA	400	0.25	80	0.2	-	-
Winelands	Winelands RMU	400/5	10P10/15VA	240	0.18	60	0.1	2400A/ 100ms	600A/ 100ms

Table E-5: Protection settings for the Sunset Vista MS feeder group

<i>Substation</i>	<i>Feeder</i>	<i>CT Ratio</i>	<i>CT Class/ Burden</i>	<i>OC PU (A)</i>	<i>OC TM</i>	<i>EF PU (A)</i>	<i>EF TM</i>	<i>OC Inst.</i>	<i>EF Inst.</i>
Sunset Vista	Transf. 1 HV	200/1	10P15/15VA	520	0.3	160	0.05	5200A/ 20ms	-
Sunset Vista	Transf. 2 HV	200/1	10P15/15VA	520	0.3	160	0.05	5200A/ 20ms	-
Sunset Vista	Transf. 3 HV	200/1	10P15/15VA	520	0.3	160	0.05	5200A/ 20ms	-
Sunset Vista	Transf. 4 HV	200/1	10P15/15VA	520	0.3	160	0.05	5200A/ 20ms	-
Sunset Vista	Transf. 1 MV	2000/5	10P20/15VA	1260	0.26	360	0.24	-	-
Sunset Vista	Transf. 2 MV	2000/5	10P20/15VA	1260	0.26	360	0.24	-	-
Sunset Vista	Transf. 3 MV	2000/5	10P20/15VA	1260	0.26	360	0.24	-	-
Sunset Vista	Transf. 4 MV	2000/5	10P20/15VA	1260	0.26	360	0.24	-	-
Sunset Vista	Recycling	300/5	10P10/15VA	225	0.23	45	0.18	-	-
Sunset Vista	Farm	400/5	10P10/15VA	200	0.3	60	0.3	-	-
Sunset Vista	Life LHS	400/5	10P10/15VA	500	0.3	120	0.3	5000A/ 100ms	1200A/ 100ms
Sunset Vista	Life RHS	400/5	10P10/15VA	500	0.3	120	0.3	5000A/ 100ms	1200A/ 100ms
Sunset Vista	Fortune	400/5	10P10/15VA	400	0.1	120	0.1	4000A/ 100ms	1200A/ 100ms
Sunset Vista	Lightning LHS	400/5	10P10/15VA	400	0.28	120	0.4	-	-
Sunset Vista	Lightning RHS	400/5	10P10/15VA	400	0.28	120	0.4	-	-
Sunset Vista	Plant 1	400/5	10P10/15VA	400	0.28	120	0.4	-	-
Sunset Vista	Plant 2	400/5	10P10/15VA	400	0.28	120	0.4	-	-
Sunset Vista	Plant 3	400/5	10P10/15VA	400	0.28	120	0.4	-	-
Sunset Vista	Plant 4	400/5	10P10/15VA	480	0.28	120	0.4	-	-
Sunset Vista	Plant 5	400/5	10P10/15VA	400	0.28	120	0.4	-	-
Sunset Vista	Plant 6	400/5	10P10/15VA	400	0.28	120	0.4	-	-
Sunset Vista	Plant 7	400/5	10P10/15VA	400	0.28	120	0.4	-	-
Sunset Vista	Forge LHS	400/5	10P10/15VA	500	0.15	120	0.3	-	-
Sunset Vista	Forge RHS	400/5	10P10/15VA	500	0.15	120	0.3	-	-
Sunset Vista	Short	400/5	10P10/15VA	400	0.25	80	0.25	-	-
Lightning	Sunset Vista 1	400/5	10P10/15VA	400	0.28	120	0.4	-	-
Lightning	Sunset Vista 2	400/5	10P10/15VA	400	0.28	120	0.4	-	-
Lightning	Fire	400/5	10P15/15VA	400	0.15	60	0.18	-	-
Lightning	Steve 1	400/5	10P15/15VA	400	0.15	120	0.27	-	-
Lightning	Steve 2	400/5	10P15/15VA	400	0.15	120	0.27	-	-
Steve	Lightning 1	400/5	10P15/15VA	400	0.15	120	0.27	-	-
Steve	Lightning 2	400/5	10P15/15VA	400	0.15	120	0.27	-	-
Steve	Fire	400/5	10P15/15VA	400	0.05	40	0.05	4000A/ 100ms	400A/ 100ms

Table E-6: Protection settings for the Workplace MS feeder group

<i>Substation</i>	<i>Feeder</i>	<i>CT Ratio</i>	<i>CT Class/ Burden</i>	<i>OC PU (A)</i>	<i>OC TM</i>	<i>EF PU (A)</i>	<i>EF TM</i>	<i>OC Inst.</i>	<i>EF Inst.</i>
Workplace	Transf. 1 HV	200/1	10P15/15VA	500	0.24	-	-	5000A/ 20ms	-
Workplace	Transf. 2 HV	200/1	10P15/15VA	500	0.3	-	-	5000A/ 20ms	-
Workplace	Transf. 1 MV	2000/5	10P20/15VA	1500	0.23	360	0.45	-	-
Workplace	Transf. 2 MV	2000/5	10P20/15VA	1500	0.23	360	0.45	-	-
Workplace	Tigress	400/5	10P10/15VA	300	0.22	80	0.22	-	-
Workplace	Gardens	400/5	10P10/15VA	400	0.25	120	0.3	-	-
Workplace	Bravo	400/5	10P10/15VA	300	0.05	120	0.05	-	-
Workplace	Smash	400/5	10P10/15VA	400	0.18	60	0.18	-	-
Workplace	British 1	400/5	10P10/15VA	400	0.25	80	0.24	-	-
Workplace	British 2	400/5	10P10/15VA	400	0.25	80	0.24	-	-
Workplace	Glassware	400/5	10P10/15VA	400	0.26	120	0.27	-	-
Workplace	Short	400/5	10P10/15VA	400	0.26	120	0.27	-	-
Workplace	Dirt	400/5	10P10/15VA	300	0.05	100	0.05	3000A/ 100ms	1000A/ 100ms
Workplace	Wozniak	400/5	10P10/15VA	400	0.2	120	0.35	-	-
Workplace	Allen	400/5	10P10/15VA	400	0.16	80	0.24	-	-
Workplace	Hundred	400/5	10P10/15VA	300	0.22	80	0.17	-	-
Short	Workplace	400/5	10P10/15VA	400	0.26	120	0.27	-	-
Short	Sunset Vista	400/5	10P10/15VA	400	0.25	80	0.25	-	-
Short	Glassware	400/5	10P10/15VA	400	0.1	120	0.1	4000A/ 100ms	1200A/ 100ms
Short	British	400/5	10P10/15VA	400	0.1	120	0.1	4000A/ 100ms	1200A/ 100ms
Short	Gru	400/5	10P10/15VA	400	0.1	120	0.1	4000A/ 100ms	1200A/ 100ms
Short	Sand	300/5	10P10/15VA	300	0.18	90	0.15	-	-
Sand	Short	300/5	10P10/15VA	300	0.18	90	0.15	-	-
Sand	Steve	400/5	10P15/15VA	320	0.1	80	0.15	-	-
Sand	Well A	100/5	10P15/15VA	100	0.05	30	0.05	-	-
Sand	Well B	100/5	10P15/15VA	100	0.05	30	0.05	-	-

Table E-7: Protection settings for the Winery MS feeder group

<i>Substation</i>	<i>Feeder</i>	<i>CT Ratio</i>	<i>CT Class/ Burden</i>	<i>OC PU (A)</i>	<i>OC TM</i>	<i>EF PU (A)</i>	<i>EF TM</i>	<i>OC Inst.</i>	<i>EF Inst.</i>
Winery	Transf. 1 HV	200/1	10P15/15VA	210	0.4	-	-	3000A/ 20ms	-
Winery	Transf. 1 MV	600/1	10P15/15VA	630	0.3	180	0.3	-	1200A/ 5000ms
Winery	Storm	400/5	10P10/15VA	52	0.05	40	0.05	600A/ 100ms	400A/ 100ms
Winery	Sunlight	400/5	10P10/15VA	252	0.05	60	0.05	1720A/ 100ms	400A/ 100ms
Winery	Yellow	400/5	10P10/15VA	252	0.05	60	0.05	1720A/ 100ms	400A/ 100ms

Table E-8: Protection settings for the Wind Turbine Incomer in the municipal network Case 2

<i>Substation</i>	<i>Feeder</i>	<i>CT Ratio</i>	<i>CT Class/ Burden</i>	<i>OC PU (A)</i>	<i>OC TM</i>	<i>EF PU (A)</i>	<i>EF TM</i>	<i>OC Inst.</i>	<i>EF Inst.</i>
Utility Sub	Wind Turbine Incomer	2000/5	10P15/15VA	1260	0.05	-	-	-	-

*No earth fault settings are assigned as the inverter unit will output 3 phase current during both three-phase and single-phase fault conditions.

Table E-9: Protection settings for the Wind Turbine Incomers in the municipal network Cases 3 and 4

<i>Substation</i>	<i>Feeder</i>	<i>CT Ratio</i>	<i>CT Class/ Burden</i>	<i>OC PU (A)</i>	<i>OC TM</i>	<i>EF PU (A)</i>	<i>EF TM</i>	<i>OC Inst.</i>	<i>EF Inst.</i>
Where applicable	Various Wind Turbine Incomers	Variable – dependent on turbine capacity	Variable	-	-	-	-	110% Rated Capacity/ 400ms	-

*No earth fault settings are assigned as the inverter unit will output 3 phase current during both three-phase and single-phase fault conditions.

*Protection settings are detailed in Tables 5-51 and 5-79.

Table E-10: Protection settings for the Utility substation feeder group

<i>Substation</i>	<i>Feeder</i>	<i>CT Ratio</i>	<i>CT Class/ Burden</i>	<i>OC PU (A)</i>	<i>OC TM</i>	<i>EF PU (A)</i>	<i>EF TM</i>	<i>OC Inst.</i>	<i>EF Inst.</i>
Utility Sub	Utility Sub Switch Yard 1	400/1	10P20/20VA	400	0.45	120	0.25	2600A/ 20ms	2600A/ 20ms
Utility Sub	Utility Sub Switch Yard 2	400/1	10P20/20VA	400	0.45	120	0.25	2600A/ 20ms	2600A/ 20ms
Utility Sub	Sunset Vista A	400/1	10P20/20VA	520	0.30	160	0.05	5200A/ 20ms	5200A/ 20ms
Utility Sub	Sunset Vista B	400/1	10P20/20VA	520	0.30	160	0.05	5200A/ 20ms	5200A/ 20ms
Utility Sub	Sunset Vista C	400/1	10P20/20VA	520	0.30	160	0.05	5200A/ 20ms	5200A/ 20ms
Utility Sub	Sunset Vista D	400/1	10P20/20VA	520	0.30	160	0.05	5200A/ 20ms	5200A/ 20ms
Utility Sub	Wozniak A	400/1	10P20/20VA	260	0.45	80	0.05	2600A/ 20ms	2600A/ 20ms
Utility Sub	Wozniak B	400/1	10P20/20VA	260	0.45	80	0.05	2600A/ 20ms	2600A/ 20ms
Utility Sub	Wozniak C	400/1	10P20/20VA	260	0.45	80	0.05	2600A/ 20ms	2600A/ 20ms
Utility Sub	Delilah 1	400/1	10P20/20VA	260	0.45	80	0.05	2600A/ 20ms	2600A/ 20ms
Utility Sub	Delilah 2	400/1	10P20/20VA	260	0.45	80	0.05	2600A/ 20ms	2600A/ 20ms
Utility Sub	Atlantic 1	1000/5	10P20/25VA	520	0.26	60	0.05	5200A/ 50ms	600A/ 50ms
Utility Sub	Atlantic 2	1000/5	10P20/25VA	520	0.26	60	0.05	5200A/ 50ms	600A/ 50ms
Utility Sub	Gardens 1	1000/5	10P20/25VA	260	0.45	80	0.05	2600A/ 20ms	2600A/ 20ms
Utility Sub	Gardens 2	1000/5	10P20/25VA	260	0.45	80	0.05	2600A/ 20ms	2600A/ 20ms
Utility Sub	Workplace 1	400/1	10P20/20VA	520	0.40	160	0.05	5200A/ 20ms	5200A/ 20ms
Utility Sub	Workplace 2	400/1	10P20/20VA	520	0.40	160	0.05	5200A/ 20ms	5200A/ 20ms
Utility Sub	Utility Source 1	400/1	10P20/20VA	1920	0.34	120	0.40	-	12A/10 s
Utility Sub	Utility Source 1	400/1	10P20/20VA	1920	0.34	120	0.40	-	12A/10 s

Appendix F: Optimisation algorithm

MATLAB code

Probability-based Incremental Learning MATLAB code used for the IEEE 14-bus system optimisation for Case 2

```
clear all

%Initialisation of variables
NumGenerations=100; %Number of generations
NumPop=50; %Number of individuals in a population

n=0;
m=0;

%Best Solution Tracker
BestPowerLoss=inf;
BestVoltProf=inf;
BestSol=[];
BestSolPF=[];
SolutionTracker=[];
OverallBestSol=[];
OverallBestPowerLoss=inf;
OverallBestVoltProf=inf;

%Set up power flow case
Network=loadcase('case14_modified_v2');

%Initialize population
GenPowerMin=0; %Min and max gen capacities
GenPowerMax=72;
GenNum=size(Network.bus); %Number of DGs to generate
GenNum=GenNum(1);
NumGenToPlace=GenNum;
GenPF=0.8; %DG power factor
MaxPF=1;
MinPF=0.8;

%PBIL Inputs
SolutionBits=7;
ProbabilityVectorGen1=0.5*ones(1,SolutionBits);
ProbabilityVectorGen2=0.5*ones(1,SolutionBits);
ProbabilityVectorGen3=0.5*ones(1,SolutionBits);
ProbabilityVectorGen4=0.5*ones(1,SolutionBits);
ProbabilityVectorGen5=0.5*ones(1,SolutionBits);
ProbabilityVectorGen6=0.5*ones(1,SolutionBits);
ProbabilityVectorGen7=0.5*ones(1,SolutionBits);
```

```

ProbabilityVectorGen8=0.5*ones(1,SolutionBits);
ProbabilityVectorGen9=0.5*ones(1,SolutionBits);
ProbabilityVectorGen10=0.5*ones(1,SolutionBits);
ProbabilityVectorGen11=0.5*ones(1,SolutionBits);
ProbabilityVectorGen12=0.5*ones(1,SolutionBits);
ProbabilityVectorGen13=0.5*ones(1,SolutionBits);
ProbabilityVectorGen14=0.5*ones(1,SolutionBits);
ProbabilityVectorGen15=0.5*ones(1,SolutionBits);
ProbabilityVectorGen16=0.5*ones(1,SolutionBits);
ProbabilityVectorGen17=0.5*ones(1,SolutionBits);
ProbabilityVectorGen18=0.5*ones(1,SolutionBits);
ProbabilityVectorGen19=0.5*ones(1,SolutionBits);
ProbabilityVectorGen20=0.5*ones(1,SolutionBits);
ProbabilityVectorGen21=0.5*ones(1,SolutionBits);
ProbabilityVectorGen22=0.5*ones(1,SolutionBits);
ProbabilityVectorGen23=0.5*ones(1,SolutionBits);
ProbabilityVectorGen24=0.5*ones(1,SolutionBits);
ProbabilityVectorGen25=0.5*ones(1,SolutionBits);
ProbabilityVectorGen26=0.5*ones(1,SolutionBits);
ProbabilityVectorGen27=0.5*ones(1,SolutionBits);
ProbabilityVectorGen28=0.5*ones(1,SolutionBits);
ProbabilityVectorGen29=0.5*ones(1,SolutionBits);
ProbabilityVectorGen30=0.5*ones(1,SolutionBits);

%Power factor
ProbabilityVectorGen1PF=0.5*ones(1,SolutionBits);
ProbabilityVectorGen2PF=0.5*ones(1,SolutionBits);
ProbabilityVectorGen3PF=0.5*ones(1,SolutionBits);
ProbabilityVectorGen4PF=0.5*ones(1,SolutionBits);
ProbabilityVectorGen5PF=0.5*ones(1,SolutionBits);
ProbabilityVectorGen6PF=0.5*ones(1,SolutionBits);
ProbabilityVectorGen7PF=0.5*ones(1,SolutionBits);
ProbabilityVectorGen8PF=0.5*ones(1,SolutionBits);
ProbabilityVectorGen9PF=0.5*ones(1,SolutionBits);
ProbabilityVectorGen10PF=0.5*ones(1,SolutionBits);
ProbabilityVectorGen11PF=0.5*ones(1,SolutionBits);
ProbabilityVectorGen12PF=0.5*ones(1,SolutionBits);
ProbabilityVectorGen13PF=0.5*ones(1,SolutionBits);
ProbabilityVectorGen14PF=0.5*ones(1,SolutionBits);

ForgettingFactor=0.05;
LearningFactor=0.1;

%Create first generation of solutions
TrialSol=rand(NumPop*(GenNum),SolutionBits);
TrialPF=rand(NumPop*(GenNum),SolutionBits);
TrialSolDec=[];
NextGenTrialSol=zeros(NumPop*(GenNum),SolutionBits);
NextGenTrialSolPF=zeros(NumPop*(GenNum),SolutionBits);

```

```

%Create binary initial solutions
TrialSol=Trialsol<0.5; %1 if >; 0 if <
TrialPF=TrialsolPF<0.5;

%Convert binary solutions to decimal
TrialSolDec=reshape(bin2dec(num2str(reshape(TrialSol,700,7))),50,14);
for a=1:NumPop
    TrialSolDec(a,:)=GenPowerMax*TrialSolDec(a,+)/sum(TrialSolDec(a,:));
end

%Limit results
for z=1:NumPop
    if sum(TrialSolDec(z,:))>GenPowerMax
        TrialSolDec(z,:)=GenPowerMax*TrialSolDec(z,+)/sum(TrialSolDec(z,:));
    end
    if sum(TrialSolDec(z,:))<GenPowerMin
        TrialSolDec(z,:)=GenPowerMin*TrialSolDec(z,+)/sum(TrialSolDec(z,:));
    end
end
%Convert limited results back to binary
TrialSol=de2bi(reshape(round(TrialSolDec),50,14),SolutionBits);

TrialPFDec=reshape(bin2dec(num2str(reshape(TrialPF,700,7))),50,14);
for a=1:NumPop
    for b=1:GenNum
        if TrialPFDec(a,b)>MaxPF*100
            TrialPFDec(a,b)=MaxPF*100;
        end
        if TrialPFDec(a,b)<MinPF*100
            TrialPFDec(a,b)=MinPF*100;
        end
    end
end
%Convert limited results back to binary
TrialPF=de2bi(reshape(round(TrialPFDec),50,14),SolutionBits);

OldGen=Network.gen;    %Save old gen configuration
VoltageProfile=[];
NewVoltageProfile=[];
VoltageProfileRef=ones(1,GenNum);
CompVoltProf=[];
NewCompVoltProf=[];
mpopt=mpoption('pf.enforce_q_lims', 1);
%mpopt=mpoption('pf.nr.max_it',100);

for s=1:NumGenerations
    for b=1:NumPop

```

```

for c=6:GenNum+5 %Account for existing Gens
    Network.gen(c,2)=(TrialPFDec(b,c-5)/100)*TrialSolDec(b,c-5); %Active Power Set
    Network.gen(c,3)=sind(acosd(TrialPFDec(b,c-5)/100))*TrialSolDec(b,c-5); %Reactive Power
Set
    Network.gen(c,4)=sind(acosd(TrialPFDec(b,c-5)/100))*TrialSolDec(b,c-5);
    Network.gen(c,5)=sind(acosd(TrialPFDec(b,c-5)/100))*TrialSolDec(b,c-5);
    Network.gen(c,8)=1; %Ensure gen turned on
end

LoadFlow=runpf(Network,mpopt); %Run load flow

Network.gen=OldGen; %Return network to original state

PowerLosses=sum(get_losses(LoadFlow)); %Get losses

for i=1:GenNum %Generate Generate Voltage Profile
    VoltageProfile=[VoltageProfile,LoadFlow.bus(i,8)];
end

CompVoltProf=sum(abs(VoltageProfileRef-VoltageProfile)); %Get Voltage Profile difference from
ideal

if abs(PowerLosses)<=abs(BestPowerLoss) && abs(CompVoltProf)<=sum(abs(VoltageProfileRef-
BestVoltProf))
    BestPowerLoss=PowerLosses; %If current solution is better than previous best; replace
    BestVoltProf=VoltageProfile;
    BestSol=[];
    BestSolPF=[];
    for z=0:13
        BestSol=[BestSol;TrialSol(b+z,:)]; %Save best performing gen configuration
    end
    BestSolGen=BestSol;
    BestSolDec=TrialSolDec(b,:);
    for z=0:13
        BestSolPF=[BestSolPF;TrialPF(b+z,:)]; %Save best performing gen configuration
    end
    BestSolPFDec=TrialPFDec(b,:);
    BestPowerLossGen=BestPowerLoss;
    BestVoltProfGen=BestVoltProf;
    Solution=LoadFlow;
    ConvergeGen=s;

end

VoltageProfile=[]; %Reset voltage profile

end

%Apply PBIL learning and forgetting factors for next gen

```

```

ProbabilityVectorGen1=(1-LearningFactor)*ProbabilityVectorGen1+LearningFactor*BestSol(1,:);
ProbabilityVectorGen1=ProbabilityVectorGen1-ForgettingFactor*(ProbabilityVectorGen1-0.05);
ProbabilityVectorGen2=(1-LearningFactor)*ProbabilityVectorGen2+LearningFactor*BestSol(2,:);
ProbabilityVectorGen2=ProbabilityVectorGen2-ForgettingFactor*(ProbabilityVectorGen2-0.05);
ProbabilityVectorGen3=(1-LearningFactor)*ProbabilityVectorGen3+LearningFactor*BestSol(3,:);
ProbabilityVectorGen3=ProbabilityVectorGen3-ForgettingFactor*(ProbabilityVectorGen3-0.05);
ProbabilityVectorGen4=(1-LearningFactor)*ProbabilityVectorGen4+LearningFactor*BestSol(4,:);
ProbabilityVectorGen4=ProbabilityVectorGen4-ForgettingFactor*(ProbabilityVectorGen4-0.05);
ProbabilityVectorGen5=(1-LearningFactor)*ProbabilityVectorGen5+LearningFactor*BestSol(5,:);
ProbabilityVectorGen5=ProbabilityVectorGen5-ForgettingFactor*(ProbabilityVectorGen5-0.05);
ProbabilityVectorGen6=(1-LearningFactor)*ProbabilityVectorGen6+LearningFactor*BestSol(6,:);
ProbabilityVectorGen6=ProbabilityVectorGen6-ForgettingFactor*(ProbabilityVectorGen6-0.05);
ProbabilityVectorGen7=(1-LearningFactor)*ProbabilityVectorGen7+LearningFactor*BestSol(7,:);
ProbabilityVectorGen7=ProbabilityVectorGen7-ForgettingFactor*(ProbabilityVectorGen7-0.05);
ProbabilityVectorGen8=(1-LearningFactor)*ProbabilityVectorGen8+LearningFactor*BestSol(8,:);
ProbabilityVectorGen8=ProbabilityVectorGen8-ForgettingFactor*(ProbabilityVectorGen8-0.05);
ProbabilityVectorGen9=(1-LearningFactor)*ProbabilityVectorGen9+LearningFactor*BestSol(9,:);
ProbabilityVectorGen9=ProbabilityVectorGen9-ForgettingFactor*(ProbabilityVectorGen9-0.05);
ProbabilityVectorGen10=(1-
LearningFactor)*ProbabilityVectorGen10+LearningFactor*BestSol(10,:);
    ProbabilityVectorGen10=ProbabilityVectorGen10-ForgettingFactor*(ProbabilityVectorGen10-0.05);
    ProbabilityVectorGen11=(1-
LearningFactor)*ProbabilityVectorGen11+LearningFactor*BestSol(11,:);
    ProbabilityVectorGen11=ProbabilityVectorGen11-ForgettingFactor*(ProbabilityVectorGen11-0.05);
    ProbabilityVectorGen12=(1-
LearningFactor)*ProbabilityVectorGen12+LearningFactor*BestSol(12,:);
    ProbabilityVectorGen12=ProbabilityVectorGen12-ForgettingFactor*(ProbabilityVectorGen12-0.05);
    ProbabilityVectorGen13=(1-
LearningFactor)*ProbabilityVectorGen13+LearningFactor*BestSol(13,:);
    ProbabilityVectorGen13=ProbabilityVectorGen13-ForgettingFactor*(ProbabilityVectorGen13-0.05);
    ProbabilityVectorGen14=(1-
LearningFactor)*ProbabilityVectorGen14+LearningFactor*BestSol(14,:);
    ProbabilityVectorGen14=ProbabilityVectorGen14-ForgettingFactor*(ProbabilityVectorGen14-0.05);

%Create next generation solutions

NextGenTrialSolRand=rand(NumPop*(GenNum),SolutionBits);

for q=1:14:NumPop*(GenNum)
    NextGenTrialSol(q,:)=ProbabilityVectorGen1>NextGenTrialSolRand(q,:);
    NextGenTrialSol(q+1,:)=ProbabilityVectorGen2>NextGenTrialSolRand(q+1,:);
    NextGenTrialSol(q+2,:)=ProbabilityVectorGen3>NextGenTrialSolRand(q+2,:);
    NextGenTrialSol(q+3,:)=ProbabilityVectorGen4>NextGenTrialSolRand(q+3,:);
    NextGenTrialSol(q+4,:)=ProbabilityVectorGen5>NextGenTrialSolRand(q+4,:);
    NextGenTrialSol(q+5,:)=ProbabilityVectorGen6>NextGenTrialSolRand(q+5,:);
    NextGenTrialSol(q+6,:)=ProbabilityVectorGen7>NextGenTrialSolRand(q+6,:);
    NextGenTrialSol(q+7,:)=ProbabilityVectorGen8>NextGenTrialSolRand(q+7,:);
    NextGenTrialSol(q+8,:)=ProbabilityVectorGen9>NextGenTrialSolRand(q+8,:);
    NextGenTrialSol(q+9,:)=ProbabilityVectorGen10>NextGenTrialSolRand(q+9,:);

```

```

NextGenTrialSol(q+10,:)=ProbabilityVectorGen11>NextGenTrialSolRand(q+10,:);
NextGenTrialSol(q+11,:)=ProbabilityVectorGen12>NextGenTrialSolRand(q+11,:);
NextGenTrialSol(q+12,:)=ProbabilityVectorGen13>NextGenTrialSolRand(q+12,:);
NextGenTrialSol(q+13,:)=ProbabilityVectorGen14>NextGenTrialSolRand(q+13,:);

end

%Apply PBIL learning and forgetting factors for next genpower
%factors
ProbabilityVectorGen1PF=(1-
LearningFactor)*ProbabilityVectorGen1PF+LearningFactor*BestSolPF(1,:);
ProbabilityVectorGen1PF=ProbabilityVectorGen1PF-ForgettingFactor*(ProbabilityVectorGen1PF-
0.05);
ProbabilityVectorGen2PF=(1-
LearningFactor)*ProbabilityVectorGen2PF+LearningFactor*BestSolPF(2,:);
ProbabilityVectorGen2PF=ProbabilityVectorGen2PF-ForgettingFactor*(ProbabilityVectorGen2PF-
0.05);
ProbabilityVectorGen3PF=(1-
LearningFactor)*ProbabilityVectorGen3PF+LearningFactor*BestSolPF(3,:);
ProbabilityVectorGen3PF=ProbabilityVectorGen3PF-ForgettingFactor*(ProbabilityVectorGen3PF-
0.05);
ProbabilityVectorGen4PF=(1-
LearningFactor)*ProbabilityVectorGen4PF+LearningFactor*BestSolPF(4,:);
ProbabilityVectorGen4PF=ProbabilityVectorGen4PF-ForgettingFactor*(ProbabilityVectorGen4PF-
0.05);
ProbabilityVectorGen5PF=(1-
LearningFactor)*ProbabilityVectorGen5PF+LearningFactor*BestSolPF(5,:);
ProbabilityVectorGen5PF=ProbabilityVectorGen5PF-ForgettingFactor*(ProbabilityVectorGen5PF-
0.05);
ProbabilityVectorGen6PF=(1-
LearningFactor)*ProbabilityVectorGen6PF+LearningFactor*BestSolPF(6,:);
ProbabilityVectorGen6PF=ProbabilityVectorGen6PF-ForgettingFactor*(ProbabilityVectorGen6PF-
0.05);
ProbabilityVectorGen7PF=(1-
LearningFactor)*ProbabilityVectorGen7PF+LearningFactor*BestSolPF(7,:);
ProbabilityVectorGen7PF=ProbabilityVectorGen7PF-ForgettingFactor*(ProbabilityVectorGen7PF-
0.05);
ProbabilityVectorGen8PF=(1-
LearningFactor)*ProbabilityVectorGen8PF+LearningFactor*BestSolPF(8,:);
ProbabilityVectorGen8PF=ProbabilityVectorGen8PF-ForgettingFactor*(ProbabilityVectorGen8PF-
0.05);
ProbabilityVectorGen9PF=(1-
LearningFactor)*ProbabilityVectorGen9PF+LearningFactor*BestSolPF(9,:);
ProbabilityVectorGen9PF=ProbabilityVectorGen9PF-ForgettingFactor*(ProbabilityVectorGen9PF-
0.05);
ProbabilityVectorGen10PF=(1-
LearningFactor)*ProbabilityVectorGen10PF+LearningFactor*BestSolPF(10,:);
ProbabilityVectorGen10PF=ProbabilityVectorGen10PF-
ForgettingFactor*(ProbabilityVectorGen10PF-0.05);

```

```

ProbabilityVectorGen11PF=(1-
LearningFactor)*ProbabilityVectorGen11PF+LearningFactor*BestSolPF(11,:);
ProbabilityVectorGen11PF=ProbabilityVectorGen11PF-
ForgettingFactor*(ProbabilityVectorGen11PF-0.05);
ProbabilityVectorGen12PF=(1-
LearningFactor)*ProbabilityVectorGen12PF+LearningFactor*BestSolPF(12,:);
ProbabilityVectorGen12PF=ProbabilityVectorGen12PF-
ForgettingFactor*(ProbabilityVectorGen12PF-0.05);
ProbabilityVectorGen13PF=(1-
LearningFactor)*ProbabilityVectorGen13PF+LearningFactor*BestSolPF(13,:);
ProbabilityVectorGen13PF=ProbabilityVectorGen13PF-
ForgettingFactor*(ProbabilityVectorGen13PF-0.05);
ProbabilityVectorGen14PF=(1-
LearningFactor)*ProbabilityVectorGen14PF+LearningFactor*BestSolPF(14,:);
ProbabilityVectorGen14PF=ProbabilityVectorGen14PF-
ForgettingFactor*(ProbabilityVectorGen14PF-0.05);

%Create next generation solutions

NextGenTrialSolRandPF=rand(NumPop*(GenNum),SolutionBits);

for q=1:14:NumPop*(GenNum)
NextGenTrialSolPF(q,:)=ProbabilityVectorGen1PF>NextGenTrialSolRandPF(q,:);
NextGenTrialSolPF(q+1,:)=ProbabilityVectorGen2PF>NextGenTrialSolRandPF(q+1,:);
NextGenTrialSolPF(q+2,:)=ProbabilityVectorGen3PF>NextGenTrialSolRandPF(q+2,:);
NextGenTrialSolPF(q+3,:)=ProbabilityVectorGen4PF>NextGenTrialSolRandPF(q+3,:);
NextGenTrialSolPF(q+4,:)=ProbabilityVectorGen5PF>NextGenTrialSolRandPF(q+4,:);
NextGenTrialSolPF(q+5,:)=ProbabilityVectorGen6PF>NextGenTrialSolRandPF(q+5,:);
NextGenTrialSolPF(q+6,:)=ProbabilityVectorGen7PF>NextGenTrialSolRandPF(q+6,:);
NextGenTrialSolPF(q+7,:)=ProbabilityVectorGen8PF>NextGenTrialSolRandPF(q+7,:);
NextGenTrialSolPF(q+8,:)=ProbabilityVectorGen9PF>NextGenTrialSolRandPF(q+8,:);
NextGenTrialSolPF(q+9,:)=ProbabilityVectorGen10PF>NextGenTrialSolRandPF(q+9,:);
NextGenTrialSolPF(q+10,:)=ProbabilityVectorGen11PF>NextGenTrialSolRandPF(q+10,:);
NextGenTrialSolPF(q+11,:)=ProbabilityVectorGen12PF>NextGenTrialSolRandPF(q+11,:);
NextGenTrialSolPF(q+12,:)=ProbabilityVectorGen13PF>NextGenTrialSolRandPF(q+12,:);
NextGenTrialSolPF(q+13,:)=ProbabilityVectorGen14PF>NextGenTrialSolRandPF(q+13,:);

end

TrialSol=NextGenTrialSol;
TrialSolDec=reshape(bin2dec(num2str(reshape(TrialSol,700,7))),50,14);

TrialPF=NextGenTrialSolPF;
TrialPFDec=reshape(bin2dec(num2str(reshape(TrialPF,700,7))),50,14);

%Limit results
for z=1:NumPop
if sum(TrialSolDec(z,:))>GenPowerMax
TrialSolDec(z,:)=GenPowerMax*TrialSolDec(z,:)/sum(TrialSolDec(z,:));

```

```

end
if sum(TrialSolDec(z,:))<GenPowerMin
    TrialSolDec(z,:)=GenPowerMin*TrialSolDec(z,:)/sum(TrialSolDec(z,:));
end
end

for a=1:NumPop
    for b=1:GenNum
        if TrialPFDec(a,b)>MaxPF*100
            TrialPFDec(a,b)=MaxPF*100;
        end
        if TrialPFDec(a,b)<MinPF*100
            TrialPFDec(a,b)=MinPF*100;
        end
    end
end

%Convert limited results back to binary
TrialSol=de2bi(reshape(round(TrialSolDec),50,14),SolutionBits);
TrialPF=de2bi(reshape(round(TrialPFDec),50,14),SolutionBits);

%Track overall best solution over the generations
if abs(BestPowerLoss)<=abs(OverallBestPowerLoss)           &&
sum(abs(BestVoltProf))<=sum(abs(OverallBestVoltProf))
    OverallBestPowerLoss=BestPowerLoss;           %If current solution is better than previous best;
replace
    OverallBestVoltProf=BestVoltProf;
    OverallBestSol=BestSol;           %Save best performing gen configuration
    OverallBestSolDec=BestSolDec;
    OverallBestSolPF=BestSolPFDec;
    SolutionFin=Solution;
    ConvergeGenFin=s;
end

end

OverallBestSol
OverallBestSolDec
OverallBestSolPF
OverallBestPowerLoss
OverallBestVoltProf
ConvergeGenFin

SolutionFin.gen(:,2)
SolutionFin.gen(:,3)

```

Differential Evolution MATLAB code used for the IEEE 14-bus system optimisation for Case 3

```
clear all
```

```
%Initialisation of variables
```

```
NumGenerations=100; %Number of generations
```

```
NumPop=50; %Number of individuals in a population
```

```
n=0;
```

```
m=0;
```

```
%Define DE parameters
```

```
F=0.5;
```

```
Lamda=0.5;
```

```
CR=0.5;
```

```
%Best Solution Tracker
```

```
BestPowerLoss=inf;
```

```
BestVoltProf=inf;
```

```
%Set up power flow case
```

```
Network=loadcase('case14_modified_v2');
```

```
%Initialize population
```

```
GenPowerMin=0; %Min and max gen capacities
```

```
GenPowerMax=72;
```

```
GenNum=size(Network.bus); %Number of DGs to generate
```

```
GenNum=GenNum(1);
```

```
GenPF=0.8; %DG power factor
```

```
MaxPF=1;
```

```
MinPF=0.8;
```

```
TrialSol=rand(NumPop,GenNum); %Create first generation of solutions - fixed bus; second column=DG  
size MVA
```

```
for a=1:NumPop
```

```
    TrialSol(a,:)=GenPowerMax*TrialSol(a,:)/sum(TrialSol(a,:));
```

```
end
```

```
TrialPF=rand(NumPop,GenNum); %Power Factor trials
```

```
TrialPF=MinPF+TrialPF*(MaxPF-MinPF);
```

```
NextGenTrialPF=zeros(NumPop,GenNum); %Next Gen Power Factor trials
```

```
NextGenTrialSol=zeros(NumPop,GenNum);
```

```
OldGen=Network.gen; %Save old gen configuration
```

```
VoltageProfile=[];
```

```
NewVoltageProfile=[];
```

```

VoltageProfileRef=ones(1,GenNum);
CompVoltProf=[];
NewCompVoltProf=[];

mpopt=mpoption('pf.enforce_q_lims', 1);
for a=1:NumGenerations
    for b=1:NumPop
        for c=6:GenNum+5
            Network.gen(c,2)=TrialPF(b,c-5)*TrialSol(b,c-5);    %Active Power Set
            Network.gen(c,3)=sind(acosd(TrialPF(b,c-5)))*TrialSol(b,c-5); %Reactive Power Set
            Network.gen(c,4)=sind(acosd(TrialPF(b,c-5)))*TrialSol(b,c-5);
            Network.gen(c,5)=sind(acosd(TrialPF(b,c-5)))*TrialSol(b,c-5);
            Network.gen(c,8)=1;
        end

        LoadFlow=runpf(Network,mpopt); %Run load flow

        Network.gen=OldGen; %Return network to original state

        PowerLosses=sum(get_losses(LoadFlow)); %Get losses

        for i=1:GenNum %Generate Generate Voltage Profile
            VoltageProfile=[VoltageProfile,LoadFlow.bus(i,8)];
        end
        CompVoltProf=sum(abs(VoltageProfileRef-VoltageProfile)); %Get Voltage Profile difference from
ideal

        if abs(PowerLosses)<=abs(BestPowerLoss) && abs(CompVoltProf)<=sum(abs(VoltageProfileRef-
BestVoltProf))
            BestPowerLoss=PowerLosses; %If current solution is better than previous best; replace
            BestVoltProf=VoltageProfile;
            BestSol=TrialSol(b,:); %Save row of best performing gen configuration
            BestSolPF=TrialPF(b,:);
            Solution=LoadFlow;
            ConvergeGen=a;
        end

        VoltageProfile=[];

        %DE Mutation
        %current-best operator

        Selector=int8(1+rand(1)*(NumPop-1));
        RandomVector1=TrialSol(Selector,:); %Select vector at random for mutation vector construction
        Selector=int8(1+rand(1)*(NumPop-1));
        RandomVector2=TrialSol(Selector,:); %Select vector at random for mutation vector construction
        BestVectorSelection=BestSol; %Select best vector for mutation vector construction

        BaseVector=BestVectorSelection-TrialSol(b,:); %Define the base vector

```

```

MutantVector=Trialsol(b,:)+F*(RandomVector1-RandomVector2)+Lamda*(BaseVector); %Define
the mutant vector

```

```

%Crossover function

```

```

ProbabilityMatrix=rand(1,GenNum*2)<CR;

```

```

for e=1:GenNum

```

```

    if ProbabilityMatrix(1,e)==0      %If Probability Vector element is 0, take element from target
vector

```

```

        NextGenTrialsol(b,e)=Trialsol(b,e);

```

```

        if NextGenTrialsol(b,e)<GenPowerMin

```

```

            NextGenTrialsol(b,e)=GenPowerMin;

```

```

        end

```

```

        if NextGenTrialsol(b,e)>GenPowerMax

```

```

            NextGenTrialsol(b,:)=GenPowerMax*NextGenTrialsol(b,:)/sum(NextGenTrialsol(b,:));

```

```

        end

```

```

    end

```

```

    if ProbabilityMatrix(1,e)==1      %If Probability Vector element is 1, take element from mutant
vector

```

```

        NextGenTrialsol(b,e)=MutantVector(1,e);

```

```

    %Limits

```

```

    if NextGenTrialsol(b,e)<GenPowerMin

```

```

        NextGenTrialsol(b,e)=GenPowerMin;

```

```

    end

```

```

    if sum(NextGenTrialsol(b,:))>GenPowerMax

```

```

        NextGenTrialsol(b,:)=GenPowerMax*NextGenTrialsol(b,:)/sum(NextGenTrialsol(b,:));

```

```

    end

```

```

end

```

```

end

```

```

%Power Factor

```

```

Selector=int8(1+rand(1)*(NumPop-1));

```

```

RandomVector1=TrialsolPF(Selector,:); %Select vector at random for mutation vector construction

```

```

Selector=int8(1+rand(1)*(NumPop-1));

```

```

RandomVector2=TrialsolPF(Selector,:); %Select vector at random for mutation vector construction

```

```

BestVectorSelection=BestSolPF; %Select best vector for mutation vector construction

```

```

BaseVector=BestVectorSelection-TrialsolPF(b,:); %Define the base vector

```

```

MutantVector=TrialsolPF(b,:)+F*(RandomVector1-RandomVector2)+Lamda*(BaseVector); %Define
the mutant vector

```

```

%Crossover function

```

```

ProbabilityMatrix=rand(1,GenNum*2)<CR;

```

```

for e=1:GenNum
    if ProbabilityMatrix(1,e)==0      %If Probability Vector element is 0, take element from target
vector
        NextGenTrialPF(b,e)=TrialSol(b,e);
        if NextGenTrialPF(b,e)>MaxPF      %Limit PF
            NextGenTrialPF(b,e)=MaxPF;
        end
        if NextGenTrialPF(b,e)<MinPF
            NextGenTrialPF(b,e)=MinPF;
        end

        end
        if ProbabilityMatrix(1,e)==1      %If Probability Vector element is 1, take element from mutant
vector
            NextGenTrialPF(b,e)=MutantVector(1,e);

            if NextGenTrialPF(b,e)>MaxPF      %Limit PF
                NextGenTrialPF(b,e)=MaxPF;
            end
            if NextGenTrialPF(b,e)<MinPF
                NextGenTrialPF(b,e)=MinPF;
            end
            end

        end

        %Try new solutions
        for c=6:GenNum+5
            Network.gen(c,2)=NextGenTrialPF(b,c-5)*NextGenTrialSol(b,c-5);      %Active Power Set
            Network.gen(c,3)=sind(acosd(NextGenTrialPF(b,c-5)))*NextGenTrialSol(b,c-5);      %Reactive
Power Set
            Network.gen(c,4)=sind(acosd(TrialPF(b,c-5)))*TrialSol(b,c-5);
            Network.gen(c,5)=sind(acosd(TrialPF(b,c-5)))*TrialSol(b,c-5);
            Network.gen(c,8)=1;
        end

        LoadFlow=runpf(Network,mpopt); %Run load flow

        Network.gen=OldGen; %Return network to original state

        NewPowerLosses=sum(get_losses(LoadFlow)); %Get losses

        for i=1:GenNum
            NewVoltageProfile=[NewVoltageProfile,LoadFlow.bus(i,8)];
        end
        NewCompVoltProf=sum(abs(VoltageProfileRef-NewVoltageProfile));

        if abs(NewPowerLosses)<abs(PowerLosses) && abs(NewCompVoltProf)<abs(CompVoltProf)
            TrialSol(b,:)=NextGenTrialSol(b,:);

```

```
    TrialPF(b,:)=NextGenTrialPF(b,:);  
end
```

```
    VoltageProfile=[];  
    NewVoltageProfile=[];
```

```
end  
end
```

```
%Display results  
BestSol  
BestPowerLoss  
BestVoltProf  
BestSolPF  
ConvergeGen  
Solution.gen(:,2)  
Solution.gen(:,3)
```

Probability-based Incremental Learning MATLAB code used for the Case Study network optimisation for Case 3

```
clear all

%Initialisation of variables
NumGenerations=100; %Number of generations
NumPop=50; %Number of individuals in a population

n=0;
m=0;

%Best Solution Tracker
BestPowerLoss=inf;
BestVoltProf=inf;
BestSol=[];
BestSolPF=[];
SolutionTracker=[];
OverallBestSol=[];
OverallBestPowerLoss=inf;
OverallBestVoltProf=inf;

%Set up power flow case
Network=loadcase('MunicipalNetwork');

%Initialize population
GenPowerMin=0; %Min and max gen capacities
GenPowerMax=72;
GenNum=size(Network.bus); %Number of DGs to generate
GenNum=GenNum(1);
NumGenToPlace=GenNum;
GenPF=0.8; %DG power factor
MaxPF=1;
MinPF=0.8;

%PBIL Inputs
SolutionBits=7;
ProbabilityVectorGen1=0.5*ones(1,SolutionBits);
ProbabilityVectorGen2=0.5*ones(1,SolutionBits);
ProbabilityVectorGen3=0.5*ones(1,SolutionBits);
ProbabilityVectorGen4=0.5*ones(1,SolutionBits);
ProbabilityVectorGen5=0.5*ones(1,SolutionBits);
ProbabilityVectorGen6=0.5*ones(1,SolutionBits);
ProbabilityVectorGen7=0.5*ones(1,SolutionBits);
ProbabilityVectorGen8=0.5*ones(1,SolutionBits);
ProbabilityVectorGen9=0.5*ones(1,SolutionBits);
ProbabilityVectorGen10=0.5*ones(1,SolutionBits);
ProbabilityVectorGen11=0.5*ones(1,SolutionBits);
```

```
ProbabilityVectorGen12=0.5*ones(1,SolutionBits);
ProbabilityVectorGen13=0.5*ones(1,SolutionBits);
ProbabilityVectorGen14=0.5*ones(1,SolutionBits);
ProbabilityVectorGen15=0.5*ones(1,SolutionBits);
ProbabilityVectorGen16=0.5*ones(1,SolutionBits);
ProbabilityVectorGen17=0.5*ones(1,SolutionBits);
ProbabilityVectorGen18=0.5*ones(1,SolutionBits);
ProbabilityVectorGen19=0.5*ones(1,SolutionBits);
ProbabilityVectorGen20=0.5*ones(1,SolutionBits);
ProbabilityVectorGen21=0.5*ones(1,SolutionBits);
ProbabilityVectorGen22=0.5*ones(1,SolutionBits);
ProbabilityVectorGen23=0.5*ones(1,SolutionBits);
ProbabilityVectorGen24=0.5*ones(1,SolutionBits);
ProbabilityVectorGen25=0.5*ones(1,SolutionBits);
ProbabilityVectorGen26=0.5*ones(1,SolutionBits);
ProbabilityVectorGen27=0.5*ones(1,SolutionBits);
ProbabilityVectorGen28=0.5*ones(1,SolutionBits);
ProbabilityVectorGen29=0.5*ones(1,SolutionBits);
ProbabilityVectorGen30=0.5*ones(1,SolutionBits);
```

%Power factor

```
ProbabilityVectorGen1PF=0.5*ones(1,SolutionBits);
ProbabilityVectorGen2PF=0.5*ones(1,SolutionBits);
ProbabilityVectorGen3PF=0.5*ones(1,SolutionBits);
ProbabilityVectorGen4PF=0.5*ones(1,SolutionBits);
ProbabilityVectorGen5PF=0.5*ones(1,SolutionBits);
ProbabilityVectorGen6PF=0.5*ones(1,SolutionBits);
ProbabilityVectorGen7PF=0.5*ones(1,SolutionBits);
ProbabilityVectorGen8PF=0.5*ones(1,SolutionBits);
ProbabilityVectorGen9PF=0.5*ones(1,SolutionBits);
ProbabilityVectorGen10PF=0.5*ones(1,SolutionBits);
ProbabilityVectorGen11PF=0.5*ones(1,SolutionBits);
ProbabilityVectorGen12PF=0.5*ones(1,SolutionBits);
ProbabilityVectorGen13PF=0.5*ones(1,SolutionBits);
ProbabilityVectorGen14PF=0.5*ones(1,SolutionBits);
ProbabilityVectorGen15PF=0.5*ones(1,SolutionBits);
ProbabilityVectorGen16PF=0.5*ones(1,SolutionBits);
ProbabilityVectorGen17PF=0.5*ones(1,SolutionBits);
ProbabilityVectorGen18PF=0.5*ones(1,SolutionBits);
ProbabilityVectorGen19PF=0.5*ones(1,SolutionBits);
ProbabilityVectorGen20PF=0.5*ones(1,SolutionBits);
ProbabilityVectorGen21PF=0.5*ones(1,SolutionBits);
ProbabilityVectorGen22PF=0.5*ones(1,SolutionBits);
ProbabilityVectorGen23PF=0.5*ones(1,SolutionBits);
ProbabilityVectorGen24PF=0.5*ones(1,SolutionBits);
ProbabilityVectorGen25PF=0.5*ones(1,SolutionBits);
ProbabilityVectorGen26PF=0.5*ones(1,SolutionBits);
ProbabilityVectorGen27PF=0.5*ones(1,SolutionBits);
ProbabilityVectorGen28PF=0.5*ones(1,SolutionBits);
```

```

ProbabilityVectorGen29PF=0.5*ones(1,SolutionBits);
ProbabilityVectorGen30PF=0.5*ones(1,SolutionBits);

ForgettingFactor=0.05;
LearningFactor=0.1;

%Create first generation of solutions
TrialSol=rand(NumPop*(GenNum-1),SolutionBits);
TrialPF=rand(NumPop*(GenNum-1),SolutionBits);
TrialSolDec=[];
NextGenTrialSol=zeros(NumPop*(GenNum-1),SolutionBits);
NextGenTrialSolPF=zeros(NumPop*(GenNum-1),SolutionBits);

%Create binary initial solutions
TrialSol=TrialSol<0.5; %1 if >; 0 if <
TrialPF=TrialPF<0.5;

%Convert binary solutions to decimal
TrialSolDec=reshape(bin2dec(num2str(reshape(TrialSol,1500,7))),50,30);
for a=1:NumPop
    TrialSolDec(a,:)=GenPowerMax*TrialSolDec(a,+)/sum(TrialSolDec(a,:));
end

%Limit results
for z=1:NumPop
    if sum(TrialSolDec(z,:))>GenPowerMax
        TrialSolDec(z,:)=GenPowerMax*TrialSolDec(z,+)/sum(TrialSolDec(z,:));
    end
    if sum(TrialSolDec(z,:))<GenPowerMin
        TrialSolDec(z,:)=GenPowerMin*TrialSolDec(z,+)/sum(TrialSolDec(z,:));
    end
end

%Convert limited results back to binary
TrialSol=de2bi(reshape(round(TrialSolDec),50,30),SolutionBits);

TrialPFDec=reshape(bin2dec(num2str(reshape(TrialPF,1500,7))),50,30);
for a=1:NumPop
    for b=1:GenNum-1
        if TrialPFDec(a,b)>MaxPF*100
            TrialPFDec(a,b)=MaxPF*100;
        end
        if TrialPFDec(a,b)<MinPF*100
            TrialPFDec(a,b)=MinPF*100;
        end
    end
end

%Convert limited results back to binary
TrialPF=de2bi(reshape(round(TrialPFDec),50,30),SolutionBits);

```

```

OldGen=Network.gen;    %Save old gen configuration
VoltageProfile=[];
NewVoltageProfile=[];
VoltageProfileRef=ones(1,GenNum);
CompVoltProf=[];
NewCompVoltProf=[];
mpopt=mpoption('pf.enforce_q_lims', 1);
%mpopt=mpoption('pf.nr.max_it',100);

for s=1:NumGenerations
    for b=1:NumPop
        for c=2:GenNum %Account for existing Gens
            Network.gen(c,2)=(TrialPFDec(b,c-1)/100)*TrialSolDec(b,c-1); %Active Power Set
            Network.gen(c,3)=sind(acosd(TrialPFDec(b,c-1)/100))*TrialSolDec(b,c-1); %Reactive Power
Set
            Network.gen(c,4)=sind(acosd(TrialPFDec(b,c-1)/100))*TrialSolDec(b,c-1);
            Network.gen(c,5)=sind(acosd(TrialPFDec(b,c-1)/100))*TrialSolDec(b,c-1);
            Network.gen(c,8)=1; %Ensure gen turned on
        end

        LoadFlow=runpf(Network,mpopt); %Run load flow

        Network.gen=OldGen; %Return network to original state

        PowerLosses=sum(get_losses(LoadFlow)); %Get losses

        for i=1:GenNum %Generate Generate Voltage Profile
            VoltageProfile=[VoltageProfile,LoadFlow.bus(i,8)];
        end

        CompVoltProf=sum(abs(VoltageProfileRef-VoltageProfile)); %Get Voltage Profile difference from
ideal

        if abs(PowerLosses)<=abs(BestPowerLoss) && abs(CompVoltProf)<=sum(abs(VoltageProfileRef-
BestVoltProf))
            BestPowerLoss=PowerLosses; %If current solution is better than previous best; replace
            BestVoltProf=VoltageProfile;
            BestSol=[];
            BestSolPF=[];
            for z=0:29
                BestSol=[BestSol;TrialSol(b+z,:)]; %Save best performing gen configuration
            end
            BestSolGen=BestSol;
            BestSolDec=TrialSolDec(b,:);
            for z=0:29
                BestSolPF=[BestSolPF;TrialPF(b+z,:)]; %Save best performing gen configuration
            end
            BestSolPFDec=TrialPFDec(b,:);

```

```

    BestPowerLossGen=BestPowerLoss;
    BestVoltProfGen=BestVoltProf;
    Solution=LoadFlow;
    ConvergeGen=s;

end

VoltageProfile=[]; %Reset voltage profile

end

%Apply PBIL learning and forgetting factors for next gen
ProbabilityVectorGen1=(1-LearningFactor)*ProbabilityVectorGen1+LearningFactor*BestSol(1,:);
ProbabilityVectorGen1=ProbabilityVectorGen1-ForgettingFactor*(ProbabilityVectorGen1-0.05);
ProbabilityVectorGen2=(1-LearningFactor)*ProbabilityVectorGen2+LearningFactor*BestSol(2,:);
ProbabilityVectorGen2=ProbabilityVectorGen2-ForgettingFactor*(ProbabilityVectorGen2-0.05);
ProbabilityVectorGen3=(1-LearningFactor)*ProbabilityVectorGen3+LearningFactor*BestSol(3,:);
ProbabilityVectorGen3=ProbabilityVectorGen3-ForgettingFactor*(ProbabilityVectorGen3-0.05);
ProbabilityVectorGen4=(1-LearningFactor)*ProbabilityVectorGen4+LearningFactor*BestSol(4,:);
ProbabilityVectorGen4=ProbabilityVectorGen4-ForgettingFactor*(ProbabilityVectorGen4-0.05);
ProbabilityVectorGen5=(1-LearningFactor)*ProbabilityVectorGen5+LearningFactor*BestSol(5,:);
ProbabilityVectorGen5=ProbabilityVectorGen5-ForgettingFactor*(ProbabilityVectorGen5-0.05);
ProbabilityVectorGen6=(1-LearningFactor)*ProbabilityVectorGen6+LearningFactor*BestSol(6,:);
ProbabilityVectorGen6=ProbabilityVectorGen6-ForgettingFactor*(ProbabilityVectorGen6-0.05);
ProbabilityVectorGen7=(1-LearningFactor)*ProbabilityVectorGen7+LearningFactor*BestSol(7,:);
ProbabilityVectorGen7=ProbabilityVectorGen7-ForgettingFactor*(ProbabilityVectorGen7-0.05);
ProbabilityVectorGen8=(1-LearningFactor)*ProbabilityVectorGen8+LearningFactor*BestSol(8,:);
ProbabilityVectorGen8=ProbabilityVectorGen8-ForgettingFactor*(ProbabilityVectorGen8-0.05);
ProbabilityVectorGen9=(1-LearningFactor)*ProbabilityVectorGen9+LearningFactor*BestSol(9,:);
ProbabilityVectorGen9=ProbabilityVectorGen9-ForgettingFactor*(ProbabilityVectorGen9-0.05);
ProbabilityVectorGen10=(1-
LearningFactor)*ProbabilityVectorGen10+LearningFactor*BestSol(10,:);
ProbabilityVectorGen10=ProbabilityVectorGen10-ForgettingFactor*(ProbabilityVectorGen10-
0.05);
ProbabilityVectorGen11=(1-
LearningFactor)*ProbabilityVectorGen11+LearningFactor*BestSol(11,:);
ProbabilityVectorGen11=ProbabilityVectorGen11-ForgettingFactor*(ProbabilityVectorGen11-
0.05);
ProbabilityVectorGen12=(1-
LearningFactor)*ProbabilityVectorGen12+LearningFactor*BestSol(12,:);
ProbabilityVectorGen12=ProbabilityVectorGen12-ForgettingFactor*(ProbabilityVectorGen12-
0.05);
ProbabilityVectorGen13=(1-
LearningFactor)*ProbabilityVectorGen13+LearningFactor*BestSol(13,:);
ProbabilityVectorGen13=ProbabilityVectorGen13-ForgettingFactor*(ProbabilityVectorGen13-
0.05);
ProbabilityVectorGen14=(1-
LearningFactor)*ProbabilityVectorGen14+LearningFactor*BestSol(14,:);

```

```

ProbabilityVectorGen14=ProbabilityVectorGen14-ForgettingFactor*(ProbabilityVectorGen14-
0.05);
ProbabilityVectorGen15=(1-
LearningFactor)*ProbabilityVectorGen15+LearningFactor*BestSol(1,:);
ProbabilityVectorGen15=ProbabilityVectorGen15-ForgettingFactor*(ProbabilityVectorGen15-
0.05);
ProbabilityVectorGen16=(1-
LearningFactor)*ProbabilityVectorGen16+LearningFactor*BestSol(2,:);
ProbabilityVectorGen16=ProbabilityVectorGen16-ForgettingFactor*(ProbabilityVectorGen16-
0.05);
ProbabilityVectorGen17=(1-
LearningFactor)*ProbabilityVectorGen17+LearningFactor*BestSol(2,:);
ProbabilityVectorGen17=ProbabilityVectorGen17-ForgettingFactor*(ProbabilityVectorGen17-
0.05);
ProbabilityVectorGen18=(1-
LearningFactor)*ProbabilityVectorGen18+LearningFactor*BestSol(3,:);
ProbabilityVectorGen18=ProbabilityVectorGen18-ForgettingFactor*(ProbabilityVectorGen18-
0.05);
ProbabilityVectorGen19=(1-
LearningFactor)*ProbabilityVectorGen19+LearningFactor*BestSol(4,:);
ProbabilityVectorGen19=ProbabilityVectorGen19-ForgettingFactor*(ProbabilityVectorGen19-
0.05);
ProbabilityVectorGen20=(1-
LearningFactor)*ProbabilityVectorGen20+LearningFactor*BestSol(5,:);
ProbabilityVectorGen20=ProbabilityVectorGen20-ForgettingFactor*(ProbabilityVectorGen20-
0.05);
ProbabilityVectorGen21=(1-
LearningFactor)*ProbabilityVectorGen21+LearningFactor*BestSol(1,:);
ProbabilityVectorGen21=ProbabilityVectorGen21-ForgettingFactor*(ProbabilityVectorGen21-
0.05);
ProbabilityVectorGen22=(1-
LearningFactor)*ProbabilityVectorGen22+LearningFactor*BestSol(2,:);
ProbabilityVectorGen22=ProbabilityVectorGen22-ForgettingFactor*(ProbabilityVectorGen22-
0.05);
ProbabilityVectorGen23=(1-
LearningFactor)*ProbabilityVectorGen23+LearningFactor*BestSol(3,:);
ProbabilityVectorGen23=ProbabilityVectorGen23-ForgettingFactor*(ProbabilityVectorGen23-
0.05);
ProbabilityVectorGen24=(1-
LearningFactor)*ProbabilityVectorGen24+LearningFactor*BestSol(4,:);
ProbabilityVectorGen24=ProbabilityVectorGen24-ForgettingFactor*(ProbabilityVectorGen24-
0.05);
ProbabilityVectorGen25=(1-
LearningFactor)*ProbabilityVectorGen25+LearningFactor*BestSol(5,:);
ProbabilityVectorGen25=ProbabilityVectorGen25-ForgettingFactor*(ProbabilityVectorGen25-
0.05);
ProbabilityVectorGen26=(1-
LearningFactor)*ProbabilityVectorGen26+LearningFactor*BestSol(6,:);

```

```

ProbabilityVectorGen26=ProbabilityVectorGen26-ForgettingFactor*(ProbabilityVectorGen26-
0.05);
ProbabilityVectorGen27=(1-
LearningFactor)*ProbabilityVectorGen27+LearningFactor*BestSol(7,:);
ProbabilityVectorGen27=ProbabilityVectorGen27-ForgettingFactor*(ProbabilityVectorGen27-
0.05);
ProbabilityVectorGen28=(1-
LearningFactor)*ProbabilityVectorGen28+LearningFactor*BestSol(8,:);
ProbabilityVectorGen28=ProbabilityVectorGen28-ForgettingFactor*(ProbabilityVectorGen28-
0.05);
ProbabilityVectorGen29=(1-
LearningFactor)*ProbabilityVectorGen29+LearningFactor*BestSol(9,:);
ProbabilityVectorGen29=ProbabilityVectorGen29-ForgettingFactor*(ProbabilityVectorGen29-
0.05);
ProbabilityVectorGen30=(1-
LearningFactor)*ProbabilityVectorGen30+LearningFactor*BestSol(10,:);
ProbabilityVectorGen30=ProbabilityVectorGen30-ForgettingFactor*(ProbabilityVectorGen30-
0.05);

```

```

%Create next generation solutions

```

```

NextGenTrialSolRand=rand(NumPop*(GenNum-1),SolutionBits);

```

```

for q=1:30:NumPop*(GenNum-1)

```

```

NextGenTrialSol(q,:)=ProbabilityVectorGen1>NextGenTrialSolRand(q,:);
NextGenTrialSol(q+1,:)=ProbabilityVectorGen2>NextGenTrialSolRand(q+1,:);
NextGenTrialSol(q+2,:)=ProbabilityVectorGen3>NextGenTrialSolRand(q+2,:);
NextGenTrialSol(q+3,:)=ProbabilityVectorGen4>NextGenTrialSolRand(q+3,:);
NextGenTrialSol(q+4,:)=ProbabilityVectorGen5>NextGenTrialSolRand(q+4,:);
NextGenTrialSol(q+5,:)=ProbabilityVectorGen6>NextGenTrialSolRand(q+5,:);
NextGenTrialSol(q+6,:)=ProbabilityVectorGen7>NextGenTrialSolRand(q+6,:);
NextGenTrialSol(q+7,:)=ProbabilityVectorGen8>NextGenTrialSolRand(q+7,:);
NextGenTrialSol(q+8,:)=ProbabilityVectorGen9>NextGenTrialSolRand(q+8,:);
NextGenTrialSol(q+9,:)=ProbabilityVectorGen10>NextGenTrialSolRand(q+9,:);
NextGenTrialSol(q+10,:)=ProbabilityVectorGen11>NextGenTrialSolRand(q+10,:);
NextGenTrialSol(q+11,:)=ProbabilityVectorGen12>NextGenTrialSolRand(q+11,:);
NextGenTrialSol(q+12,:)=ProbabilityVectorGen13>NextGenTrialSolRand(q+12,:);
NextGenTrialSol(q+13,:)=ProbabilityVectorGen14>NextGenTrialSolRand(q+13,:);
NextGenTrialSol(q+14,:)=ProbabilityVectorGen15>NextGenTrialSolRand(q+14,:);
NextGenTrialSol(q+15,:)=ProbabilityVectorGen16>NextGenTrialSolRand(q+15,:);
NextGenTrialSol(q+16,:)=ProbabilityVectorGen17>NextGenTrialSolRand(q+16,:);
NextGenTrialSol(q+17,:)=ProbabilityVectorGen18>NextGenTrialSolRand(q+17,:);
NextGenTrialSol(q+18,:)=ProbabilityVectorGen19>NextGenTrialSolRand(q+18,:);
NextGenTrialSol(q+19,:)=ProbabilityVectorGen20>NextGenTrialSolRand(q+19,:);
NextGenTrialSol(q+20,:)=ProbabilityVectorGen21>NextGenTrialSolRand(q+20,:);
NextGenTrialSol(q+21,:)=ProbabilityVectorGen22>NextGenTrialSolRand(q+21,:);
NextGenTrialSol(q+22,:)=ProbabilityVectorGen23>NextGenTrialSolRand(q+22,:);
NextGenTrialSol(q+23,:)=ProbabilityVectorGen24>NextGenTrialSolRand(q+23,:);

```

```

NextGenTrialSol(q+24,:)=ProbabilityVectorGen25>NextGenTrialSolRand(q+24,:);
NextGenTrialSol(q+25,:)=ProbabilityVectorGen26>NextGenTrialSolRand(q+25,:);
NextGenTrialSol(q+26,:)=ProbabilityVectorGen27>NextGenTrialSolRand(q+26,:);
NextGenTrialSol(q+27,:)=ProbabilityVectorGen28>NextGenTrialSolRand(q+27,:);
NextGenTrialSol(q+28,:)=ProbabilityVectorGen29>NextGenTrialSolRand(q+28,:);
NextGenTrialSol(q+29,:)=ProbabilityVectorGen30>NextGenTrialSolRand(q+29,:);

```

```
end
```

```
%Apply PBIL learning and forgetting factors for next genpower
```

```
%factors
```

```
ProbabilityVectorGen1PF=(1-
```

```
LearningFactor)*ProbabilityVectorGen1PF+LearningFactor*BestSolPF(1,:);
```

```
ProbabilityVectorGen1PF=ProbabilityVectorGen1PF-ForgettingFactor*(ProbabilityVectorGen1PF-0.05);
```

```
ProbabilityVectorGen2PF=(1-
```

```
LearningFactor)*ProbabilityVectorGen2PF+LearningFactor*BestSolPF(2,:);
```

```
ProbabilityVectorGen2PF=ProbabilityVectorGen2PF-ForgettingFactor*(ProbabilityVectorGen2PF-0.05);
```

```
ProbabilityVectorGen3PF=(1-
```

```
LearningFactor)*ProbabilityVectorGen3PF+LearningFactor*BestSolPF(3,:);
```

```
ProbabilityVectorGen3PF=ProbabilityVectorGen3PF-ForgettingFactor*(ProbabilityVectorGen3PF-0.05);
```

```
ProbabilityVectorGen4PF=(1-
```

```
LearningFactor)*ProbabilityVectorGen4PF+LearningFactor*BestSolPF(4,:);
```

```
ProbabilityVectorGen4PF=ProbabilityVectorGen4PF-ForgettingFactor*(ProbabilityVectorGen4PF-0.05);
```

```
ProbabilityVectorGen5PF=(1-
```

```
LearningFactor)*ProbabilityVectorGen5PF+LearningFactor*BestSolPF(5,:);
```

```
ProbabilityVectorGen5PF=ProbabilityVectorGen5PF-ForgettingFactor*(ProbabilityVectorGen5PF-0.05);
```

```
ProbabilityVectorGen6PF=(1-
```

```
LearningFactor)*ProbabilityVectorGen6PF+LearningFactor*BestSolPF(6,:);
```

```
ProbabilityVectorGen6PF=ProbabilityVectorGen6PF-ForgettingFactor*(ProbabilityVectorGen6PF-0.05);
```

```
ProbabilityVectorGen7PF=(1-
```

```
LearningFactor)*ProbabilityVectorGen7PF+LearningFactor*BestSolPF(7,:);
```

```
ProbabilityVectorGen7PF=ProbabilityVectorGen7PF-ForgettingFactor*(ProbabilityVectorGen7PF-0.05);
```

```
ProbabilityVectorGen8PF=(1-
```

```
LearningFactor)*ProbabilityVectorGen8PF+LearningFactor*BestSolPF(8,:);
```

```
ProbabilityVectorGen8PF=ProbabilityVectorGen8PF-ForgettingFactor*(ProbabilityVectorGen8PF-0.05);
```

```
ProbabilityVectorGen9PF=(1-
```

```
LearningFactor)*ProbabilityVectorGen9PF+LearningFactor*BestSolPF(9,:);
```

```
ProbabilityVectorGen9PF=ProbabilityVectorGen9PF-ForgettingFactor*(ProbabilityVectorGen9PF-0.05);
```

```

ProbabilityVectorGen10PF=(1-
LearningFactor)*ProbabilityVectorGen10PF+LearningFactor*BestSolPF(10,:);
ProbabilityVectorGen10PF=ProbabilityVectorGen10PF-
ForgettingFactor*(ProbabilityVectorGen10PF-0.05);
ProbabilityVectorGen11PF=(1-
LearningFactor)*ProbabilityVectorGen11PF+LearningFactor*BestSolPF(11,:);
ProbabilityVectorGen11PF=ProbabilityVectorGen11PF-
ForgettingFactor*(ProbabilityVectorGen11PF-0.05);
ProbabilityVectorGen12PF=(1-
LearningFactor)*ProbabilityVectorGen12PF+LearningFactor*BestSolPF(12,:);
ProbabilityVectorGen12PF=ProbabilityVectorGen12PF-
ForgettingFactor*(ProbabilityVectorGen12PF-0.05);
ProbabilityVectorGen13PF=(1-
LearningFactor)*ProbabilityVectorGen13PF+LearningFactor*BestSolPF(13,:);
ProbabilityVectorGen13PF=ProbabilityVectorGen13PF-
ForgettingFactor*(ProbabilityVectorGen13PF-0.05);
ProbabilityVectorGen14PF=(1-
LearningFactor)*ProbabilityVectorGen14PF+LearningFactor*BestSolPF(14,:);
ProbabilityVectorGen14PF=ProbabilityVectorGen14PF-
ForgettingFactor*(ProbabilityVectorGen14PF-0.05);
ProbabilityVectorGen15PF=(1-
LearningFactor)*ProbabilityVectorGen15PF+LearningFactor*BestSolPF(15,:);
ProbabilityVectorGen15PF=ProbabilityVectorGen15PF-
ForgettingFactor*(ProbabilityVectorGen15PF-0.05);
ProbabilityVectorGen16PF=(1-
LearningFactor)*ProbabilityVectorGen16PF+LearningFactor*BestSolPF(16,:);
ProbabilityVectorGen16PF=ProbabilityVectorGen16PF-
ForgettingFactor*(ProbabilityVectorGen16PF-0.05);
ProbabilityVectorGen17PF=(1-
LearningFactor)*ProbabilityVectorGen17PF+LearningFactor*BestSolPF(17,:);
ProbabilityVectorGen17PF=ProbabilityVectorGen17PF-
ForgettingFactor*(ProbabilityVectorGen17PF-0.05);
ProbabilityVectorGen18PF=(1-
LearningFactor)*ProbabilityVectorGen18PF+LearningFactor*BestSolPF(18,:);
ProbabilityVectorGen18PF=ProbabilityVectorGen18PF-
ForgettingFactor*(ProbabilityVectorGen18PF-0.05);
ProbabilityVectorGen19PF=(1-
LearningFactor)*ProbabilityVectorGen19PF+LearningFactor*BestSolPF(19,:);
ProbabilityVectorGen19PF=ProbabilityVectorGen19PF-
ForgettingFactor*(ProbabilityVectorGen19PF-0.05);
ProbabilityVectorGen20PF=(1-
LearningFactor)*ProbabilityVectorGen20PF+LearningFactor*BestSolPF(20,:);
ProbabilityVectorGen20PF=ProbabilityVectorGen20PF-
ForgettingFactor*(ProbabilityVectorGen20PF-0.05);
ProbabilityVectorGen21PF=(1-
LearningFactor)*ProbabilityVectorGen21PF+LearningFactor*BestSolPF(21,:);
ProbabilityVectorGen21PF=ProbabilityVectorGen21PF-
ForgettingFactor*(ProbabilityVectorGen21PF-0.05);

```

```

ProbabilityVectorGen22PF=(1-
LearningFactor)*ProbabilityVectorGen22PF+LearningFactor*BestSolPF(12,:);
ProbabilityVectorGen22PF=ProbabilityVectorGen22PF-
ForgettingFactor*(ProbabilityVectorGen22PF-0.05);
ProbabilityVectorGen23PF=(1-
LearningFactor)*ProbabilityVectorGen23PF+LearningFactor*BestSolPF(13,:);
ProbabilityVectorGen23PF=ProbabilityVectorGen23PF-
ForgettingFactor*(ProbabilityVectorGen23PF-0.05);
ProbabilityVectorGen24PF=(1-
LearningFactor)*ProbabilityVectorGen24PF+LearningFactor*BestSolPF(14,:);
ProbabilityVectorGen24PF=ProbabilityVectorGen24PF-
ForgettingFactor*(ProbabilityVectorGen24PF-0.05);
ProbabilityVectorGen25PF=(1-
LearningFactor)*ProbabilityVectorGen25PF+LearningFactor*BestSolPF(1,:);
ProbabilityVectorGen25PF=ProbabilityVectorGen25PF-
ForgettingFactor*(ProbabilityVectorGen25PF-0.05);
ProbabilityVectorGen26PF=(1-
LearningFactor)*ProbabilityVectorGen26PF+LearningFactor*BestSolPF(2,:);
ProbabilityVectorGen26PF=ProbabilityVectorGen26PF-
ForgettingFactor*(ProbabilityVectorGen26PF-0.05);
ProbabilityVectorGen27PF=(1-
LearningFactor)*ProbabilityVectorGen27PF+LearningFactor*BestSolPF(3,:);
ProbabilityVectorGen27PF=ProbabilityVectorGen27PF-
ForgettingFactor*(ProbabilityVectorGen27PF-0.05);
ProbabilityVectorGen28PF=(1-
LearningFactor)*ProbabilityVectorGen28PF+LearningFactor*BestSolPF(4,:);
ProbabilityVectorGen28PF=ProbabilityVectorGen28PF-
ForgettingFactor*(ProbabilityVectorGen28PF-0.05);
ProbabilityVectorGen29PF=(1-
LearningFactor)*ProbabilityVectorGen29PF+LearningFactor*BestSolPF(5,:);
ProbabilityVectorGen29PF=ProbabilityVectorGen29PF-
ForgettingFactor*(ProbabilityVectorGen29PF-0.05);
ProbabilityVectorGen30PF=(1-
LearningFactor)*ProbabilityVectorGen30PF+LearningFactor*BestSolPF(6,:);
ProbabilityVectorGen30PF=ProbabilityVectorGen30PF-
ForgettingFactor*(ProbabilityVectorGen30PF-0.05);

```

```

%Create next generation solutions

```

```

NextGenTrialSolRandPF=rand(NumPop*(GenNum-1),SolutionBits);

```

```

for q=1:30:NumPop*(GenNum-1)

```

```

NextGenTrialSolPF(q:)=ProbabilityVectorGen1PF>NextGenTrialSolRandPF(q,:);
NextGenTrialSolPF(q+1,:)=ProbabilityVectorGen2PF>NextGenTrialSolRandPF(q+1,:);
NextGenTrialSolPF(q+2,:)=ProbabilityVectorGen3PF>NextGenTrialSolRandPF(q+2,:);
NextGenTrialSolPF(q+3,:)=ProbabilityVectorGen4PF>NextGenTrialSolRandPF(q+3,:);
NextGenTrialSolPF(q+4,:)=ProbabilityVectorGen5PF>NextGenTrialSolRandPF(q+4,:);
NextGenTrialSolPF(q+5,:)=ProbabilityVectorGen6PF>NextGenTrialSolRandPF(q+5,:);
NextGenTrialSolPF(q+6,:)=ProbabilityVectorGen7PF>NextGenTrialSolRandPF(q+6,:);

```

```

NextGenTrialSolPF(q+7,:)=ProbabilityVectorGen8PF>NextGenTrialSolRandPF(q+7,:);
NextGenTrialSolPF(q+8,:)=ProbabilityVectorGen9PF>NextGenTrialSolRandPF(q+8,:);
NextGenTrialSolPF(q+9,:)=ProbabilityVectorGen10PF>NextGenTrialSolRandPF(q+9,:);
NextGenTrialSolPF(q+10,:)=ProbabilityVectorGen11PF>NextGenTrialSolRandPF(q+10,:);
NextGenTrialSolPF(q+11,:)=ProbabilityVectorGen12PF>NextGenTrialSolRandPF(q+11,:);
NextGenTrialSolPF(q+12,:)=ProbabilityVectorGen13PF>NextGenTrialSolRandPF(q+12,:);
NextGenTrialSolPF(q+13,:)=ProbabilityVectorGen14PF>NextGenTrialSolRandPF(q+13,:);
NextGenTrialSolPF(q+14,:)=ProbabilityVectorGen15PF>NextGenTrialSolRandPF(q+14,:);
NextGenTrialSolPF(q+15,:)=ProbabilityVectorGen16PF>NextGenTrialSolRandPF(q+15,:);
NextGenTrialSolPF(q+16,:)=ProbabilityVectorGen17PF>NextGenTrialSolRandPF(q+16,:);
NextGenTrialSolPF(q+17,:)=ProbabilityVectorGen18PF>NextGenTrialSolRandPF(q+17,:);
NextGenTrialSolPF(q+18,:)=ProbabilityVectorGen19PF>NextGenTrialSolRandPF(q+18,:);
NextGenTrialSolPF(q+19,:)=ProbabilityVectorGen20PF>NextGenTrialSolRandPF(q+19,:);
NextGenTrialSolPF(q+20,:)=ProbabilityVectorGen21PF>NextGenTrialSolRandPF(q+20,:);
NextGenTrialSolPF(q+21,:)=ProbabilityVectorGen22PF>NextGenTrialSolRandPF(q+21,:);
NextGenTrialSolPF(q+22,:)=ProbabilityVectorGen23PF>NextGenTrialSolRandPF(q+22,:);
NextGenTrialSolPF(q+23,:)=ProbabilityVectorGen24PF>NextGenTrialSolRandPF(q+23,:);
NextGenTrialSolPF(q+24,:)=ProbabilityVectorGen25PF>NextGenTrialSolRandPF(q+24,:);
NextGenTrialSolPF(q+25,:)=ProbabilityVectorGen26PF>NextGenTrialSolRandPF(q+25,:);
NextGenTrialSolPF(q+26,:)=ProbabilityVectorGen27PF>NextGenTrialSolRandPF(q+26,:);
NextGenTrialSolPF(q+27,:)=ProbabilityVectorGen28PF>NextGenTrialSolRandPF(q+27,:);
NextGenTrialSolPF(q+28,:)=ProbabilityVectorGen29PF>NextGenTrialSolRandPF(q+28,:);
NextGenTrialSolPF(q+29,:)=ProbabilityVectorGen30PF>NextGenTrialSolRandPF(q+29,:);

end

TrialSol=NextGenTrialSol;
TrialSolDec=reshape(bin2dec(num2str(reshape(TrialSol,1500,7))),50,30);

TrialPF=NextGenTrialSolPF;
TrialPFDec=reshape(bin2dec(num2str(reshape(TrialPF,1500,7))),50,30);

%Limit results
for z=1:NumPop
    if sum(TrialSolDec(z,:))>GenPowerMax
        TrialSolDec(z,:)=GenPowerMax*TrialSolDec(z,:)/sum(TrialSolDec(z,:));
    end
    if sum(TrialSolDec(z,:))<GenPowerMin
        TrialSolDec(z,:)=GenPowerMin*TrialSolDec(z,:)/sum(TrialSolDec(z,:));
    end
end

for a=1:NumPop
    for b=1:GenNum-1
        if TrialPFDec(a,b)>MaxPF*100
            TrialPFDec(a,b)=MaxPF*100;
        end
        if TrialPFDec(a,b)<MinPF*100
            TrialPFDec(a,b)=MinPF*100;
        end
    end
end

```

```

    end
  end
end

%Convert limited results back to binary
TrialSol=de2bi(reshape(round(TrialSolDec),50,30),SolutionBits);
TrialPF=de2bi(reshape(round(TrialPFDec),50,30),SolutionBits);

%Track overall best solution over the generations
if      abs(BestPowerLoss)<=abs(OverallBestPowerLoss)      &&
sum(abs(BestVoltProf))<=sum(abs(OverallBestVoltProf))
    OverallBestPowerLoss=BestPowerLoss;      %If current solution is better than previous best;
replace
    OverallBestVoltProf=BestVoltProf;
    OverallBestSol=BestSol;      %Save best performing gen configuration
    OverallBestSolDec=BestSolDec;
    OverallBestSolPF=BestSolPFDec;
    SolutionFin=Solution;
    ConvergeGenFin=s;
end

end

OverallBestSol
OverallBestSolDec
OverallBestSolPF
OverallBestPowerLoss
OverallBestVoltProf
ConvergeGenFin

SolutionFin.gen(:,2)
SolutionFin.gen(:,3)

```

Differential Evolution MATLAB code used for the Case Study network optimisation for Case 4

```
clear all

%Initialisation of variables
NumGenerations=100; %Number of generations
NumPop=50; %Number of individuals in a population

n=0;
m=0;

%Define DE parameters
F=0.5;
Lamda=0.5;
CR=0.5;

%Best Solution Tracker
BestPowerLoss=inf;
BestVoltProf=inf;

%Set up power flow case
Network=loadcase('MunicipalNetwork');

%Initialize population
GenPowerMin=0; %Min and max gen capacities
GenPowerMax=72;
GenNum=size(Network.bus); %Number of DGs to generate
GenNum=GenNum(1);
GenPF=0.8; %DG power factor
MaxPF=1;
MinPF=0.8;

TrialSol=rand(NumPop,GenNum-1); %Create first generation of solutions - fixed bus; second
column=DG size MVA
for a=1:NumPop
    TrialSol(a,:)=72*TrialSol(a,+)/sum(TrialSol(a,:));
end
TrialPF=rand(NumPop,GenNum-1); %Power Factor trials
TrialPF=MinPF+TrialPF*(MaxPF-MinPF);

NextGenTrialPF=zeros(NumPop,GenNum-1); %Next Gen Power Factor trials
NextGenTrialSol=zeros(NumPop,GenNum-1);

OldGen=Network.gen; %Save old gen configuration
VoltageProfile=[];
NewVoltageProfile=[];
```

```

VoltageProfileRef=ones(1,GenNum);
CompVoltProf=[];
NewCompVoltProf=[];

mpopt=mpoption('pf.enforce_q_lims', 1);
for a=1:NumGenerations
    for b=1:NumPop
        for c=2:GenNum
            Network.gen(c,2)=TrialPF(b,c-1)*TrialSol(b,c-1);    %Active Power Set
            Network.gen(c,3)=sind(acosd(TrialPF(b,c-1)))*TrialSol(b,c-1); %Reactive Power Set
            Network.gen(c,4)=sind(acosd(TrialPF(b,c-1)))*TrialSol(b,c-1);
            Network.gen(c,5)=sind(acosd(TrialPF(b,c-1)))*TrialSol(b,c-1);
            Network.gen(c,8)=1;
        end

        LoadFlow=runpf(Network,mpopt); %Run load flow

        Network.gen=OldGen; %Return network to original state

        PowerLosses=sum(get_losses(LoadFlow)); %Get losses

        for i=1:GenNum %Generate Generate Voltage Profile
            VoltageProfile=[VoltageProfile,LoadFlow.bus(i,8)];
        end
        CompVoltProf=sum(abs(VoltageProfileRef-VoltageProfile)); %Get Voltage Profile difference from
ideal

        if abs(PowerLosses)<=abs(BestPowerLoss) && abs(CompVoltProf)<=sum(abs(VoltageProfileRef-
BestVoltProf))
            BestPowerLoss=PowerLosses; %If current solution is better than previous best; replace
            BestVoltProf=VoltageProfile;
            BestSol=TrialSol(b,:); %Save row of best performing gen configuration
            BestSolPF=TrialPF(b,:);
            Solution=LoadFlow;
            ConvergeGen=a;
        end

        VoltageProfile=[];

        %DE Mutation
        %current-best operator

        Selector=int8(1+rand(1)*(NumPop-1));
        RandomVector1=TrialSol(Selector,:); %Select vector at random for mutation vector construction
        Selector=int8(1+rand(1)*(NumPop-1));
        RandomVector2=TrialSol(Selector,:); %Select vector at random for mutation vector construction
        BestVectorSelection=BestSol; %Select best vector for mutation vector construction

        BaseVector=BestVectorSelection-TrialSol(b,:); %Define the base vector

```

```

MutantVector=Trialsol(b,:)+F*(RandomVector1-RandomVector2)+Lamda*(BaseVector); %Define
the mutant vector

```

```

%Crossover function

```

```

ProbabilityMatrix=rand(1,GenNum*2)<CR;

```

```

for e=1:GenNum-1

```

```

    if ProbabilityMatrix(1,e)==0      %If Probability Vector element is 0, take element from target
vector

```

```

        NextGenTrialsol(b,e)=Trialsol(b,e);

```

```

        if NextGenTrialsol(b,e)<GenPowerMin

```

```

            NextGenTrialsol(b,e)=GenPowerMin;

```

```

        end

```

```

        if NextGenTrialsol(b,e)>GenPowerMax

```

```

            NextGenTrialsol(b,:)=GenPowerMax*NextGenTrialsol(b,:)/sum(NextGenTrialsol(b,:));

```

```

        end

```

```

    end

```

```

    if ProbabilityMatrix(1,e)==1      %If Probability Vector element is 1, take element from mutant
vector

```

```

        NextGenTrialsol(b,e)=MutantVector(1,e);

```

```

        if NextGenTrialsol(b,e)<GenPowerMin

```

```

            NextGenTrialsol(b,e)=GenPowerMin;

```

```

        end

```

```

        if NextGenTrialsol(b,e)>GenPowerMax

```

```

            NextGenTrialsol(b,:)=GenPowerMax*NextGenTrialsol(b,:)/sum(NextGenTrialsol(b,:));

```

```

        end

```

```

    end

```

```

end

```

```

%Power Factor

```

```

Selector=int8(1+rand(1)*(NumPop-1));

```

```

RandomVector1=TrialsolPF(Selector,:); %Select vector at random for mutation vector construction

```

```

Selector=int8(1+rand(1)*(NumPop-1));

```

```

RandomVector2=TrialsolPF(Selector,:); %Select vector at random for mutation vector construction

```

```

BestVectorSelection=BestSolPF; %Select best vector for mutation vector construction

```

```

BaseVector=BestVectorSelection-TrialsolPF(b,:); %Define the base vector

```

```

MutantVector=TrialsolPF(b,:)+F*(RandomVector1-RandomVector2)+Lamda*(BaseVector); %Define
the mutant vector

```

```

%Crossover function

```

```

ProbabilityMatrix=rand(1,GenNum*2)<CR;

```

```

for e=1:GenNum-1

```

```

        if ProbabilityMatrix(1,e)==0      %If Probability Vector element is 0, take element from target
vector
        NextGenTrialPF(b,e)=TrialSol(b,e);
        if NextGenTrialPF(b,e)>MaxPF      %Limit PF
            NextGenTrialPF(b,e)=MaxPF;
        end
        if NextGenTrialPF(b,e)<MinPF
            NextGenTrialPF(b,e)=MinPF;
        end

        end
        if ProbabilityMatrix(1,e)==1      %If Probability Vector element is 1, take element from mutant
vector
        NextGenTrialPF(b,e)=MutantVector(1,e);

        if NextGenTrialPF(b,e)>MaxPF      %Limit PF
            NextGenTrialPF(b,e)=MaxPF;
        end
        if NextGenTrialPF(b,e)<MinPF
            NextGenTrialPF(b,e)=MinPF;
        end
        end

    end

    %Try new solutions
    for c=2:GenNum
        Network.gen(c,2)=NextGenTrialPF(b,c-1)*NextGenTrialSol(b,c-1);    %Active Power Set
        Network.gen(c,3)=sind(acosd(NextGenTrialPF(b,c-1)))*NextGenTrialSol(b,c-1);    %Reactive
Power Set
        Network.gen(c,4)=sind(acosd(TrialPF(b,c-1)))*TrialSol(b,c-1);
        Network.gen(c,5)=sind(acosd(TrialPF(b,c-1)))*TrialSol(b,c-1);
        Network.gen(c,8)=1;
    end

    LoadFlow=runpf(Network,mpopt); %Run load flow

    Network.gen=OldGen; %Return network to original state

    NewPowerLosses=sum(get_losses(LoadFlow)); %Get losses

    for i=1:GenNum
        NewVoltageProfile=[NewVoltageProfile,LoadFlow.bus(i,8)];
    end
    NewCompVoltProf=sum(abs(VoltageProfileRef-NewVoltageProfile));

    if abs(NewPowerLosses)<abs(PowerLosses) && abs(NewCompVoltProf)<abs(CompVoltProf)
        TrialSol(b,:)=NextGenTrialSol(b,:);
        TrialPF(b,:)=NextGenTrialPF(b,:);
    end

```

```
end
```

```
VoltageProfile=[];
```

```
NewVoltageProfile=[];
```

```
end
```

```
end
```

```
%Display results
```

```
BestSol
```

```
BestPowerLoss
```

```
BestVoltProf
```

```
BestSolPF
```

```
ConvergeGen
```

```
Solution.gen(:,2)
```

```
Solution.gen(:,3)
```

Appendix G: Additional results for the network simulations

Voltage profiles for the modified IEEE network cases

Table G-1: The bus results for the modified IEEE 14-bus system for Case 1

<i>Busbar</i>	<i>3-phase Voltage Magnitude (kV)</i>	<i>3-phase Voltage Angle (°)</i>
Bus 1	139.920	0.
Bus 2	137.940	-5.1867
Bus 3	133.320	-15.713
Bus 4	134.447	-9.481
Bus 5	134.841	-8.081
Bus 6	35.310	-12.331
Bus 7	1.0586	-13.199
Bus 8	11.990	-13.198
Bus 9	34.639	-15.138
Bus 10	34.393	-15.440
Bus 11	35.095	-12.595
Bus 12	34.946	-13.021
Bus 13	34.791	-13.029
Bus 14	33.569	-16.959

Table G-2: The bus results for the modified IEEE 14-bus system for Case 2

<i>Busbar</i>	<i>3-phase Voltage Magnitude (kV)</i>	<i>3-phase Voltage Angle (°)</i>
Bus 1	133.261	0.
Bus 2	130.782	-4.029
Bus 3	129.533	-14.426
Bus 4	127.977	-7.086
Bus 5	128.418	-5.819
Bus 6	33.047	-7.333
Bus 7	0.989	-9.655
Bus 8	10.892	-8.892
Bus 9	32.610	-11.523
Bus 10	32.488	-11.708
Bus 11	33.268	-6.946
Bus 12	32.842	-7.953
Bus 13	32.655	-7.896
Bus 14	31.724	-13.342

Table G-3: The bus results for the modified IEEE 14-bus system for Case 3

<i>Busbar</i>	<i>3-phase Voltage Magnitude (kV)</i>	<i>3-phase Voltage Angle (°)</i>
Bus 1	132.747	0.000
Bus 2	130.350	-3.967
Bus 3	130.420	-14.192
Bus 4	127.122	-7.216
Bus 5	127.410	-6.094
Bus 6	32.682	-9.454
Bus 7	0.988	-8.985
Bus 8	10.849	-8.579
Bus 9	32.555	-10.657
Bus 10	32.583	-10.619
Bus 11	32.522	-9.668
Bus 12	32.466	-10.066
Bus 13	32.407	-9.934
Bus 14	31.686	-12.005

Voltage profiles for the municipal network cases

Case 1

Table G-4: The bus results for the 33 kV Utility substation for the municipal network for Case 1

<i>Busbar</i>	<i>3-phase Voltage Magnitude (kV)</i>	<i>3-phase Voltage Angle (°)</i>
Utility Sub Front LHS	33.000	0.000
Utility Sub Front RHS	33.000	0.000
Utility Sub Rear	33.000	0.000
Utility Sub Switchyard	33.000	0.000

Table G-5: The bus results for the Atlantic substation group for the municipal network for Case 1

<i>Busbar</i>	<i>3-phase Voltage Magnitude (kV)</i>	<i>3-phase Voltage Angle (°)</i>
Atlantic LHS	11.623	-30.680
Atlantic RHS	11.652	-30.792
Ares	11.620	-30.686
Bushes	11.621	-30.685
Forest	11.648	-30.802
Hula	11.648	-30.798
Parcel	11.621	-30.685
Poles	11.651	-30.794
Queen	11.651	-30.793
Rain	11.641	-30.804
Spring	11.644	-30.800
Squad	11.619	-30.687
Twenty	11.623	-30.680
Youth	11.650	-30.796

Table G-6: The bus results for the Delilah substation group for the municipal network for Case 1

<i>Busbar</i>	<i>3-phase Voltage Magnitude (kV)</i>	<i>3-phase Voltage Angle</i>
Delilah LHS	11.656	-30.472
Delilah RHS	11.658	-30.321
Bull	11.653	-30.477
Caramel	11.653	-30.477
Dollar	11.656	-30.472
Loop	11.652	-30.482
Ninety	11.658	-30.322
Shimmer	11.657	-30.323
Tortoise	11.655	-30.325
Trees	11.655	-30.325
Wind	11.655	-30.474

Table G-7: The bus results for the Gardens substation group for the municipal network for Case 1

<i>Busbar</i>	<i>3-phase Voltage Magnitude (kV)</i>	<i>3-phase Voltage Angle</i>
Gardens LHS	11.657	-30.521
Gardens RHS	11.653	-31.037
Addition	11.651	-31.046
Allen	11.651	-31.046
Bean	11.651	-31.046
Benjamin	11.657	-30.521
Brush	11.653	-30.529
Gardevoir	11.650	-31.044
Gas	11.651	-31.042
Goth	11.651	-31.046
Night	11.654	-30.526
Oracle	11.656	-30.523
Place	11.648	-31.045
Rose	11.651	-31.040
Royalty	11.657	-30.521
Sam	11.651	-31.046
Show	11.657	-30.521
Thirty	11.657	-30.521
Town	11.653	-31.037
West 1	11.657	-30.521
West 2	11.623	-30.680

Table G-8: The bus results for the Wozniak substation group for the municipal network for Case 1

<i>Busbar</i>	<i>3-phase Voltage Magnitude (kV)</i>	<i>3-phase Voltage Angle</i>
Wozniak A	11.618	-30.417
Wozniak B	11.618	-30.417
Wozniak C	11.629	-30.313
Construction	11.615	-30.420
Mat	11.623	-30.318
Weet	11.618	-30.417
Winelands	11.615	-30.422
Winelands RMU 1	11.615	-30.422

Table G-9: The bus results for the Sunset Vista substation group for the municipal network for Case 1

<i>Busbar</i>	<i>3-phase Voltage Magnitude (kV)</i>	<i>3-phase Voltage Angle</i>
Sunset Vista A	11.473	27.924
Sunset Vista B	11.473	27.924
Sunset Vista C	11.546	28.966
Sunset Vista D	11.546	28.966
Farm	11.473	27.924
Fire	11.465	27.918
Forge LHS	11.473	27.924
Forge RHS	11.473	27.924
Fortune	11.472	27.924
Urban	11.465	27.918
Life LHS	11.471	27.910
Life RHS	11.470	27.889
Lightning LHS	11.465	27.918
Lightning RHS	11.470	27.922
Mine	11.391	27.836
Plant 1	11.471	27.922
Plant 2	11.470	27.922
Plant 3	11.471	27.922
Plant 4	11.470	27.913
Plant 5	11.473	27.924
Plant 6	11.544	28.964
Plant 7	11.544	28.964
Recycling	11.451	27.882
Steve LHS	11.465	27.918
Steve RHS	11.470	27.922

Table G-10: The bus results for the Workplace substation group for the municipal network for Case 1

<i>Busbar</i>	<i>3-phase Voltage Magnitude (kV)</i>	<i>3-phase Voltage Angle</i>
Workplace A	11.640	-32.729
Workplace B	11.640	-32.729
Bravo	11.631	-32.748
British	11.603	-32.841
Dirt	11.638	-32.733
Glassware	11.640	-32.729
Gru	11.635	-32.746
Hundred	11.640	-32.730
Sand	11.613	-32.849
Short	11.612	-32.843
Smash	11.635	-32.746
Tigress	11.633	-32.744

Table G-11: The bus results for the Winery substation group for Case 1 for the municipal network

<i>Busbar</i>	<i>3-phase Voltage Magnitude (kV)</i>	<i>3-phase Voltage Angle</i>
Winery 11 kV LHS	11.686	-30.225
Winery 11 kV RHS	11.686	-30.225
FM	11.634	-30.609
GM	11.634	-30.610
Grounds	11.634	-30.606
High Road	11.647	-30.507
Low Road	11.647	-30.507
PM	11.634	-30.609
Paste RMU 1	11.634	-30.609
Paste RMU 2	11.634	-30.609
Storm	11.686	-30.225
Sunlight	11.676	-30.239
Yellow	11.647	-30.507

Case 2

Table G-12: The bus results for the 33 kV Utility substation for the municipal network for Case 2

<i>Busbar</i>	<i>3-phase Voltage Magnitude (kV)</i>	<i>3-phase Voltage Angle (°)</i>
Utility Sub Front LHS	33.000	0
Utility Sub Front RHS	33.000	0
Utility Sub Rear	33.000	0
Utility Sub Switchyard	33.000	0

Table G-13: The bus results for the Atlantic substation group for the municipal network for Case 2

<i>Busbar</i>	<i>3-phase Voltage Magnitude (kV)</i>	<i>3-phase Voltage Angle (°)</i>
Atlantic LHS	11.623	-30.680
Atlantic RHS	11.652	-30.792
Ares	11.620	-30.686
Bushes	11.621	-30.685
Forest	11.648	-30.802
Hula	11.648	-30.798
Parcel	11.621	-30.685
Poles	11.651	-30.794
Queen	11.651	-30.793
Rain	11.641	-30.804
Spring	11.644	-30.800
Squad	11.619	-30.687
Twenty	11.623	-30.680
Youth	11.650	-30.796

Table G-14: The bus results for the Delilah substation group for the municipal network for Case 2

<i>Busbar</i>	<i>3-phase Voltage Magnitude (kV)</i>	<i>3-phase Voltage Angle</i>
Delilah LHS	11.656	-30.472
Delilah RHS	11.658	-30.321
Bull	11.653	-30.477
Caramel	11.653	-30.477
Dollar	11.656	-30.472
Loop	11.652	-30.482
Ninety	11.658	-30.322
Shimmer	11.657	-30.323
Tortoise	11.655	-30.325
Trees	11.655	-30.325
Wind	11.655	-30.474

Table G-15: The bus results for the Gardens substation group for the municipal network for Case 2

<i>Busbar</i>	<i>3-phase Voltage Magnitude (kV)</i>	<i>3-phase Voltage Angle</i>
Gardens LHS	11.657	-30.521
Gardens RHS	11.653	-31.037
Addition	11.651	-31.046
Allen	11.651	-31.046
Bean	11.651	-31.046
Benjamin	11.657	-30.521
Brush	11.653	-30.529
Gardevoir	11.650	-31.044
Gas	11.651	-31.042
Goth	11.651	-31.046
Night	11.654	-30.526
Oracle	11.656	-30.523
Place	11.648	-31.045
Rose	11.651	-31.040
Royalty	11.657	-30.521
Sam	11.651	-31.046
Show	11.657	-30.521
Thirty	11.657	-30.521
Town	11.653	-31.037
West 1	11.657	-30.521
West 2	11.623	-30.680

Table G-16: The bus results for the Wozniak substation group for the municipal network for Case 2

<i>Busbar</i>	<i>3-phase Voltage Magnitude (kV)</i>	<i>3-phase Voltage Angle</i>
Wozniak A	11.618	-30.417
Wozniak B	11.618	-30.417
Wozniak C	11.629	-30.313
Construction	11.615	-30.420
Mat	11.623	-30.318
Weet	11.618	-30.417
Winelands	11.615	-30.422
Winelands RMU 1	11.615	-30.422

Table G-17: The bus results for the Sunset Vista substation group for the municipal network for Case 2

<i>Busbar</i>	<i>3-phase Voltage Magnitude (kV)</i>	<i>3-phase Voltage Angle</i>
Sunset Vista A	11.473	27.924
Sunset Vista B	11.473	27.924
Sunset Vista C	11.546	28.966
Sunset Vista D	11.546	28.966
Farm	11.473	27.924
Fire	11.465	27.918
Forge LHS	11.473	27.924
Forge RHS	11.473	27.924
Fortune	11.472	27.924
Urban	11.465	27.918
Life LHS	11.471	27.911
Life RHS	11.470	27.891
Lightning LHS	11.465	27.918
Lightning RHS	11.470	27.922
Mine	11.391	27.836
Plant 1	11.471	27.922
Plant 2	11.470	27.922
Plant 3	11.471	27.922
Plant 4	11.470	27.914
Plant 5	11.473	27.924
Plant 6	11.544	28.964
Plant 7	11.544	28.964
Recycling	11.451	27.882
Steve LHS	11.465	27.918
Steve RHS	11.470	27.922

Table G-18: The bus results for the Workplace substation group for the municipal network for Case 2

<i>Busbar</i>	<i>3-phase Voltage Magnitude (kV)</i>	<i>3-phase Voltage Angle</i>
Workplace A	11.640	-32.729
Workplace B	11.640	-32.729
Bravo	11.631	-32.748
British	11.608	-32.833
Dirt	11.638	-32.732
Glassware	11.627	-32.775
Gru	11.635	-32.745
Hundred	11.640	-32.729
Sand	11.614	-32.830
Short	11.613	-32.824
Smash	11.635	-32.745
Tigress	11.633	-32.744

Table G-19: The bus results for the Winery substation group for the municipal network for Case 2

<i>Busbar</i>	<i>3-phase Voltage Magnitude (kV)</i>	<i>3-phase Voltage Angle</i>
Winery 11 kV LHS	11.686	-30.225
Winery 11 kV RHS	11.686	-30.225
FM	11.634	-30.609
GM	11.634	-30.610
Grounds	11.634	-30.606
High Road	11.647	-30.507
Low Road	11.647	-30.507
PM	11.634	-30.609
Paste RMU 1	11.634	-30.609
Paste RMU 2	11.634	-30.609
Storm	11.686	-30.225
Sunlight	11.676	-30.239
Yellow	11.647	-30.507

Case 3

Table G-20: The bus results for the 33 kV Utility substation for the municipal network for Case 3

<i>Busbar</i>	<i>3-phase Voltage Magnitude (kV)</i>	<i>3-phase Voltage Angle (°)</i>
Utility Sub Front LHS	33.000	0.000
Utility Sub Front RHS	33.000	0.000
Utility Sub Rear	33.000	0.000
Utility Sub Switchyard	33.001	0.000

Table G-21: The bus results for the Atlantic substation group for the municipal network for Case 3

<i>Busbar</i>	<i>3-phase Voltage Magnitude (kV)</i>	<i>3-phase Voltage Angle (°)</i>
Atlantic LHS	11.681	-28.791
Atlantic RHS	11.686	-29.342
Ares	11.678	-28.797
Bushes	11.678	-28.796
Forest	11.682	-29.352
Hula	11.682	-29.349
Parcel	11.678	-28.796
Poles	11.685	-29.345
Queen	11.685	-29.344
Rain	11.676	-29.355
Spring	11.678	-29.350
Squad	11.676	-28.798
Twenty	11.680	-28.791
Youth	11.685	-29.346

Table G-22: The bus results for the Delilah substation group for the municipal network for Case 3

<i>Busbar</i>	<i>3-phase Voltage Magnitude (kV)</i>	<i>3-phase Voltage Angle</i>
Delilah LHS	11.679	-28.200
Delilah RHS	11.856	-29.132
Bull	11.676	-28.205
Caramel	11.676	-28.205
Dollar	11.679	-28.200
Loop	11.674	-28.211
Ninety	11.855	-29.132
Shimmer	11.855	-29.133
Tortoise	11.853	-29.135
Trees	11.853	-29.135
Wind	11.678	-28.202

Table G-23: The bus results for the Gardens substation group for the municipal network for Case 3

<i>Busbar</i>	<i>3-phase Voltage Magnitude (kV)</i>	<i>3-phase Voltage Angle</i>
Gardens LHS	11.693	-30.310
Gardens RHS	11.709	-30.757
Addition	11.706	-30.766
Allen	11.706	-30.766
Bean	11.706	-30.766
Benjamin	11.693	-30.310
Brush	11.689	-30.319
Gardevoir	11.706	-30.763
Gas	11.707	-30.762
Goth	11.706	-30.766
Night	11.690	-30.315
Oracle	11.692	-30.312
Place	11.704	-30.765
Rose	11.707	-30.760
Royalty	11.693	-30.310
Sam	11.706	-30.766
Show	11.693	-30.310
Thirty	11.693	-30.310
Town	11.709	-30.757
West 1	11.693	-30.310
West 2	11.681	-28.791

Table G-24: The bus results for the Wozniak substation group for the municipal network for Case 3

<i>Busbar</i>	<i>3-phase Voltage Magnitude (kV)</i>	<i>3-phase Voltage Angle</i>
Wozniak A	11.632	-30.330
Wozniak B	11.632	-30.330
Wozniak C	11.625	-28.293
Construction	11.629	-30.333
Mat	11.619	-28.298
Weet	11.632	-30.330
Winelands	11.628	-30.335
Winelands RMU 1	11.628	-30.335

Table G-25: The bus results for the Sunset Vista substation group for the municipal network for Case 3

<i>Busbar</i>	<i>3-phase Voltage Magnitude (kV)</i>	<i>3-phase Voltage Angle</i>
Sunset Vista A	11.568	28.483
Sunset Vista B	11.568	28.483
Sunset Vista C	11.612	29.346
Sunset Vista D	11.612	29.346
Farm	11.568	28.483
Fire	11.561	28.477
Forge LHS	11.568	28.483
Forge RHS	11.568	28.483
Fortune	11.568	28.483
Urban	11.561	28.477
Life LHS	11.567	28.470
Life RHS	11.565	28.450
Lightning LHS	11.561	28.477
Lightning RHS	11.566	28.481
Mine	11.487	28.396
Plant 1	11.566	28.482
Plant 2	11.565	28.481
Plant 3	11.566	28.481
Plant 4	11.566	28.473
Plant 5	11.568	28.483
Plant 6	11.610	29.344
Plant 7	11.610	29.344
Recycling	11.547	28.442
Steve LHS	11.561	28.477
Steve RHS	11.566	28.481

Table G-26: The bus results for the Workplace substation group for the municipal network for Case 3

<i>Busbar</i>	<i>3-phase Voltage Magnitude (kV)</i>	<i>3-phase Voltage Angle</i>
Workplace A	11.651	-32.037
Workplace B	11.651	-32.037
Bravo	11.642	-32.056
British	11.619	-32.141
Dirt	11.649	-32.041
Glassware	11.638	-32.083
Gru	11.646	-32.054
Hundred	11.650	-32.038
Sand	11.625	-32.138
Short	11.624	-32.132
Smash	11.646	-32.054
Tigress	11.644	-32.052

Table G-27: The bus results for the Winery substation group for the municipal network for Case 3

<i>Busbar</i>	<i>3-phase Voltage Magnitude (kV)</i>	<i>3-phase Voltage Angle</i>
Winery 11 kV LHS	11.793	-29.416
Winery 11 kV RHS	11.793	-29.416
FM	11.794	-29.427
GM	11.794	-29.428
Grounds	11.794	-29.424
High Road	11.794	-29.422
Low Road	11.794	-29.422
PM	11.794	-29.427
Paste RMU 1	11.794	-29.427
Paste RMU 2	11.794	-29.427
Storm	11.793	-29.416
Sunlight	11.783	-29.430
Yellow	11.794	-29.422

Case 4

Table G-28: The bus results for the 33 kV Utility substation for the municipal network for Case 4

<i>Busbar</i>	<i>3-phase Voltage Magnitude (kV)</i>	<i>3-phase Voltage Angle (°)</i>
Utility Sub Front LHS	33.000	0
Utility Sub Front RHS	33.000	0
Utility Sub Rear	33.000	0
Utility Sub Switchyard	33.001	0

Table G-29: The bus results for the Atlantic substation group for the municipal network for Case 4

<i>Busbar</i>	<i>3-phase Voltage Magnitude (kV)</i>	<i>3-phase Voltage Angle (°)</i>
Atlantic LHS	11.658	-30.493
Atlantic RHS	11.673	-29.600
Ares	11.655	-30.499
Bushes	11.656	-30.498
Forest	11.669	-29.610
Hula	11.669	-29.607
Parcel	11.656	-30.498
Poles	11.672	-29.603
Queen	11.672	-29.602
Rain	11.662	-29.613
Spring	11.665	-29.608
Squad	11.654	-30.500
Twenty	11.658	-30.493
Youth	11.671	-29.604

Table G-30: The bus results for the Delilah substation group for the municipal network for Case 4

<i>Busbar</i>	<i>3-phase Voltage Magnitude (kV)</i>	<i>3-phase Voltage Angle</i>
Delilah LHS	11.675	-30.445
Delilah RHS	11.658	-30.321
Bull	11.672	-30.450
Caramel	11.671	-30.450
Dollar	11.675	-30.445
Loop	11.670	-30.455
Ninety	11.658	-30.322
Shimmer	11.657	-30.323
Tortoise	11.655	-30.325
Trees	11.655	-30.325
Wind	11.674	-30.447

Table G-31: The bus results for the Gardens substation group for the municipal network for Case 4

<i>Busbar</i>	<i>3-phase Voltage Magnitude (kV)</i>	<i>3-phase Voltage Angle</i>
Gardens LHS	11.712	-30.033
Gardens RHS	11.697	-30.699
Addition	11.695	-30.708
Allen	11.695	-30.708
Bean	11.695	-30.708
Benjamin	11.712	-30.033
Brush	11.708	-30.042
Gardevoir	11.694	-30.705
Gas	11.695	-30.704
Goth	11.695	-30.708
Night	11.708	-30.038
Oracle	11.710	-30.035
Place	11.692	-30.707
Rose	11.695	-30.702
Royalty	11.712	-30.033
Sam	11.695	-30.708
Show	11.712	-30.033
Thirty	11.711	-30.034
Town	11.697	-30.699
West 1	11.712	-30.033
West 2	11.658	-30.493

Table G-32: The bus results for the Wozniak substation group for the municipal network for Case 4

<i>Busbar</i>	<i>3-phase Voltage Magnitude (kV)</i>	<i>3-phase Voltage Angle</i>
Wozniak A	11.665	-29.992
Wozniak B	11.665	-29.992
Wozniak C	11.627	-28.866
Construction	11.661	-29.995
Mat	11.621	-28.871
Weet	11.664	-29.992
Winelands	11.661	-29.997
Winelands RMU 1	11.661	-29.997

Table G-33: The bus results for the Sunset Vista substation group for the municipal network for Case 4

<i>Busbar</i>	<i>3-phase Voltage Magnitude (kV)</i>	<i>3-phase Voltage Angle</i>
Sunset Vista A	11.520	28.558
Sunset Vista B	11.520	28.558
Sunset Vista C	11.557	29.365
Sunset Vista D	11.557	29.365
Farm	11.520	28.558
Fire	11.512	28.552
Forge LHS	11.520	28.558
Forge RHS	11.520	28.558
Fortune	11.520	28.558
Urban	11.512	28.552
Life LHS	11.518	28.545
Life RHS	11.517	28.525
Lightning LHS	11.512	28.552
Lightning RHS	11.517	28.556
Mine	11.439	28.471
Plant 1	11.518	28.557
Plant 2	11.517	28.556
Plant 3	11.518	28.557
Plant 4	11.517	28.548
Plant 5	11.520	28.558
Plant 6	11.554	29.363
Plant 7	11.554	29.363
Recycling	11.498	28.517
Steve LHS	11.512	28.552
Steve RHS	11.517	28.556

Table G-34: The bus results for the Workplace substation group for the municipal network for Case 4

<i>Busbar</i>	<i>3-phase Voltage Magnitude (kV)</i>	<i>3-phase Voltage Angle</i>
Workplace A	11.656	-31.206
Workplace B	11.656	-31.206
Bravo	11.647	-31.225
British	11.619	-31.317
Dirt	11.654	-31.209
Glassware	11.656	-31.206
Gru	11.651	-31.222
Hundred	11.655	-31.207
Sand	11.629	-31.325
Short	11.628	-31.319
Smash	11.651	-31.222
Tigress	11.649	-31.221

Table G-35: The bus results for the Winery substation group for the municipal network for Case 4

<i>Busbar</i>	<i>3-phase Voltage Magnitude (kV)</i>	<i>3-phase Voltage Angle</i>
Winery 11 kV LHS	11.669	-30.025
Winery 11 kV RHS	11.669	-30.025
FM	11.669	-30.036
GM	11.669	-30.038
Grounds	11.669	-30.034
High Road	11.669	-30.031
Low Road	11.669	-30.031
PM	11.669	-30.036
Paste RMU 1	11.669	-30.036
Paste RMU 2	11.669	-30.036
Storm	11.669	-30.025
Sunlight	11.658	-30.039
Yellow	11.669	-30.031

Additional grading results for the municipal network cases

Case 1

a) Protection grading results for the 33 kV Utility substation rear busbar

The three-phase fault current level for the Utility substation rear busbar is 13.001 kA. This results in the incomers sharing the fault current equally, tripping in 1.928 seconds.

The earth-fault current level is 4.849 kA. This results in the incomers sharing the fault current equally and each tripping in 0.907 seconds.

b) Protection grading results for the Addition substation

The grading for a three-phase fault of 4.112 kA and a single-phase-to-ground fault of 1.000 kA at the Addition substation is shown below.

Table G-36: Branch currents and trip times for a three-phase fault at Addition SS for the municipal network for Case 1

<i>Substation</i>	<i>Feeder</i>	<i>Voltage Level (kV)</i>	<i>Fault Level Magnitude Contribution (kA)</i>	<i>OCEF relay calculated trip time (s)</i>
Allen	Addition	11.66	4.112	0.120
Allen	Gardens	11.66	4.112	0.528
Gardens	Allen	11.66	4.112	0.734
Gardens	Transformer 2 MV	11.66	4.113	1.098
Gardens	Transformer 2 HV	33	1.453	1.420
Utility Sub	Gardens 2	33	1.453	1.799
Utility Sub	Incomer 1	33	0.880	N/A
Utility Sub	Incomer 2	33	0.880	N/A

Table G-37: Branch currents and trip times for a single-phase fault at Addition SS for the municipal network for Case 1

<i>Substation</i>	<i>Feeder</i>	<i>Voltage Level (kV)</i>	<i>Fault Level Magnitude Contribution (kA)</i>	<i>OCEF relay calculated trip time (s)</i>
Allen	Addition	11.66	1.000	0.120
Allen	Gardens	11.66	1.000	0.485
Gardens	Allen	11.66	1.000	1.131
Gardens	Transformer 2 MV	11.66	1.000	1.805
Gardens	Transformer 2 HV	33	0.232	28.572
Utility Sub	Gardens 2	33	0.232	N/A
Utility Sub	Incomer 1	33	0.461	N/A
Utility Sub	Incomer 2	33	0.461	N/A

c) **Protection grading results for the Tortoise substation**

The grading for a three-phase fault of 3.981 kA and a single-phase-to-ground fault of 1.163 kA at the Tortoise substation is shown below.

Table G-38: Branch currents and trip times for a three-phase fault at Tortoise SS for the municipal network for Case 1

<i>Substation</i>	<i>Feeder</i>	<i>Voltage Level (kV)</i>	<i>Fault Level Magnitude Contribution (kA)</i>	<i>OCEF relay calculated trip time (s)</i>
Delilah	Tortoise	11.66	3.981	0.120
Delilah	Transformer 2 MV	11.66	3.983	0.857
Delilah	Transformer 2 HV	33	1.407	0.937
Utility Sub	Delilah 2	33	1.407	1.834
Utility Sub	Incomer 1	33	0.894	N/A
Utility Sub	Incomer 2	33	0.894	N/A

Table G-39: Branch currents and trip times for a single-phase fault at Tortoise SS for the municipal network for Case 1

<i>Substation</i>	<i>Feeder</i>	<i>Voltage Level (kV)</i>	<i>Fault Level Magnitude Contribution (kA)</i>	<i>OCEF relay calculated trip time (s)</i>
Delilah	Tortoise	11.66	1.163	0.120
Delilah	Transformer 2 MV	11.66	1.163	1.289
Delilah	Transformer 2 HV	33	0.246	N/A
Utility Sub	Delilah 2	33	0.246	N/A
Utility Sub	Incomer 1	33	0.476	N/A
Utility Sub	Incomer 2	33	0.476	N/A

d) **Protection grading results for the Steve LHS substation**

The grading for a three-phase fault of 9.387 kA and a single-phase-to-ground fault of 1.167 kA at the Steve LHS substation is shown below.

Table G-40: Branch currents and trip times for a three-phase fault at Steve LHS SS for the municipal network for Case 1

<i>Substation</i>	<i>Feeder</i>	<i>Voltage Level (kV)</i>	<i>Fault Level Magnitude Contribution (kA)</i>	<i>OCEF relay calculated trip time (s)</i>
Lightning LHS	Steve LHS	11.66	9.387	0.340
Sunset Vista	Lightning LHS	11.66	9.392	0.635
Sunset Vista	Transformer A MV	11.66	4.784	1.346
Sunset Vista	Transformer B MV	11.66	4.783	1.346
Sunset Vista	Transformer A HV	33	1.690	1.761
Sunset Vista	Transformer B HV	33	1.690	1.761
Utility Sub	Sunset Vista A	33	1.690	1.761
Utility Sub	Sunset Vista B	33	1.690	1.761
Utility Sub	Incomer 1	33	1.792	N/A
Utility Sub	Incomer 2	33	1.792	N/A

Table G-41: Branch currents and trip times for a single-phase fault at Steve LHS SS for the municipal network for Case 1

<i>Substation</i>	<i>Feeder</i>	<i>Voltage Level (kV)</i>	<i>Fault Level Magnitude Contribution (kA)</i>	<i>OCEF relay calculated trip time (s)</i>
Lightning LHS	Steve LHS	11.66	1.167	0.812
Sunset Vista	Lightning LHS	11.66	1.167	1.203
Sunset Vista	Transformer A MV	11.66	0.584	3.460
Sunset Vista	Transformer B MV	11.66	0.584	3.460
Sunset Vista	Transformer A HV	33	0.231	N/A
Sunset Vista	Transformer B HV	33	0.231	N/A
Utility Sub	Sunset Vista A	33	0.231	N/A
Utility Sub	Sunset Vista B	33	0.231	N/A
Utility Sub	Incomer 1	33	0.476	N/A
Utility Sub	Incomer 2	33	0.476	N/A

e) Protection grading results for the Mine substation

The grading for a three-phase fault of 3.576 kA and a single-phase-to-ground fault of 0.761 kA at the Mine substation is shown below.

Table G-42: Branch currents and trip times for a three-phase fault at Mine SS for the municipal network for Case 1

<i>Substation</i>	<i>Feeder</i>	<i>Voltage Level (kV)</i>	<i>Fault Level Magnitude Contribution (kA)</i>	<i>OCEF relay calculated trip time (s)</i>
Recycling	Mine	11.66	3.576	0.113
Sunset Vista	Recycling	11.66	3.576	0.566
Sunset Vista	Transformer A MV	11.66	2.051	3.717
Sunset Vista	Transformer B MV	11.66	2.051	3.718
Sunset Vista	Transformer A HV	33	0.725	6.313
Sunset Vista	Transformer B HV	33	0.725	6.316
Utility Sub	Sunset Vista A	33	0.725	6.308
Utility Sub	Sunset Vista B	33	0.725	6.311
Utility Sub	Incomer 1	33	0.950	N/A
Utility Sub	Incomer 2	33	0.950	N/A

Table G-43: Branch currents and trip times for a single-phase fault at Mine SS for the municipal network for Case 1

<i>Substation</i>	<i>Feeder</i>	<i>Voltage Level (kV)</i>	<i>Fault Level Magnitude Contribution (kA)</i>	<i>OCEF relay calculated trip time (s)</i>
Recycling	Mine	11.66	0.761	0.120
Sunset Vista	Recycling	11.66	0.761	0.433
Sunset Vista	Transformer A MV	11.66	0.381	29.962
Sunset Vista	Transformer B MV	11.66	0.381	29.962
Sunset Vista	Transformer A HV	33	0.191	N/A
Sunset Vista	Transformer B HV	33	0.191	N/A
Utility Sub	Sunset Vista A	33	0.191	N/A
Utility Sub	Sunset Vista B	33	0.191	N/A
Utility Sub	Incomer 1	33	0.440	N/A
Utility Sub	Incomer 2	33	0.440	N/A

f) **Protection grading results for the Paste RMU 1 substation**

The grading for a three-phase fault of 2.848 kA and a single-phase-to-ground fault of 0.754 kA at the Paste RMU 1 substation is shown below.

Table G-44: Branch currents and trip times for a three-phase fault at Paste RMU 1 SS for the municipal network for Case 1

<i>Substation</i>	<i>Feeder</i>	<i>Voltage Level (kV)</i>	<i>Fault Level Stage 1 Magnitude Contribution (kA)</i>	<i>OCEF Relay Stage 1 Calculated Trip Time (s)</i>	<i>Fault Level Stage 2 Magnitude Contribution (kA)</i>	<i>OCEF Relay Stage 2 Calculated Trip Time (s)</i>	<i>Overall Trip Time (s)</i>
Winery	Yellow	11.66	0.969	0.256	1.346	0.205	0.248
Winery	Transformer 1 MV	11.66	0.971	4.836	1.347	2.741	2.835
Atlantic	Transformer 1 MV	11.66	2.012	1.788	0.062	N/A	N/A
Atlantic	Grounds (Yellow/Paste)	11.66	1.977	0.216	0	N/A	0.216
Winery	Transformer 1 HV	33	0.343	5.679	0.476	3.393	3.480
Atlantic	Transformer 1 HV	33	0.711	2.268	0.022	N/A	N/A
Utility Sub	Atlantic 1	33	0.711	5.811	0.022	N/A	N/A
Utility Sub	Utility Sub Sw. Yard 1	33	0.170	N/A	0.237	N/A	N/A
Utility Sub	Utility Sub Sw. Yard 2	33	0.172	N/A	0.239	N/A	N/A
Utility Sub	Incomer 1	33	0.818	N/A	0.588	N/A	N/A
Utility Sub	Incomer 2	33	0.818	N/A	0.588	N/A	N/A

Table G-45: Branch currents and trip times for a single-phase fault at Paste RMU 1 SS for the municipal network for Case 1

<i>Substation</i>	<i>Feeder</i>	<i>Voltage Level (kV)</i>	<i>Fault Level Stage 1 Magnitude Contribution (kA)</i>	<i>OCEF Relay Stage 1 Calculated Trip Time (s)</i>	<i>Fault Level Stage 2 Magnitude Contribution (kA)</i>	<i>OCEF Relay Stage 2 Calculated Trip Time (s)</i>	<i>Overall Trip Time (s)</i>
Winery	Yellow	11.66	0.240	0.249	0.284	0.222	0.248
Winery	Transformer 1 MV	11.66	0.240	5.020	0.284	4.578	4.599
Atlantic	Transformer 1 MV	11.66	0.514	2.971	0	N/A	N/A
Atlantic	Grounds (Yellow/Paste)	11.66	0.514	0.237	0	N/A	0.237
Winery	Transformer 1 HV	33	0.059	N/A	0.059	N/A	N/A
Atlantic	Transformer 1 HV	33	0.124	N/A	0.023	N/A	N/A
Utility Sub	Atlantic 1	33	0.124	N/A	0.023	N/A	N/A
Utility Sub	Utility Sub Sw. Yard 1	33	0.029	N/A	0.029	N/A	N/A
Utility Sub	Utility Sub Sw. Yard 2	33	0.030	N/A	0.030	N/A	N/A
Utility Sub	Incomer 1	33	0.440	N/A	0.400	N/A	N/A
Utility Sub	Incomer 2	33	0.440	N/A	0.400	N/A	N/A

Case 2

a) Protection grading results for the 33 kV Utility substation rear busbar

The three-phase fault current level for the Utility substation rear busbar is 13.212 kA. This results in the incomers each carrying an equal fault current of 5.888 kA with a calculated trip time of 2.100 for this stage. The wind turbine contributes 1.512 kA and trips in 4.019 seconds.

The earth-fault current level is 4.859 kA. This results in the incomers sharing the fault current equally at 2.430 kA with a calculated trip time of 0.907 seconds for the first stage. The wind turbine does not contribute any fault current to the earth fault condition at this bus.

b) Protection grading results for the Addition substation

The grading for a three-phase fault of 4.121 kA and a single-phase-to-ground fault of 1.000 kA at the Addition substation is shown below.

Table G-46: Branch currents and trip times for a three-phase fault at Addition SS for the municipal network for Case 2

Substation	Feeder	Voltage Level (kV)	Fault Level Magnitude Contribution (kA)	OCEF relay calculated trip time (s)
Allen	Addition	11.66	4.121	0.120
Allen	Gardens	11.66	4.122	0.528
Gardens	Allen	11.66	4.122	0.733
Gardens	Transformer 2 MV	11.66	4.123	1.097
Gardens	Transformer 2 HV	33	1.457	1.418
Utility Sub	Gardens 2	33	1.457	1.797
Utility Sub	Wind Turbine	33	1.290	N/A
Utility Sub	Incomer 1	33	0.404	N/A
Utility Sub	Incomer 2	33	0.404	N/A

Table G-47: Branch currents and trip times for a single-phase fault at Addition SS for the municipal network for Case 2

Substation	Feeder	Voltage Level (kV)	Fault Level Magnitude Contribution (kA)	OCEF relay calculated trip time (s)
Allen	Addition	11.66	1.000	0.120
Allen	Gardens	11.66	1.000	0.485
Gardens	Allen	11.66	1.000	1.131
Gardens	Transformer 2 MV	11.66	1.000	1.805
Gardens	Transformer 2 HV	33	0.232	28.561
Utility Sub	Gardens 2	33	0.232	N/A
Utility Sub	Wind Turbine	33	1.261	N/A
Utility Sub	Incomer 1	33	0.323	N/A
Utility Sub	Incomer 2	33	0.323	N/A

c) **Protection grading results for the Tortoise substation**

The grading for a three-phase fault of 3.989 kA and a single-phase-to-ground fault of 1.163 kA at the Tortoise substation is shown below.

Table G-48: Branch currents and trip times for a three-phase fault at Tortoise SS for the municipal network for Case 2

<i>Substation</i>	<i>Feeder</i>	<i>Voltage Level (kV)</i>	<i>Fault Level Magnitude Contribution (kA)</i>	<i>OCEF relay calculated trip time (s)</i>
Delilah	Tortoise	11.66	3.989	0.120
Delilah	Transformer 2 MV	11.66	3.992	0.856
Delilah	Transformer 2 HV	33	1.411	0.936
Utility Sub	Delilah 2	33	1.411	1.832
Utility Sub	Wind Turbine	33	1.290	N/A
Utility Sub	Incomer 1	33	0.361	N/A
Utility Sub	Incomer 2	33	0.361	N/A

Table G-49: Branch currents and trip times for a single-phase fault at Tortoise SS for the municipal network for Case 2

<i>Substation</i>	<i>Feeder</i>	<i>Voltage Level (kV)</i>	<i>Fault Level Magnitude Contribution (kA)</i>	<i>OCEF relay calculated trip time (s)</i>
Delilah	Tortoise	11.66	1.163	0.120
Delilah	Transformer 2 MV	11.66	1.163	1.289
Delilah	Transformer 2 HV	33	0.246	N/A
Utility Sub	Delilah 2	33	0.246	N/A
Utility Sub	Wind Turbine	33	1.261	N/A
Utility Sub	Incomer 1	33	0.323	N/A
Utility Sub	Incomer 2	33	0.323	N/A

d) **Protection grading results for the Steve LHS substation**

The grading for a three-phase fault of 9.433 kA and a single-phase-to-ground fault of 1.167 kA at the Steve LHS substation is shown below.

Table G-50: Branch currents and trip times for a three-phase fault at Steve LHS SS for the municipal network for Case 2

<i>Substation</i>	<i>Feeder</i>	<i>Voltage Level (kV)</i>	<i>Fault Level Magnitude Contribution (kA)</i>	<i>OCEF relay calculated trip time (s)</i>
Lightning LHS	Steve LHS	11.66	9.433	0.340
Sunset Vista	Lightning LHS	11.66	9.438	0.635
Sunset Vista	Transformer A MV	11.66	4.807	1.341
Sunset Vista	Transformer B MV	11.66	4.806	1.341
Sunset Vista	Transformer A HV	33	1.699	1.754
Sunset Vista	Transformer B HV	33	1.698	1.754
Utility Sub	Sunset Vista A	33	1.698	1.753
Utility Sub	Sunset Vista B	33	1.698	1.754
Utility Sub	Wind Turbine	33	1.328	N/A
Utility Sub	Incomer 1	33	3.447	N/A
Utility Sub	Incomer 2	33	3.447	N/A

Table G-51: Branch currents and trip times for a single-phase fault at Steve LHS SS for the municipal network for Case 2

<i>Substation</i>	<i>Feeder</i>	<i>Voltage Level (kV)</i>	<i>Fault Level Magnitude Contribution (kA)</i>	<i>OCEF relay calculated trip time (s)</i>
Lightning LHS	Steve LHS	11.66	1.167	0.814
Sunset Vista	Lightning LHS	11.66	1.167	1.203
Sunset Vista	Transformer A MV	11.66	0.584	3.459
Sunset Vista	Transformer B MV	11.66	0.584	3.459
Sunset Vista	Transformer A HV	33	0.231	N/A
Sunset Vista	Transformer B HV	33	0.231	N/A
Utility Sub	Sunset Vista A	33	0.231	N/A
Utility Sub	Sunset Vista B	33	0.231	N/A
Utility Sub	Wind Turbine	33	1.261	N/A
Utility Sub	Incomer 1	33	0.328	N/A
Utility Sub	Incomer 2	33	0.328	N/A

e) Protection grading results for the Mine substation

The grading for a three-phase fault of 3.580 kA and a single-phase-to-ground fault of 0.762 kA at the Mine substation is shown below.

Table G-52: Branch currents and trip times for a three-phase fault at Mine SS for the municipal network for Case 2

<i>Substation</i>	<i>Feeder</i>	<i>Voltage Level (kV)</i>	<i>Fault Level Magnitude Contribution (kA)</i>	<i>OCEF relay calculated trip time (s)</i>
Recycling	Mine	11.66	3.580	0.113
Sunset Vista	Recycling	11.66	3.580	0.566
Sunset Vista	Transformer A MV	11.66	2.053	3.710
Sunset Vista	Transformer B MV	11.66	2.053	3.711
Sunset Vista	Transformer A HV	33	0.725	6.294
Sunset Vista	Transformer B HV	33	0.725	6.296
Utility Sub	Sunset Vista A	33	0.725	6.289
Utility Sub	Sunset Vista B	33	0.725	6.291
Utility Sub	Wind Turbine	33	1.278	N/A
Utility Sub	Incomer 1	33	0.344	N/A
Utility Sub	Incomer 2	33	0.344	N/A

Table G-53: Branch currents and trip times for a single-phase fault at Mine SS for the municipal network for Case 2

<i>Substation</i>	<i>Feeder</i>	<i>Voltage Level (kV)</i>	<i>Fault Level Magnitude Contribution (kA)</i>	<i>OCEF relay calculated trip time (s)</i>
Recycling	Mine	11.66	0.762	0.120
Sunset Vista	Recycling	11.66	0.762	0.433
Sunset Vista	Transformer A MV	11.66	0.381	29.615
Sunset Vista	Transformer B MV	11.66	0.381	29.615
Sunset Vista	Transformer A HV	33	0.191	N/A
Sunset Vista	Transformer B HV	33	0.191	N/A
Utility Sub	Sunset Vista A	33	0.191	N/A
Utility Sub	Sunset Vista B	33	0.191	N/A
Utility Sub	Wind Turbine	33	1.260	N/A
Utility Sub	Incomer 1	33	0.323	N/A
Utility Sub	Incomer 2	33	0.323	N/A

f) **Protection grading results for the Paste RMU 1 substation**

The grading for a three-phase fault of 2.851 kA and a single-phase-to-ground fault of 0.754 kA at the Paste RMU 1 substation is shown below.

Table G-54: Branch currents and trip times for a three-phase fault at Paste RMU 1 SS for the municipal network for Case 2

<i>Substation</i>	<i>Feeder</i>	<i>Voltage Level (kV)</i>	<i>Fault Level Stage 1 Magnitude Contribution (kA)</i>	<i>OCEF Relay Stage 1 Calculated Trip Time (s)</i>	<i>Fault Level Stage 2 Magnitude Contribution (kA)</i>	<i>OCEF Relay Stage 2 Calculated Trip Time (s)</i>	<i>Overall Trip Time (s)</i>
Winery	Yellow	11.66	0.970	0.256	1.346	0.205	0.248
Winery	Transformer 1 MV	11.66	0.972	4.824	1.348	2.740	2.833
Atlantic	Transformer 1 MV	11.66	2.014	1.786	0	N/A	N/A
Atlantic	Grounds (Yellow/Paste)	11.66	1.980	0.215	0	N/A	0.215
Winery	Transformer 1 HV	33	0.343	5.666	0.476	3.391	2.477
Atlantic	Transformer 1 HV	33	0.712	2.266	0	N/A	N/A
Utility Sub	Atlantic 1	33	0.711	5.790	0	N/A	N/A
Utility Sub	Utility Sub Sw. Yard 1	33	0.171	N/A	0.237	N/A	N/A
Utility Sub	Utility Sub Sw. Yard 2	33	0.172	N/A	0.239	N/A	N/A
Utility Sub	Wind Turbine	33	1.278	N/A	1.267	N/A	N/A
Utility Sub	Incomer 1	33	0.188	N/A	0.155	N/A	N/A
Utility Sub	Incomer 2	33	0.188	N/A	0.155	N/A	N/A

Table G-55: Branch currents and trip times for a single-phase fault at Paste RMU 1 SS for the municipal network for Case 2

<i>Substation</i>	<i>Feeder</i>	<i>Voltage Level (kV)</i>	<i>Fault Level Stage 1 Magnitude Contribution (kA)</i>	<i>OCEF Relay Stage 1 Calculated Trip Time (s)</i>	<i>Fault Level Stage 2 Magnitude Contribution (kA)</i>	<i>OCEF Relay Stage 2 Calculated Trip Time (s)</i>	<i>Overall Trip Time (s)</i>
Winery	Yellow	11.66	0.240	0.249	0.284	0.222	0.248
Winery	Transformer 1 MV	11.66	0.240	5.020	0.284	4.578	4.599
Atlantic	Transformer 1 MV	11.66	0.514	2.971	0	N/A	N/A
Atlantic	Grounds (Yellow/Paste)	11.66	0.514	0.237	0	N/A	0.237
Winery	Transformer 1 HV	33	0.059	N/A	0.059	N/A	N/A
Atlantic	Transformer 1 HV	33	0.124	N/A	0	N/A	N/A
Utility Sub	Atlantic 1	33	0.124	N/A	0	N/A	N/A
Utility Sub	Utility Sub Sw. Yard 1	33	0.029	N/A	0.029	N/A	N/A
Utility Sub	Utility Sub Sw. Yard 2	33	0.030	N/A	0.030	N/A	N/A
Utility Sub	Wind Turbine	33	1.260	N/A	1.260	N/A	N/A
Utility Sub	Incomer 1	33	0.323	N/A	0.323	N/A	N/A
Utility Sub	Incomer 2	33	0.323	N/A	0.323	N/A	N/A

Case 3

a) Protection grading results for the 33 kV Utility substation rear busbar

The three-phase fault current level for the Utility substation rear busbar is 13.376 kA. This results in the Utility incomers each carrying an equal fault current of 5.979 kA with a calculated trip time of 2.071 seconds for this stage. All the installed wind turbine incomers throughout the network pickup and trip in 0.420 seconds.

Table G-56: Branch currents and trip times for a three-phase fault at the Utility substation for the municipal network for Case 3

Substation	Feeder	Voltage Level (kV)	Stage 1 Fault Level Magnitude Contribution (kA)	Stage 1 OCEF relay calculated trip time (s)	Stage 2 Fault Level Magnitude Contribution (kA)	Stage 2 OCEF relay calculated trip time (s)	Overall Trip Time (s)
Various	All Installed Wind Turbines	33/11.66	Various	0.420	0	N/A	0.420
Utility Sub	Incomer 1	33	5.979	2.071	6.500	1.928	1.957
Utility Sub	Incomer 2	33	5.979	2.071	6.500	1.928	1.957

The earth-fault current level is 4.866 kA. This results in the Utility substation incomers sharing the fault current equally at 2.433 kA with a calculated trip time of 0.907 seconds for the first stage. The wind turbines do not contribute any fault current to the earth fault condition at this bus but continues generating normal three-phase power before and after the Utility substation incomers have tripped. Once the wind turbine relays have tripped, the fault current slightly decreases to 4.849 kA with the current being shared equally between the incomers. The calculated trip time remains 0.907 seconds.

b) Protection grading results for the Addition substation

The grading for a three-phase fault of 4.141 kA and a single-phase-to-ground fault of 1.005 kA at the Addition substation is shown below.

Table G-57: Branch currents and trip times for a three-phase fault at Addition SS for the municipal network for Case 3

Substation	Feeder	Voltage Level (kV)	Fault Level Magnitude Contribution (kA)	OCEF relay calculated trip time (s)
Allen	Addition	11.66	4.141	0.120
Allen	Gardens	11.66	4.142	0.527
Gardens	Allen	11.66	4.142	0.731
Gardens	Transformer 2 MV	11.66	4.122	1.097
Gardens	Wind Turbine - RHS LV	11.66	0.033	0.420
Gardens	Transformer 2 HV	33	1.456	1.418
Utility Sub	Gardens 2	33	1.418	1.825
Utility Sub	Incomer 1	33	0.563	N/A
Utility Sub	Incomer 2	33	0.563	N/A

Table G-58: Branch currents and trip times for a single-phase at Addition SS for the municipal network for Case 3

<i>Substation</i>	<i>Feeder</i>	<i>Voltage Level (kV)</i>	<i>Fault Level Magnitude Contribution (kA)</i>	<i>OCEF relay calculated trip time (s)</i>
Allen	Addition	11.66	1.005	0.120
Allen	Gardens	11.66	1.005	0.484
Gardens	Allen	11.66	1.005	1.128
Gardens	Transformer 2 MV	11.66	1.005	1.800
Gardens	Wind Turbine - RHS LV	11.66	0.027	N/A
Gardens	Transformer 2 HV	33	0.227	35.942
Utility Sub	Gardens 2	33	0.201	N/A
Utility Sub	Incomer 1	33	0.237	N/A
Utility Sub	Incomer 2	33	0.237	N/A

c) Protection grading results for the Tortoise substation

The grading for a three-phase fault of 4.064 kA and a single-phase-to-ground fault of 1.183 kA at the Tortoise substation is shown below.

Table G-59: Branch currents and trip times for a three-phase fault at Tortoise SS for the municipal network for Case 3

<i>Substation</i>	<i>Feeder</i>	<i>Voltage Level (kV)</i>	<i>Fault Level Magnitude Contribution (kA)</i>	<i>OCEF relay calculated trip time (s)</i>
Delilah	Tortoise	11.66	4.064	0.120
Delilah	Transformer 2 MV	11.66	3.967	0.859
Delilah	Wind Turbine - RHS LV	11.66	0.144	0.420
Delilah	Transformer 2 HV	33	1.402	0.940
Utility Sub	Delilah 2	33	1.354	1.878
Utility Sub	Incomer 1	33	0.520	N/A
Utility Sub	Incomer 2	33	0.520	N/A

Table G-60: Branch currents and trip times for a single-phase fault at Tortoise SS for the municipal network for Case 3

<i>Substation</i>	<i>Feeder</i>	<i>Voltage Level (kV)</i>	<i>Fault Level Magnitude Contribution (kA)</i>	<i>OCEF relay calculated trip time (s)</i>
Delilah	Tortoise	11.66	1.183	0.120
Delilah	Transformer 2 MV	11.66	1.183	1.277
Delilah	Wind Turbine - RHS LV	11.66	0.120	N/A
Delilah	Transformer 2 HV	33	0.226	N/A
Utility Sub	Delilah 2	33	0.207	N/A
Utility Sub	Incomer 1	33	0.238	N/A
Utility Sub	Incomer 2	33	0.238	N/A

d) **Protection grading results for the Steve LHS substation**

The grading for a three-phase fault of 9.524 kA and a single-phase-to-ground fault of 1.177 kA at the Steve LHS substation is shown below.

Table G-61: Branch currents and trip times for a three-phase fault at Steve LHS SS for the municipal network for Case 3

<i>Substation</i>	<i>Feeder</i>	<i>Voltage Level (kV)</i>	<i>Fault Level Magnitude Contribution (kA)</i>	<i>OCEF relay calculated trip time (s)</i>
Lightning LHS	Steve LHS	11.66	9.524	0.340
Sunset Vista	Lightning LHS	11.66	9.529	0.635
Sunset Vista	Transformer A MV	11.66	4.755	1.352
Sunset Vista	Transformer B MV	11.66	4.760	1.351
Sunset Vista	Wind Turbine - LHS LV	11.66	0.221	0.420
Sunset Vista	Transformer A HV	33	1.680	1.770
Sunset Vista	Transformer B HV	33	1.682	1.769
Utility Sub	Sunset Vista A	33	1.668	1.781
Utility Sub	Sunset Vista B	33	1.649	1.799
Utility Sub	Incomer 1	33	1.347	N/A
Utility Sub	Incomer 2	33	1.347	N/A

Table G-62: Branch currents and trip times for a single-phase fault at Steve LHS SS for the municipal network for Case 3

<i>Substation</i>	<i>Feeder</i>	<i>Voltage Level (kV)</i>	<i>Fault Level Magnitude Contribution (kA)</i>	<i>OCEF relay calculated trip time (s)</i>
Lightning LHS	Steve LHS	11.66	1.177	0.809
Sunset Vista	Lightning LHS	11.66	1.177	1.198
Sunset Vista	Transformer A MV	11.66	0.589	3.399
Sunset Vista	Transformer B MV	11.66	0.589	3.399
Sunset Vista	Wind Turbine - LHS LV	11.66	0.196	N/A
Sunset Vista	Transformer A HV	33	0.196	N/A
Sunset Vista	Transformer B HV	33	0.198	N/A
Utility Sub	Sunset Vista A	33	0.177	N/A
Utility Sub	Sunset Vista B	33	0.147	N/A
Utility Sub	Incomer 1	33	0.238	N/A
Utility Sub	Incomer 2	33	0.238	N/A

e) **Protection grading results for the Mine substation**

The grading for a three-phase fault of 3.615 kA and a single-phase-to-ground fault of 0.768 kA at the Mine substation is shown below.

Table G-63: Branch currents and trip times for a three-phase fault at Mine SS for the municipal network for Case 3

<i>Substation</i>	<i>Feeder</i>	<i>Voltage Level (kV)</i>	<i>Fault Level Magnitude Contribution (kA)</i>	<i>OCEF relay calculated trip time (s)</i>
Recycling	Mine	11.66	3.615	0.113
Sunset Vista	Recycling	11.66	3.615	0.564
Sunset Vista	Transformer A MV	11.66	1.967	4.069
Sunset Vista	Transformer B MV	11.66	1.972	4.044
Utility Sub	Wind Turbine - LHS LV	11.66	0.199	N/A
Sunset Vista	Transformer A HV	33	0.695	7.230
Sunset Vista	Transformer B HV	33	0.697	7.161
Utility Sub	Sunset Vista A	33	0.675	8.043
Utility Sub	Sunset Vista B	33	0.640	10.084
Utility Sub	Incomer 1	33	0.343	N/A
Utility Sub	Incomer 2	33	0.343	N/A

Table G-64: Branch currents and trip times for a single-phase fault at Mine SS for the municipal network for Case 3

Substation	Feeder	Voltage Level (kV)	Fault Level Magnitude Contribution (kA)	OCEF relay calculated trip time (s)
Recycling	Mine	11.66	0.768	0.120
Sunset Vista	Recycling	11.66	0.768	0.432
Sunset Vista	Transformer A MV	11.66	0.384	26.014
Sunset Vista	Transformer B MV	11.66	0.384	26.014
Utility Sub	Wind Turbine - LHS LV	33	0.196	N/A
Sunset Vista	Transformer A HV	33	0.156	N/A
Sunset Vista	Transformer B HV	33	0.158	N/A
Utility Sub	Sunset Vista A	33	0.137	N/A
Utility Sub	Sunset Vista B	33	0.106	N/A
Utility Sub	Incomer 1	33	0.237	N/A
Utility Sub	Incomer 2	33	0.237	N/A

f) Protection grading results for the Paste RMU 1 substation

The grading for a three-phase fault of 2.904 kA and a single-phase-to-ground fault of 0.761 kA at the Paste RMU 1 substation is shown below.

Table G-65: Branch currents and trip times for a three-phase fault at Paste RMU 1 SS for the municipal network for Case 3

Substation	Feeder	Voltage Level (kV)	Fault Level Stage 1 Magnitude Contribution (kA)	OCEF Relay Stage 1 Calculated Trip Time (s)	Fault Level Stage 2 Magnitude Contribution (kA)	OCEF Relay Stage 2 Calculated Trip Time (s)	Overall Trip Time (s)
Winery	Yellow	11.66	0.969	0.256	1.362	0.204	0.247
Winery	Transformer 1 MV	11.66	0.910	5.697	1.301	2.876	2.981
Atlantic	Transformer 1 MV	11.66	1.912	1.870	0	N/A	N/A
Atlantic	Grounds (Yellow/Paste)	11.66	2.016	0.213	0	N/A	0.213
Atlantic	Wind Turbine - LHS LV	11.66	0.181	0.420	0	N/A	N/A
Winery	Transformer 1 HV	33	0.321	6.552	0.460	3.547	3.645
Atlantic	Transformer 1 HV	33	0.676	2.368	0	N/A	N/A
Utility Sub	Atlantic 1	33	0.650	8.127	0	N/A	N/A
Utility Sub	Utility Sub Sw. Yard 1	33	0.119	N/A	0.188	N/A	N/A
Utility Sub	Utility Sub Sw. Yard 2	33	0.120	N/A	0.190	N/A	N/A
Utility Sub	Incomer 1	33	0.240	N/A	0.019	N/A	N/A
Utility Sub	Incomer 2	33	0.240	N/A	0.019	N/A	N/A

Table G-66: Branch currents and trip times for a single-phase fault at Paste RMU 1 SS for the municipal network for Case 3

Substation	Feeder	Voltage Level (kV)	Fault Level Stage 1 Magnitude Contribution (kA)	OCEF Relay Stage 1 Calculated Trip Time (s)	Fault Level Stage 2 Magnitude Contribution (kA)	OCEF Relay Stage 2 Calculated Trip Time (s)	Overall Trip Time (s)
Winery	Yellow	11.66	0.242	0.247	0.287	0.220	0.246
Winery	Transformer 1 MV	11.66	0.242	5.020	0.287	4.467	4.493
Atlantic	Transformer 1 MV	11.66	0.519	2.946	0	N/A	N/A
Atlantic	Grounds (Yellow/Paste)	11.66	0.519	0.236	0	N/A	0.236
Atlantic	Wind Turbine - LHS LV	11.66	0.153	N/A	0	N/A	N/A
Winery	Transformer 1 HV	33	0.047	N/A	0.052	N/A	N/A
Atlantic	Transformer 1 HV	33	0.085	N/A	0	N/A	N/A
Utility Sub	Atlantic 1	33	0.073	N/A	0	N/A	N/A
Utility Sub	Utility Sub Sw. Yard 1	33	0.050	N/A	0.052	N/A	N/A
Utility Sub	Utility Sub Sw. Yard 2	33	0.050	N/A	0.052	N/A	N/A
Utility Sub	Incomer 1	33	0.238	N/A	0.236	N/A	N/A
Utility Sub	Incomer 2	33	0.238	N/A	0.236	N/A	N/A

Case 4

a) Protection grading results for the 33 kV Utility substation rear busbar

The three-phase fault current level for the Utility substation rear busbar is 13.324 kA. This results in the Utility Sub incomers each carrying an equal fault current of 6.206 kA with a calculated trip time of 2.005 seconds for this stage. All the installed wind turbine incomers throughout the network pickup and trip in 0.420 seconds.

Table G-67: Branch currents and trip times for a three-phase fault at the Utility substation for the municipal network for Case 4

Substation	Feeder	Voltage Level (kV)	Stage 1 Fault Level Magnitude Contribution (kA)	Stage 1 OCEF relay calculated trip time (s)	Stage 2 Fault Level Magnitude Contribution (kA)	Stage 2 OCEF relay calculated trip time (s)	Overall Trip Time (s)
Various	All Installed Wind Turbines	33/11.66	Various	0.420	0	N/A	0.420
Utility Sub	Incomer 1	33	6.206	2.005	6.500	1.928	1.944
Utility Sub	Incomer 2	33	6.206	2.005	6.500	1.928	1.944

The earth-fault current level is 4.863 kA. This results in the Utility substation incomers sharing the fault current equally at 2.343 kA with a calculated trip time of 0.907 seconds for the first stage. The wind turbines do not contribute any fault current to the earth fault condition. Thus the total trip time for the fault is defined completely by the Utility substation incomers' 0.907 second trip time.

b) Protection grading results for the Addition substation

The grading for a three-phase fault of 4.136 kA and a single-phase-to-ground fault of 1.004 kA at the Addition substation is shown below.

Table G-68: Branch currents and trip times for a three-phase fault at Addition SS for the municipal network for Case 4

Substation	Feeder	Voltage Level (kV)	Fault Level Magnitude Contribution (kA)	OCEF relay calculated trip time (s)
Allen	Addition	11.66	4.136	0.120
Allen	Gardens	11.66	4.136	0.527
Gardens	Allen	11.66	4.136	0.732
Gardens	Transformer 2 MV	11.66	4.114	1.098
Gardens	Wind Turbine - RHS LV	11.66	0.037	0.420
Gardens	Transformer 2 HV	33	1.454	1.419
Utility Sub	Gardens 2	33	1.452	1.800
Utility Sub	Incomer 1	33	0.702	N/A
Utility Sub	Incomer 2	33	0.702	N/A

Table G-69: Branch currents and trip times for a single-phase fault at Addition SS for the municipal network for Case 4

<i>Substation</i>	<i>Feeder</i>	<i>Voltage Level (kV)</i>	<i>Fault Level Magnitude Contribution (kA)</i>	<i>OCEF relay calculated trip time (s)</i>
Allen	Addition	11.66	1.004	0.120
Allen	Gardens	11.66	1.004	0.484
Gardens	Allen	11.66	1.004	1.129
Gardens	Transformer 2 MV	11.66	1.004	1.801
Gardens	Wind Turbine - RHS LV	11.66	0.031	N/A
Gardens	Transformer 2 HV	33	0.225	40.777
Utility Sub	Gardens 2	33	0.216	N/A
Utility Sub	Incomer 1	33	0.100	N/A
Utility Sub	Incomer 2	33	0.100	N/A

c) Protection grading results for the Tortoise substation

The grading for a three-phase fault of 3.986 kA and a single-phase-to-ground fault of 1.163 kA at the Tortoise substation is shown below.

Table G-70: Branch currents and trip times for a three-phase fault at Tortoise SS for the municipal network for Case 4

<i>Substation</i>	<i>Feeder</i>	<i>Voltage Level (kV)</i>	<i>Fault Level Magnitude Contribution (kA)</i>	<i>OCEF relay calculated trip time (s)</i>
Delilah	Tortoise	11.66	3.986	0.120
Delilah	Transformer 2 MV	11.66	3.989	0.856
Delilah	Transformer 2 HV	33	1.410	0.936
Utility Sub	Delilah 2	33	1.410	1.832
Utility Sub	Incomer 1	33	0.675	N/A
Utility Sub	Incomer 2	33	0.675	N/A

Table G-71: Branch currents and trip times for a single-phase fault at Tortoise SS for the municipal network for Case 4

<i>Substation</i>	<i>Feeder</i>	<i>Voltage Level (kV)</i>	<i>Fault Level Magnitude Contribution (kA)</i>	<i>OCEF relay calculated trip time (s)</i>
Delilah	Tortoise	11.66	1.163	0.120
Delilah	Transformer 2 MV	11.66	1.163	1.289
Delilah	Transformer 2 HV	33	0.246	N/A
Utility Sub	Delilah 2	33	0.246	N/A
Utility Sub	Incomer 1	33	0.115	N/A
Utility Sub	Incomer 2	33	0.115	N/A

d) **Protection grading results for the Steve LHS substation**

The grading for a three-phase fault of 9.505 kA and a single-phase-to-ground fault of 1.173 kA at the Steve LHS substation is shown below.

Table G-72: Branch currents and trip times for a three-phase fault at Steve LHS SS for the municipal network for Case 4

<i>Substation</i>	<i>Feeder</i>	<i>Voltage Level (kV)</i>	<i>Fault Level Magnitude Contribution (kA)</i>	<i>OCEF relay calculated trip time (s)</i>
Lightning LHS	Steve LHS	11.66	9.505	0.340
Sunset Vista	Lightning LHS	11.66	9.510	0.635
Sunset Vista	Transformer A MV	11.66	4.753	1.353
Sunset Vista	Transformer B MV	11.66	4.753	1.353
Sunset Vista	Wind Turbine - LHS LV	11.66	0.226	0.420
Sunset Vista	Transformer A HV	33	1.679	1.771
Sunset Vista	Transformer B HV	33	1.679	1.771
Utility Sub	Sunset Vista A	33	1.670	1.779
Utility Sub	Sunset Vista B	33	1.661	1.787
Utility Sub	Incomer 1	33	1.544	N/A
Utility Sub	Incomer 2	33	1.544	N/A

Table G-73: Branch currents and trip times for a single-phase fault at Steve LHS SS for the municipal network for Case 4

<i>Substation</i>	<i>Feeder</i>	<i>Voltage Level (kV)</i>	<i>Fault Level Magnitude Contribution (kA)</i>	<i>OCEF relay calculated trip time (s)</i>
Lightning LHS	Steve LHS	11.66	1.173	0.810
Sunset Vista	Lightning LHS	11.66	1.173	1.201
Sunset Vista	Transformer A MV	11.66	0.586	3.428
Sunset Vista	Transformer B MV	11.66	0.586	3.428
Sunset Vista	Wind Turbine - LHS LV	11.66	0.195	N/A
Sunset Vista	Transformer A HV	33	0.198	N/A
Sunset Vista	Transformer B HV	33	0.198	N/A
Utility Sub	Sunset Vista A	33	0.183	N/A
Utility Sub	Sunset Vista B	33	0.179	N/A
Utility Sub	Incomer 1	33	0.112	N/A
Utility Sub	Incomer 2	33	0.112	N/A

e) **Protection grading results for the Mine substation**

The grading for a three-phase fault of 3.605 kA and a single-phase-to-ground fault of 0.765 kA at the Mine substation is shown below.

Table G-74: Branch currents and trip times for a three-phase fault at Mine SS for the municipal network for Case 4

<i>Substation</i>	<i>Feeder</i>	<i>Voltage Level (kV)</i>	<i>Fault Level Magnitude Contribution (kA)</i>	<i>OCEF relay calculated trip time (s)</i>
Recycling	Mine	11.66	3.605	0.113
Sunset Vista	Recycling	11.66	3.605	0.564
Sunset Vista	Transformer A MV	11.66	1.962	4.092
Sunset Vista	Transformer B MV	11.66	1.961	4.096
Utility Sub	Wind Turbine - LHS LV	11.66	0.211	0.420
Sunset Vista	Transformer A HV	33	0.693	7.293
Sunset Vista	Transformer B HV	33	0.693	7.305
Utility Sub	Sunset Vista A	33	0.677	7.943
Utility Sub	Sunset Vista B	33	0.673	8.101
Utility Sub	Incomer 1	33	0.568	N/A
Utility Sub	Incomer 2	33	0.568	N/A

Table G-75: Branch currents and trip times for a single-phase fault at Mine SS for the municipal network for Case 4

Substation	Feeder	Voltage Level (kV)	Fault Level Magnitude Contribution (kA)	OCEF relay calculated trip time (s)
Recycling	Mine	11.66	0.765	0.120
Sunset Vista	Recycling	11.66	0.765	0.432
Sunset Vista	Transformer A MV	11.66	0.382	27.776
Sunset Vista	Transformer B MV	11.66	0.382	27.776
Utility Sub	Wind Turbine - LHS LV	33	0.194	N/A
Sunset Vista	Transformer A HV	33	0.158	N/A
Sunset Vista	Transformer B HV	33	0.158	N/A
Utility Sub	Sunset Vista A	33	0.143	N/A
Utility Sub	Sunset Vista B	33	0.139	N/A
Utility Sub	Incomer 1	33	0.076	N/A
Utility Sub	Incomer 2	33	0.076	N/A

f) Protection grading results for the Paste RMU 1 substation

The grading for a three-phase fault of 2.863 kA and a single-phase-to-ground fault of 0.755 kA at the Paste RMU 1 substation is shown below.

Table G-76: Currents and trip times for a three-phase fault at Paste RMU 1 SS for the municipal network for Case 4

Substation	Feeder	Voltage Level (kV)	Fault Level Stage 1 Magnitude Contribution (kA)	OCEF Relay Stage 1 Calculated Trip Time (s)	Fault Level Stage 2 Magnitude Contribution (kA)	OCEF Relay Stage 2 Calculated Trip Time (s)	Overall Trip Time (s)
Winery	Yellow	11.66	0.968	0.257	1.348	0.205	0.249
Winery	Transformer 1 MV	11.66	0.970	4.849	1.350	2.735	2.829
Atlantic	Transformer 1 MV	11.66	1.998	1.798	0	N/A	N/A
Atlantic	Grounds (Yellow/Paste)	11.66	1.989	0.215	0	N/A	0.215
Atlantic	Wind Turbine - LHS LV	11.66	0.033	0.420	0	N/A	N/A
Winery	Transformer 1 HV	33	0.343	5.693	0.477	3.386	3.473
Atlantic	Transformer 1 HV	33	0.706	2.281	0	N/A	N/A
Utility Sub	Atlantic 1	33	0.700	6.115	0	N/A	N/A
Utility Sub	Utility Sub Sw. Yard 1	33	0.140	N/A	0.209	N/A	N/A
Utility Sub	Utility Sub Sw. Yard 2	33	0.142	N/A	0.212	N/A	N/A
Utility Sub	Incomer 1	33	0.469	N/A	0.218	N/A	N/A
Utility Sub	Incomer 2	33	0.469	N/A	0.218	N/A	N/A

Table G-77: Currents and trip times for a single-phase fault at Paste RMU 1 SS for the municipal network for Case 4

Substation	Feeder	Voltage Level (kV)	Fault Level Stage 1 Magnitude Contribution (kA)	OCEF Relay Stage 1 Calculated Trip Time (s)	Fault Level Stage 2 Magnitude Contribution (kA)	OCEF Relay Stage 2 Calculated Trip Time (s)	Overall Trip Time (s)
Winery	Yellow	11.66	0.240	0.249	0.284	0.221	0.248
Winery	Transformer 1 MV	11.66	0.240	5.020	0.284	4.571	4.592
Atlantic	Transformer 1 MV	11.66	0.515	2.967	0	N/A	N/A
Atlantic	Grounds (Yellow/Paste)	11.66	0.515	0.237	0	N/A	0.237
Atlantic	Wind Turbine - LHS LV	11.66	0.028	N/A	0	N/A	N/A
Winery	Transformer 1 HV	33	0.056	N/A	0.059	N/A	N/A
Atlantic	Transformer 1 HV	33	0.117	N/A	0	N/A	N/A
Utility Sub	Atlantic 1	33	0.108	N/A	0	N/A	N/A
Utility Sub	Utility Sub Sw. Yard 1	33	0.028	N/A	0.030	N/A	N/A
Utility Sub	Utility Sub Sw. Yard 2	33	0.029	N/A	0.030	N/A	N/A
Utility Sub	Incomer 1	33	0.077	N/A	0.042	N/A	N/A
Utility Sub	Incomer 2	33	0.077	N/A	0.042	N/A	N/A

Appendix H: IDMT curve results

IEEE 14-bus network

Case 1

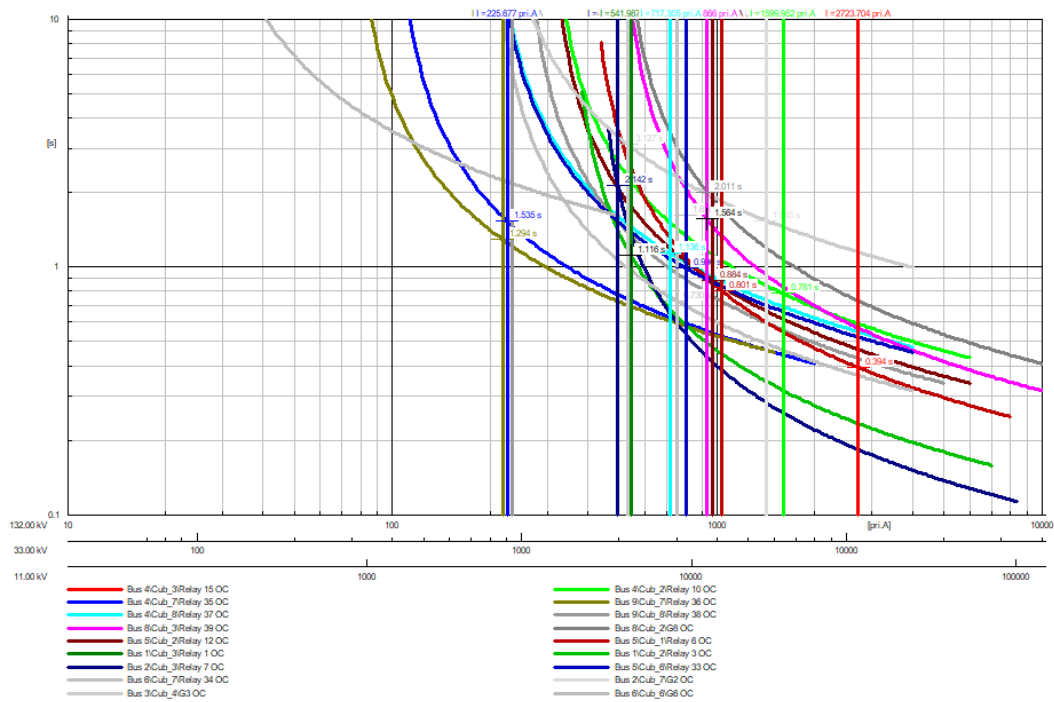


Figure H.1: The OC relay grading for a three-phase fault at Bus 4

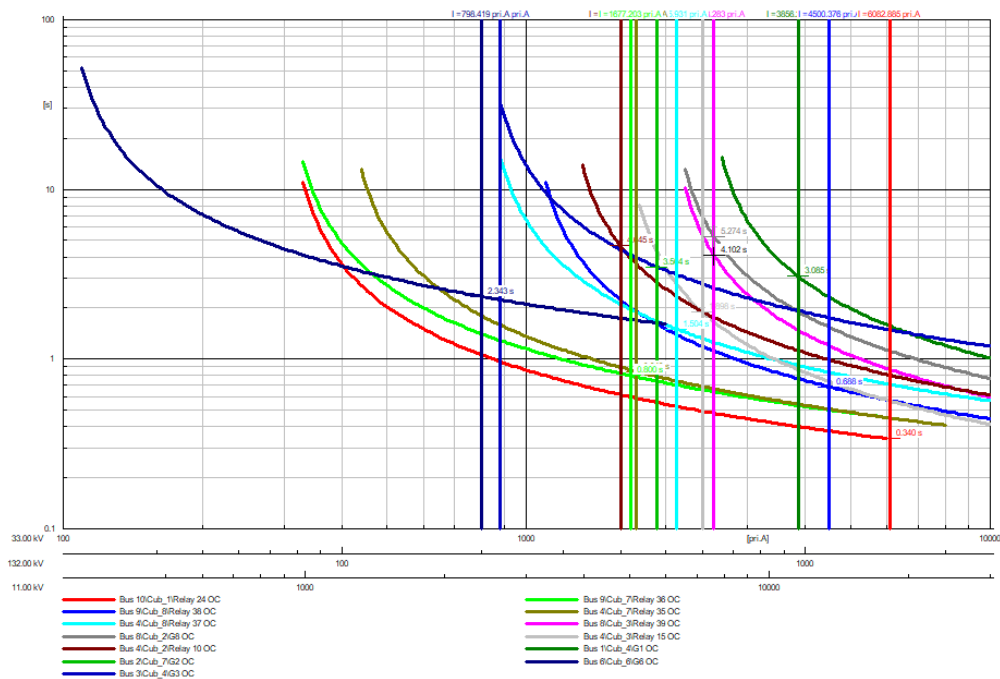


Figure H.2: The OC relay grading for a three-phase fault at Bus 10

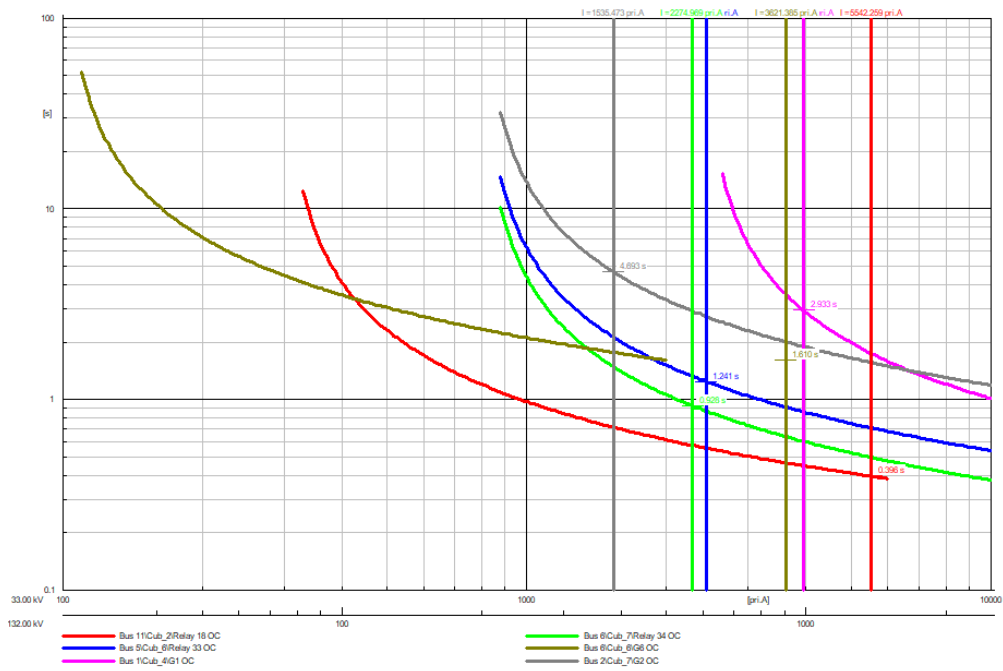


Figure H.3: The OC relay grading for a three-phase fault at Bus 11

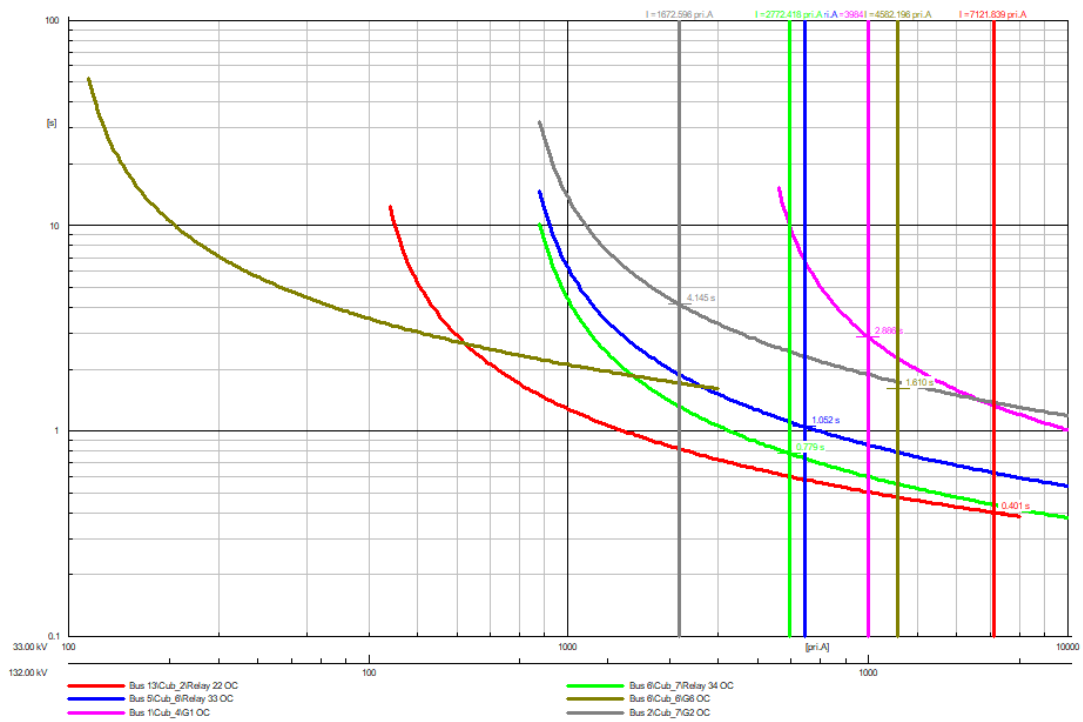


Figure H.4: The OC relay grading for a three-phase fault at Bus 13

Case 2

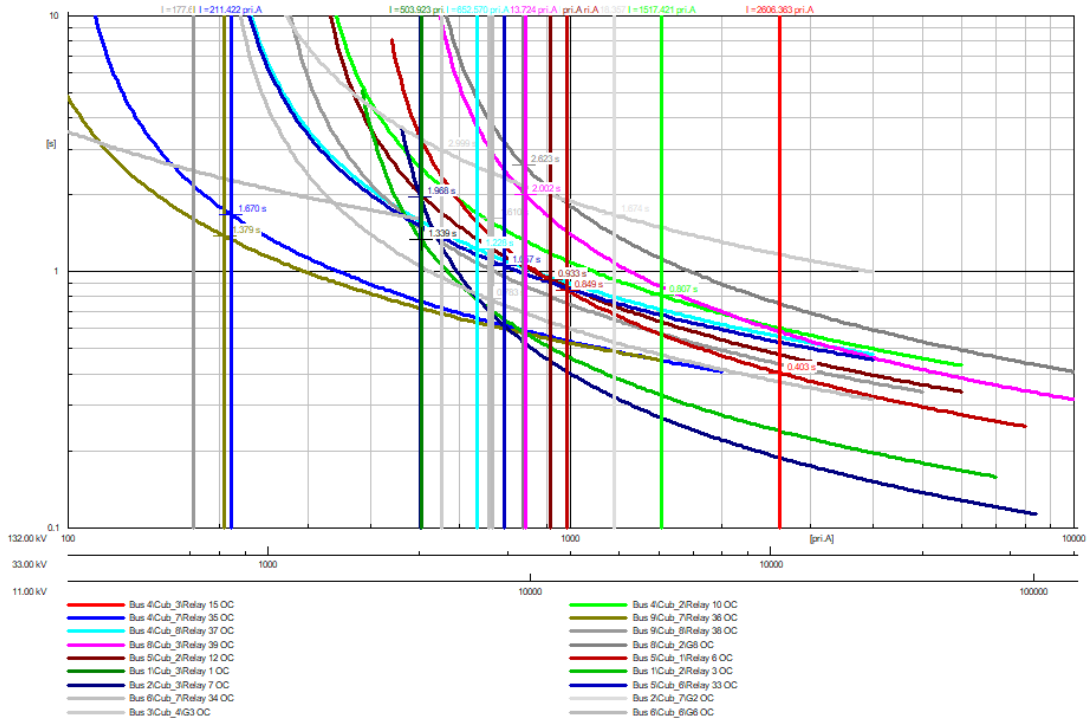


Figure H.5: The OC relay grading for a three-phase fault at Bus 4

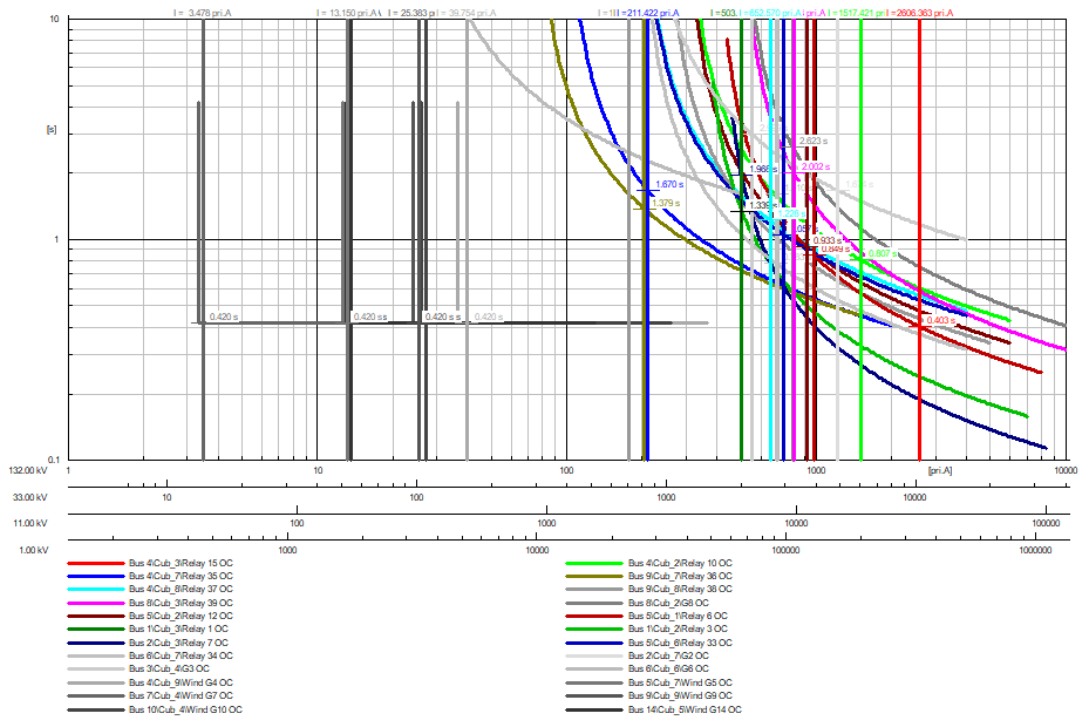


Figure H.6: The OC relay grading for a three-phase fault at Bus 10

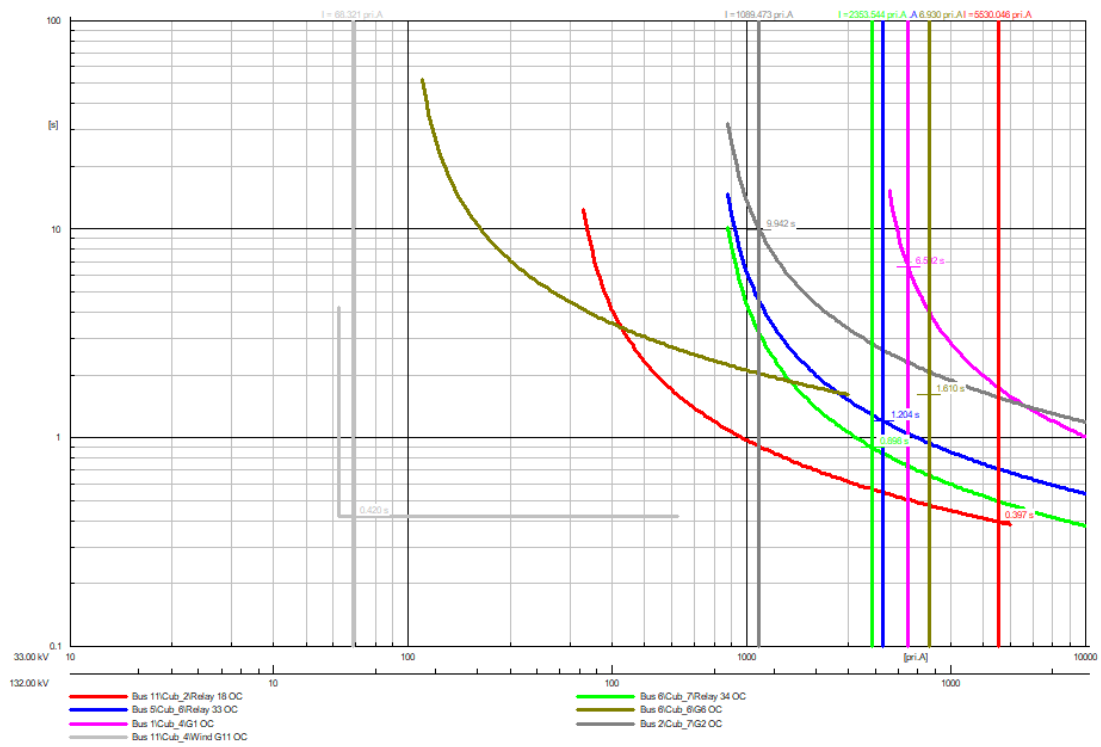


Figure H.7: The OC relay grading for a three-phase fault at Bus 11

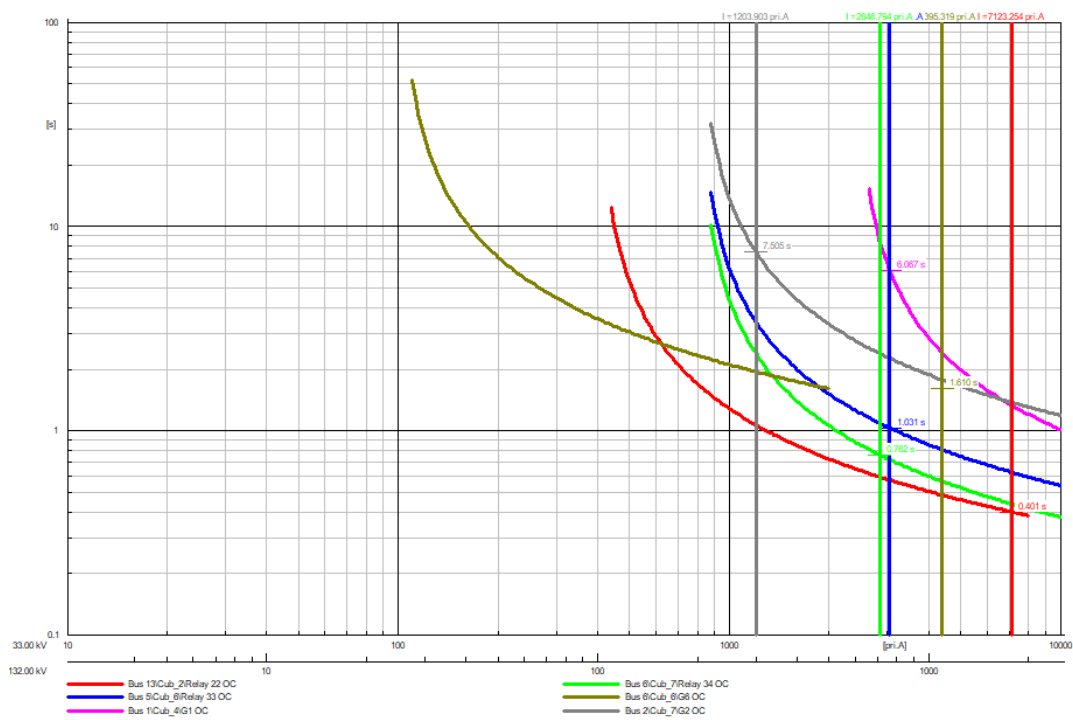


Figure H.8: The OC relay grading for a three-phase fault at Bus 13

Case 3

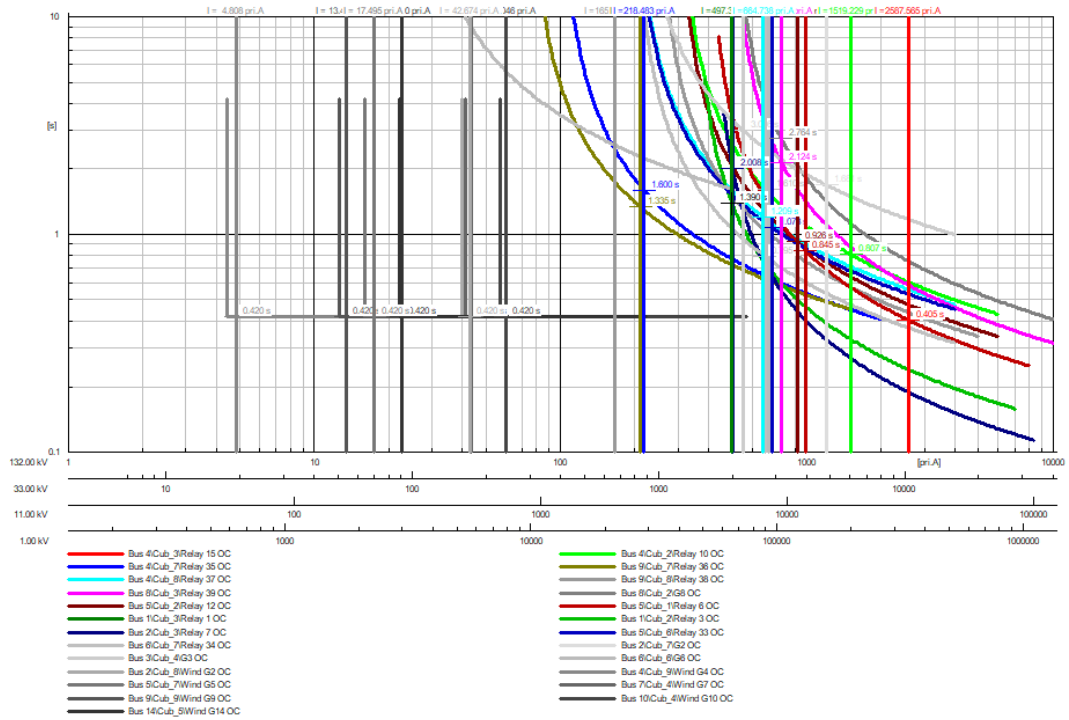


Figure H.9: The OC relay grading for a three-phase fault at Bus 4

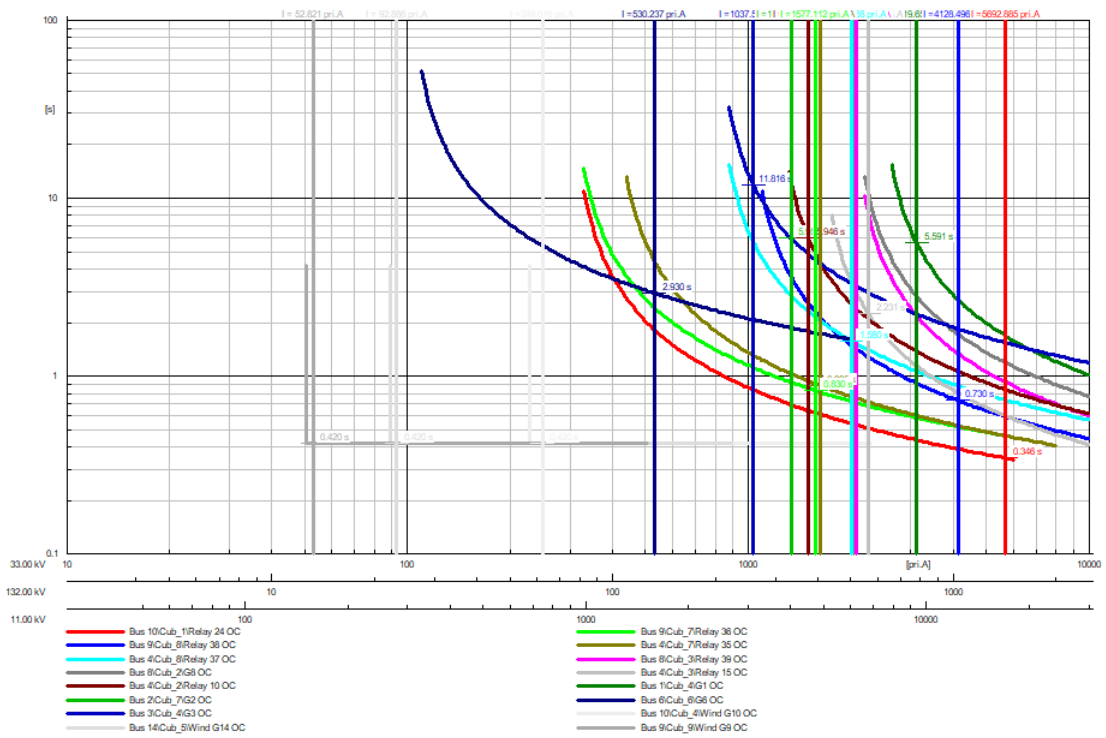


Figure H.10: The OC relay grading for a three-phase fault at Bus 10

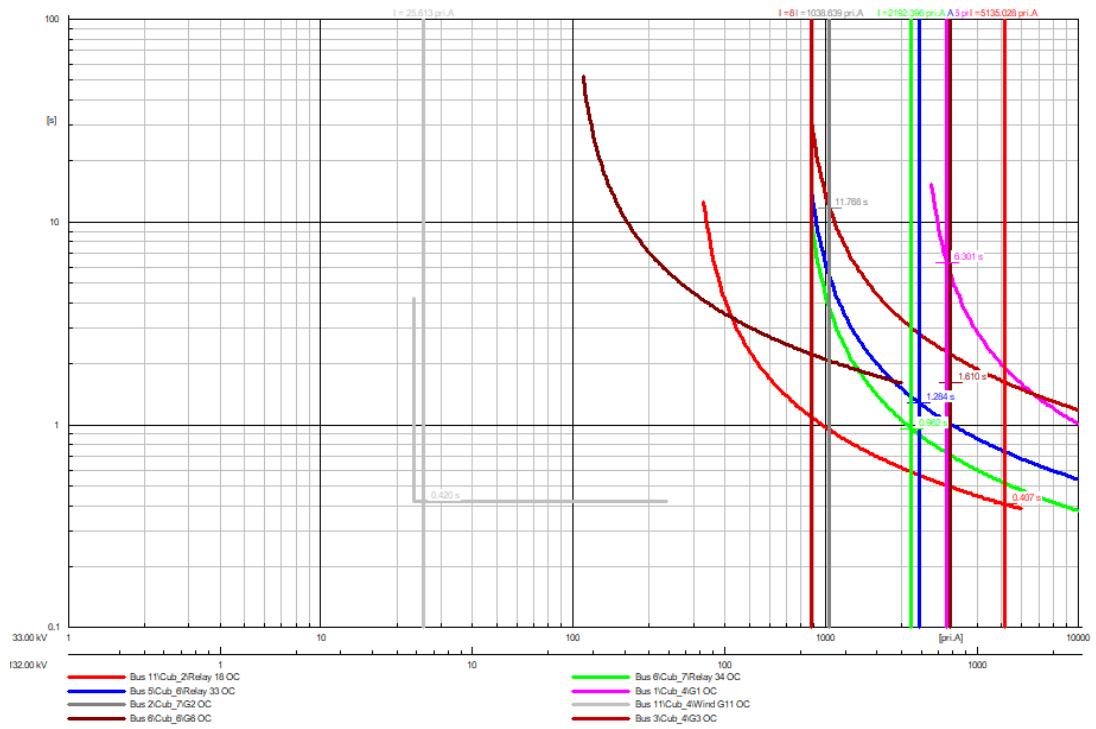


Figure H.11: The OC relay grading for a three-phase fault at Bus 11

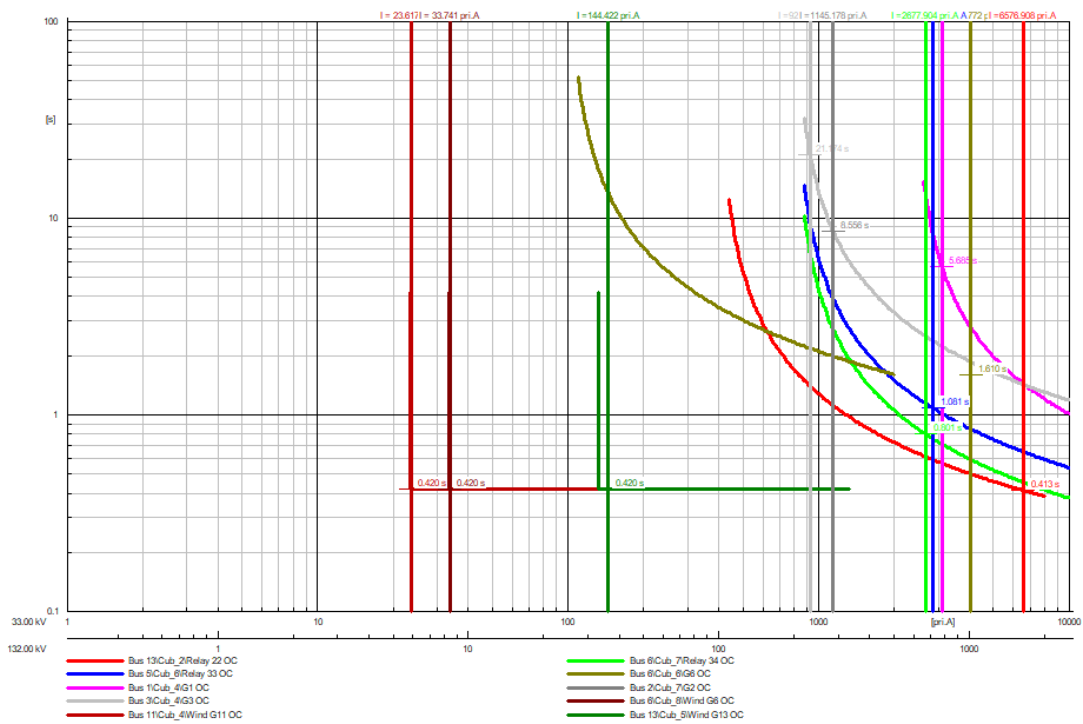


Figure H.12: The OC relay grading for a three-phase fault at Bus 13

Case Study Network

Case 1

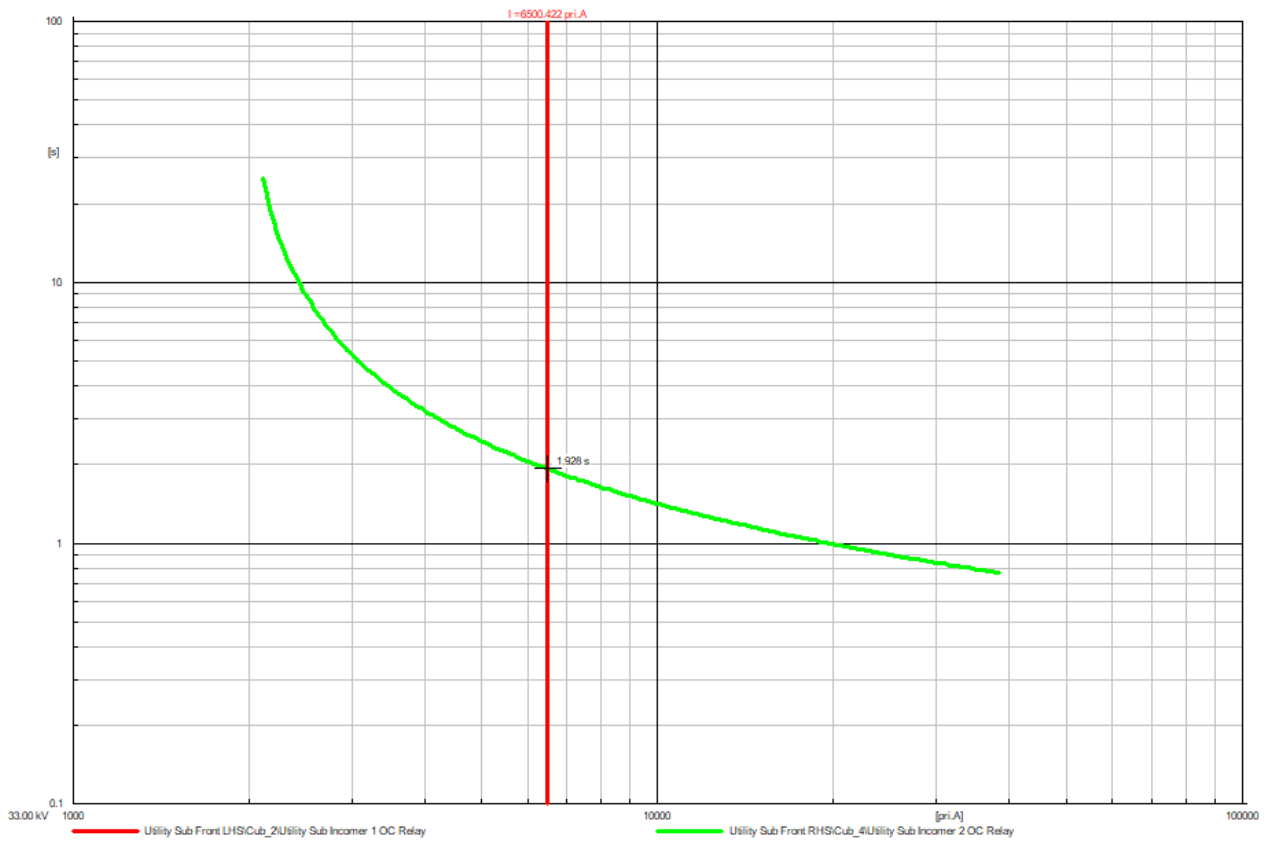


Figure H.13: The OC relay grading for a three-phase fault at the Utility Sub

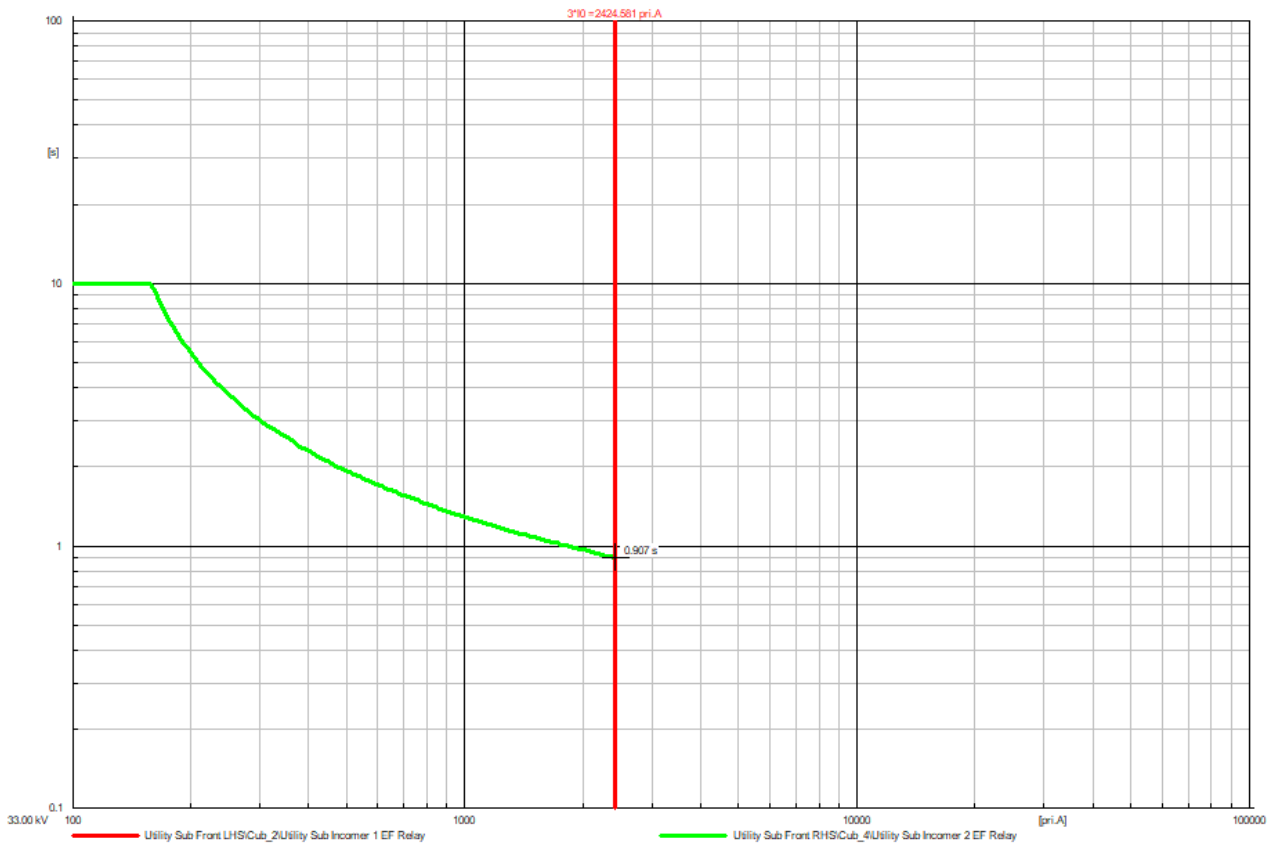


Figure H.14: The EF relay grading for a single-phase fault at the Utility Sub

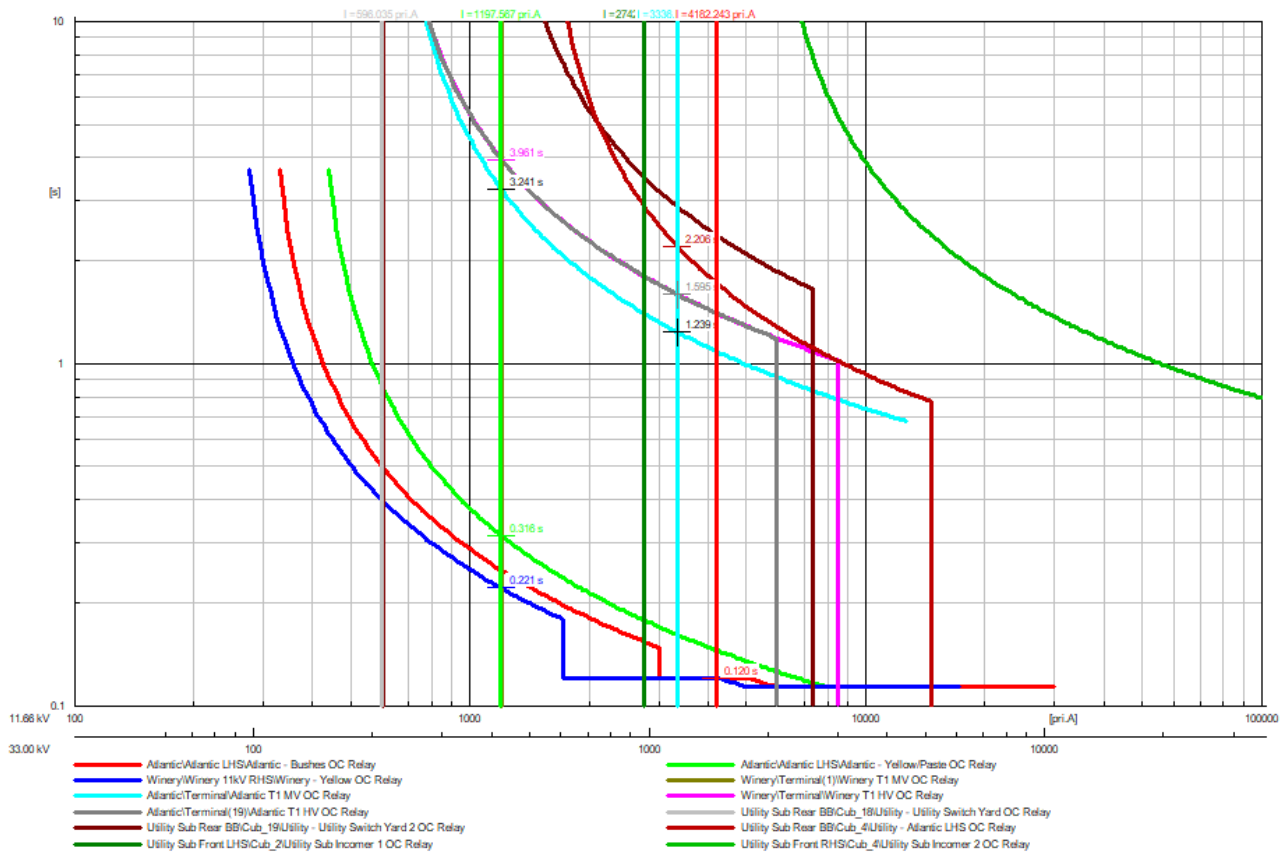


Figure H.15: The OC relay grading for a three-phase fault at Bushes SS

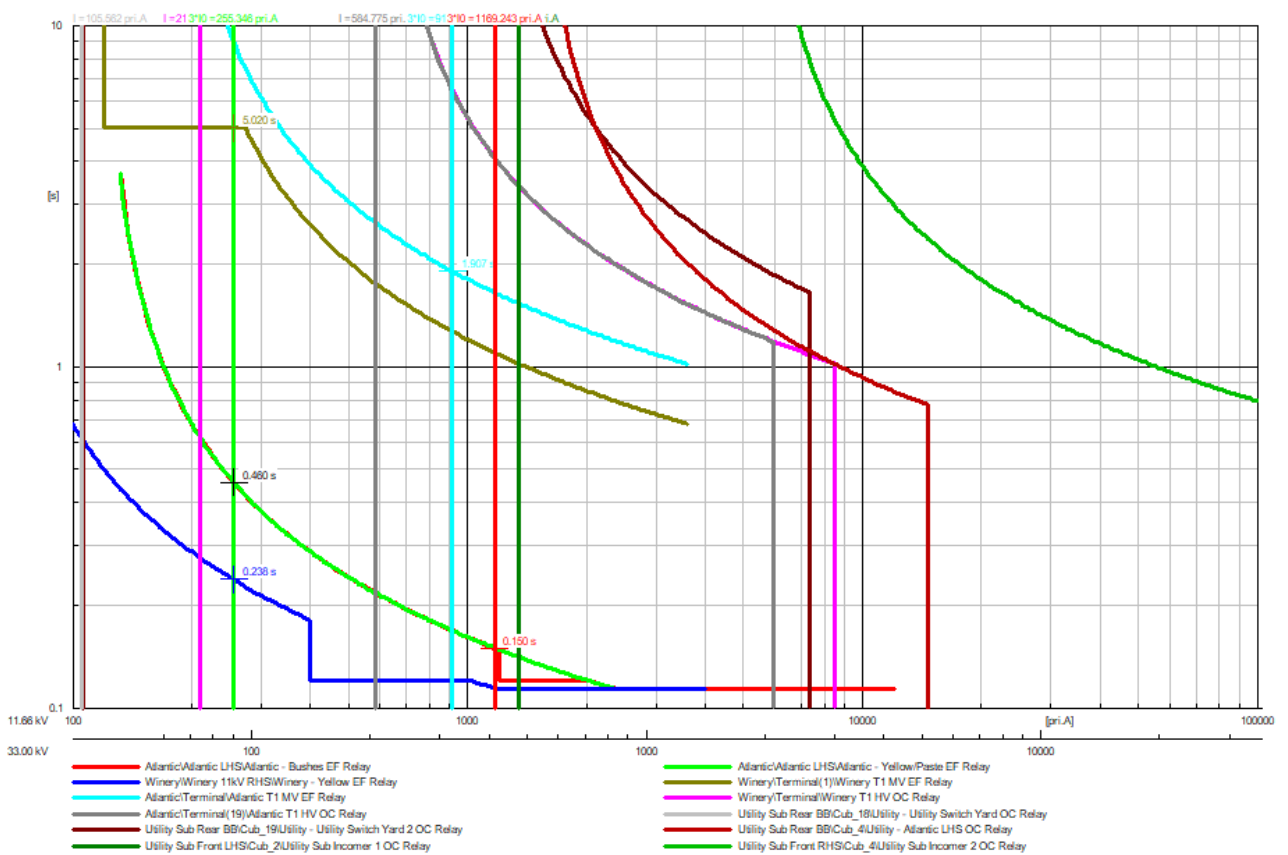


Figure H.16: The EF relay grading for a single-phase fault at Bushes SS

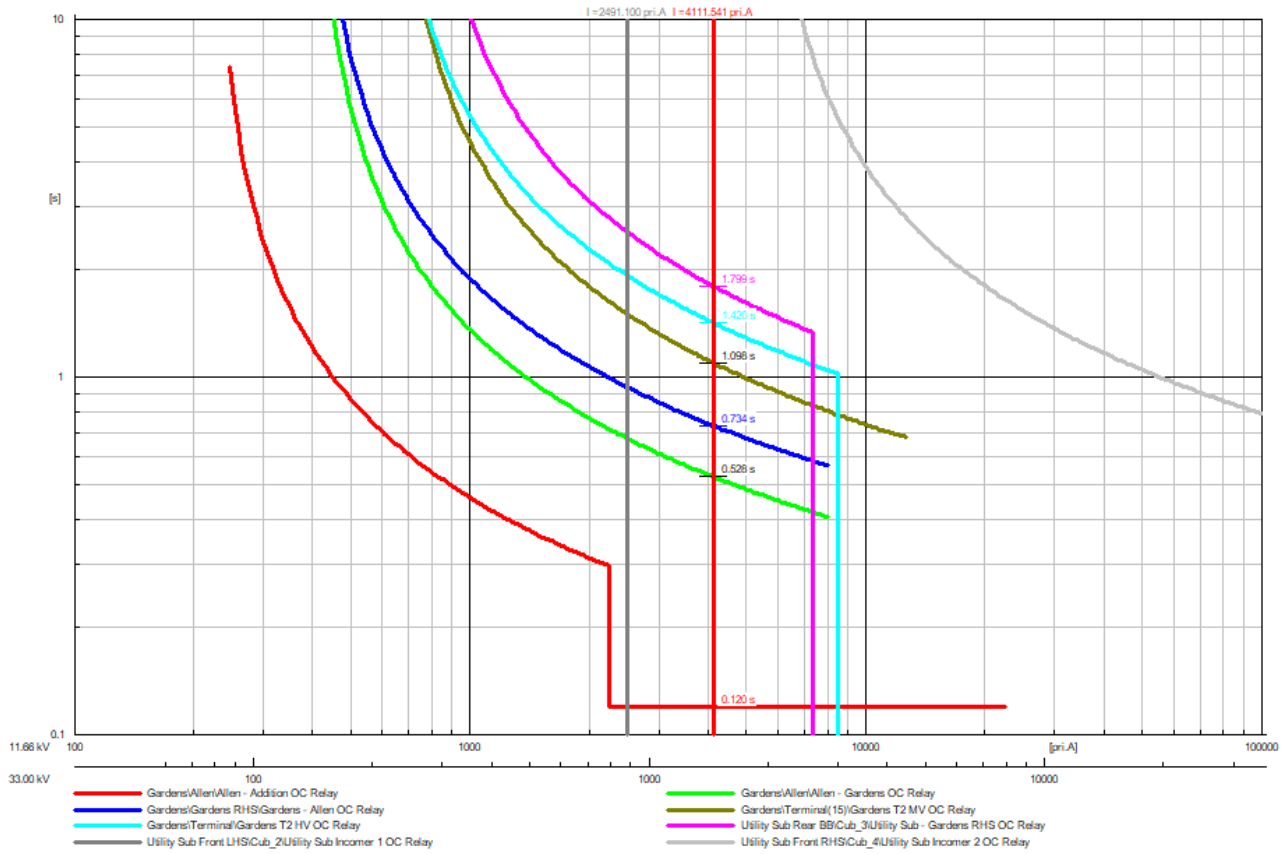


Figure H.17: The OC relay grading for a three-phase fault at Addition SS

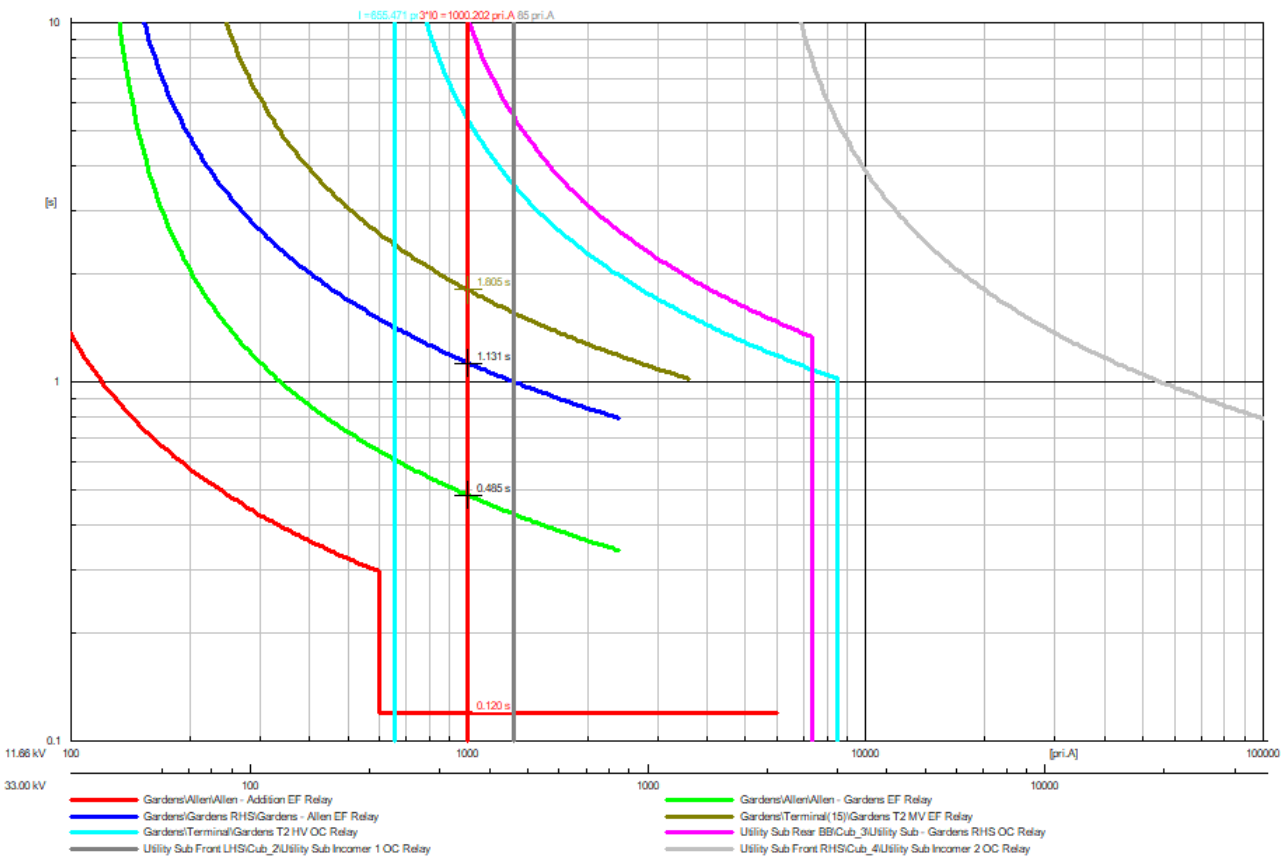


Figure H.18: The EF relay grading for a single-phase fault at Addition SS

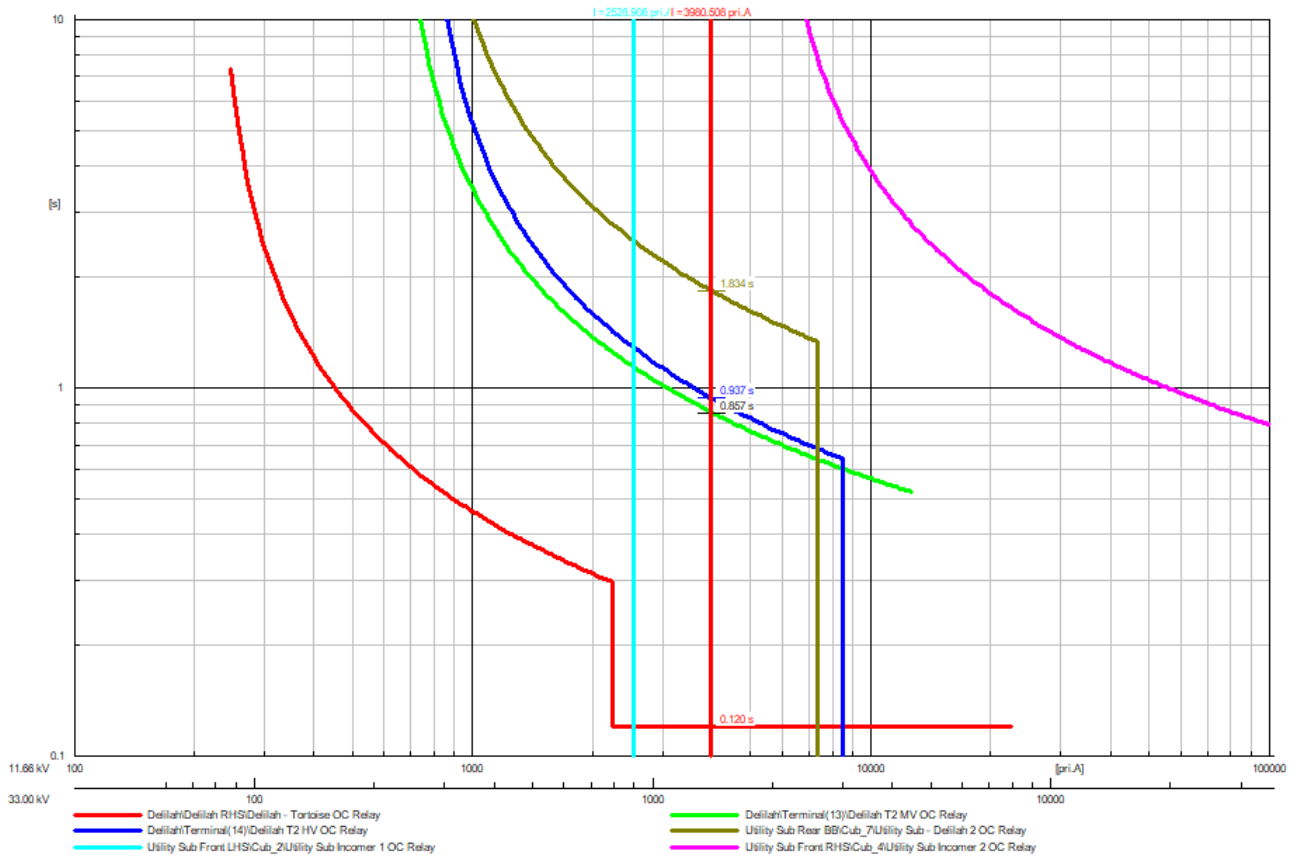


Figure H.19: The OC relay grading for a three-phase fault at Tortoise SS

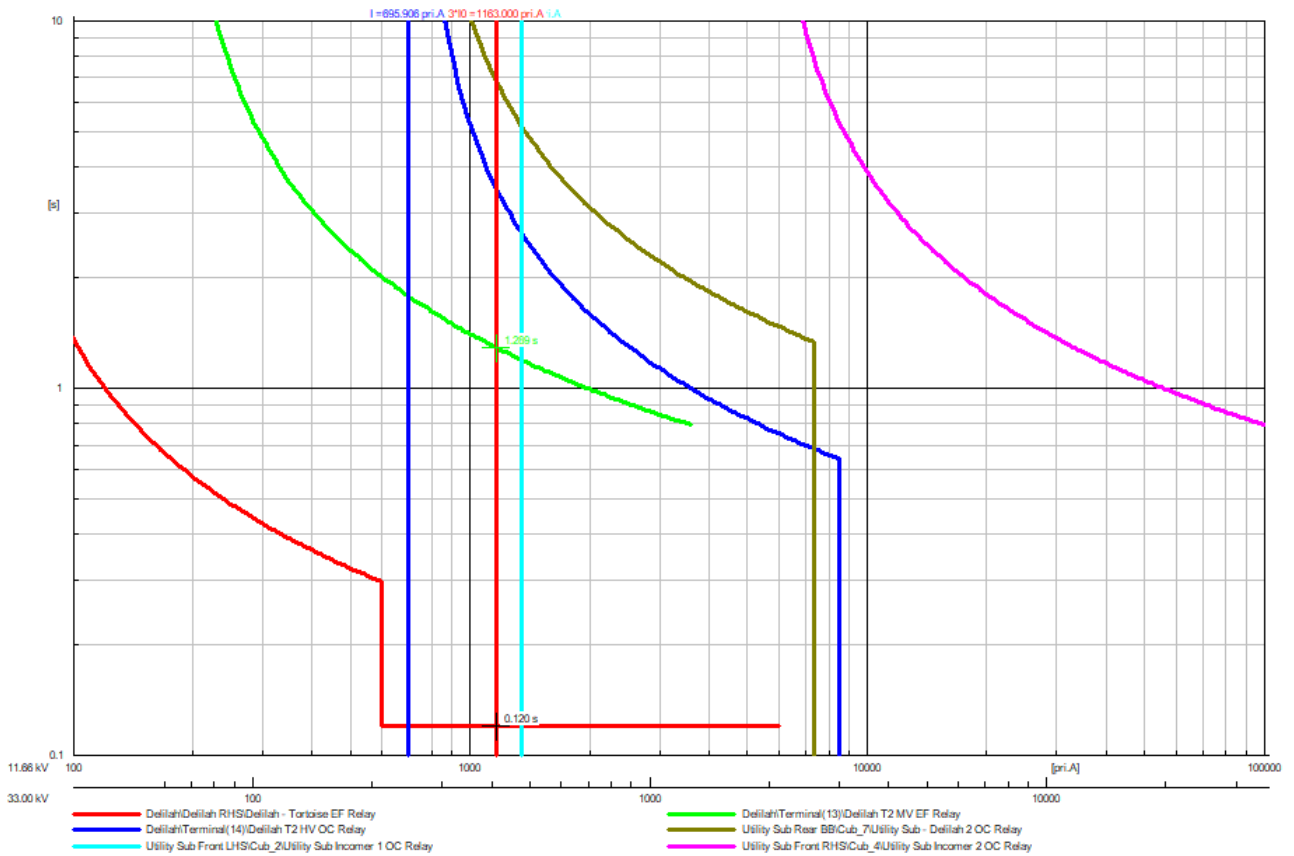


Figure H.20: The EF relay grading for a single-phase fault at Tortoise SS

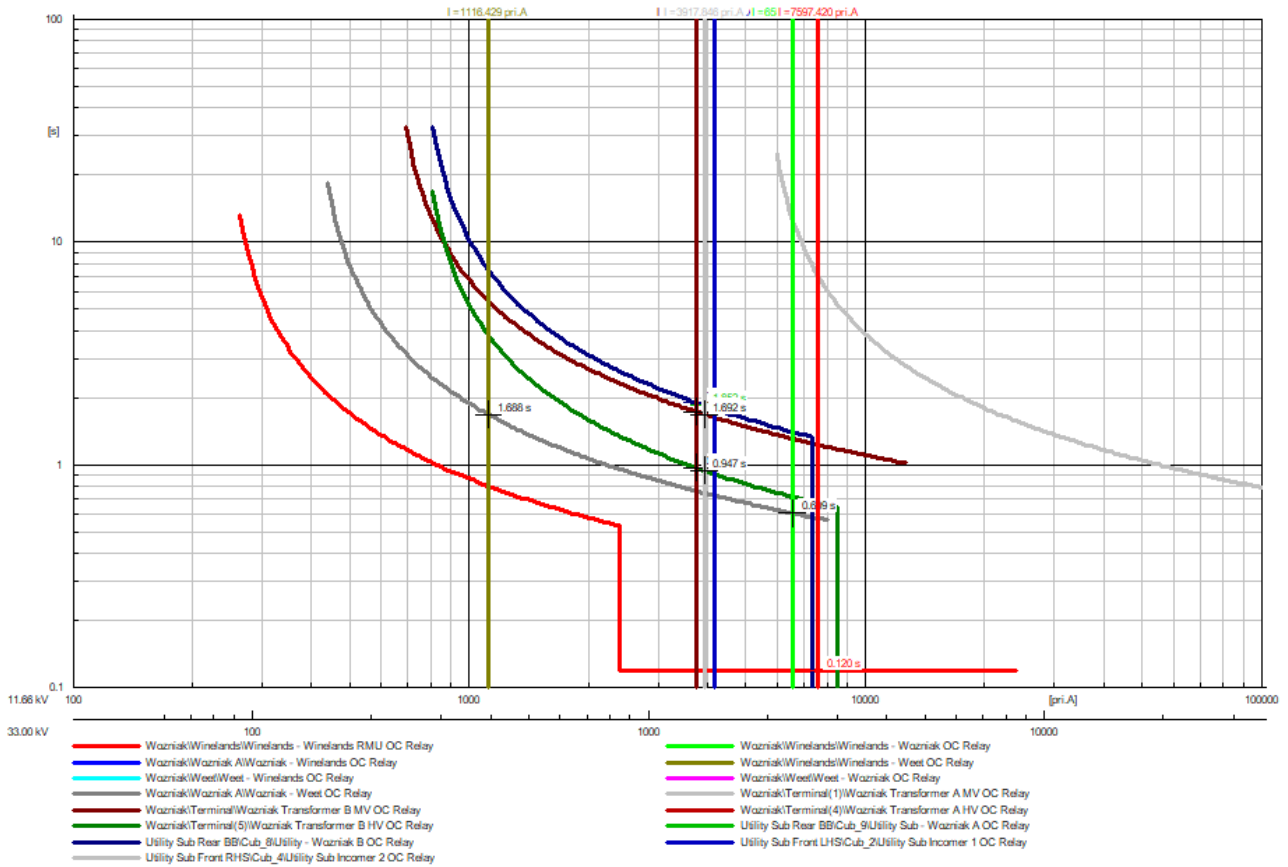


Figure H.21: The OC relay grading for a three-phase fault at Winelands RMU 1 SS

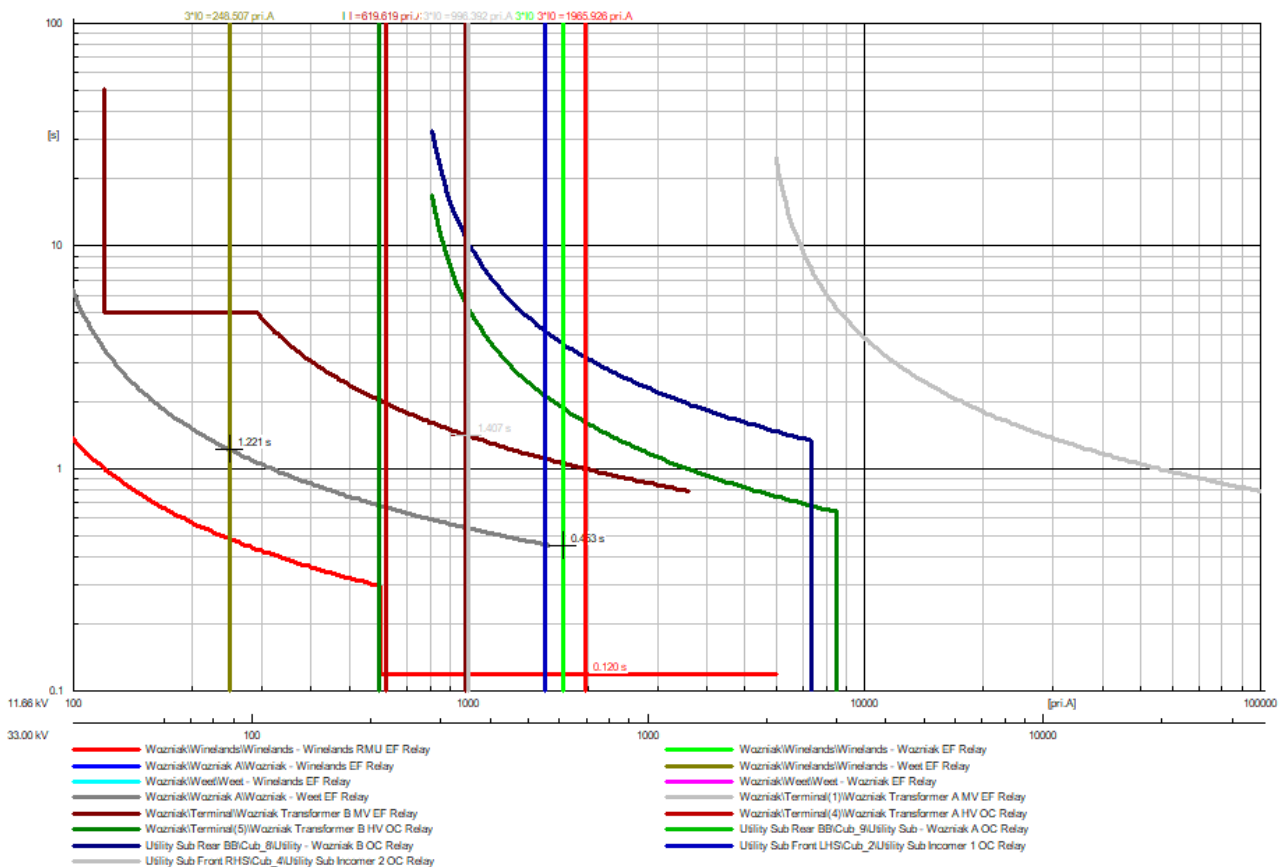


Figure H.22: The EF relay grading for a single-phase fault at Winelands RMU 1 SS

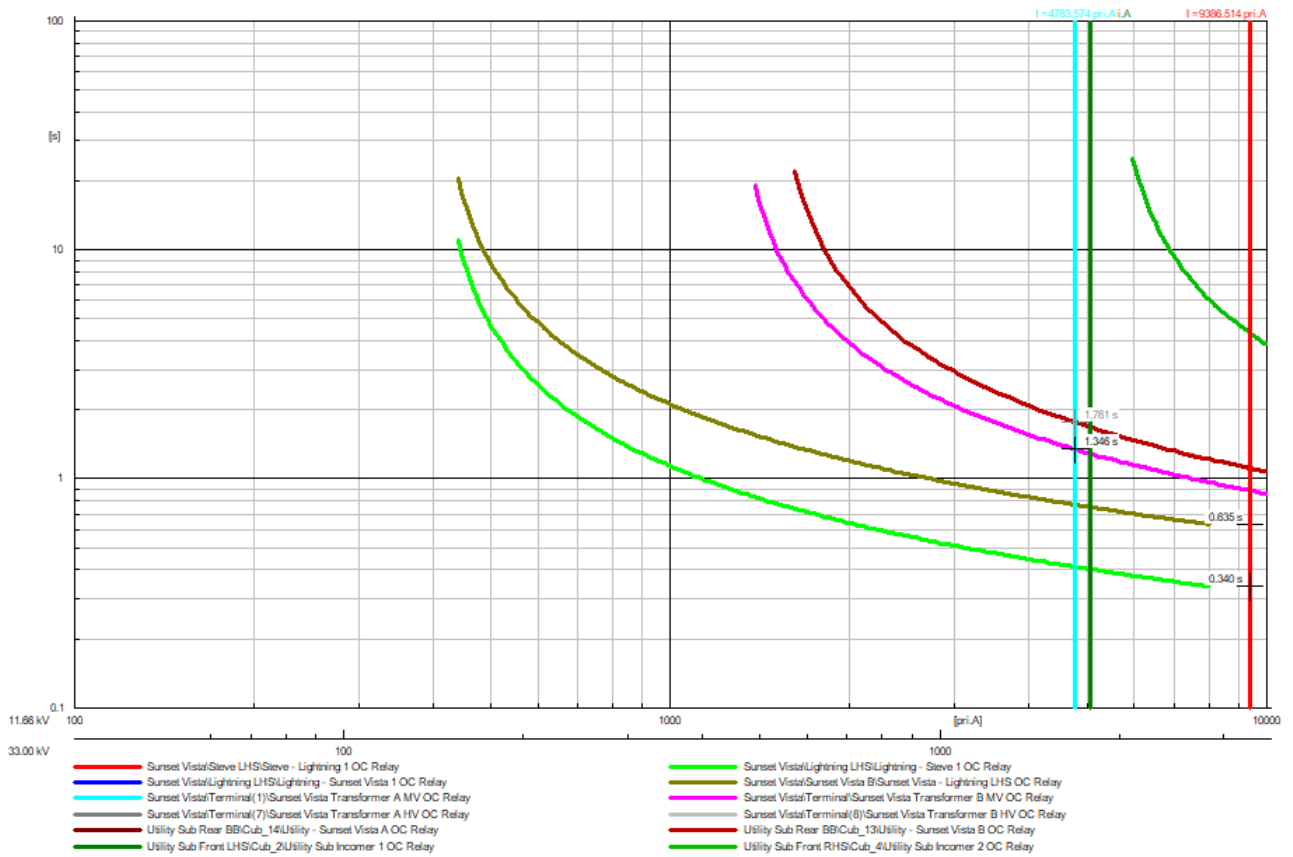


Figure H.23: The OC relay grading for a three-phase fault at Steve LHS SS

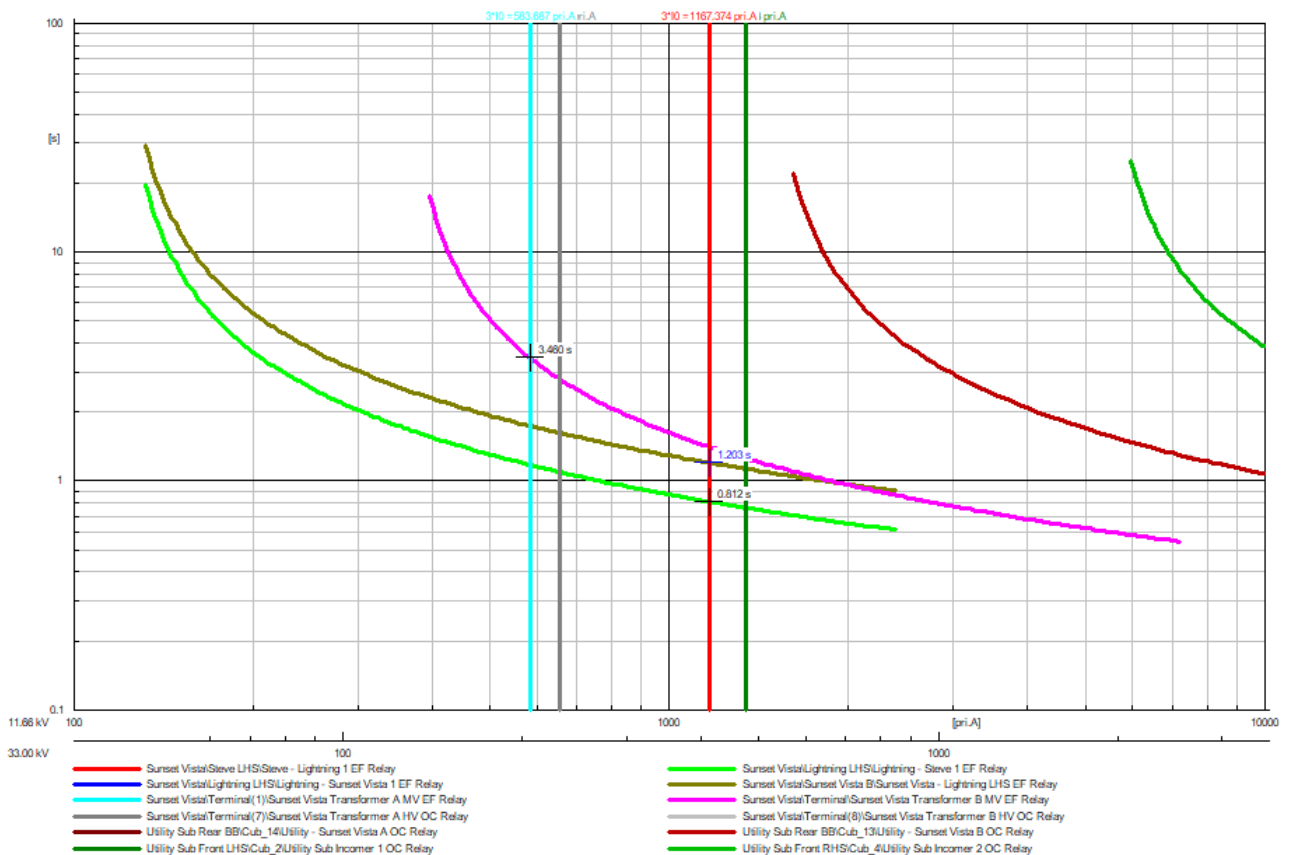


Figure H.24: The EF relay grading for a single-phase fault at Steve LHS SS

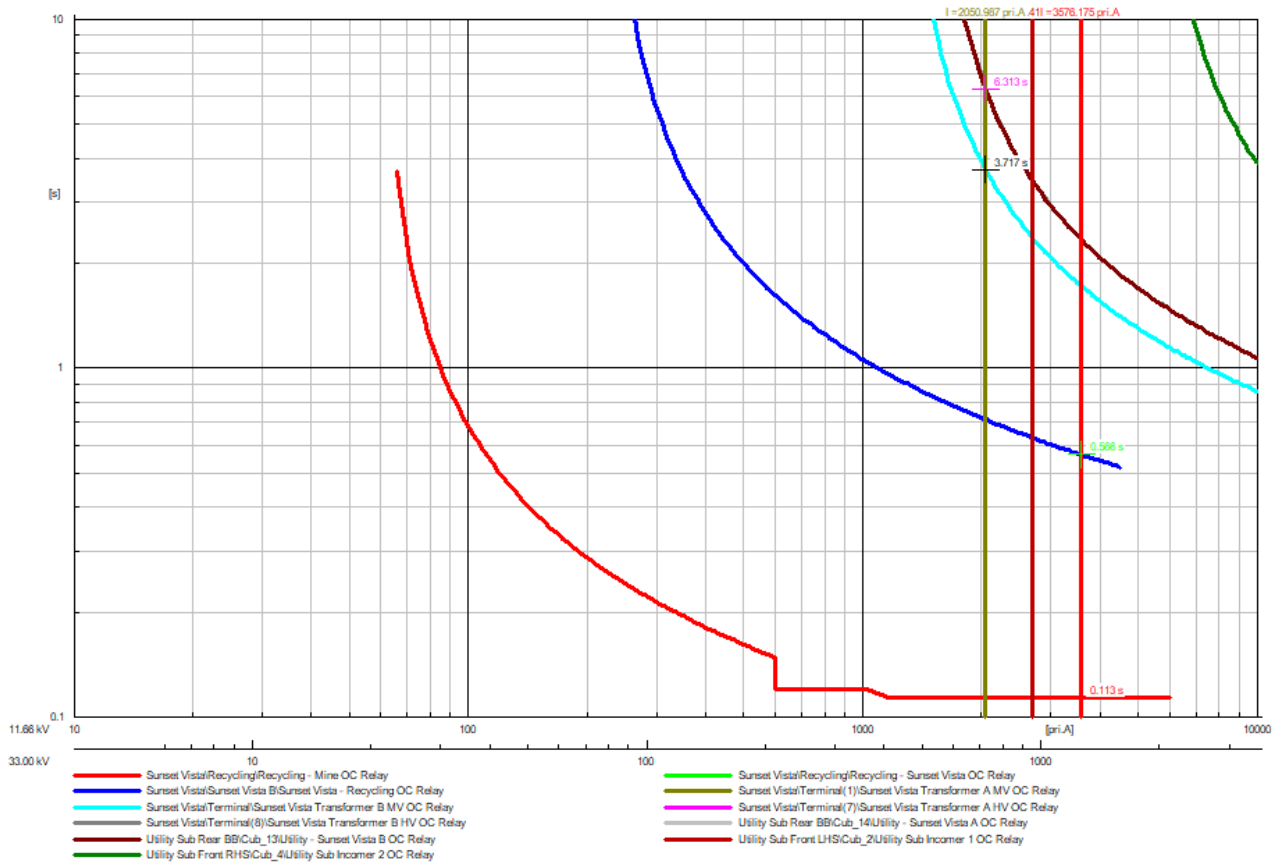


Figure H.25: The OC relay grading for a three-phase fault at Mine SS

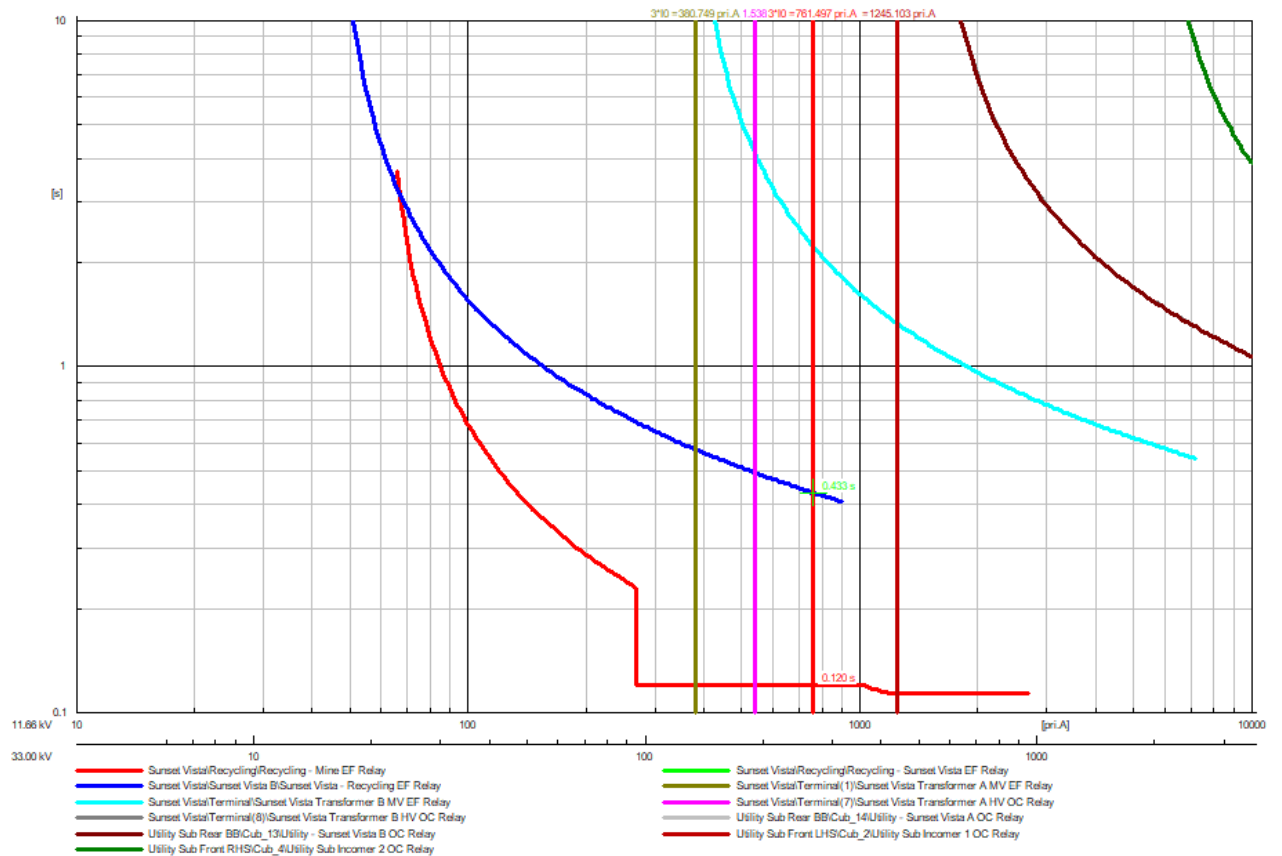


Figure H.26: The EF relay grading for a single-phase fault at Mine SS

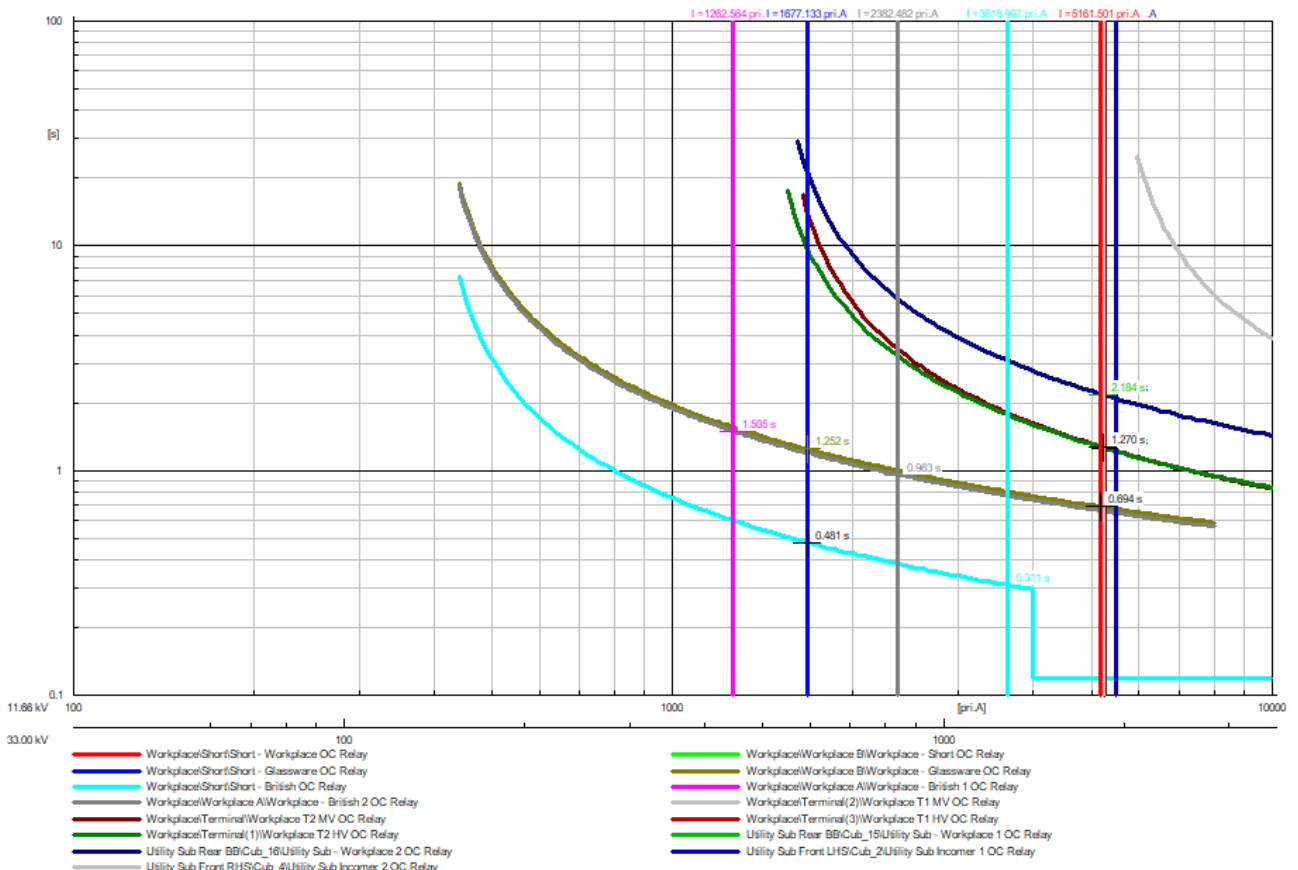


Figure H.27: The OC relay grading for a stage 1 three-phase fault at Short SS

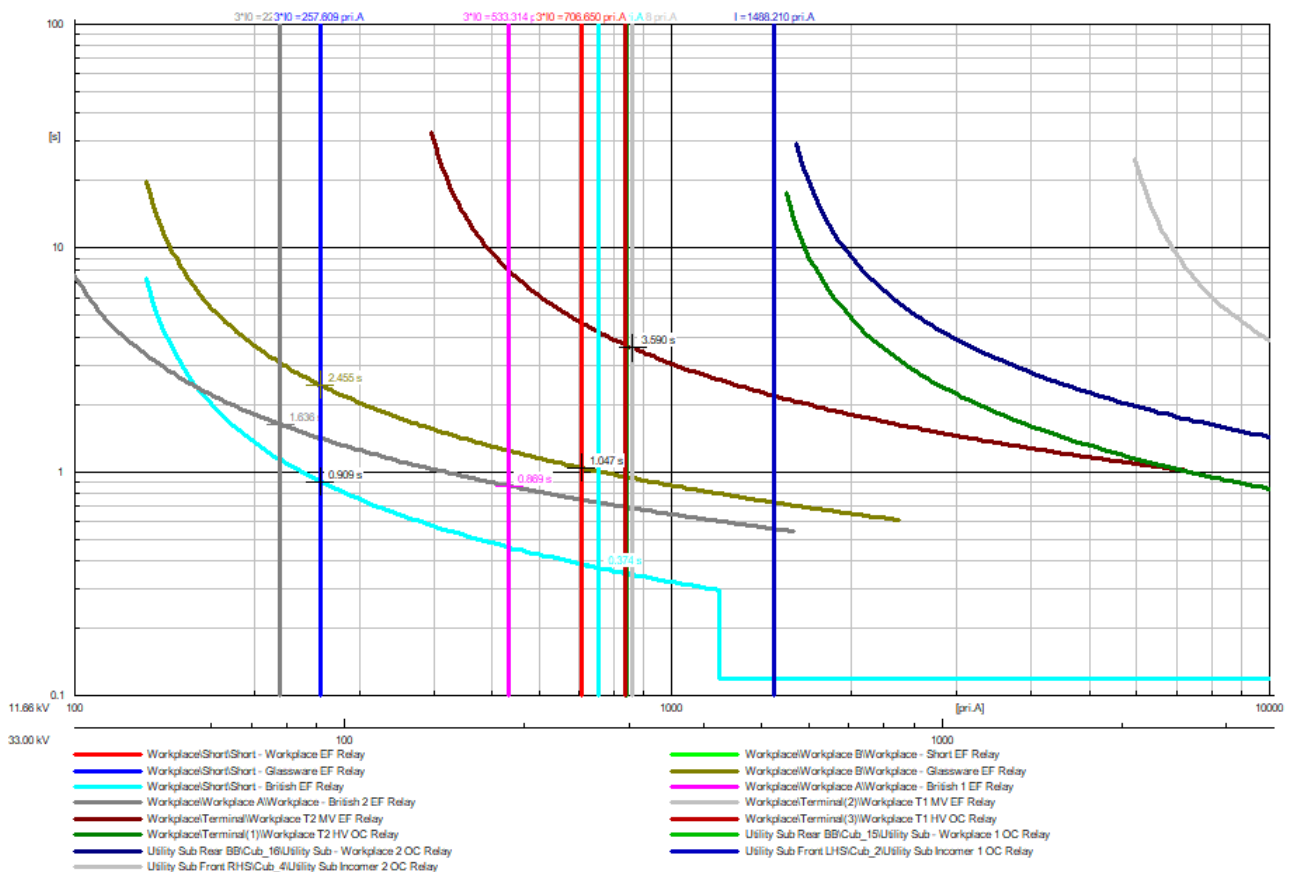


Figure H.28: The EF relay grading for a stage 1 single-phase fault at Short SS

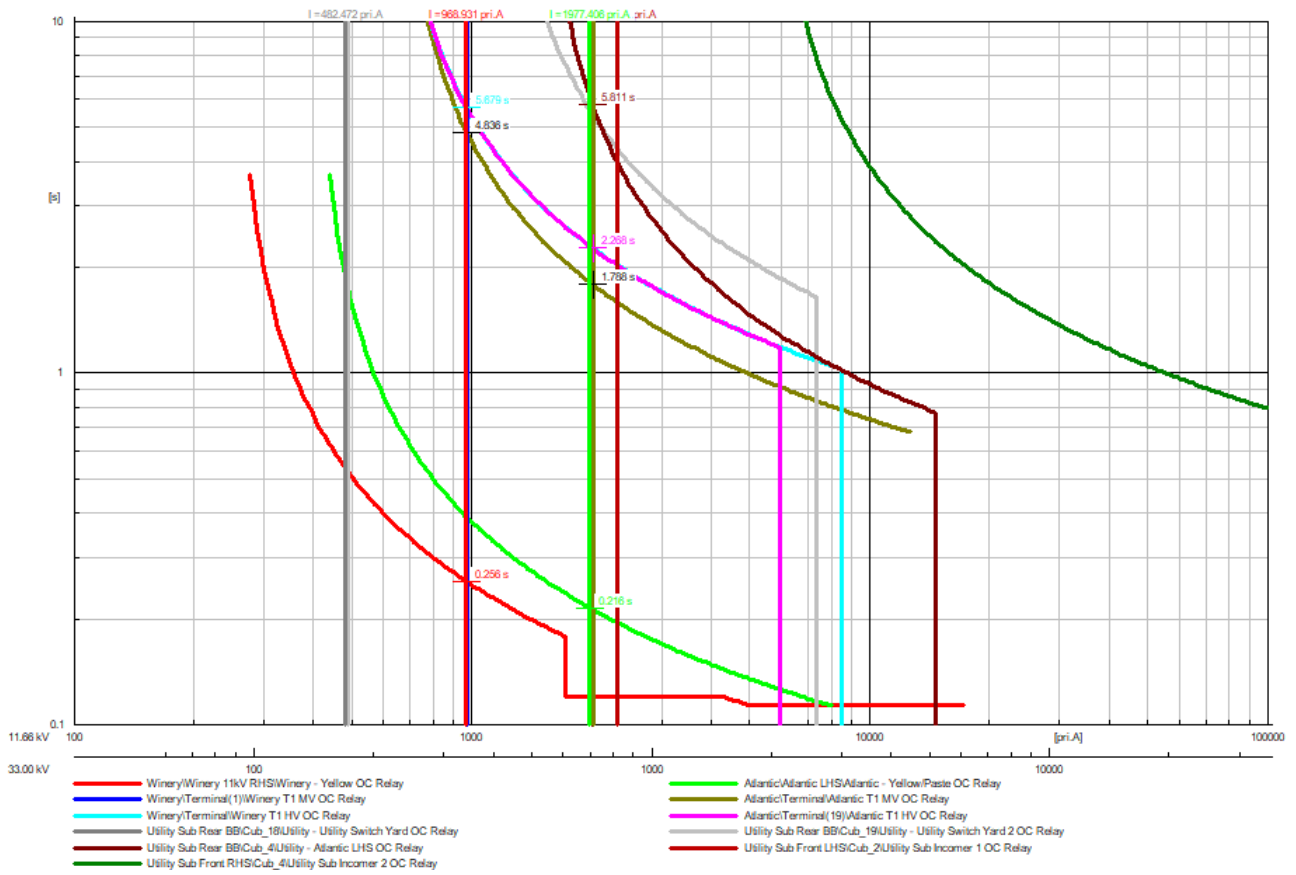


Figure H.29: The OC relay grading for a three-phase fault at Paste RMU 1 SS

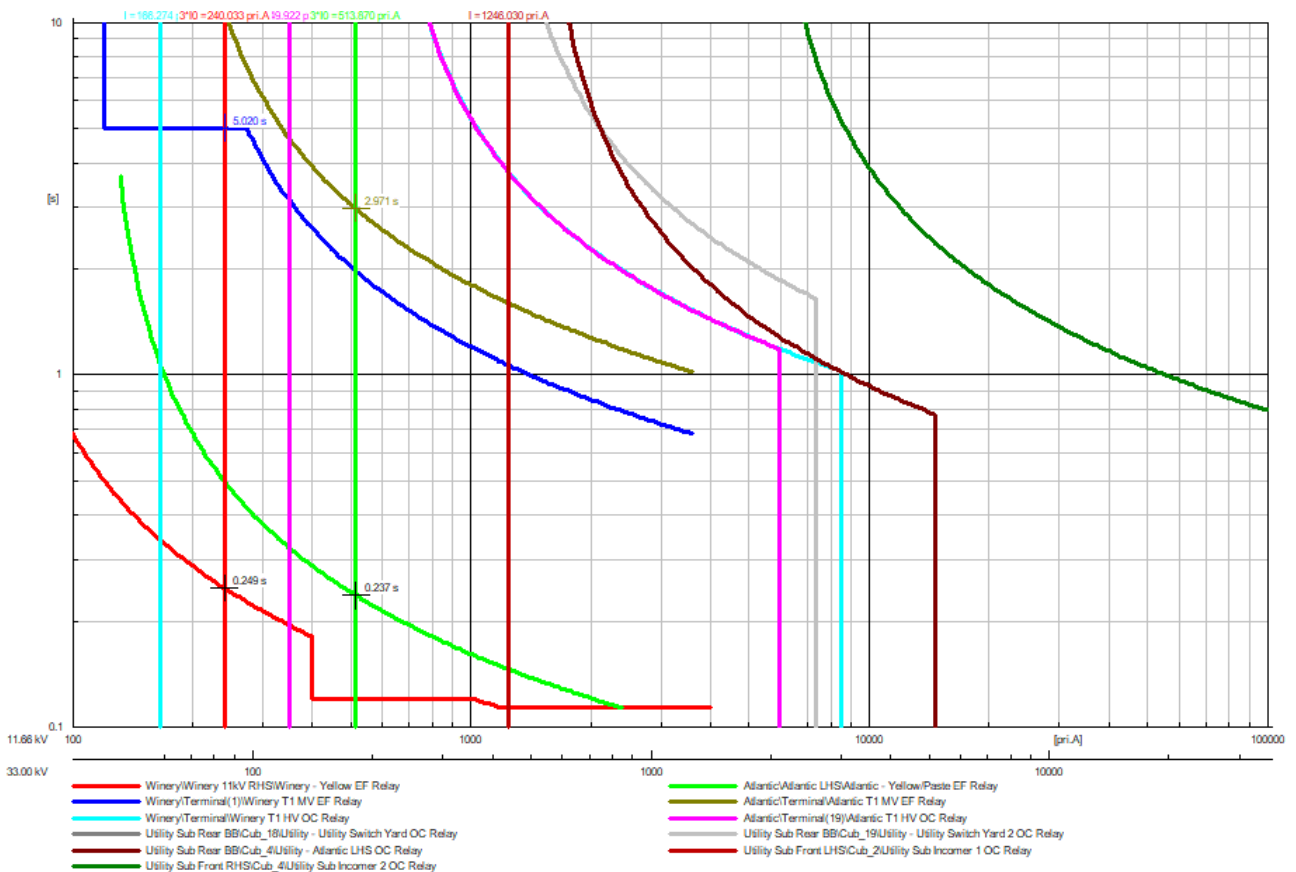


Figure H.30: The EF relay grading for a single-phase fault at Paste RMU 1 SS

Case 2

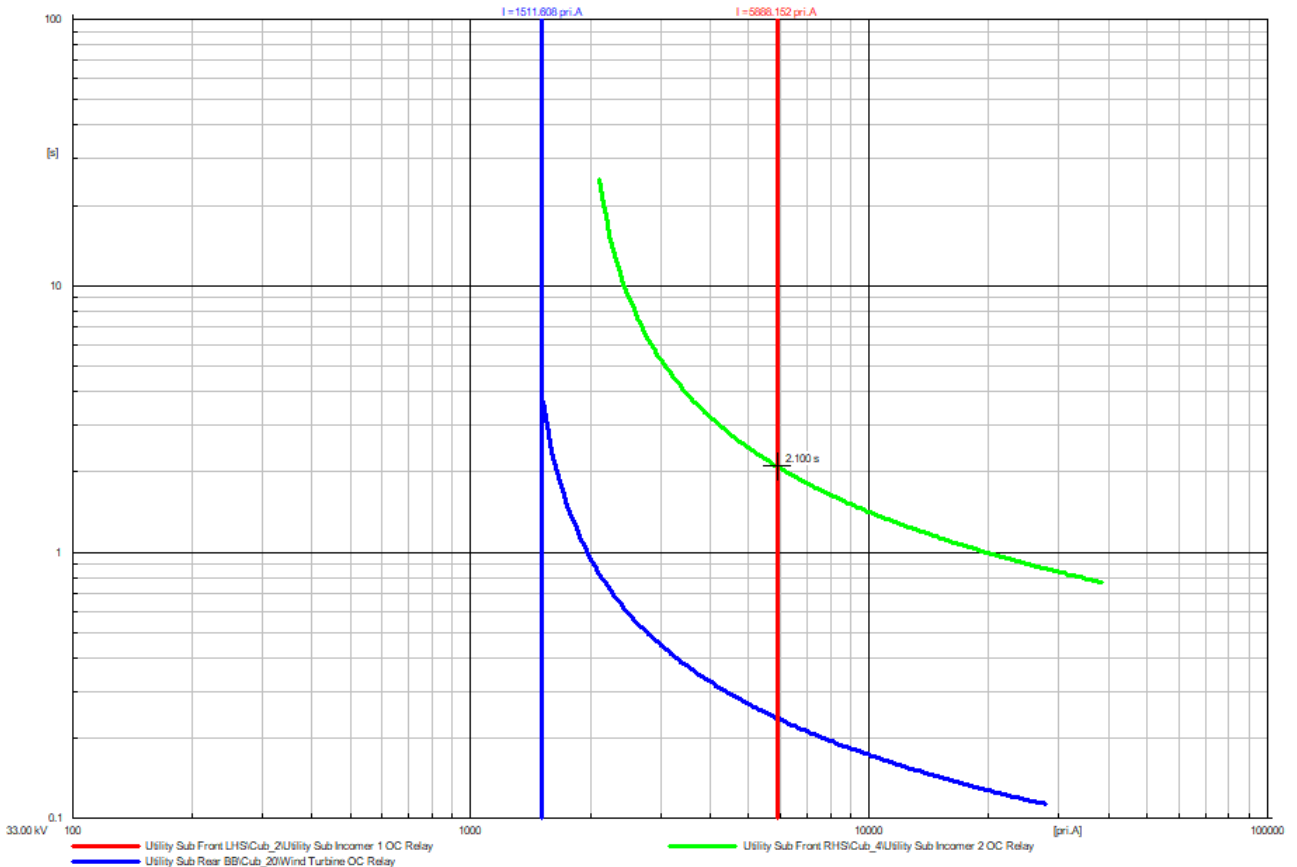


Figure H.31: The OC relay grading for a three-phase fault at the Utility Sub

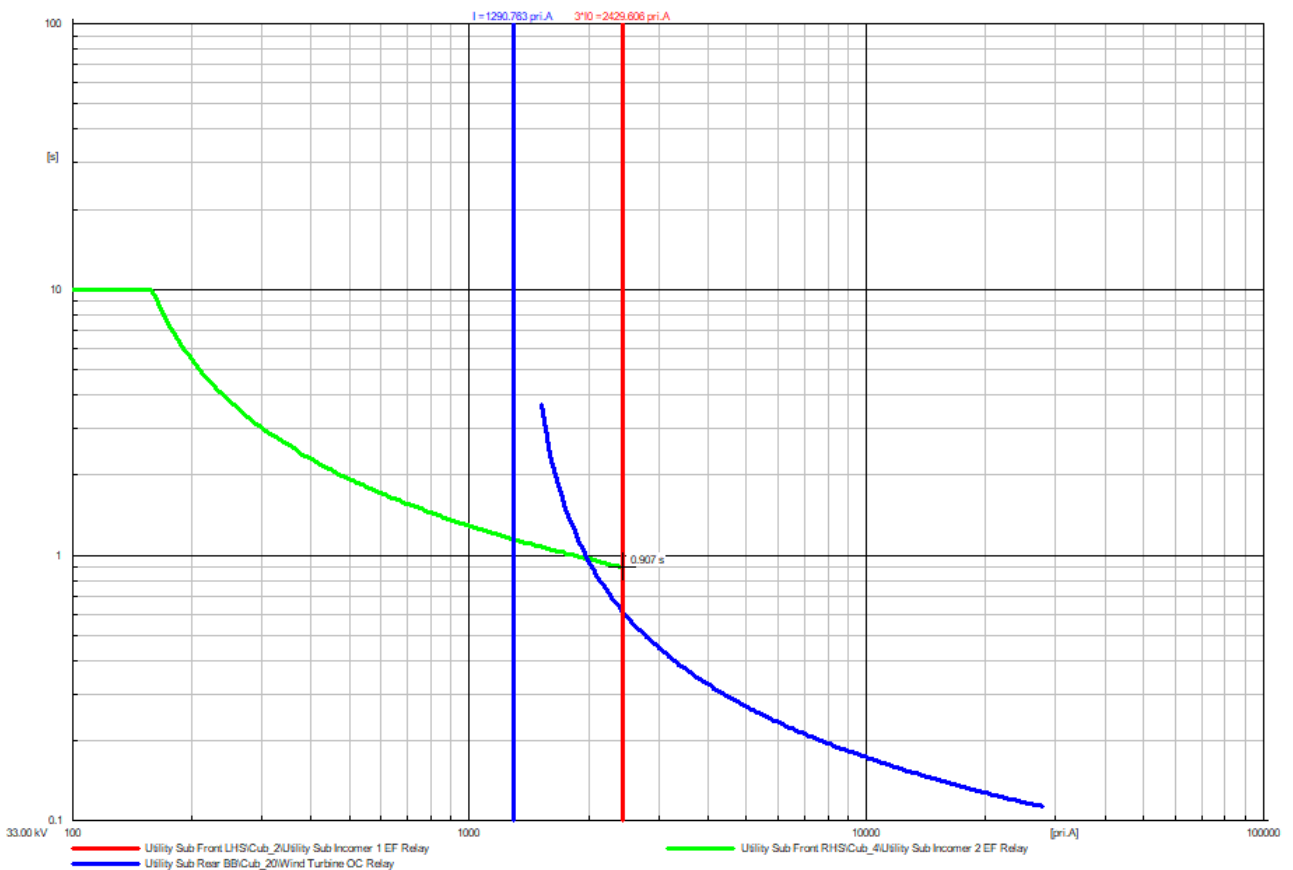


Figure H.32: The EF relay grading for a single-phase fault at the Utility Sub

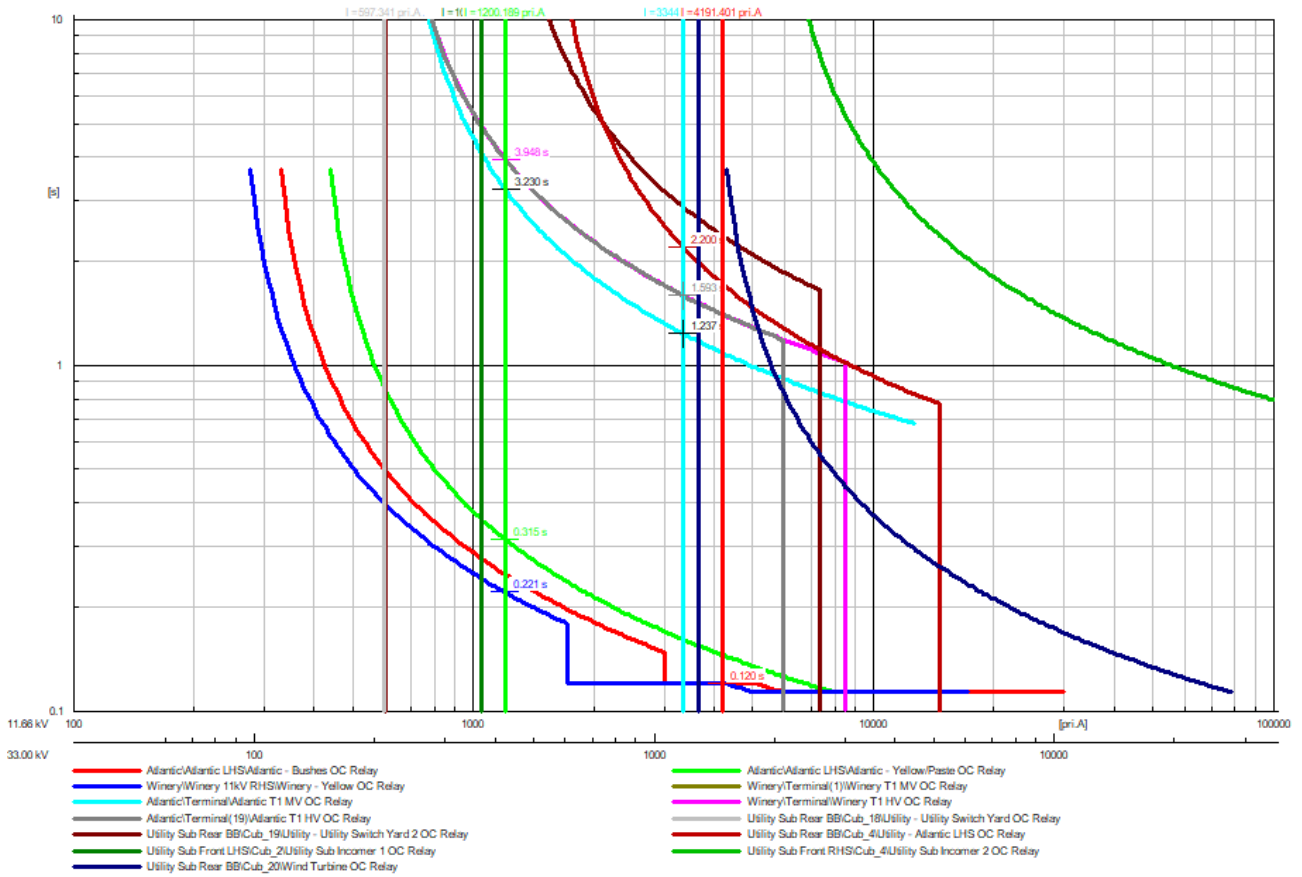


Figure H.33: The OC relay grading for a three-phase fault at Bushes SS

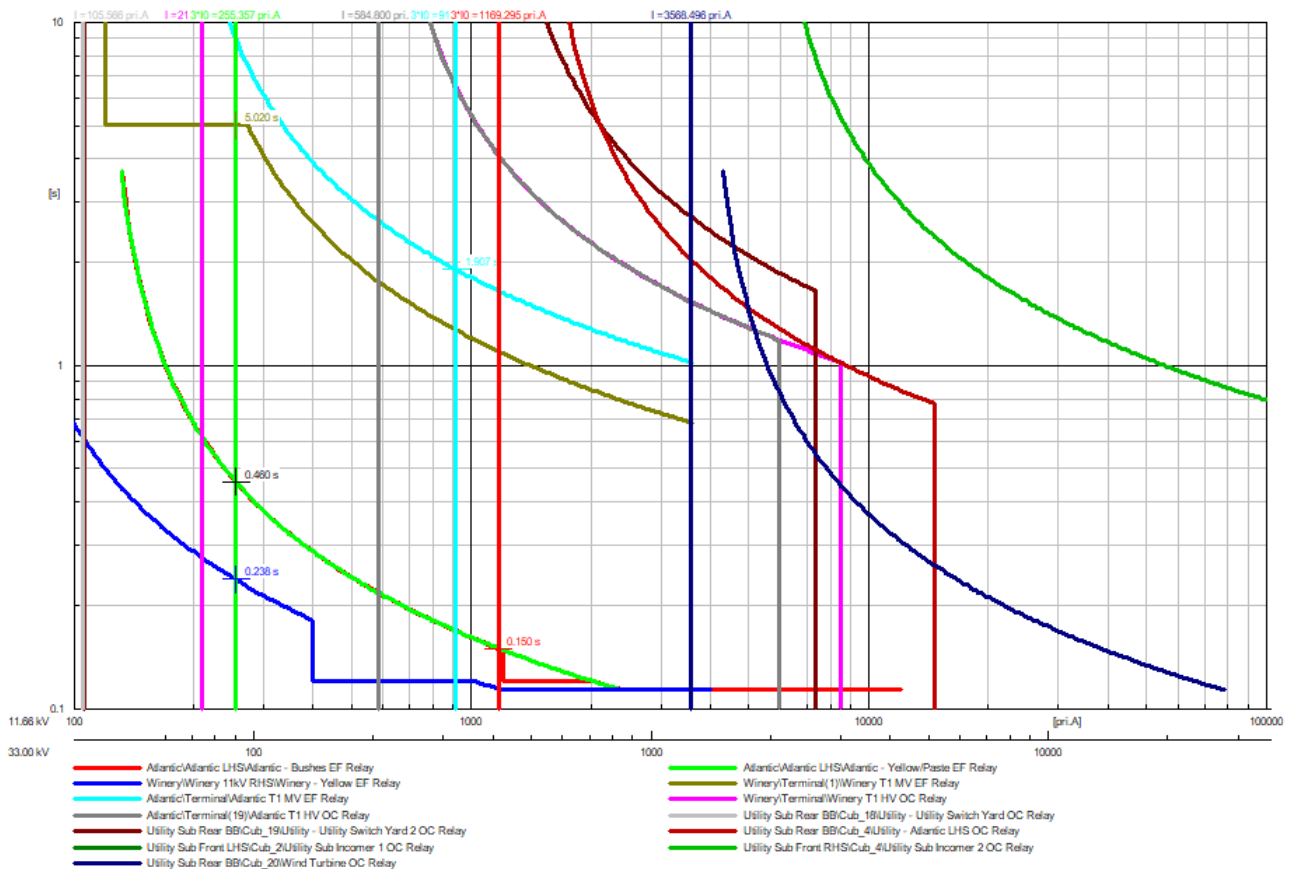


Figure H.34: The EF relay grading for a single-phase fault at Bushes SS

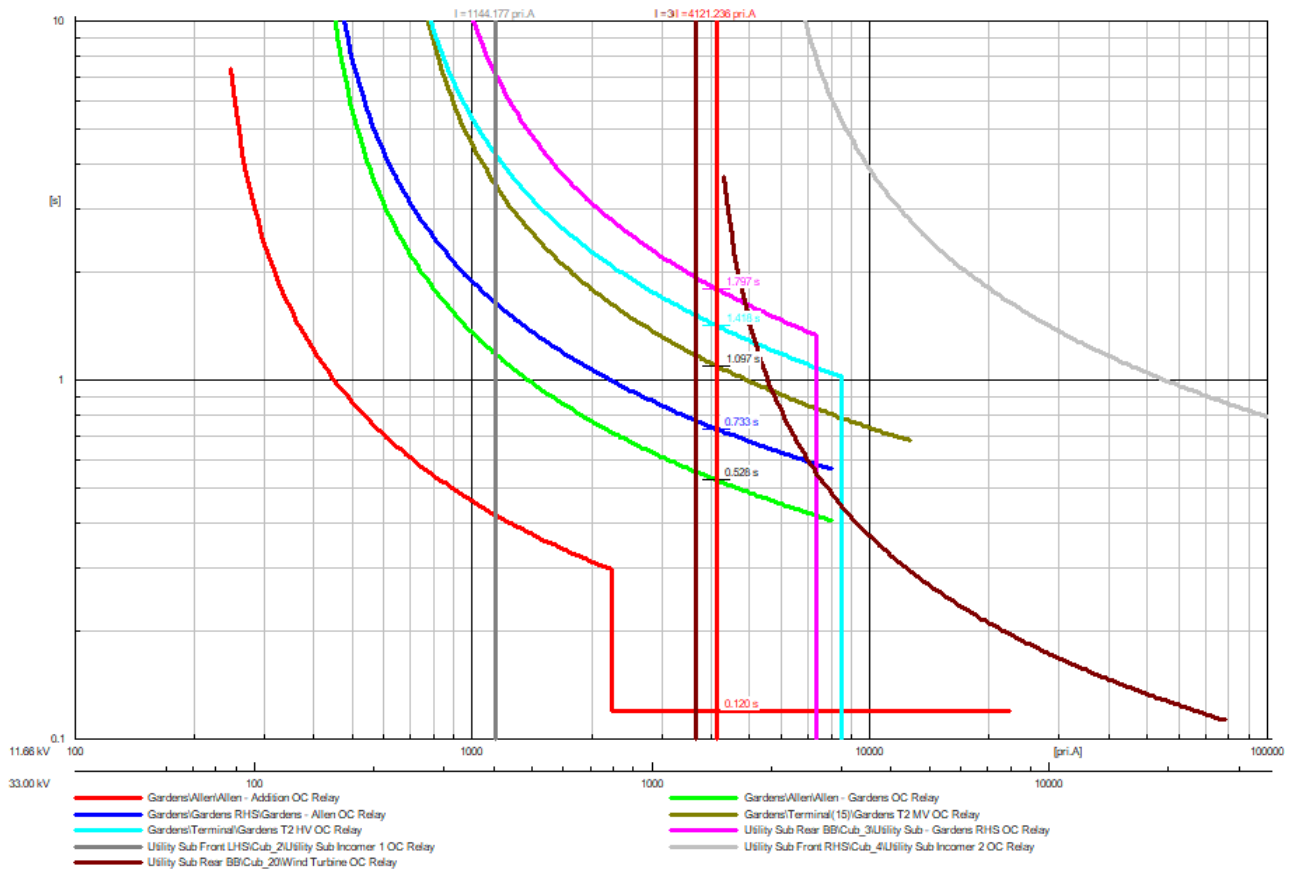


Figure H.35: The OC relay grading for a three-phase fault at Addition SS

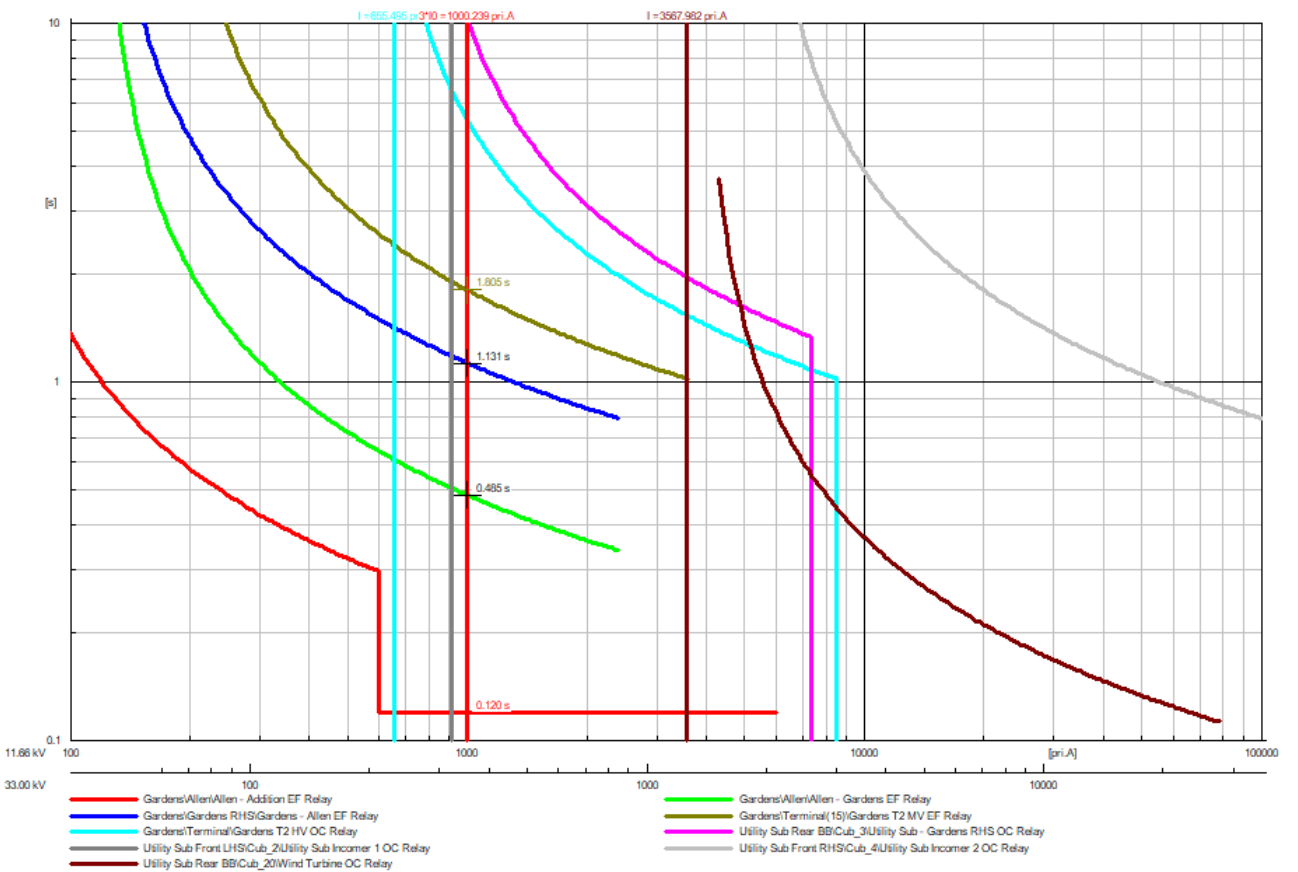


Figure H.36: The EF relay grading for a single-phase fault at Addition SS

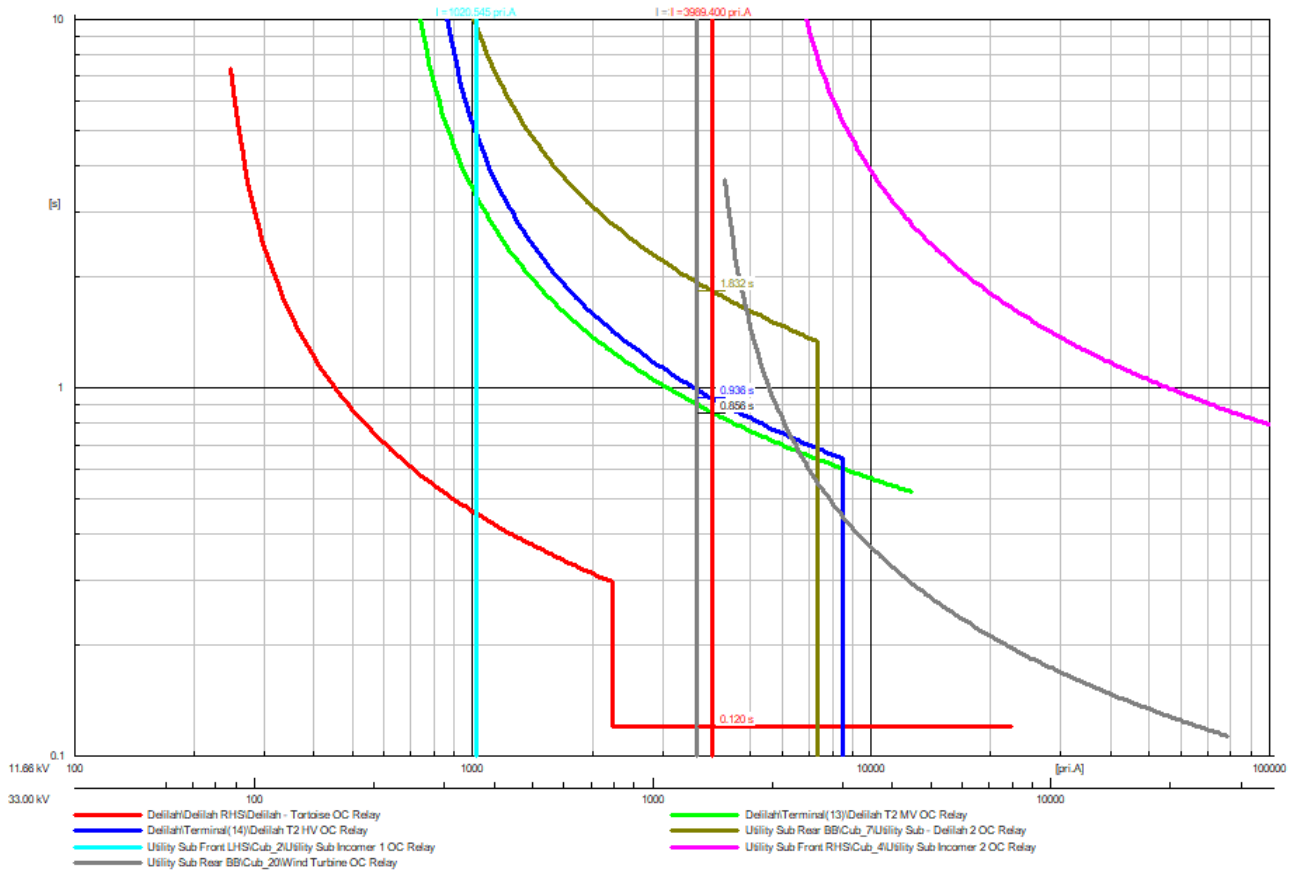


Figure H.37: The OC relay grading for a three-phase fault at Tortoise SS

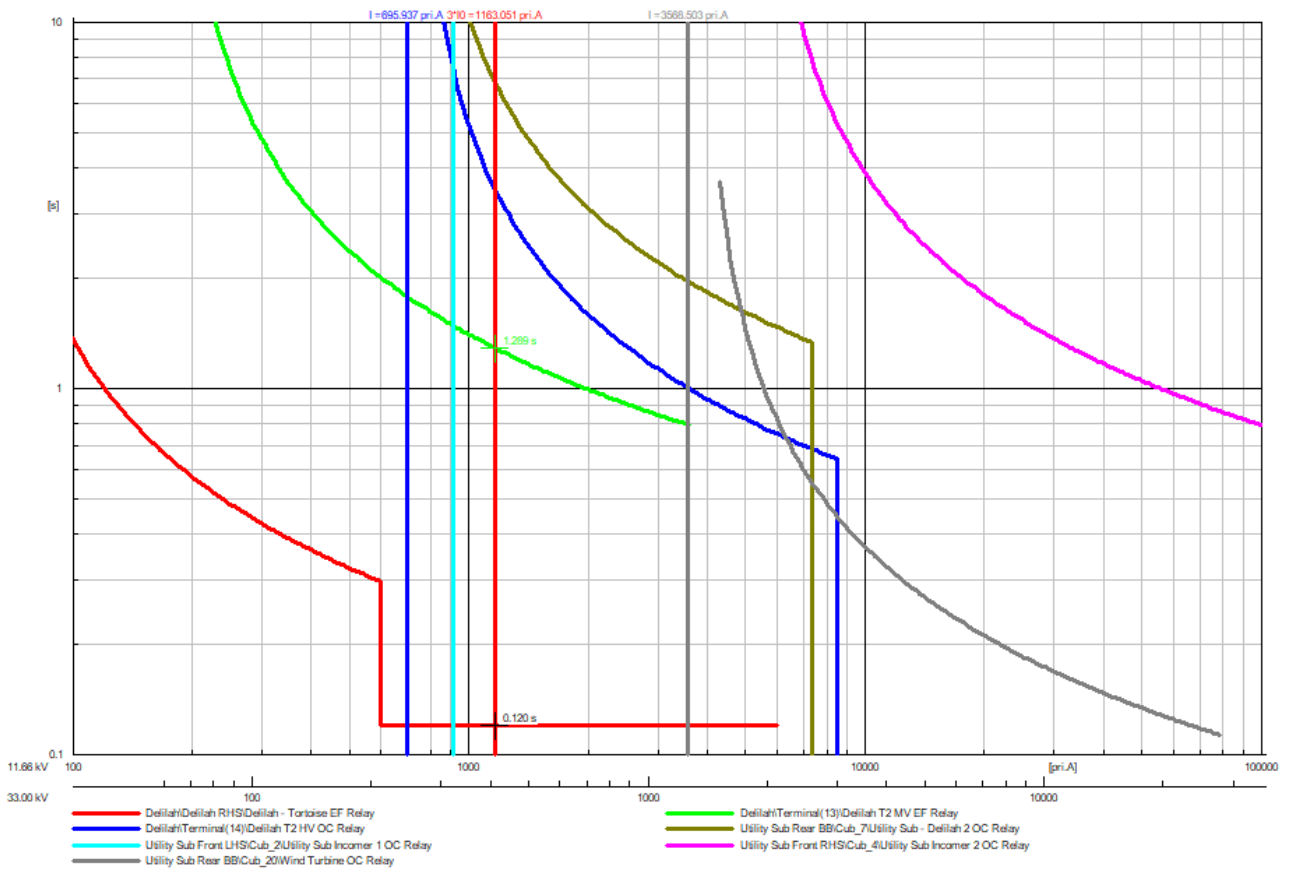


Figure H.38: The EF relay grading for a single-phase fault at Tortoise SS

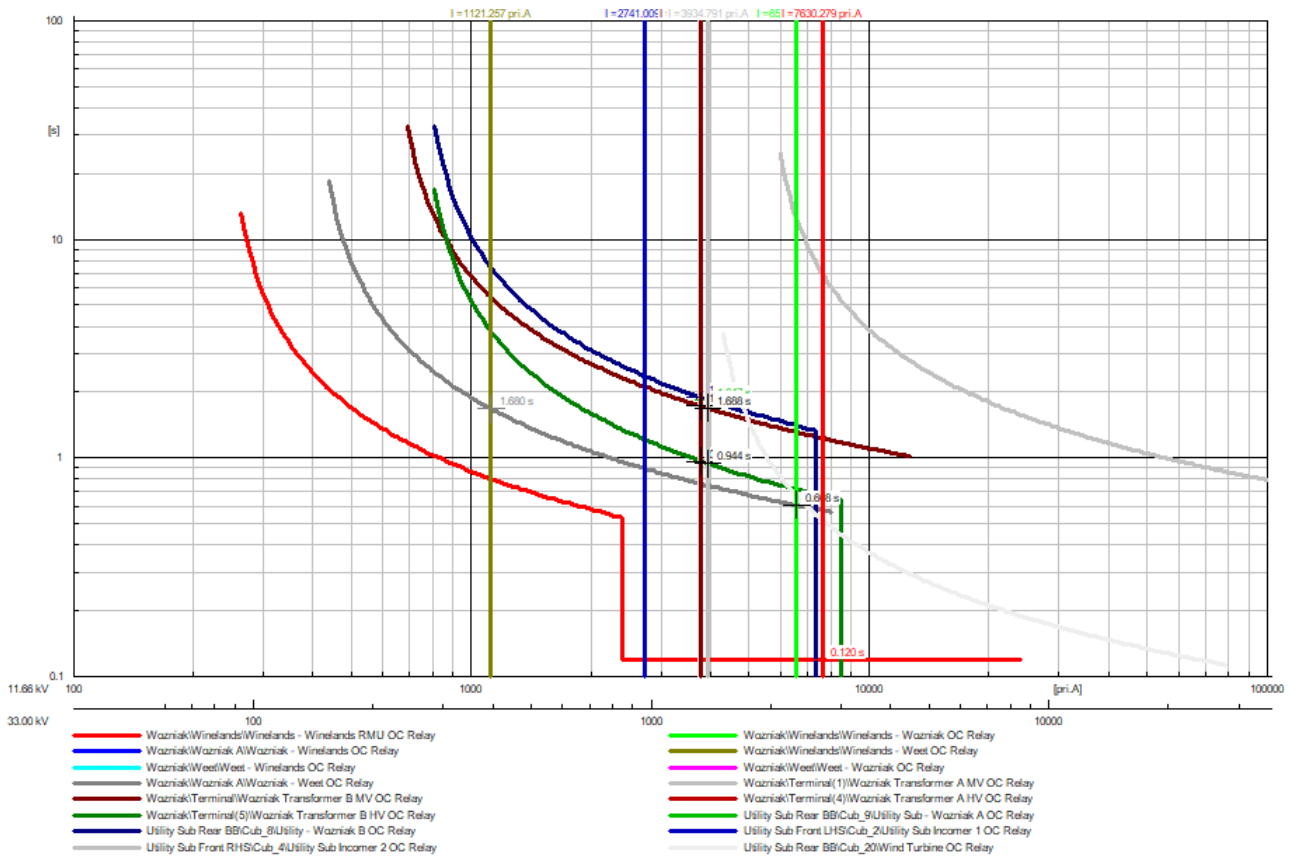


Figure H.39: The OC relay grading for a three-phase fault at Winelands RMU 1 SS

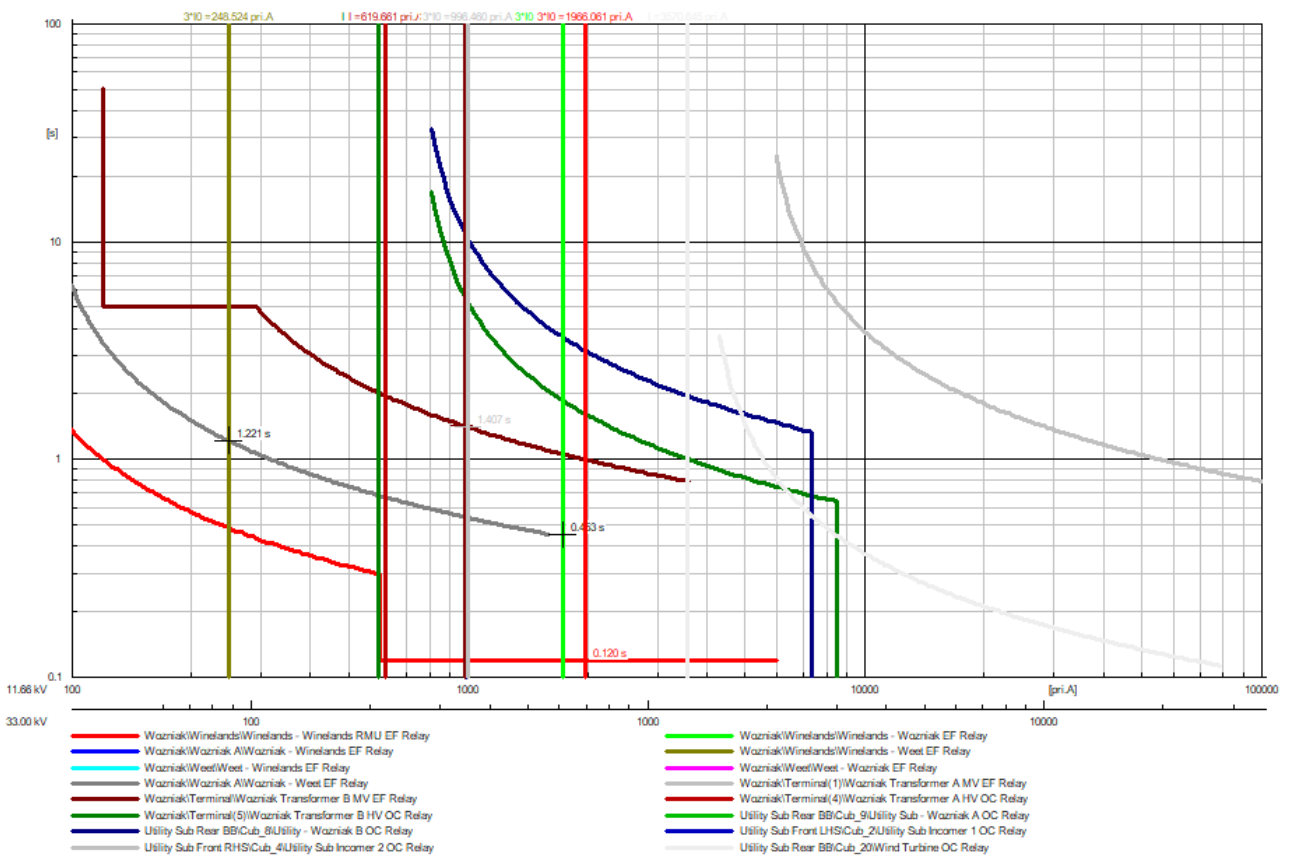


Figure H.40: The EF relay grading for a single-phase fault at Winelands RMU 1 SS

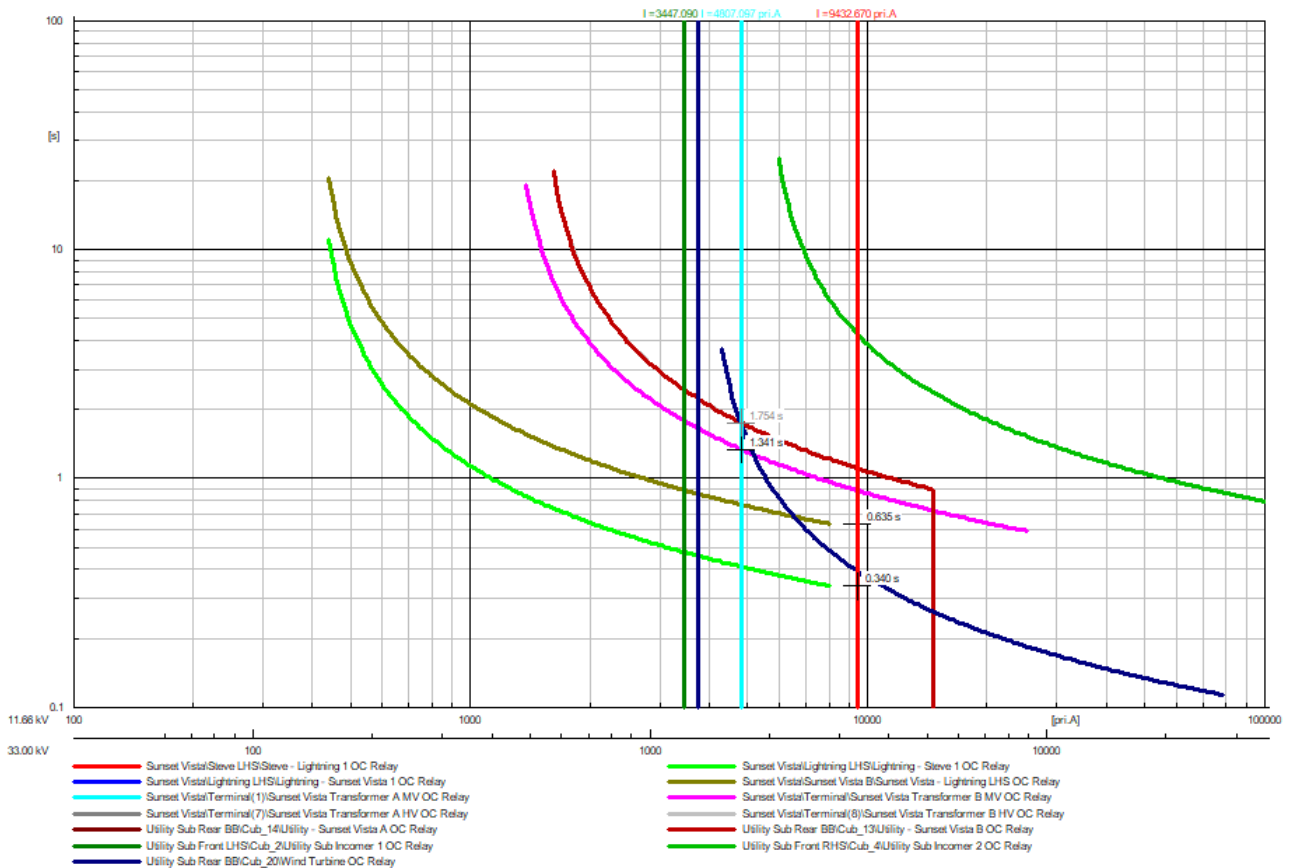


Figure H.41: The OC relay grading for a three-phase fault at Steve LHS SS

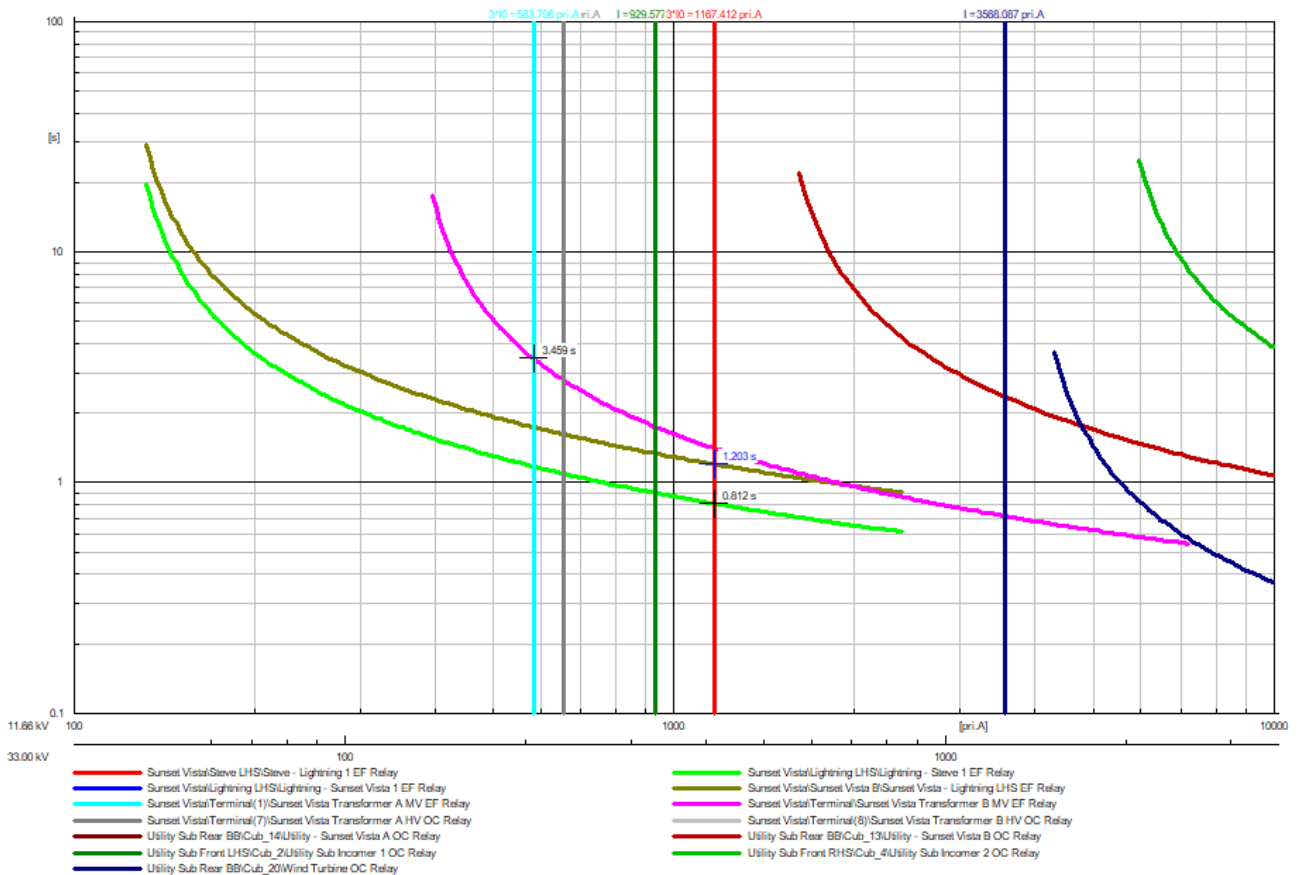


Figure H.42: The EF relay grading for a single-phase fault at Steve LHS SS

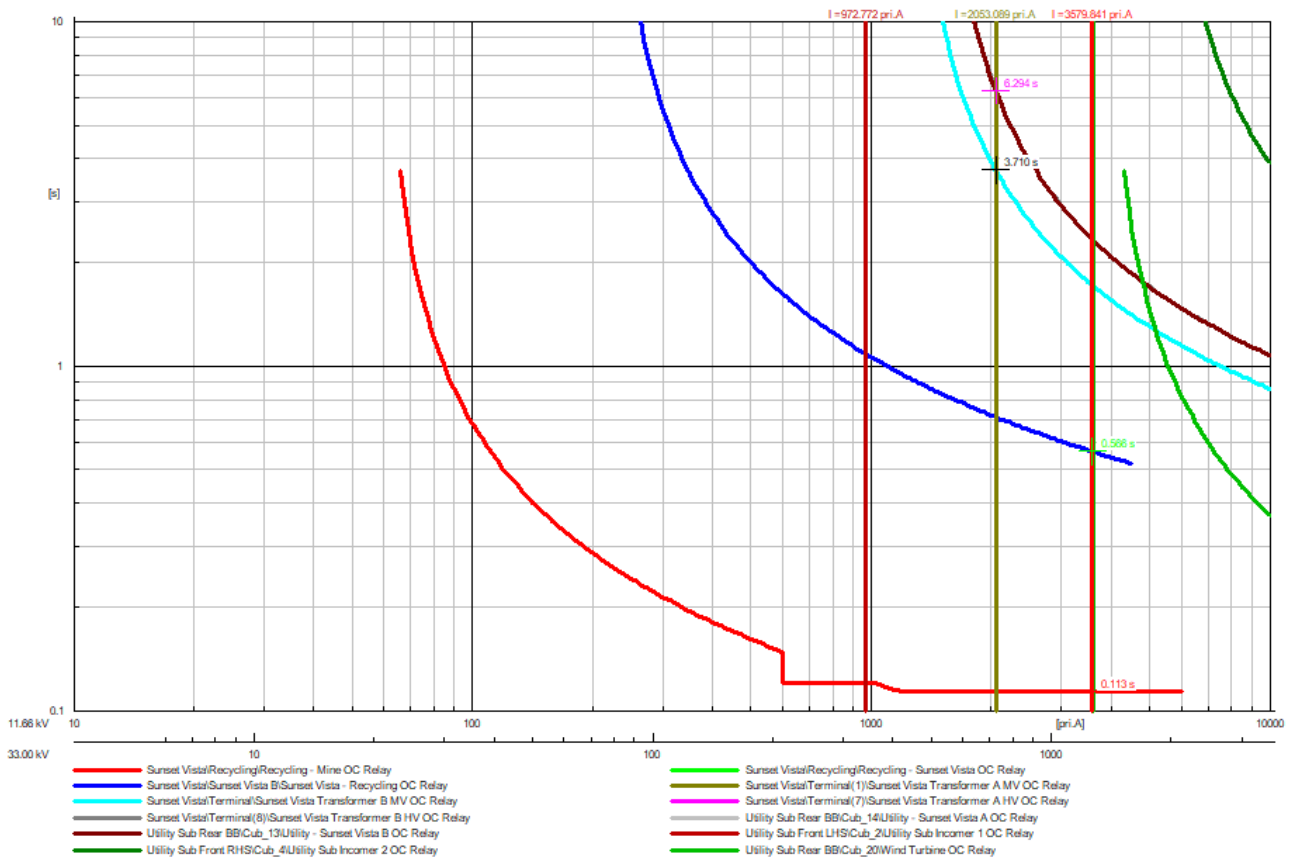


Figure H.43: The OC relay grading for a three-phase fault at Mine SS

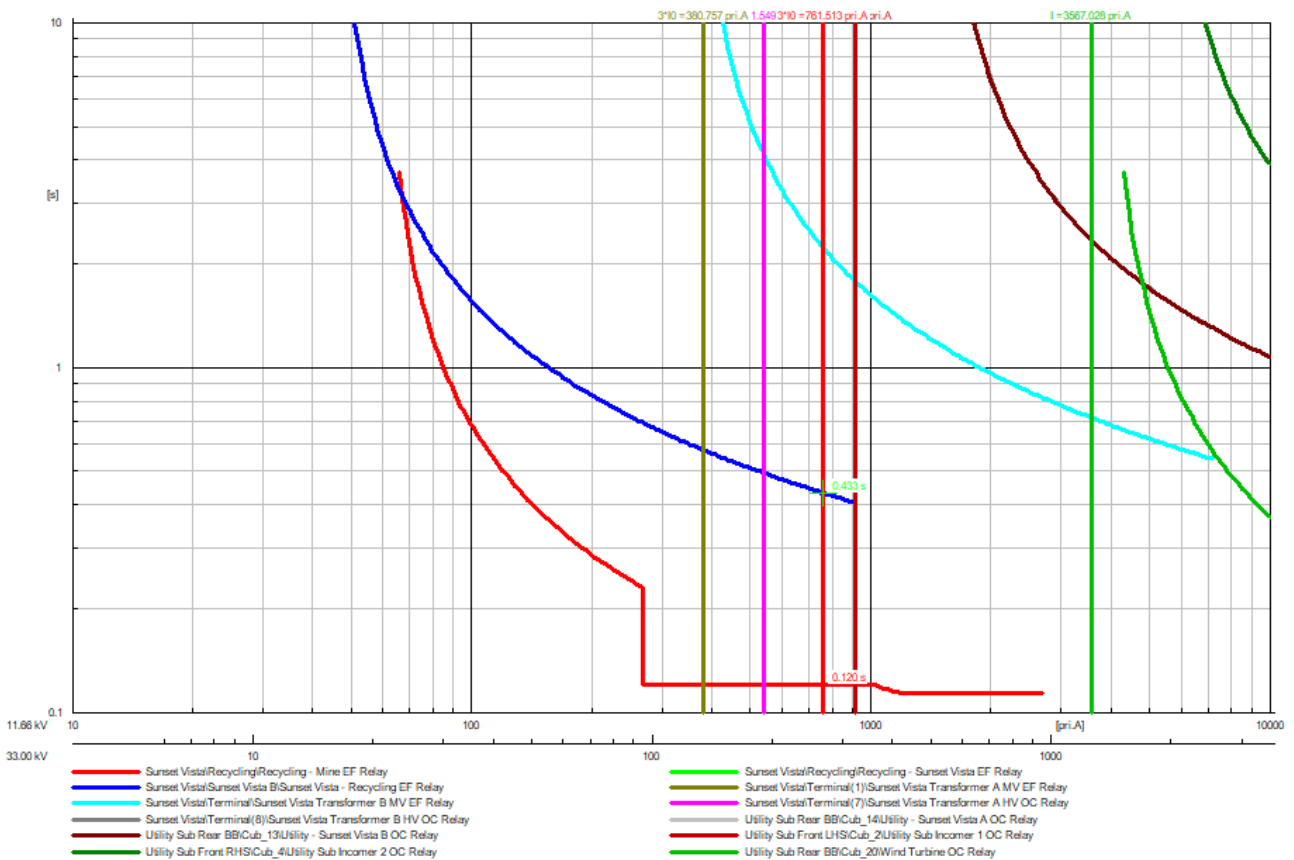


Figure H.44: The EF relay grading for a single-phase fault at Mine SS

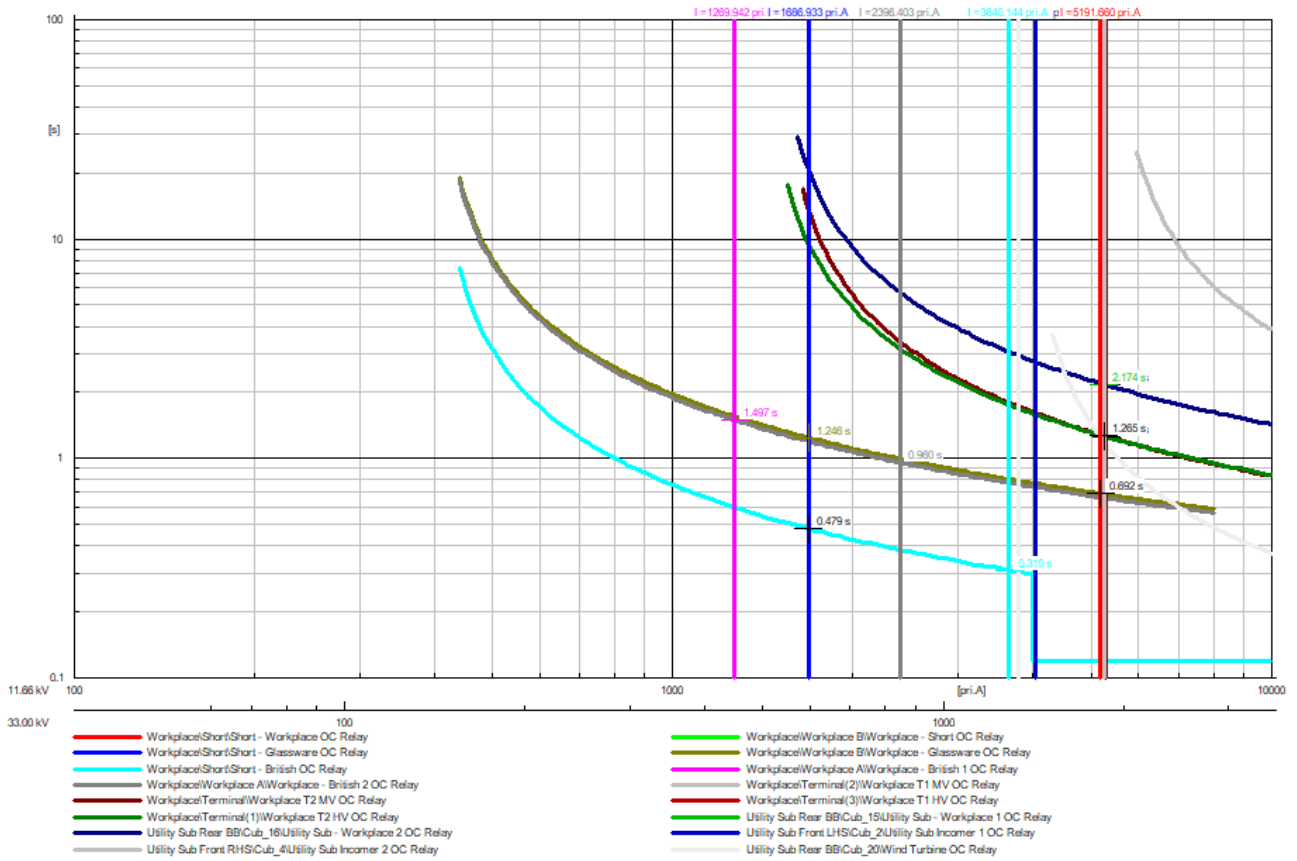


Figure H.45: The OC relay grading for a stage 1 three-phase fault at Short SS

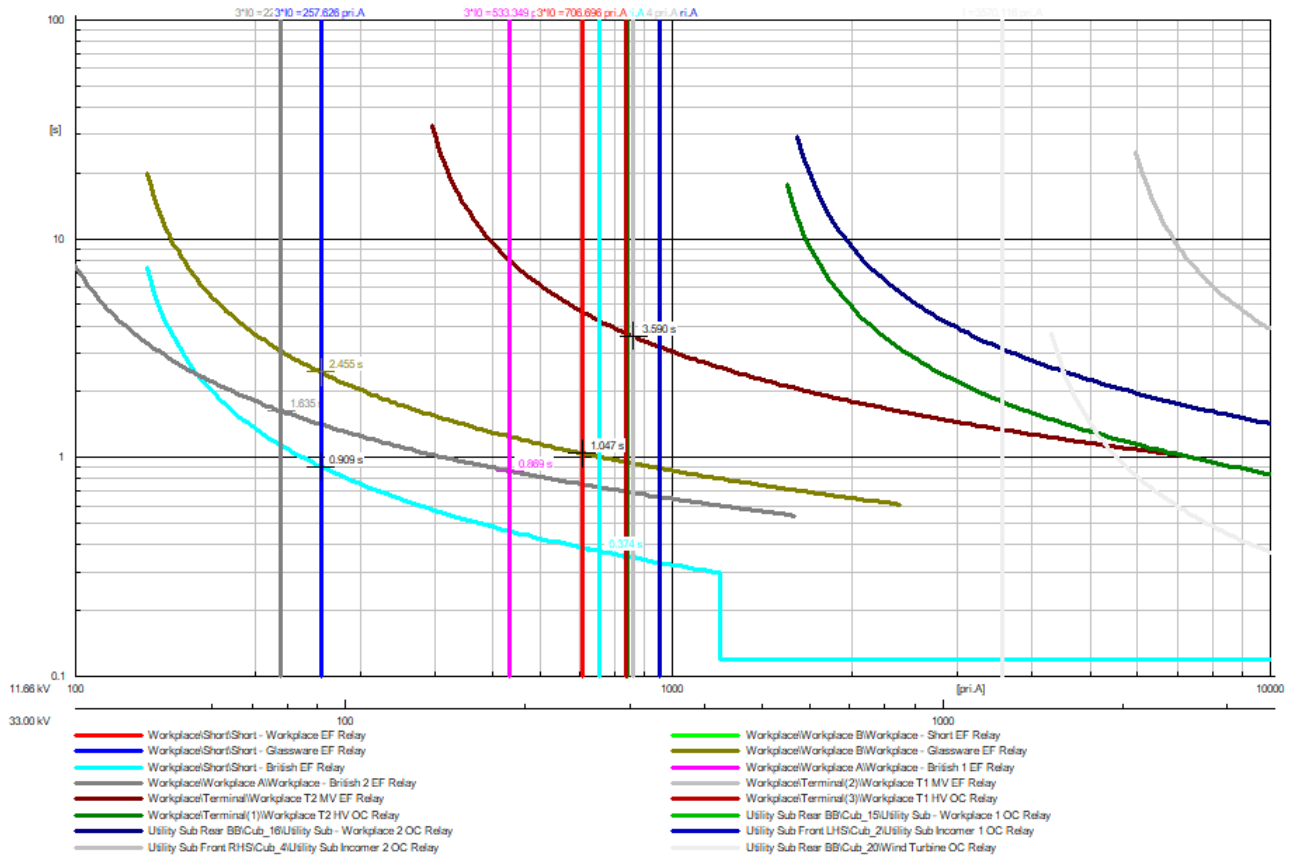


Figure H.46: The EF relay grading for a stage 1 single-phase fault at Short SS

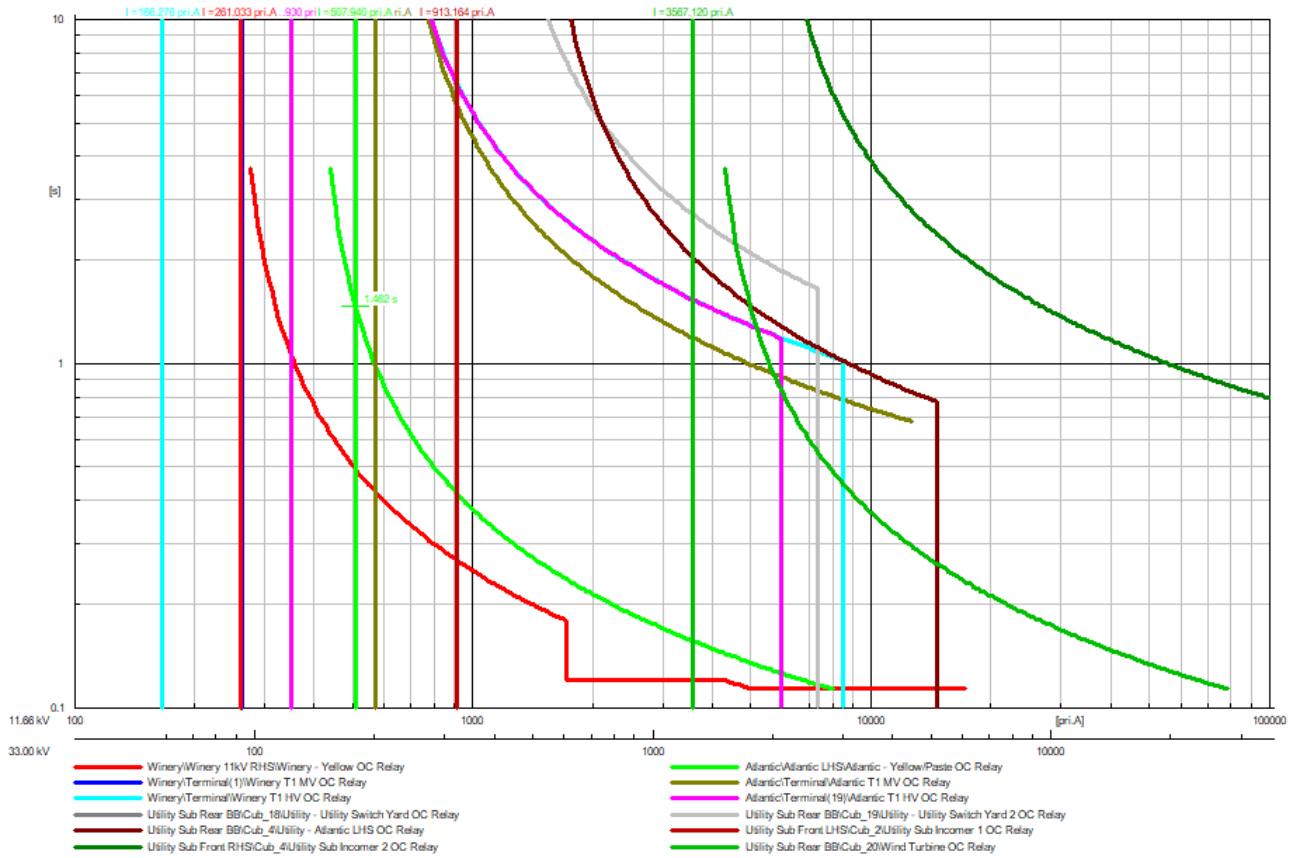


Figure H.47: The OC relay grading for a three-phase fault at Paste RMU 1 SS

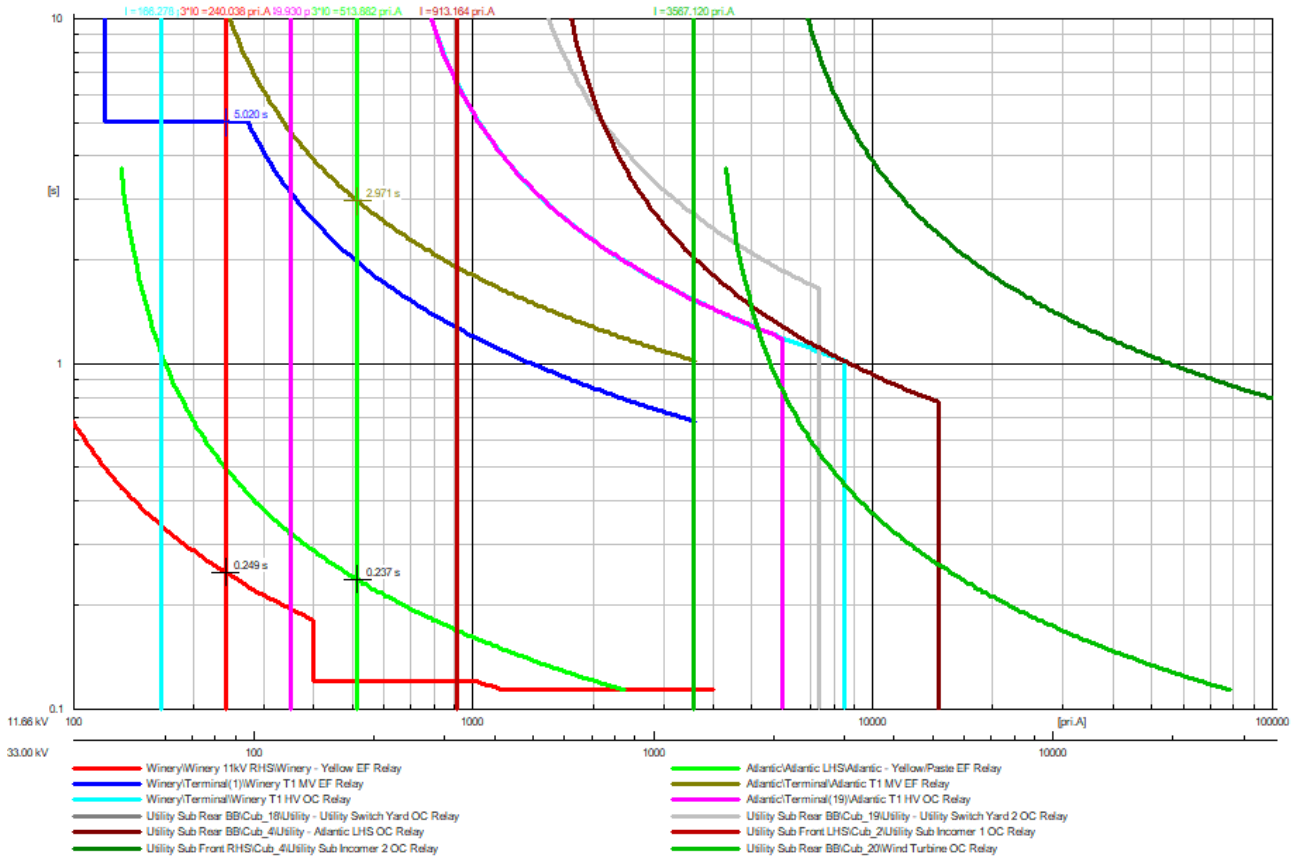


Figure H.48: The EF relay grading for a single-phase fault at Paste RMU 1 SS

Case 3

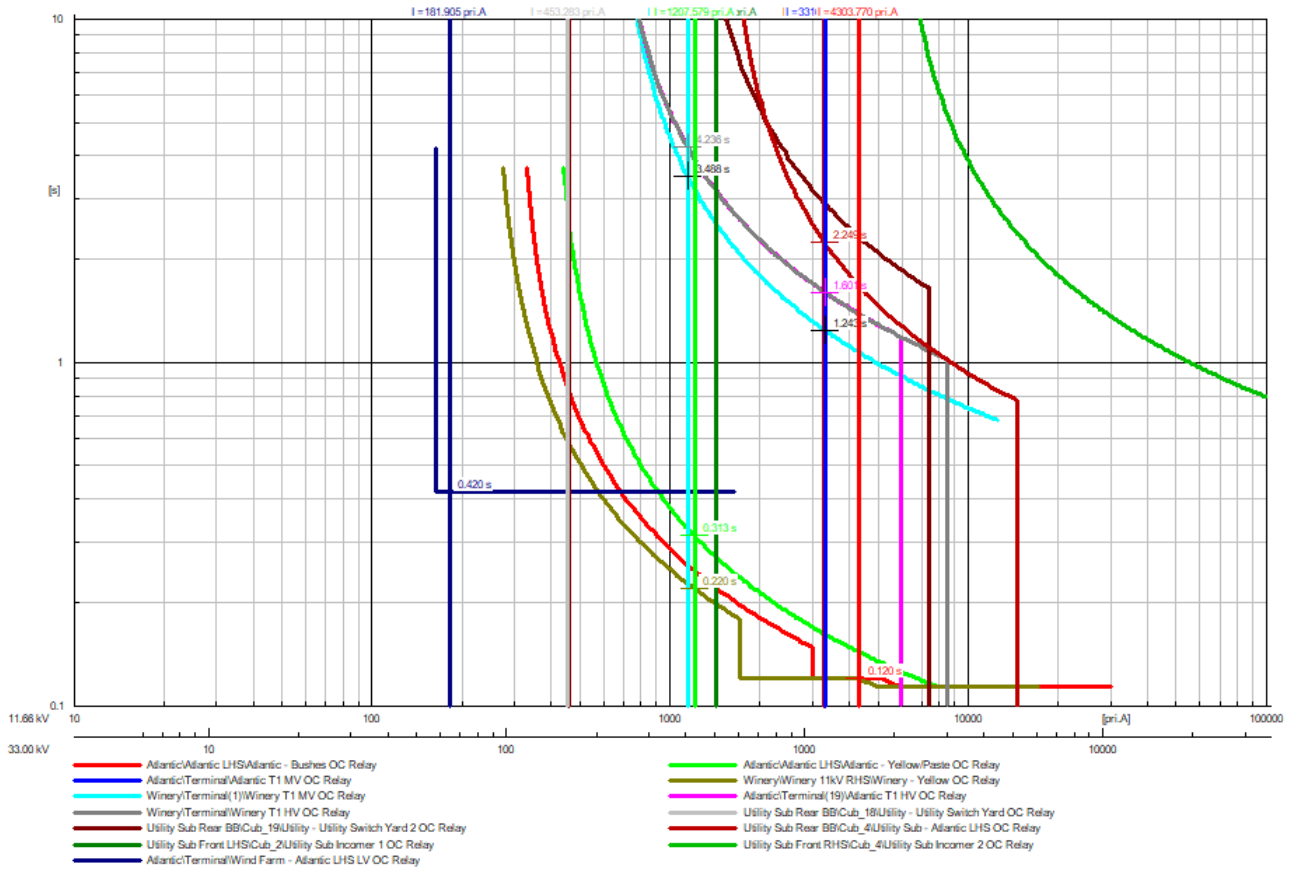


Figure H.49: The OC relay grading for a three-phase fault at Bushes SS

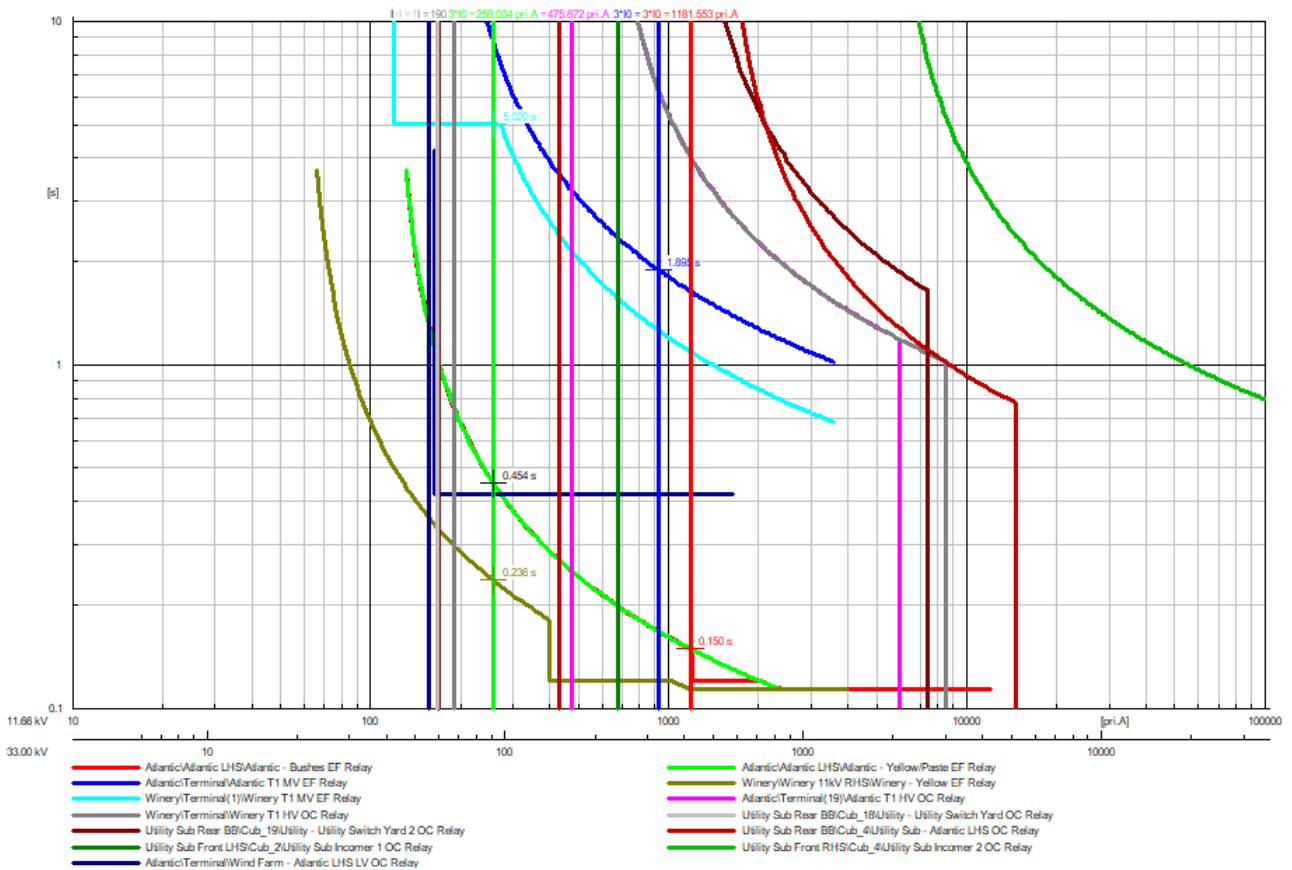


Figure H.50: The EF relay grading for a single-phase fault at Bushes SS

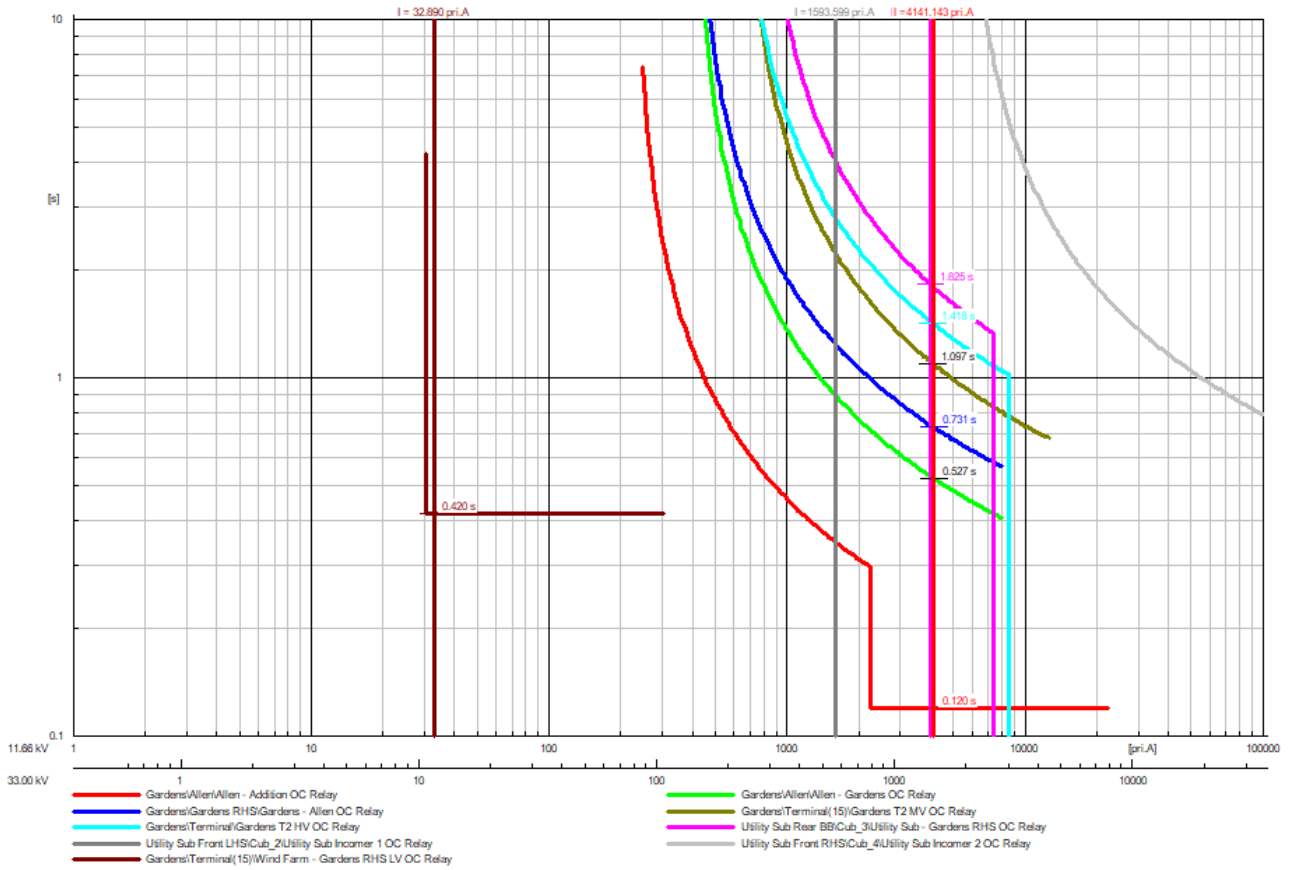


Figure H.51: The OC relay grading for a three-phase fault at Addition SS

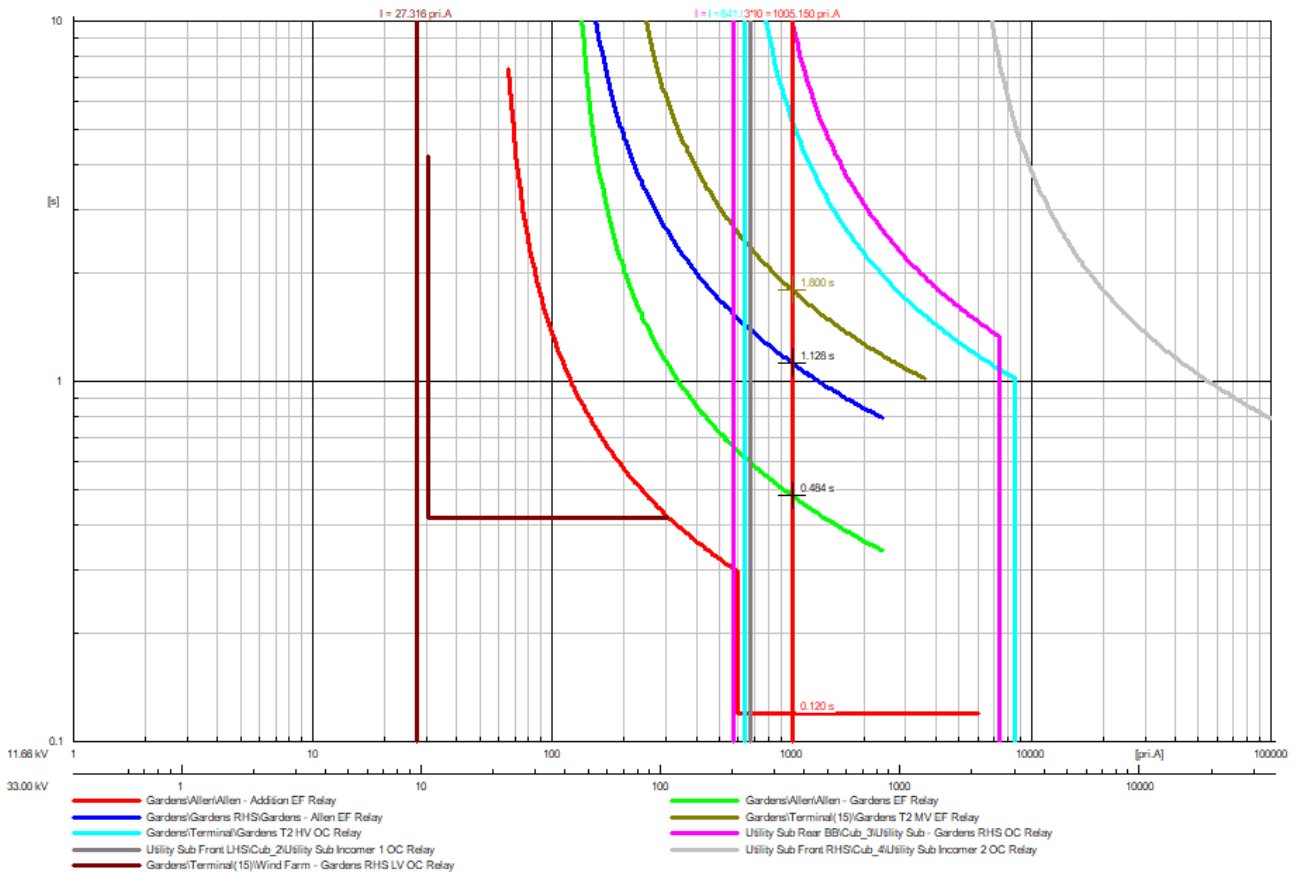


Figure H.52: The EF relay grading for a single-phase fault at Addition SS

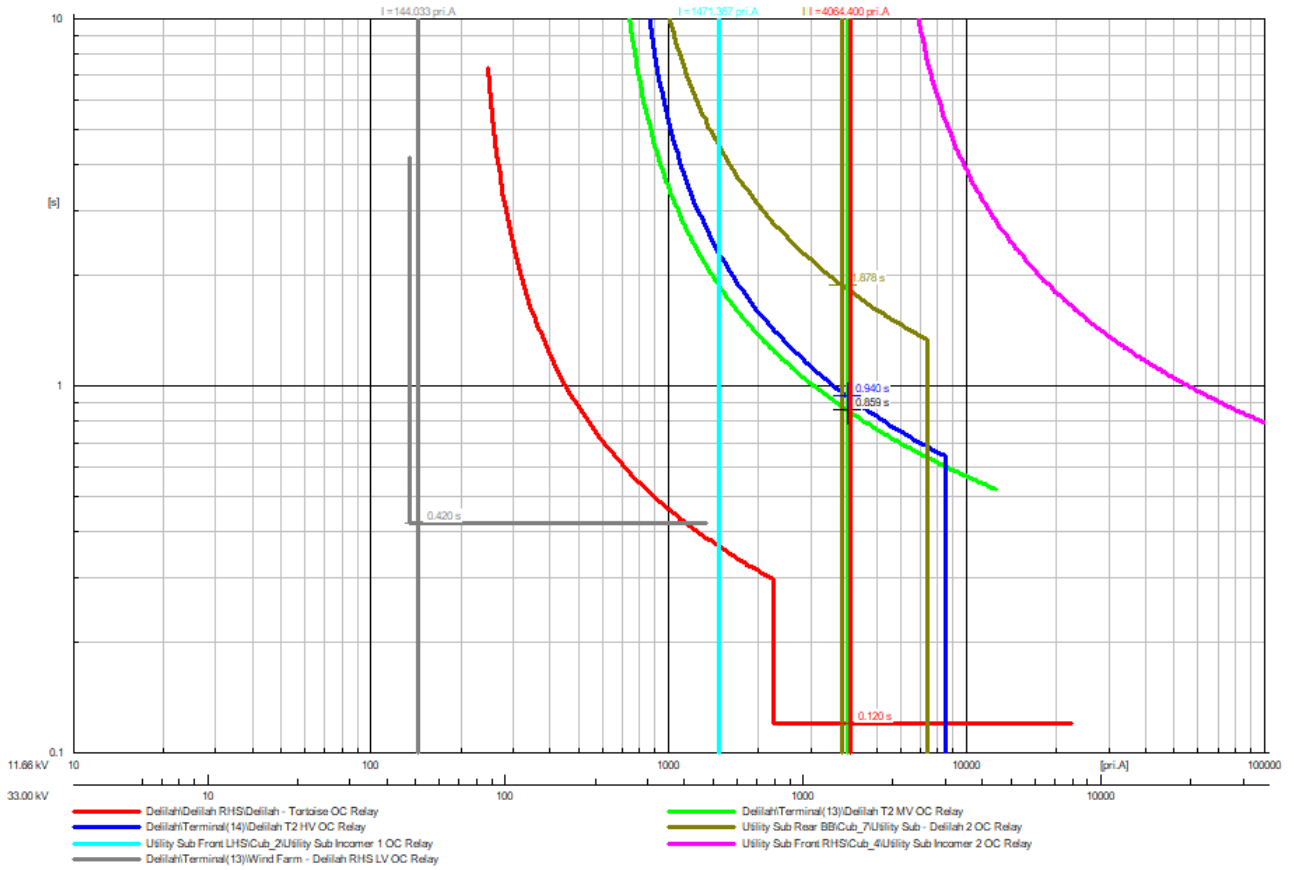


Figure H.53: The OC relay grading for a three-phase fault at Tortoise SS

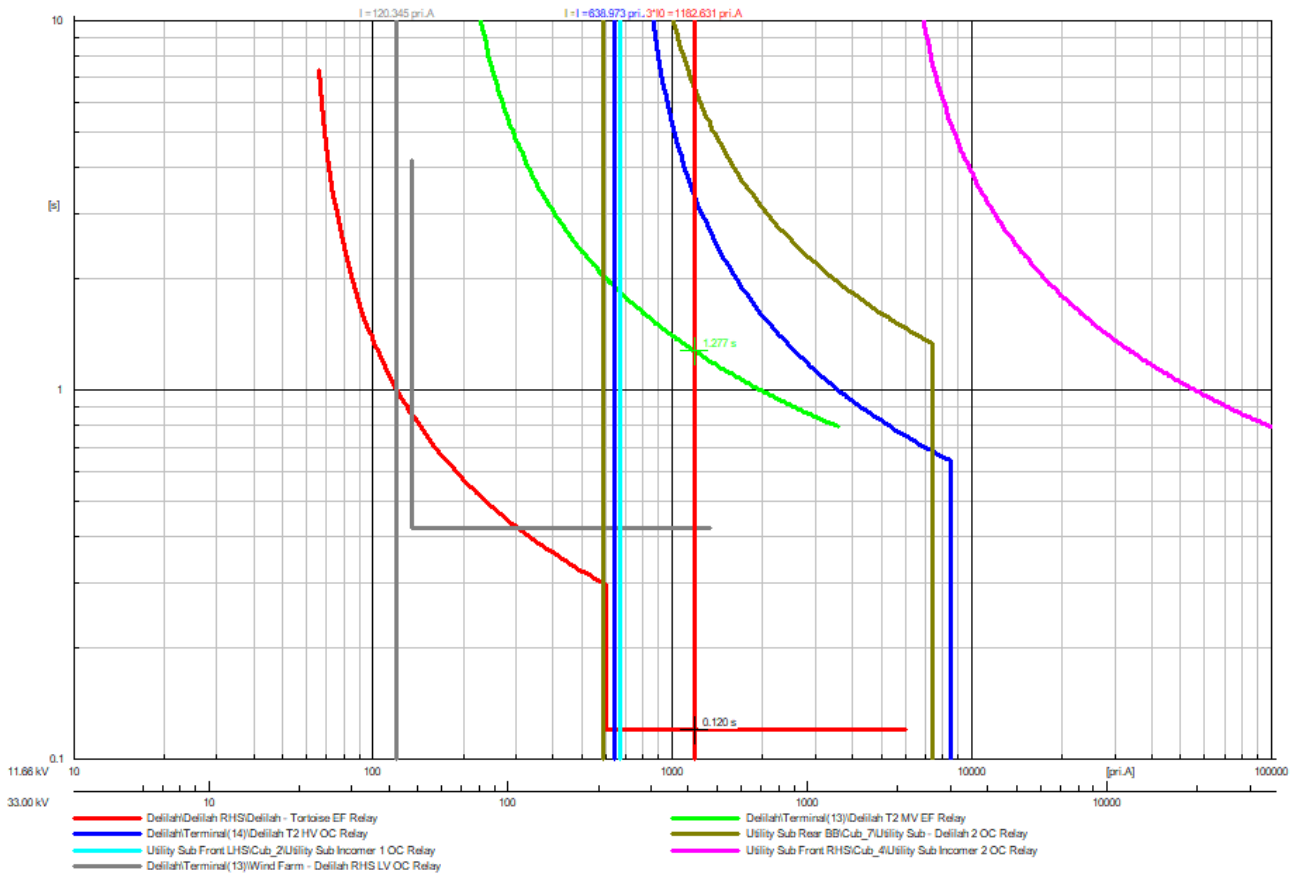


Figure H.54: The EF relay grading for a single-phase fault at Tortoise SS

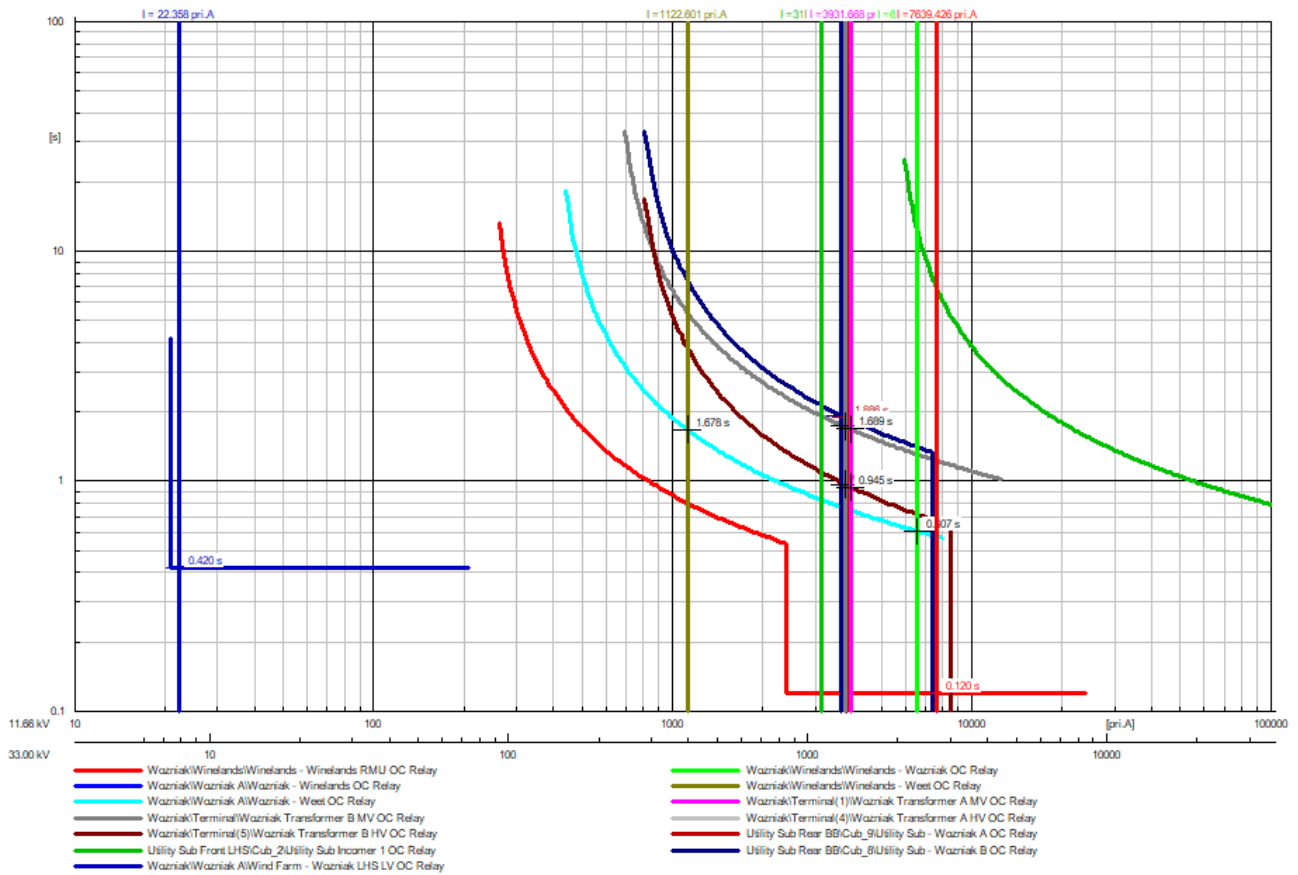


Figure H.55: The OC relay grading for a three-phase fault at Winelands RMU 1 SS

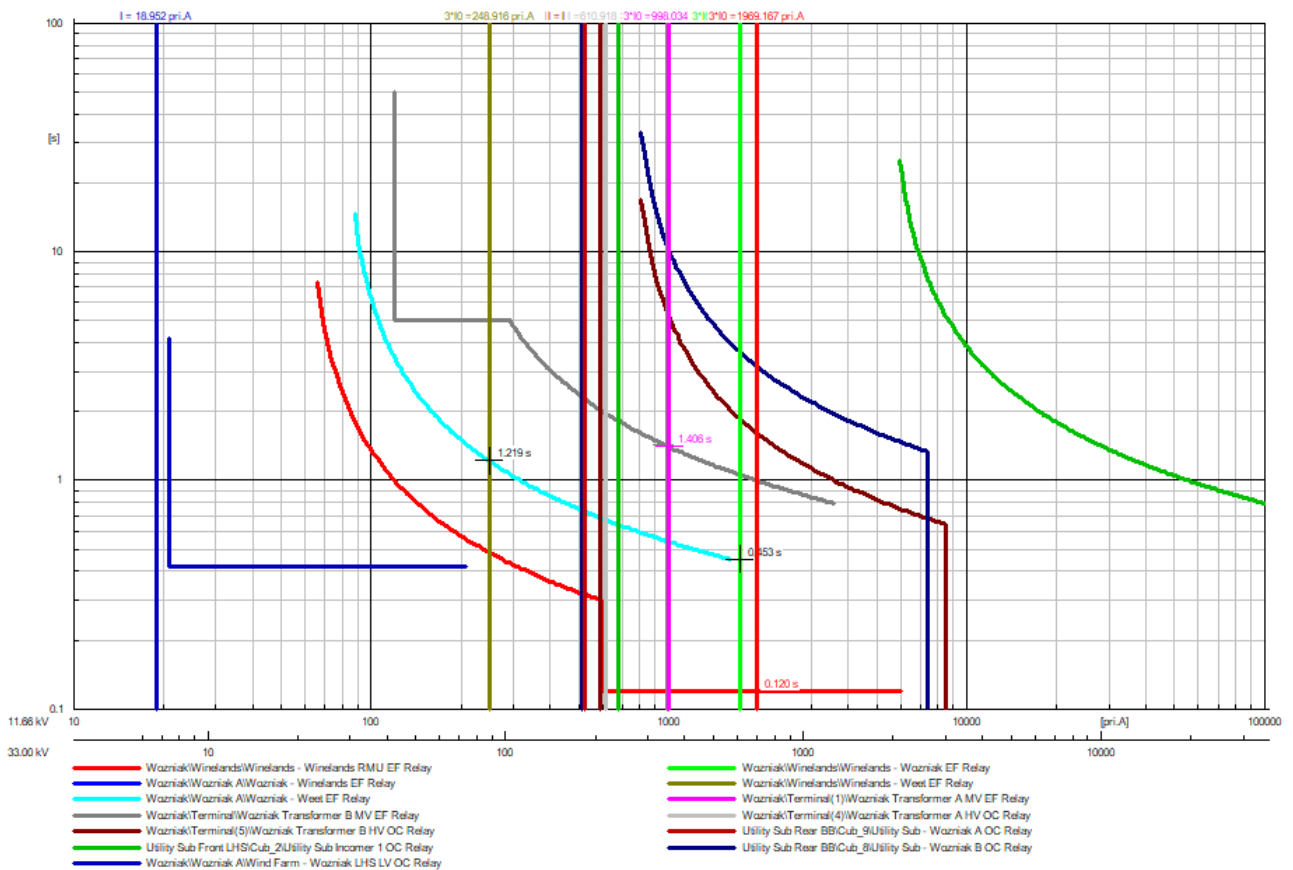


Figure H.56: The EF relay grading for a single-phase fault at Winelands RMU 1 SS

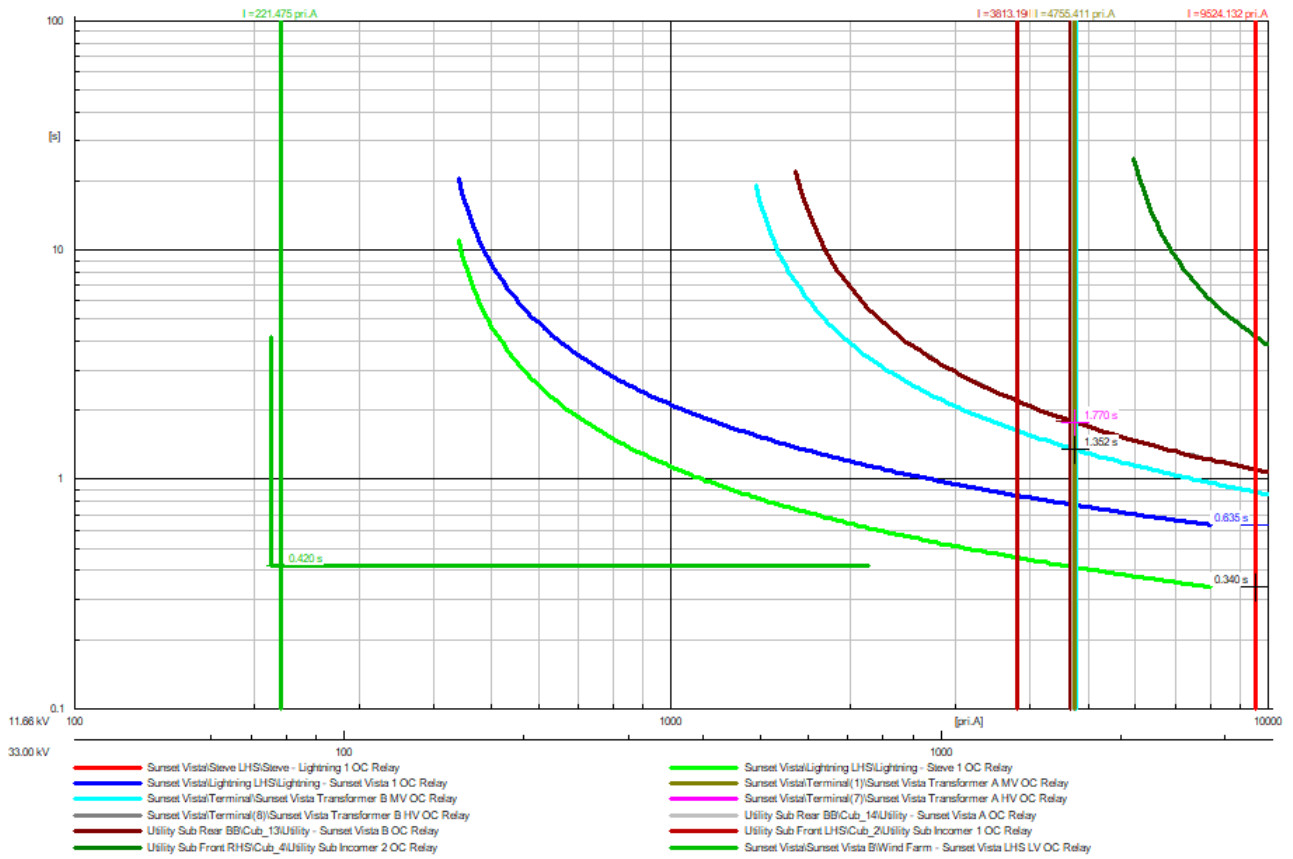


Figure H.57: The OC relay grading for a three-phase fault at Steve LHS SS

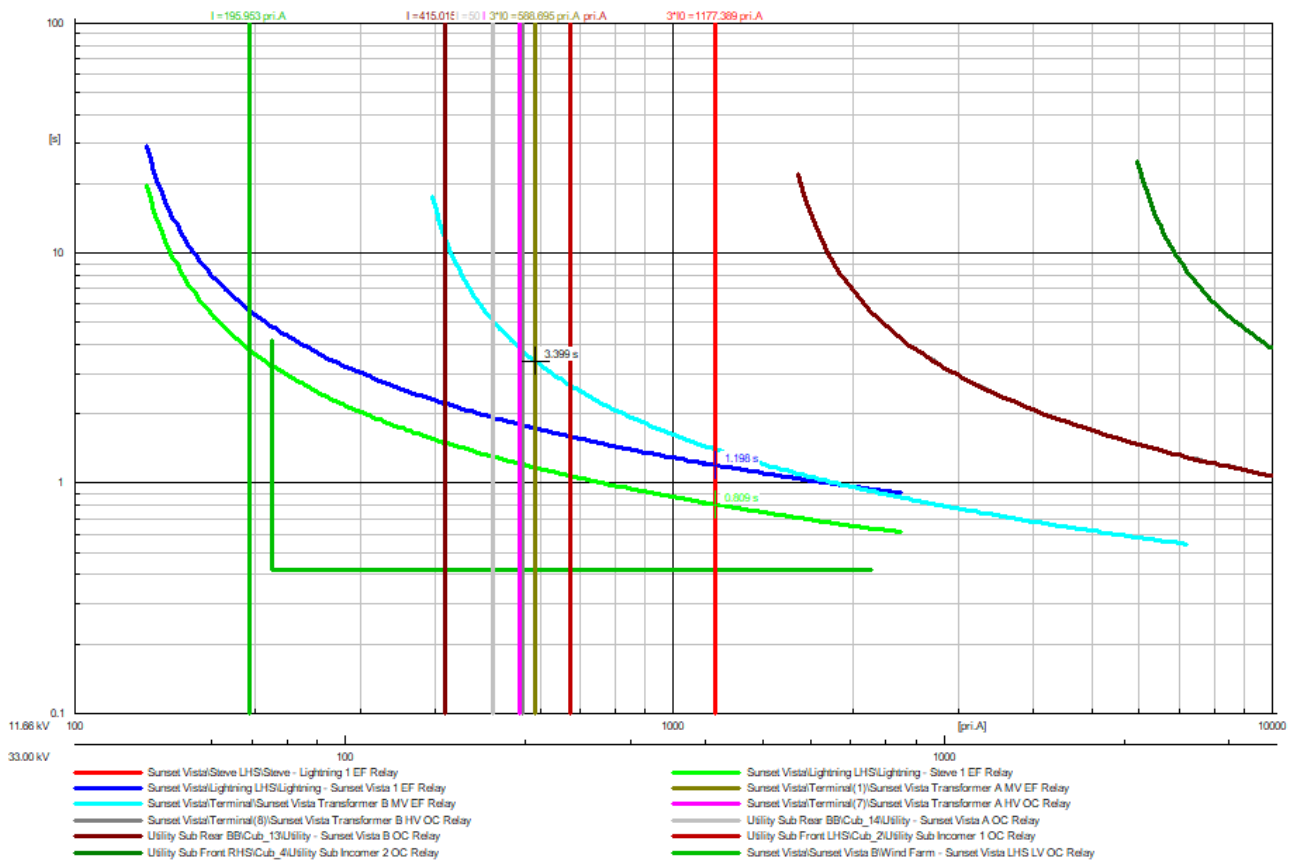


Figure H.58: The EF relay grading for a single-phase fault at Steve LHS SS

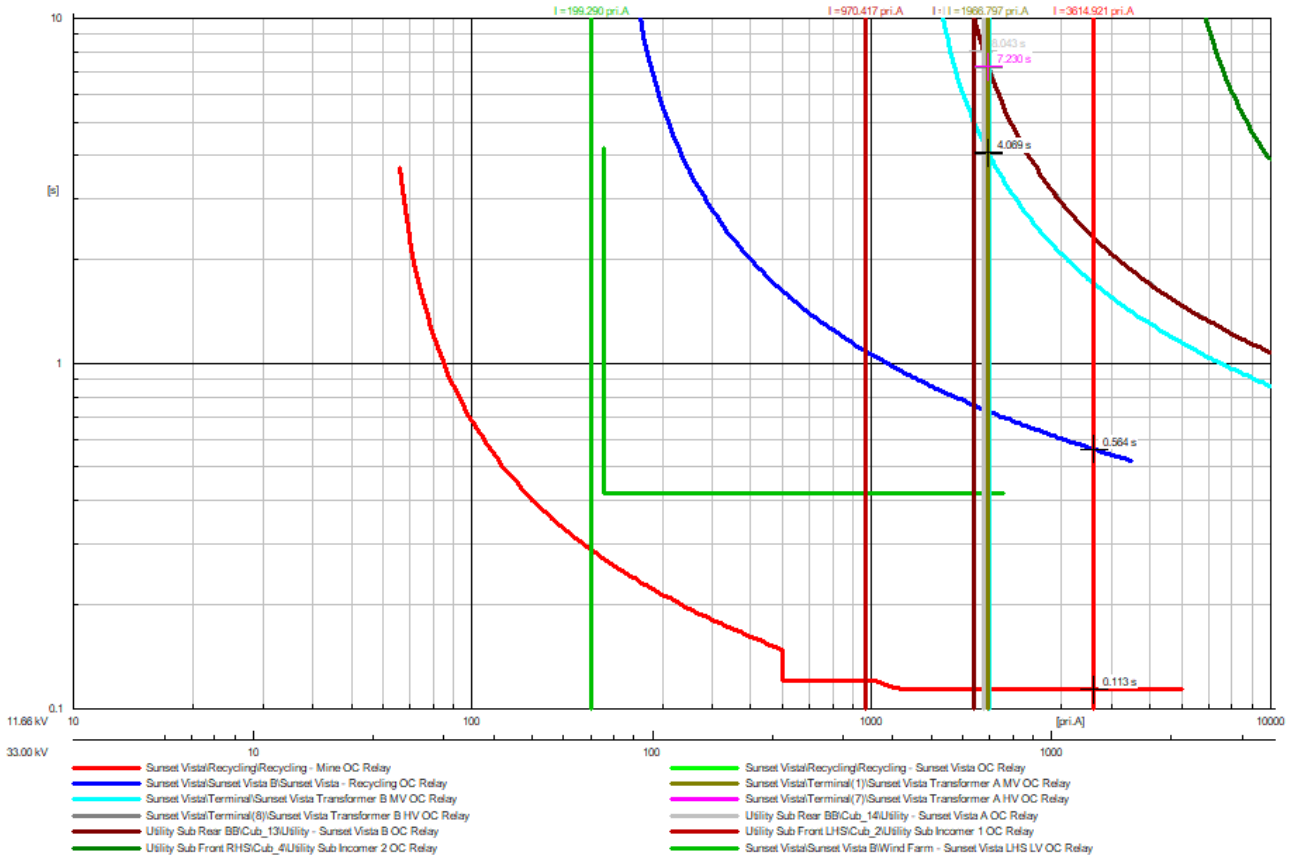


Figure H.59: The OC relay grading for a three-phase fault at Mine SS

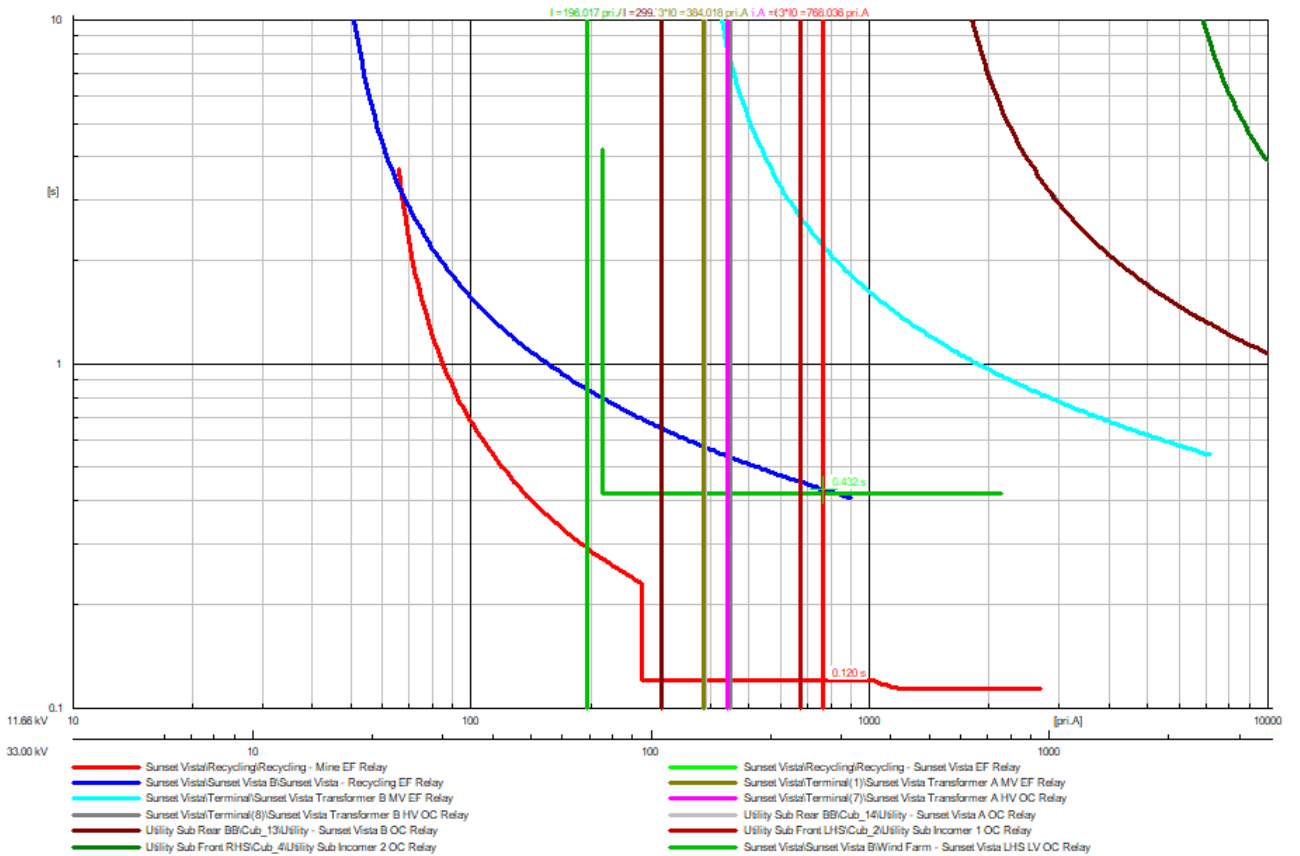


Figure H.60: The EF relay grading for a single-phase fault at Mine SS

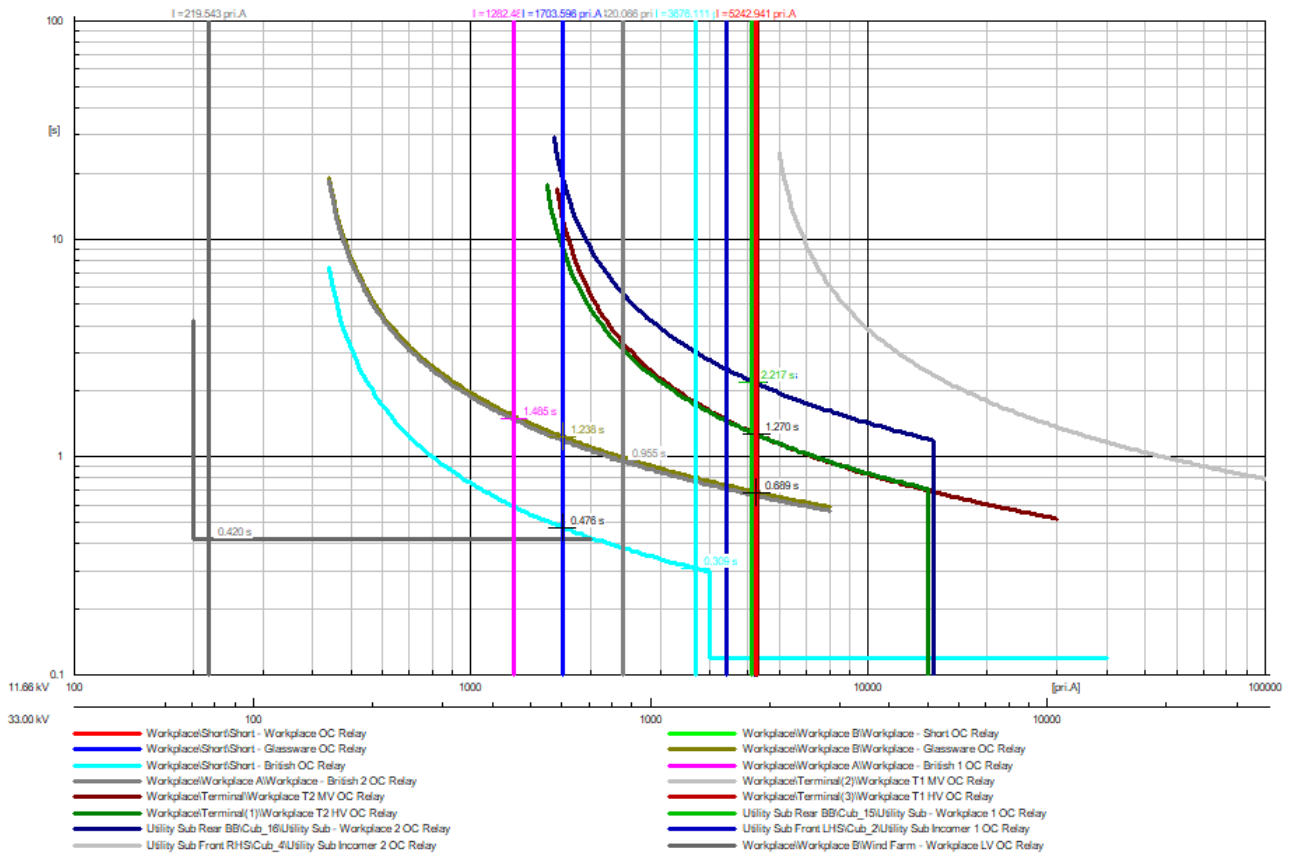


Figure H.61: The OC relay grading for a stage 1 three-phase fault at Short SS

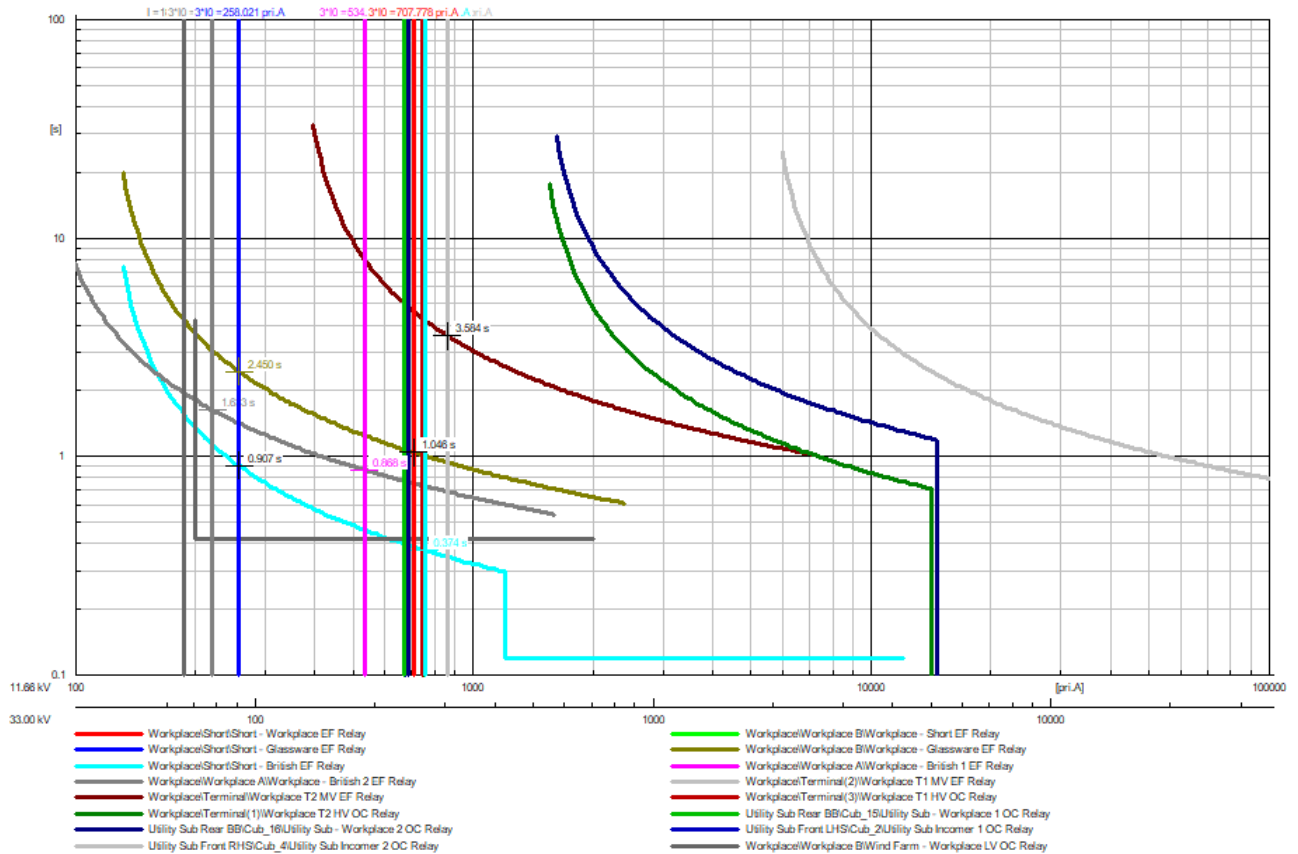


Figure H.62: The EF relay grading for a stage 1 single-phase fault at Short SS

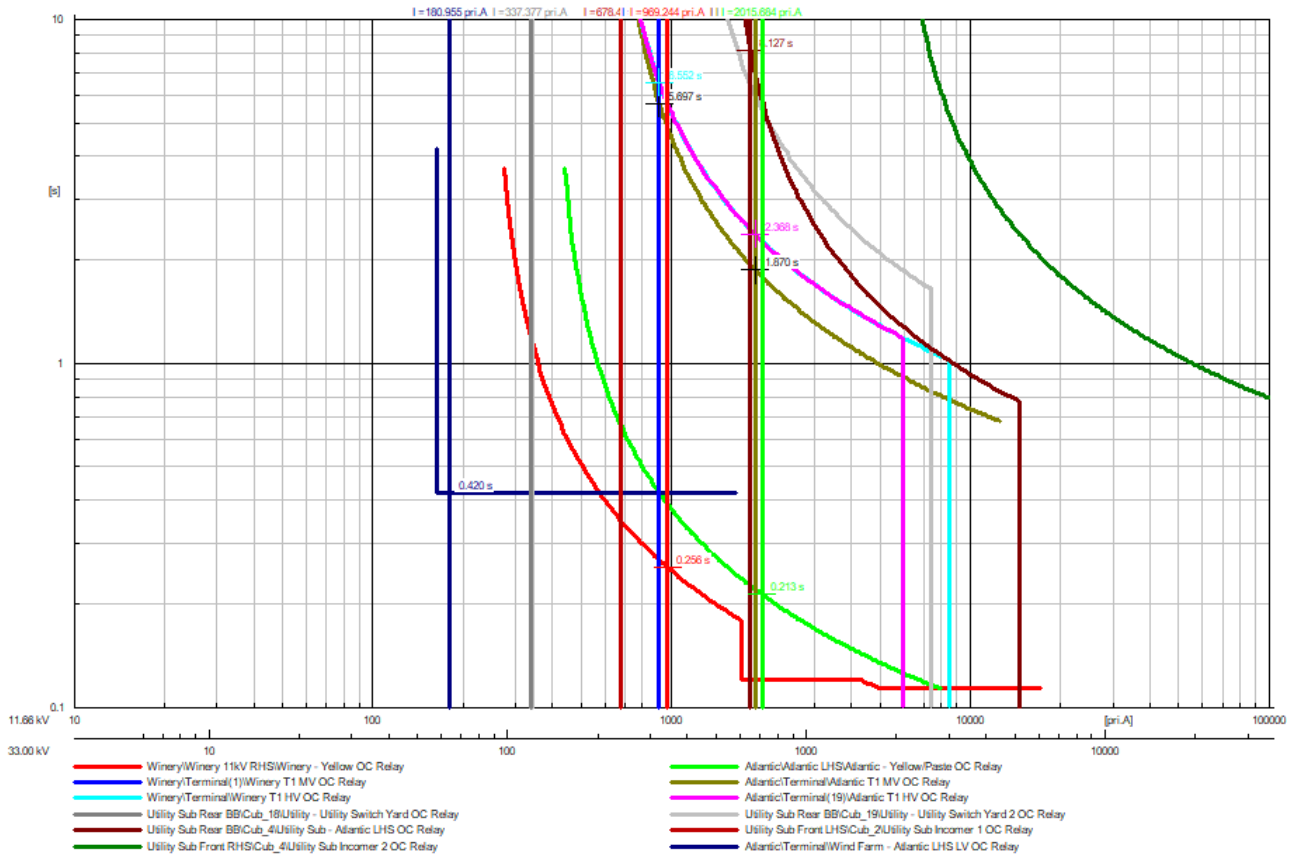


Figure H.63: The OC relay grading for a three-phase fault at Paste RMU 1 SS

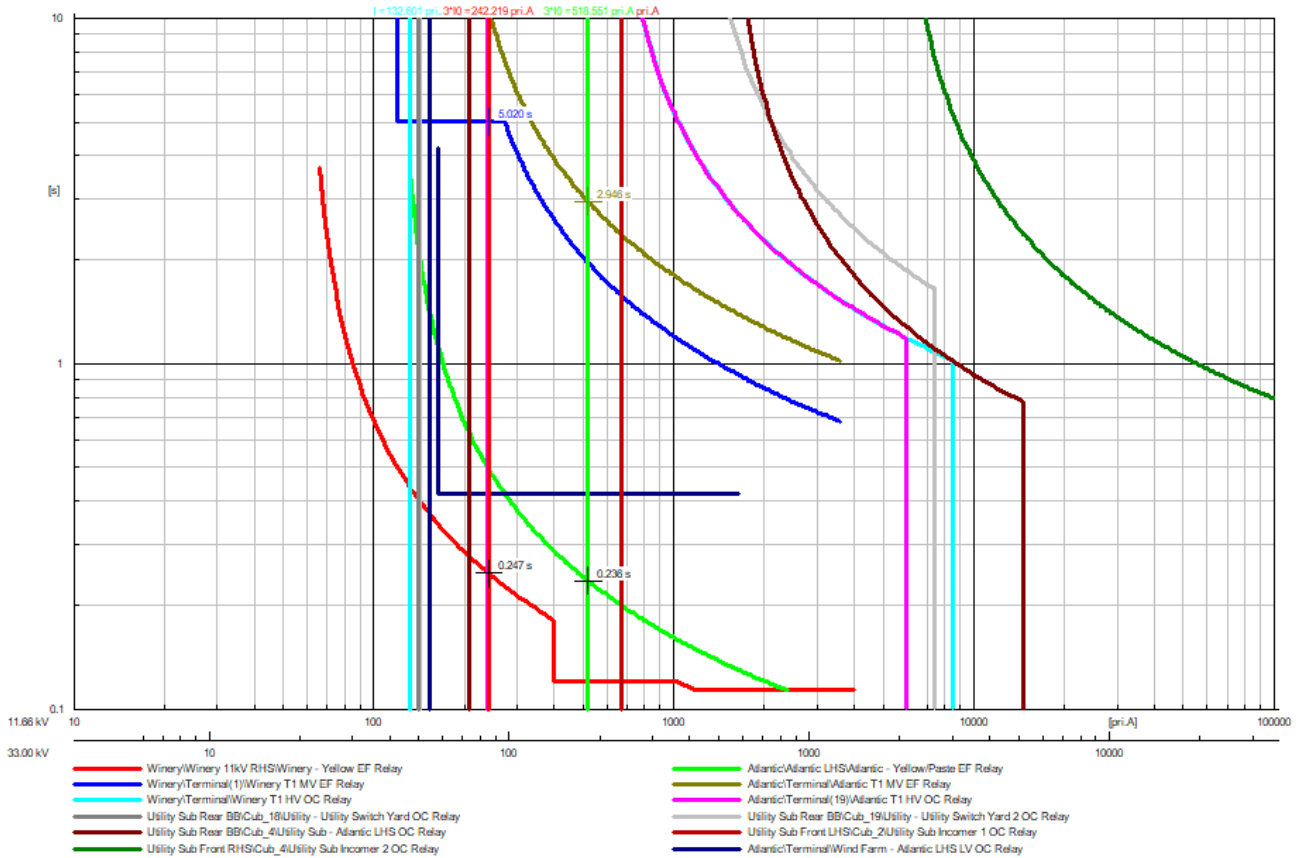


Figure H.64: The EF relay grading for a single-phase fault at Paste RMU 1 SS

Case 4

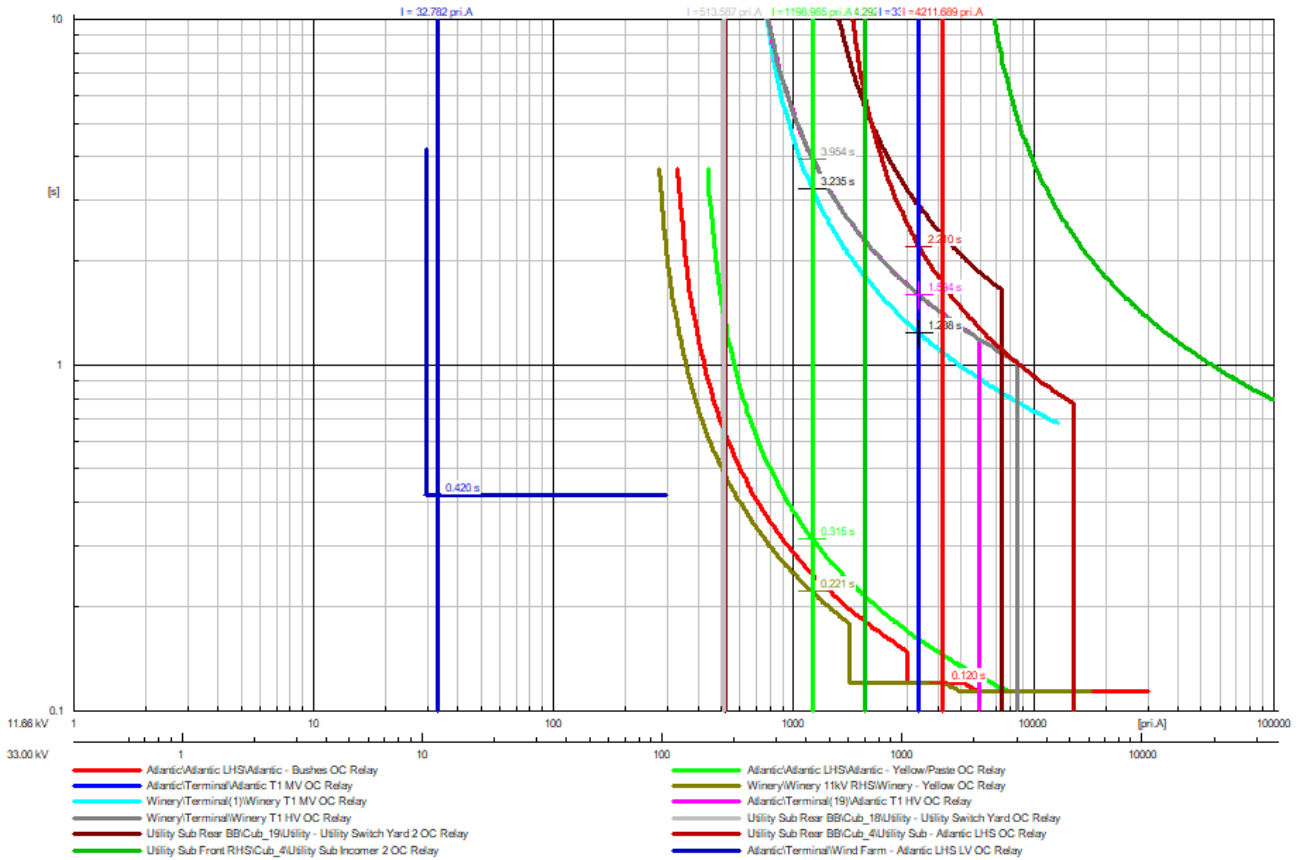


Figure H.65: The OC relay grading for a three-phase fault at Bushes SS

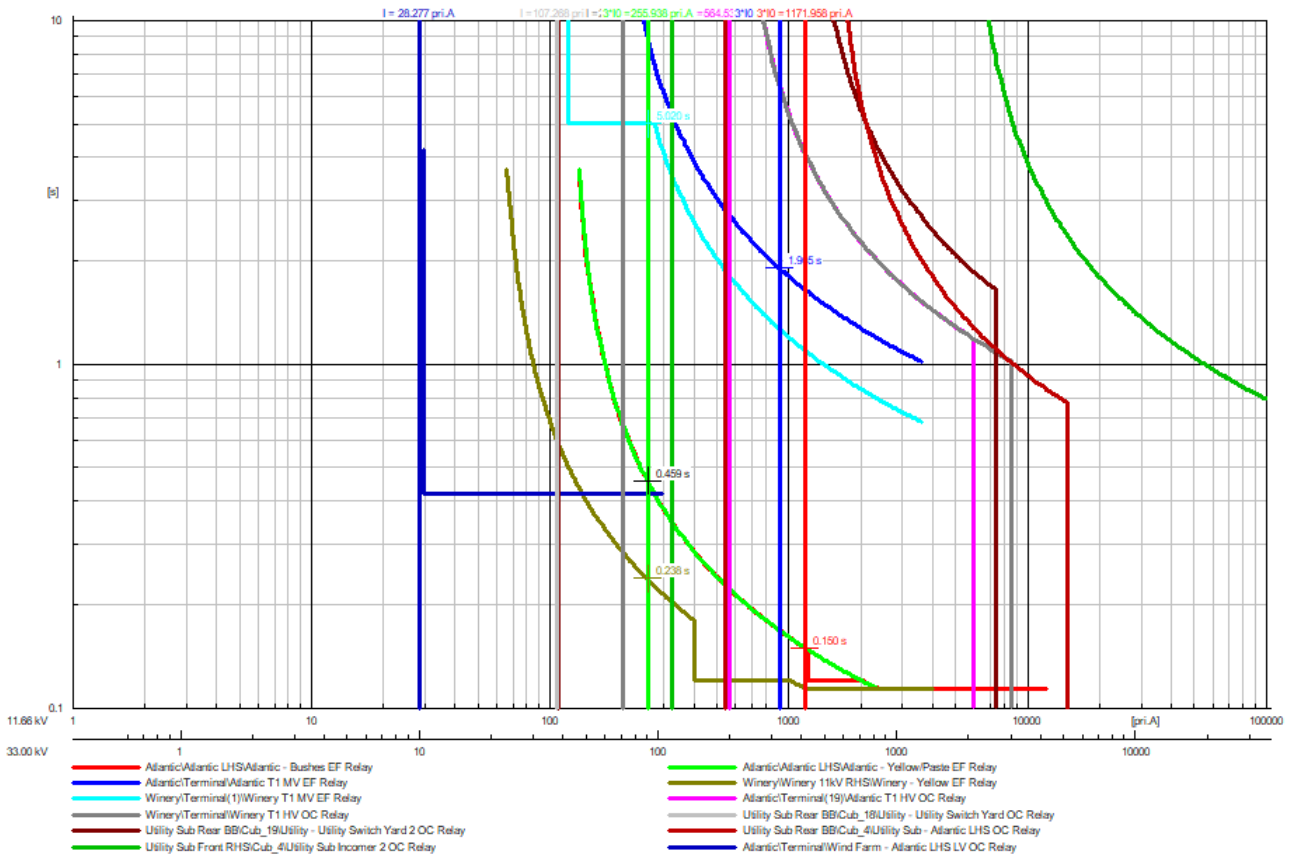


Figure H.66: The EF relay grading for a single-phase fault at Bushes SS

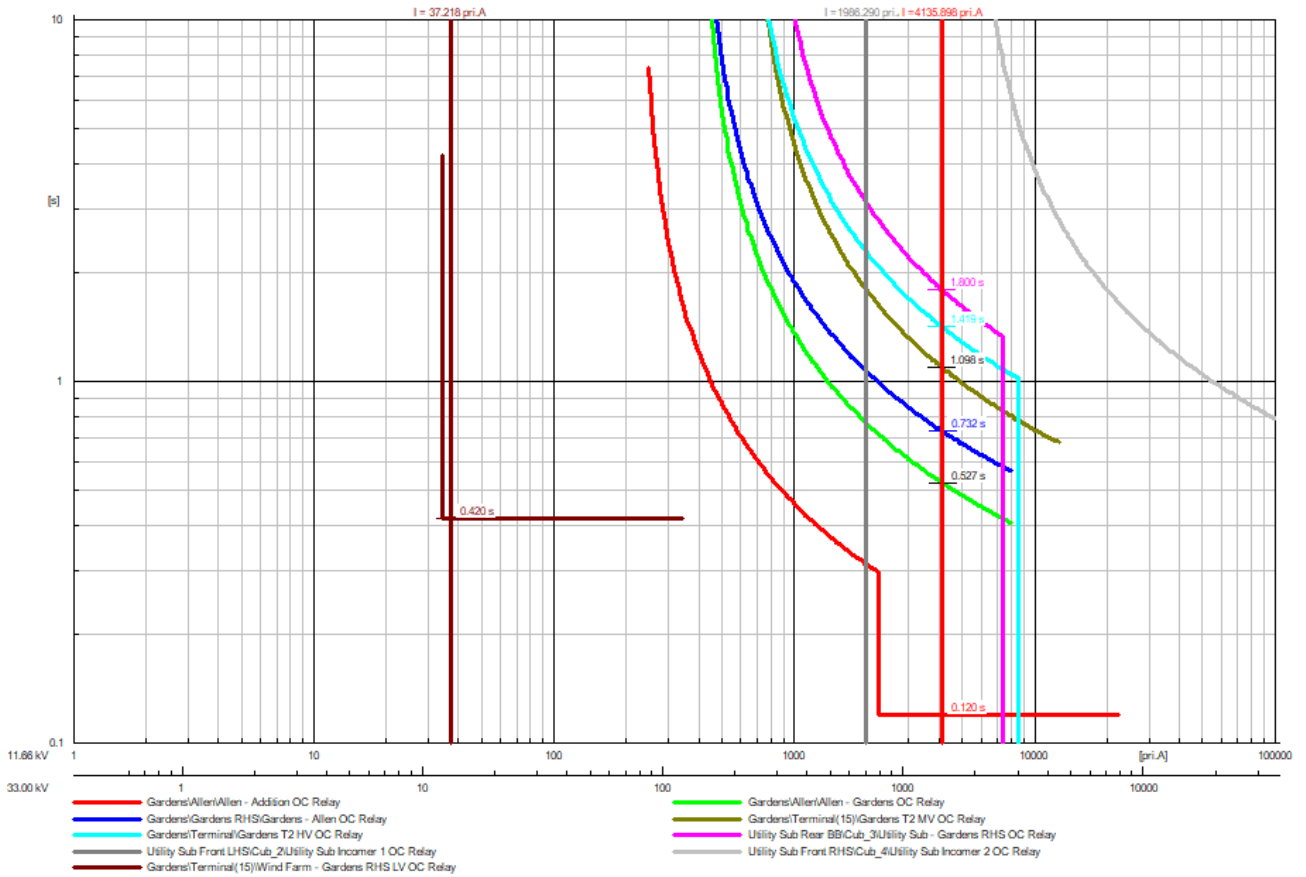


Figure H.67: The OC relay grading for a three-phase fault at Addition SS

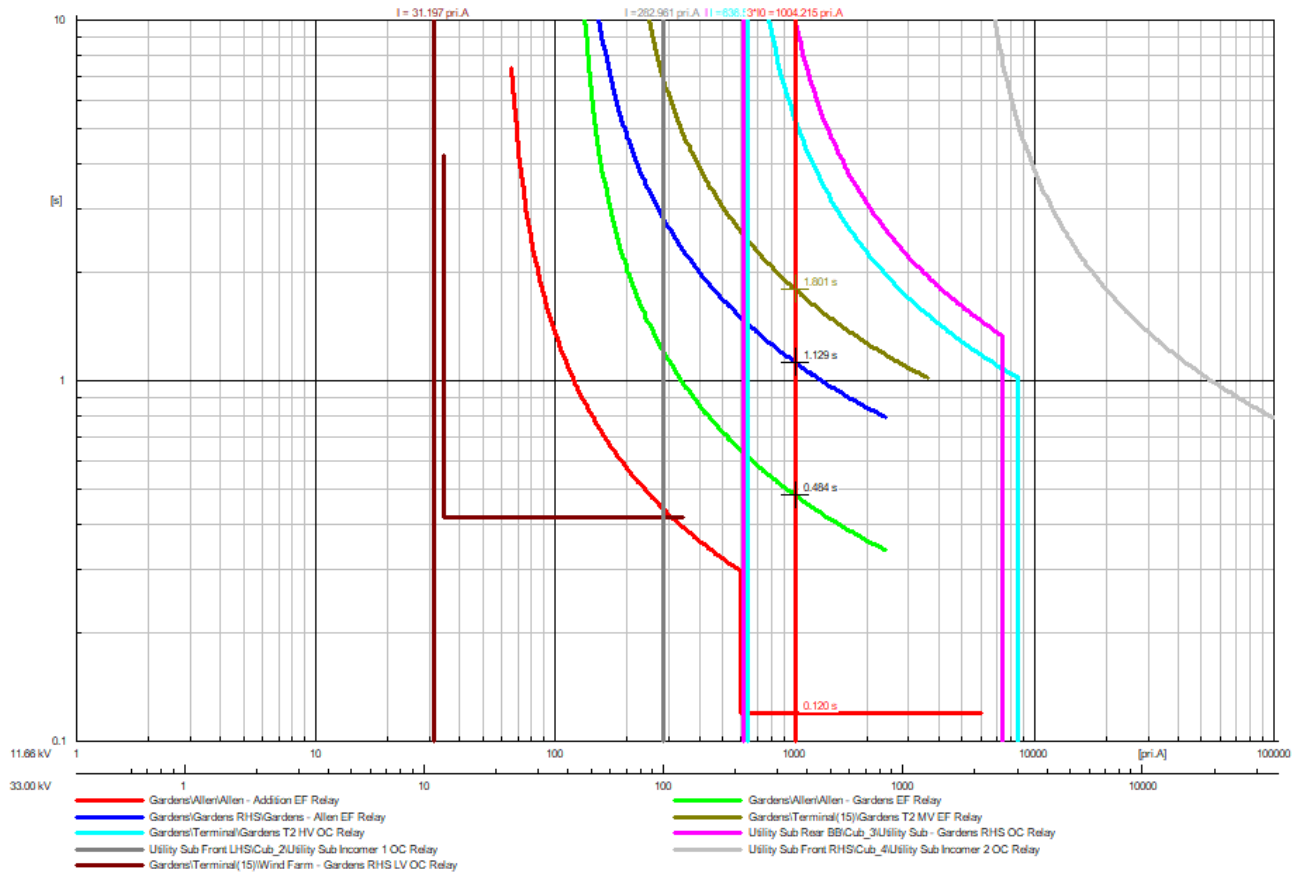


Figure H.68: The EF relay grading for a single-phase fault at Addition SS

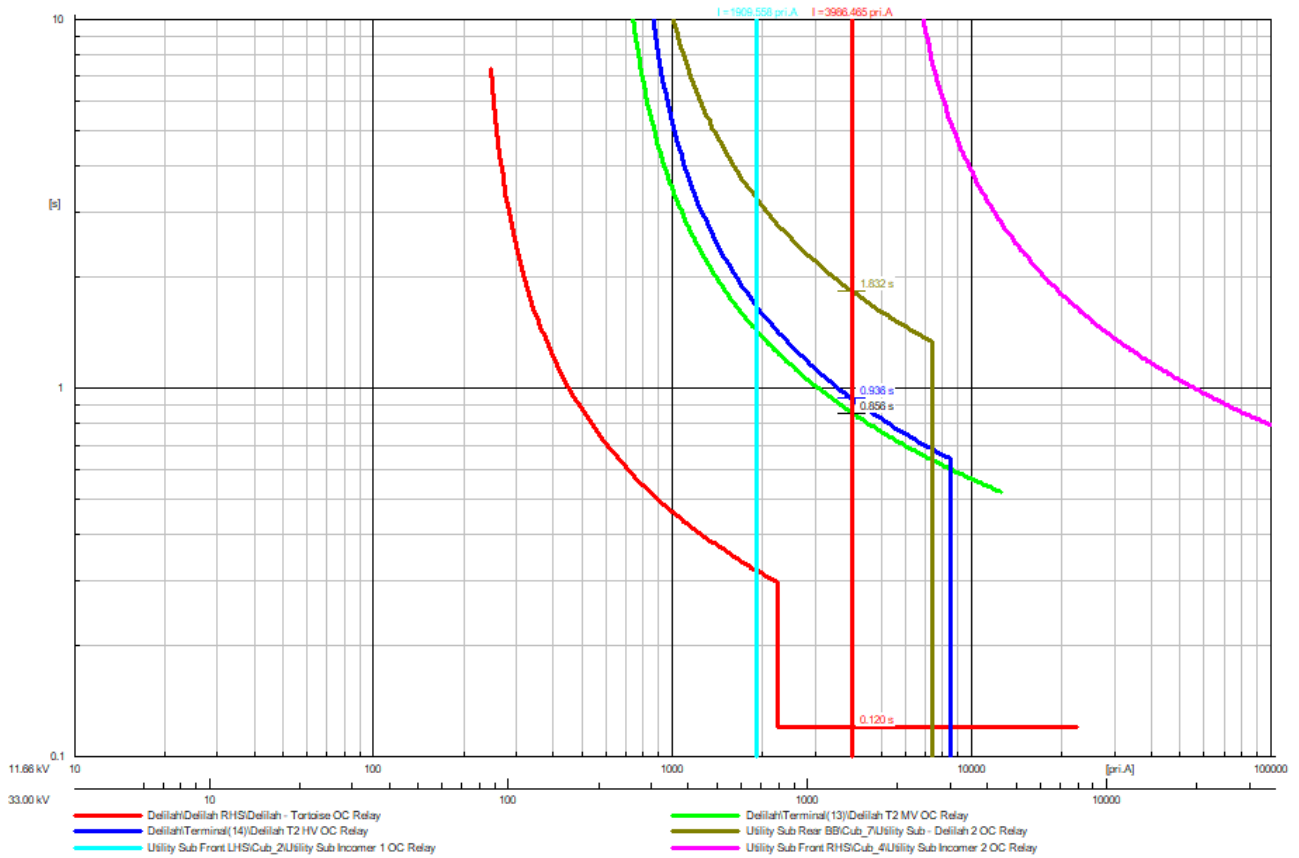


Figure H.69: The OC relay grading for a three-phase fault at Tortoise SS

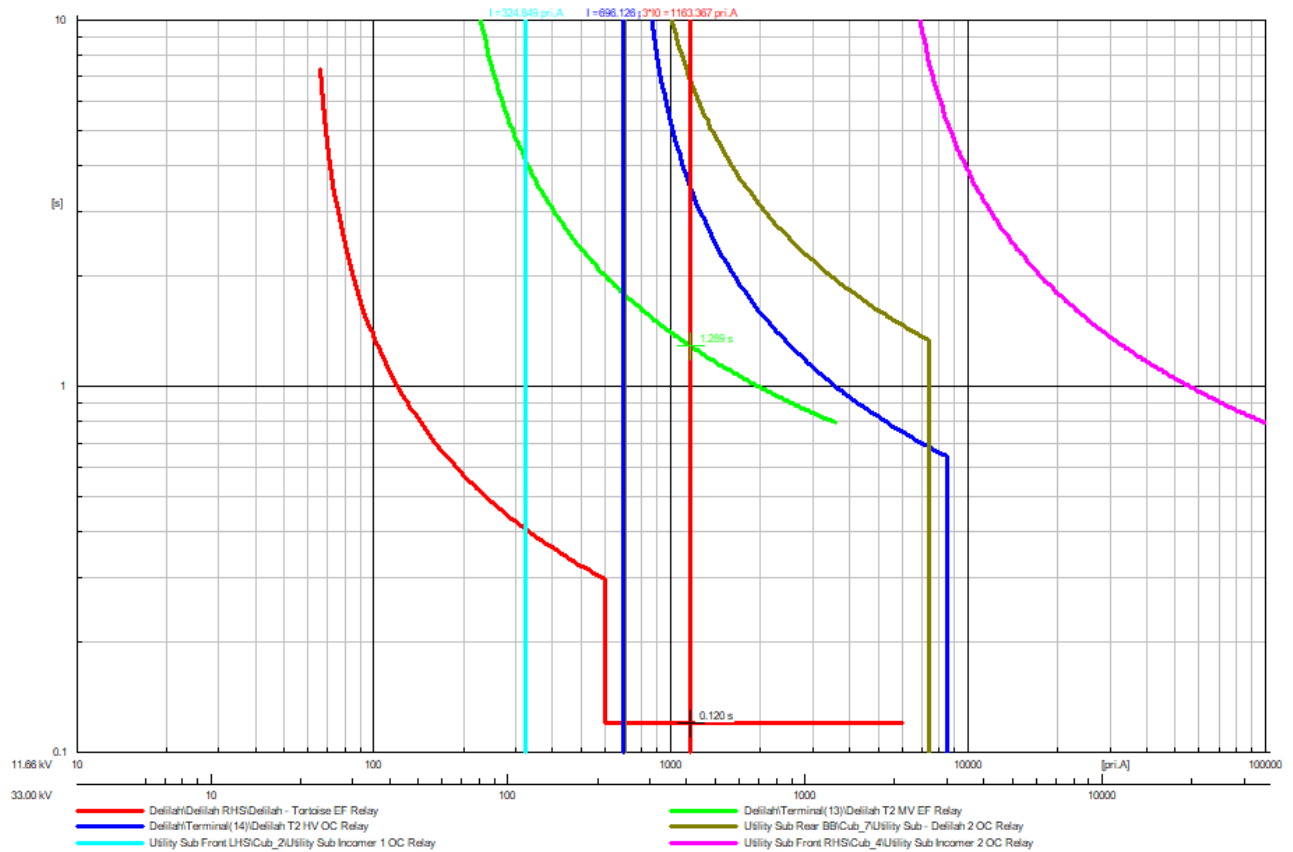


Figure H.70: The EF relay grading for a single-phase fault at Tortoise SS

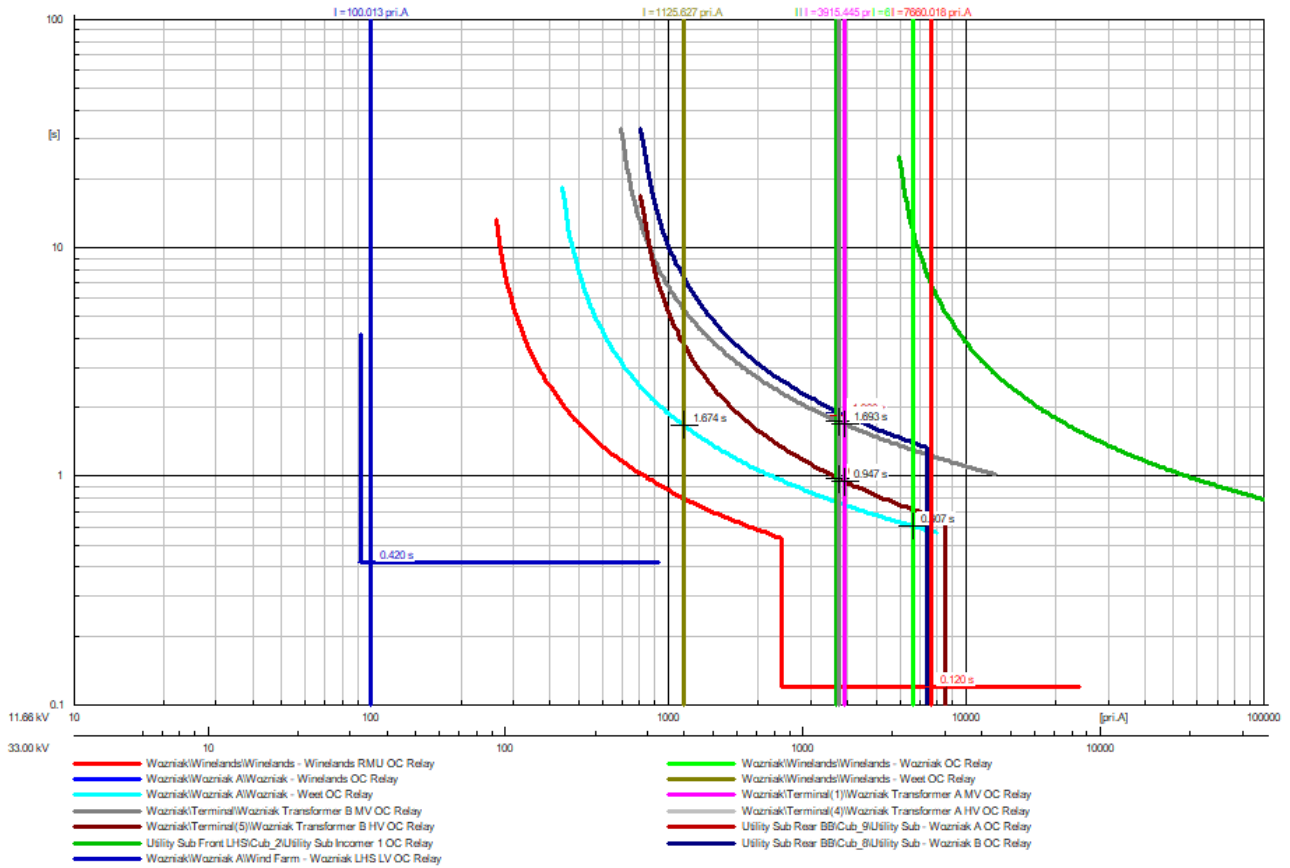


Figure H.71: The OC relay grading for a three-phase fault at Winelands RMU 1 SS

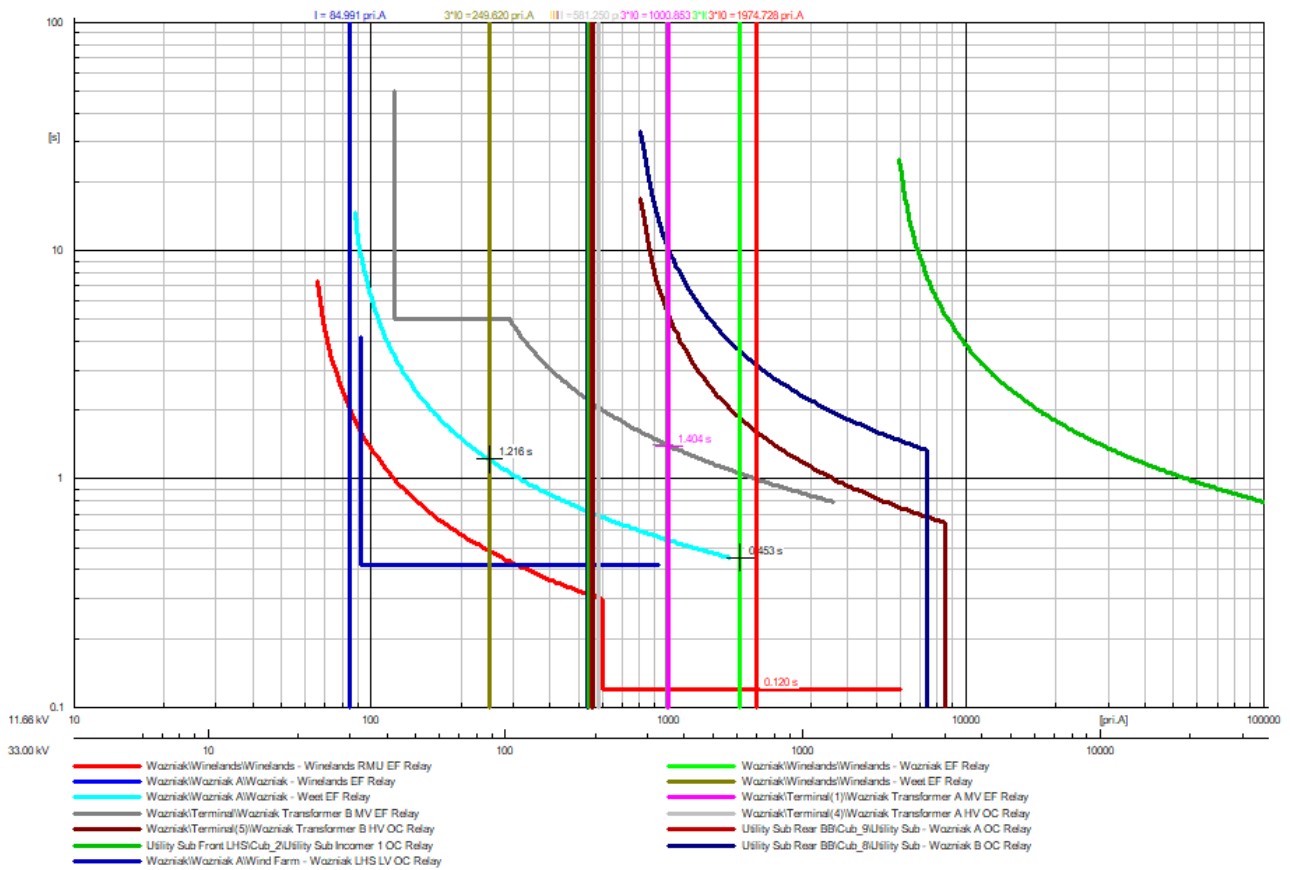


Figure H.72: The EF relay grading for a single-phase fault at Winelands RMU 1 SS

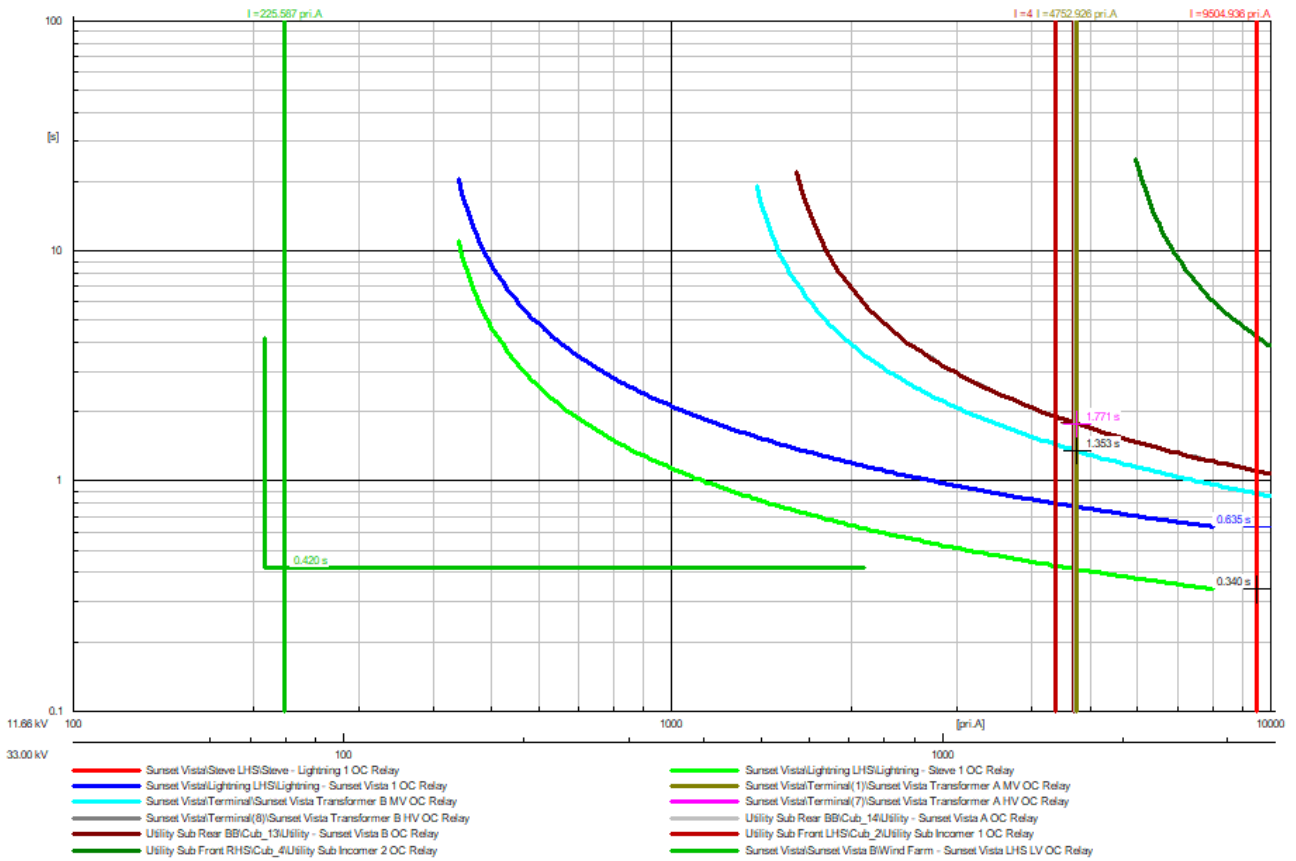


Figure H.73: The OC relay grading for a three-phase fault at Steve LHS SS

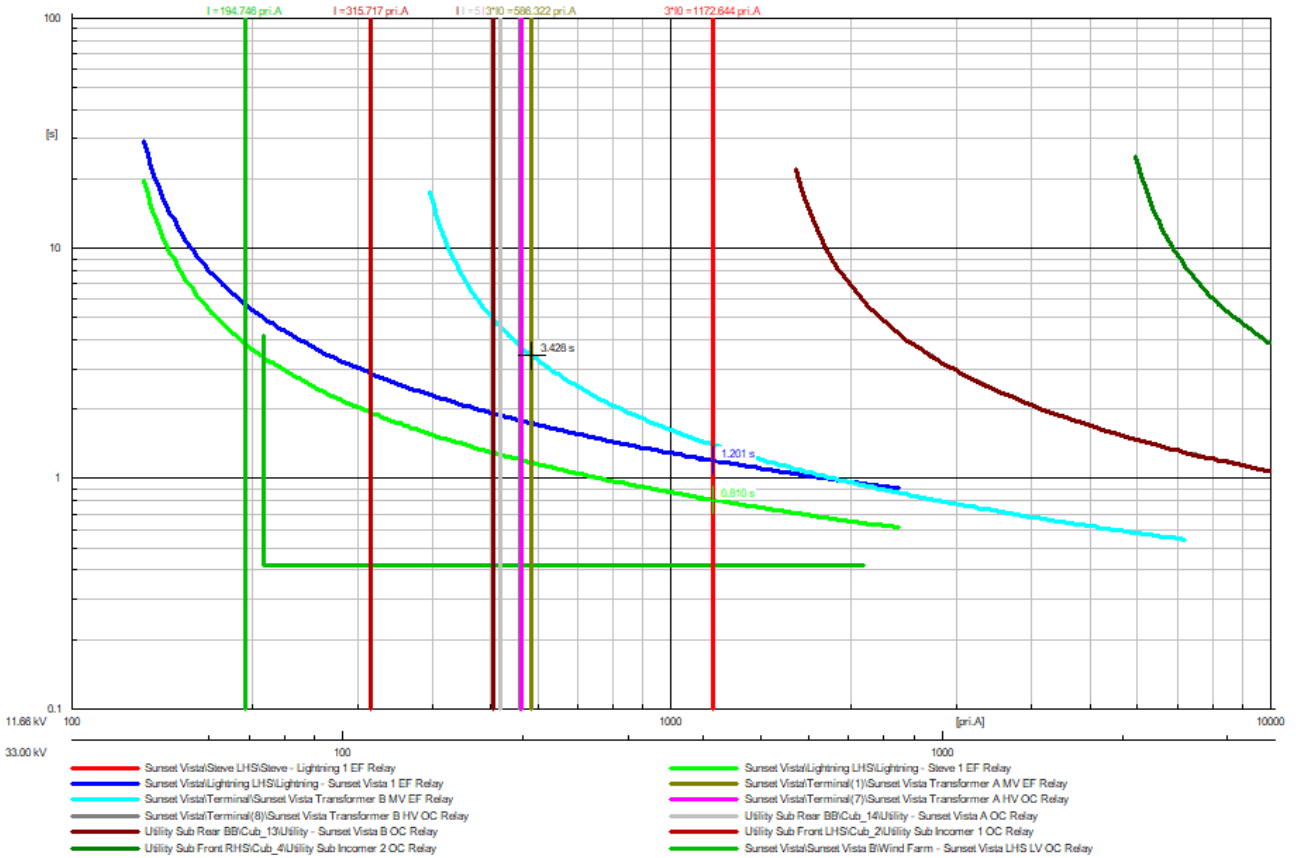


Figure H.74: The EF relay grading for a single-phase fault at Steve LHS SS

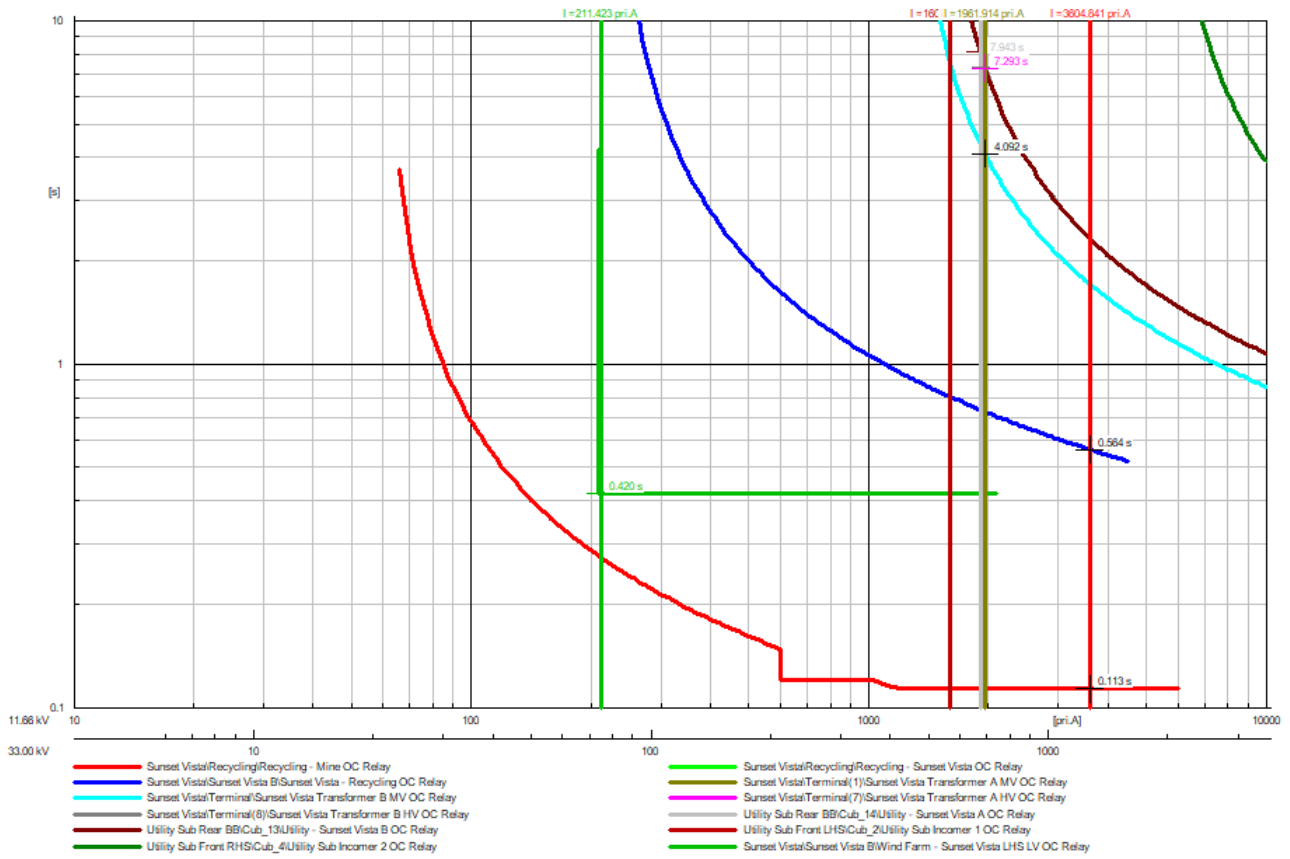


Figure H.75: The OC relay grading for a three-phase fault at Mine SS

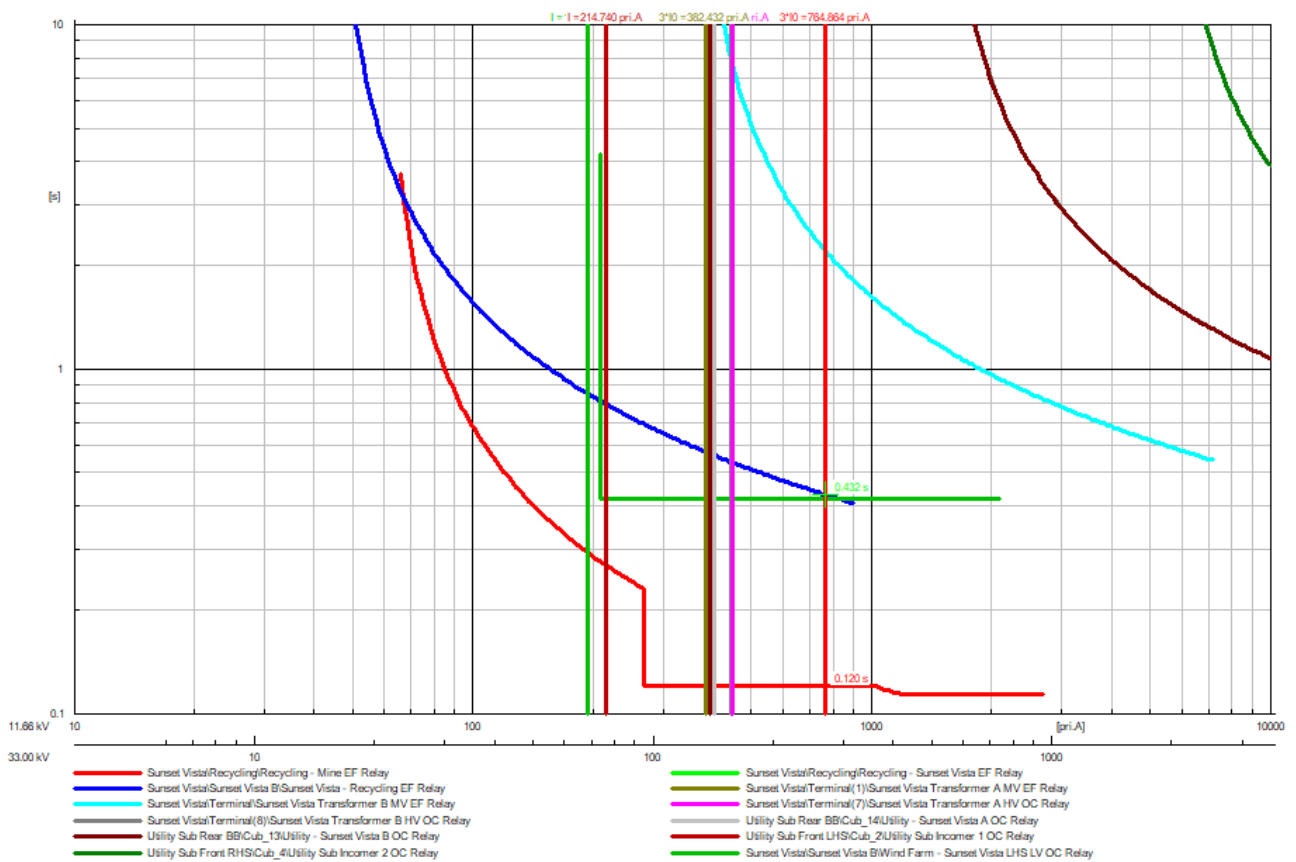


Figure H.76: The EF relay grading for a single-phase fault at Mine SS

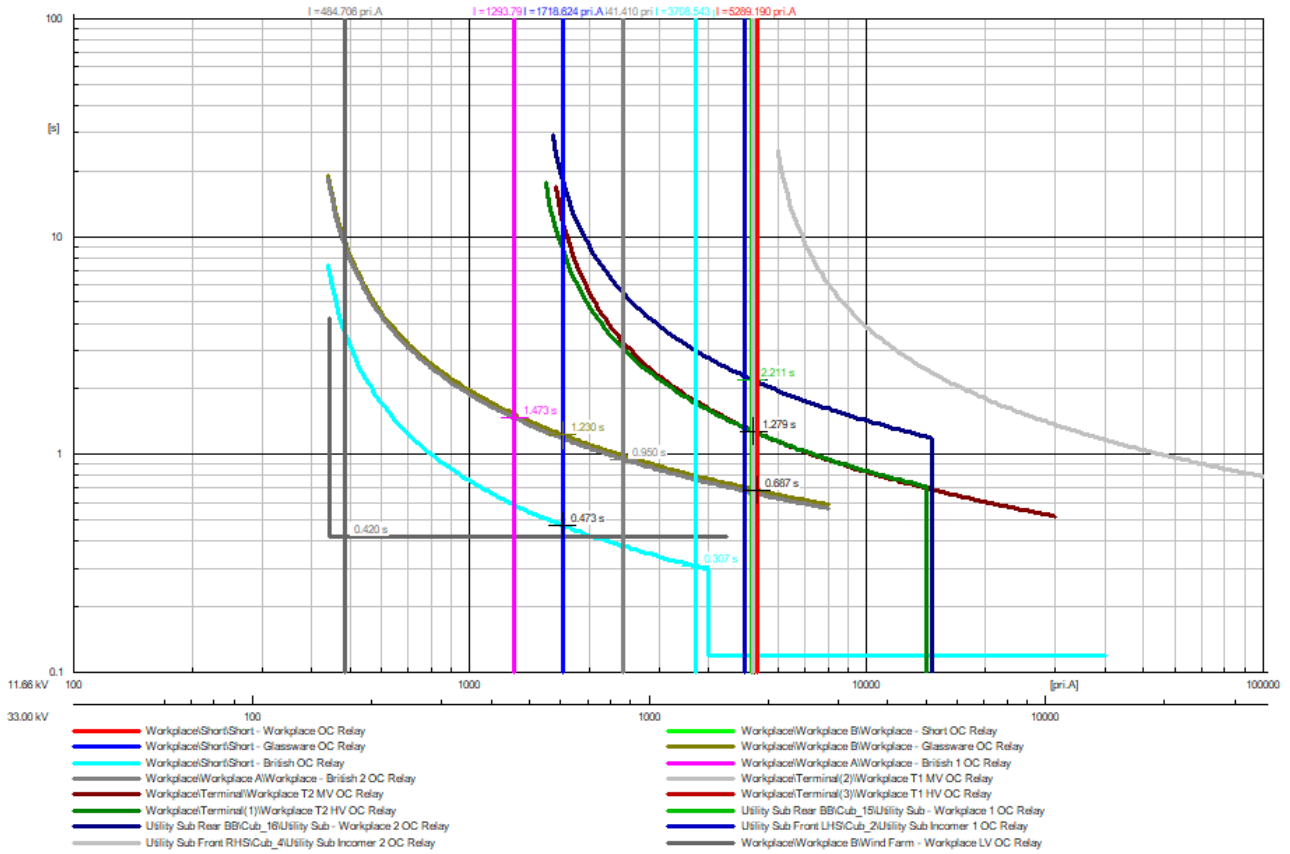


Figure H.77: The OC relay grading for a stage 1 three-phase fault at Short SS

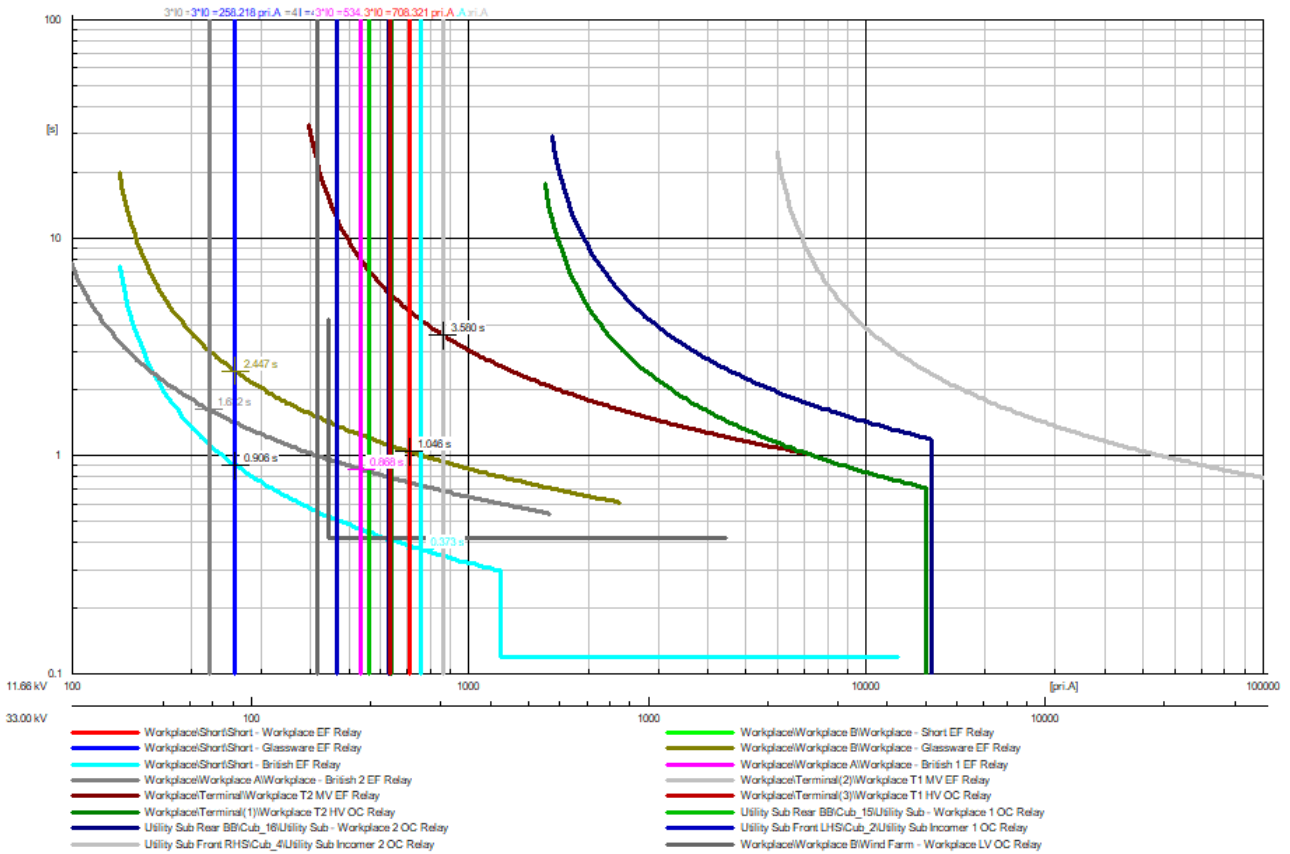


Figure H.78: The EF relay grading for a stage 1 single-phase fault at Short SS

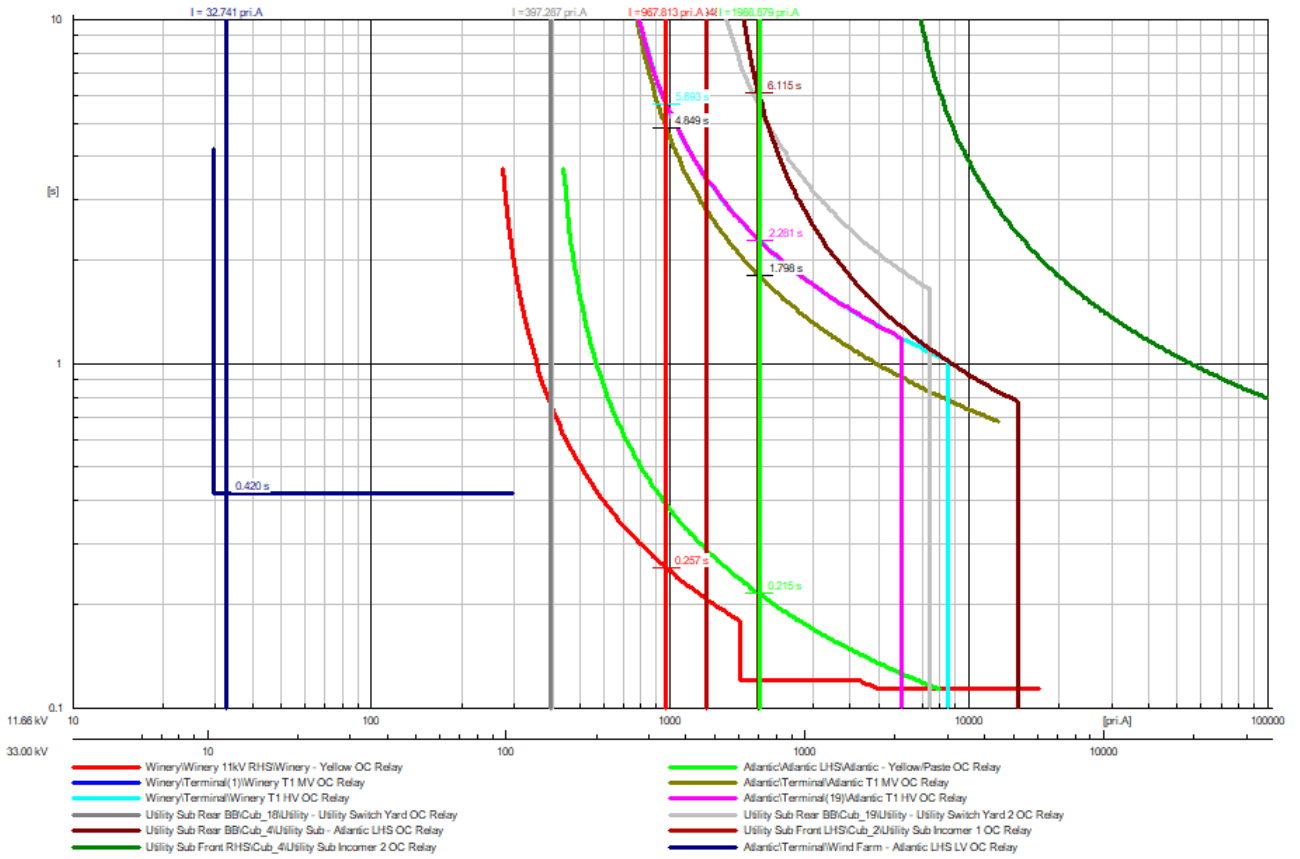


Figure H.79: The OC relay grading for a three-phase fault at Paste RMU 1 SS

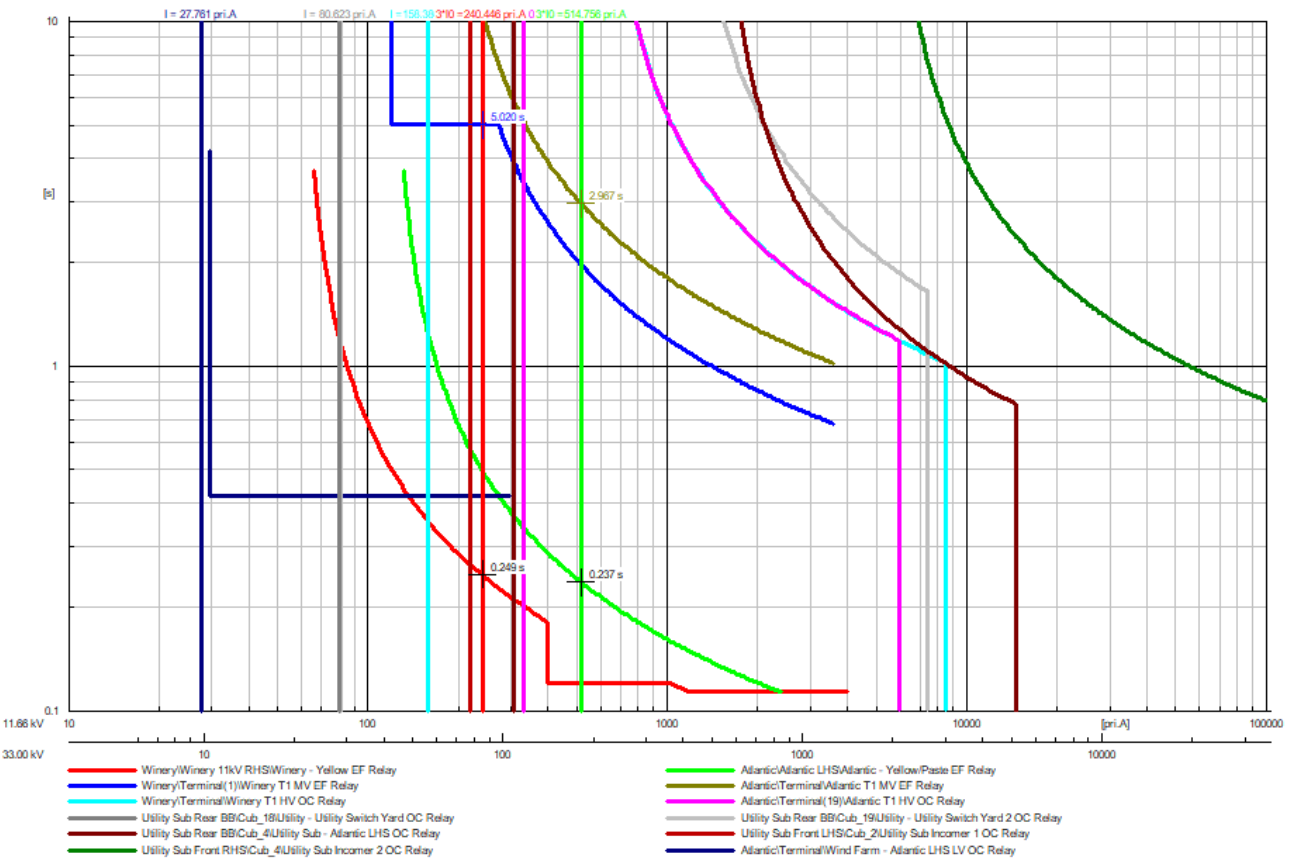


Figure H.80: The EF relay grading for a single-phase fault at Paste RMU 1 SS